Investigation into the weathering of organic coated steel and application of mathematical modelling to the data.

Wijdekop, Maarten

Investigation into the weathering of organic coated steel and application of mathematical modelling to the data.

Maarten Wijdekop

EngD Thesis

2004

University of Wales, Swansea

Department of Materials Engineering

ProQuest LLC.
789 East Eisenhower Parkway
P.O. Box 1346
Ann Arbor, MI 48106 – 1346

Acknowledgements

I would like to thank the people in the Department of Materials Engineering in Swansea University, in Corus' WTC labs in Port Talbot (now known as ECM^2), and in Akzo Nobel's labs in Darwen for their support over the 4 years that I worked on this project. First of all I would like to thank Swansea University's Dr Cris Arnold for his academic supervision, for his suggestions that were always good and for the time he spent on correcting the thesis and other publications. Another thanks goes to Dr Mark Evans for his advice on statistics and probability theory, and to Dr Dave Worsley for sharing some of his knowledge on photo-degradation processes in coatings with me and for looking after the interests of the EngD students in general.
In Corus I would like to thank Vernon John for his continuous support and Gaynor Miasik for sharing her technical expertise with me during the first two years of the project. During my trips to Akzo Nobel in Darwen I have learned a lot about paints and coatings, which was important for my understanding of the project, so thank you Anthony Lloyd and Anis Zakarias for showing me the ropes.

The four years on the EngD scheme have been a period in which I have learned a lot, but it was also fun, so I would like to thank Mel, Clare, Paul, Paul, Andrew, Andrew, John, Jon, Richard and Nathan for a good time, especially during the trips we made and the courses we did together. A special thanks has to go to Mel, Jon and Andrew R. for putting up with my antics whilst sharing an office with me and for sitting all the way through my presentations three times a year.

Most of all though, I would like to thank my parents, Kees and Margreet, and my sister Femke, for their unconditional love and support. With the benefit of hindsight I can now say that I think I have made the right choices in my life (although being a sailor or a pilot might have been fun for a while…), and your guidance played a big part in that. Thanks!
And last but not least, thank you, Opa Cor, for your support while I was a student and for your example of how hard work pays off. I hope to continue following your example.

Table of contents

Nomenclature

Some Definitions regarding Paints and Coatings:

Solution: Mix at the molecular scale

Dispersion (or emulsion): Mix at a larger than molecular scale

Polymer: A long chain of many repeating units

Monomer: A repeating unit from which a polymer is made

Oligomer: A chain of few repeating units

Polymerisation: Joining together monomers to form a polymer

Homopolymer: Polymer made with one type of monomer

Copolymer: Polymer with several types of monomers

Bleeding: Staining of a paint film by a colour from a previous coat of paint. A typical situation in which this could occur is when a red paint is over-coated with white paint (because many red pigments are sensitive to solvents).

Chalking: A thin powdery layer formed on the surface of a film after exposure to weathering. It is due to breakdown of the resin by UV light. Pigments have a big influence on chalking tendencies. Black paints show a similar breakdown defect called sooting.

Sooting: A thin powdery layer formed on the surface of a black film after exposure to weathering and due to breakdown of the resin by UV light. It is very common with films of bitumen.

Clear coating: An unpigmented coating

Flatting or sanding: Abrasion of a painted film intended to produce a level surface prior to applying finishing coats.

Floating or flooding: Partial separation of different pigments during film drying. This can result in a change of colour during drying so that the film colour is different from that of the wet paint.

Flocculation: Spontaneous reversal of pigment dispersion. To prevent it the presence of a suitable surfactant agent is often required.

Gloss: The reflectivity of the surface of a film, measured at an angle.

Mar resistance: The ability to resist minor surface scratching. It is not directly related to film hardness and can sometimes be improved by a small addition of wax.

Matt: Describes a film very low gloss.

Medium: A general term for the continuous phase in which the pigment is dispersed. Often it is called the vehicle in a liquid paint and the binder in a dry film.

Plasticiser: A liquid that can dissolve a resin but which is non-volatile and becomes part of the dry film, where it enhances the flexibility of the coating (so that it is less vulnerable to temperature changes that make steel expand and shrink, stretching the coating).

Opacity: The ability to obscure background.

Some Definitions regarding Colour Measurement:

Brightness: Brightness is the term used to describe the colour sensation as being bright or dim. It is a measure of the ability of the light entering the eye to stimulate the achromatic response from the light sensitive cells.

Hue: Hue is the term used to describe the similarity between a colour and one or more of the primary sensations: red, yellow, green or blue.

Colourfulness: The colourfulness of a colour sensation is difficult to define precisely. It can be thought as a measure of the concentration of the hue sensation. The neutral greys running from white to black are achromatic, they have zero colourfulness.

Saturation: Saturation describes the relative proportion of colourfulness to the brightness of the colour sensation. In other words every colour is regarded as mixture of the "saturated" hue and white. The colour is more saturated the smaller the content of white.

Lightness: Lightness is judged by the brightness of the object compared to that of a white viewed under the same condition. The adjectives associated with lightness are light and dark.

Chroma: The chroma is judged by the colourfulness of an object compared to the brightness of a white viewed under the same conditions. The adjectives associated with chroma are strong and weak.

SUMMARY

This EngD project is an investigation into how the aesthetic properties of organic coated strip steel are influenced by the weather. A commercial PVC plastisol coating system with a wide range of pigment loadings has been tested. The two main objectives in this work were to investigate the correlation between the pigmentations and the weathering properties of the commercial PVC plastisol coating, and to investigate the correlation between natural and accelerated weathering.

The colour fastness and gloss retention of these coatings were evaluated after exposure to natural weathering (in the UK) and to accelerated weathering (in QUV testers). Reflectance spectrometry was used for the colour measurements, as this technique gives most information about colours and is therefore most apt when attempting to correlate colour changes to the chemical processes that take place in coatings during weathering. Three processes that take place in the coating during weathering which can cause colour changes were identified with reflectance spectrometry: PVC dehydrochlorination, organic pigment degradation and chalking of inorganic pigments. A model is proposed to estimate the relative intensities of these processes from the reflectance spectra taken before and after weathering of a coating. With these relative intensities of the three processes the correlations between different types of weathering were investigated.

Gloss retention during natural and accelerated weathering was compared, and the correlation of gloss loss and plasticizer degradation was examined and confirmed.
The shades with the worst weathering performance were those containing low concentrations of a phthalocyanine green pigment combined with an inorganic yellow Cr-Sb-Ti Oxide. This is thought to be because the inorganic yellow Cr-Sb-Ti Oxide itself is relatively photo-active for a commercial pigment, and on top of that is photo-sensitised by the organic green phthalocyanine. This was confirmed with experiments that measured the photo-electrical response of pigmented PVC coatings using a dye-sensitised solar cell set-up. This concept seems to be a quick and easy way to test the photo-activity of paints.

1 INTRODUCTION

More than half of the worldwide production of organically coated strip steel is used in the construction sector, the rest goes to the domestic appliances industry (such as microwaves and fridges), to the automotive sector and to general engineering applications.

Manufacturers of coated strip steel want to give a long term quality guarantee on their product. They also need to respond to the market-driven requirement for new colours and shades. Because of this, there is a need to test new shades before they can be introduced onto the market, in order to evaluate their resistance to weathering. This EngD project is driven by this need. Its aim was to investigate the possibility of predicting service lifetimes of PVC plastisol coatings on strip steel with variable pigmentations. The stability of the visual properties (colour fastness and gloss retention) of the coatings is routinely evaluated by exposing them to natural weathering and accelerated weathering. Natural weathering is when coated strip steel panels are placed on racks outdoors and exposed to the weather. Accelerated weathering can be performed in a range of high intensity UV systems, though in this research project it is performed in a UV fluorescent tube tester (a QUV-cabinet). In this device coated panels are exposed to UV-A irradiation and condensation. This process is aimed at simulating the real weather conditions while accelerating the degradation effects on the coatings. The correlation between the performance of the shades and their pigmentations is investigated, as is the correlation between the effects of natural weathering and accelerated weathering on the coatings.

Colours of coatings are not measured using CIE L*a*b* values, as is usually done when coatings are tested for their weathering performance, but with reflectance spectroscopy. A reflectance spectrum of a coating contains all the fundamental information of the colour of that coating, so it is very useful when investigating the effects of weathering on the microscopic and chemical properties of a coating that influence its colour. In this way, attempts are made to correlate the visual changes that take place in the coatings during weathering to the different chemical reactions that can take place in a coating

during weathering, such as pigment degradation or dehydrochlorination of PVC. Other analysis techniques that have been used in this research are Infra-Red spectroscopy, Scanning Electron Microscopy, Gas Chromatography combined with Mass Spectrometry, and gloss measurements.

In chapter 2, there is a literature review with general backgrounds of this research project. An overview is given there of topics such as organic coatings of strip steel, paints, pigments, weathering, colour measurement and other methods used for analysing coatings Then in chapter 3, the materials and methods that are used in this research are discussed. In chapter 4, the results of the analysis of the PVC plastisol coatings that have been subjected to the weathering experiments are given. In chapter 5, these results are discussed, and correlations between natural weathering and accelerated weathering are explored. Also discussed is how the visual changes in gloss and colour that the coatings undergo during weathering are correlated to their pigmentations, and which photochemical reactions can be associated with those changes. In chapter 6, the results and background of a separate set of experiments are given, in which the photo-electrical response of the different pigments in PVC was tested in a Graetzel cell set-up. The results of this investigation have shown that this could be a new, quick and cheap way to measure the photo-activity of pigment combinations in new shades. In chapter 7, conclusions are drawn from the research that has been conducted, and some recommendations are made for future research activities in this area.

2 LITERATURE REVIEW AND BACKGROUND

The earth's crust contains about 5% iron, which is the earth's fourth most abundant element (after oxygen, silicon and aluminium). In addition to its abundance, it is relatively easy to process and has a very useful range of mechanical properties, however metallic iron is unstable in the atmosphere and it will be oxidized when it makes contact with oxygen and water, a process that is called corrosion. This eagerness to react is the reason that iron in nature is only found bound to other atoms, usually oxygen, to form ores (mostly Fe_2O_3). People have been extracting iron from its ores for thousands of years, but the techniques to produce high-quality uniform steel were developed only from 1700 AD onwards.

Nowadays, steel is widely used in many manufacturing sectors, due to its superior engineering properties. It is made from iron ores in two stages: The first 'ironmaking' stage is reducing the iron ores in a blast furnace by heating it in the presence of coke and limestone to produce pig iron. The second 'steelmaking' stage is a controlled oxidation where the high levels of carbon and other elements in the pig iron are removed to give the steel its desired properties [1, 2].

Once the steel is made, it is susceptible to corrosion. This can be prevented (at least temporarily) by isolating the steel from the atmosphere with a coating. Depending on the end-user requirements, this coating can be metallic or organic. This research is focused on organic coatings (paints), applied to strip steel that is used in the construction sector.

2.1 Organically Coated Steel

About 50% of all metal components receiving protection against corrosion rely on paint for this. A paint can be regarded as a pigmented material that, when applied as a liquid to a surface, forms a dry adherent film after drying or curing. Its principal functions are protective (corrosion resistance) and aesthetic (colour, gloss).

Steelmakers paint their strip steel in order to move their business downstream and to offer their customers a more valuable product. This is done on large coil-coating lines, and has many benefits; one can think of time and energy savings because of the scale on which the painting is done, well co-ordinated solvent extraction and recycling, and of course the immediate protection of the steel against corrosion from the moment the paint is applied.

In Europe, the construction industry accounts for 70% of the total consumption of pre-painted organic coated steel [3]. To increase the value of their product, manufacturers are giving their customers product performance guarantees on their pre-painted strip steel products of up to 30 years. These guarantees are based on the quality of the coating systems, the geographical location of the building that they are used in (i.e. the climate), and the way that the panels are used in the building (e.g. in the roof, on a wall, on a tilted surface, and the geographical orientation of the coating). The guarantees increase the amount of product development and testing that needs to be done before new shades can be introduced to the market. This is the driving force behind research into weathering resistance.

The coatings that are investigated here are based on poly(vinyl chloride) (PVC), which is used in a wide range of applications, such as pipe and fittings, films and sheet, coatings, flooring and insulation materials [4]. When PVC based systems are used as coatings on strip steel it is usually for outdoor applications such as construction and the automotive sector, because of the good weathering resistance. The coating system applied to the strip

steel in this research is a PVC plastisol, this is a commercial paint system with additives in it that modify all the important properties.

Poly(vinylidene fluoride) (PVDF) is also used in coil coatings, in a plastisol-like dispersion, and its co-polymers find use in powder coatings [5]. These coatings also provide good weathering resistance, and are a bit more 'high tech' than the PVC-based plastisols (PVDF can be applied in a 20 microns layer to give the same performance as 200 microns of PVC plastisol).

Polyurethane coatings are widely used for coatings, where they can be applied from solvent, by hot melt or by powder coating technology [4]. Their usefulness is based on characteristics that are different from most other binders available for coatings, like the potential to form stable intermolecular hydrogen bonds between polymer chains [5]. This makes polyurethane a good material for primers (the coating between the metal and the topcoat) [6, 7].

Poly(ethylene terephthalate) (PET) is a polyester, it also has many applications (plastic bottles, packaging film). When it is used as a coating for strip steel, it is generally for indoor applications, such as home furnishings and white goods [4].

2.2 Pre-painted Strip Steel for the Construction Industry

The steel substrate that is coated for construction purposes is typically 0.7 mm thick for roofing applications, and 0.55 mm for wall cladding [3]. It is coated with multiple layers on both sides.

The first layer that is applied is a zinc coating. This metallic coating provides sacrificial galvanic protection at the cut edge of the panels, and in areas where the coating is damaged. The process mostly used for applying the zinc layer is called hot dip galvanizing; the strip steel is fed through a bath of molten zinc at high speed, after which the layers of zinc that are formed on the surface on both sides of the strip steel are reduced to 10 - 20 μm with air knives.

Then the strip is treated with a chromate solution, which is done to increase the adhesion of the paint layers to the metal and to act as a corrosion inhibitor. For reasons to do with environmental legislation this process will need to be replaced with an alternative in the near future.

After this, the primer is applied to the strip by coil coating. For PVC plastisols, the primer is usually an acrylic-based system, applied in a 5 μm thick layer, but polyurethanes can also be used. The reverse side of the strip can also have a primer, which is usually polyester based.

In coated strip steel used in construction, the external facing side (that is exposed to the weather) is coated with a different layer than the internal facing side. For the internal face generally a 10 μm polyester back-coat is applied. For the panels that are being investigated in this project, the external face has been coated with a 200 μm top-coat of a commercial PVC plastisol paint system. This is a high performance paint that has been developed continually since the mid 1960s by Corus and its partners.

The different layers on strip steel are schematically represented in Figure 2.1.

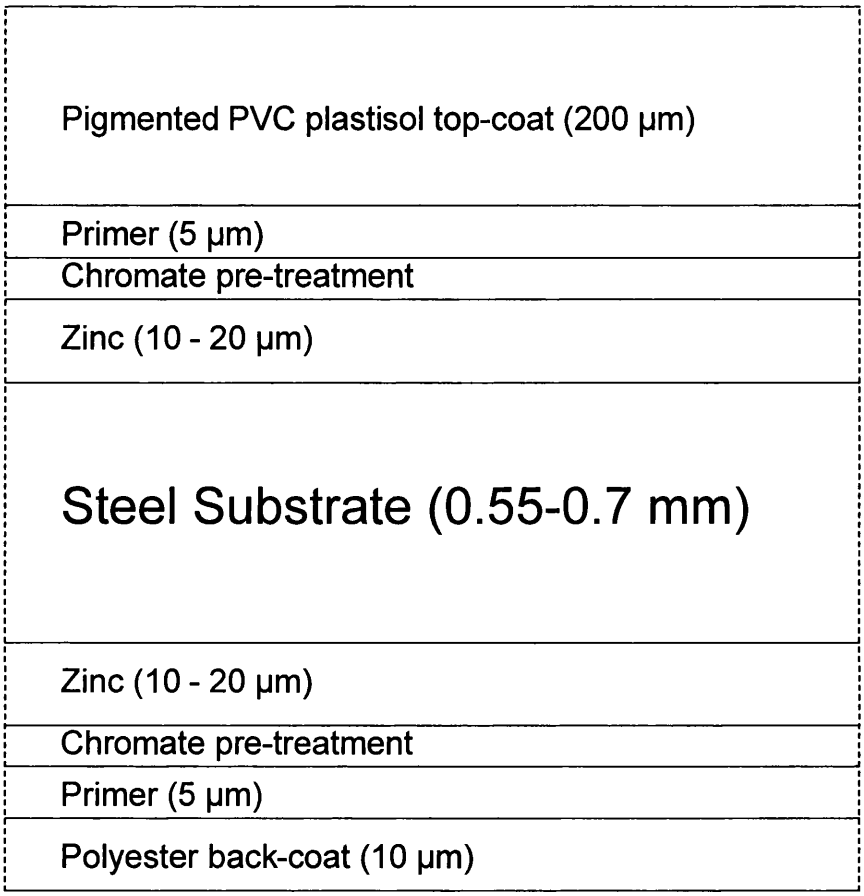

Figure 2.1 Schematic representation of the multiple layers applied to strip steel

2.3 Paints

The principal components of paints are binders, pigments and dyes, solvents, plasticisers and additives [8]. Binders form the matrix that holds the film together. Pigments and dyes provide colour and opacity. Solvents facilitate application and evaporate during drying/curing. Plasticisers make the paint film flexible and additives have specific functions like plasticization, UV protection and fire retardation. In the following paragraphs, the functions and properties of these components are described in more detail, as they are found in the commercial PVC plastisol paint that is investigated here.

2.3.1 Binders

The term binder reflects a functional role in the paint of binding together the paint's other components. Alternative terms that can be used are film former, resin and vehicle.In the case of plastisol, the binder is a polymer called poly(vinyl chloride) (PVC). PVC plastisol paint systems are widely used, because their properties are easily adjustable, they have good weathering resistance, and they are relatively cheap [9]. The structure of PVC, the homopolymer of vinyl chloride, is a simple carbon chain with a chlorine atom on every second carbon (Fig. 2.2):

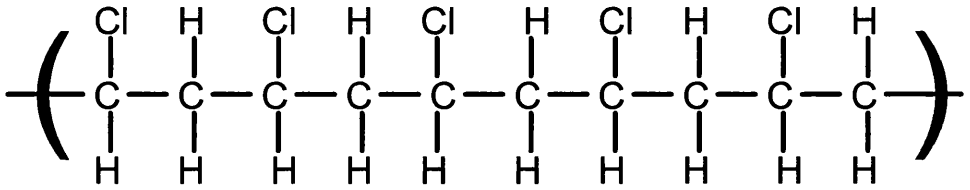

Figure 2.2 : Structure of PVC

With PVC (and other polymers), an important parameter is the polymer molecular weight. The viscosity of the polymer is dependent upon the structure and the molecular

weight distribution (low molecular weight gives fluid resins (low viscosity), and high molecular weight gives very viscous (thick) resins). Viscosity of course is a critical property in the coil coating process. The presence of pigments, solvents and additives in paints also influences the viscosity of the resin.

When a PVC-based coating is attached to the strip steel substrate after curing of the resin, another factor comes into play. Polymers have glassy and rubbery states; the transition point between these states is at the glass transition temperature, usually called Tg. Below Tg films are hard and glassy, tending to break rather than deform under stress. They have reduced impact resistance, flexibility and poor formability. On the other hand chemical resistance is maximised and permeability is low. Above Tg films are rubbery, relaxed and they deform easily under stress. They have good impact resistance, flexibility and formability, permeability is high and adhesion is maximised [9].

For low molecular weight polymers, the Tg increases with the molecular weight. This happens because as the chains get longer, they get more intertwined and will experience more resistance when they are dislocated. This makes the film more rigid, and increases Tg, the temperature needed to reach the rubbery, flexible state. However it is characteristic that above a certain molecular weight, Tg stops rising and reaches a plateau, as at this point elongation of the chains will not increase the resistance between them anymore. The Tg of unplasticized PVC is generally between 75 and 105°C [9].

In plastisols, the Tg is lowered by addition of plasticisers (see section 2.3.3). These are relatively small organic molecules that can lower the intramolecular friction of the polymer chains as they move alongside each other; one can think of their function as 'lubrication'. Another effect of plasticisers being present in the coating is that there is not one Tg point for the plastisol, but a Tg range. The temperatures to which the plastisol coating is normally exposed, will be within this range, so that the PVC film finds itself in between the glassy and the rubbery state.

During weathering of PVC plastisol coatings, plasticiser degradation will increase the resistance between the PVC chains, as will cross-linking reactions. This will increase the Tg, so that the coating will find itself in the glassy state, which will lead to embrittlement and cracking of the film.

Another process that takes place during weathering is chain breakage of the polymer; this will shorten the PVC chains and lower their molecular weight, and with that the Tg will decrease. However, this process starts playing a role relatively late in the weathering process of a PVC-plastisol coating, so it will not have a big impact.

2.3.2 Solvents

Solvents are used to dissolve the other components. In solvent-based systems they are used to dissolve the resin and to adjust the viscosity of the liquid paint to suit the method of application.There are true and latent solvents; a true solvent will dissolve the resin of interest, whereas a latent solvent enhances the solving capacity of a true solvent but is not able to dissolve the resin on its own. A solvent will enable the paint to have a higher resin content at the same viscosity or a lower viscosity at the same resin content. Solvents are added to improve the rheology of the paint for the coil coating operation.A dry film from a resin with a good true solvent will be clear, smooth and glossy [8].

2.3.3 Plasticisers

Of the substances that make up a PVC plastisol commercial paint, plasticisers are added to the resin in the largest volume fraction. Their function is to 'plasticize', i.e. to make the dry paint film more flexible and to prevent cracks from forming on the surface [10].

Plasticisers are very important because they greatly differentiate and diversify the properties of PVC-based products.

Plasticisers act to reduce the glass transition temperature (Tg) of PVC. In rigid, unplasticized PVC, strong interactions exist between neighbouring polymeric chains, resulting in a rigid network. When the PVC is heated, these interactions are lost, resulting in a flowable and formable melt. Unplasticized PVC will regain its rigidity when it is cooled again, as the interactions between the PVC chains are reformed. If the PVC is heated in the presence of a plasticiser, an intimate mix of polymer and plasticiser is formed in the melt. When this melt is cooled, the plasticiser molecules set up their own interactions with the PVC chain. The plasticiser molecules usually have long alkyl chains, which screen the PVC chains from each other, preventing them from forming the chain-chain interactions which give the unplasticized polymer its rigidity. As long as there is sufficient compatibility between the polymer and the plasticiser, the plasticiser will be retained and the system will be flexible [11].

Plasticisers are not chemically bound to a polymer [12]; the ester groups attached to the benzene ring can attach themselves temporarily to a polymer chain by inter-molecular forces, while the flexible alkyl groups provide a separation between different polymer chains [13]. In this way the polymer chains are able to move alongside each other with less friction, which makes the coating more flexible. Because the plasticiser molecules are relatively small and mobile, they can escape from the resin by leaching and evaporation. Plasticisers are often the first components to be degraded by UV-irradiation, and this is often the main cause of plasticiser loss. These are common problems in the paint industry that can result in microcracking and delamination of the paint film[14, 15].

Plasticisers are typically oily organic liquids with a high boiling point, often esters [10, 13]. The main plasticiser of relevance for this project is DIDP (di-isodecyl phthalate), a phthalate ester (Fig. 2.3):

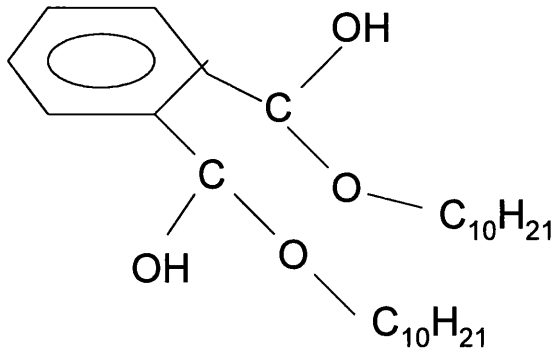

Figure 2.3 structure of DIDP

This plasticiser is popular because of its ability to keep PVC soft and pliable at temperatures as low as -30 °C and to endure prolonged temperatures up to 95°C, its low volatility, and its resistance to UV degradation and fungus attack [10].

Some examples of other commercial and classic plasticisers are shown in Table 2.1:

Table 2.1 : Plasticisers used in PVC applications [13].

Plasticiser	Chemical name	Molecular structure	Purity	Molecular weight
DBA	Di-butyl adipate	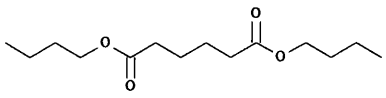	96%	258.36
DBP	Di-butyl phthalate	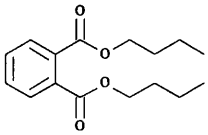	99%	278.35
DIOP	D-iso octyl phthalate	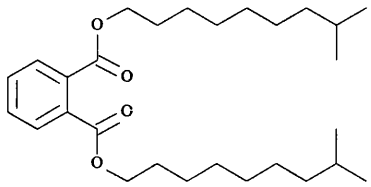	Isomeric mixture	444
TBP	Tri-butyl phosphate	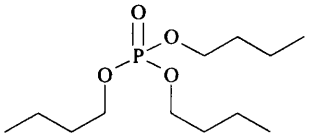	98%	266.32

Dibutyl adipate (DBA) is an adipate plasticiser and usually consists of esters of adipic acid or hexanedioic acid. Dibutyl phthalate (DBP) is a phthalate plasticiser and as such is a member of the larger of the plasticiser types, like DIDP and DIOP. Di-isooctyl phthalate (DIOP) is a commercially available plasticiser used in many PVC applications. Phthalates are manufactured from phthalic anhydride and many commercial plasticisers consist of an isomeric mixture.

Tributyl phosphate (TBP) is a phosphate based plasticiser: In the early days phosphates were found to be effective PVC plasticisers and were adopted along with the phthalates into PVC technology. However they were incapable of competing with the cost effectiveness of the phthalates for general purpose use and so are now considered a speciality plasticiser used mainly for their fire resistance qualities [13].

2.3.4 Other Additives

Additives, also known as modifiers, can be thought of as substances added in small quantities to a coating material to improve or modify one or more properties. Plasticisers can also be thought of as additives, but because of the importance of their function and their relatively large concentration they were described separately in the previous section. Here, the functions and chemistry of these other additives will be described.

PVC plastisol systems that are exposed to sunlight need UV protection to slow down photo-degradation of the PVC chains and the plasticiser molecules [9]. UV protection can be achieved by UV screening, where the high energetic UV light is prevented from reaching the photo-active sites. This can be achieved by the use of inorganic pigments in the paint (such as TiO_2), which generally reflect the UV radiation back out of the coating.

.

Another way of doing this is by UV absorption, where Ultra Violet Absorbers (UVAs) are added to polymer paint systems. UVAs are chemicals that would ideally absorb light of wavelengths between 295 and 400 nm, and then transform it into a harmless form with wavelengths greater than 400 nm. Compounds used for this include oxanilides and benzotriazoles (Fig. 2.4).

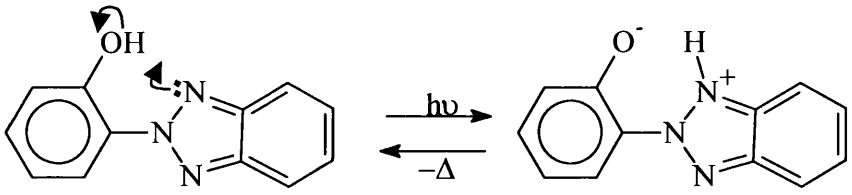

Figure 2.4 : UV-protection by absorption followed by dissipation of harmless energy (heat) by a benzotriazole [13].

UV and heat stabilisation of PVC systems can be achieved in different ways; one of them is excited-state quenching: This is when the decay of the excited state of a photodegradable molecule is accelerated by a quencher, so that the chance of that

molecule actually starting the degradation reaction is minimised. Quenchers that can be added to PVC systems include nickel- and cobalt chelates [9].

Scavenging of reactive molecules is another way of UV and heat stabilisation. This is when for example free radicals or HCl molecules are neutralised by reaction with the scavenging agent.

Mono- and Dibutyltin thioesters are added to PVC systems for UV and heat stabilisation. These substances can provide dual action stabilisation; they react with HCl, and are involved in addition reactions with polyenes. This way, they can reverse the dehydrochlorination of PVC (Fig. 2.5).

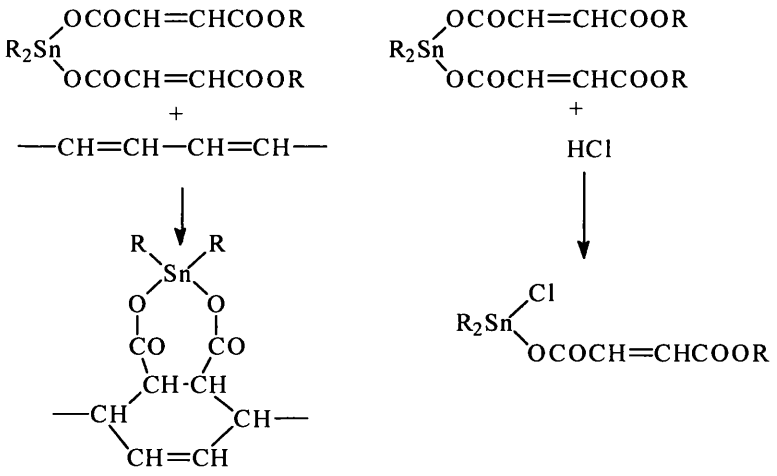

Figure 2.5 : Dual action stabilisation of tin maleates ,an addition reaction with polyene and HCl scavenging [13].

Outdoor coatings also need to have protection against fungi and other micro-organisms. This is done by adding biocides and fungicides to the paints. Substances that are used for this include tin, arsenic and antimony compounds. Bactericides are also added and include chlorinated hydroxyl-phenyl esters and tin compounds [10].

Organic coatings used in buildings by law need to meet European fire resistance standards; PVC plastisols contain fire retardants to slow down the spreading of a fire and increase the safety of the building.

Antimony trioxide (Sb_2O_3) has historically been used as a fire retardant. However, in future formulations, this substance will be removed to comply with new environmental legislation. Metal borates also find use as fire retardants, but these substances have multiple functions in light- and temperature stabilising and as fungicides and biocides.

In commercial PVC paints, mixtures of additives are used to gain the most efficient stabilisation. Stabilisers often have multiple functions, and it is recognised that the result of different stabilisers combined is greater than the sum of their individual performances.

2.4 Pigments and Dyes

Colorants can be divided into two types: pigments and dyes. Dyes are soluble in the application medium, where they are present in their molecular state. Pigments are insoluble in the application medium, where they are present in a colloidal state [16].

Pigments and dyes are catalogued in the "The Colour Index" which is published by The Society of Dyers and Colourists [17]. They are catalogued by chemical type and given a systematic name, sub-types are given a number. All the known commercial pigments and dyes are listed here, with useful information on the application methods and the fastness properties. The Colour Index is regularly updated and universally accepted as the most important reference for colorants.

Dyes are mostly used for the coloration of textiles, where they are usually applied through an aqueous medium. Pigments are typically used in paints, inks and plastics. They are applied through a (usually organic) medium in which they are dispersed, not dissolved. Their small, but solid particles are held in their place mechanically, usually in the matrix of a polymer [16].

Pigments can be classified according to a variety of different criteria. There are organic and inorganic pigments, and they can be of natural or synthetic origin. In the paint industry synthetic pigments are better and more economical than natural ones, so they are generally preferred. Organic and inorganic pigments are roughly equally important in the paint industry.

Inorganic pigments provide excellent resistance to heat, light, weathering, solvents and chemicals, and they are generally cheaper than organic pigments. The range of modern inorganic pigments is dominated by metallic oxides (titanium, of course, and iron and chromium), along with some lead chromates and cadmium sulphides. Inorganic pigments

generally exhibit high opacities, which can be attributed to the compact atomic arrangement in their crystal structure [16].

Organic pigments are generally found to have more colour strength and brightness than inorganic ones, and they are generally preferred when the appearance is relevant. However, they are generally unable to provide the degree of opacity that inorganic pigments offer, because of the lower refractive index associated with organic crystals. Amide (-NHCO-) groups feature prominently in the chemical structures of organic pigments, and enhance the fastness to solvents, light and heat. The incorporation of metal ions and halogen substituents in appropriate places in the chemical structure can also increase the fastness of organic pigments. The colour fastness that organic pigments offer is variable; high performance organic pigments with good durability tend to be expensive. [16]

Important properties of pigments in paints are [8] :

- Chemical nature and reactivity. Obviously the ideal pigment would be stable and inert to reactions with other components in the paint.
- Light fastness. This is a measure of the permanence of a colour during irradiation with (sun) light; it may vary with the presence of other pigments in the paint.
- Thermal stability. This is a measure of a pigment's inertness to colour and/or structural change with temperature.
- Crystal structure. This influences the interactions of the pigment with light.
- Particle size and particle size distribution. It is very difficult to find pigments with a uniform particle size; they have a range of sizes that is usually denoted by an average size. If greater precision is required then the size range can be defined by a particle size distribution, which is usually a skewed distribution that can be described with a lognormal function. The particle size of a pigment will influence its light absorbing and scattering properties.
- Particle shape. The shape of a pigment can vary from acicular (needle-like) to cubic, spherical or plate-like. It will influence the light absorption and scattering properties, and will have an important bearing on the rheological and dispersion properties of pigments.

- Refractive index. The refractive index of a pigment relative to that of its environment determines the light scattering properties. If the refractive index of the pigment matches that of the binder then the pigment becomes transparent. The larger the refractive index difference between the dispersed and the continuous phases is, the greater the amount of the light the pigment will scatter. This effect is similar to that of small bubbles of air (RI = 1) causing water (RI=1.33) to become white as in a foam.
- Critical pigment volume concentration. When the properties of a paint film are examined, such as gloss, film hardness, permeability, corrosion protection, flexibility etc., the following is observed. As pigment is added to the binder, there is a gradual change in these properties until a certain pigment volume concentration is reached; then a rapid change in properties occurs over a very small change in the pigment volume concentration. This concentration is called the critical pigment volume concentration (CPVC). The CPVC is the region when close packed pigment particles have just enough binder to fill the voids in between themselves. Beyond the CPVC there is not enough binder to surround all the pigment particles.

The most important blue and green pigments are phthalocyanines. This is the most important chromophoric system used in the industry, because of their intense, bright colours, and their high stability. They were accidentally discovered in 1928 by Scottish Dyes, and have been studied extensively ever since. C.I. Pigment Blue 15 (Fig. 2.6) is the blue pigment tested in this research. It has the basic phthalocyanine structure with a copper ion in the middle, and is by far the most important blue pigment, finding almost universal use in paints, inks and plastics.

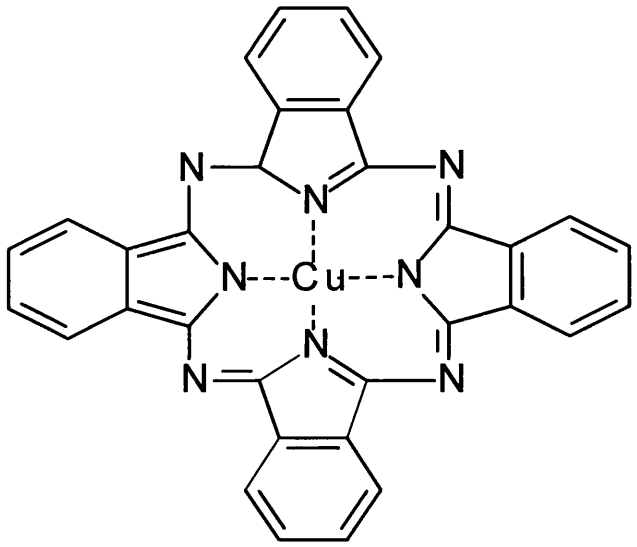

Figure 2.6 : structure of C.I. Pigment Blue 15 (copper-phthalocyanine)

The green pigment tested in this research is also a copper-phthalocyanine. In CI Pigment Green 7, the 16 ring hydrogen atoms are virtually all replaced by chlorine (Fig. 2.7), which makes it hexadecachloro-copper-phthalocyanine.

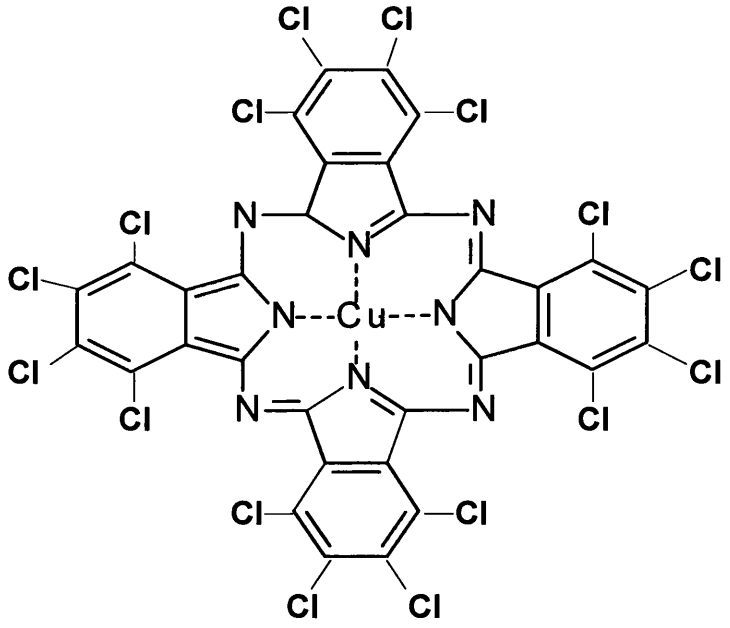

Figure 2.7: structure of C.I. Pigment Green 7 (hexadecachloro-copper-phthalocyanine)

Substituents on the aromatic rings in the C.I. Pigment Green 7 shift the absorption band to longer wavelengths, resulting in a shift from blue to green.

There is a high level of symmetry in the phthalocyanine molecules, which is increased by the presence of Copper in the centre. This results in very narrow absorption bands and in colours that are perceived as very bright. The extensive resonance stabilisation throughout the system might well account for the high stability of phthalocyanines. In addition, copper phthalocyanines are relatively cheap to produce, in spite of their complex structures, because their synthesis is straightforward and they give high yields from inexpensive, commodity starting materials[16].

Red pigments, including the one tested in this research, are often based on diketopyrrolo-pyrrol (DPP), as shown in Fig. 2.8. This is a group of high performance pigments with properties similar to the phthalocyanines. They were discovered in 1974, after which an intensive research study at CIBA led to an effective 'one pot' synthesis procedure from readily available starting materials.

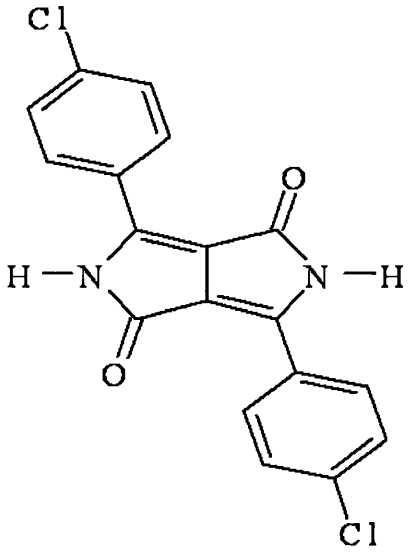

Figure 2.8 : structure of C.I. Pigment Red 254 (diketopyrrolo-pyrrol)

The two fused five-membered ketopyrrol rings are the essential structural feature of DPP pigments, which, through appropriate substituent variation, are also capable of providing orange, and violet-blue shades [16].

The commercial yellow pigments are often inorganic, such as chromium-, nickel- or antimony-doped titanium dioxide (one of these is tested in this research and will be discussed below), cadmium sulphide and lead chromate.

The organic yellows are generally azo-pigments (containing -N-N- or -N=N- groups), or conjugated systems consisting of five-and six membered rings, such as C.I. Pigment Yellow 138 (Fig 2.9). This pigment, which is tested in this research, is a Quinophthalone structure with eight chlorine atoms in the molecule.

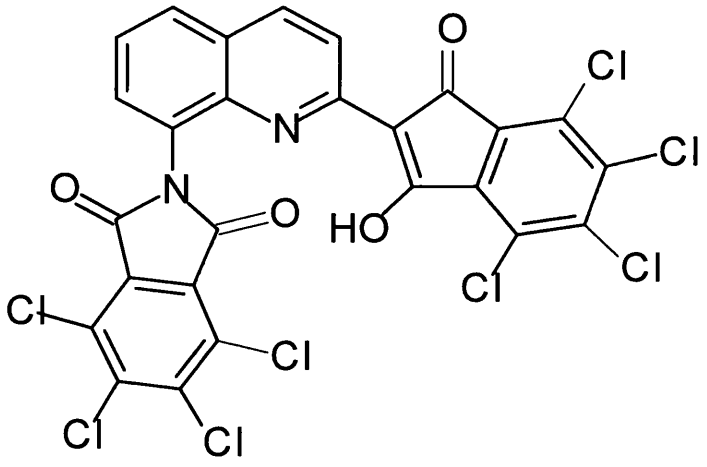

Figure 2.9 : structure of C.I. Pigment Yellow 138 (quinophthalone)

Titanium dioxide (C.I Pigment White 6) is by far the most important opaque white pigment, due to its whiteness (high scattering and low absorbance), and its excellent durability and non-toxicity. It accounts for two thirds of the total inorganic pigment trade worldwide [8]. Titanium dioxide is manufactured in two polymorphic forms: rutile and anatase (Fig. 2.10). The rutile form has a more compact atomic arrangement, which gives it a higher refractive index and with that more opacity. The rutile form is also more

durable and less photo-active, so it is commercially far more important than the anatase form. Anatase is used in paper and synthetic fibres. The white pigment that is tested in this research is a high performance rutile TiO_2 grade.

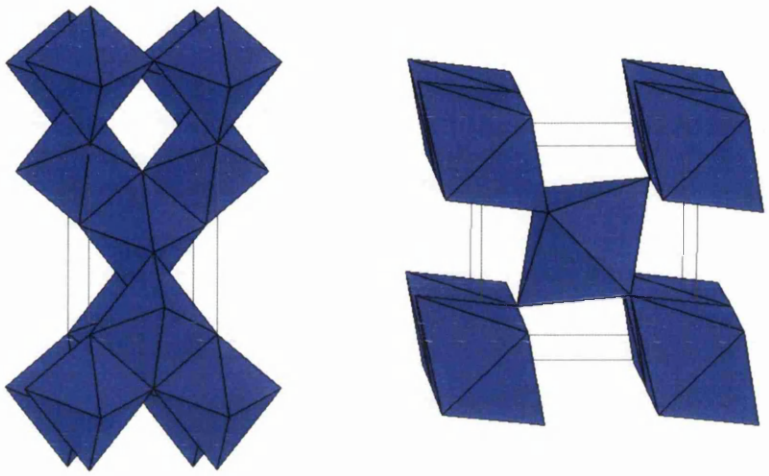

Figure 2.10 : anatase (left) and rutile (right) structures of titanium dioxide (ref)

Titanium occurs in many abundant minerals, like ilmenite ($FeTiO_3$), leucoxene (TiO_2 .$xFeO.yH_2O$), and in the rutile and anatase TiO_2 forms themselves. Traditionally, titanium dioxide was won from ilmenite ore with the so-called Sulphate process, which is a low tech labour intensive batch process based on aqueous chemistry. A new technology, called the Chloride Process, was developed by Dupont in the 1950s. It is based on flame technology and offers waste disposal, quality and energy advantages over the Sulphate process.Both processes now are equally important on a worldwide basis.

As mentioned above, an inorganic yellow (or brown) pigment is also tested in this research. This is C.I. Pigment Brown 24, a titanium / chromium / antimony oxide. It is based a rutile TiO_2 mother-structure, where approximately 1 in 10 of the Ti (IV) cations are substituted by either a chromium (III) or an antimony (V) cation (a process called 'doping').

Rutile pigments are manufactured from anatase TiO_2, or titanium dioxide hydrolysate containing sulfuric acid. Finely divided metal oxides, hydroxides or carbonates are mixed in and the homogeneous mixture is calcined continuously in rotary furnaces at a temperature of 1100 to 1200 °C. Atmospheric oxygen is blown in to oxidize the trivalent antimony. This substitution doesn't change the basic structure of the host TiO_2 lattice, but it changes the dimensions of the unit cell in the lattice [18].The influence of the octahedral oxygen ion field on the d-electrons of the Chromium cations shortens the band-gap of the material compared to that of TiO_2 , which means that light of a longer wavelength than 400 nm (the cut-off point for TiO_2) can be absorbed by the pigment [19]. This causes the yellow-brown colour of the pigment. The Sb(V) cations are added to balance the valencies and achieve electro-neutrality in the lattice.

2.5 Weathering

Almost every polymer, and consequently every polymer-based coating, deteriorates when exposed to solar irradiation. It is commonly accepted that the ultra-violet (UV) part of the sunlight causes most of the damage in coatings during weathering, while oxygen, moisture and heat also play a part in most degradation reactions [20-23]. Another parameter that has a large influence on the degradation of a coating exposed to the weather can be termed the "severity of cycling". Climates with repeated or severe changes in temperature, humidity and irradiation can fatigue the specimen, causing more deterioration in the coating than steady-state climates. Atmospheric contaminants (dirt, soot, smog, etc.) also play their part in the degradation and discolouration of coatings.

The testing of the resistance of coatings to weathering can be done by natural weathering (where coated panels are put on racks outdoors and exposed to the elements) and by accelerated weathering (where coated panels are placed in cabinets where they are subjected to irradiation with UV-lamps and condensation cycles).

Light plays an important role in this research, both in the irradiation during the weathering process and in some of the techniques that are used to analyse the coatings. To clarify some of the issues, the next section sheds some light upon the electromagnetic spectrum, which contains all forms of electromagnetic radiation.

2.5.1 The Electromagnetic Spectrum

The electromagnetic spectrum contains all forms of electromagnetic radiation (Fig. 2.11). The higher the wavelength, the lower the frequency of the radiation and the lower its energy will be. The spectrum starts at wavelengths of 10^{-13} m with highly energetic gamma rays, which can be found near radio-active elements. Then, there is the X-ray region, followed by the ultra violet (UV), visible and infra red (IR) regions. At the low

energy end of the spectrum there are microwaves, used in radar and in (of course) microwave cookers, and then there are the very low energetic radio waves, which have wavelengths of 0.1-10 m, and are used in radio communication.

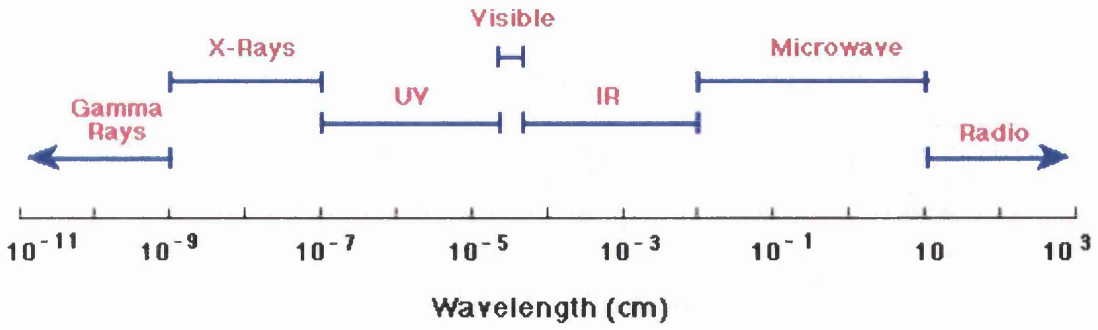

Figure 2.11 : The electromagnetic spectrum.

The UV, visible and IR regions of the electromagnetic spectrum play a role in this project. The solar radiation that reaches the earth is spread over these three regions (Fig. 2.12).

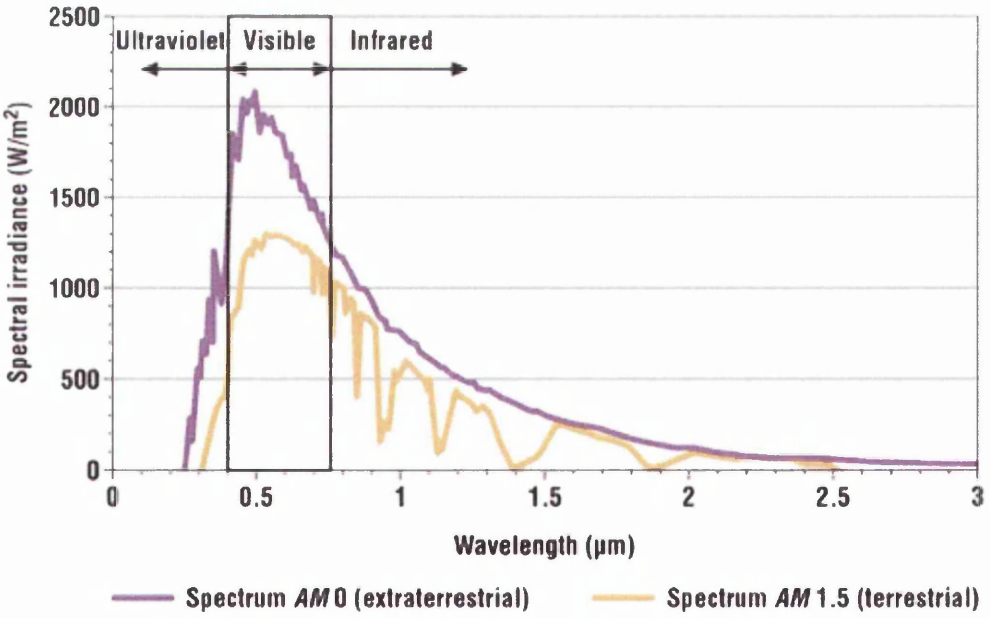

Figure 2.12: The irradiance spectrum of extraterrestrial sunlight and that of sunlight that reaches the surface of the earth[24].

There are two spectra in Figure 2.12, The extraterrestrial AM0 spectrum is the spectrum of sunlight that falls onto a plane perpendicular to the direction of the sun's rays just outside of the earth's atmosphere, before any absorption can take place in the atmosphere. The terrestrial AM1.5 spectrum is a spectrum of sunlight that reaches the earth's surface. Components in the atmosphere absorb radiation of certain wavelengths. These wavelengths correspond with electronic transitions or vibration energies of the radiation-absorbing molecules in the atmosphere (ozone, water, nitrogen and oxygen). This causes the absorption bands that are clearly visible in the AM1.5 spectrum.

'AM' stands for 'Air Mass'; if the sun's rays are perpendicular to the earth's surface, which can only happen in the tropics, sunlight only has to pass through the vertical air mass (AM) of the atmosphere once. Therefore, this state is called AM 1. In all other cases, the route of the solar radiation through the atmosphere is longer. How much longer depends on the sun's altitude angle, γ_s. (Fig. 2.13)

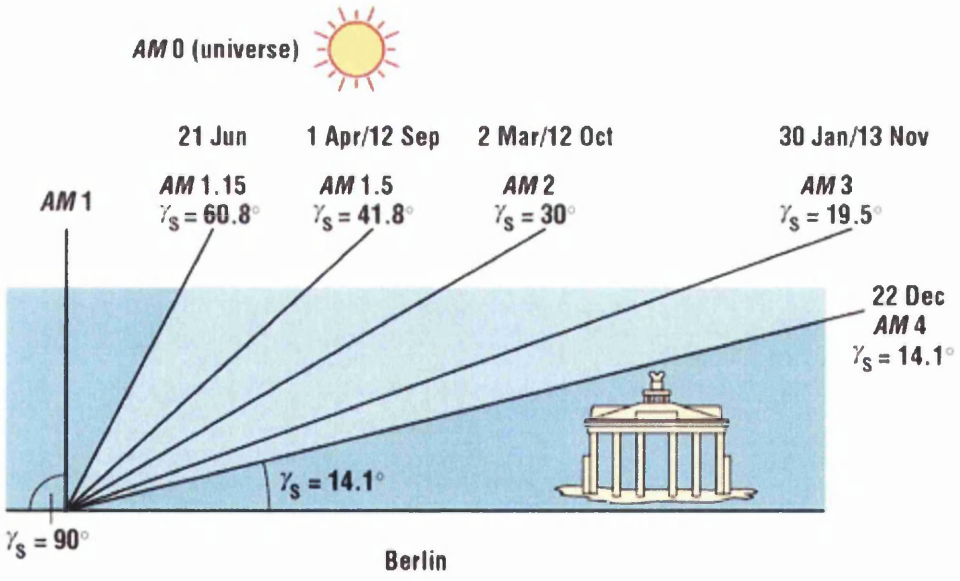

Figure 2.13: The concept of Air Mass explained with the solar altitude angle measured in Berlin on different days in the year when the sun is at its highest point [24].

The sun's altitude angle can be calculated when the latitude of the location, the date and the time are known. How this is done is shown in Chapter 3, where the yearly γ_s profiles for Darwen (Lancashire) and Rye (East Sussex), the outdoor exposure sites that have been used in this research, are calculated. With this angle, the air mass can be calculated with a simple formula (also given in Chapter 3). AM1.5 indicates that the path of the sunlight through the atmosphere is 1.5 times that of AM1, the shortest route to the earth's surface (when $\gamma_s = 90°$). This is the length that the rays must travel when the sun's altitude angle γ_s is 41.8° [24].

The AM1.5 spectrum is a standard solar irradiance spectrum, used for calculations on solar cells etc, and in this research it is used to estimate the amount of UV-irradiation that coatings receive when they are exposed to the weather at different locations in the United Kingdom.

The cut-off point of terrestrial solar irradiation is at 295 nm, so the part between there and 400 nm is in the UV region of the electromagnetic spectrum. This is the highest energetic part of the sunlight, which causes people to tan, but can also cause skin cancer and eye damage. Not surprisingly this part is responsible for most of the damage that is done in coatings during weathering.

Then there is the visible region, which runs from 400 nm to 750 nm. Light in this region can be perceived by the human eye, which happens when we see objects that are illuminated by sunlight: What is seen is the visible part of the solar irradiation that is reflected by the object. The colour of an object is determined by which wavelengths in the visible region are absorbed and which ones are reflected by the object. Only if the object is white is there no absorption, and all the visible light is reflected.In reflectance spectroscopy these properties are measured and analysed; more on this will follow in section 2.7.1.

The energy of sunlight in the UV and visible regions (295-750 nm) is in the same order as the excitation energy of binding and non-binding valence electrons. When a molecule absorbs a photon (a light particle) in this region, an electron is brought into an excited

state, which can cause the molecule to react. This is more so when UV light is absorbed because it has more energy than visible light. In this way, polymers like PVC are prone to degradation reactions when irradiated with UV light.

In the visible region, the energies are lower and less likely to trigger degradation reactions. Pigments and dyes have electron transitions with energies in this region, enabling them to absorb visible light at certain wavelengths while reflecting it at other wavelengths. This property gives them their colour.

A large part of the sunlight that reaches the earth has wavelengths greater than 750 nm, which makes it part of the IR region. This light is not visible, and the energy of the photons in this region is generally too low to excite electrons and trigger reactions. It is at the level of the vibration and rotation energies of molecules. The IR part of sunlight is responsible for most of the warming up of objects that are irradiated, as the vibrating of molecules generates heat. In IR spectroscopy the absorption of IR light by a substance is measured and then correlated to characteristic vibrations of different groups of atoms in the molecule. More on this subject will follow in section 2.7.2.

2.5.2 Chemical reactions during Weathering

Photo-degradation is perceived as the principal reaction that takes place in coatings during weathering [8, 25]. In this process the organic components of the coating, such as the PVC and the plasticisers and some of the pigments, can get involved in a chemical reaction because they are irradiated with light from the sun or from UV-lamps, with oxygen and/or water also playing a part in this process. The activation energy needed to trigger these reactions, is generated by the absorption of the light. The end-products of photo-degradation are usually water and carbon dioxide, but the process is generally a multi-step reaction with many intermediary compounds.

The spectral irradiance distribution of the light that is absorbed by the coating during weathering plays an important role in determining which reactions will take place in the coating during irradiation. Because of this, it is important that the spectral irradiance distribution of the artificial light source that is used in accelerated weathering resembles that of sunlight as closely as possible. It is possible to demonstrate the effects of different wavelength regions in the electromagnetic spectrum on the photochemical reactions that take place in a specific polymer during irradiation [25, 26].

Thermal degradation is another important process that takes place in coatings that are weathered, as irradiated coatings will warm up during weathering. Thermal degradation of PVC happens at temperatures far below those of pyrolytic decomposition [9], and its main outward manifestations are the evolution of hydrogen chloride, discolouration (usually yellowing or browning) of the coating, and deterioration of its physical, chemical and electrical properties. The process is called dehydrochlorination (Fig. 2.14), and involves progressive 'unzipping' of neighbouring chlorine and hydrogen atoms along the polymer chain, where double bonds between the carbon atoms are formed. A free radical mechanism is favoured by some investigators [27, 28], and an ionic one by others [29]. The discolouration taking place is attributed to the formation of a conjugated double bond system in the backbone of the polymer during this process. The polyene structure formed in this way absorbs at around 320 nm, but when the polyene concentration in the coating increases this absorption peak broadens into the visible region of the electromagnetic spectrum; this results in darkening of the colour of the coating.

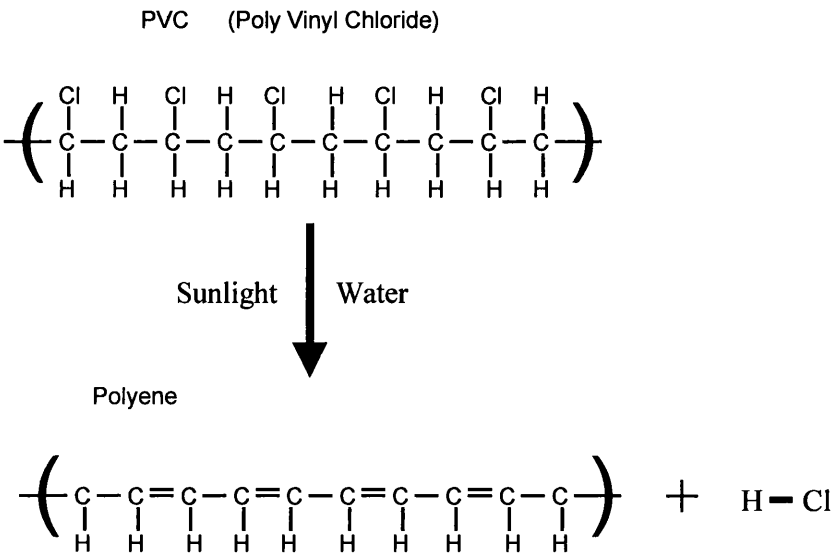

Figure 2.14 : Dehydrochlorination of PVC

Thermal dehydrochlorination can occur at temperatures as low as 100°C. It is catalysed by the HCl that evolves in the reaction (autocatalysis), and can be promoted or initiated by other strong acids [9]. Thermal degradation of PVC in the presence of oxygen can lead to oxidation reactions and the formation of hydroperoxide and ketone groups, some of which can provide additional sites for initiation of dehydrochlorination.

Most of the external manifestations associated with the photochemical degradation of PVC are the same as those associated with thermal degradation (discolouration, dehydrochlorination, deterioration of properties). Compared to thermal degradation, there is more variability in the occurrence and relative intensities of these reactions [9]. When the exposure to light is associated with weathering, additional factors such as the presence of water and dirt particles, and salt in maritime climates, further complicate this situation.

Photo-degradation of PVC in air generally starts with photo-oxidation which results in the formation of hydroperoxide, ketone and aldehyde groups through a free-radical mechanism. The presence of these hydrophilic groups is thought to play a part in the

disruptive effects of atmospheric water during the weathering of PVC based coatings.Dehydrochlorination occurs at an early stage, but the conjugated double bond sequences formed here are likely to react with oxygen from the air. Chain scission and cross-linking reactions can also take place. Exudation of plasticisers has been associated to their reduced affinity with cross-linked structures, leading to embrittlement of the coating [9]. Prior degradation by heat can enhance and accelerate later photo-degradation, as can impurities in the paint [30].

Photo-oxidation is a free radical process and, like polymerisation, consists of initiation, propagation and termination steps. Initiation requires absorption of UV radiation by the polymer or some component in the coating, to produce an excited species that can then undergo bond cleavage to give free radicals. Carbon radicals rapidly react with oxygen (especially at the coating surface) to produce peroxide radicals. The propagation reactions are influenced by the susceptibility of the PVC to hydrogen and chloride abstraction. The PVC is subjected both to chain scission reactions and chain cross-linking reactions. A termination occurs when two radicals meet each other and form a bond.

Apart from causing thermal degradation and dehydrochlorination, a general effect of heat is that it accelerates the photochemical processes taking place in the coatings. As a rule of thumb, a 10°C increase in temperature will double the reaction-rate [31]. In QUV machines (weathering cabinets containing UV tubes that simulate solar irradiation and that can produce moisture to simulate rain, see section 2.5.4) it is often found that a 10°C increase in UV exposure temperature doubles the rate of UV degradation in the coating [32]. Most of the reactions that take place in a coating during weathering can be caused both by heat and by the absorption of light; as irradiation of a coating will automatically increase its temperature, the reactions that take place in this coating are best considered to be a result of the combination of both effects.

Water can have at least three kinds of effects during weathering: it can play a role in destroying the bond between polymers and fillers (such as pigments), it can hydrolyse

unstable bonds in the PVC, and it can generate hydroxyl radicals or other reactive species like peroxides which can then initiate free radical chain reactions[21, 25].

As mentioned earlier, plasticisers and organic pigments are also susceptible to degradation reactions during weathering. In general, plasticisers will degrade under the influence of light, water and air in a multi-step reaction to give carbon dioxide and water (Fig 2.15).

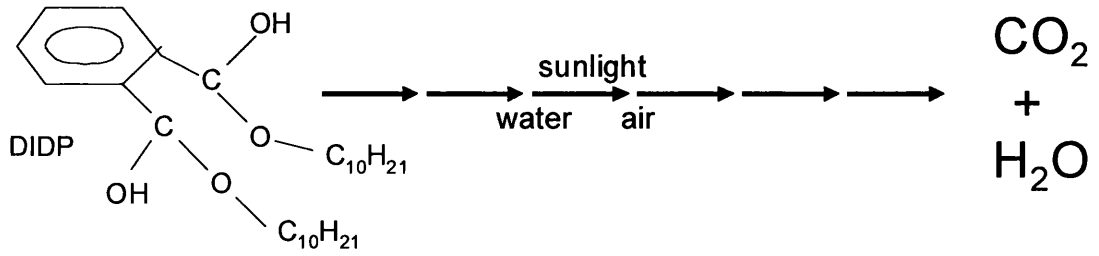

Fig 2.15: The multi-step degradation of DIDP.

For the coating, plasticiser degradation can have important consequences, like embrittlement, delamination, crack formation and gloss loss [10, 13, 33-35].

In the case of pigments, degradation will lead to loss of the colour strength of the coating; the colour of the coating will fade, or loose its brightness, because the degraded pigment molecules will have lost their chromophoric function [36]. Another consequence of this is that the pigment will give less protection to the coating system against irradiation.

2.5.3 Natural Weathering

Exterior durability refers to the resistance of coatings to the elements of the weather. Outdoor exposure tends to cause undesirable changes to the coating, including delamination, discoloration, embrittlement, chalking, absorption of dirt and other contaminations from the atmosphere, and loss of gloss.

During conventional outdoor testing, samples are exposed to the weather on tests sites (Fig. 2.16), where average daily temperature, average daily relative humidity, daily rainfall and total daily solar radiation are measured. The following parameters seem to be of particular interest [21, 37]:

- Altitude. If a sample is weathered far above the sea level, the sunlight has to travel through less air to reach the sample; this results in a higher UV intensity.
- Geographical latitude. This will affect the intensity of the solar irradiation that a panel will receive; in general closer to the equator means more UV.
- Orientation of the sample. To receive as much sunlight as possible, panels exposed in the northern hemisphere are mostly south facing when they are weathered.
- Local climate. This can vary substantially; a panel exposed at the coast will suffer the effects of salt that is solved in atmospheric water, while a panel exposed 50 miles away in an industrial area will suffer the effects of chemical pollutants in the air.
- Mounting angle. Coatings generally give a better performance when mounted at 90° or 45° (relative to the earth's surface) compared to 0 degrees. This is thought to be due to the 'ponding' effect; a horizontal surface will be wet for a longer time after rainfall than a non-horizontal surface, where the water can slide off. A mounting angle of 45° is mostly used in outdoor weathering.
- Environment. Apart from the obvious effects of different climates at various exposure sites, the immediate environment of a test fence can impose different kind of test conditions. Grass, bare earth and cement beneath the mounting stand have different reflective properties and can affect the panel temperature as well as humidity and moisture concentration.
- Season at start test. There is evidence from artificial testing that the order in which parameters such as heat and light are supplied can be relevant.
- Random year-on-year variation in the weather. A harsh year can cause up to double the deterioration in a coating than a mild year
- Local geographical features such as wind and dew.
- Type of coating.: Different types have different sensitivities to various climates.

All these factors should be taken into account when comparing results from different sites.

Figure 2.16 : Natural weathering on an outdoor site

In attempting to shorten the exposure time required for degradation, while avoiding the need to change the natural spectral distribution of sunlight, schemes have been devised to concentrate natural sunlight on test samples in order to increase the intensity of irradiation. A well known system is called EMMA (Equatorial Mount with Mirrors for Acceleration), which is based on a Fresnel-reflecting solar concentrator, employing ten flat mirrors that focus the light onto the samples with an intensity of approximately eight suns. This set-up is used in conjunction with an equatorial amount of solar irradiation. Forced air-cooling minimises overheating of samples. The energy distribution of sunlight that is incident upon samples tested with the EMMA system varies throughout the day and throughout the year, as does natural sunlight [21, 38, 39]. Experiments with this

technique have shown that the correlation between yellowing under normal sunlight exposure and EMMA exposure strongly depends upon the formulation that is tested. EMMA, like other accelerated weathering tools, distorts test results by putting too much emphasis on irradiation while underestimating the effect of temperature, oxygen availability, and moisture.

The EMMAQUA (Equatorial Mount with Mirrors for Acceleration plus water) is a method similar to EMMA, but here water is sprayed on the samples in order to simulate rain. It has the same weaknesses as EMMA, but gives quick results as can be expected from strong irradiation in combination with water.

2.5.4 Accelerated Weathering

Accelerated weathering is the term used for procedures that test the weatherability of coatings by simulating the effects of real outdoor weathering in machines that are usually operated indoors. The aim of this is, as the name says, to accelerate the deterioration process of the coatings in order to obtain quicker test results. There are a number of different types of these machines: Three of the most commonly used types are UV fluorescent tube testers, full spectrum Xenon Arc testers and salt spray testers.

UV fluorescent tube testers provide exposure to irradiation with UV light, often with an optional mode that subjects the panels to condensation in order to simulate rain. The effects of moisture during weathering are very important: Even for phenomena like gloss loss and colour change, which are mostly considered to be UV-induced changes, the presence of moisture during the weathering process tends to make a big difference [31]. In general, a synergistic effect between UV irradiation and condensation during weathering is often found. Materials that are resistant to UV irradiation alone and to condensation alone often fail when they are subjected to both [32].

The testers that were used in this research are called QUV cabinets (Fig. 2.17), after the manufacturer, the Q-Panel Company. In these machines, the tested panels can be subjected to UV irradiation alone, or to a continuous cycle of condensation and UV irradiation. The machines can be loaded with UV-A tubes or with UV-B tubes. UV-A tubes irradiate light with wavelengths of 295 to 420 nm, UV-B tubes irradiate light with wavelengths of 270 to 400 nm. The UV-A and UV-B lamps simulate the effects of the sunlight in the UV region (Figs 2.18 and 2.19).

Figure 2.17: Accelerated weathering in a QUV cabinet

UV-B lamps emit most of their light in the UV-B region. This is the region where the shortest wavelengths of sunlight are found. Photons with wavelengths in this region are highly energetic and therefore responsible for most of the damage done in coatings during weathering. For this reason, UV-B lamps give fast weathering results. Part of the light that UV-B lamps emit has wavelengths shorter than the solar cut-off, which means that the photons have more energy than those of sunlight. This means that they can

trigger reactions in coatings that normally would not take place in sunlight. The spectral irradiance distribution of a UV-B lamp, and that of its predecessor, the FS-40 lamp, can be seen in Fig. 2.18, together with that of sunlight.

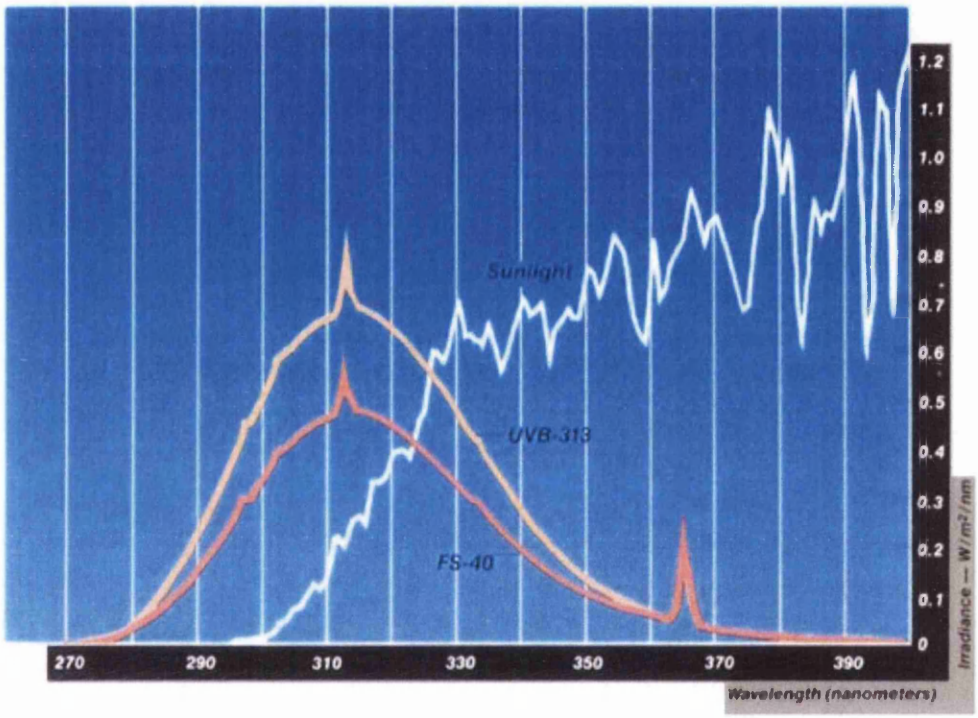

Figure 2.18 : Spectral irradiance distribution of UV-B and FS-40 tubes [40]

UV-A lamps have no UV output below the normal solar cut-off of 295 nm, as can be seen in Fig. 2.19. UVA-340 lamps are the best available simulation of sunlight in the critical short-wavelength UV region between 365 nm and the solar cut-off at 295 nm [40]. For this reason they give a better correlation with natural weathering than UV-B lamps. This was recognised by Skerry in 1988 [41], but in industrial testing labs UV-B lamps have often stayed the preferred method in order to reduce testing times; the deterioration of the coatings when irradiated with UV-A lamps is slower because the photons are not as energetic as those of UV-B lamps, so it takes longer to obtain the testing results when UV-A lamps are used.

Research by Torikai and Hasegawa [42] has shown that accelerated photodegradation under long-wavelength irradiation similar to sunlight after a pre-irradiation with short-wavelength light can give some useful results. The threshold wavelength of PVC chain scission was seen to move to a longer wavelength after pre-irradiation.

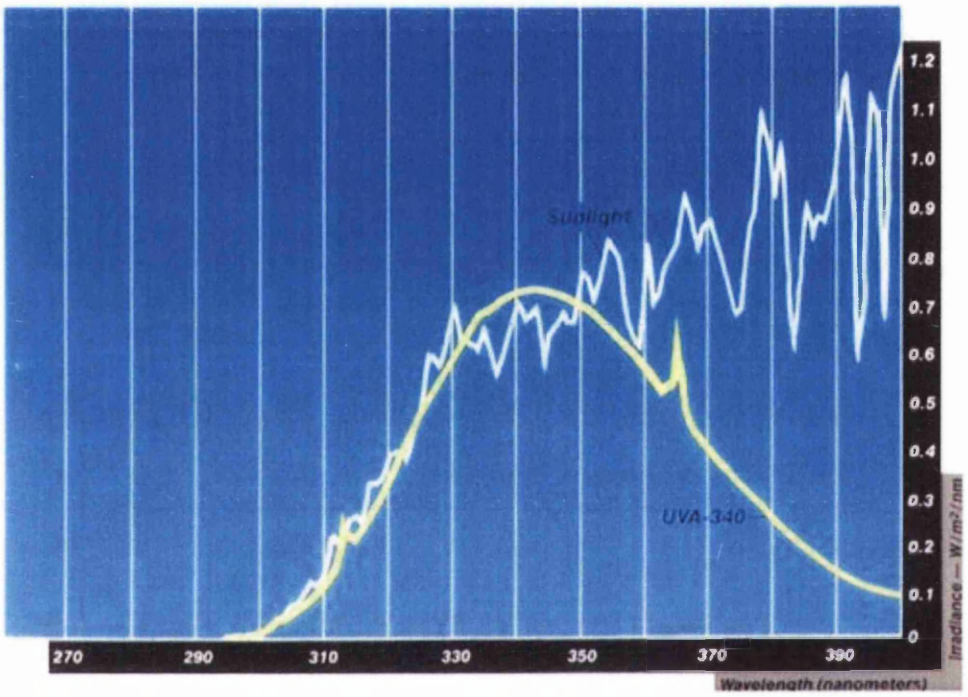

Figure 2.19: Spectral irradiance distribution of UV-A tube [40]

The Xenon Arc tester uses a light source (xenon arc) that simulates the sunlight in the UV region, as well as in the visible and infra-red regions of the electromagnetic spectrum. This method is especially used for the testing of pigments [20]. It has not been used in this research, because it is expensive and the availability is limited.

The classic salt spray test was developed in 1914 and involves a continuous exposure to a 5% salt fog at 35° C. As such it is primarily used to study corrosion rather than UV-induced degradation. This testing procedure's results do not correlate well with actual atmospheric exposures. It was found possible to improve the correlation by using a

mixture of commonly occurring atmospheric salts: A one-hour spray of a mixture containing 0.40% ammonium sulphate and 0.05% sodium chloride by weight at an ambient temperature, followed by one hour of a dry environment at 35° C was found to provide a good correlation with real weathering results from industrial environments. This test is commonly known as the prohesion test [43].

Another way to use salt spray tests is to combine them with a UV exposure cycle; this procedure is called the cyclic corrosion test [44]. The idea here is to incorporate degradation from UV light exposure into a prohesion test. It is based on the assumption that UV light degrades coatings to the point that they become more susceptible to a corrosion attack. During a series of experiments carried out with this method by Skerry and others [41] it was found that the morphology of the corrosion products were similar to those seen with outdoor testing. Salt spray testing has not been used in this research, again due to limited availability of testing space.

2.5.5 Correlation between Natural and Accelerated Weathering

It can be relatively easy to simulate a simple, monotonous climate (one can think of simulating a desert climate by exposing the samples to UV irradiation in a fluorescent tube tester) and find a good correlation. Most climates however are not monotonous.As was explained in section 2.5.3, a lot of factors can influence the effect that outdoor exposure has on a coating. This makes it very difficult to correlate accelerated weathering, which is generally either a constant condition, or a repeating cycle of two events, to the real weather, which in most places on earth is very variable. Looking for a simple conversion factor between hours of accelerated weathering and hours of outdoor exposure would be an oversimplification [26, 31, 32, 37].

For most climates found in Western Europe and North America, it is difficult to find an accelerated weathering method that gives reliable results. The successes in correlating

accelerated weathering to natural weathering that were reported in the previous paragraph refer to individual cases where huge efforts were made to simulate the weathering of relatively simple materials under very particular conditions. Work done by Kamal [20] in the 1960s showed that a good correlation could be found when a coating is artificially weathered repeatedly while playing with the parameters of this process (varying temperature, wetness fraction and wetness time per cycle); this is done in order to find the accelerated weathering cycle that produces results that provide the best fit with the real weathering results for that specific material weathered in that specific outdoor location. Inherent to this approach is that the optimum correlation found can not be extrapolated to different materials or different outdoor weathering locations.

A statistical approach is less labour intensive and will give less specific results, but can be useful if one wants to make a service lifetime prediction of a coating. This approach involves defining pass/fail criteria for the critical properties of the coatings that are tested. For example, a pass criterion could be that the gloss retention is more than 50% or that the change in colour (ΔE) is less than 2 units. When this is done, a Spearman rank correlation test can be done [45]. In this test, two identical batches of coatings with different formulations are weathered, one outdoors and one indoors (accelerated); then, in both batches, the panels are ranked in the order in which they fail the criterion of a chosen parameter. The correlation coefficient of the ranking of the accelerated weathered batch with that of the naturally weathered batch can then be calculated; if this Spearman rank correlation coefficient is close to 1, there is a good correlation between both types of weathering, if it is 0, there is no correlation at all.

In the testing of modern coatings, the stresses applied during accelerated testing are usually greater than those of natural weathering. If a large batch of identical coatings is tested in this way, the 'time to failure' values of the samples regarding a chosen criterion of a relevant parameter, can be measured for every sample. These measured 'time to failure' values will follow an extreme value distribution, if the batch of the tested specimen is large enough. In these cases, the Weibull distribution has proven to be very suitable to fit these data, and provides a model for product life of the coating [46].

Publications on sophisticated methods to translate accelerated weathering data into real weathering predictions are hard to find. An exception is a paper by Guseva and others on service life prediction of aircraft coatings [47]. In this paper the goal is to determine the 'normal use' (real weathering) probability density function from accelerated life test data (accelerated weathering) rather than from data obtained under normal use conditions. To accomplish this, a relationship is sought that allows extrapolating from data collected at accelerated conditions to use-level conditions, the so-called life-stress relationship. The life-stress relationships in accelerated life testing discussed here were Arrhenius (used when the temperature is an accelerating factor), inverse power law (usually used for non-thermal accelerated stresses) and Eyring (used for thermal or humidity stresses). After evaluating the specific qualities of the different models, a model was proposed for calculating the service life for organic coatings under service conditions that incorporated three stress types; temperature, UV and aerosol. With this model, the mean life and the 90% warranty time (the time at which only 10% of the panels have reached the failure criterion) regarding the gloss-loss for aircraft coatings were calculated. For both parameters, the experimental results were in good agreement with the proposed model.

In past research, a lot of the developed procedures are empirical and lack sufficient scientific foundation; too much emphasis has been placed on measuring the macroscopic, visible properties of the coatings, instead of the microscopic and chemical (spectral) properties that can be related directly to changes in the composition of a coating [21]. This is reflected in the literature that was found regarding the weathering and degradation of PVC coatings; surprisingly, only a few papers were found that reported the use of sophisticated techniques such as IR- and UV-VIS (reflectance) spectroscopy. These are outlined below:

Research that has been done by Cunningham and Hansen [48], where Electron Spectroscopy for Chemical Analysis ESCA and Fourier Transform Infrared Spectroscopy (FT-IR) have been used, shows that early changes in the chemical structure of both

naturally and artificially weathered coatings can be detected. The photo-oxidation of PVC was perceived to be taking place in the first 10 nm of the coating surface.

Cho and Choi [49] have used UV-VIS spectroscopy, FT-IR spectroscopy and Scanning Electron Microscopy to investigate the photo-catalytic degradation of PVC-TiO_2 composites. They found that the presence of TiO_2 accelerated the photo-degradation, and that it caused the formation of chloride containing degradation products other than HCl.

Birer [50] used FT-IR, UV-VIS and XPS spectroscopy to investigate the discolouration and increase in electrical conductivity in PVC coatings after exposure to high-energy photons. It was confirmed that the dehydrochlorination of the PVC caused by this irradiation is responsible for the discoloration and the increase in electrical conductivity.

Beltran [51] studied the thermal decomposition of PVC-plastisols with FT-IR. First, the bands in the IR spectrum associated with the plasticisers disappeared, and then the pyrolysis of the PVC resin was observed by the appearance of absorption peaks of C=C stretch vibrations. All in all it was proposed that the presence of plasticisers in PVC-plastisol delays the pyrolysis of the PVC-resin, but at the same time, at high temperatures, the PVC pyrolysis effects take place more markedly in a PVC-plastisol coating than in a coating based on just PVC-resin (without plasticisers).

Gesenhues [52] investigated the influence of TiO_2 particles on the photo-degradation of PVC while using UV-VIS spectroscopy and Scanning Electron Microscopy. His research concluded that the surface chemistry of TiO_2 is important when the weathering process is investigated, and that the intensity of rainfall during weathering might have a big influence on the photocatalytic activity of TiO_2.

Bierwagen and others [53, 54] have written papers on the choice and measurement of aircraft coating system properties. They used spectral, optical and electrochemical techniques to evaluate the deterioration of the properties of coating systems during

simulated and real exposure. Here both reflectance spectrometry and the CIE L*a*b* system have been used to evaluate colour changes.

The fact that it was hard to find publications on sophisticated statistical techniques to correlate accelerated weathering and real weathering, and publications on evaluation of colour changes during weathering of coatings using reflectance spectrometry, was surprising. It could be that the leading-edge research that is done in this area by the large paint companies is not published for confidentiality reasons.

2.6 Colour Measurement

Colour is of great importance in the visually oriented society of today. In the case of coated strip steel used in construction, architects are generally very keen on their buildings having the right colour composition, and of course they want these colours to stay the same during weathering.

Different ways have been developed to measure colours and assign numerical values to them. This was driven by the need of colourists and dyers to communicate with each other and their customers (because of the vast number of different colours that can be distinguished by the human eye, it would not be much good to tell your paint producer to make you a bright green, as there are hundreds of different colours that fit this description). The most widely used system to measure colour nowadays is the CIE L*a*b* system[8, 55].

2.6.1 The CIE L*a*b* system

In the CIE L*a*b* system, every colour is represented by a point in an imaginary three-dimensional colour space (Fig. 2.20). The three axes that define this colour space are:

- L=lightness
- a =redness (-a=greenness)
- b=yellowness (-b=blueness)

The L, a and b axes are perpendicular to each other (Cartesian co-ordinates).
Instead of a and b, the cylindrical co-ordinates C and h can be used: C is chroma or colour-saturation, and h is the hue angle, which is related to the nature of a colour.

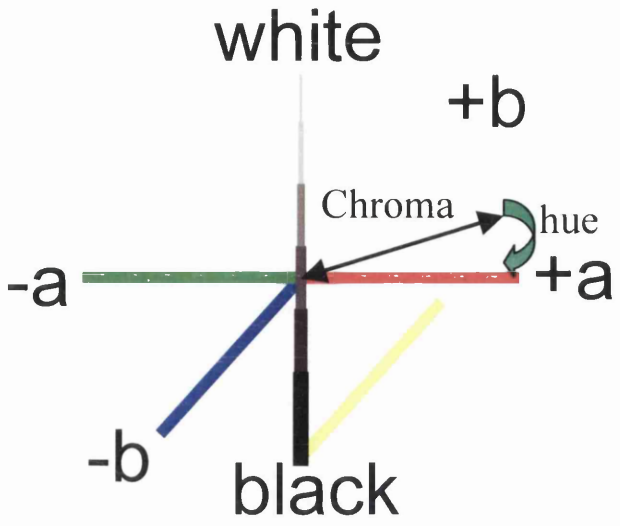

Figure 2.20 : The CIE L*a*b* Colour Space

The following formulas relate the chroma C and the hue angle h to the a and b values:

$$h = \arctan(\frac{b}{a})$$

$$C = \sqrt{a^2 + b^2}$$

The value of chroma, C, is zero at the origin of the colour space and increases with the distance from this point. The hue angle h, expressed in degrees, is defined as starting at the +a axis and is positive in the anti-clockwise direction. In this way, 0° would be +a (red), 90° would be +b (yellow), 180° would be -a (green) and 270° would be -b (blue).

The colour difference between two colours is quantified by the distance between the two points representing those colours in the colour space. This distance, expressed as ΔE, is determined using the laws of right-angled triangles:

$$\Delta E = \sqrt{dL^2 + da^2 + db^2}$$

where dL is the difference of the L co-ordinates of the two points, da is the difference of the a co-ordinates and db is the difference of the b co-ordinates.

The scaling of the colour space is such that if two samples had a colour-difference value of $\Delta E=1$ between them, this difference would be perceived by 50% of the observers. The other 50% of the observers would not see a difference between the colours.

In this research, initial modelling of the changes in the colours of coatings due to the effects of weathering with these parameters has not been very successful. This is not surprising because the CIE L*a*b* system was designed to describe the way that people perceive colour; it is a bio-physical description of colour based on the human eye.

The most fundamental, physically exact way to describe the colour of an object is by its reflectance spectrum. The position of a colour in the L*a*b* space is connected to its reflectance spectrum by the XYZ tristimulus system, which is another way of measuring colour and will be described in the next section.

2.6.2 The XYZ tristimulus system

An older way of representing colour is the XYZ tristimulus system.The XYZ system in turn was derived from the RGB primary light sources system. The RGB system was developed in the 19^{th} century and was the first system to describe colours numerically. Every monochromatic colour in the spectrum could be matched by adding and subtracting the three primary light sources which were red, green and blue. The RGB system however was impractical to use and therefore replaced by the XYZ tristimulus values system. This system works the same as the RGB primaries, but now every monochromatic colour can be matched by just adding the X, Y and Z tristimulus values (instead of adding and subtracting as was the case with the RGB system). The XYZ primaries are not real light sources like the RGB primaries; they cannot be physically created. Therefore they are called imaginary primaries.

The tristimulus values XYZ of an object can be derived from its reflectance spectrum R with the following differential equations:

$$X = k\int_0^\infty SRxd\lambda$$

$$Y = k\int_0^\infty SRyd\lambda$$

$$Z = k\int_0^\infty SRzd\lambda$$

The constant k is a normalisation constant, its function is to ensure that for a perfect white sample (with a 100% reflection at all wavelengths) the value for Y equals 100:

$$k = \frac{100}{\int S(\lambda).y(\lambda)d\lambda}$$

S represents the power distribution of the illuminant, usually the daylight simulators D50 or D65. Their spectral power distributions can be seen in Fig 2.21.

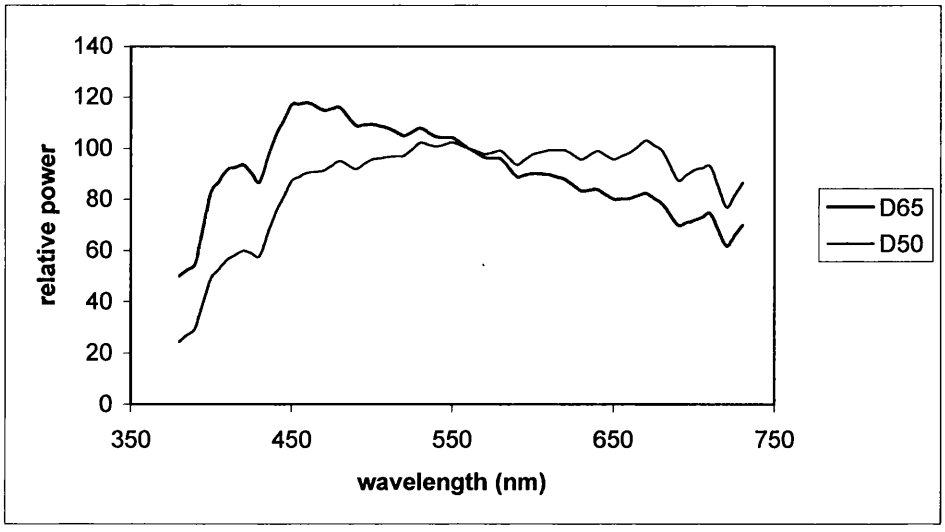

Figure 2.21 : Spectral power distribution of the illuminants D65 and D50 [55]

R represents the reflectance spectrum of the test sample (reflectance spectra will be further explained in the next section), and x, y and z are the colour matching functions for the X, Y and Z stimuli. These functions are plotted in Fig. 2.22.

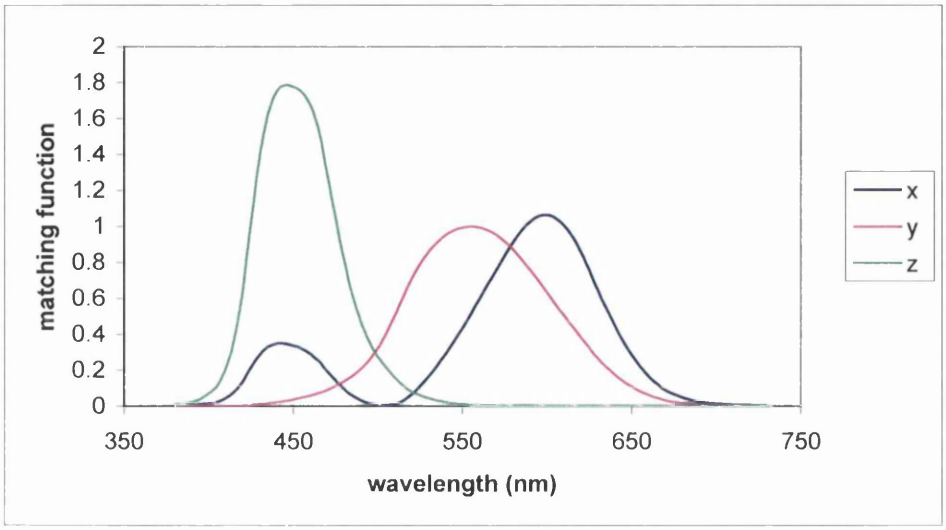

Figure 2.22: The colour matching functions x, y and z [55].

These colour matching x, y and z give the amounts of the X, Y and Z stimuli at each wavelength needed to match a monochromatic light source of this particular wavelength. So, the XYZ tristimulus values can be calculated from the reflectance spectrum, if the power distribution S of the illuminant that is used is known.

The L*a*b* system is directly correlated to the XYZ tristimulus values. The formulas that describe the relationships between the L*a*b* values and the XYZ tristimulus values are given below:

$$L = 116Fy - 16$$
$$a = 500(Fx - Fy)$$
$$b = 200(Fy - Fz)$$

$$Fx = (\frac{X}{X_o})^{1/3}$$
$$Fy = (\frac{Y}{Y_o})^{1/3}$$
$$Fz = (\frac{Z}{Z_o})^{1/3}$$

Xo, Yo and Zo are the tristimulus values of a perfect white sample (which reflects 100% at all wavelengths) under the chosen illuminant. The value of Y is set to be 100 for a perfect white sample (so Yo=100), and 0 for a perfect black sample.

With these formulas, CIE L*a*b* values can be converted into XYZ tristimulus values and vice versa.

2.6.3 Reflectance Spectra

The most fundamental way of looking at the colour of an object is to use its reflectance spectrum R. This is the spectrum of the light that is reflected by the object if it is illuminated by a specified light source.

In general, any form of electromagnetic radiation can be characterized by its wavelength. The visible region of the electromagnetic radiation spectrum runs from about 380 to 750 nm. The light in different sections of this visible region is perceived as the following colours (Table 2.2):

Table 2.2 : different colours in the UV-VIS region of the electromagnetic spectrum.

wavelength	300-380 nm:	380-450 nm:	450-490 nm:	490-560 nm:	560-590 nm:	590-630 nm:	630-750 nm:
Colour	Ultraviolet	Violet	Blue	Green	Yellow	Orange	Red

As an example the reflectance spectra of some of the green shades used in this project are given in Fig. 2.23, together with the spectrum of the clear PVC base:

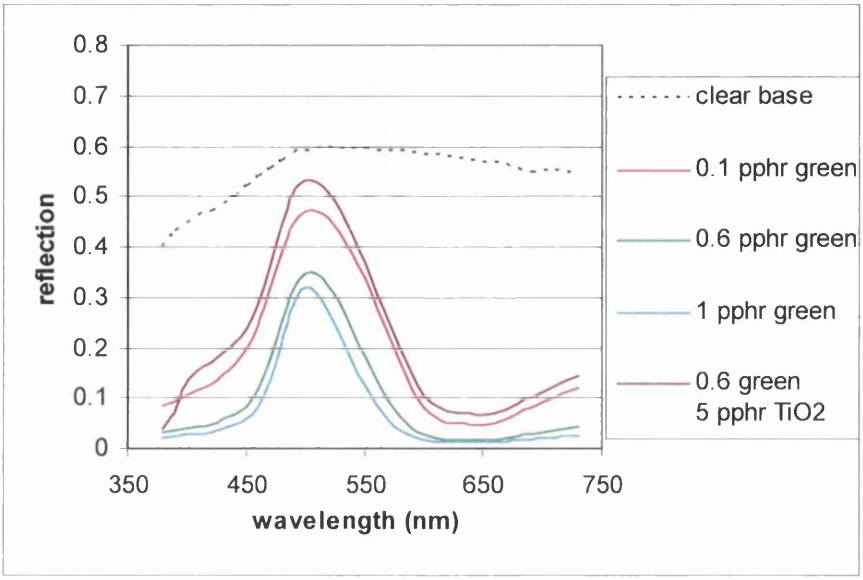

Figure 2.23 : Reflectance spectra of some green shades.

The reflectance spectra of the shades containing the green pigment all have peaks at 500 nm. This is because the green pigment does not absorb the incident light at this wavelength as much as the light at other wavelengths of the visible spectrum, so most of the incident light that is reflected by this pigment has a wavelength of around 500 nm, which we perceive as green.

So, it is in fact the light-absorbing properties of the green pigment that determine the colour of the shade. This is confirmed by the fact that the peak at 500 nm of the 1 pphr green shade is lower than that of the 0.6 pphr green shade; because the first shade has a higher concentration of green pigment, it absorbs more of the incident light than the second shade, so the peak in the reflection spectrum of the first shade is lower than that of the second shade. The 0.6 pphr green shade in turn is lower than the 0.1 pphr green shade, the latter having a broad spectrum, closest to the spectrum of the clear base, because it has the lowest green pigment concentration of all the shades.

The effect of the whitener TiO_2 is clearly visible as well; the reflectance spectrum of the 0.6 pphr green 5 pphr TiO_2 shade is above that of the 0.6 pphr shade throughout the visible region, so the titanium dioxide increases the reflection properties at all wavelengths of the visible spectrum.

It doesn't hold for all the spectra that a higher pigment concentration means a lower reflectance peak, as can be seen in the reflectance spectra of some of the red shades in Fig. 2.24:

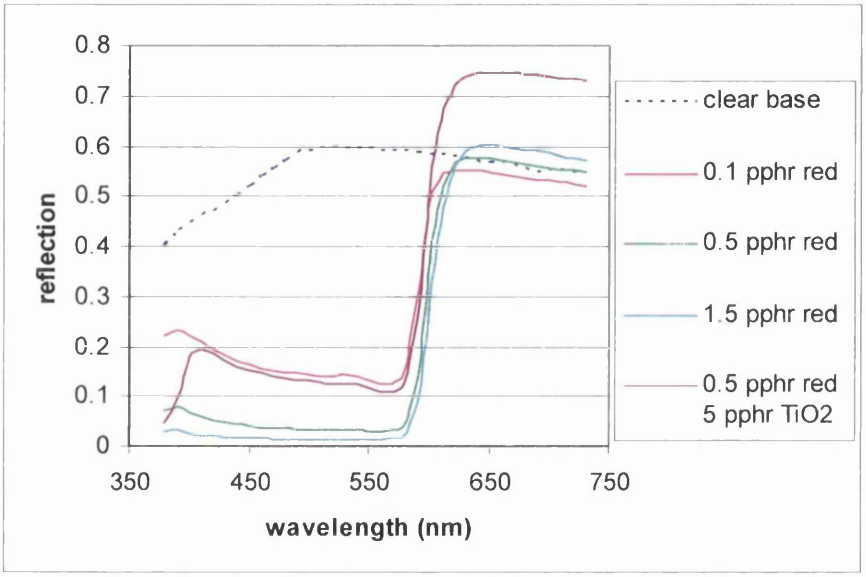

Figure 2.24 : : Reflectance spectra of some red shades

Here it is shown that for the absorbing part of the spectra of the red pigment shades (below 600 nm), the same trend can be seen as with the green shades; a higher pigment concentration results in more light absorption and thus a lower reflectance value. However, in the part of the spectra where the red pigment reflects light, above 600 nm, the opposite trend occurs; a higher pigment concentration here results in more light reflection, thus a higher reflectance value. This phenomenon has been found for the red and yellow pigments used in this project, which both have reflectance peaks at the high wavelength end of the spectrum; this could indicate that the red and yellow pigments function by absorbing low wavelength light (high energy), and then, after some intrinsic

quenching, irradiate light at a higher wavelength (lower energy). This process is known as fluorescence.

The green and blue pigments used in this project, that have reflectance peaks at 500 and 450 nm respectively, show less reflection over the whole spectrum if the pigment concentration increases.

A reflectance spectrum really is a set of reflectance values, in this case, 36 values taken every 10 nm from 380 to 730 nm. It is thought that the colour change in coatings is best monitored using the reflectance spectra to describe the colours, as they hold all the information about a colour (in comparison, with the CIE L*a*b* and XYZ tristimulus system, a colour is described with only 3 parameters). Once the reflectance spectrum of a colour is known, the XYZ tristimulus values can be calculated, and from this the CIE L*a*b* values. Unfortunately, this is not possible the other way around, because differential equations are used to derive the XYZ tristimulus values from the reflectance spectrum of a shade. In principle, an infinite number of different reflectance spectra belonging to different colours can lead to the same set of XYZ tristimulus values (and with that, the same set of CIE L*a*b* values). These colours will be perceived as the same by the human eye, this phenomenon is called mesomery [55].

2.6.4 Effects of Weathering on Colours of Coatings

There are chemical reactions in organic coatings that occur during weathering which have an effect on the colour of the coating, these have been mentioned in section 2.5.2.

Dehydrochlorination of PVC will form polyenes in the coating which absorb light around 320 nm. If the concentration of the polyenes in the coating increases, this absorption expands into the visible spectrum, decreasing the reflection spectrum of the coating over

the whole visible region. This effect is called 'yellowing' or 'browning', because that is how the colour changes are perceived.

Photo-degradation of organic pigments will decrease the concentration of 'active' organic pigments. This will cause the colour of the coating to fade (loose its strength, have weaker chroma). This means that the colour of the coating will get closer to that of the clear (unpigmented) base paint, which is grey. In the reflectance spectrum, photo-degradation of organic pigments will result in the spectrum of the shade to come closer to that of the clear base, which can be seen in Figure 2.24.

Another effect taking place during weathering that chances the colour of a coating is chalking. This can only take place in coatings containing TiO_2 or other inorganic pigments. It is caused by the breaking down of the resin in the top layer of a coating during weathering, after which a thin layer of the inorganic pigment can be formed on top of the coating [56]. Chalking (in the case of TiO_2) results in the coating becoming lighter. It is as if more TiO_2 is added to the coating because more TiO_2 particles have become visible as they have moved to the top of the coating. The reflectance spectrum of the coating in the visible region (above 400 nm) will increase, as TiO_2 reflects all the light here.

These three effects, PVC dehydrochlorination, organic pigment degradation and chalking, will be further discussed in Chapter 5, where an attempt is made to model the colour changes of coatings during weathering using reflectance spectra.

The search for publications about the colour change of coatings due to weathering has not returned much specific information. There are some useful reviews on lifetime prediction of coating systems [57-59] and pieces on general paint performance [60, 61] but these were focussing more on physical deterioration of coatings and not on colour change due to weathering. Other publications were found on the weathering of polymers [62-65], but here the chemical mechanisms and the formulation aspects highlighted, with only the yellowing process as a consequence of polyene formation included. In other areas

however there were publications specifically on the correlation between colour change and deterioration of materials due to exposure. One area is the paper industry [66-68], and another is the conservation (museum) sector [68-72].

The few publications that were found on colour change in polymers were again to do with exposure indoors (in musea) and mainly involved dyes instead of pigments, so they are not much particularly relevant [36, 73, 74]. This leads to the belief that any specific research into the colour dynamics of coatings during weathering that has been done by paint manufacturers is not published for confidentiality reasons.

The correlation between the pigmentation of a paint layer its colour can be modelled with the Schuster, Kubelka Munk theory of diffuse reflection [8]. This theory was presented by Kubelka and Munk in 1931 [75] and was based on a theory by proposed Schuster in 1905 that studied the passage of light through scattering and absorbing layers [76]. In this model, the scattering coefficients and the absorption coefficients of the different pigments in the paint are all calculated relative to the scattering coefficient of TiO_2 , and relative to the pigment's concentration. Then, the reflectance spectrum of a paint with a known pigmentation can be modelled with these coefficients, as is described in some more recent publications [77, 78]. The Kubelka-Munk theory has not been applied in this research, because the reflectance spectra of the tested coatings have all been measured here, so there was no need to model them. As all the spectra before and after weathering have been collected, it has been attempted in chapter 5 to model the changes that they undergo during weathering with the characteristics of the three weathering processes that influence the colour (dehydrochlorination, organic pigment degradation and chalking). There was no need to introduce the Kubleka-Munk theory here, as it would have made the model overcomplicated.

2.7 Techniques for Analysing Coatings

There are several techniques available to analyse the coatings that have been exposed to weathering. Already mentioned was reflectance spectroscopy, which is really a form of UV-VIS spectroscopy. Other techniques that have been used in this research are IR spectroscopy, gloss measurements, Gas Chromatography combined with Mass Spectrometry and Scanning Electrode Microscopy.

2.7.1 UV-VIS Spectroscopy

As described earlier, the visible and ultraviolet spectra of organic compounds are associated with transitions between electronic energy levels [79]. A group of atoms in a molecule that contains the electrons that are being excited during the absorption of UV-VIS light is called a chromophore. The transitions are generally between a bonding or lone-pair orbital and an unfilled non-bonding or anti-bonding orbital. Light with wavelengths of 200 nm and higher can excite electrons from p- and d-orbitals and particularly (conjugated) π-orbitals to give informative spectra. An absorption peak in a UV-VIS spectrum is usually broad because of superposition of a vibrational and rotational fine structure.

In this research, UV-spectroscopy has not been used, but reflectance spectroscopy in the visible region has been applied every time that a colour was measured. The polyenes formed during the dehydrochlorination of PVC in coatings as described in paragraph 2.5.2 are of course a conjugated π system. Polyenes absorb at 320 nm, but this peak broadens as their concentration increases in the coating. When this happens, the absorption peak of the polyenes can expand into the visible region of the electromagnetic spectrum. Here they can be detected by reflectance spectroscopy, as they lower the reflectance spectrum, making the colour of the coating darker.

For a pigment, the most important property is of course its specific chromophoric function, which gives the pigment its colour. When a pigment reacts during weathering it will loose this chromophoric function, which can also be picked up by reflectance spectroscopy (if the pigment concentration in a coating decreases its reflectance spectrum will move closer to that of a clear unpigmented base).

2.7.2 Infra Red Spectroscopy

Most molecular vibrations and rotations have energies that correspond to the infra red (IR) region of the electromagnetic spectrum [79]. The most useful vibrations for analysis in organic chemistry occur between 2500 and 16000 nm. In IR spectroscopy, the position of an absorption band in the electromagnetic spectrum is usually expressed in reciprocal centimetres (cm^{-1}). This is a unit that is proportional to frequency and inversely proportional to wavelength; 2500 nm corresponds with 4000 cm^{-1} and 16000 nm with 625 cm^{-1}. When reciprocal centimetres are used, the IR spectra are plotted going from high energy (4000 cm^{-1}) on the left of the spectrum to low energy (500 cm^{-1}) on the right.

IR spectroscopy is a simple, reliable and quick method that can identify many functional groups by their characteristic vibration frequencies. These functional group frequencies can be found from about 3700 cm^{-1} to 1500 cm^{-1}. The stretching vibrations of single, double and triple bonds between C, O, N and H atoms cause typical absorption peaks in specific regions of the spectrum. The surroundings of these bonds in a molecule will determine the exact wavenumber of the absorption peak.

A number of different studies on the evaluation of photo-degradation of pigmented PVC with IR spectroscopy has been found [48-51]. In research conducted by Matuana and others [80], the UV weathering performance of composites of PVC and wood-fiber has been evaluated using IR spectroscopy. Different absorption bands have been assigned to functional groups that are typical for weathered and unweathered PVC. A typical FTIR

spectrum of unweathered PVC showed two characteristic bands: a very broad one at 691 cm^{-1}, probably due to C-Cl stretching, and a sharp band at 1434 cm^{-1}, probably due to C-H deformation vibrations. The stretching frequencies of the C-H bonds are located around 2900 cm^{-1}[79]. The appearance of new absorption bands was clearly seen in the difference spectra of weathered and unweathered samples: C=C stretching mode frequencies associated with the formation of alkene or polyene linkages were easily recognized between 1409–1478 cm^{-1} and at 875 cm^{-1}. The appearance of polyene units on the surface of the samples is indicative of photo-degradation of the samples upon exposure to UV light. A frequency for a more specific C=C group, that of $HC=CH_2$ (located at the end of a chain), was found to be at 1640 cm^{-1} [81]. This group would emerge if chain scission reactions have taken place in the PVC.

Some oxygenated structures were also detected in the PVC chain by Matuana [80], with absorption around 1733 cm^{-1} and 1791 cm^{-1}, which can be attributed to carbonyl (C=O) groups. In the case of PVC plastisol, the plasticisers that are present contain carbonyl groups, so here the size of the C=O bands tends to be proportionate to the amount of plasticiser that is present in the coating, as the amount of carbonyl groups added by oxidation of the PVC chain is negligible compared to this.

When plasticiser degradation takes place in PVC plastisol during weathering, these carbonyl groups get hydrolysed; the resulting O-H groups have stretch vibrations between 3300 and 3500 cm^{-1} [81].

2.7.3 Gloss Measurements

The gloss of a coating is an important aesthetic property. It reflects the overall surface roughness; a smooth surface will have a high gloss level, making the coating look shiny by reflecting a large portion of the light that falls onto the coating, especially when the reflection of the light is examined at an angle. During weathering, as the binder and the

plasticisers get photo-oxidised, pits and cracks occur on the surface. This phenomenon, called microcracking, will make the surface rough and will therefore decrease the gloss level of the coating.

Gloss can be measured with a simple device. For this research, a Minolta Multi-Gloss 268 was used. This apparatus is placed on a coating, and when a measurement is performed, a tungsten filament lamp (2.5 V 60 mA) emits a light flash which hits the surface of the coating at an angle. Naturally this light flash is reflected by the surface of the coating at the same angle, where it is measured by a silicon photo-element (Fig. 2.25). The angle at which the gloss is measured with the Minolta Multi-Gloss 268 can be chosen between 20°, 60° and 85° to the normal of the surface of the coating. Normally the gloss level at 60° is used in the evaluation of coatings.

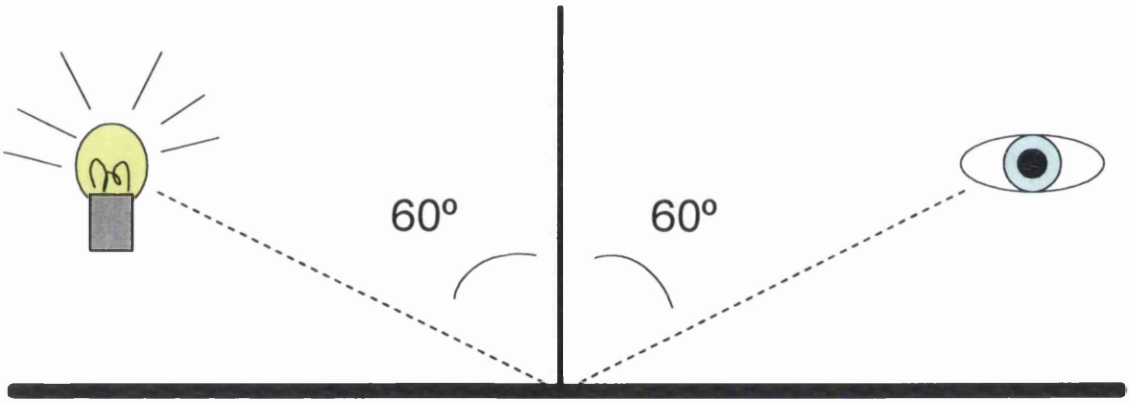

Figure 2.25 : Schematic representation of the 60° gloss measurement of a coating.

In weathering experiments, the gloss retention is the standard way to state the durability of coatings. It is usually stated as the amount of weathering after which the 60° gloss value of a coating is 50% of its original value.

2.7.4 Gas Chromatography / Mass Spectrometry

Chromatography is a technique that is used to separate substances in a mixture based on their differences in solubility in and affinity with the phases that are present in the chromatograph separation column. With this technique substances in a mixture can be separated and their amounts measured.

Mass Spectrometry is a technique that brings the molecules of the substance that is investigated into the gas phase in a vacuum. These molecules are then bombarded with electrons which can result in ionisation, when the molecule loses one or more electrons. The ions that are formed in this way are then accelerated in an electric field after which they are led through a magnetic field that is perpendicular to the direction they travel in. This will result in a Lorentz force exerted on the ions which will cause the ions to follow a circular trajectory, where the radius of that circle is determined by the ratio of the mass and the charge (m/z) of the ion. The ions are then separated according to their m/z ratio, making use of the different radii of their trajectories, and plotted in a spectrum. In this mass spectrum the ratio of the mass and charge of the ions (derived from the radius of the path that the ions followed) is plotted on the x-axis versus the intensity of the received signal by the detector, which is proportional to the number of ions with that m/z ratio that is detected. A specific molecule has a typical way of breaking down when it is bombarded with electrons, which leads to a characteristic mass spectrum for that molecule.

The GC/MS technique combines an analysis of the identity of a substance with that of the quantity of that substance. In this research it has been used to analyse the concentration of plasticisers in coatings after weathering.

2.7.5 Scanning Electron Microscopy

A scanning electron microscope works, as the name says, by scanning the surface of a specimen with a finely focused electron beam to produce an image of the surface. This happens in a nearly evacuated chamber, which is necessary in order to prevent significant electron scattering. Nowadays scanning electron microscopes can have a resolving power of 1 nm and magnify over 400000 times (for comparison; a modern light microscope enables the eye to resolve objects separated by 200 nm and magnifies 1000 times).

In general, when the electrons from the beam strike the specimen, five phenomena can occur:

1) primary electrons from the beam are reflected (backscattered electrons)
2) primary electrons from the beam are absorbed
3) secondary electrons are emitted from the specimen because of the impact of the primary electrons from the beam
4) the specimen emits X-rays
5) the specimen emits photons (light).

The backscattered electrons (BSE) are high in energy compared to the secondary electrons that the specimen emits. They are detected by a so-called solid state detector, where the minute signal produced by the backscattered electrons is amplified. In the specimen, heavy (high atomic weight) atoms will bounce back more electrons from the beam than light (low atomic weight) atoms, which are more likely to absorb the incoming primary electrons. For this reason (as the number of backscattered electrons is translated into an intensity of light) particles made of heavy elements in the specimen will appear lighter in an SEM scan than particles consisting of light elements. The image produced by the back scatter electrons thus provides a contour map based on atomic weight; in this way, the titanium dioxide particles can be distinguished from the PVC base. As their atoms are heavier the titanium dioxide particles will appear white against a dark background of PVC in the image produced by the backscattered electrons.

This makes the BSE response of a scanning electron microscope a good tool to monitor the migration and chalking effects of titanium dioxide and the antimony/chromium/titanium oxide in PVC during weathering.

3 MATERIALS AND METHODS

In this chapter the materials and methods that were used in this research project will be described. This includes the paints that were tested, where an indication of the formulation of the commercial PVC plastisol base paint will be given, and of the pigments that have been used to colour this base.

The fluorescent tube testers that were used for accelerated weathering are discussed, with the parameters (such as temperature, irradiation intensity) under which they were operated in this research.
The amount of UV irradiation that is involved with the different types of weathering that the coatings have been subjected to will be evaluated.

Also discussed are the devices that were used to measure colour and gloss changes, and the way these measurements were evaluated for their validity.

3.1 The Colour Dynamics Predictive Database

This research project started in October 2000 for a duration of four years. The initiative to make up a large batch of paints in a systematic way in order to investigate the correlation between colour fastness during weathering and the pigmentation of the exposed paints was taken 2 years earlier, when Akzo Nobel started its Colour Dynamics Predictive Database (CDPD) project. This database, originally consisting of 300 paints that are based on a commercial PVC plastisol paint, has been the pivot of this research; its paints have been used to coat panels that were exposed in Darwen (Lansashire) and Rye (East Sussex), and in the QUV machines. During this research, the CDPD has been expanded with 50 paints, mostly low pigment concentration shades, to obtain a more complete coverage of all the possible pigmentations.

3.1.1 The Commercial PVC Plastisol Base Paint

The paints in the CDPD were all based on the same commercial PVC plastisol paint system, which was made of the following ingredients.

Three different types of PVC are used in the tested paint system; together they account for 67% of the weight of the base. The concentrations of the other components in the paint are usually given in amounts relative to this concentration (in pphr, parts per hundred resin, by weight relative to PVC).

The solvents used are white spirit and butyl dioxitol acetate; together they account for around 3% of the weight of the base paint.

The main plasticiser used is DIDP, which has been described in section 2.3.3. Two other plasticisers used in the commercial paint system are hexanedioic acid (a polymer with 1,4-butanediol, 1,3-propanediol, 2,2-dimethyl and isononanol) and 2,2,4-trimethyl-1,3-

pentanediol-diisobutyrate. The three plasticisers together account for 22.6% of the weight of the base paint, or 34.7 pphr (when the base is pigmented later this will be increased to 44 pphr by addition of DIDP through the stainer).

Antimony trioxide (Sb_2O_3) is added as a fire retardant. Another fire retardant that is added is barium metaborate monohydrate, but this substance has multiple functions; it is also a light- and temperature stabiliser and a fungicide/biocide. Both fire retardants account for less than 3% of the weight of the paint base.

In the investigated commercial paint system, an oxanilide is added as a UV absorber (UVA) and makes up a small fraction (<0.5%) of the paint base. Mono- and Dibutyltin thioesters are added for UV and heat stabilisation. These substances can provide dual action stabilisation; they react with HCl, and are involved in addition reactions with polyenes. This way, they can delay the dehydrochlorination of PVC. In total they account for around 1% of the weight of the paint base.

An acid scavenger is added to absorb reactive acidic molecules in the resin that can accelerate the degradation of the plasticisers or the polymers. Its chemical name is 3,4-epoxy cyclohexyl methyl-3,4-epoxy cyclohexyl carboxylate, and it makes up around 2% of the weight of the paint base.

The coil coating process was simulated by bar-coating a 200 micron thick layer of this PVC plastisol paint to a primed steel substrate, which was then cured at a PMT (Peak Metal Temperature) of around 210° C. At this temperature, the plasticisers in the formulation will fuse with the PVC to give a flexible product. After curing the panels were taken out of the oven and quickly quenched in water.

3.1.2 The Pigments used in the CDPD

Six different commercial pigments have been used in the CDPD, which have been added to the commercial PVC plastisol base in different concentrations and combinations. Four of the pigments were organic, two were inorganic (titanium dioxide and Yellow 2, a titanium/chromium/antimony oxide). The a* and b* axes in the CIE L*a*b* colour space are covered by a red, a blue, a green and two yellow pigments, and the amount of titanium dioxide that is added as a whitener and will determine the L* co-ordinate (lightness) of a shade.The pigments are listed in Table 3.1, with the one letter symbols as they are used in the CDPD.

Table 3.1: The pigments that are tested in the commercial paint system

Colour and symbol	CI Class	Chemical Type	(In)Organic
Blue (B)	Blue 15:3	β Cu phthalocyanine	Organic
Green (G)	Green 7	Phthalocyanine	Organic
Red (R)	Red 254	Diketopyrrolo-pyrrol	Organic
Yellow 1 (P)	Yellow 138	Quinophthalone	Organic
Yellow 2 (S)	Brown 24	Ti/Cr/Sb Oxide	Inorganic
Titanium Dioxide (N)	White 6	TiO_2 (rutile)	Inorganic

3.1.3 Pigmentations of Paints in the CDPD

When the CDPD was started up in 1998, it consisted of 300 paints; 60 of these paints consisted of a single red, yellow, green or blue pigment, with additions of the whitener titanium dioxide. The four organic pigments were used here. For each of these four pigments there were 15 paints in the CDPD, made by combining three different pigment concentrations with five titanium dioxide concentrations. When this EngD research project started, it was felt that the number of single pigment shades in the CDPD needed

to be expanded, especially in the lower pigment concentration area. For this reason, six new paints were added for each pigment, two new (lower) pigment concentrations combined with three titanium dioxide concentrations (0, 1 and 5 pphr TiO_2). Originally, there were no single pigment paints with the inorganic Yellow 2 pigment in the CDPD. This pigment was used in the yellow-green shades (discussed later), whereas the Yellow 1 pigment was used in the orange shades and in the single yellow pigment shades of the CDPD. For this reason, during this EngD research project, 21 single pigment paints were made with this Yellow 2 pigment, so that this pigment was represented like the others in the CDPD. Also added to the CDPD were five new paints containing just titanium dioxide (in the 5 concentrations that are used all the way through the CDPD; 0, 1, 5, 10 and 15 pphr).

The other 240 of the original paints were two-pigment shades. The shades orange, cyan, magenta and yellow-green were manufactured by mixing two pigments (respectively Red and Yellow 1, Green and Blue, Red and Blue, and Yellow 2 and Green). Each of the four shades had 60 different pigment combinations. In each shade 12 different combinations of two pigments were made (3 ratios between the pigments concentrations with 4 different pigment concentrations each) and these 12 combinations were combined again with 5 different titanium dioxide concentrations (0,1,5,10 and 15 pphr TiO_2) to obtain 60 different compositions per shade.

3.1.4 Selection of CDPD Shades to be Investigated

After the addition of 50 paints during this research, the CDPD consisted of 350 paints. Panels were drawn with all of these paints in Darwen and these have been exposed on a weathering site there. Then, in the spring of 2002 at WTC the paints were transported to Corus' Welsh Technology Centre in Port Talbot, South Wales, where panels were coated with a selection of 158 paints from the CDPD. The paints used from the CDPD to draw these sheets were:

1) All the single pigment shades with all different TiO_2 concentrations (5 different pigments, 21 different combinations per pigment =>105 panels)
2) All the two pigment shades with no TiO_2 (4 different shades, 12 different combinations per shade => 48 panels)
3) The base plastisol with 0, 1, 5, 10, and 15 pphr TiO_2 (=> 5 panels)

So, the two-pigment shades (orange, yellow-green, cyan and magenta) with titanium dioxide additions were left out of this set, because the time-limitations made it necessary to make a selection of the paints that were to be investigated.

With every one of the 158 selected paints, 2 A4-sized primed strip steel sheets were coated, and reflectance spectra have been recorded of all these sheets. Then, the sheets were cut up into smaller panels. Two panels of each shade were transported to Rye to be weathered at Corus' outdoor weathering site there. The starting date for this exposure was July 2002. In June 2003, after 11 months of exposure, one copy of every shade was brought back to be measured. In May 2004, the other panels were brought back, after a total of 22 months of exposure. The rest of the panels that were cut out of the A4 sheets were subjected to accelerated weathering in the QUV machines at WTC.

The 158 shades selected from the CDPD can be seen in Fig. 3.1, where they are pictured attached to racks before they were transported to Rye.

Figure 3.1: The 158 selected shades from the CDPD that were weathered in Rye and in the QUV machines in Port Talbot.

The pigmentations of the 158 paints that were selected from the CDPD are given Tables 3.2 to 3.11. Here the systematic names of the paints are given in the first column; these names consist of a letter followed by a number.

'N' is used for the whites (No pigment, just the whitener titanium dioxide in these paints), 'R' for the Reds, 'B' for the Blues, 'G' for the Greens, 'P' for the organic (Paliotol) yellows, 'S' for the inorganic yellows, 'Y' for the Yellow-Greens, 'M' for the Magentas, 'C' for the Cyans and 'O' for the Orange paints.

Table 3.2: Pigmentations of the white shades

White shades	Red	Blue	Green	Yellow 1	Yellow 2	TiO_2	Org. Pig.	Inorg. Pig.	Total Pig.
N1						0		0	0
N2						1		1	1
N3						5		5	5
N4						10		10	10
N5						15		15	15

Table 3.3: Pigmentations of the red shades

Red shades	Red	Blue	Green	Yellow 1	Yellow 2	TiO_2	Org. Pig.	Inorg. Pig.	Total Pig.
R1	0.1						0.1		0.1
R2	0.1					1	0.1	1	1.1
R3	0.1					5	0.1	5	5.1
R4	0.25						0.25		0.25
R5	0.25					1	0.25	1	1.25
R6	0.25					5	0.25	5	5.25
R7	0.5						0.5		0.5
R8	0.5					1	0.5	1	1.5
R9	0.5					5	0.5	5	5.5
R10	0.5					10	0.5	10	10.5
R11	0.5					15	0.5	15	15.5
R12	1.5						1.5		1.5
R13	1.5					1	1.5	1	2.5
R14	1.5					5	1.5	5	6.5
R15	1.5					10	1.5	10	11.5
R16	1.5					15	1.5	15	16.5
R17	2.5						2.5		2.5
R18	2.5					1	2.5	1	3.5
R19	2.5					5	2.5	5	7.5
R20	2.5					10	2.5	10	12.5
R21	2.5					15	2.5	15	17.5

Table 3.4: Pigmentations of the blue shades

Blue shades	Red	Blue	Green	Yellow 1	Yellow 2	TiO_2	Org. Pig.	Inorg. Pig.	Total Pig.
B1		0.05					0.05		0.05
B2		0.05				1	0.05	1	1.05
B3		0.05				5	0.05	5	5.05
B4		0.1					0.1		0.1
B5		0.1				1	0.1	1	1.1
B6		0.1				5	0.1	5	5.1
B7		0.2					0.2		0.2
B8		0.2				1	0.2	1	1.2
B9		0.2				5	0.2	5	5.2
B10		0.2				10	0.2	10	10.2
B11		0.2				15	0.2	15	15.2
B12		0.6					0.6		0.6
B13		0.6				1	0.6	1	1.6
B14		0.6				5	0.6	5	5.6
B15		0.6				10	0.6	10	10.6
B16		0.6				15	0.6	15	15.6
B17		1					1		1
B18		1				1	1	1	2
B19		1				5	1	5	6
B20		1				10	1	10	11
B21		1				15	1	15	16

Table 3.5: Pigmentations of the green shades

Green shades	Red	Blue	Green	Yellow 1	Yellow 2	TiO_2	Org. Pig.	Inorg. Pig.	Total Pig.
G1			0.05				0.05		0.05
G2			0.05			1	0.05	1	1.05
G3			0.05			5	0.05	5	5.05
G4			0.1				0.1		0.1
G5			0.1			1	0.1	1	1.1
G6			0.1			5	0.1	5	5.1
G7			0.2				0.2		0.2
G8			0.2			1	0.2	1	1.2
G9			0.2			5	0.2	5	5.2
G10			0.2			10	0.2	10	10.2
G11			0.2			15	0.2	15	15.2
G12			0.6				0.6		0.6
G13			0.6			1	0.6	1	1.6
G14			0.6			5	0.6	5	5.6
G15			0.6			10	0.6	10	10.6
G16			0.6			15	0.6	15	15.6
G17			1				1		1
G18			1			1	1	1	2
G19			1			5	1	5	6
G20			1			10	1	10	11
G21			1			15	1	15	16

Table 3.6: Pigmentations of the organic yellow shades

Org.Yellow shades	Red	Blue	Green	Yellow 1	Yellow 2	TiO_2	Org. Pig.	Inorg. Pig.	Total Pig.
P1				0.25			0.25		0.25
P2				0.25		1	0.25	1	1.25
P3				0.25		5	0.25	5	5.25
P4				1			1		1
P5				1		1	1	1	2
P6				1		5	1	5	6
P7				2			2		2
P8				2		1	2	1	3
P9				2		5	2	5	7
P10				2		10	2	10	12
P11				2		15	2	15	17
P12				6			6		6
P13				6		1	6	1	7
P14				6		5	6	5	11
P15				6		10	6	10	16
P16				6		15	6	15	21
P17				10			10		10
P18				10		1	10	1	11
P19				10		5	10	5	15
P20				10		10	10	10	20
P21				10		15	10	15	25

Table 3.7: Pigmentations of the inorganic yellow shades

Inorg.Yellow shades	Red	Blue	Green	Yellow 1	Yellow 2	TiO_2	Org. Pig.	Inorg. Pig	Total Pig.
S1					0.25			0.25	0.25
S2					0.25	1		1.25	1.25
S3					0.25	5		5.25	5.25
S4					1			1	1
S5					1	1		2	2
S6					1	5		6	6
S7					2.5			2.5	2.5
S8					2.5	1		3.5	3.5
S9					2.5	5		7.5	7.5
S10					2.5	10		12.5	12.5
S11					2.5	15		17.5	17.5
S12					5			5	5
S13					5	1		6	6
S14					5	5		10	10
S15					5	10		15	15
S16					5	15		20	20
S17					10	0		10	10
S18					10	1		11	11
S19					10	5		15	15
S20					10	10		20	20
S21					10	15		25	25

Table 3.8: Pigmentations of the yellow-green shades

Yellow-green shades	Red	Blue	Green	Yellow 1	Yellow 2	TiO_2	Org. Pig.	Inorg. Pig.	Total Pig.
Y1			0.05		0.5		0.05	0.5	0.55
Y2			0.2		2		0.2	2	2.2
Y3			0.5		5		0.5	5	5.5
Y4			1		10		1	10	11
Y5			0.02		0.5		0.02	0.5	0.52
Y6			0.08		2		0.08	2	2.08
Y7			0.2		5		0.2	5	5.2
Y8			0.4		10		0.4	10	10.4
Y9			0.05		0.25		0.05	0.25	0.3
Y10			0.1		0.5		0.1	0.5	0.6
Y11			0.5		2.5		0.5	2.5	3
Y12			1		5		1	5	6

Table 3.9: Pigmentations of the magenta shades

Magenta shades	Red	Blue	Green	Yellow 1	Yellow 2	TiO_2	Org. Pig.	Inorg. Pig.	Total Pig.
M1	0.25	0.05					0.3		0.3
M2	0.5	0.1					0.6		0.6
M3	2.5	0.5					3		3
M4	5	1					6		6
M5	0.1	0.05					0.15		0.15
M6	0.2	0.1					0.3		0.3
M7	1	0.5					1.5		1.5
M8	2	1					3		3
M9	0.25	0.01					0.26		0.26
M10	1	0.04					1.04		1.04
M11	2	0.08					2.08		2.08
M12	5	0.2					5.2		5.2

Table 3.10: Pigmentations of the cyan shades

Cyan shades	Red	Blue	Green	Yellow 1	Yellow 2	TiO_2	Org. Pig.	Inorg. Pig.	Total Pig.
C1		0.05	0.05				0.1		0.1
C2		0.1	0.1				0.2		0.2
C3		0.5	0.5				1		1
C4		1	1				2		2
C5		0.02	0.05				0.07		0.07
C6		0.04	0.1				0.14		0.14
C7		0.2	0.5				0.7		0.7
C8		0.4	1				1.4		1.4
C9		0.05	0.02				0.07		0.07
C10		0.1	0.04				0.14		0.14
C11		0.5	0.2				0.7		0.7
C12		1	0.4				1.4		1.4

Table 3.11: Pigmentations of the orange shades

Orange shades	Red	Blue	Green	Yellow 1	Yellow 2	TiO_2	Org. Pig.	Inorg. Pig.	Total Pig.
O1	1			0.1			1.1		1.1
O2	2			0.2			2.2		2.2
O3	3			0.3			3.3		3.3
O4	5			0.5			5.5		5.5
O5	0.25			0.1			0.35		0.35
O6	0.5			0.2			0.7		0.7
O7	0.75			0.3			1.05		1.05
O8	1.25			0.5			1.75		1.75
O9	0.05			0.1			0.15		0.15
O10	0.1			0.2			0.3		0.3
O11	0.15			0.3			0.45		0.45
O12	0.25			0.5			0.75		0.75

3.2 The QUV Accelerated Weathering Machines

Three QUV machines were available in Port Talbot for accelerated weathering of the CDPD shades; two 'normal' QUV machines, where panels are placed in an almost vertical position (Fig 3.2). These cabinets have two sets of four UV-tubes at either side to irradiate the panels. If a condensation cycle is introduced here, water from the bottom of the cabinet is heated up and vaporised, after which it condensates onto the panels. From here the droplets can flow back down to the reservoir at the bottom. These machines were operated both with UV irradiation only and with an 8 hrs UV / 4 hrs condensation cycle.

At first, UV-B lamps were used in the QUV machines, as this was the usual practice in Port Talbot. The light emitted by these lamps was found to be too strong (see section 2.5.4), which resulted in quick browning of the panels, probably caused by dehydrochlorination (see section 2.5.2). After this discovery, only UV-A lamps were used for irradiation in the QUV machines. Only the results from accelerated weathering with UV-A lamps are reported in this thesis.

The two normal QUV machines are equipped with Solar Eye irradiance control [82]. Two 'solar eyes' can be seen in the black vertical bar in the middle of the cabinet in Fig. 3.2. This system continuously monitors the UV intensity, and maintains the programmed irradiance level by adjusting the power to the lamps. During the experiments, the irradiance intensity was programmed to be 0.68 $W/m^2/nm$ at 340 nm for the UV-A lamps.The temperature that the normal QUV machines were operated at was 40°C, both during irradiation and condensation.

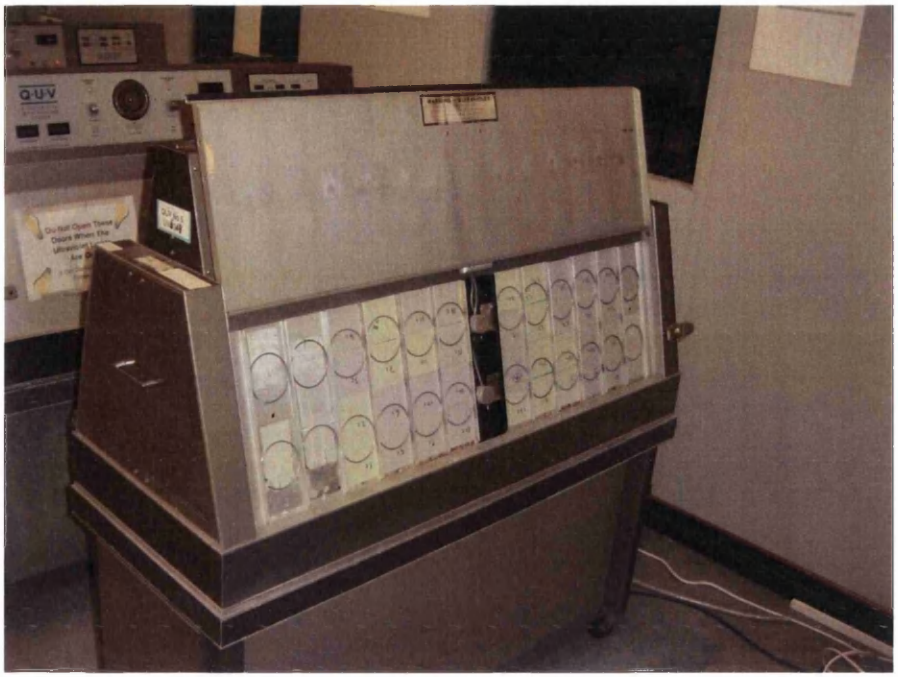

Figure 3.2: A QUV machine in Port Talbot loaded with panels.

The third fluorescent tube tester that was used in Port Talbot is unique in the world, it is called the QUV 'ponding' machine and has been made especially for Corus (Fig. 3.3). This cabinet has two pull-out drawers at either side on which the panels are placed horizontally, facing up. When the drawers are closed the panels are irradiated by a set of four UV-A tubes at either side. If a condensation cycle is introduced, a thin layer of water will cover the shades, which explains why the word 'ponding' is used here. This is done to simulate the weathering of coated strip steel used in horizontal roofing. This machine was used with an 8 hrs irradiation / 4 hrs condensation cycle with UV-A tubes. As there is no Solar Eye irradiance control installed in the QUV ponding machine, new lamps were put in at the beginning of each experiment. The irradiance intensity at 340 nm was measured at 1.0 $W/m^2/nm$ for new lamps, and after 2000 irradiation hours, the irradiation intensity was measured to be 0.75 $W/m^2/nm$, because the lamps had lost power with age.The temperature that the horizontal QUV was operated at was 45°C during condensation and 55°C during UV-irradiation.

Figure 3.3: The QUV 'ponding' machine, unique in the world

Every accelerated weathering experiment in this research, in both the normal and the horizontal QUV and with and without a condensation cycle, consisted of 2000 irradiation hours.

3.2.1 Evaluation of UV Irradiation Intensity

The most important parameter to look at when organic coatings are weathered is the amount of UV irradiation that is received by the coating. This is because UV light is capable of initiating degradation reactions in organic coatings, as has been described in section 2.5.2. It is therefore important to evaluate the amounts of UV irradiation that are involved during natural weathering in Rye and Darwen and during accelerated weathering in the two types of QUV machines that were used.

The UV-A lamps used in the QUV machines match the terrestrial solar irradiance spectrum well from the solar cut-off point at 295 nm to about 350 nm (Fig. 2.19). Above 350 nm, the irradiance of the UV-A lamps decreases, while that of sunlight keeps increasing.The amounts of UV irradiation that the coatings have been exposed to during accelerated weathering in the two normal QUV machines and in the horizontal QUV machine that were used in this research was evaluated in the following way:

The two normal QUV machines are equipped with Solar Eye irradiance control [82]. This system continuously monitors the UV intensity, and maintains the programmed irradiance level by adjusting the power to the lamps. The lamps that have been used in the machines are UVA-340 tubes. These have the peak of their irradiance intensity at 340 nm. The irradiance controllers on the QUV machines were programmed to maintain the 340 nm irradiance at 0.68 $W/m^2/nm$. At this irradiance level, the total amount of UV irradiation power (radiation with wavelengths smaller than 400 nm) is estimated at 36.3 W/m^2. This number is obtained by estimating the surface area under the spectral irradiance distribution of an UV-A lamp (Fig. 2.19) when the 340 nm irradiation intensity is 0.68 $W/m^2/nm$. With this value, the accumulated UV energy that is received by a panel during a 500 hrs exposure period to UV irradiation can be calculated: $36.3*500*3600/1000000= 65.4\ MJ/m^2$. The accumulated UV energies in a normal QUV machine over a 2000 hrs exposure period are given in Table 3.12.

On the horizontal QUV machine, there was no irradiance controller installed. At the beginning of each experiment, new lamps were put in, and the irradiance intensity at 340 nm was measured at 1.0 $W/m^2/nm$. After 2000 irradiation hours, the irradiation intensity was measured again; it was now 0.75 $W/m^2/nm$, because the lamps had worn out. This meant that the lamps on average lost 0.0125% of their intensity per hour. This decrease in intensity had to be incorporated into the estimations of the amounts of UV irradiation received by panels in the horizontal weathering machine after 500, 1000, 1500 and 2000 irradiation hours. The estimated accumulated UV irradiation energies received by coatings in the horizontal QUV machine as they were used in this research are given in Table 3.12.

Table 3.12: The accumulated UV irradiation energies estimated for the two QUV machines

Irradiation hours	accumulated UV irradiation (MJ/m2)	
	Normal QUV	Horizontal QUV
500	65.4	91.4
1000	130.8	177.1
1500	196.1	257.2
2000	261.5	331.7

In the normal QUV machines, two experiments were conducted. One was a 2000 hrs non stop UV-A irradiation, and the other one was an 8 hrs UV-A / 4 hrs condensation cycle, also amounting to a total of 2000 irradiation hours. In the horizontal QUV machine, an 8 hrs UV-A / 4 hrs condensation cycle was operated, but the condensation here is likely to have more impact because of the 'ponding' effect.

The weathering sites used in this research are Rye in East Sussex and Darwen in Lancashire (Fig. 3.4).

Fig 3.4: The natural weathering sites are located in Darwen and Rye.

The Met Office records weathering data at weathering stations spread over the UK. Some data are available for free on its website, but these are not recorded on the exact locations of the weathering sites. The data for Darwen given in Table 3.13 are obtained by averaging those of the weather stations in Manchester Airport and in Malham Tarn. The data for Rye in Table 3.14 are obtained by averaging those of the weather stations in Eastbourne and Bognor Regis. All these data found on the Met Office web site [83] are averages of a 30 year period, running from 1971 to 2000.

Table 3.13: The weather data for Darwen

Darwen	Max Temp	Min Temp	Days of Air frost	Sunshine	Rainfall	Days of rainfall >= 1mm
Month	[deg C]	[deg C]	[days]	[hours]	[mm]	[days]
Jan	5.5	0.5	13.6	43.0	118.3	15.8
Feb	5.7	0.5	12.3	59.9	83.7	12.3
Mar	7.9	1.8	8.9	87.2	99.1	14.3
Apr	10.4	3.3	4.7	128.0	69.9	11.7
May	14.2	6.1	0.8	176.6	69.3	11.2
Jun	16.5	8.8	0.1	156.8	81.8	12.7
Jul	18.7	11.0	0.0	164.3	77.2	11.5
Aug	18.4	10.9	0.0	158.4	96.9	12.7
Sep	15.6	8.9	0.1	116.7	99.9	12.8
Oct	12.1	6.1	1.3	88.2	119.2	14.9
Nov	8.3	2.9	6.7	55.1	119.1	15.6
Dec	6.3	1.3	10.6	37.9	128.4	15.7
Year	11.7	5.2	58.7	1271.7	1162.5	161.0

Table 3.14: The weather data for Rye

Rye	Max Temp	Min Temp	Days of Air frost	Sunshine	Rainfall	Days of rainfall >= 1mm
Month	[deg C]	[deg C]	[days]	[hours]	[mm]	[days]
Jan	7.7	3.3	5.8	67.9	78.7	12.5
Feb	7.6	2.9	5.4	86.9	50.4	9.5
Mar	9.7	4.3	2.3	130.2	57.9	10.0
Apr	12.0	5.6	0.6	190.1	47.0	8.4
May	15.4	8.9	0.0	236.4	44.7	8.0
Jun	18.0	11.6	0.0	232.8	52.3	7.8
Jul	20.3	13.9	0.0	244.9	42.8	6.5
Aug	20.6	14.0	0.0	239.6	49.0	7.1
Sep	18.2	12.1	0.0	171.5	69.1	9.2
Oct	14.9	9.4	0.1	129.3	92.5	10.8
Nov	11.0	5.9	1.8	87.3	85.4	11.1
Dec	8.8	4.4	4.1	59.1	84.1	11.8
Year	13.7	8.0	20.0	1875.8	753.6	112.4

The average maximum and minimum temperatures in the two sites are 2-3°C apart, which seems a small difference as Darwen is located 200 miles north of Rye. There is a more

substantial difference in sunshine and rainfall between the sites, as can be seen in Figs 3.5 and 3.6.

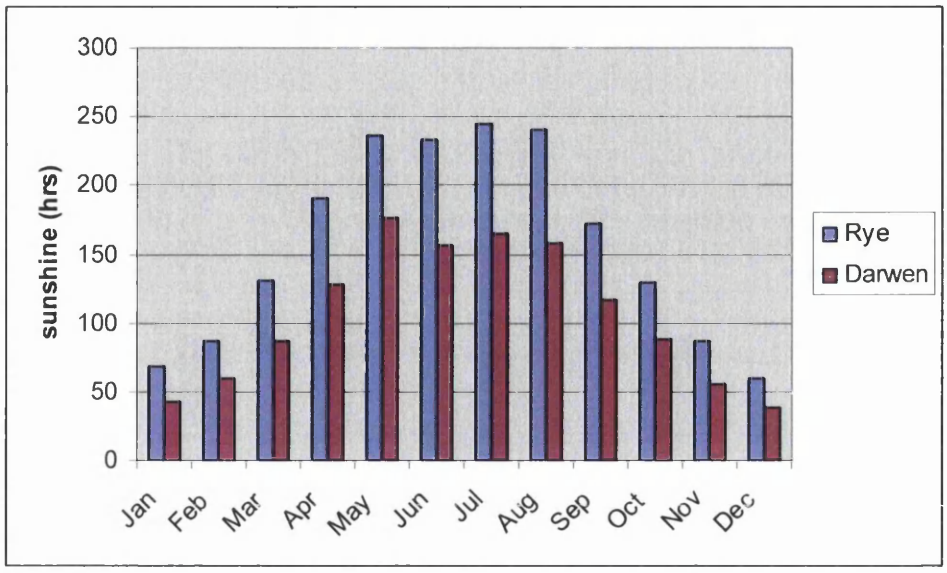

Figure 3.5: Yearly distribution of sun hours in Rye and Darwen.

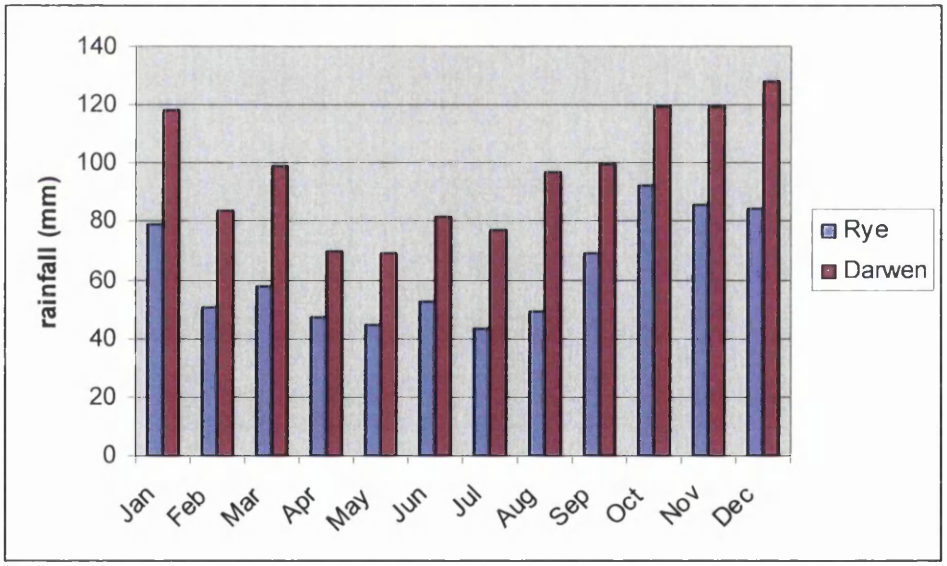

Figure 3.6: Yearly distribution of rainfall in Rye and Darwen

As could be expected Rye, which is located in the region that receives the most solar irradiation in the UK , has 47% more sun hours in a year than Darwen. Darwen on the other hand has 54% more rain fall in a year than Rye.As mentioned previously, the most important facet of weathering of organic coatings is the UV irradiation intensity. Even

though UV constitutes just 5% of the sunlight falling onto the earth, it is responsible for virtually all the damage done to polymers. The UV irradiation that is received by the natural weathering sites in Darwen and Rye has been estimated in the following way:

Because part of the UV light is absorbed by the air in the atmosphere, the amount of solar UV irradiation that reaches the earth's surface can be estimated when the air mass, through which the light has to travel to reach the earth's surface, is known. The air mass can be calculated when the sun's altitude angle γ_s is known (see section 2.5.1). Here, Rozenberg's empirical relation is used [84] :

$$AM = 1/(\sin(\gamma_s) + 0.025 * e^{-11*\sin(\gamma_s)})$$

The air mass is 40 at a γ_s of 0°, and 1 at a γ_s of 90°, the correlation is given in Fig 3.7:

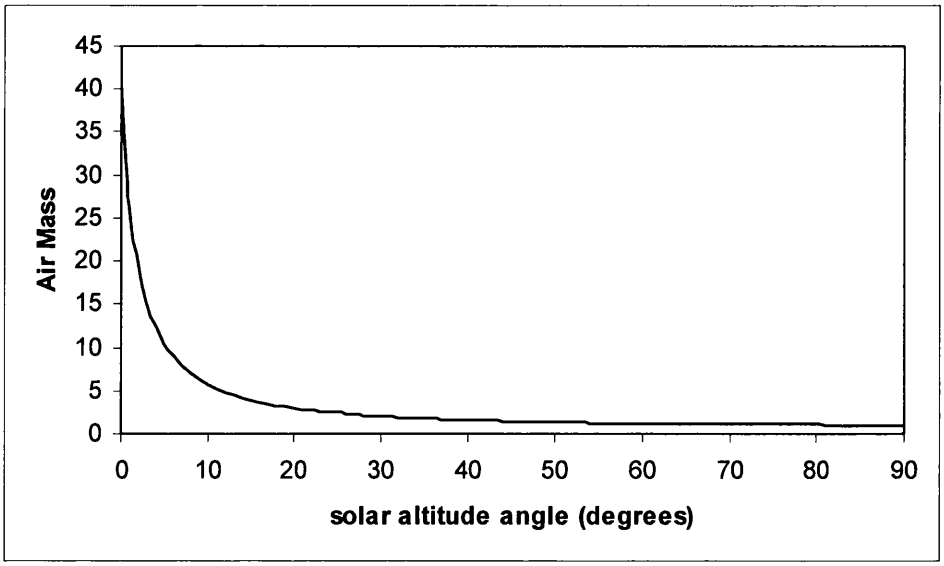

Fig 3.7: Correlation of Air Mass that solar irradiation has to go through and the solar altitude angle γ_s according to Rozenberg's empirical relationship.

The sun's altitude angle γ_s can be calculated at any moment in time when the geographical latitude of the location, the day in the year and the time in the day are

known. The formulas used here have been obtained from the Geography Department of the Free University in Amsterdam, the Netherlands [85]:

When the day of the year is known, the solar declination angle (SolDec) can be calculated with this formula:

$$SolDec = -23.4.\cos(360 * \frac{(day + 10)}{365})$$

The solar declination function describes the annual fluctuation of the sunlight between the two tropics, which is the cause for the four seasons in a year. (Fig. 3.8).

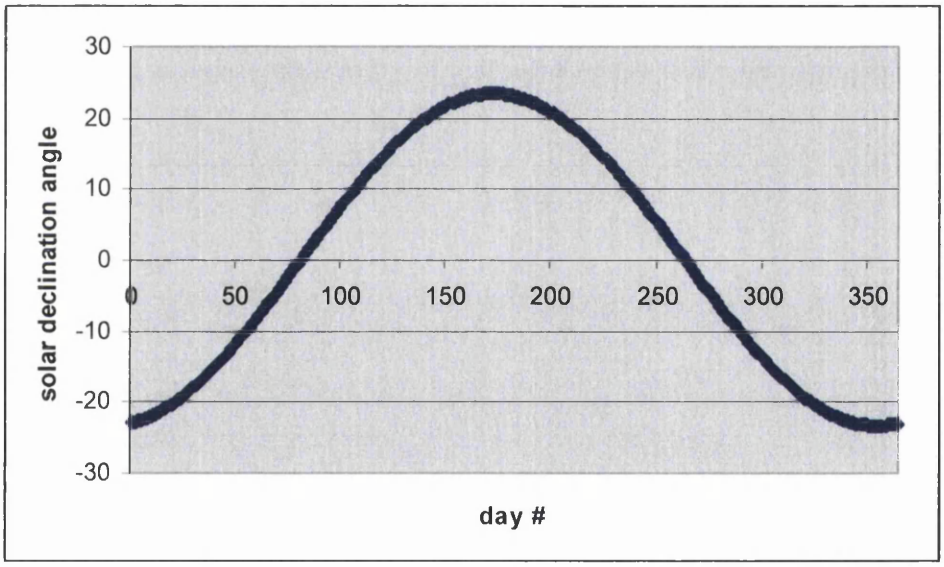

Fig 3.8: The solar declination angle as a function of the days in a year, (day #1 = Jan 1st).

The effect of the earth spinning around its axis makes the sun appear to move from east to west in the sky during the day. The hour angle (HourAngle) describes this movement of the sun around the earth in 24 hrs, with 15 degrees longitude per hour (360°/24hrs):

$$HourAngle = 15 * (Hour - 12)$$

So, the solar declination angle and the hour angle are calculated with the date in the year and the time in the day. When the geographical latitude of the location is also known, the solar altitude angle γ_s can be calculated with this formula:

$$\gamma_s = a\sin(\sin(Lat) * \sin(SolDec) + \cos(Lat) * \cos(SolDec) * \cos(HourAngle))$$

The solar altitude angle γ_s has been calculated for every day of the year, every 15 minutes, for Darwen and Rye, the two locations in the UK where panels have been exposed to the weather. The latitude of Rye is 50.9°, and that of Darwen is 53.7°.

To illustrate this, the solar altitude angle is plotted against time on the longest day in the year (21st June), the shortest day (21st December) and the equinox (21st March/ 22nd September) for both Darwen and Rye in Fig. 3.9.

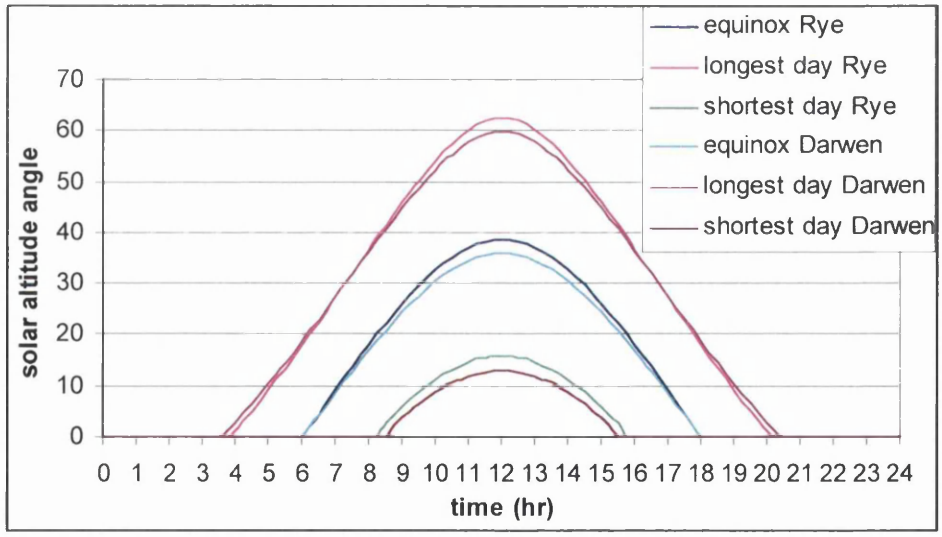

Figure 3.9: The solar altitude angle in Rye and Darwen on the longest day, the shortest day and the equinox.

The American Society for Testing and Materials (ASTM) has defined a standard terrestrial solar spectral irradiance distribution (AM1.5) for the global irradiance of a

plane tilted by 37° facing the equator. The conditions selected for this standard were considered to be a reasonable average for the 48 contiguous states of the United States of America over a period of one year (the tilt angle selected is approximately the average latitude for the contiguous states of the U.S.A.). In Britain, the racks on which panels are mounted during natural weathering are tilted by 45° to the south, to compensate for Britain's higher latitude. This justifies using the ASTM standard global solar irradiance spectrum for estimations of UV irradiation intensity here in Britain, as long as the difference in air mass is corrected for. The way in which this is done will be described in the next paragraphs.

The ASTM standard global irradiance spectrum is modelled using the 'Simple Model for Atmospheric Transmission of Sunshine' of Gueymard [86, 87]. 'Global irradiance' means that this spectrum consists of all the direct and diffuse solar irradiance within a hemispherical field of view of the tilted plane. The data for this standard spectrum are found in a document called ASTM G-173-03, which was downloaded from the website of the National Renewable Energy Laboratory in the United States [88]. The UV part of this spectrum is plotted in Fig. 3.10 together with that of the extraterrestrial AM0 spectrum, which is also developed by Gueymard [89].

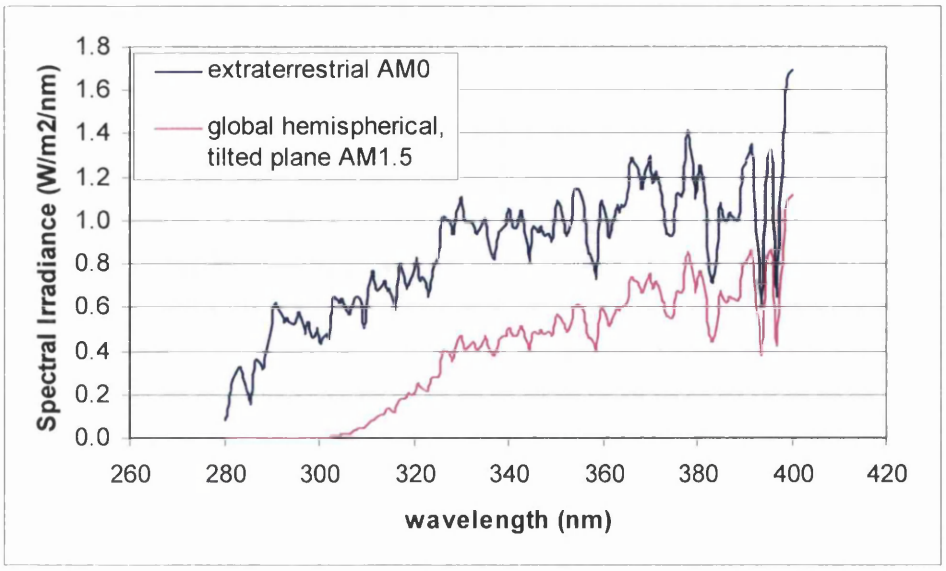

Figure 3.10: The UV part of the extraterrestrial AM0 spectrum and that of the global hemispherical AM1.5 spectrum

The amount of solar UV irradiance power (wavelength smaller than 400 nm) per square meter per second for an air mass 0 and an air mass 1.5 can be calculated from these spectra; this is done by a numerical integration, which gives the surface under the spectra in Fig. 3.10 . The value calculated for the AM0 spectrum is 113.15 Wm^{-2} and that for the AM1.5 spectrum is 51.06 Wm^{-2}. This means that, if the air mass is 1.5, 51.06 Wm^{-2} of global UV irradiation reaches the earth's surface, out of the potential 113.15 Wm^{-2} of UV irradiation that reaches the outer layer of the atmosphere.

With these two values, a model is proposed to calculate the global UV irradiance power on a plane tilted to face the equator by the same angle as the latitude of the location for an air mass other than 1.5:The air absorbs part of the UV-light, so the Lambert-Beer [79] law can be applied here, which correlates the fraction of light that is absorbed by a medium to the pathlength (in this case the air mass) that the light travels through this medium.. This is a simplification, as it assumes that the air is uniform in constitution in the atmosphere. This is not the case, as there is ozone which has a specific UV absorbing function in the outer layers of the atmosphere, and of course the density of the air (air

pressure) varies with altitude. However, as there are only two data points available to make an estimation, this is seems an appropriate solution.

The two known data points are fitted into a Lambert-Beer absorption equation in order to obtain the absorption constant (in conventional use of Lambert-Beer's law this constant equals the product of the molar extinction coefficient and the concentration of the medium). The constant is calculated to be 0.53 (obtained by filling in 51.06 Wm^{-2} for P_{UV} when AM equals 1.5, as is the case in the ASTM standard global solar irradiance spectrum). Of course, the zero-absorption irradiation power is 113.15 $W\,m^{-2}$, as this is the case when the air mass equals zero. Now, the UV irradiance power P_{UV} can be calculated with any value for the air mass (AM):

$$P_{UV}(W.m^{-2}) = 113.15 * e^{-0.53*AM}$$

Now, as the solar altitude angle γ_s has been calculated for Darwen and Rye, every day of the year, every 15 minutes, using the given set of formulas, the time-based daily average of this parameter was calculated for every quarter of an hour that the value of γ_s was higher than 1°. This was done for every day in the year, and these daily averages were subsequently merged into 12 monthly averages. These monthly averages for the solar altitude angle γ_s are given in the first column in Tables 3.15 and 3.16.

From the monthly average solar altitude angle the monthly average air mass is calculated (second column in Tables) with Rozenberg's empirical relationship.The average air mass over a year that the sun's rays have to travel through in order to reach Rye is 2.90, and that of Darwen is 3.20. The difference, 0.3, tells us that over a hypothetical year without any clouds in the sky, 85% of the UV irradiation that reaches Rye will reach Darwen (as $e^{-0.53*0.3} = 0.85$).

In the third column the number of monthly sun hours is given, based on the data from the Met Office. The total number of sun hours over a year in Darwen (1272 hrs), is 68% of that in Rye (1876 hrs).

In the fourth column, the average power of the UV irradiation, P_{UV} (inW/m^2) that falls onto a tilted south facing panel during a calendar-month is calculated with the formula that was proposed earlier in this paragraph. This value is an estimate of the average UV irradiation power in a calendar month when there are no clouds to block the solar irradiation, calculated with the average air mass of that month that the sun's rays have to go through.

In the fifth column, the UV irradiation energy in MJ/m^2 (E_{UV}) that a panel receives in the month, is calculated by multiplying the average UV irradiation power with the number of monthly sun hours, then multiplying by 3600 (seconds in an hour) and dividing by a million (to obtain Mega Joules).

$$E_{UV}(MJ.m^{-2}) = P_{UV} * (sunhours) * 3600/10^6$$

In the last column the accumulated UV irradiation energy is given, i.e. the energy that a panel would accumulate during a year when it would be exposed on January 1st.

Table 3.15: calculated data for Rye

Rye	average Solar altitude angle (°)	Calculated Average Air Mass	sunshine monthly (hours)	calculated UV irradiation power (Puv) (W/m2)	Calculated monthly UV irradiation energy (Euv) (MJ/m2)	accumulated UV irradiation energy (Euv) (MJ/m2)
Jan	12.18	4.69	67.90	9.42	2.30	2.30
Feb	16.83	3.44	86.85	18.22	5.70	8.00
Mar	23.21	2.53	130.20	29.49	13.82	21.82
Apr	29.46	2.03	190.05	38.48	26.33	48.15
May	33.64	1.80	236.40	43.43	36.96	85.11
Jun	35.31	1.73	232.80	45.19	37.87	122.99
Jul	34.62	1.76	244.90	44.48	39.22	162.21
Aug	31.34	1.92	239.60	40.81	35.20	197.41
Sep	25.73	2.30	171.45	33.37	20.59	218.00
Oct	19.01	3.06	129.30	22.27	10.37	228.37
Nov	13.42	4.27	87.30	11.73	3.69	232.05
Dec	10.89	5.21	59.05	7.14	1.52	233.57

Table 3.16: calculated data for Darwen

Darwen	average Solar altitude angle (°)	calculated average Air Mass	sunshine monthly (hours)	calculated UV irradiation power (Puv) (W/m2)	calculated monthly UV irradiation energy (Euv) (MJ/m2)	accumulated UV irradiation energy (Euv) (MJ/m2)
Jan	10.42	5.43	42.95	6.36	0.98	0.98
Feb	15.09	3.82	59.90	14.90	3.21	4.20
Mar	21.57	2.72	87.15	26.77	8.40	12.59
Apr	27.96	2.13	127.95	36.52	16.82	29.41
May	32.13	1.88	176.55	41.73	26.53	55.94
Jun	33.82	1.80	156.75	43.62	24.62	80.56
Jul	33.11	1.83	164.30	42.85	25.35	105.90
Aug	29.84	2.01	158.40	38.97	22.23	128.13
Sep	24.12	2.45	116.70	30.92	12.99	141.12
Oct	17.29	3.35	88.20	19.10	6.07	147.18
Nov	11.65	4.89	55.05	8.47	1.68	148.86
Dec	9.13	6.13	37.85	4.37	0.60	149.46

Fig. 3.11 gives a graphical representation of the UV irradiation power (P_{UV}) that is estimated for the different natural and accelerated weathering experiments that were conducted in this research. The time axis is the number of irradiation hours, and the

natural weathering curves represent one year of outdoor exposure, with the dots in the lines representing the monthly averages. The starting date of the exposure is chosen to be January 1st.

The lines that represent accelerated weathering have dots after every 500 irradiation hours, when the samples are taken out and measured. The line representing the normal QUV machine is at a constant value of 36.3 Wm^{-2}, because of the solar-eye irradiance control that is installed here. The line representing the horizontal QUV, which lacks solar-eye irradiance control, has a descending slope because the UV-A lamps' intensities decrease during the experiment, as is explained before.

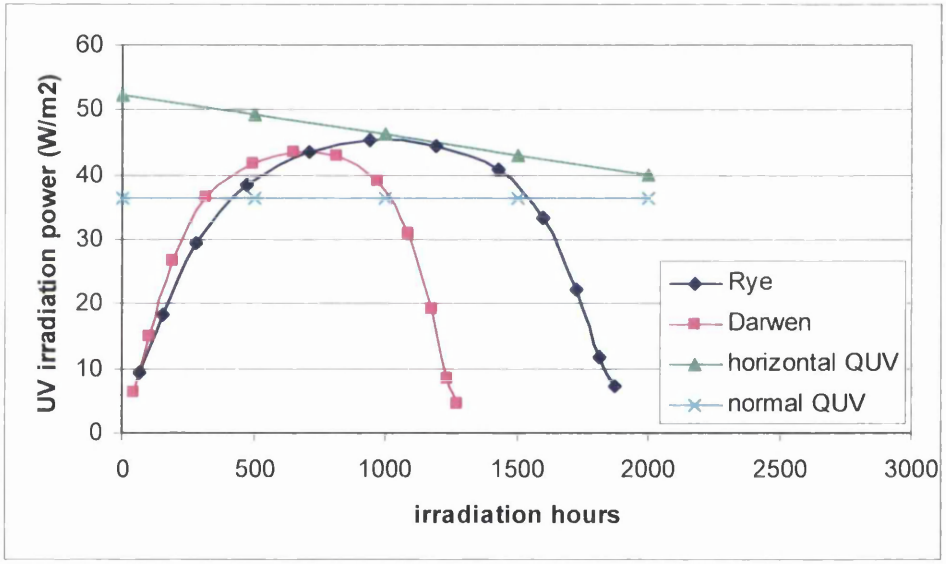

Figure 3.11: The UV irradiation power as a function of the number of irradiation hours (natural weathering started on January 1st)

In the same way, the accumulated UV irradiation energy is plotted in Fig. 3.12.This plot enables to compare the total amount of UV irradiation energy that a coating accumulates during natural and accelerated weathering as a function of the number of irradiation hours. In real time, the curves for the natural weathering exposures represent a year, while the line linked with accelerated weathering represent 18 weeks (3000 hrs) when a

condensation cycle is used, and 12 weeks (2000 hrs) when the experiment is irradiation-only.

There is an important difference between irradiation hours and real hours for natural weathering. During hours without irradiation (during the night, in cloudy weather), time-based factors such as oxygen and water diffusion into the coating come into play much more for natural weathering than for accelerated weathering, where the time-base is much shorter. This is an important reason why it is so difficult to find good correlations between natural and accelerated weathering [57].

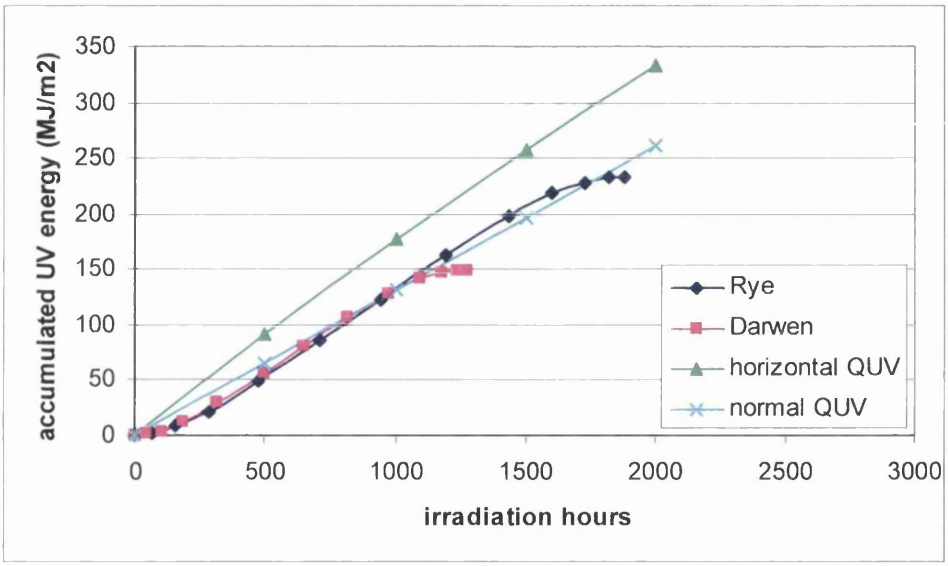

Figure 3.12: The accumulated UV irradiation energy as a function of the number of irradiation hours (natural weathering started on January 1st)

The modelling of the UV irradiation received in Rye and Darwen so far has been done with a daily, time based average value for the solar altitude angle from which the average air mass was calculated. With this average air mass the average UV irradiation power was calculated. This method seems adequate, but it might overestimate the amount of UV irradiation that can actually do damage to the coatings: UV damage occurs largely when the sun is high in the sky; if this is the case, the air mass is low, which increases the intensity of the UV-irradiation and moves the solar cut-off to a shorter wavelength

(higher energy). This happens in the hours around noon during the summer time, and all year around in latitudes close to the equator. Many hours of bright sunlight at a low solar altitude angle cause little or no photo-degradation, while a few hours of sunlight at a high angle can cause substantial degradation [32].

By counting all the time during the day that the solar altitude angle is greater than 1°, the calculated amount of damaging (high solar altitude angle/low air mass)) UV irradiation is overestimated. So, in order to fine-tune this UV irradiation estimation, a model is proposed when only the solar UV irradiation is 'counted' that is received when the solar altitude angle is greater than 30° (which means that the air mass is smaller than 2). This is done in the same way as the previous model, and the results of these calculations are given in Table 3.17:

Table 3.17:The calculated irradiation data for Rye and Darwen counting only irradiation received when γ_s>30°

	Darwen % potential sunhours γ>30°	calculated monthly irradiation energy (MJ/m2)	accumulated irradiation energy (MJ/m2)		**Rye** % potential sunhours γ>30°	calculated monthly irradiation energy (MJ/m2)	accumulated Irradiation energy (MJ/m2)
Jan	0.00	0.00	0.00		0.00	0.00	0.00
Feb	0.00	0.00	0.00		0.47	0.05	0.05
Mar	25.87	3.43	3.43		35.93	7.43	7.48
Apr	49.94	11.40	14.83		52.62	18.36	25.84
May	55.83	19.09	33.92		57.79	26.98	52.82
Jun	56.46	17.69	51.61		58.12	27.50	80.32
Jul	56.76	18.36	69.98		58.40	28.68	109.01
Aug	52.97	15.57	85.54		55.25	25.16	134.16
Sep	39.78	7.57	93.11		45.05	13.08	147.24
Oct	3.56	0.42	93.53		10.88	1.98	149.22
Nov	0.00	0.00	93.53		0.00	0.00	149.22
Dec	0.00	0.00	93.53		0.00	0.00	149.22

The calculated monthly irradiation energies are derived from the real monthly sun hours (given in the previous Tables 3.5 and 3.6) and the percentage of the monthly sun hours with γ_s>30°. An additional benefit of this method is that only irradiations that travel

through air masses smaller than 2 are counted, limiting the error introduced by the proposed formula that calculates the UV irradiance power from the air mass.

Both the models (γ_s>30° and γ_s>1°) will be used when natural weathering is compared to accelerated weathering, in order to evaluate their competence.

3.3 Measurements on Coatings

Reflectance spectroscopy, which is really a form of UV-VIS spectroscopy, has been used to measure the colour changes of the coatings during weathering. This was the main technique used in this research project. Other methods for analysing the coatings that have been used are IR spectroscopy, gloss measurements, Gas Chromatography combined with Mass Spectrometry and Scanning Electron Microscopy.

3.3.1 Colour Measurements

Until December 2001, the colours of the panels in the CDPD were only measured with the colour measuring device that is used at Akzo Nobel's paintlab in Darwen. This apparatus can only measure the CIE L*a*b* values of a colour. As has been explained in section 2.5 this is not detailed enough when one is interested in explaining the colour changes with the chemical processes that take place during weathering.

From December 2001 onwards, a reflectance spectrometer belonging to the Welsh Printing Group (attached to the School of Engineering at the University of Wales Swansea), has been used to record the spectra of weathered and unweathered panels coated with paints from the CDPD. This reflectance spectrometer is a Gretag-MacBeth SPM50.

The Gretag-MacBeth SPM50 has a 45°/0° geometry, which means that the measured coating is illuminated with a collimated beam of light at a 45° angle with the surface normal, and the reflective response of the coating is measured at a 0° angle with the surface normal (at a 90° angle to the surface of the coating). This means that the gloss reflectance (the 'mirror' effect which will reflect the incident beam from the coating at a 45° angle in the opposite direction) is excluded from the measurement.

3.3.2 Evaluation of Reflectance Measurements

The colour changes of the samples due to weathering are quite small. This brings the accuracy and the repeatability of the spectrometer measurements in question.

To evaluate the repeatability of the measurements of the reflectance spectra, some experiments were conducted to investigate the variation in measurements taken on the same location of a coating (caused by the spectrometer), and the variation in measurements taken on different locations of a coating (caused by both the spectrometer and by variations in the coating).

According to Gretag-MacBeth, the accuracy of its SPM50 spectrometer is 0.02 reflection units. This was tested by measuring the exact same spot on a coating ten times and then calculating the standard deviation of the reflectance in these ten measurements at every wavelength. This was done for 15 different coatings. The average standard deviation obtained in this way was 0.000173 reflection units, which means that the repeatability of the Gretag-MacBeth SPM50 spectrometer is (2.8*0.000173=) 0.0005 reflection units.

To evaluate the influence of variations between different places on the same coating on the reflection measurements, 10 measurements were taken on different spots each of the same 15 coatings that were used before; Now, the average standard deviation of the 15 panels was 0.006442 reflection units, which means a repeatability of (2.8*0.006442) 0.018. From this it is clear that on average 36 times (0.018/0.0005) more variation is introduced by variations in the samples than by variations in the measurements.

So, if reflectance spectra are taken of different locations on the coating of a panel, they will have a certain variance, mainly caused by differences in the reflection properties on the different locations of the coating.

The difference between two measurements on the same panel is best evaluated by looking at the maximum difference in reflectance between these two spectra over the

entire spectrum. This is done because the maximum difference between two measurements of the same sample is usually found at the wavelength of the reflection peaks of the spectra, which defines the 'nature' of the colour.

To investigate the distribution of the maximum differences between different spectra taken of one panel, the 45 absolute maximum differences (9+8+7+6+5+4+3+2+1) for each set of two measurements within the group of 10 measurements on one coating are calculated. These values can be plotted in a histogram, which is done here for a panel coated with base 15 pphr TiO_2 (Fig. 3.12)

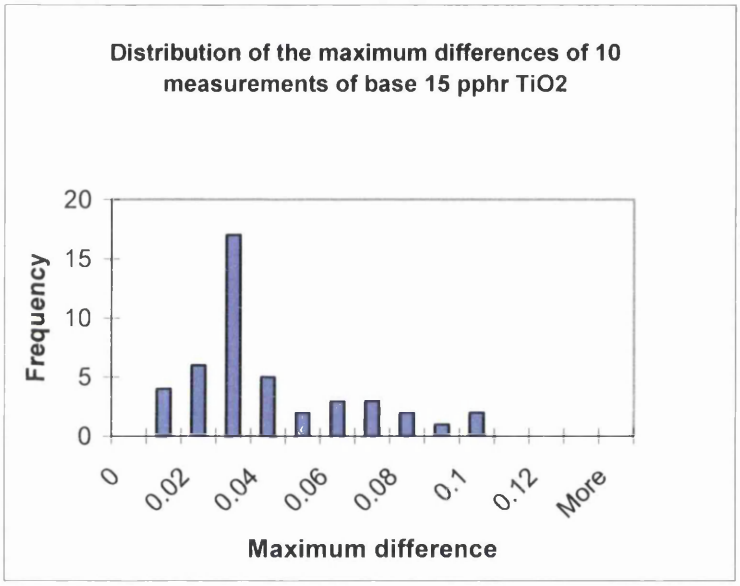

Figure 3.12: Histogram of the maximum differences between spectra taken of the same coating (15 pphr TiO_2 in PVC plastisol)

In general, if you take extreme values out of any distribution and plot them, like has been done here by picking out the maximum difference in reflectance over the whole spectrum for each set of two measurements within a group of 10 measurements, you will find an extreme value distribution. With the 45 maximum differences calculated for the set of ten measurements of the panel coated with base 15 pphr TiO_2, a probability plot of the extreme value distribution can be calculated (Fig. 3.13), with the help of Weibull distribution theory as described by Nelson [46]: This probability density function is matching the histogram of the data.

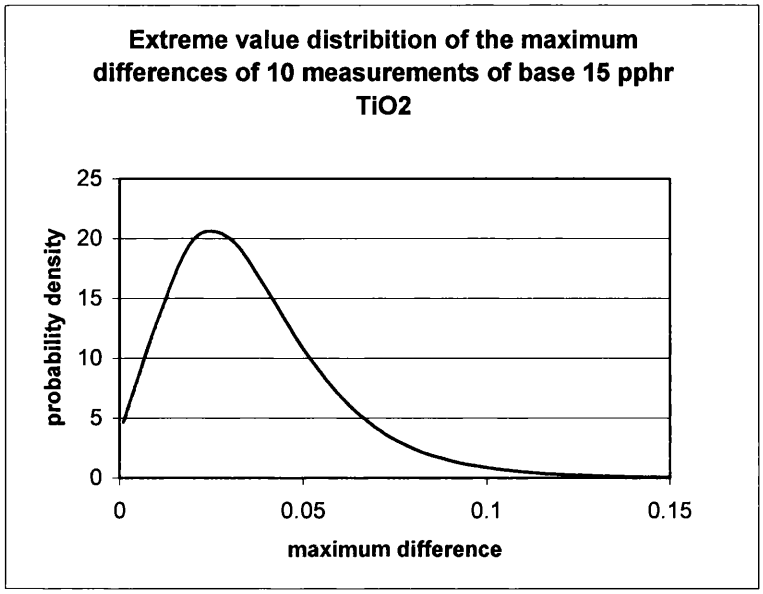

Figure 3.13: Extreme value distribution of the maximum differences

The reason that this subject is raised, is the following. After weathering in the QUV cabinets, the panels were measured. Because this was done frequently (after every 500 UV hours), only two measurements were taken of each panel. The average of the two measurements was calculated to give the end result, and the maximum difference between them was calculated to get an indication of the reliability of this end result. A high maximum difference calculated in this way would indicate a low reliability for that particular set of measurements.

Because the data are used to evaluate changes in the reflectance spectra due to weathering, and these changes tend to be quite small, it is important to eliminate outliers ('bad' measurements that are not representative for the sample). If this is done the data are 'purified' and the modelling done with the purified data will have a better quality.

For outliers to be eliminated, there has to be a cut-off point, a maximum allowable difference between the two spectra of a duplo measurement. This maximum allowable difference value is different for panels painted with different paints, because the variance

in reflectance properties will depend on the pigments used, the concentrations of these pigments and how well these pigments are dispersed in the paint.

Of all the A4 sized sheets that were coated in Port Talbot with the 158 selected paints from the CDPD, 7 different reflectance measurements were taken before any weathering had taken place. This gives 21 maximum differences between the 7 spectra (6+5+4+3+2+1) per sample to calculate the extreme value distribution for the measurements of that coating with. Once these distributions have been established, the cut-off points can be calculated for every paint, by inputting a chosen fraction, 0.995, into the primitive (accumulative) of the extreme value probability density function [46]. This will return a value, and 99.5% of the maximum differences between any two measurements of that panel will be smaller than that value (based on the seven measurements that were taken of the panel). This value will be called the maximum allowable difference of a duplo measurement.

With these calculated maximum allowable differences, the duplo measurement of a panel weathered in the QUV machine can be evaluated by comparing maximum difference of the duplo measurement with the maximum allowable value calculated for that panel. If the ratio of the maximum difference of the duplo measurements and the maximum allowable difference is greater than one, the duplo measurements belong to the 0.5% that are considered to be outliers. If this is the case than the spectrum is regarded as suspicious, and it is excluded from the modelling that is done later.

In the tables in Appendix I, the maximum allowable differences (MAD), are given for all the 158 coatings made from the paints chosen from the CDPD. There are two values for every shade, because two A4 sheets were drawn with every shade; one of these two was used to cut out panels that were exposed in Rye, and the other was used to cut out panels that were exposed in the QUV machines in Port Talbot.

The duplo measurements that have a maximum difference between the spectra greater than 0.02 reflection units are also treated as suspicious, as this is the spectrometer's accuracy (given by the manufacturer of the Gretag SPM 50).

For the reflectance spectra taken of the coatings that were exposed in Rye and Darwen, three measurements have been taken. From these three measurements, the median is taken as the end result, as this is a more robust estimator (the presence of an outlier in a set of three measurements will not influence the quality of the median). For every one of the 158 coatings, the maximum difference between highest and the lowest of the three spectra over the whole spectrum is calculated. On average, the maximum difference between three measurements is 1.5 times that of the maximum allowable difference between two measurements, so here the maximum allowable ratio of the maximum difference of the triplo measurements and the calculated maximum allowable (duplo) difference is set to be 1.5. If this ratio is greater than 1.5, the maximum difference of the triplo measurement belongs to the 0.5% 'outlier' group, which makes the measurement suspicious and excludes it from modelling. With the same rationale, the triplo measurements where the maximum difference exceeds 0.03 (1.5 times the spectrometer's accuracy of 0.02) are suspicious too.

3.3.3 Other Devices Used for Analysing Coatings

For gloss measurements in this research project, a Minolta Multi-Gloss 268 was used. This was operated in the 60° mode (section 2.5.3).

For the IR reflection measurements, a Spectrum One FTIR Spectrometer was used, manufactured by Perkin Elmer Instruments. This device is located in the Chemistry Department of the University of Wales Swansea.

For the measurement of plasticiser contents in weathered coatings, a Hewlett Packard 5890 Series II Chromatograph combined with a 5971A Mass Selective Detector (GC-

MS) was used, and for gravimetrical analysis a Gerhardlt Soxtherm 2000 was used. This work was carried out by Testing Solutions Wales, based in the ECM^2 building (the former Welsh Technology Centre) on the Corus site in Port Talbot.

The Scanning Electron Microscopy analyses were carried out in a Philips XL30CP, based in the Department of Materials Engineering of the University of Wales Swansea.

4 COLOUR CHANGE RESULTS AND DISCUSSION

4.1 Measurement of Visual Properties during Weathering

This project has generated a large amount of data on the coatings that were investigated. As the objective is to investigate the visual properties of coatings, and how they change during weathering, the bulk of the collected data are reflectance spectra that represent the colours of the coatings, and gloss measurements. These measurements were taken of 158 newly made (unweathered) coatings with variable pigmentations (see Chapter 3 for details). Identical copies of these coatings were then exposed to different types of natural and accelerated weathering, where their gloss measurements and reflectance spectra were recorded repeatedly after subsequent exposure periods. Natural weathering took place in Rye and Darwen, where the panels were measured every year (every 11 months in the case of Rye due to circumstances). Accelerated weathering took place in three different ways: UV-A irradiation only, UV-A irradiation in combination with a condensation cycle (8 hrs UV-A / 4 hrs condensation), and UV-A irradiation in combination with a condensation cycle in a horizontal set-up (in order to create the 'ponding' effect, also 8 hrs UV-A / 4 hrs condensation).

4.1.1 Reflection Spectra

The reflectance spectra of the 158 panels that were investigated are given in Appendix I. For every panel, the reflectance spectrum before weathering is given by the dark blue line (in the legend the pigmentation of this panel is given). The five coloured lines then give the reflectance spectra of that panel after exposure to the five different types of weathering. In general, a panel was measured after every year of outdoor exposure and after every 500 hours of UV-A irradiation in accelerated weathering. Because the total number of measurements is too high for all of them to be plotted, only the reflectance spectrum recorded after the maximum amount of each type of weathering is given in

Appendix I. This is 2000 UV-A hours for the three different types of accelerated weathering: a light blue line ('UVA') indicates QUV without condensation, a magenta line ('UVA-C') indicates QUV with condensation and a brown line ('UVA-C h') indicates the horizontal 'ponding' QUV machine. The two types of natural weathering are indicated with a yellow line ('22 months Rye') for natural weathering the maritime climate of Rye, and a pink line ('.. months Darwen') for natural weathering in the industrial climate of Darwen, because the maximum exposure time of the shades varies.

Before the spectra can be discussed, a few points have to be made:

The spectra of the unweathered panels are the medians of seven measurements. In the legend the pigment concentrations of the shade are given in pphr (parts per hundred, equal to weight percentage) relative to the PVC concentration.

The spectra of the "Rye" panels are the median of three measurements. The maximum exposure time for all the Rye panels is 22 months.

The spectra of the "Darwen" panels are also the median of three measurements.The maximum exposure times in Darwen of the shades vary; they can be 24, 36 or 48 months, because the starting dates of the exposure vary. The shades in Darwen have been exposed at an industrial site where dirt uptake from the soil and the air is known to take place. Even though the panels have been washed and softly scrubbed before the reflectance measurements were carried out, this contamination can still be present in the top layer of the coating and cause the shade to appear darker (and the reflectance spectrum to be lower).

The spectra of the panels weathered in the QUV machines are all the average of two measurements. For convenience, the pigmentations of the 158 shades are given in the tables in Appendix I, together with the calculated maximum allowable differences (MAD) for the panels exposed in the QUV machines and in Rye (see section 3.3.2). Then for each shade the maximum difference between the spectra is given; this value is printed

bold when it exceeds 0.02 (in the case of the duplo QUV measurements) or 0.03 (in the case of the triplo Rye measurements, see section 3.3.2). The ratios of these values and the MADs of the shades have been given in the next column., These ratios have been printed bold when they exceed 1 (in the case of the duplo QUV measurements) or 1.5 (in the case of the triplo Rye measurements). So the spectra of weathered shades that have bold-printed maximum differences or bold-printed ratios of maximum differences with MADs after certain types of weathering are treated as suspicious and excluded from the modelling.

The shades weathered in Darwen could not be evaluated in this way because they were exposed to the weather before this project started, so there are no unweathered spectra available for these shades to calculate the MAD values with. All that could be done here was to exclude the triplo measurements with a maximum difference of 0.03 between the highest and the lowest spectrum from the modelling.

The entities and units of the axes are not given in the graphs, in order to create more space for the spectra to make them look clearer. In all graphs, the x-axis represents the wavelength of the reflected light in nanometers (nm), and the y-axis represents the amount of reflected light relative to the incident light, expressed in reflectance units.

The scale of the y-axis runs from 0 to 1 in for the single pigment shades and for the orange shade, but not for the cyan, yellow-green and magenta shades. In the case of the last three shades the scale of the axis has been rescaled, because the reflectance values of these shades were small. This was done in order to enable the reader to distinguish the spectra properly.

4.1.2 Changes of Reflection Spectra During Weathering

Now, the general trends that are observed in the changes of the reflectance spectra after weathering are discussed:

Base TiO_2 shades:

The base TiO_2 shade spectra seem to have a regular downward trend after weathering. This makes sense because there are no organic pigments in this paint, so the only processes that could change the colour are dehydrochlorination and chalking. Because the impact of the chalking process is very small compared to that of dehydrochlorination, the spectra generally become lower after weathering. The correlation between the lowering of the reflectance spectra due to dehydrochlorination and the UV exposure time for pigmentless base will be examined later by introducing the Spectrum Surface Integral (SSI), which is defined as the surface under the reflectance spectrum of a weathered sample minus the surface under the reflectance spectrum of an unweathered sample.

Only the spectra taken after 2000 hrs UVA and after 22 months Rye of the 1 pphr TiO_2 shade have risen after weathering (Fig. 4.1). This can be explained by the chalking process, and will be shown later in this chapter with some SEM scans.

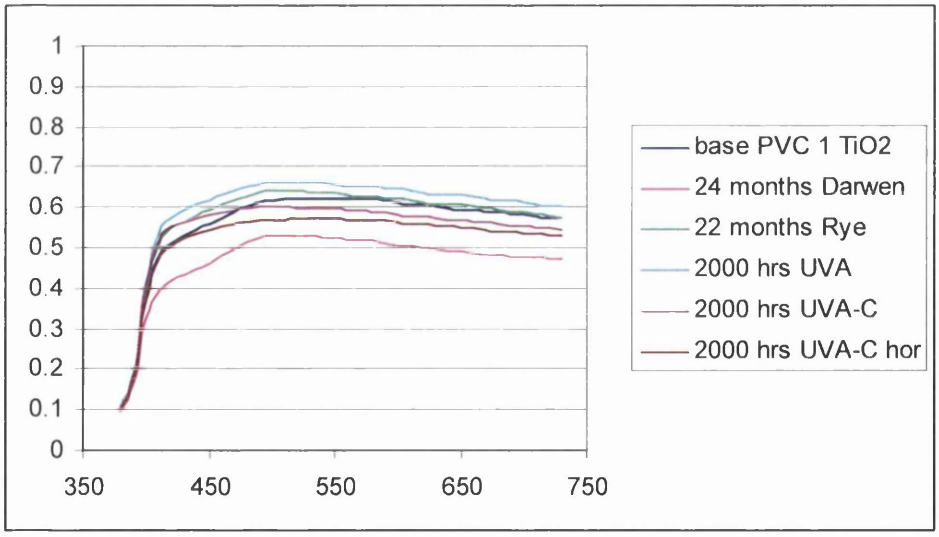

Figure 4.1 Spectra of base PVC plastisol with 1 pphr TiO_2

It has to be noted that the measurements taken of the base shades have shown a very high variance (in the table in appendix I, the values for the max. variance for 99.5% of the

population are high). This means that there is a lot of variation in the reflectance properties on the panel, probably caused by the absence of light-absorbing pigments.

Green shades:

The green shades with low green pigment concentrations (0.05, 0.1 and 0.2 pphr) show a lower reflectance spectrum after accelerated weathering with condensation, which is caused by dehydrochlorination. This is especially the case with the spectra taken after QUV weathering with condensation (both horizontal and normal) and after weathering in Darwen (Fig. 4.2).

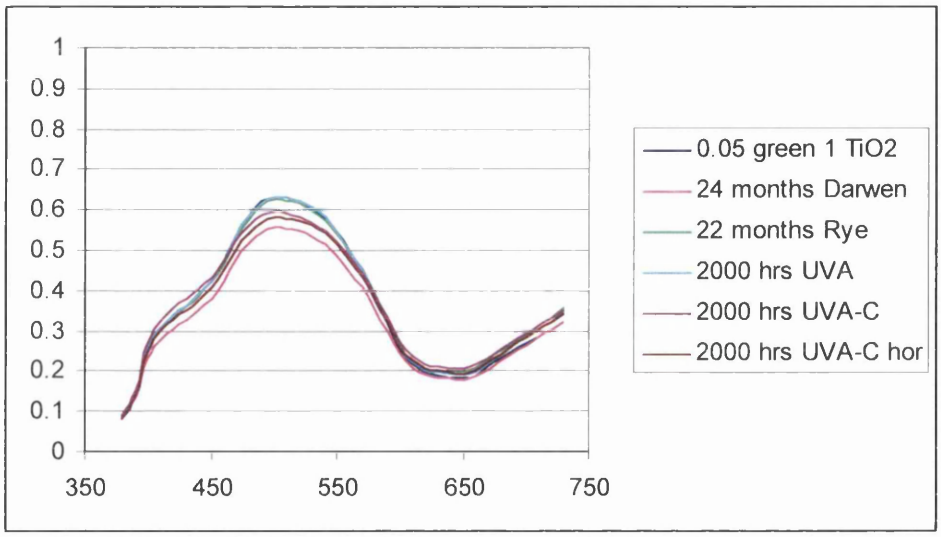

Figure 4.2 Spectra of 0.05 pphr green 1 pphr TiO_2

When TiO_2 is added to the shades, this lowering is less because of shielding by the inorganic pigment. At low green pigment concentrations, the reflectance spectra after 2000 hrs of UV-A light without condensation are the same as those before weathering, so it seems that there is no pigment reaction caused by photo-degradation of the green pigment molecules in these shades. The spectra of the low green concentration panels weathered in Darwen are significantly lower than those weathered in Rye, so this reinforces the idea that dirt uptake in an industrial environment depresses reflectance spectra.

At the higher green concentrations (0.6 and 1 pphr), the spectra don't change as much in a downward direction. This is due to a better protection of the PVC base by the pigment, so that less dehydrochlorination is taking place. On the other hand, because there is more green pigment in the coating, there is a bigger chance of green pigment molecules in the excited state reacting. This would elevate the reflection spectrum, as the green pigment reflection peak increases with decreasing pigment concentration.

Some of the spectra of the higher pigment shades after weathering have a higher spectrum after weathering than before, in these cases it is likely that more pigment degradation has taken place than dehydrochlorination in the coating. At high concentrations of both TiO_2 and the green pigment, there is hardly any change in the spectra at all.

Blue shades:

The same trends apply for the blue shades as for the green pigment shades:

The shades with low blue pigment concentrations (0.05 and 0.1 pphr) show a lower reflectance spectrum after accelerated weathering with condensation, caused by dehydrochlorination (Fig. 4.3).

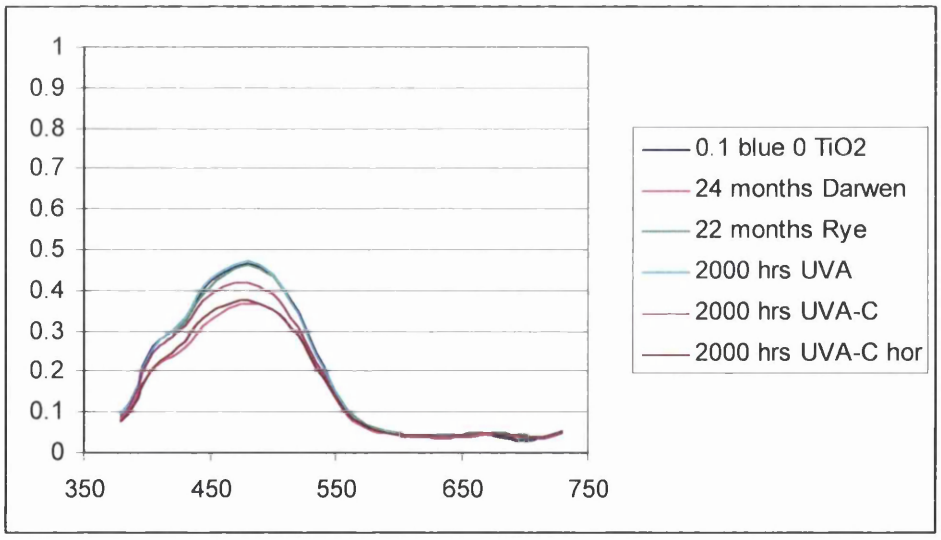

Figure 4.3 Spectra of 0.1 blue 0 TiO_2

At higher TiO_2 concentrations, this lowering is less because of shielding. At low concentrations, the reflectance spectra after 2000 hrs of UV-A light without condensation are virtually the same as those before weathering, so it seems that there is no pigment reaction caused by photodegradation of the blue pigment molecules at these concentrations. At blue pigments concentrations of 0.2 , 0.6 and 1 pphr, the spectra seem to go up and down after weathering, indicating that reaction of the blue pigment (this would elevate the reflection spectrum, as the blue pigment reflection peak increases with decreasing pigment concentration), is happening alongside PVC dehydrochlorination. Again, at high concentrations of both TiO_2 and the blue pigment, there is hardly any change in the spectra at all.

Red shades:

For the absorbing part of the spectra of the red pigment shades (below 600 nm), the same rule applies as with the green and blue shades; a higher pigment concentration results in more light absorption and thus a lower reflectance value. However, in the part of the spectra where the red pigment reflects light, above 600 nm, the opposite trend occurs; a higher pigment concentration results in more light reflection, thus a higher reflectance value. This phenomenon has been found for the organic red and yellow pigments used in the CDPD, which both have reflectance peaks at the high wavelength end of the spectrum. Above 600 nm, the reflectance of the 2.5 pphr red / 0 pphr TiO_2 shade is even higher than the reflectance of the pigmentless base (Fig. 4.4). The reason for this could be that the red pigment has a 'fluorescence' effect; it absorbs the high energy part of the standard D65 light that the spectrometer emits during a measurement at the lower wavelengths, and then transforms it into a lower energy light, which is then emitted by the pigment at a higher wavelength.

For this reason, the red pigment, like both the yellow pigments used in the CDPD, has a positive correlation between the reflection peak size and the pigment concentration (the reflection peak increases when the pigment concentration increases). This means that both the weathering effects that influence the reflectance spectrum of the coating have the same result at high wavelengths; they will depress the reflectance spectra.

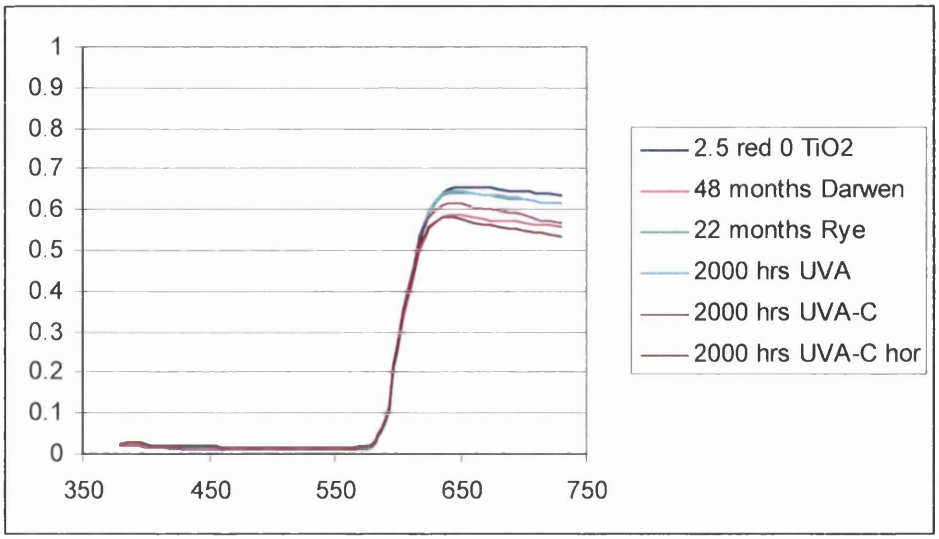

Figure 4.4 Spectra of 2.5 red 0 TiO_2

In the low red pigment concentrations (0.1 , 0.25 and 0.5 pphr red) it is clear that the reflection peaks get smaller after weathering. Generally, the spectra after 2000 hrs UV-A light without condensation and those after outdoor exposure in Rye show a smaller change than the spectra recorded after 2000 UV-A hrs with condensation, after outdoor exposure in Darwen, and after weathering in the horizontal QUV ponding machine. This indicates the difference that the presence of water makes during weathering. Dehydrochlorination seems to be the process that has the biggest impact on the colour change during weathering.

The higher pigment concentrations (1.5 and 2.5 pphr red) show depression of the reflectance spectra, but to a lesser extent. One outlier seems to be the 1.5 red 10 TiO_2 shade after 2000 UV-A hrs with condensation. Checking in Appendix I reveals that the maximum difference between the duplos is high (0.029), so it seems best not to take this measurement too seriously. As usual, the TiO_2 seems to have a shielding effect; there is less spectrum depression after weathering for higher TiO_2 concentrations than for the lower ones.

1-yellow shades:

The organic 1-yellow gives basically the same story as the red pigment; the reflection peak increases when the pigment concentration increases (Fig. 4.5). This means that both the weathering effects that influence the reflectance spectrum of the coating have the same result in the long wavelength region where the reflection peak is located; they will depress the reflectance spectra.

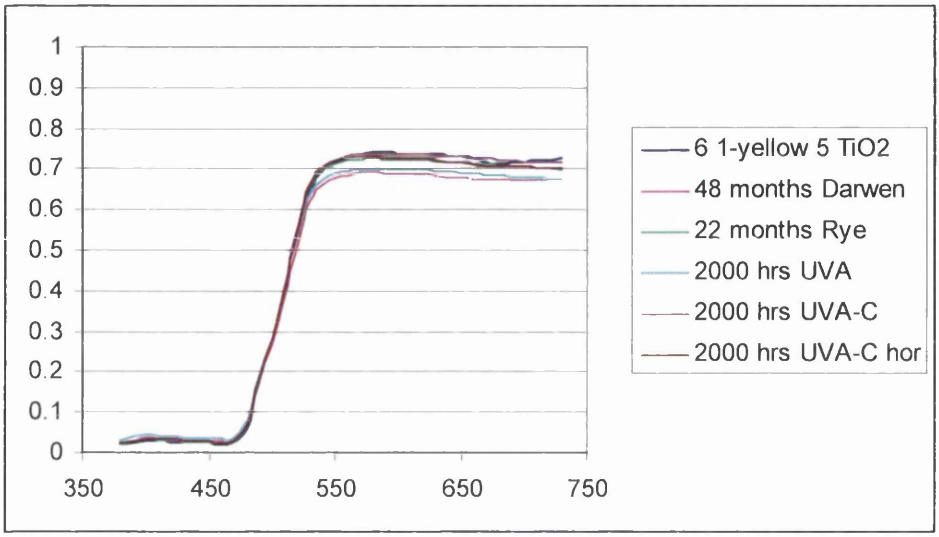

Figure 4.5 6 1-yellow 5 TiO_2

The trends can be explained in the usual manner; a higher TiO_2 concentration means more shielding and less decreasing of the spectrum after weathering, and at high concentrations of the 1-yellow pigment, there is hardly any change in the spectra after weathering.

2-yellow shades:

The 2-yellow pigment is the only inorganic pigment used in the CDPD, apart from the TiO_2 of course. It is a Cr-Ti-Sb Oxide, which itself should be inert to photochemical reactions during weathering. For this reason, it is fair to assume that most of the changes in the reflectance spectra of the 2-yellow shades are caused by the dehydrochlorination of PVC (Fig 4.6). Chalking is the other process that can take place, as the pigment is inorganic.

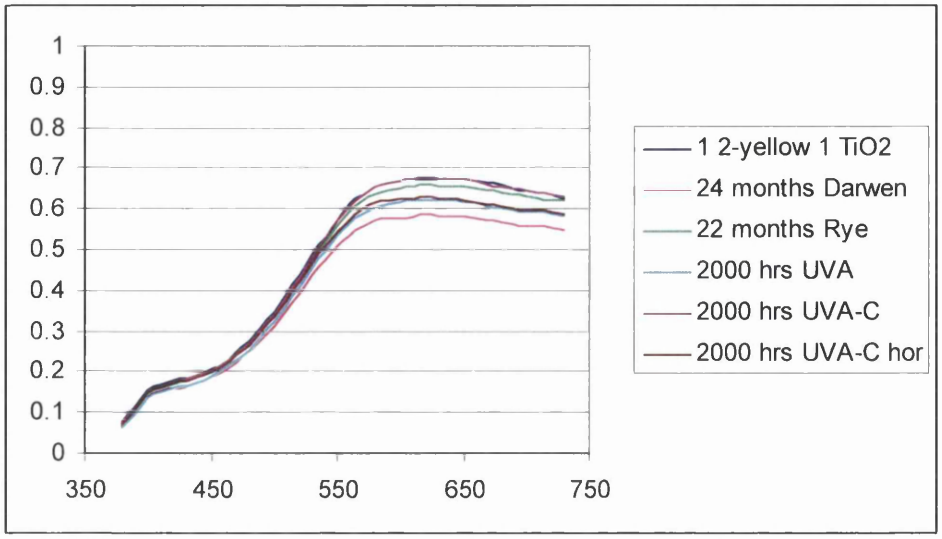

Figure 4.6 Spectra of 1 2-yellow 1 TiO_2

The 2-yellow pigment has the same shielding function as the TiO_2 has. This can be seen when the shades with 0.25, 1, 2.5, 5, and 10 pphr Si-yellow (all with 0 pphr TiO_2) are compared; the higher the Si-yellow concentration gets, the less the spectra are decreased after weathering because of the dehydrochlorination of PVC.

Magenta shades:

The spectra of the magenta shades (mixtures of the blue and the red pigment, without TiO_2) are mostly increasing after weathering, but this happens in small amounts (Fig 4.7, remember the vertical axes here are adapted to smaller scales).

This indicates that most of the colour change is caused by the reaction of the blue pigment, since this is the only known photochemical reaction in these shades that can cause an increase of the spectra after weathering. Of course the (absorbing) short wavelength end of the red pigments increases too when the red pigment concentration decreases, but this goes together with a decrease of the long wavelength part of the spectrum where the reflection peak of the red pigment is, and a decrease in this region is not observed in the magenta shades. The only exceptions are the spectra of the low concentrations magenta shades after 2000 hrs of weathering in the horizontal QUV

ponding machine. Below a wavelength of 550 nm, these spectra are lower than the ones taken before weathering. This can only be explained with dehydrochlorination of PVC, as the pigments cannot protect the PVC base well enough at low concentrations, and the QUV ponding machine is the type of weathering that causes the most dehydrochlorination.

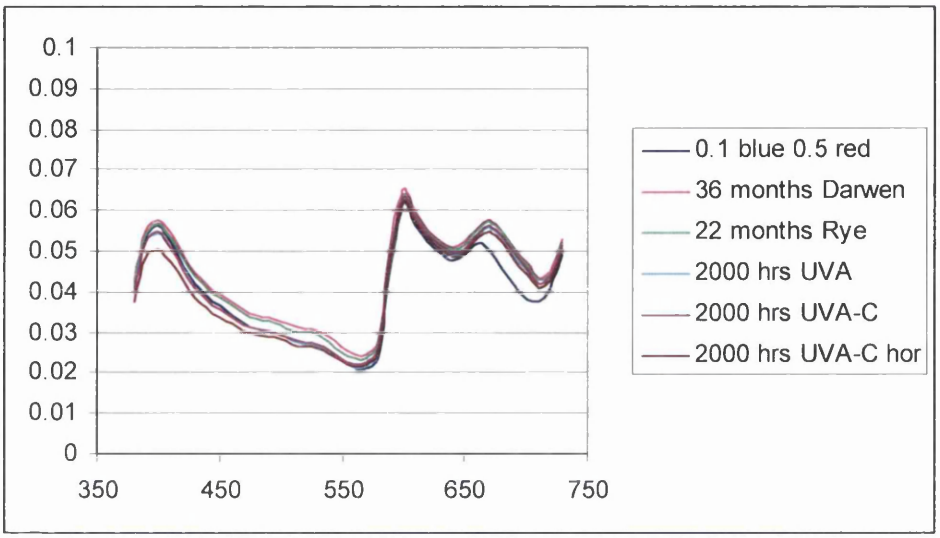

Figure 4.7 Spectra of 0.1 blue 0.5 red

As usual, high pigment concentrations decrease the amount of change in the reflectance spectra due to weathering.

Orange shades:

The orange shades (mixtures of the red pigment and the 1-yellow pigment without TiO_2) are straightforward to analyse; both pigments have reflectance peaks that increase when the pigment concentrations increase, so the spectra at longer wavelengths should decrease after weathering, after pigment reaction or PVC dehydrochlorination.

This is what can be seen in the spectra; all the spectra of the shades decrease after weathering (the low concentration ones more than the high concentration ones, Fig. 4.8).

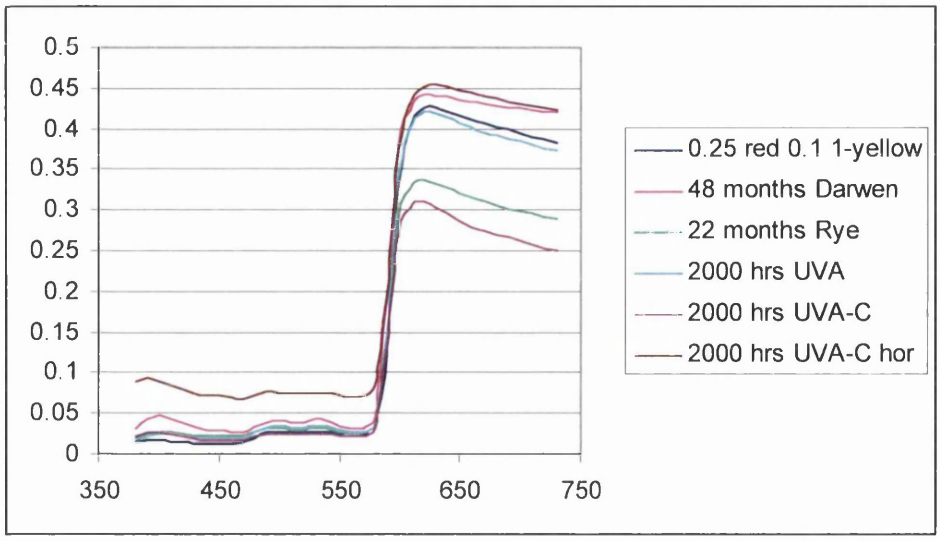

Figure 4.8 Spectra of 0.25 red 0.1 1-yellow

Most changed are generally the spectra after 2000 UV-A hrs with condensation and after 2000 UV-A hrs in the horizontal ponding machine. This again shows the strength of weathering in the ponding machine.

Cyan shades:

The cyan shades (mixtures of the blue and the green pigment, no TiO_2) all show a lot of changes in their reflectance spectra after weathering, but remember that the vertical axes here are adapted to smaller scales. Consisting of the two pigments that have a negative correlation between the pigment concentration and the reflectance peak size (higher pigment concentration gives lower peaks), the reaction of the pigments here will result in elevation of the reflectance. For most shades, this is what happens after 2000 UV-A hrs without condensation in the QUV weathering cabinets and after 22 months of outdoor exposure in Rye (Fig. 4.9).

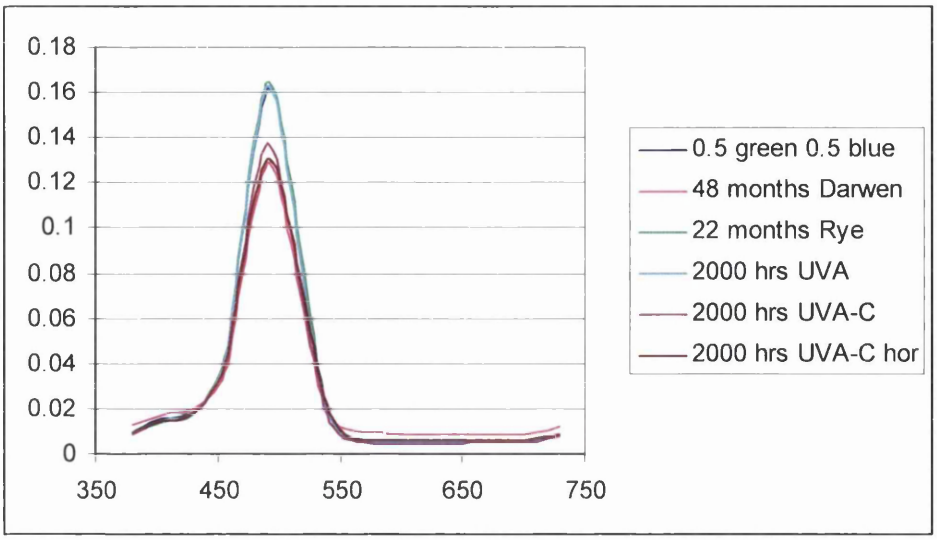

Figure 4.9 Spectra of 0.5 green 0.5 blue

The spectra of the panels weathered in Darwen, in the QUV cabinet with condensation and in the horizontal QUV ponding machine, have all decreased, indicating that PVC dehydrochlorination is the main photochemical process that is going on here. In most cases, the QUV ponding machine causes the most changes in the spectra.

Yellow-green shades:

The yellow-green shades (mixtures of the 2-yellow pigment and the green pigment, no TiO_2) show big changes in the reflectance spectra after weathering when the pigment concentrations are low (<1 pphr, Fig 4.10), but virtually none when they are higher (again, the vertical axes here are adapted to smaller scales).

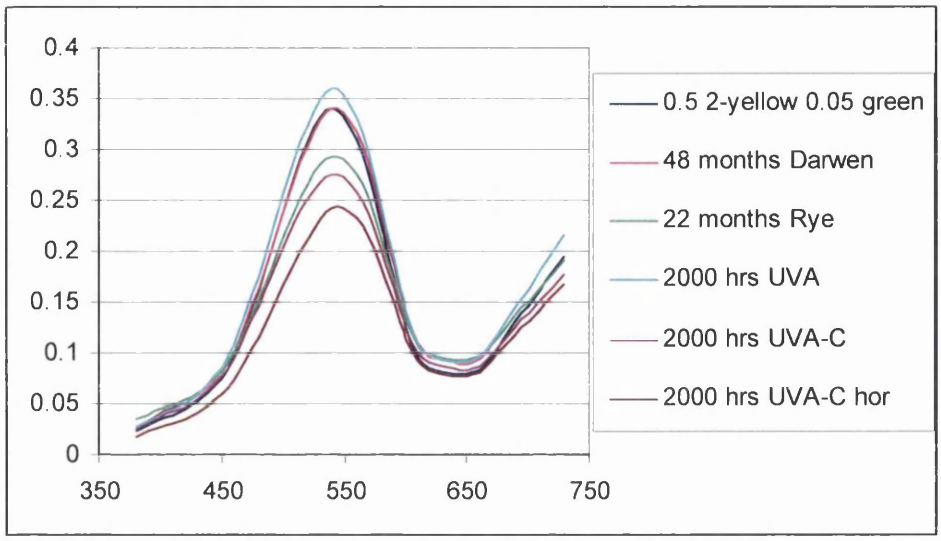

Figure 4.10 Spectra of 0.5 2-yellow 0.05 green

Because the inorganic 2-yellow pigment is inert, and the green pigment's reflection peak increases when its concentration decreases due to a photochemical reaction, the same pattern arises for the low concentration yellow-green shades as with the cyan shades: After 2000 UV-A hrs without condensation, the reflectance spectra tend to rise, due to loss of the green pigment, and after the same amount of time in the QUV cabinet with condensation and in the horizontal QUV ponding machine, the spectra decrease, indicating that PVC dehydrochlorination is the main photochemical process caused by these types of 'wet' weathering.

The low-concentration yellow-green shades that were weathered in the horizontal 'ponding' QUV also became brittle after 1500 UVA hours. This would indicate the loss of plasticiser from the coating due to photo-degradation. This phenomenon was further investigated by measuring the plasticiser concentrations in the coatings using GC-MS. The results of this were very interesting; the concentration of the DIDP plasticiser was found to have strongly decreased after weathering in the horizontal ponding QUV machine for the yellow-green shades with low pigment concentrations. Details of this are discussed later in this chapter.

4.1.3 Gloss Retention Measurements

The gloss values have been measured every 500 UVA hours during accelerated weathering, and every year in natural weathering. These values are given in Appendix II, together with those measured after the first two years of outdoor exposure in Rye and Darwen. In the appendix, the 60° gloss values are given of the unweathered panels. For the weathered panels, the gloss retention values are given. This is done because the initial unweathered 60° gloss values can vary substantially (mainly due to small differences in the curing process), so the gloss value of a weathered panel needs to be related to the initial gloss value before weathering of that specific panel to be relevant. The gloss retention is calculated with a simple formula:

$$\text{Gloss retention (\%)} = 100 * (\text{Gloss}_{\text{weathered}} / \text{Gloss}_{\text{unweathered}})$$

These data have been analysed as follows. In order to compare the gloss retentions of coatings that have been exposed to different types of weathering, every calculated gloss retention value in Appendix II was divided by the amount of irradiation that the coating had been exposed to when the measurement was taken (see section 3.2.1) to obtain the 'corrected gloss retention'. These values now indicate for every shade the amount of gloss loss that the coating has displayed relative to the irradiation it has received.

As the gloss measurements tend to have a big variation, for every weathering process the median of the obtained corrected gloss retention values of a shade was taken (generally there are 4 values for the accelerated weathering processes and two for the natural weathering processes). This median value was then considered the best estimate for the corrected gloss retention of that shade exposed to that particular weathering process. The reasoning behind this is that by taking the median of the calculated 'corrected gloss retention' values, the outlier gloss measurements will be excluded from the analysis.

These median corrected gloss retention values were subjected to a correlation analysis. It was found that the exposure of the panels in Rye had good correlations with all three

types of accelerated weathering regarding the gloss retention properties of the coating. The correlation coefficient of natural weathering in Rye with QUV weathering without condensation is 0.84, that with QUV weathering with a condensation cycle is 0.92, and that with horizontal QUV weathering with condensation is 0.90. Correlation plots are given in Figures 4.11, 4.12 and 4.13.

On the other hand, the correlations of weathering in Darwen with the three types of accelerated weathering were poor: The correlation coefficient of natural weathering in Darwen with QUV weathering without condensation is -0.13, that with QUV weathering with a condensation cycle is -0.01, and that with horizontal QUV weathering with condensation is -0.02.

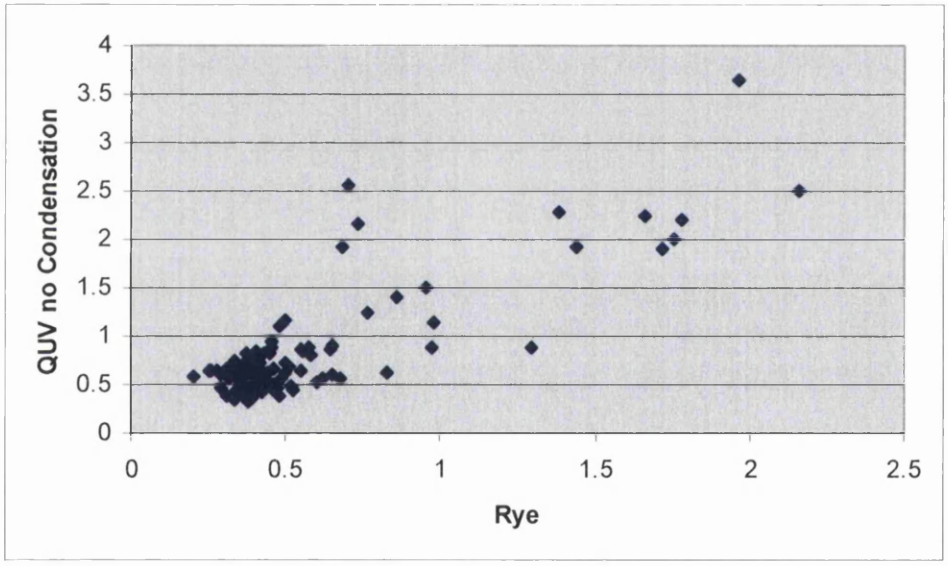

Figure 4.11 correlation plot for the calculated corrected gloss retention values of weathering in Rye and QUV weathering without condensation

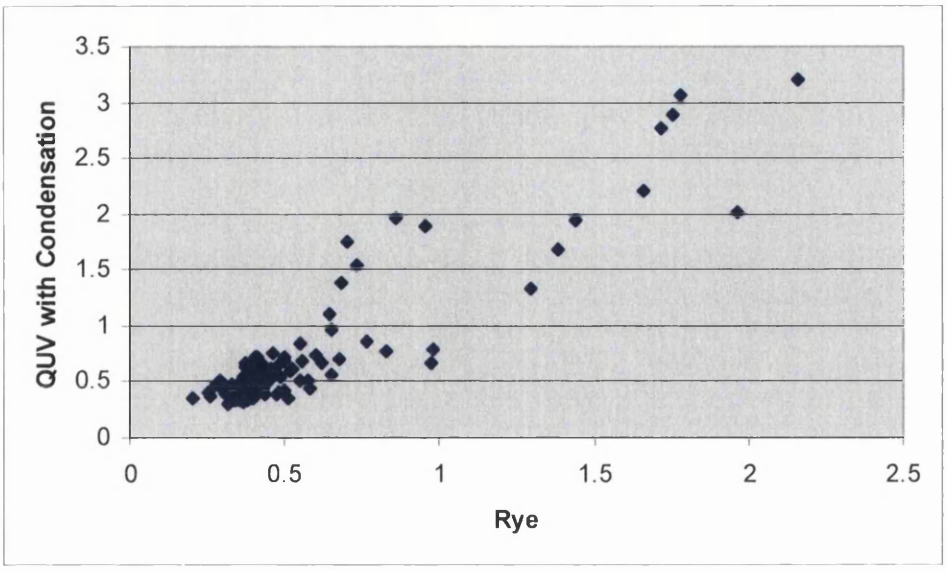

Figure 4.12 correlation plot for the calculated corrected gloss retention values of weathering in Rye and QUV weathering with condensation

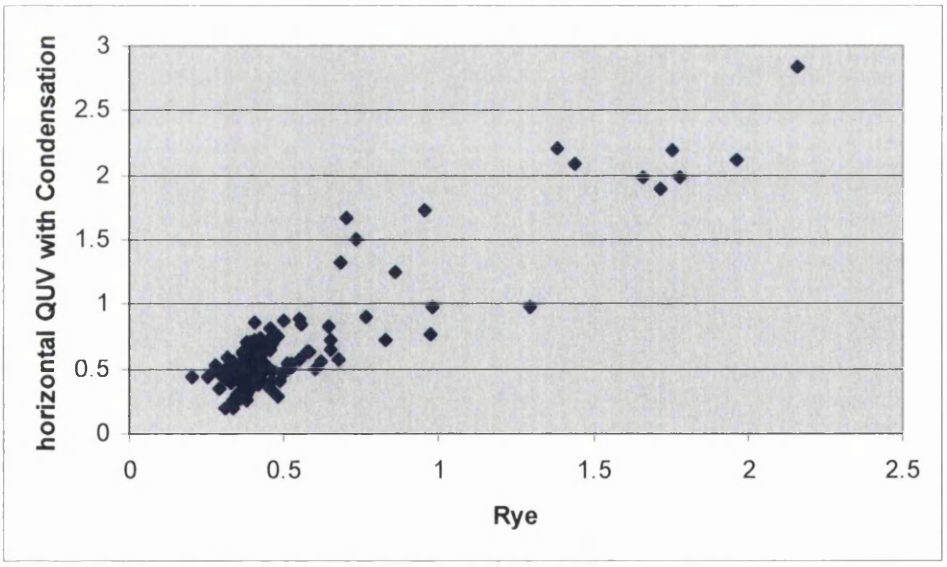

Figure 4.13 correlation plot for the calculated corrected gloss retention values of weathering in Rye and horizontal QUV weathering with condensation

In the correlation plots shown here, the corrected gloss retention values calculated for weathering in Rye were obtained using the irradiation energies calculated with the solar altitude angle $\gamma_s>1^\circ$ irradiation model. The same was done with the $\gamma_s>30^\circ$ irradiation

model, which makes the calculated corrected gloss retention larger because the gloss retentions are divided by a smaller amount of irradiation energy (the γ_s>30° irradiation model only 'counts' the energy when the solar altitude angle is higher than 30°, see section 3.2.1). In order to evaluate which of the solar irradiation models has a closer similarity with the irradiation received during weathering in the QUV machines, the ratio of the corrected gloss retention after QUV weathering and that after weathering in Rye was calculated for all the exposed panels. When the γ_s>30° irradiation model was used for the estimation of the solar irradiation energy received in Rye, the average ratios were 1.20, 1.32 and 1.37 for weathering in Rye and QUV weathering without condensation, with condensation and horizontal QUV with condensation. When the γ_s>1° irradiation model was used they were 0.75, 0.82 and 0.85 respectively. This indicates that the γ_s>30° irradiation model probably underestimates the amount of solar irradiation that is capable of damaging the coatings, while the γ_s>1° irradiation model overestimated it.

4.2 Plasticiser Degradation, Gloss Loss and Dehydrochlorination in the Yellow-Green Shades

As stated in the previous section, some of the yellow-green shades showed a lot of deterioration during the weathering in the horizontal QUV machine. Here the experiments and the analysis that is done on these shades following those observations is reported.

4.2.1 DIDP Concentration Measurements

Some of the coatings that were weathered in the horizontal 'ponding' QUV became brittle after 1500 UVA hours. This was mainly the case in the low concentration yellow-green shades, pigmented with the inorganic yellow Cr-Sb-Ti oxide, and with the polychloro copper phthalocyanine green. These coatings partially delaminated from the primer and became so brittle that they would break off on minimal contact (Fig 4.14).

Figure 4.14 Yellow- green shades delaminate and become brittle after weathering in the horizontal QUV machine.

When this deterioration was observed, these yellow-green coatings, and some other shades, were submitted to Testing Solutions in Port Talbot, to analyse them for their DIDP contents (DIDP is the main plasticiser used in the tested PVC plastisol base). This was done using a GC-MS set-up (see section 2.7.4). The DIDP concentrations that were measured in this way are given in Appendix III. The GC-MS measures the concentrations in weight %. The initial DIDP concentration in the PVC plastisol paints was 18.7% (28 pphr PVC). The samples indicated with 'a' and 'b' in the table are measurements of different parts of the same coating, this is done in order to evaluate the accuracy of the method. In general the method seems reasonably accurate, the 'a' and 'b' measurements of R13 and B8 are close together, those of P13 have some discrepancy. As expected, the DIDP concentrations in the weathered coatings are lower than the initial value of 18.7%, and in most cases they decrease gradually after progressive weathering. However there are exceptions, like the 2000 hrs horizontal QUV measurement of the S1 shade. These outliers could be caused by the method (P13a and P13b had a difference of 3.6), or by a non-homogeneous distribution of the plasticiser in the coating.

4.2.2 Correlation of Plasticiser Degradation and Gloss Loss.

The loss of plasticiser content has an effect on the gloss value of the coatings. When the plasticiser concentrations decrease and the PVC matrix becomes less flexible, microcracking occurs. Microcracking is the formation of little cracks in the coating. This roughens the surface of the coating and makes it less glossy, so loss of gloss can indicate plasticiser loss in a coating. The measured plasticiser concentrations and the gloss retention values of the yellow-green shades weathered for 1500 and 2000 UV-A hrs in the horizontal QUV machine are given in table 4.1.

Table 4.1 DIDP concentrations and gloss retention values of the yellow-green shades weathered in the horizontal QUV machine.

Horizontal QUV		DIDP concentration		Gloss retention	
		1500 UV-A hrs	2000 UV-A hrs	1500 UV-A hrs	2000 UV-A hrs
Y1	0.5 2-yellow 0.05 green	7.2	2	68.9	77.6
Y2	2 2-yellow 0.2 green	11.6	9.1	93.2	28.7
Y3	5 2-yellow 0.5 green	17.7	17.1	97.6	94.4
Y4	10 2-yellow 1 green	18.4	13	90.1	74.8
Y5	0.5 2-yellow 0.02 green	2.1	1.2	50.9	38.7
Y6	2 2-yellow 0.08 green	14.4	2.9	90.0	52.1
Y7	5 2-yellow 0.2 green	18.5	13.3	101.4	74.6
Y8	10 2-yellow 0.4 green	21.5	10.4	94.4	71.3
Y9	0.25 2-yellow 0.05 green	16.1	1.8	44.2	53.1
Y10	0.5 2-yellow 0.1 green	8.6	3.5	51.9	49.4
Y11	2.5 2-yellow 0.5 green	18.3	1.3	82.0	87.2
Y12	5 2-yellow 1 green	19.3	11.2	97.2	96.1

The 12 yellow green panels are divided in three groups of 4 that have a yellow:green pigment concentration ratio of 10:1 (Y1-Y4), 25:1 (Y5-Y8) and 5:1 (Y9-Y12) respectively.

In the table, it can be seen that the DIDP levels all decrease going from 1500 UV-A hrs to 2000 UV-A hrs. The low concentration yellow-greens have the most plasticiser degradation, whereas in the higher pigment concentration yellow-greens, plasticiser degradation does not take place as much because the plasticiser molecules are shielded by the pigments.

The gloss retention values in the CDPD have never been known for their accuracy, as the gloss can vary substantially on different locations of the same panel. These effects can be caused by the oven that was used to cure the panels not having a homogeneous temperature distribution. In the table, trends are visible though for the gloss values. The majority of the gloss retention values decrease going from 1500 to 2000 UV-A hrs. As with the DIDP concentrations, the lowest gloss retention values are generally found in the low concentration yellow-green shades, such as Y1, Y5, Y9 and Y10.

The DIDP values and the gloss retention values after 1500 and 2000 UV hrs in the ponding machine are plotted together in the scatter plot below. Now the correlation between the gloss retention values and the DIDP levels can be examined. A correlation coefficient of 0.61 was calculated for this set of values (Fig. 4.15), which provides evidence for the earlier mentioned correlation between gloss loss and plasticiser loss, due to microcracking.

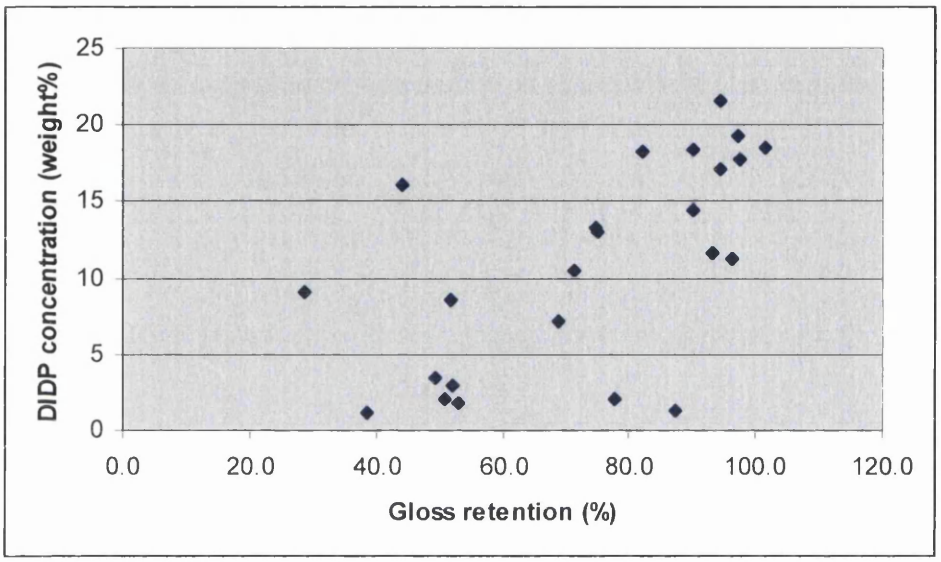

Figure 4.15 Correlation plot for the gloss retention and the DIDP concentration of the yellow-green shades after weathering in the horizontal QUV machine

4.2.3 Correlation of Dehydrochlorination and Plasticiser Degradation

In Figure 4.16 it can be seen that the reflectance spectra of the pigmentless PVC base after accelerated weathering in a QUV-cabinet (subjected to a 8 hrs UV-A / 4 hrs condensation cycle) are lower than that of the PVC base coated before weathering. This PVC base is not protected by any pigment, so dehydrochlorination is likely to take place at a higher rate than in pigmented coatings. The formation of polyenes during dehydrochlorination of the PVC chain is likely to be the reason that the reflectance spectra are lower after weathering. As explained before, the polyenes absorb light in the

visible spectrum, which will make the coatings look darker and lower their reflectance spectra.

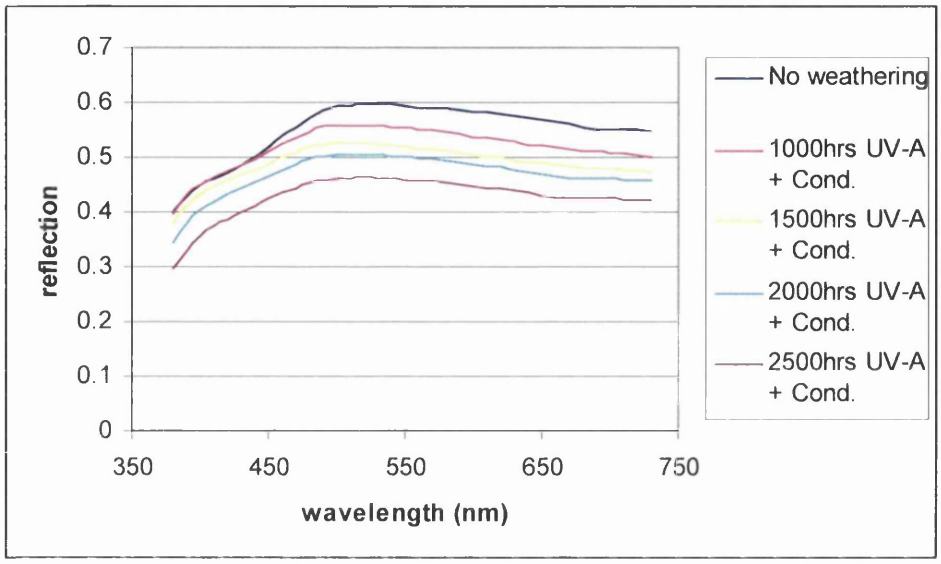

Figure 4.16 Reflectance spectra of base PVC plastisol after progressive weathering

A way of quantifying the level of dehydrochlorination in a coating could be to calculate the Spectrum Surface Integral (SSI). This is defined as the surface under the reflectance spectrum of a weathered sample minus the surface under the reflectance spectrum of an unweathered sample. This way, a negative SSI would indicate that a spectrum has decreased after weathering, and the negative value of the SSI would say something about the polyene content in the plastisol (and about the amount of dehydrochlorination that has taken place in the PVC chain).

Figure 4.17 shows how the SSI is calculated, using the pigmentless PVC base spectra from the previous graph. It is shown here to be the difference between the surface under the spectrum that was taken after 1000 UV hrs with condensation (the yellow line) and that under the spectrum of the unweathered sample (the blue line). The SSI for 1000 UV hrs with condensation is equal to the area between these lines, accentuated with the double headed arrows in the graph:

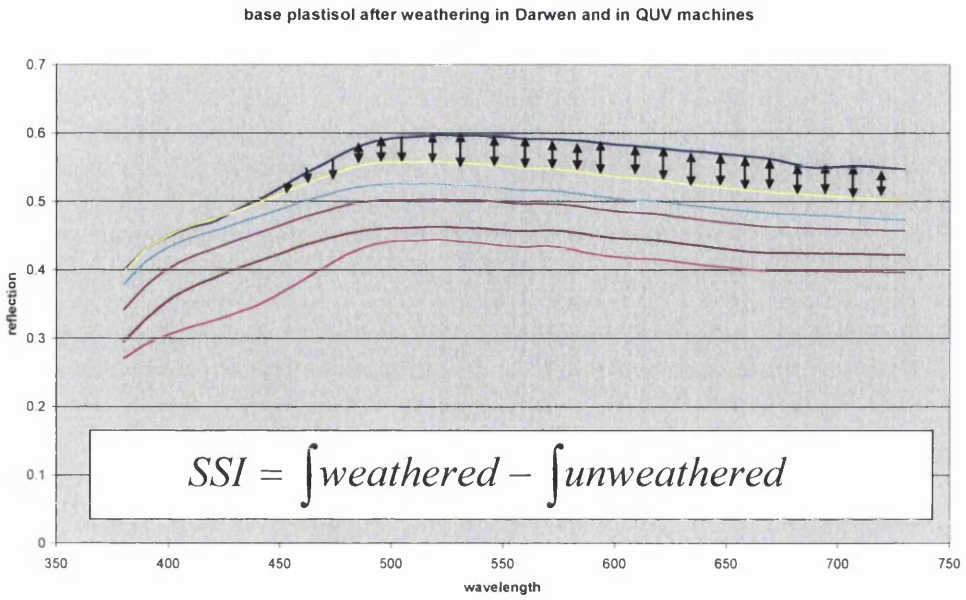

Figure 4.17 The Spectrum Surface Integral (SSI)

The SSI values for the base PVC after 1000, 1500, 2000 and 2500 UV hrs in the QUV machines have been calculated and plotted against the UV exposure time in Figure 4.18.

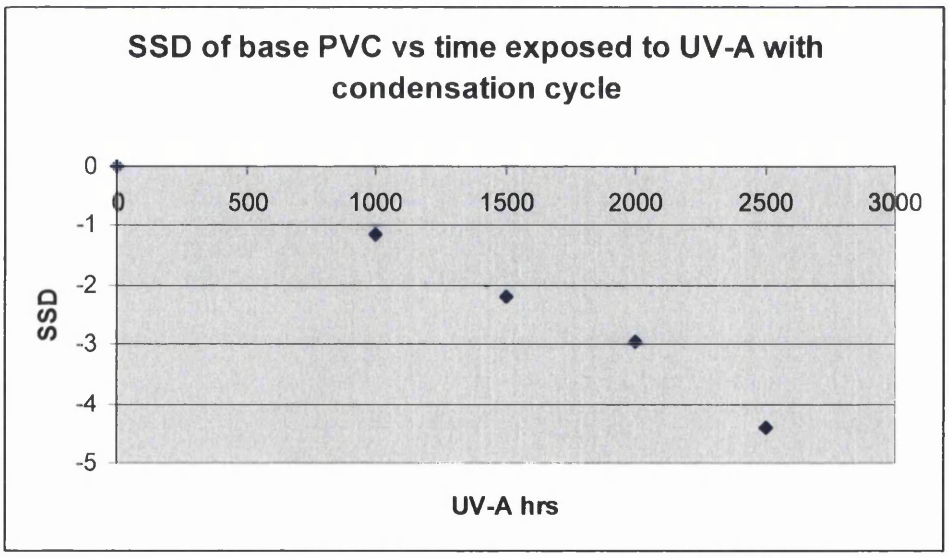

Figure 4.18 Calculated SSI values of base PVC plastisol plotted against the weathering time in UV-A hrs

From this it shows that there seems to be a linear correlation between the rate of darkening of the base PVC and the exposure time in the QUV machine.

The measured platicizer levels of the yellow green panels can also be plotted against the calculated Spectrum Surface Integrals for those panels. This plot would give an indication of the order in which the different processes (plasticiser degradation and PVC dehydrochlorination) take place during weathering and what the influence of the pigment concentration on this is.

In Table 4.2, the measured DIDP concentrations and the calculated SSI values are given of the yellow green shades, together with some single pigment yellow and single pigment green shades and with the pigmentless PVC base.

Table 4.2 DIDP levels and calculated SSI values after weathering

		1500 UV hrs		2000 UV hrs	
		DIDP levels	SSD	DIDP levels	SSD
Y1	0.5 yellow 0.05 green	7.2	-0.796	2	-1.290
Y2	2 yellow 0.2 green	11.6	-0.002	9.1	0.141
Y3	5 yellow 0.5 green	17.7	0.091	17.1	0.111
Y4	10 yellow 1 green	18.4	0.105	13	0.289
Y5	0.5 yellow 0.02 green	2.1	-1.918	1.2	-1.008
Y6	2 yellow 0.08 green	14.4	-0.168	2.9	-0.049
Y7	5 yellow 0.2 green	18.5	0.052	13.3	0.111
Y8	10 yellow 0.4 green	21.5	0.119	10.4	0.353
Y9	0.25 yellow 0.05 green	16.1	-0.651	1.8	-0.693
Y10	0.5 yellow 0.1 green	8.6	-0.806	3.5	-0.832
Y11	2.5 yellow 0.5 green	18.3	0.071	1.3	0.077
Y12	5 yellow 1 green	19.3	0.088	11.2	0.238
	base PVC	13.6	-3.145	8.7	-5.337
	1 yellow	12.9	-1.425	3	-1.837
	2.5 yellow	15.4	-2.795	12.9	-0.873
	0.05 green	14.9	-1.144	7.4	-2.053
	0.1 green	10.9	-0.588	8.3	-0.815

The DIDP levels and the SSI values for the yellow-green shades are plotted in Figure 4.19. For each shade, the point after 1500 UV hrs is connected to that after 2000 UV hrs with a colour that refers to the legend of the plot (in all the cases, the measured DIDP level after 2000 UV hrs is lower than that after 1500 hrs, so for every shade the point corresponding to 2000 UV hrs is positioned to the left of that corresponding to 1500 UV hrs in the graph).

The dotted line gives the trend of the points after 1500 UV hrs of weathering and the solid line gives the trend of the points after 2000 UV hrs.

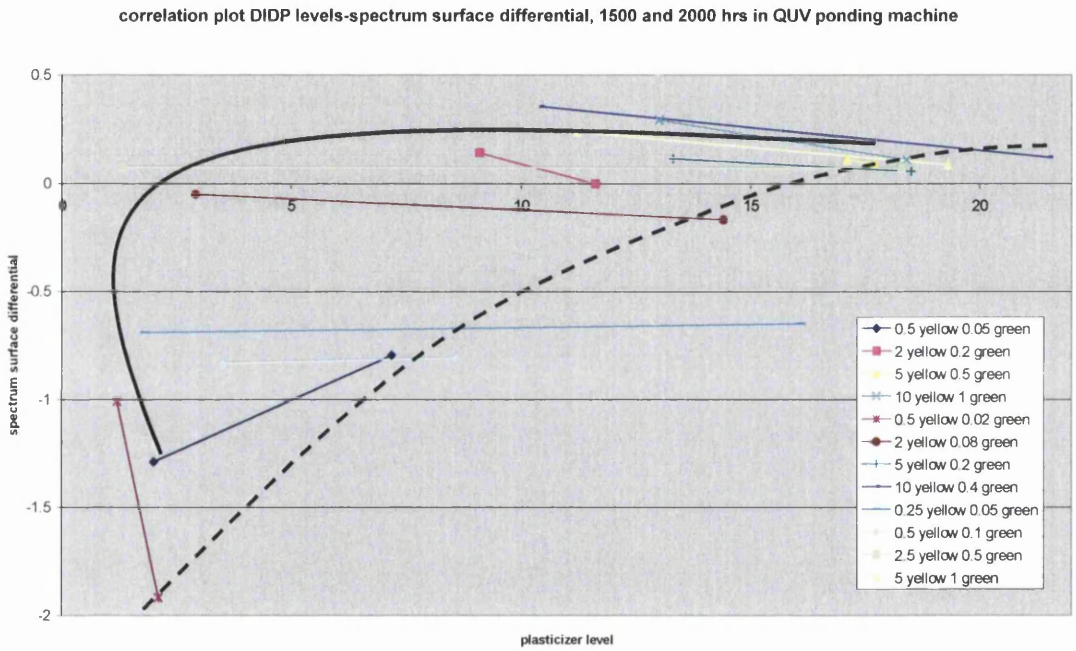

Figure 4.19 Calculated SSI values plotted against the DIDP levels after weathering

In the plot it can be seen that low pigment concentration yellow green-shades (Y1, Y5, Y9 and Y10) show PVC degradation and plasticiser loss simultaneously within 1500 UV-A hrs. High pigment concentration yellow green-shades show no PVC degradation at all, and plasticiser losses are starting to occur mostly after 1500 UV-hrs.

Figure 4.20 gives the same yellow-green shades as the last one, but now the points for two single yellow and two single green pigment shades, and for the base PVC have been

added (because of this addition the vertical axis has a different scale). The added data points are connected with a thicker line than the old yellow-green data points, in order to distinguish them.

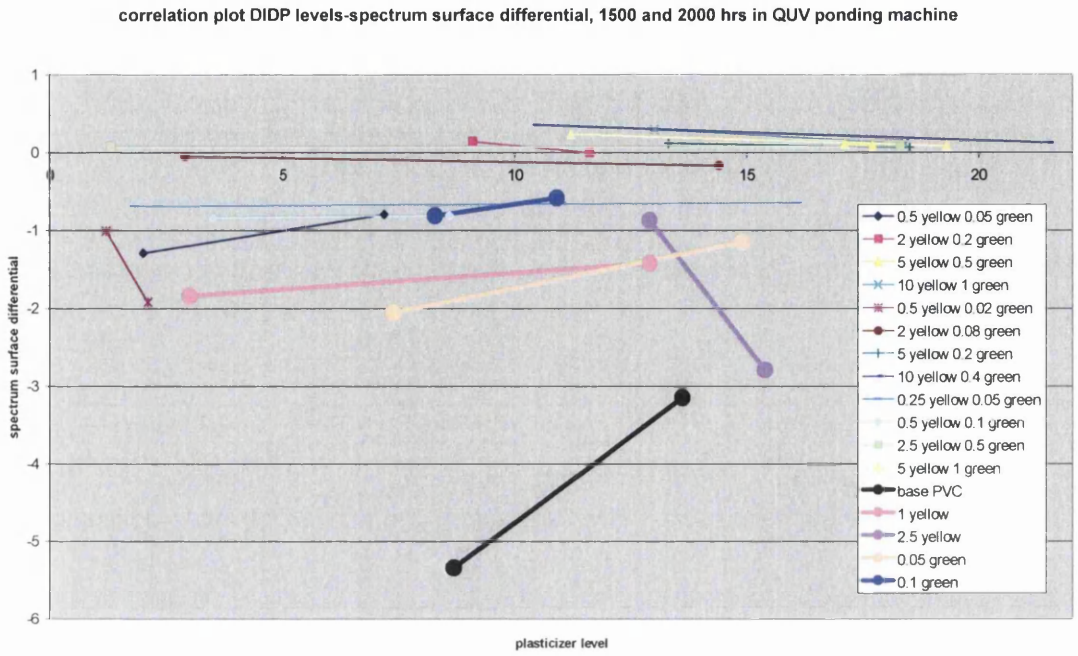

Figure 4.20 SSI/DIDP plot with single pigment shades and pigmentless base PVC datapoints added.

First of all, it strikes the eye that the base PVC has more darkening than any of the pigmented shades (the calculated SSI value is more negative). This indicates that most PVC dehydrochlorination takes place in the PVC base, which makes sense because the PVC base doesn't have any pigment to shield it from irradiation. However, the DIDP levels of the base PVC after weathering have remained higher than those of the low concentration yellow-green shades. So, even though the yellow-green shades are shielded by their pigments, and the base PVC is not, there is more plasticiser degradation in the low concentration yellow-green shades. This could indicate that the photo-degradation of the DIDP plasticiser molecules is enhanced by the inorganic yellow pigment (rutile Cr-Sb-Ti Oxide) that is used in the yellow-green shades. It could be that the relatively small, mobile DIDP plasticiser molecules are photo-catalysed by the inorganic yellow pigment.

This process could be envisioned as a DIDP molecule, being able to move around the PVC matrix because of its small size, coming into contact with an excited Cr-Sb-Ti Oxide surface, after which an energy transfer process takes place from the excited Cr-Sb-Ti Oxide to the DIDP plasticiser. The DIDP molecule now becomes excited, and can react from this excited shade.

This hypothesis is strengthened by the fact that the single pigment 1 pphr yellow shade had a plasticiser content of 3 pphr after 2000 hrs in the ponding machine, while the plasticiser contents of the single pigment green shades stayed above 7 pphr after the same amount of time, like that of the base PVC.

The plasticiser content of the 2.5 pphr yellow shade stays high (12.9 pphr), too, after 2000 UV hrs; this could be because the pigment concentration here is sufficiently high to shield the plasticiser molecules from the irradiation. This would mean that the Cr-Sb-Ti Oxide has two effects in the PVC coating. At low concentrations it can enhance plasticiser degradation by photo-catalysis, and at high concentrations it prevents this from happening by shielding. The very strong deterioration of the yellow-green shades during weathering indicates that the organic green pigment contributes to the high photo-activity of these coatings. The organic green pigment seems to enhance the photo-catalytic activity of the inorganic yellow pigments. This is thought to be done by a process called sensitisation, which means that the organic green absorbs light and then passes the energy on to the inorganic yellow, thus increasing the portion of the sunlight that the inorganic yellow can absorb. This issue has been further explored with some experiments based on dye-sensitized solar cells, which are reported in Chapter 5.

4.3 Infra Red Spectroscopy

Infra Red spectroscopy has been used to investigate the processes that take place in the coatings during weathering further. The principles of this technique and relevant frequencies for this project are given in section 2.7.2. The recorded IR spectra are given in Appendix IV, as are the tables where the sizes of the relevant peaks sizes in these spectra are given.

The peaks that were analysed were at 3400 cm^{-1} (O-H stretch vibration), 2900 cm^{-1} (C-H stretch vibration), 1730 cm^{-1} (C=O) and 1640 cm^{-1} ($HC=CH_2$ located at the end of a chain). This last vibration emerges if chain scission reactions have taken place in the PVC chain to form end-group double bonds. The ratio of this peak and the peak belonging to the C-H stretch vibration is an indication of the amount of PVC dehydrochlorination that has taken place in the coating.

The plasticisers that are present in PVC plastisol contain carbonyl groups, so here the size of the C=O bands tends to be proportionate to the amount of plasticiser that is present in the coating, as the amount of carbonyl groups added by oxidation of the PVC chain is negligible compared to this. When these carbonyl groups are hydrolysed during plasticiser degradation, OH groups are formed. Therefore, the ratio of the O-H peak and the C=O is an indication of the amount of plasticiser degradation that has taken place in the coating. These two ratios are calculated for all the coatings that were investigated with IR spectroscopy, and are shown in Table 4.3.

With the ratios in Table 4.3, for every shade the difference between the O-H/C=O ratio and the $HC=CH_2$/C-H ratio before weathering and after weathering is calculated. These differences are plotted in Figures 4.21 to 4.32. It can be seen in these figures that weathering in the horizontal QUV causes the most change in the calculated differences between the ratios, which means that according to the IR spectra this type of weathering causes the most plasticiser degradation and PVC dehydrochlorination. This is consistent

with the other methods that were used to evaluate the effects of weathering, and the general observations of the strength of weathering in the horizontal QUV machine.

As for the differences between the shades, it seems that the pigmentless base, the yellow-green shades and the low concentration single pigment shades show the most plasticiser degradation and PVC dehydrochlorination with this method, which is again consistent with the earlier observations. On the other hand, some negative values were also calculated for the differences in O-H/C=O and $HC=CH_2$/C-H ratios. This was mainly the case for the base TiO_2 shades, and is probably caused by high O-H/C=O and $HC=CH_2$/C-H ratios for the measured unweathered panels of these shades.

IR spectroscopy seems to be a good technique to use while investigating the weathering of coatings, but it is most useful in combination with other analysis methods.

Table 4.3 The O-H/C=O and HC=CH2/C-H ratios calculated from the IR spectra in Appendix IV

IR absorption peak ratios	0.05 green		0.1 green		0.25 2-yel 0.05 green		0.5 2-yellow 0.02 green	
	O-H/C=O	HC=H2/C-H	O-H/C=O	HC=H2/C-H	O-H/C=O	HC=H2/C-H	O-H/C=O	HC=H2/C-H
unweathered	0.19	0.16	0.16	0.15	0.17	0.14	0.15	0.18
11 months Rye	0.32	0.16	0.28	0.19	0.27	0.22	0.28	0.23
22 months Rye	0.17	0.22	0.19	0.19	0.35	0.25	0.37	0.28
24 months Darwen	0.09	0.23	0.09	0.15				
2000 hrs UVA	0.37	0.20	0.39	0.21	1.07	0.66	0.35	0.23
2000 hrs UVA hor cond	0.28	0.28	0.75	0.53	0.32	0.40	0.63	0.39
2500 hrs UVA cond,	0.24	0.22	0.21	0.25	0.20	0.29	0.27	0.46
	0 TiO2		0.25 2-yellow		1 2-yellow		2.5 2-yellow	
	O-H/C=O	HC=H2/C-H	O-H/C=O	HC=H2/C-H	O-H/C=O	HC=H2/C-H	O-H/C=O	HC=H2/C-H
unweathered	0.20	0.26	0.15	0.13	0.16	0.19	0.14	0.18
11 months Rye	0.34	0.21	0.27	0.19	0.24	0.19	0.23	0.15
22 months Rye	0.23	0.16	0.21	0.20	0.20	0.19	0.22	0.23
24 months Darwen	0.08	0.15	0.11	0.18	0.09	0.18	0.07	0.15
2000 hrs UVA	0.42	0.17	0.38	0.20	0.37	0.17	0.39	0.20
2000 hrs UVA hor cond	0.68	0.64	0.32	0.54	0.28	0.42	1.48	1.67
2500 hrs UVA cond,	0.23	0.17	0.24	0.26	0.24	0.32	0.22	0.36
	1 TiO2		5 TiO2		10 TiO2		15 TiO2	
	O-H/C=O	HC=H2/C-H	O-H/C=O	HC=H2/C-H	O-H/C=O	HC=H2/C-H	O-H/C=O	HC=H2/C-H
unweathered	0.20	0.30	0.20	0.29	0.15	0.30	0.24	0.46
11 months Rye	0.24	0.25	0.27	0.21	0.41	0.31	0.24	0.22
22 months Rye	0.20	0.18	0.15	0.22	0.14	0.16	0.14	0.20
24 months Darwen	0.08	0.15	0.07	0.15	0.07	0.15	0.09	0.15
2000 hrs UVA	0.36	0.28	0.38	0.19	0.39	0.20	0.36	0.19
2000 hrs UVA hor cond	0.31	0.26	0.20	0.28	0.23	0.25	0.35	0.32
2500 hrs UVA cond,	0.18	0.22	0.17	0.24	0.17	0.21	0.26	0.37
	0.25 2-yellow 1 TiO2		1 2-yellow 1 TiO2		0.25 2-yellow 5 TiO2		1 2-yellow 5 TiO2	
	O-H/C=O	HC=H2/C-H	O-H/C=O	HC=H2/C-H	O-H/C=O	HC=H2/C-H	O-H/C=O	HC=H2/C-H
unweathered	0.16	0.15	0.13	0.15	0.16	0.16	0.13	0.14
11 months Rye	0.24	0.15	0.23	0.16	0.18	0.20	0.20	0.16
22 months Rye	0.16	0.11	0.17	0.15	0.23	0.22	0.18	0.16
24 months Darwen	0.08	0.15	0.09	0.15	0.08	0.17	0.09	0.18
2000 hrs UVA	0.33	0.22	0.43	0.19	0.33	0.24	0.47	0.14
2000 hrs UVA hor cond	0.39	0.51	0.24	0.32	0.22	0.30	0.23	0.30
2500 hrs UVA cond,	0.15	0.23	0.24	0.32	0.19	0.31	0.23	0.16

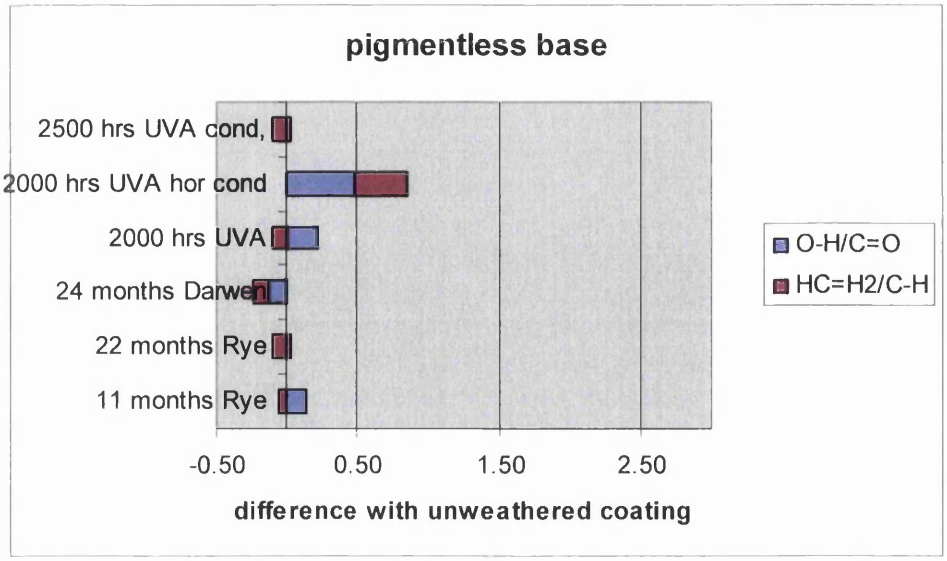

Figure 4.21 The O-H/C=O and HC=H₂/C-H ratios for pigmentless PVC plastisol base

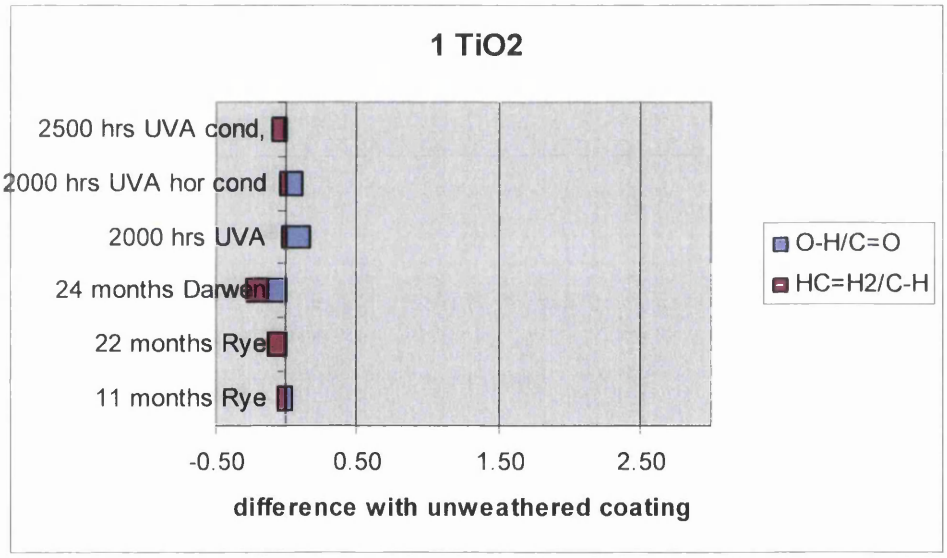

Figure 4.22 The O-H/C=O and HC=H₂/C-H ratios for 1 TiO_2

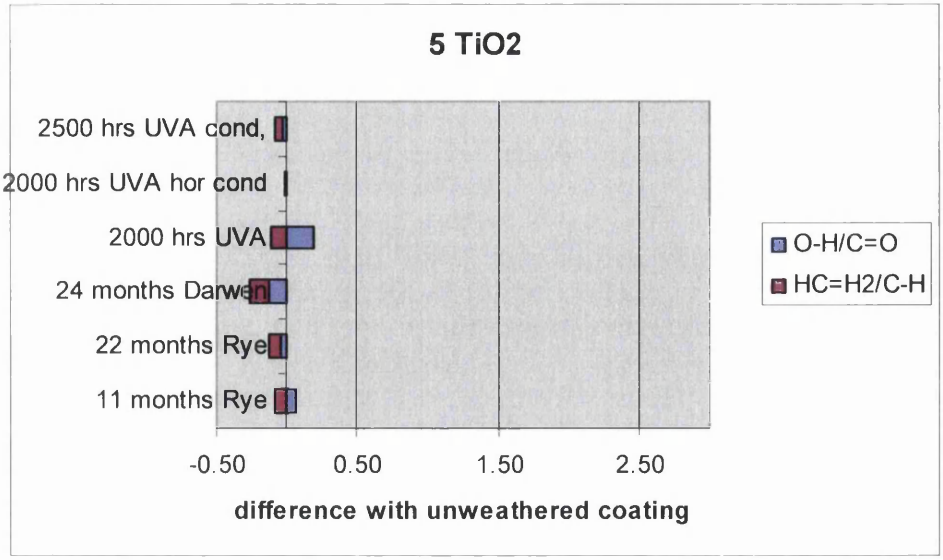

Figure 4.23 The O-H/C=O and HC=H2/C-H ratios for 5 TiO_2

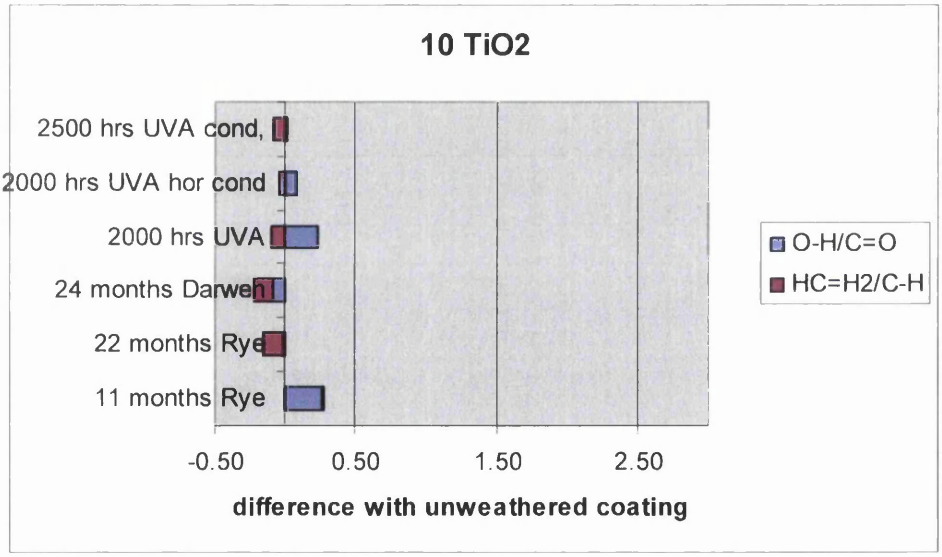

Figure 4.24 The O-H/C=O and HC=H2/C-H ratios for 10 TiO_2

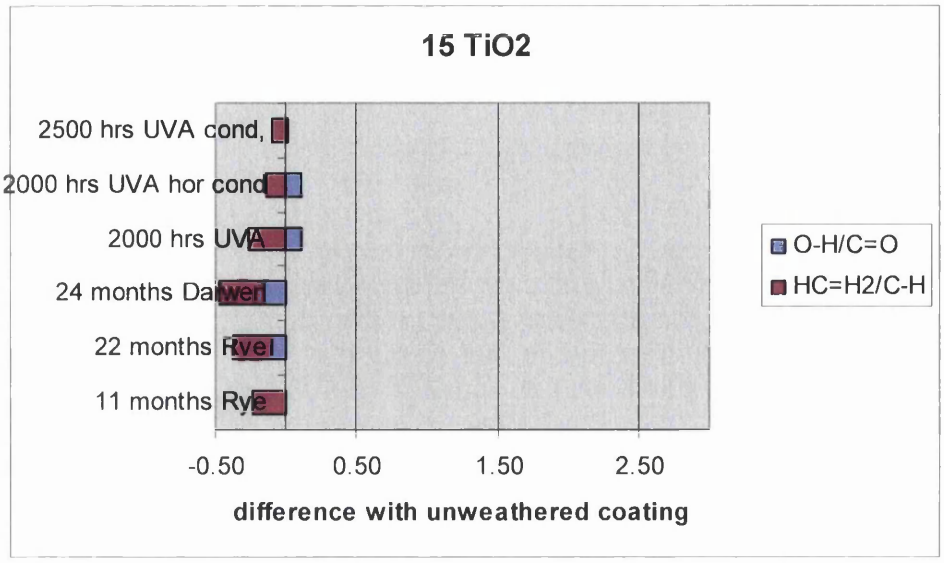

Figure 4.25 The O-H/C=O and HC=H₂/C-H ratios for 15 TiO_2

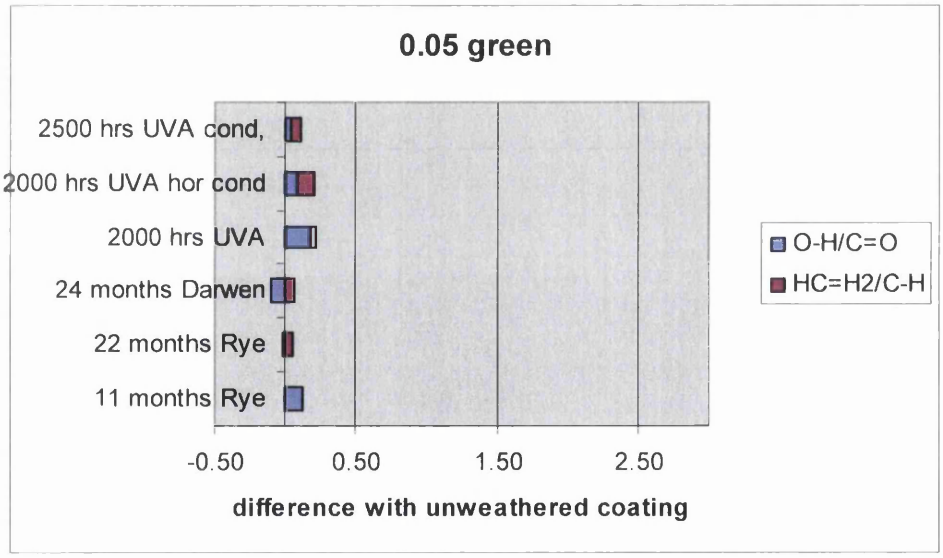

Figure 4.26 The O-H/C=O and HC=H₂/C-H ratios for 0.05 green

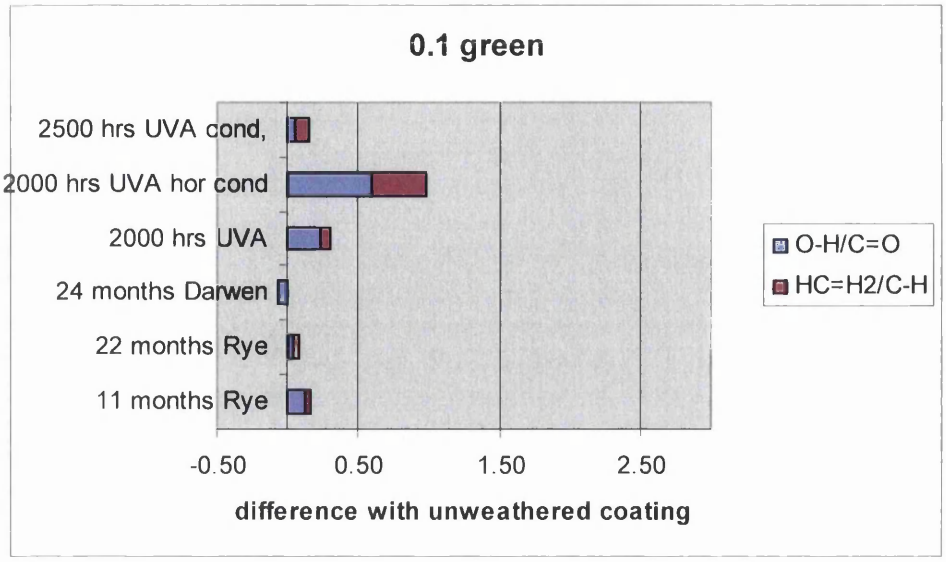

Figure 4.27 The O-H/C=O and HC=H2/C-H ratios for 0.1 green

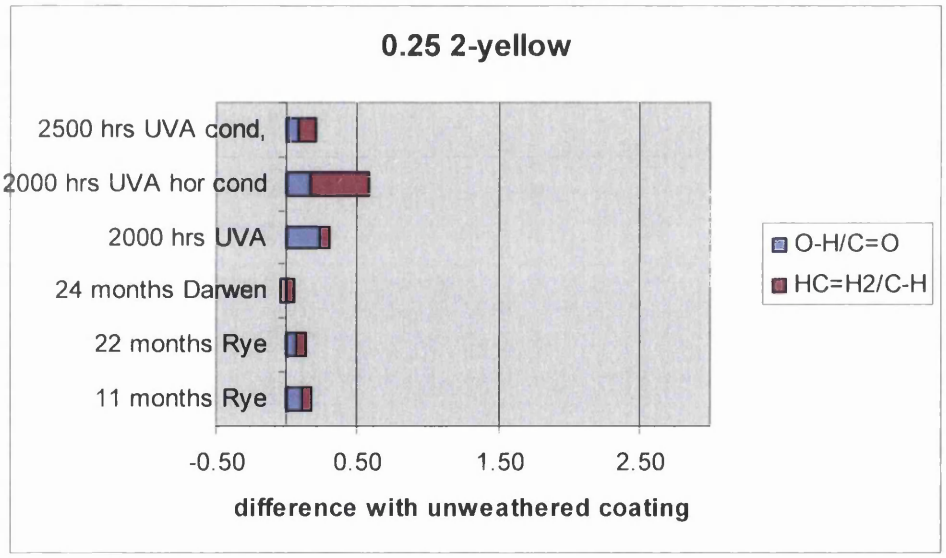

Figure 4.28 The O-H/C=O and HC=H2/C-H ratios for 0.25 2-yellow

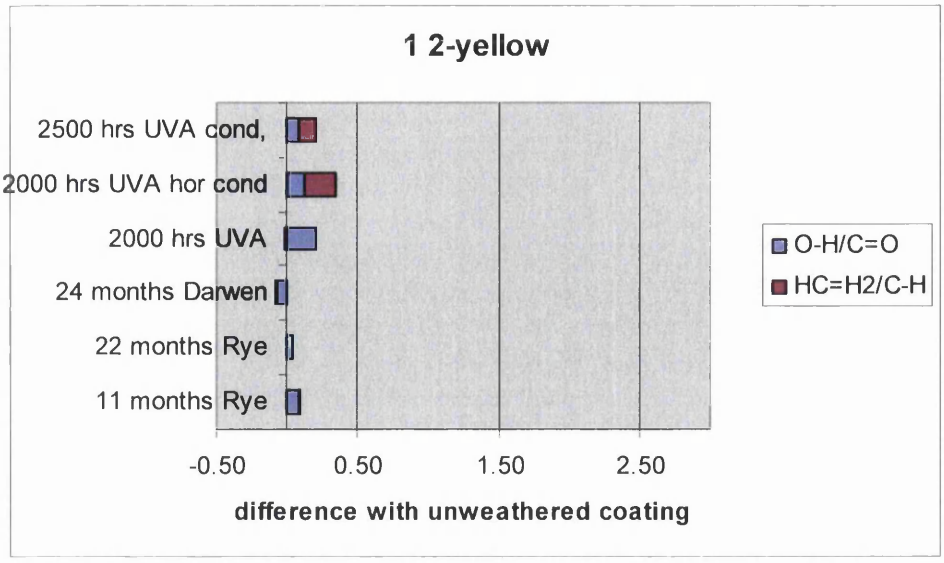

Figure 4.29 The O-H/C=O and HC=H2/C-H ratios for 1 2-yellow

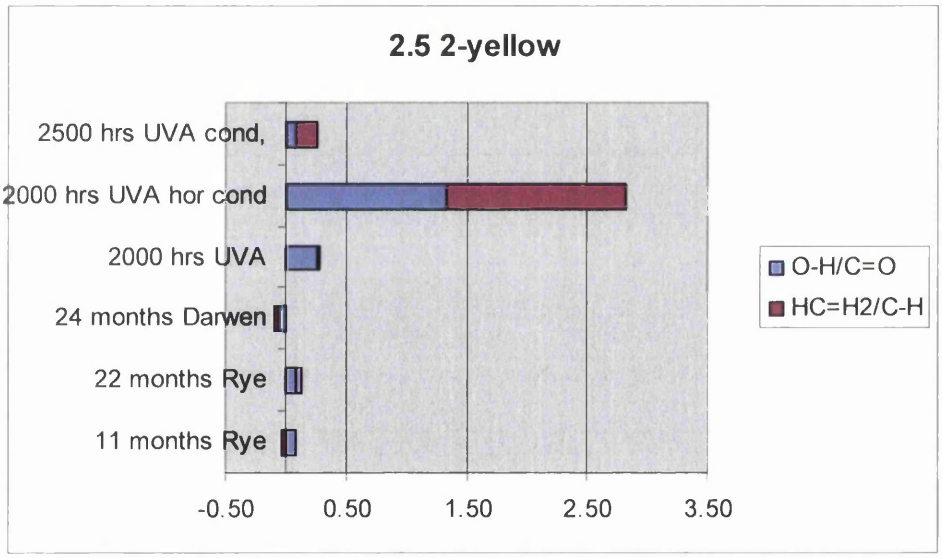

Figure 4.30 The O-H/C=O and HC=H2/C-H ratios for 2.5 2-yellow

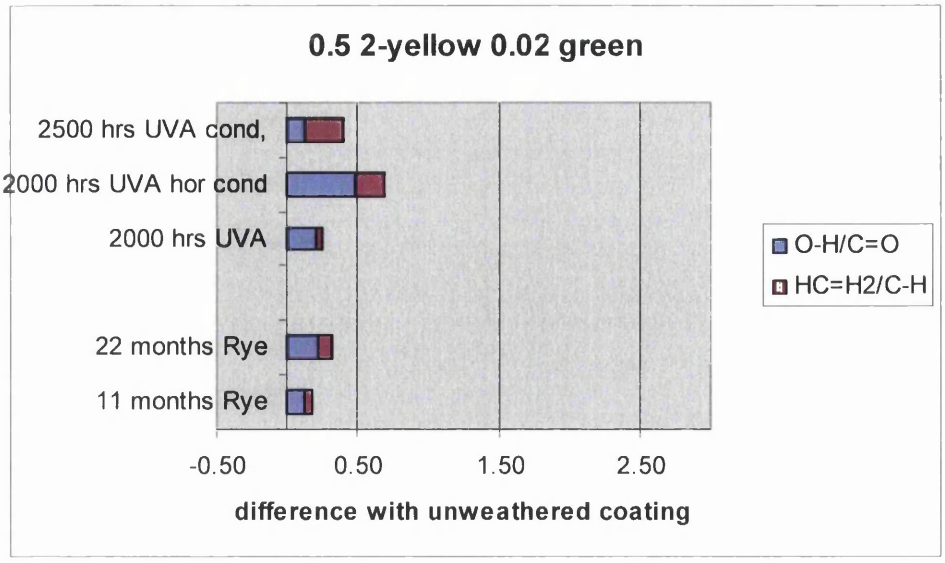

Figure 4.31 The O-H/C=O and HC=H2/C-H ratios for 0.5 2-yellow 0.02 green

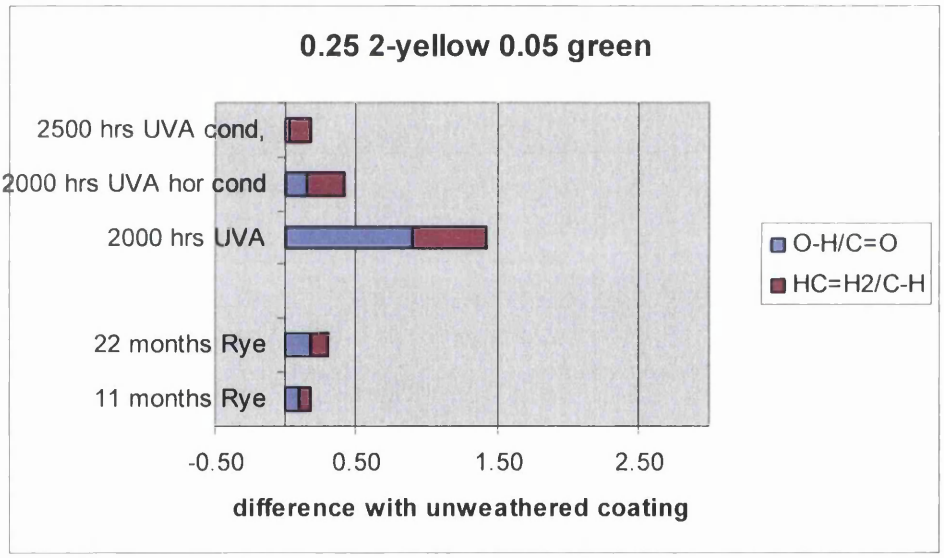

Figure 4.32 The O-H/C=O and HC=H2/C-H ratios for 0.25 2-yellow 0.05 green

4.4 Scanning Electron Microscopy

When the colour changes of coatings were evaluated with reflectance spectrometry, some spectra changed in a way that could not be explained with organic pigment degradation or PVC dehydrochlorination. These spectra generally belonged to shades that contained only inorganic pigments, so pigment degradation was not possible, and they increased after weathering, so this change could not be explained by dehydrochlorination either, because this process decreases the spectrum. Figure 4.33 shows the reflectance spectra of base PVC plastisol with 1 pphr TiO_2 increasing after weathering in the QUV without condensation, after weathering in Rye, and even having been stored in a dark cupboard for two years (the '2 yrs ref' spectrum).

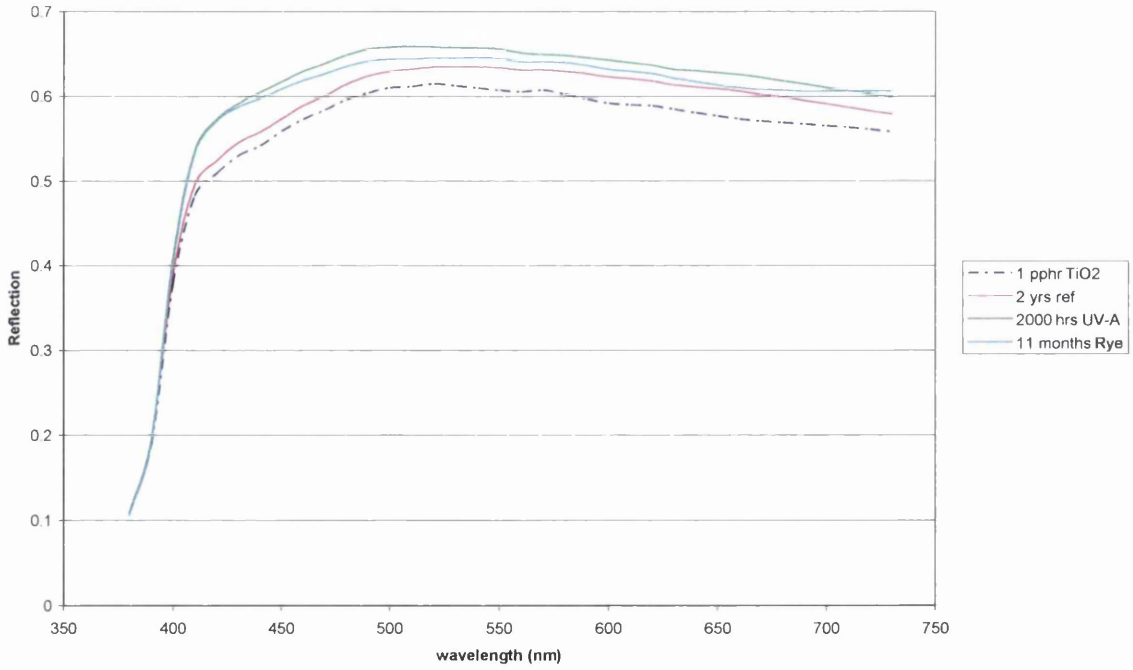

Figure 4.33 Spectra of base with 1 pphr TiO_2

The only way that these changes in the reflectance spectra could be explained was with a process called 'chalking'. This is the breaking down of the resin in the top layer of a

coating during weathering, after which a thin layer of the inorganic pigment can be formed on top of the coating (see section 2.6.5). Chalking (in the case of TiO_2) results in the coating becoming lighter. It is as if more TiO_2 is added to the coating because more TiO_2 particles have become visible as they have migrated to the top of the coating.

Scanning Electron Microscopy (section 2.7.5) was used to investigate this phenomenon, Figure 4.34 gives the scan of the unweathered 1 pphr TiO_2 shade 2 years after drawing (corresponding with the '2 yrs ref' spectrum in Fig. 4.33) and Figure 4.35 gives the scan of this shade after 2000 UV-A hrs in the QUV without condensation. The Back-scattered electron mode was used to pick up the atomic-number contrast between the pigment particles and the base PVC.

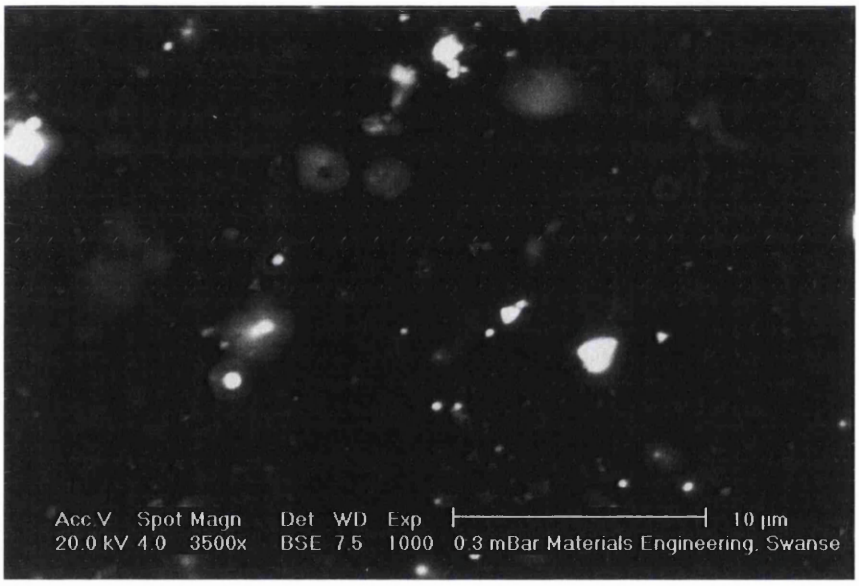

Figure 4.34 Scan of unweathered 1 pphr TiO_2 2 years after drawing of the panel

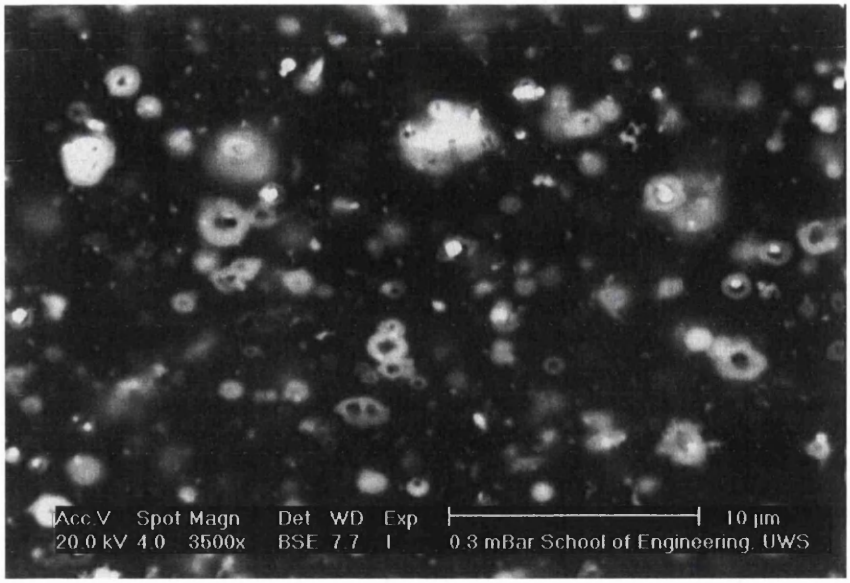

Figure 4.35 Scan of 1 pphr TiO_2 after 2000 UV-A hrs in the QUV without condensation

So, with the use of Scanning Electron Microscopy, it has been established that chalking is a process that can influence the colour of coatings pigmented with inorganic pigments. The effect of chalking on the colour of a coating is that it makes the coating look like the concentration of the inorganic pigment in it has increased, because its particles have migrated to the surface of the coating.

5 MODELLING OF REFLECTANCE SPECTRA

The amount of data (reflectance spectra, gloss values) that has been generated is so big that there is a need to focus on certain aspects of weathering, because the amount of time that available for analysis has been limited. It is also important to take into account the general difficulties that are associated with predicting the service lives of coating systems, as is pointed out in the review by Martin, Saunders, Floyd and Wineburg [57]. First of all, no study has ever found outdoor weathering itself is reproducible, even if specimens are exposed for the same period at the same time of the year, but starting in different years [90]. The weather is an enormously complicated system which does not display any cyclical patterns over any timescale [91].

Not surprisingly, no laboratory-based experimental procedure has consistently produced a high correlation with long term outdoor weathering results [92, 93].And on top of that, the variability in the loss-of-appearance characteristics of nominally identical coated panels that are subjected to identical weathering can be considerable [94]. This is due to the fact that variables regarding manufacturing, processing and application of coatings are not controlled or controllable [57].

The chosen approach here is, as explained in Chapter 3, to quantify the weathering that the coatings are subjected to in terms of the accumulated amounts of UV irradiation per square meter that the coatings absorb. This was done as it is thought that UV irradiation is the dominant weathering factor in loss-of-appearance processes that take place in coatings [57]. The ultimate goal of this research is to predict the ways in which colours of pigmented coatings change during both natural and accelerated weathering. Given the poor success rate of previous attempts, this goal may seem very ambitious. However, it is thought that when colours are measured with reflectance spectrometry, the colour changes can be correlated to chemical processes that take place in the coating during weathering, so that the correlations between natural and accelerated weathering can be investigated better

5.1 Modelling Reflectance Spectra

As stated in section 2.6.5, three phenomena have been identified that take place in a coating during weathering and that can change the colour of a coating; PVC dehydrochlorination, organic pigment degradation and chalking. It is proposed here that these three effects are separable. In this modelling exercise, it is attempted to explain the change of the reflectance spectra during weathering by estimating the relative amounts in which the three identified weathering processes take place.

5.1.1 Modelling of Dehydrochlorination

PVC dehydrochlorination, the formation of polyenes while HCl is released (see Chapter 2 for details) is best evaluated by examining the reflectance spectra of clear pigmentless PVC plastisol base before and after weathering (Fig. 5.1).

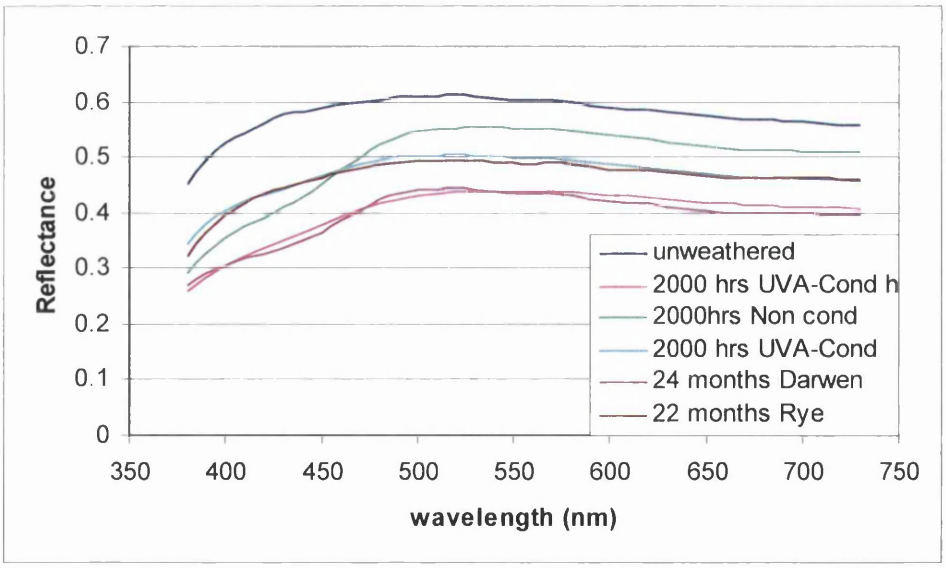

Fig. 5.1 Reflectance spectra of pigmentless PVC plastisol base after exposure to different types of weathering.

As can be seen in Figure 5.1, the reflectance spectra all decrease after weathering, as the polyenes that are formed by dehydrochlorination absorb light. If one takes a closer look, the way in which the spectra change is different for each type of weathering, which is thought to be a consequence of the characteristics of each particular type of weathering.

The change of the spectra due to dehydrochlorination seen here is very large, as there is no pigment present at all to protect the PVC plastisol. It is proposed that dehydrochlorination will take place in pigmented coatings when exposed to a certain type of weathering, in a way which is the same as for this pigmentless coating when exposed to the same weathering type, but to a lesser extent because of the protection offered by the pigmentation. It is attempted here to model the change of the spectrum of a shade due to dehydrochlorination by introducing a dehydrochlorination vector that we will call A, which belongs to a type of weathering. This vector is a set of 36 values (380 to 730 nm with intervals of 10 nm), every variable in this vector is obtained by calculating the difference between the reflectance spectrum of the weathered base and that of the unweathered base, and divide this number by the reflectance spectrum of the unweathered base. This is done for every one of the 36 values that a spectrum consists of to obtain the 36 variable vector:

$$A = (Rbase_{weathered} - Rbase_{unweathered}) / Rbase_{unweathered}$$

The vectors for the different types of weathering are calculated and plotted in Figure 5.2.

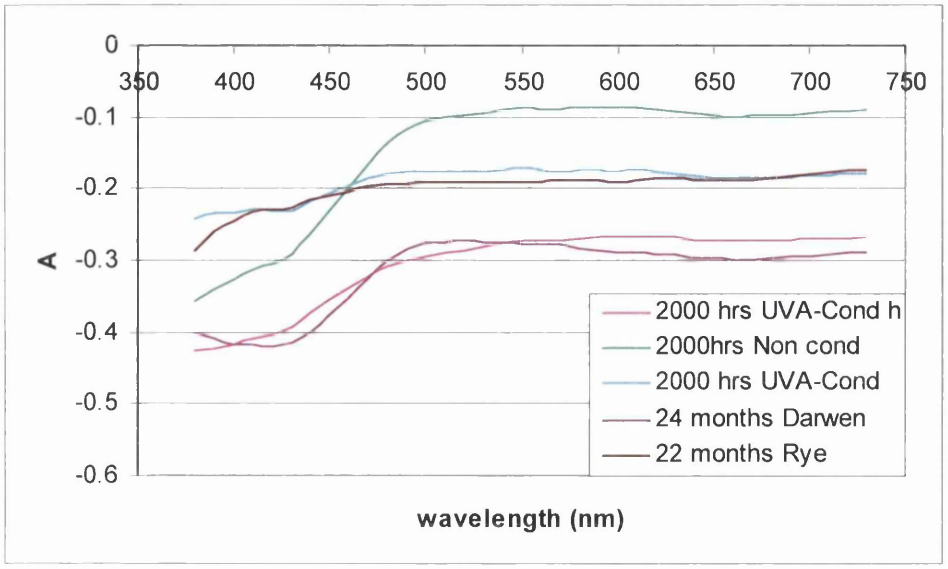

Figure 5.2 The calculated dehydrochlorination vectors A for the different types of weathering.

Now with this vector, the relative amount of dehydrochlorination (the dehydrochlorination variable a) of a weathered panel can be calculated by solving the following equation:

$$R_{weathered} = R_{unweathered} * (1+a*A)$$

$R_{weathered}$ and $R_{unweathered}$ (the reflectance spectra of the panel before and after weathering), and the dehydrochlorination vector A for the type of weathering that the panel has been subjected to have to be known, in order to calculate the dehydrochlorination variable a. This calculation is done with a trial and error method, by using the SOLVER function in Microsoft Excel.

5.1.2 Modelling of Organic Pigment Loss

Another vector needs to be defined to account for the change in the reflectance spectra of coatings due to organic pigment degradation. In order to do that, let's take a look at the

reflectance spectra of PVC plastisol pigmented with different concentrations of the organic blue pigment (Fig. 5.3).

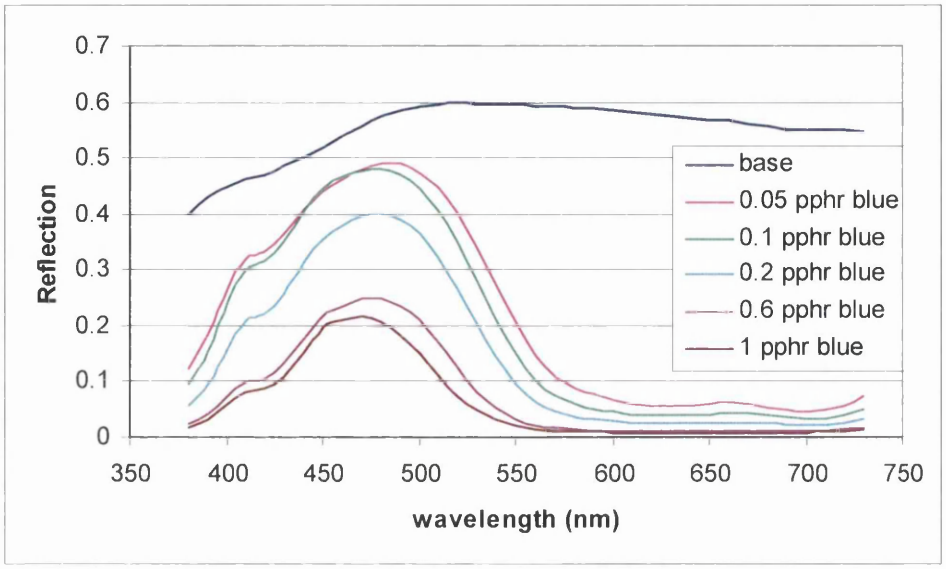

Figure 5.3 Reflectance spectra of PVC plastisol containing different concentrations of blue pigment.

As has been explained in section 2.6.3, pigments obtain their colour by absorbing more light at certain wavelengths than at others, and in the case of reds and yellows sometimes reflecting more light than they absorb at the long wavelength end of the spectrum, due to fluorescence effects. Here it can be seen that a high concentration of the blue pigment will result in a low reflectance spectrum, giving a dark colour. The lower the concentration of the organic blue gets, the higher the reflectance spectrum becomes and the lighter the colour. If organic pigments are involved in degradation reactions, the pigment concentration in a coating decreases, so in the case of the organic blue pigment the reflectance spectrum will get higher.

In general a lower pigment concentration will bring the reflectance spectrum closer to that of the pigmentless plastisol base. This leads to propose the definition of the organic pigment loss vector B to be as follows:

$B = (R_{base} - R_{pigmented}) / R_{base}$

This is based on the rationale that, when the difference between the reflection of the pigmented coating and that of the base coating is large at a certain wavelength, a decrease in pigment concentration (due to organic pigment loss) in the pigmented coating will have more impact at this particular wavelength. This can be seen in Figure 5.4, where the calculated B values have the highest negative value for the highest concentration of the blue pigment.

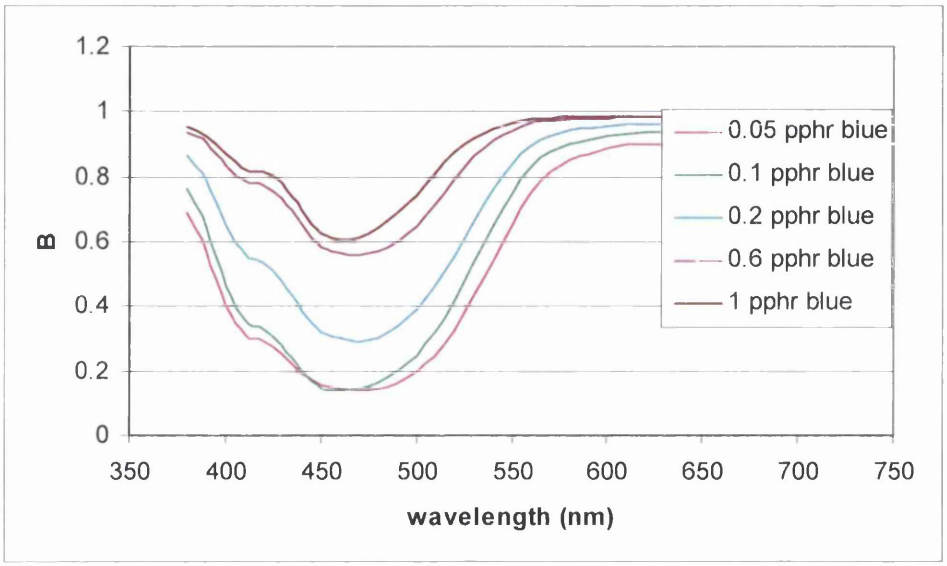

Figure 5.4 The organic pigment loss vector B for the blue pigment at different concentrations.

To clarify the fluorescence-issue with yellow and red pigments, the organic pigment loss vector B is calculated for the investigated organic red pigment. The reflectance spectra are given in Figure 5.5 and the B-vectors in Figure 5.6.

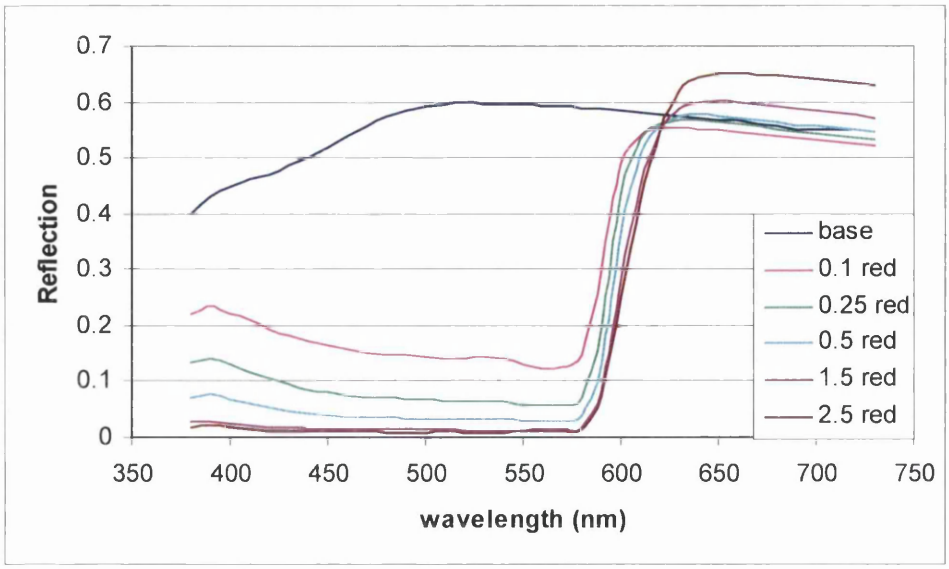

Figure 5.5 The reflectance spectra of PVC plastisol containing different concentrations of red pigment.

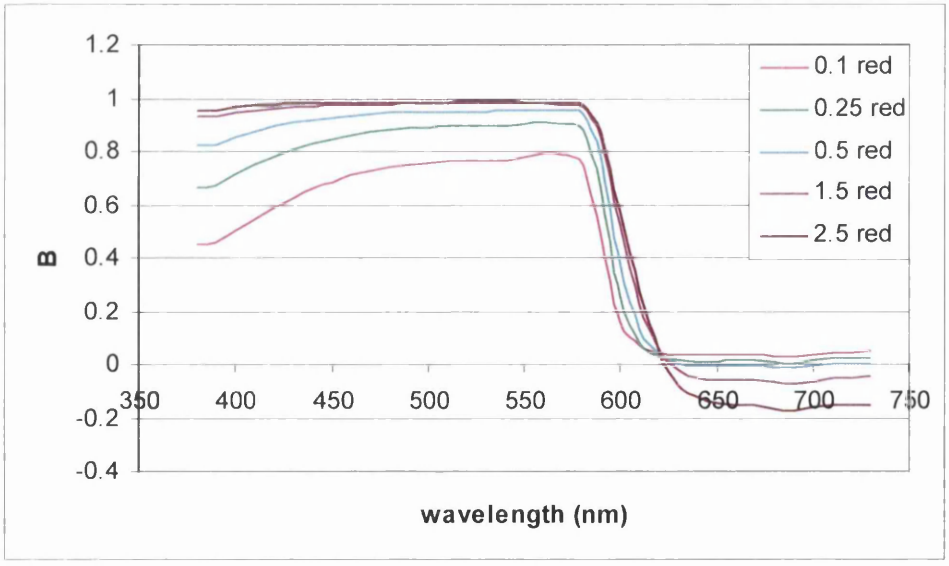

Figure 5.6 The organic pigment loss vectors B for different concentrations of the red pigment.

As can be seen in Figure 5.6, the organic pigment loss B at long wavelengths is negative for high concentrations of the red pigment, so this means that if there is red pigment loss the reflectance values at these wavelengths will decrease (in order to come closer to the spectrum of the pigmentless base).

Now that the organic pigment loss vector is defined, the relative amount of organic pigment loss (the organic pigment loss variable b) of a weathered panel together with the dehydrochlorination variable (a) can be calculated by solving the following equation by using the SOLVER function in Microsoft Excel.

$$R_{weathered} = R_{unweathered} * (1+a*A) * (1+b*B)$$

5.1.3 Modelling of Chalking

A third effect that influences the colour of a coating is chalking. This is the migration of inorganic pigment particles to the surface of the coating, which makes it seem like there is an increase in the concentration of the inorganic pigment. In Figure 5.7 the reflectance spectra of the base with different concentrations of titanium dioxide are given

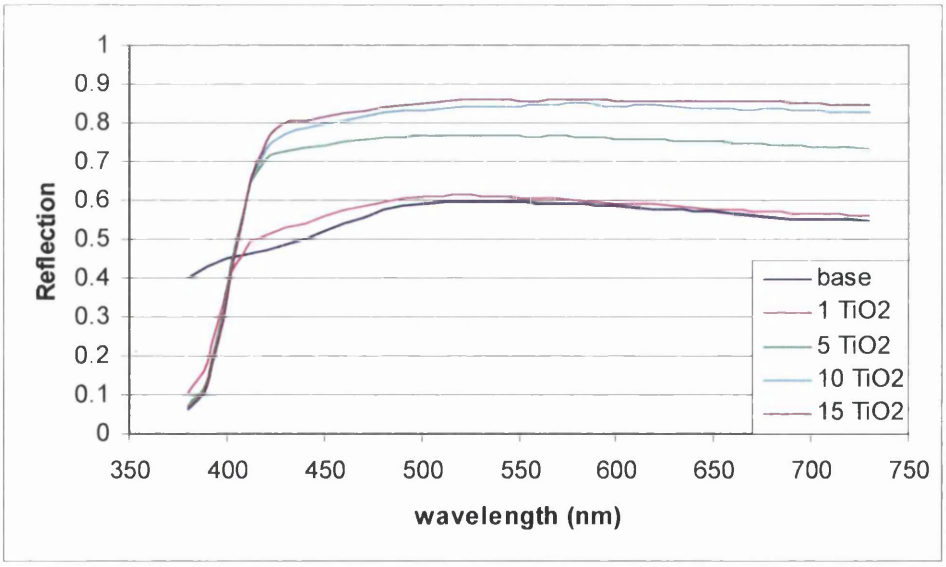

Figure 5.7 The reflectance spectra of PVC plastisol base with different concentrations of titanium dioxide.

Because the chalking effect increases the perceived pigment concentration in the coating, the chalking vector C is defined as follows:

$$C = (R_{TiO2} - R_{base}) / R_{base}$$

The chalking vectors C were calculated for the different titanium dioxide concentrations, and plotted in Figure 5.8:

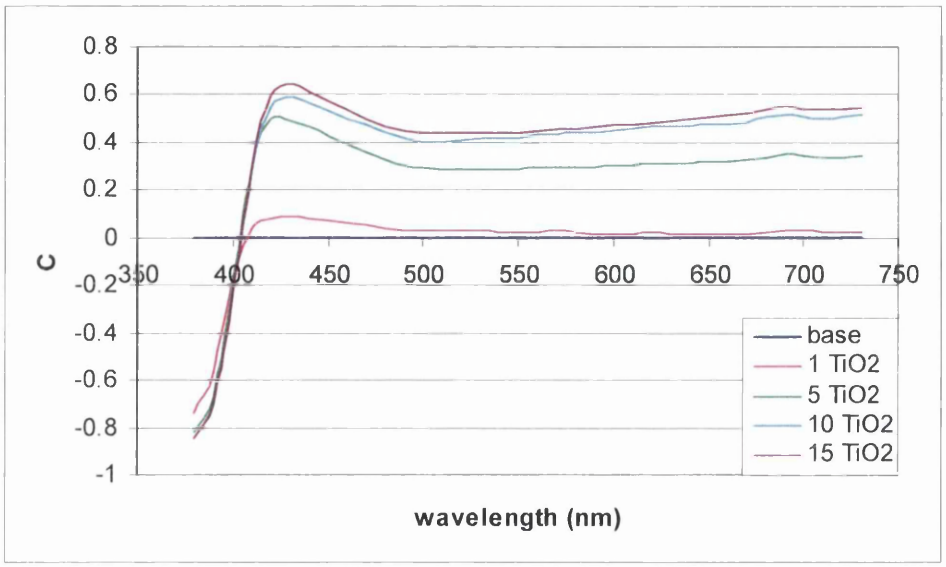

Figure 5.8 The calculated chalking vectors

So now that all three vectors are defined, the relative amount of chalking (the chalking variable c), that of organic pigment loss (the organic pigment loss variable b) and that of dehydrochlorination (the dehydrochlorination variable a) of a weathered panel can be calculated by solving the following equation by using the SOLVER function in Microsoft Excel:

$$R_{weathered} = R_{unweathered} * (1+a*A) * (1+b*B) * (1+c*C)$$

The spectrum of the weathered panel, that of the unweathered panel, and the vectors A, B and C are known.

5.2 Modelling Results Matched with Measurements

The model introduced in the previous section has been applied to all the spectra that were obtained after natural weathering in Darwen and Rye and after the three types of accelerated weathering. Some examples of how successful this was are given in the Figures 5.9 and 5.10. In the Figures it can be seen that the modelled spectra match the real spectra of the weathered green shade very well; the modelled spectra are almost superimposed on the real ones.

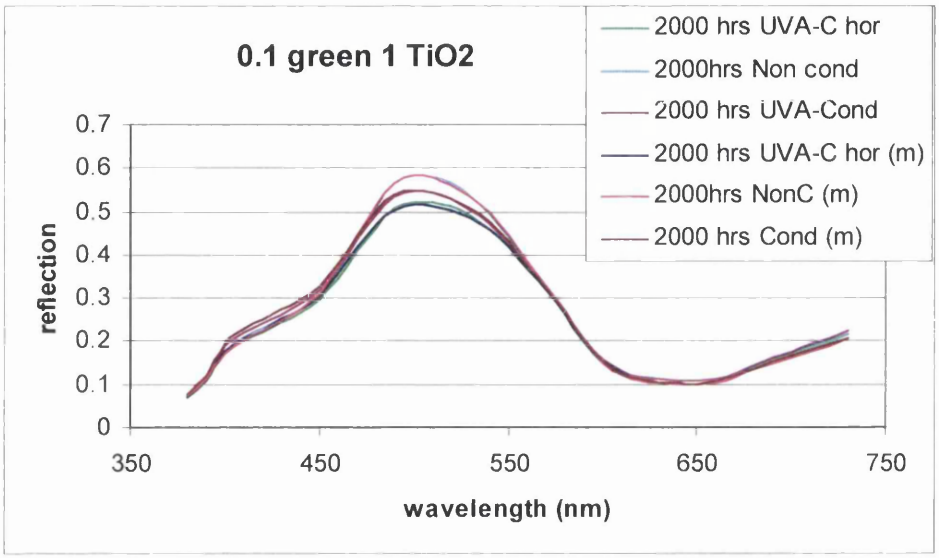

Figure 5.9 The measured and the modelled (m) spectra for 0.1 green 1 TiO_2 weathered in the QUV

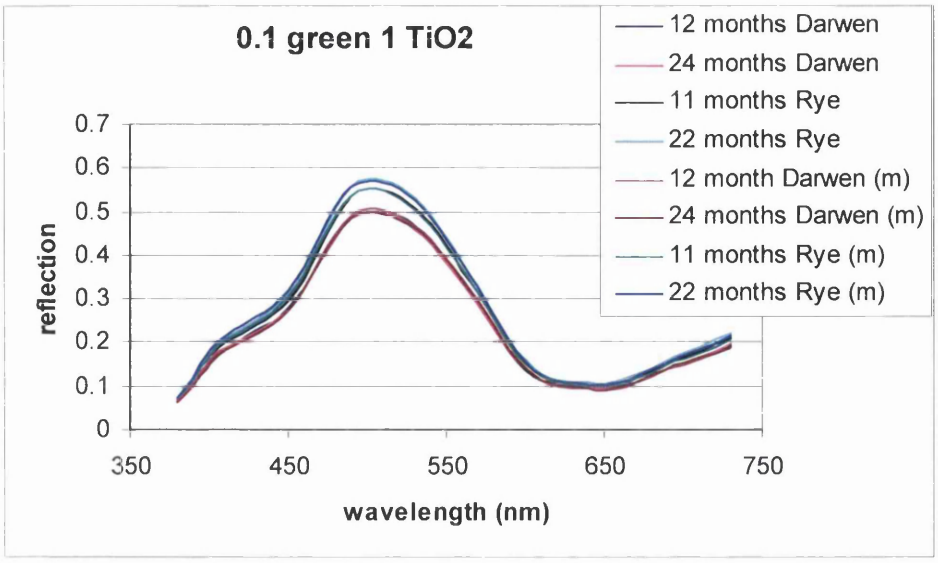

Figure 5.10 The measured and the modelled (m) spectra for 0.1 green 1 TiO_2 weathered in Darwen and Rye

In Table 5.1, the values for a, b and c that belong to the modelled spectra shown in Figure 5.9 and 5.10 are given:

Table 5.1 The a b and c coefficients for the modelled spectra of 0.1 green 1 TiO_2

	a	b	c
2000 hrs UVA-C hor (m)	0.2938	0.6482	0.0000
2000hrs UVA (m)	0.0629	0.3681	0.0000
2000 hrs UVA-C (m)	0.2222	0.7577	0.0000
12 month Darwen (m)	0.2179	0.7230	0.0000
24 months Darwen (m)	0.2757	0.8112	0.0000
11 months Rye (m)	0.1470	0.5728	0.0000
22 months Rye (m)	0.1656	0.4144	0.0085

With the values of the coefficients some observations can be made. The b coefficient indicates organic pigment degradation and is high for weathering in the horizontal QUV, weathering in the normal QUV and weathering at Darwen. The a coefficient, which stands for dehydrochlorination, is high for the same types, and has the highest value after 24 months in rainy Darwen. The c coefficient, corresponding with chalking, is zero for all

weathering types except for 22 months exposure in Rye, the highest UV region in the UK.

Like the green shades shown in Figure 5.9 and 5.10, the other shades in the CDPD generally showed a good match between the measured reflectance spectra of the weathered panels and the modelled reflectance spectra.

5.3 Correlating Natural and Accelerated Weathering with the ABC Model

What has been done in this section is the following: The a, b and c values were multiplied by 100 so that they were expressed as a percentage rather than a fraction. These values have been divided by the estimated amount of irradiation energy (in MJ) that the coatings had been exposed to up to the time that the measurement was taken for that particular type of weathering. Now that the a, b and c values were corrected for different amounts of UV exposure, the median of the available values was taken for every type of weathering, for every shade. Measurements that were judged as unreliable (see section 3.3.2) were excluded from these calculations of the median values. The median values of the a, b and c coefficients of a shade calculated for one type of weathering could now be plotted against those calculated for another type, in order to investigate the correlation between the weathering types. These plots for the correlations of accelerated weathering in the normal QUV (C) with weathering in Darwen (D) and Rye (R) green pigment shades are given in Figures 5.11 to 5.16.

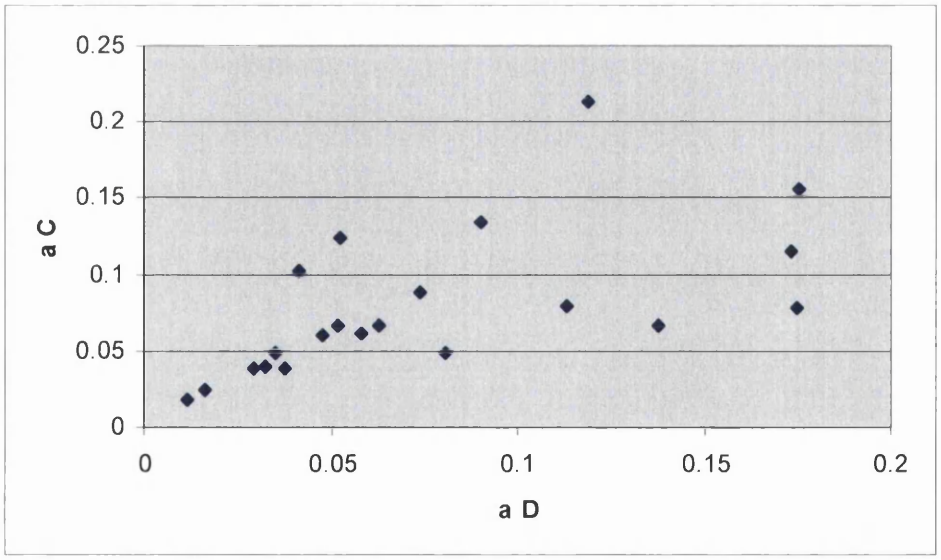

Figure 5.11 Correlations of the a coefficients of the green shades after weathering in Darwen (D) and in the QUV with condensation (C)

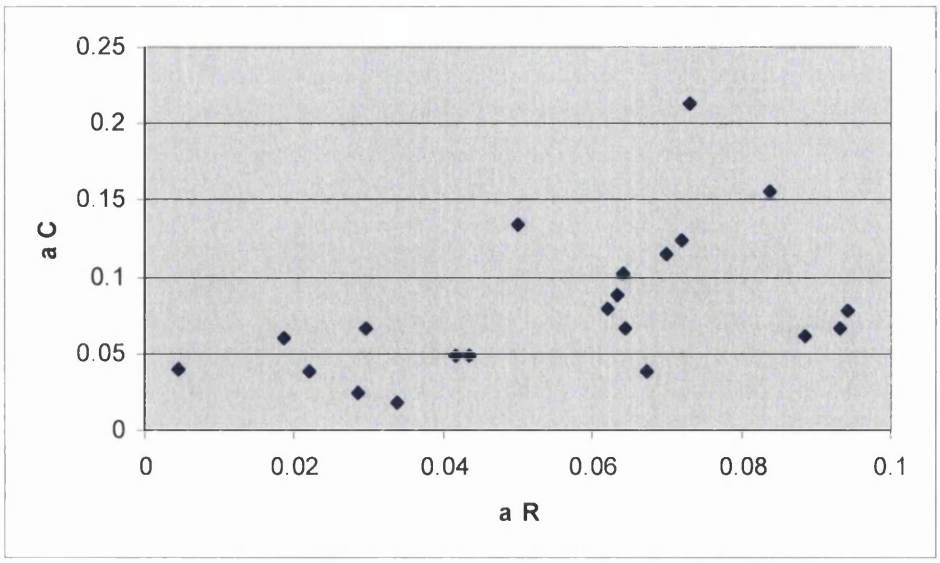

Figure 5.12 Correlations of the a coefficients of the green shades after weathering in Rye (R) and in the QUV with condensation (C)

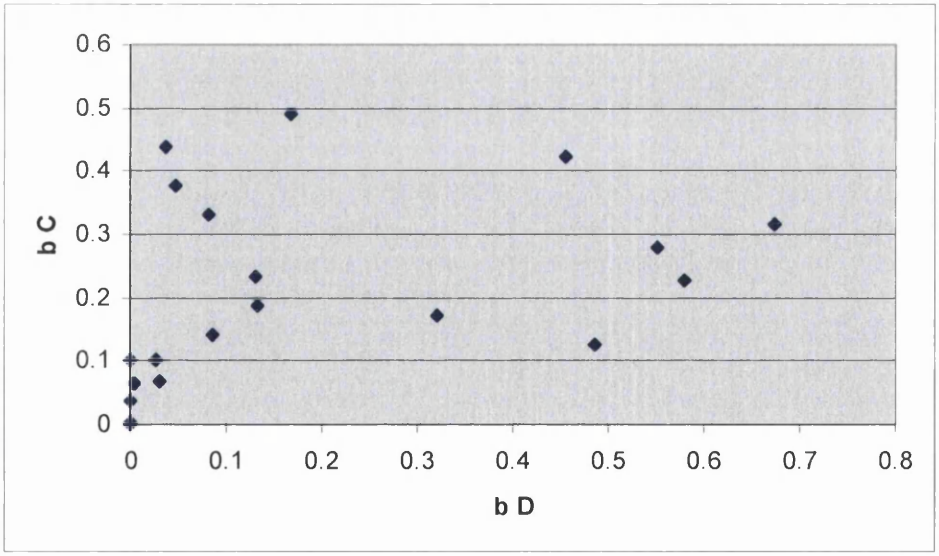

Figure 5.13 Correlations of the b coefficients of the green shades after weathering in Darwen (D) and in the QUV with condensation (C)

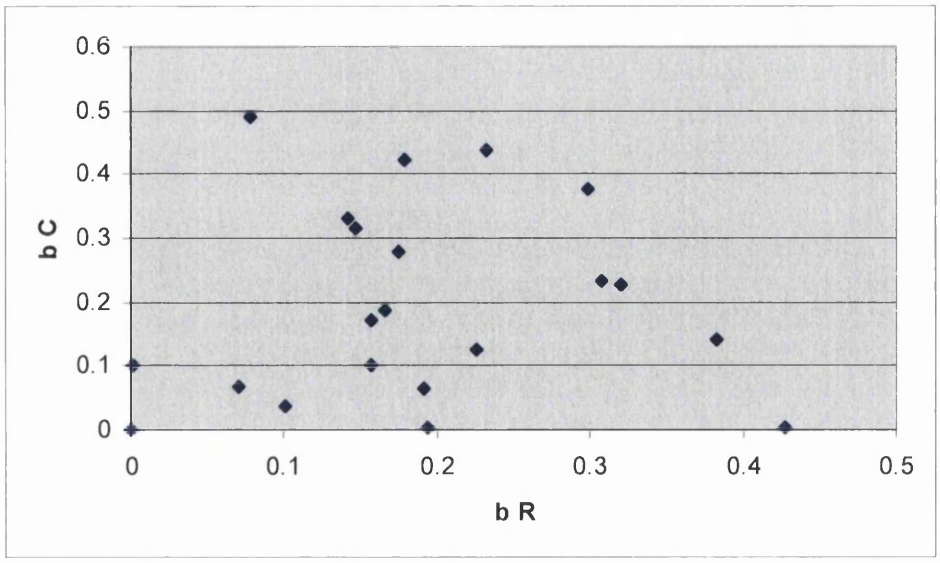

Figure 5.14 Correlations of the b coefficients of the green shades after weathering in Rye (R) and in the QUV with condensation (C)

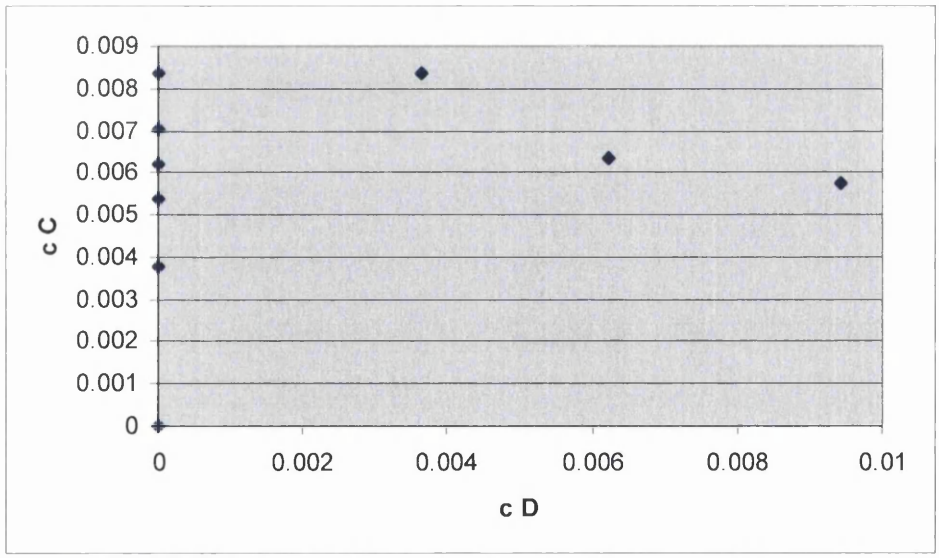

Figure 5.15 Correlations of the c coefficients of the green shades after weathering in Darwen (D) and in the QUV with condensation (C)

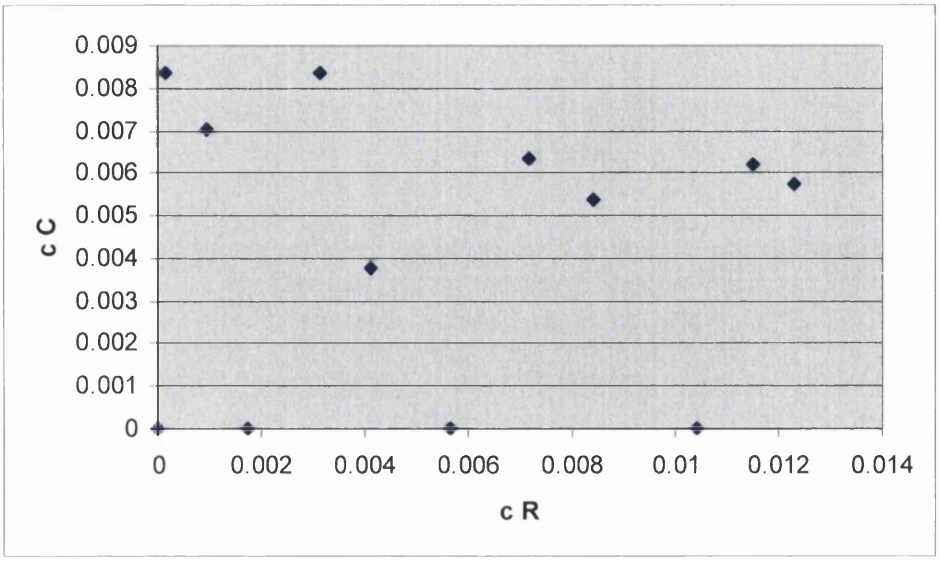

Figure 5.16 Correlations of the c coefficients of the green shades after weathering in Rye (R) and in the QUV with condensation (C)

For natural weathering in Darwen and Rye the coefficients that were plotted here were corrected with the irradiation energies calculated for a solar altitude angle of 30°, because these values matched those for accelerated weathering better than when they were calculated with the 1° solar altitude angle model.

Some observations can be made from these plots: The correlation of the calculated 'a' coefficients after weathering in Rye and QUV weathering is reasonable, and that of weathering in Darwen and QUV weathering seems to be good.

The correlations of the 'b' coefficients are reasonable. In the plot of Figure 5.13 there seem to be two different trends. This could be a differentiation between low and high pigment concentrations. The correlations of the 'c' coefficients are not good, especially those of weathering in Darwen with QUV (Fig. 5.15).

The correlations found for other shades using this method were sometimes good, and sometimes not so good. It seems that this method has potential to become a useful tool to compare different types of weathering while separating the effects that the different types of weathering have on the colours (reflectance spectra) of the shades. One thing that could be done is to re-define the vectors A, B and C that were introduced in section 5.1 to

see if the correlations improve. Especially vector B, which is related to the colour change caused by organic pigment degradation, seems to have scope for improvement (the definition of vector B that has been proposed here was the most successful out of a number of different possibilities that were tried out).

This modelling is a trial-and-error process, and unfortunately in this EngD project there was not enough time to investigate this any further.

6 PHOTO-ACTIVITY MEASUREMENTS OF PIGMENTED PVC COATINGS USING THE DYE SOLAR CELL PRINCIPLE.

As an intermezzo from all the pigmented coatings, colour measurements and weathering processes, some research was conducted into the possibilities of evaluating the photo-activity of thin pigmented PVC layers using photo-electrochemistry. The connection to this research project is that the photo-activity of a pigmented PVC layer is correlated to its weatherability: If a coating is photo-active, it generates a high number of excited electrons under irradiation. In terms of weatherability, a high number of excited electrons mean that degradation reactions are likely to take place in the coatings.

The approach of this investigation was to measure the photo-electrical response of PVC coatings that contained semi-conductors such as titanium dioxide and its doped derivatives such as chromium/antimony/titanium oxide (the inorganic Yellow 2 pigment used in the CDPD). This was done using an experimental set-up that was based on the Grätzel solar cell [95-97]. This is a well known electrochemical cell that can transform light into electricity with an efficiency of approximately 10%. The idea was to implement the pigmented PVC layer into a Grätzel solar cell set-up, and to measure the voltage and the current when this device was irradiated with UV-A light and with normal light.

This is a preliminary investigation that took place over a period of five weeks in the spring of 2004. Even though the results were very encouraging there was no time to pursue this any further, as thesis writing became the number one priority in the last six months of the EngD project.

6.1 Introduction

Different grades of titanium dioxide and a doped TiO_2 yellow pigment were tested in a PVC base for their photo-activity by applying a thin layer (appr. 10 microns) of the

model paint onto a glass plate with a transparent conducting oxide (TCO) on the surface. This forms one electrode, and is attached to the second electrode; this is another glass plate with a TCO layer on the surface, onto which a graphite layer is applied to improve its conducting properties (Fig. 6.1).

Between the two electrodes an electrolyte solution is injected, which makes it a conducting device that can absorb light and transform it into an electric current, very similar to the well known Grätzel cell (Fig. 6.2). The difference is that here the titanium dioxide is held together by a PVC matrix, while in the Grätzel cell the titanium dioxide particles are sintered onto the glass.

Also, in the Grätzel cell the titanium dioxide particles are impregnated by a red dye, so that they can be sensitized when that dye absorbs light outside of the absorption region of TiO_2 (> 400 nm). This way, a bigger part of the solar spectrum can be harvested by the cell. In this set of experiments the commercial green pigment that was tested in the CDPD has been added to some of the mixtures of TiO_2 and PVC in order to investigate how it influences the conductivity and light-absorption properties of the paint systems.

Figure 6.1: A layer of pigmented PVC is applied on one electrode, and a layer of graphite on the other.

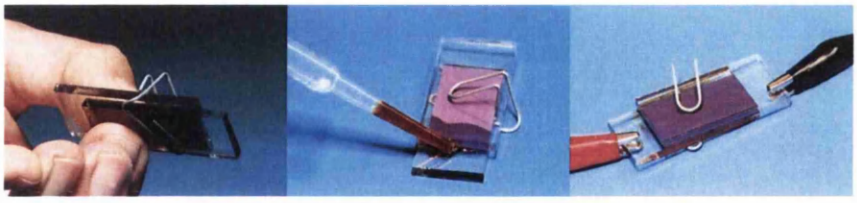

Figure 6.2: The two electrodes are held together, an electrolyte fluid is sucked between them, and the cell is connected to a voltmeter.

The cell can be connected to a voltmeter, so that the open circuit electric potential and the short circuit electric current can be measured. This was done while the cell was irradiated with UV-A light and with normal light (Fig. 6.3).

Figure 6.3: Measurement of the photo-electrical response during irradiation with UV-A light and with normal light.

The kit used for this is purchased from Man Solar in the Netherlands, the information in the next section is obtained from their website [98] and will provide some background on Grätzel's dye-sensitized solar cell.

6.2 The Dye-Sensitized Solar Cell.

The working principle of the dye solar cell is explained in Figure 6.4

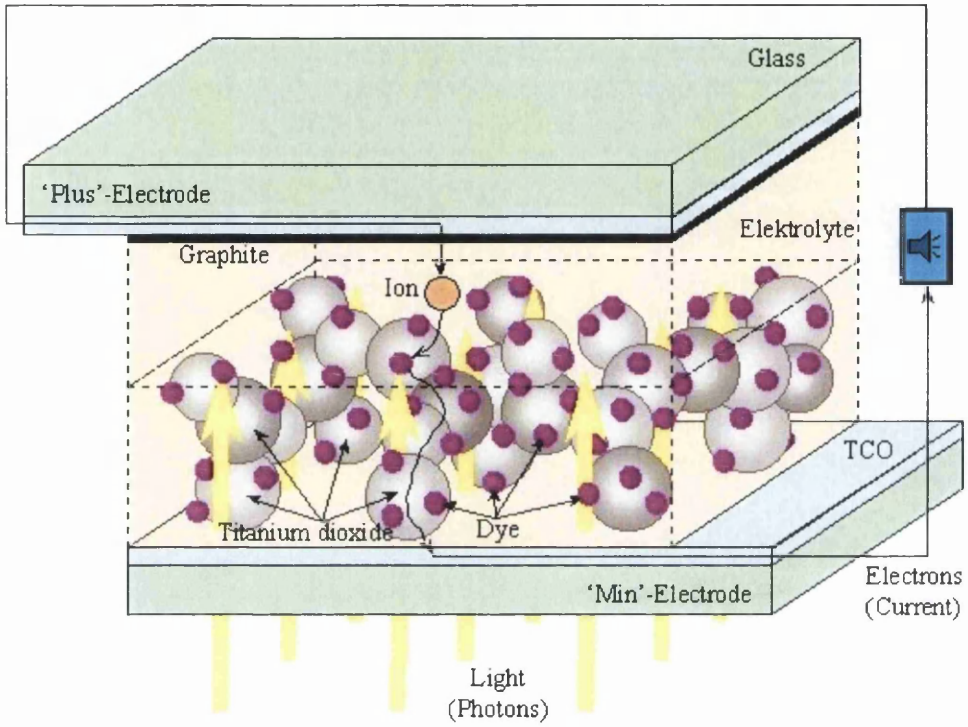

Figure 6.4: A schematic drawing of Grätzel's dye-sensitized solar cel.

TCO stands for transparent conducting oxide, a thin coating which is electrically conducting.

The dye solar cell consists of a thin layer (appr. 10 micrometer thickness) randomly stacked titanium dioxide particles (appr. 20 nm sized) to which organic dye molecules are chemically attached. The titanium dioxide particles form a three dimensional network which is electrically conducting when illuminated. This layer is attached to a TCO coated glass substrate. This TCO layer has been coated onto the glass beforehand and is essential to transport the produced current of the solar cell to the power consuming device, for example a calculator. This glass plate with the coloured titanium dioxide on it is called the photo electrode and this is the negative pole of the solar cell. To complete the solar

cell (and the electrical circuit) also a counter electrode and an electrolyte liquid are required. This will be explained later.

The transformation of the energy of light into electrical energy works as follows in the dye solar cell: a dye molecule absorbs a small amount of light. The energy present in this light is transferred to one electron in this dye molecule. Upon this energy transfer the electron has become mobile and is able to leave its defined bond. The electron possesses enough energy to migrate through the titanium dioxide and the TCO to the current consuming device. In order to have an electrical current run a closed circuit is required. This means that electrons, after they have transferred their energy to a consuming device, have to return to the spot where they were released. To realize this, a counter electrode is required which absorbs the electrons from the consuming device. These electrons return via the electrolyte to the dye molecules that are missing an electron. The counter electrode absorbs the electrons and transfers them to ions present in the electrolyte liquid. To let this process run efficiently, a catalyst is required. This is a layer of graphite from a pencil, deposited on the TCO of the counter electrode. The "charged" ions carry the electrons through the liquid and the pores of the titanium dioxide network until they meet with a dye molecule missing an electron. The electron is then transferred from the ion to the dye. This final step closes the electrical circuit and the dye is ready again to carry out the process of transforming light into electricity. The dye solar cell has been invented in the group of prof. Michael Grätzel in Switzerland and is often referred to as Grätzel-cell. After the discovery in 1991 [95] in many research laboratories natural alternatives to the synthetic dye are investigated [97] and also the educational value has been discovered [96].

6.3 The Grätzel Cell and the PVC Based Cell: Differences

As stated in section 6.1, the presence of PVC itself is the main difference between the two cells. This however has significant consequences for the conductive properties of the cell. The electric conductivity of the Grätzel cell, where the TiO_2 particles are sintered onto the glass, is higher than that of the PVC based cell, which in most of the experiments conducted here contains 30 weight% TiO_2. This is because the electron transport will take place through 'pathways' formed by chains of TiO_2 particles; in the sintered (~100%) TiO_2 structure there will be more of these pathways than in the PVC matrix where the TiO_2 content is lower. This means that resistance of the PVC cells will be much higher, and therefore the current that will flow through them will be lower.

The other difference is that in the Grätzel cell, a dye is used in order to maximise the photochemical response of the cell; in the PVC cell, the green pigment that was added in some of the tests is a commercial pigment used in paints. This means that this pigment has been developed for its protective properties and its colour strength. The effect of the addition of the commercial green pigment to the PVC/TiO_2 matrix on the photo-electric response and the conductivity of the paint-layer have been investigated here and compared to that of the red sensitizing dye.

Both these differences will cause the photo-electric response of the PVC cell to be different to that of the Grätzel cell. However, the response is still measurable and makes it possible to compare the photo-activity of PVC based paints with different pigmentations in a relatively simple experimental set-up.

6.4 Experimental.

Three grades of titanium dioxide were tested: Kronos 2220, TR60 and Degussa P25. The doped TiO_2 yellow pigment was the inorganic Yellow 2, a chromium-antimony-titanium oxide. The commercial colorant that was added to some of the paints is the organic green Green pigment that has ben tested in the CDPD, a beta-copper-phthalocyanine. The PVC was purchased from the Aldrich Chemical Company.

The 'make your own solar cells' kit was purchased from the Man Solar BV company [98] in the Netherlands. This kit contained the glass plates with the transparent conducting layer on it (made of fluorine doped tin oxide), the electrolyte solution (iodine and sodium iodide in ethanol), the voltmeter (a Ferm digital multimeter) and the electric wires with crocodile clips that are used to connect the cells to the voltmeter. It also contained some ready made glass electrodes (4 by 2 cm) for the Grätzel cell, with a layer (appr. 10 microns) of TiO_2 (mainly anatase, with an average primary particle size of 25 nm) already sintered onto the conducting side of the glass plates. The red dye comes from the leaves of dried hibiscus flowers, which is used as a colorant for herbal tea. It is extracted with hot water, after which the sintered TiO_2 particles on the negative electrode can be impregnated with the dye by letting them soak in the dye solution in water for 20 minutes.

The pigmented PVC coatings were applied to the electrodes by applying two pieces of tape to the long sides of the conducting glass, covering a strip with a 3 mm width. Then a few drops of the PVC based model paint were dropped onto the glass with a pasteur pipette, after which the coating layer was formed by dragging a microscope glass along the length of the glass surface while it is touching the tape layers on the side (Fig. 6.1). This way, an area of 5 cm^2 was coated. After this, the electrode was left to dry overnight. Then, the other glass electrode (with a graphite layer deposited onto the conducting side) could be attached by using a deformed paper clip, after which the electrolyte was added by sucking it into the space between the electrodes by using capillary forces (Fig. 6.2). The cell is 'alive' now and its photo-activity can be tested.

Twelve cells have been tested. The first cell is a Grätzel cell, which is done in order to have a reference to compare the PVC based cells with. Then the TiO_2 grades of Kronos 2220, TR60, and Degussa P25 were tested in a 30 weight% concentration in PVC, as was the Yellow 2 pigment. The Degussa P25 grade was done in a 60 weight% concentration too, in order to investigate the change of the conductive properties of the cell when the pigment load is increased.

Then, the addition of different concentrations of Green to 30 weight% Yellow 2 was investigated. The reason for this is that Yellow-Green shades have shown a lot of delamination in accelerated weathering experiments (especially in the horizontal QUV ponding machine), which indicates photo-degradation of plasticisers and therefore high photo-catalytic activity of the pigments. The yellow to green ratios that were tested are 10:1, 25:1 and 5:1 respectively.A mixture of 1 weight% Green and 30 weight% Degussa P25 in PVC has also been tested.

The last two tested cells were Green impregnated onto 30 weight% Degussa P25 (by letting the glass electrode coated with the P25/PVC matrix soak in a solution of Green in THF overnight), and the red dye from the Grätzel cell impregnated onto 30 weight% Degussa P25 (by letting the glass electrode coated with the P25/PVC matrix soak in a solution of the red dye in water for 20 minutes, like is done with the Grätzel cell).

6.5 Results

For every tested cell, the resistance, the open circuit voltage and the short circuit current was measured in three conditions:

1) while the cell was in the dark,
2) while it was irradiated with a 60W tungsten-filament light bulb (placed 11cm above the cell)
3) while it was irradiated with 6 8W UV-A lamps implemented into a half-cylindrical holder with a radius of 6 cm

The set ups with the light-bulb and the UV-A lamps are pictured in Fig. 6.3. The measurements were carried out over three consecutive days after the cells were fabricated. The results could vary substantially over these three days, probably because the cells are 'wet' (due to the electrolyte) which makes their electrochemical properties vary with time (eg. the penetration of the electrolyte into the PVC / TiO_2 membrane takes time, and the electrolyte can dry up). In order to get consistent results, the measurements done on the third day after the cell was made are given here.

Table 6.1: measured electrical properties of the tested cells in the dark, and under irradiation of a lightbulb and UV-A light.

	dark			lightbulb			UV-A		
	R (k Ohm)	Voc (mV)	Isc (μA)	R (k Ohm)	Voc (mV)	Isc (μA)	R (k Ohm)	Voc (mV)	Isc (μA)
Graetzel cell	9.9	0.4	0	12.7	287	187	19.4	300	500
Kronos 2220 30%	127	2	0	98	-38	-0.1	61.1	34	0.5
TR 60 30 %	114	12	0.1	86.6	-47	-0.2	46.7	-73.5	-1
P25 30%	168	29.2	0.1	130	142	0.3	141.7	310	6.7
P25 60%	112	38	0.1	88	135	0.8	84	216	9.6
Sicotan Yellow 30%	110	6.9	0	85.5	10.5	0.05	98	258	9
Sicotan Yellow 30% Irgalite green 3 %	109.6	12.7	0.05	86.6	50	0.2	18.7	275	16.4
Sicotan Yellow 30% Irgalite green 1.2%	117.4	5.8	0.05	81.5	63	0.05	19.1	242	8
Sicotan Yellow 30% Irgalite green 6%	100	0.3	0	77	-55	-0.25	18.9	-78	-2.3
P25 30% Irgalite green 1%	15.5	65	0.5	13.4	-19	-0.4	10.8	-90	-5.3
Irgalite green impr. on P25 30%	8.6	16	0.05	7.4	-68	-1.4	8.1	-99	-4.6
red dye Graetzel cell impr. on P25 30%	110	6.9	0	85.5	10.5	0.05	98	258	9

6.6 Theory and Assumptions

The Grätzel cell has the biggest open circuit voltage and short circuit current out of all the cells, as can be expected for reasons discussed earlier.

A lot of the measured voltages and currents in the table are negative. This means that the net current through these cells is flowing in the opposite direction of that in the Grätzel cell; the excited electrons from the TiO_2 in the PVC matrix, instead of flowing to the 'minus' electrode of the cell (the photo-electrode to which the coating is attached and through which the light enters the cell), are in fact absorbed by positive ions in the electrolyte and transported to the 'plus' counter-electrode.

It is likely that excited electrons from the TiO_2 in the PVC matrix can be transported to either electrode, and that what we measure is the 'net' current, the difference between the total electron flow in one direction and that in the other direction. The sign of the net flow tells us which of the processes is the dominant one, which of the two possible directions is the energetically most favourable one for the electrons to follow.

Normally, the net number of electrons per second that are excited in the PVC / TiO_2 matrix and that have enough energy to complete the electrical circuit (N_{sc}) can be calculated by dividing the short circuit current over the elementary charge constant:

$N_{sc} = I_{sc} / 1.602*10^{-19}$

However, in the PVC cells the short circuit currents are very low compared to that in the Grätzel cell, due to the lower conductivity in the PVC cells. Because of this, it would not be right to use these values as an indication for the photo-activity of the model paint, as the large resistance of the PVC based cell forms too big an obstacle for most of the excited electrons to complete the electrical circuit.

The open circuit voltages of the PVC cells are measurable quantities, and the following simplification is proposed to estimate from the measured open circuit voltage the net number of electrons per second in the PVC matrix that are excited with enough energy to reach the negative electrode in the cell (N_{oc}).

If the open circuit voltage is measured, no current flows through the sytem. The cell can regarded as a parallel-plate capacitor with a source of electromotance between the plates (this source being the light that excites a certain amount of electrons of the TiO_2 / PVC matrix every second). From here, these electrons can go to either glass electrode, but they are likely to have a 'preferred pathway' to the energetically most favourable position (like with the short circuit current). This will cause more electrons to go to one electrode than the other, which will result in a charge separation within the cell; the open circuit voltage is a measure for the amount of charge separation that takes place during the irradiation of the cell.

Even when it is accepted that part of the flux of electrons towards one electrode is cancelled out by the flux in the opposite direction, a very photo-active coating will have big fluxes flowing through the matrix, and therefore the net flux (the difference between the dominant flux and the flux in the opposite direction) will also be big. The amount of charge separation between the electrodes is directly correlated to the size of the net flux of electrons through the matrix, and so is the measured open circuit voltage. Following this rationale, the open circuit voltage is an indicator for the photo-activity of TiO_2 / PVC matrix in the cell

An estimate of the net flux of electrons flowing through the matrix between the electrodes can be made when the assumption of a parallel-plate capacitor is continued:

Within seconds after irradiation of a PVC-based cell, the open circuit voltage reaches a constant value. When this happens, the system is in a steady state; the net current through the TiO_2 / PVC matrix caused by the irradiation of the cell equals the naturally occurring 'reaction' current that discharges the parallel-plate capacitor.

In a capacitor, the formula for the current when it is discharged through an external resistance is:

$I_{discharge} = Q_0 / (R.C) * e^{(-t/RC)}$

Where Q_0 is the charge of the capacitor at t=0, R is the resistance and C is the capacity of the capacitor.

In the case of a PVC cell in a steady state, the charge Q is constant, the discharge takes place through the internal resistance of the cell (between the electrodes), and the discharge current is constant and equal to the net current caused by the excited electrons from the TiO_2 / PVC matrix (I_{oc}) flowing in the opposite direction. The formula for the current becomes:

$I_{discharge} = I_{oc} = Q / (R.C)$

For a capacitor, the relationship between the charge and the electric potential is as follows:

$Q = C * V$

This is substituted into the previous formula to give:

$I_{discharge} = I_{oc} = V_{oc} / R$

This is of course the most fundamental relationship used in electrical engineering.
So now, with the open clamp voltage and the internal resistance of an irradiated cell, we can calculate the (theoretical) net current of electrons within the cell that reaches the negative electrode. Again, by dividing this current over the electrical charge constant, we

can calculate the net number of electrons that are excited per second in the PVC / TiO_2 matrix and that have enough energy to reach the negative electrode (N_{oc}).

$N_{oc} = I_{oc} / 1.602*10^{-19} = V_{oc} / (1.602*10^{-19} * R)$

6.7 Modified Results

The measured open circuit voltages and short circuit currents of the cell in the dark, called the 'dark current' (given in Table 6.1, caused by chemical imbalances), were subtracted from the values measured during irradiation to obtain the 'net' open circuit voltage and the 'net' short circuit current caused by the light absorption of the cell. These net currents and voltages measured for the 12 tested cells, together with the calculated values for the net open circuit currents and the net number of excited electrons per second, are given in Table 6.2.

Table 6.2: net open circuit voltages and short circuit currents given for cells irradiated with a lightbulb and with UV-A light, with the calculated values for open circuit currents and excited electrons per second (Noc).

	lightbulb					UV-A				
	R (k Ohm)	Voc (mV) (net)	Isc (μA) (net)	Ioc (μA) (calculated)	Noc (10^12/sec)	R (k Ohm)	Voc (mV) (net)	Isc (μA) (net)	Ioc (μA) (calculated)	Noc (10^12/sec)
Graetzel cell	12.7	286.6	187.0	22.6	140.9	19.4	299.6	500.0	15.4	96.4
Kronos 2220 30%	98.0	-40.0	-0.1	-0.4	-2.5	61.1	32.0	0.5	0.5	3.3
TR 60 30 %	86.6	-59.0	-0.3	-0.7	-4.3	46.7	-85.5	-1.1	-1.8	-11.4
P25 30%	130.0	112.8	0.2	0.9	5.4	141.7	280.8	6.6	2.0	12.4
P25 60%	88.0	97.0	0.7	1.1	6.9	84.0	178.0	9.5	2.1	13.2
Sicotan Yellow 30%	85.5	3.6	0.1	0.0	0.3	98.0	251.1	9.0	2.6	16.0
Sicotan Yellow 30% Irgalite green 3 %	86.6	37.3	0.2	0.4	2.7	18.7	262.3	16.4	14.0	87.6
Sicotan Yellow 30% Irgalite green 1.2%	81.5	57.2	0.0	0.7	4.4	19.1	236.2	8.0	12.4	77.2
Sicotan Yellow 30% Irgalite green 6%	77.0	-55.3	-0.3	-0.7	-4.5	18.9	-78.3	-2.3	-4.1	-25.9
P25 30% Irgalite green 1%	13.4	-84.0	-0.9	-6.3	-39.1	10.8	-155.0	-5.8	-14.4	-89.6
Irgalite green impregnated on P25 30%	7.4	-84.0	-1.5	-11.4	-70.9	8.1	-115.0	-4.7	-14.2	-88.6
red dye from Graetzel cell impregnated on P25 30%	85.5	3.6	0.1	0.0	0.3	98.0	251.1	9.0	2.6	16.0

The fact that some of the N_{oc} values are negative means that the open circuit currents and the open circuit voltages that they were calculated from were negative. This means that the net stream of the electrons is flowing through the electrolyte to the counter-electrode, and not to the photo-electrode like in the Grätzel cell, as is explained previously.

6.8 Discussion

Of the TiO_2 grades, the Kronos 2220 is known to be the least photo-active of the three, the TR60 grade is more photo-active, and the Degussa P25 is the most photo-active. This is reflected in the N_{oc} values both during irradiation with normal light and with UV-A light. The (absolute) N_{oc} values for Degussa P25 30% (5.4 $*10^{12}s^{-1}$ lightbulb / 12.4 $*10^{12}s^{-1}$UV-A) are bigger than those for TR60 30% (-4.3 / -11.4) which are bigger than those for Kronos 2220 30% (-2.5 / 3.3), and the same trend is observed for the measured short circuit currents during UV-A irradiation. The trend is displayed in Figs. 6.5 and 6.6, which show the absolute values of the measured open circuit voltages and short circuit currents.

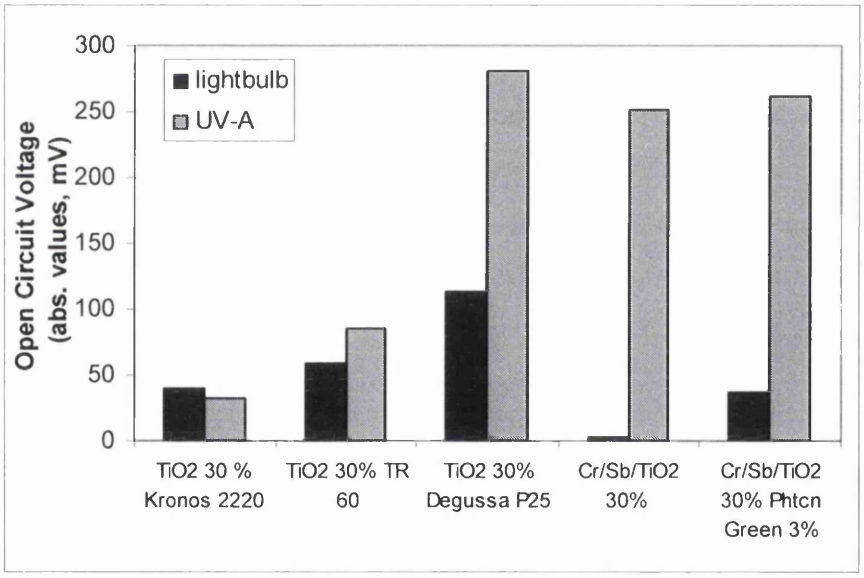

Figure 6.5: absolute values of some measured open circuit voltages

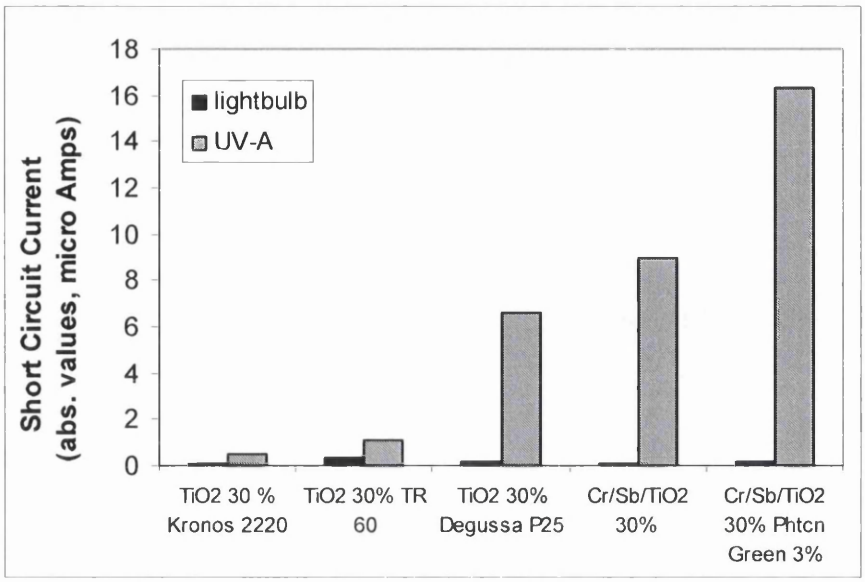

Figure 6.6: Absolute values of some measured short circuit currents

The resistances in the Degussa P25 cell (130 kOhm lightbulb/ 141.7 kOhm UV-A) under irradiation are higher than those of the other TiO_2 grades (86.6 / 46.7 for TR60 and 98 / 61.1 for Kronos 2220). This will decrease the value of the open circuit current, as this is calculated by dividing the net open circuit voltage over the resistance of the cell measured while it is irradiated. It is therefore to be expected that the relative photo-activity of the Degussa P25 compared to the other TiO_2 grades is higher than the ratio of the calculated open circuit currents would suggest.

In general, the potential of a pigment to catalyze the photo-degradation of organic molecules in a coating will depend both on the ability of the pigment to absorb light and bring its electrons to a higher energy level (the photo-activity), and on the chance of an excited electron to meet an organic molecule and initiate the degradation reaction. The latter will depend on the ability of the molecules to travel through the PVC / TiO_2 matrix, and on the ability of the excited electrons to do the same. In a PVC / TiO_2 matrix with a low electrical resistance, the excited electrons will travel well and have a bigger chance of meeting other molecules and initiate their degradation, so more photo-degradation will take place.

How much the photo-activity and how much the electrical resistance of different grades of TiO_2 'count' when their potential to catalyse photo-degradation in a PVC matrix is evaluated, is unknown, but the currents and voltages measured using the solar cell set-up seem to give results that reflect both these properties.

The N_{oc} values for Degussa P25 60% (6.9 / 13.2) are higher than those of Degussa P25 30% (5.4 / 12.4), which is to be expected as there is double the amount of TiO_2 in it. This would theoretically double the number of photo-active sites in the coating and increase the conductivity of the PVC / TiO_2 matrix.

The fact that the short circuit current during UV-A irradiation of 60% Degussa P25 in PVC (9.5 μA) is only 44% higher than that with half the Degussa P25 loading (6.6 μA) indicates that that there is a saturation concentration for the number of photo-active sites in a cell. The resistances of the 60% Degussa P25 cell (88 / 84) under irradiation are lower than those of the 30% cell (130 / 141.7), as was to be expected because more TiO_2 in the matrix means more 'pathways' for the excited electrons to travel on.

The 30% Yellow 2 (Cr/Sb/TiO_2) in PVC has a very low electrical response to the light bulb irradiation, but its response to the UV-A light is remarkably high for a commercial pigment (short circuit current 9 μA / open circuit current 16 μA), it is comparable to the Degussa P25 responses. When the different amounts of the Green pigment were added to the 30% Yellow 2, the photo-response under UV-A irradiation rose dramatically, and the response under light-bulb irradiation rose to substantial levels, too. It is proposed that the addition of Green (beta-copper-phthalocyanine) increases both the light absorption properties and the conductivity of the Yellow 2 / PVC matrix. The first seems to happen in the Yellow-Greens that are irradiated by the lightbulb: While the resistance of the cells does not change much compared to that of the 30% Yellow 2 cell (Fig. 6.7), the calculated N_{oc} values of the Yellow-Greens are between 9 and 15 times higher than that of the 30% Yellow 2 cell. This indicates that the increase in photo response is due to sensitisation of the Yellow 2 by the Green; The green, being a phthalocyanine, finds it easy to absorb light and bring its electrons into a higher energy state. It can transfer these

excited electrons to the Yellow 2 molecules so that these in turn get into an excited state. In this way, the green pigment increases the portion of the light that the Yellow 2 molecules can absorb.

When the Yellow-Greens were irradiated with the UV-A light, the resistance of the cells dropped to under 20 k Ohm (Fig. 6.7), compared to 98 k Ohm of the 30% Yellow 2 cell irradiated with UV-A light. It is proposed that the lowering of the resistance is due to the excitation of a big number of electrons in the green phthalocyanine molecules by the high-energetic UV-A light. When these electrons are in the excited state, they have more freedom to move, both within the molecules and between different molecules, and this will enhance the conductivity of the cell as a whole.

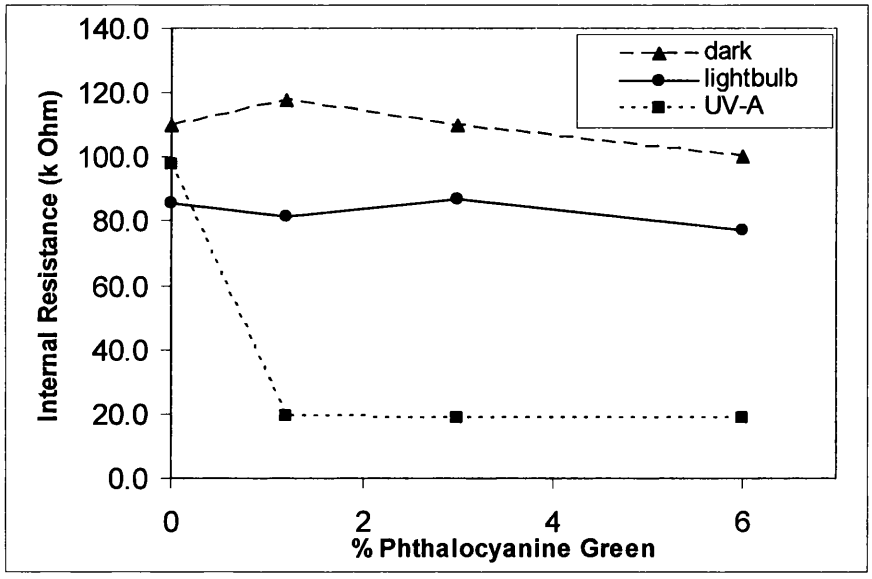

Figure 6.7: The internal resistance of a 30% Cr/Sb/Ti Oxide in PVC as a function of the Phthalocyanine Green concentration.

In the 30% Yellow 2 6% Green shade, the electrons prefer to move towards the counter-electrode, as the measured currents and voltages are negative. Since this is the highest concentration of the green pigment of the three tested Yellow/Green ratios, it looks like the green promotes the movement of electrons in this direction. It could be that the green

pigment facilitates the transfer of electrons from the PVC / Yellow 2 matrix to the electrolyte ions, which then transport the electrons to the counter electrode.

This is confirmed by the measured negative currents and voltages of the next two cells that both contain the green pigment (30% P25 / 1% Green and the Green impregnated onto 30% P25). Both these cells have a low resistance as well, during light bulb irradiation and UV-A irradiation. Under irradiation with the tungsten filament lightbulb, the (absolute) measured short circuit current is 4.5 times bigger in the 30% Degussa P25 where 1% Green was added, and the (absolute) calculated N_{oc} values are 7 times higher, indicating a sensitizing effect as Degussa P25 without any addition can only absorb light with wavelength smaller than 400nm).

Under UV-A irradiation, the (absolute) measured short circuit current is a bit lower than that of 30% Degussa P25 without Green (indicating that the sensitising effect of the green on the already UV-A photo-active Degussa P25 is small), but the (absolute) calculated N_{oc} values are seven times higher again, due to the lower resistance in the cell with the green pigment.

The 30% Degussa P25 cell with the Green impregnated onto it has the lowest resistance of all the tested cells (7.4 k Ohm under a light bulb and 8.1 k Ohm under UV-A light). The impregnated green pigment-molecules in this cell will be located in the lop layer of the PVC / TiO_2 matrix (as it was already attached to the glass electrode while it was soaked in the Green / THF solution). This indicates that the resistance 'bottleneck' in the cell is the transfer of the electrons from the PVC / TiO_2 matrix to the ions in the electrolyte; in this cell there are plenty of the green pigment molecules present in the region where the electrolyte and the PVC come together to facilitate this process, which results in the lowest resistance out of all the cells tested.

The impregnation of the red dye used in the Grätzel cell (made from hot water and dried hibiscus flowers) onto 30% Degussa P25 in PVC had no increasing effect on the currents flowing through the cell during irradiation with the light bulb, but increased the measured

short circuit current and the calculated N_{oc} value by 30% during UV-A irradiation. This is likely to be due to a decrease of the cell resistance by 30% that was measured after impregnation with the red dye.

The observed decreases of the resistance of the PVC based cells when they are irradiated seem happen for two reasons: light and heat. When the light bulb was used to irradiate the cells, the samples did not take long to heat up as the distance between the lamp and the cells was only 11 cm. When the sample was shielded from the light, but still hot, its resistance would go back up slowly while it was cooling down. The heating up of the samples was not a big issue when the UV-A lamps were used, so the increased conductivity here was more likely to be due to the effect of the light itself.

6.9 Conclusions of the Dye Solar Cell Experiment

The idea to test pigmented PVC systems for their photo-activity by using a Grätzel cell set-up and measuring the open circuit voltages, short circuit currents and electrical resistances seems to have potential. The benefits are that the testing samples are quick and easy to prepare and that the tests themselves are simple and fast. The downside is that the photo-response of the cells varies with time after the cells are made, because the cell is 'wet' and things like the penetration of the electrolyte into the PVC matrix and evaporation of the electrolyte are processes that change the electrochemical properties of the cell with time.

Also, the heating up of the cell during irradiation changes its conductivity and with that the electrical response that is measured. All these issues point at the necessity to have a strict testing protocol when the investigation into this technique is taken further, so that every sample is made in the same way, and every test is done with the same timing.

The results in this set of experiments have shown that with this technique it is possible to evaluate different grades of titanium dioxide for their photo-activity and electrical conductivity, as was done with the Kronos 2220, TR60, Degussa P25 and Yellow 2 Pigments. Out of these four Kronos 2220 was shown to be the least photo-active, followed by TR60.

It is also possible to evaluate model paint systems made up of organic and inorganic pigments. The addition of the Green dye to 30% Degussa P25 titanium dioxide and to 30% Yellow 2 pigment in PVC have been shown to decrease the electrical resistance of the cells, and to increase their photo-activity by sensitisation, the latter mainly during irradiation by a light bulb.

7 CONCLUSIONS

In this EngD project the influence of weathering on the aesthetic properties of organic coated strip has been investigated. A wide range of PVC plastisol coatings with variable experimental pigment combinations was tested. The colour fastness and gloss retention of these coatings were evaluated after exposure to natural weathering in Darwen and Rye and to accelerated weathering in the QUV testers.

The objectives of this research project (to investigate the correlation between the pigmentations and the weathering properties of the commercial PVC plastisol coating, and to investigate the correlation between natural and accelerated weathering) were defined quite broadly. Also, the way in which to go about investigating this was not specified in the description of the project; in the project proposal it was assumed that colour would be measured in CIE L*a*b* values. One year into this project, it was established that evaluating the colour change in coatings using these parameters was not going to be successful. This is because the CIE L*a*b* system describes colours based on the way they are perceived by the human eye.

Reflectance spectrometry was then introduced for the colour measurements on the weathered panels. This technique gives a more fundamental, physical description of colours and is therefore more suitable when attempting to correlate colour changes to the chemical processes that take place in coatings during weathering. With reflectance spectrometry, the effects of dehydrochlorination, organic pigment degradation and chalking on the way that the colours of panels change during weathering could be analysed.

Dehydrochlorination of PVC leads to darkening of the coating. It is a process that involves progressive 'unzipping' of neighbouring chlorine and hydrogen atoms along the polymer chain, while double bonds are formed between the carbon atoms. The discolouration that is taking place is attributed to the formation of a conjugated double bond system in the backbone of the polymer during this process. The polyene structure

formed in this way absorbs light with wavelengths around 320 nm, but when the polyene concentration in the coating increases, this absorption peak broadens into the visible region of the electromagnetic spectrum; this results in darkening of the colour of the coating and a decrease of the reflectance spectrum.

Organic pigment degradation leads to loss of the colour strength of the coating; the colour of the coating will fade, because the degraded pigment molecules will have lost their chromophoric function. The reflectance spectrum will get closer to that of the pigmentless PVC plastisol base. Another consequence of this is that there will be less protection for the coating system against irradiation.

Chalking can only take place in coatings containing TiO_2 or other inorganic pigments. It is caused by the breaking down of the resin in the top layer of a coating during weathering, after which a thin layer of the inorganic pigment can be formed on top of the coating. In the case of TiO_2, chalking will make the coating appear lighter because more TiO_2 particles have become visible as they have migrated to the top of the coating. This has been demonstrated with some SEM scans of a coating pigmented with TiO_2 taken before and after exposure to UV-A irradiation in a QUV cabinet. Because of chalking, the reflectance spectrum of the coating in the visible region (above 400 nm) will increase, as TiO_2 reflects all the light in this region.

A model has been proposed that can calculate three coefficients which give an indication of the relative amounts in which the identified processes take place in a coating during weathering. These coefficients are called 'a' (PVC dehydrochlorination), 'b' (organic pigment degradation) and 'c' (chalking). This has been done by defining a 36-dimensional vector for each of the three processes (called 'A', 'B' and 'C' respectively), which are a mathematical representation of how that particular process affects the reflectance spectrum of the coating (the vector has 36 values because a reflectance spectrum also consists of 36 reflection values, running from 380 to 730 nm with 10 nm intervals). When the reflectance spectrum of a coating before weathering and after weathering is known, the coefficients 'a', 'b' and 'c' of a weathered coating can be

calculated by solving the following equation by using the SOLVER function in Microsoft Excel:

$$R_{weathered} = R_{unweathered} * (1+a*A) * (1+b*B) * (1+c*C)$$

In general, the shades in the CDPD (Colour Dynamics Predictive Database) showed a good match between the measured reflectance spectra of the weathered panels and the reflectance spectra reconstructed with the calculated coefficients. Also, natural weathering was compared to accelerated weathering by plotting the values of the 'a', 'b' and 'c' coefficients calculated for natural weathering against those calculated for accelerated weathering. This was done after the coefficients had been corrected for the amounts of UV-A irradiation that they had been exposed to. It was found here that the coefficients for natural weathering in Darwen and Rye that were corrected with the irradiation energies calculated with the $\gamma_s>30°$ solar irradiation model (which counts solar irradiation only when the solar altitude angle (γ_s) is greater than 30°, this means that the Air Mass that the rays travel through is less than 2) had a better match with those for accelerated weathering than when they were corrected with the $\gamma_s>1°$ solar irradiation model. This seems logical as the $\gamma_s>1°$ solar irradiation model is thought to overestimate the solar irradiation. The correlations between natural and accelerated weathering that were found using this method were sometimes good, and sometimes not so good. It seems that this method has potential to become a useful tool to compare different types of weathering while separating the effects that the different types of weathering have on the colours (reflectance spectra) of the shades, but unfortunately there was not enough time left in this EngD project to investigate this further.

The correlation between the gloss loss caused by different types of weathering has also been investigated for all the weathered panels. The gloss retention values were corrected for the amounts of UV irradiation. It was found that the exposure of the panels in Rye had good correlations with all three types of accelerated weathering regarding the gloss retention properties of the coating. The correlation coefficient of natural weathering in Rye with QUV weathering without condensation is 0.84, that with QUV weathering with

a condensation cycle is 0.92, and that with horizontal QUV weathering with condensation is 0.90. On the other hand, it was found that the exposure of the panels in Darwen had poor correlations with all three types of accelerated weathering. This is thought to be because the amount of UV-A irradiation that panels receive from the sun in Darwen is far less than what panels receive in Rye. The amounts of UV-A received in Rye are comparable to those that panels receive during weathering in the QUV machines, whereas the amounts received in Darwen are not. Because the main cause for gloss loss is plasticiser degradation in the coating, which is triggered by absorption of UV irradiation by the plasticiser molecules, this is likely to make a big difference.

In order to evaluate which of the solar irradiation models has a closer similarity with the irradiation received during weathering in the QUV machines, the ratio of the corrected gloss retention after QUV weathering and that after weathering in Rye was calculated for all the exposed panels. When the $\gamma_s>30°$ solar irradiation model was used for the estimation of the solar irradiation energy received in Rye, the average ratios were 1.20, 1.32 and 1.37 for weathering in Rye and QUV weathering without condensation, with condensation and horizontal QUV with condensation. When the $\gamma_s>1°$ solar irradiation model was used they were 0.75, 0.82 and 0.85 respectively. This indicates that, according to the gloss-loss correlation analysis, the $\gamma_s>30°$ solar irradiation model underestimates the amount of solar irradiation that is capable of damaging the coatings, while the $\gamma_s>1°$ solar irradiation model overestimates it.

Gloss loss is caused by degradation of the plasticisers in the coating. Plasticisers are susceptible to degradation reactions during weathering. In general, plasticisers will degrade under the influence of UV light, water and air in a multi-step reaction to give carbon dioxide and water. For a coating, plasticiser degradation can have important consequences, like embrittlement, delamination, crack formation and gloss loss. The most extreme case of plasticiser degradation was found for the low concentration yellow-green shades that were weathered in the horizontal 'ponding' QUV machine. These yellow-green coatings became very brittle after 1500 UV-hours of irradiation. For these yellow-green panels, the correlation between the gloss retention values and the plasticiser levels (which were measured using GC-MS) was examined, and a correlation coefficient of 0.61

was calculated for this set of values. This is because the degradation of plasticiser molecules results into the formation of small cracks in the surface of the coating (microcracking), which on a macroscopic level is perceived as the loss of gloss.

The correlation between the plasticiser levels in the yellow-green shades and the amount of darkening caused by PVC dehydrochlorination (quantified with a proposed Spectrum Surface Integral (SSI) value) after weathering in the horizontal QUV machine was also investigated. Unpigmented base PVC showed more darkening caused by dehydrochlorination than the yellow-green shades, which is expected, because in the yellow-green shades the PVC base is shielded by the pigmentation. It was also found that the low concentration yellow-green shades showed more plasticiser degradation than unpigmented base PVC plastisol. This indicates that the photo-degradation of the plasticiser molecules is enhanced by the inorganic yellow pigment (rutile Cr-Sb-Ti Oxide) that is used in the yellow-green shades. It is thought that the particles of the inorganic yellow pigment in turn are sensitised by the organic green pigment: This means that the organic green absorbs light and then passes the energy on to the inorganic yellow, thus increasing the portion of the sunlight that the inorganic yellow can absorb. This process could be envisioned as a plasticiser molecule, being able to move around the PVC matrix because of its small size, coming into contact with an excited Cr-Sb-Ti Oxide surface, after which an energy transfer process takes place from the excited Cr-Sb-Ti Oxide to the plasticiser. The plasticiser molecule now becomes excited, and can react from this excited state.

The observations of the strong deterioration of the yellow-green shades triggered the idea of conducting some experiments to measure the photo-activity of pigmented PVC layers by using a Grätzel cell set-up. In this initiative, different grades of titanium dioxide and the inorganic yellow-2 pigment (which is a doped TiO_2) were tested in a PVC base for their photo-activity. This was done by applying a thin layer (appr. 10 microns) of the model paint (which consisted of PVC with a 30% or 60% inorganic pigment loading) onto a glass plate with a transparent conducting oxide (TCO) on the surface. This forms one electrode, and is attached to the second electrode, which is another glass plate with a

TCO layer on the surface, onto which a graphite layer is applied to improve its conducting properties. Between the two electrodes an electrolyte solution is injected, which makes it a conducting device that can absorb light and transform it into an electric current, very similar to the well known Grätzel cell. The difference is that here the titanium dioxide is held together by a PVC matrix, while in the Grätzel cell the titanium dioxide particles are sintered onto the glass. Also, in the Grätzel cell the titanium dioxide particles are impregnated by a red dye, so that they can be sensitized when that dye absorbs light outside of the absorption region of TiO_2 (> 400 nm). This way, a bigger part of the solar spectrum can be harvested by the cell. In this set of experiments the organic green pigment that was tested in the CDPD has been added to some of the mixtures of TiO_2 and PVC in order to investigate how it influences the conductivity and light-absorption properties of the paint systems. With this experimental set-up the open circuit voltages, short circuit currents and electrical resistances of the tested coatings were measured while they were irradiated with UV-A light and with a normal incandescent light bulb. The results in this set of experiments have shown that with this technique it is possible to evaluate different grades of titanium dioxide for their photo-activity and electrical conductivity. This was done with the Kronos 2220, TR60, and Degussa P25 titanium dioxide grades and with the inorganic yellow-2 pigment. Out the three titanium dioxides, Kronos 2220 was shown to be the least photo-active, followed by TR60. This is in accordance with their known weathering performances in coatings. The photo-activity of the inorganic yellow-2 pigment under UV-A irradiation was comparable with that the Degussa P25 titanium dioxide grade. This is remarkable because this grade is mainly anatase and therefore very photo-active, but it is consistent with the bad weathering performance of the yellow-2 pigment. The additions of the green pigment to 30% Degussa P25 titanium dioxide and to 30% inorganic yellow-2 pigment in PVC have been shown to decrease the electrical resistance of the cells, and to increase their photo-activity by sensitisation, the latter mainly during irradiation by a light bulb. From this it seems that, in the yellow-green shades, the green pigment enhances the deterioration during weathering both by sensitisation of the inorganic yellow particles, and by lowering the electrical resistance of the coating (which enables excited electrons more freedom to travel to 'active sites').

The benefits of this concept are that the testing samples are quick and easy to prepare and that the tests themselves are simple and fast. The downside is that the photo-response of the cells varies with time after the cells are made, because the cell is 'wet' and things like the penetration of the electrolyte into the PVC matrix and evaporation of the electrolyte are processes that change the electrochemical properties of the cell with time. Also, the heating up of the cell during irradiation changes its conductivity and with that the electrical response that is measured. All these issues point at the necessity to have a strict testing protocol when the investigation into this technique is taken further, so that every sample is made in the same way, and every test is done with the same timing.

Infra Red spectroscopy has been used to investigate the processes that take place in the coatings during weathering further. The peaks that were analysed were at 3400 cm^{-1} (O-H stretch vibration), 2900 cm^{-1} (C-H stretch vibration), 1730 cm^{-1} (C=O) and 1640 cm^{-1} ($HC=CH_2$ located at the end of a chain). The ratio of the $HC=CH_2$ peak and the peak belonging to the C-H stretch vibration is calculated to give an indication of the amount of PVC dehydrochlorination that has taken place in the coating. The ratio of the O-H peak and the C=O is calculated to give an indication of the amount of plasticiser degradation that has taken place in the coating. These two ratios are calculated for some low concentration yellow-green shades, and some low concentration single pigment inorganic yellow-2 and single pigment organic green shades. The pigmentless PVC plastisol base and four white shades (1, 5, 10, 15 pphr TiO_2) were also investigated. It was found that weathering in the horizontal QUV causes the most change in the calculated differences between the ratios, which means that according to the IR spectra this type of weathering causes the most plasticiser degradation and PVC dehydrochlorination. This is consistent with the other methods that were used to evaluate the effects of weathering, and with the general observations of the strength of weathering in the horizontal QUV machine. The coatings pigmented with TiO_2 generally showed less dehydrochlorination and plasticiser degradation than the yellow-green, the single pigment yellow and single pigment green coatings. IR spectroscopy seems to be a good technique to use while investigating the weathering of coatings, but it is most useful in combination with other analysis methods.

BIBLIOGRAPHY

1. Moore, C., Marshall, R.I., *Modern steelmaking methods.* 1980, London: Institute of Metallurgists.
2. Turkdogan, E.T., *Fundamentals of Steelmaking.* 1996, London: Institute of Materials.
3. B.S., *The Colorcoat Building.* 1995, British Steel Strip Products.
4. Ulrich, H., *Introduction to industrial polymers.* 1982: Hanser Publishers.
5. Wicks, Z.W., Jones, F.N., Pappas, S.P., *Organic coatings, science and technology.* 1992: John Wiley & sons.
6. Gaske, J.E., *Coil Coatings.* 1987, Blue Bell, PA: Federation of Societies for Coatings Technology.
7. Munekata, S., Prog. Org. Coat., 1988. **16**: p. 113.
8. PRA, *Notes from Paint Technology training Course.* 2000.
9. Titov, W.V., *PVC Technology (Fourth Edition).* 1984: Elsevier Applied Sciences Publishers, London and New York.
10. Sears, J.K., Darby, J.R., *The Technology of Plasticisers.* 1982: Wiley and Sons, New York.
11. *Plastics Additives, an A-Z reference.* Polymer science and technology, ed. G. Pritchard. 1998, London: Chapman & Hall.
12. Wilson, A.S., *Plasticisers: Principles and Practice.* 1995, The Institute of Materials: London.
13. Searle, J.R., *Titanium Dioxide Pigment Photocatalysed Degradation of PVC and Plasticised PVC Coatings*, in *Dept. of Materials Engineering.* 2002, University of Wales, Swansea: Swansea.
14. Howick, C., Plastics, Rubber and Composites Processing and Applications, 1995(23): p. 53.
15. Braun, D., Pure & Applied Chem., 1981(53): p. 549.
16. Christie, R.M., *Colour Chemistry.* 2001: The Royal Society of Chemistry.
17. *The Colour Index.* 3rd revision ed. Vol. 1-9. 1988, Society of Dyers and Colorists: Bradford.
18. BASF, *Sicotan, the Nickel, Chromium and Manganese rutile pigments of BASF*, H. Endriss, Editor. 2000, BASF: Ludwigshafen.
19. Hocken, J., Proft, B., *Clean Surfaces by the Application of the Photocatalytic Effect, a new application for fine Titanium Dioxide and Zinc Sulfide*, Sachtleben Chemie GmbH: Duisburg.
20. Kamal, M.R., *Effect of variables in artificial weathering on the degradation of selected plastics.* Polymer engineer and science, 1966.
21. Kamal, M.R., Saxon, R. *Recent Development in the Analysis and Prediction of the Weatherability of Plastics.* in *Applied Polymer Symposia N. 4.* 1967.
22. Matsumoto, S., Ohshima, H., Hasuda, Y., *Natural and induced weathering of plasticised Polyvinyl Chloride.* Journal of Polymer Science, 1984. **22**(Polymer Chemistry Edition): p. 869-871.
23. Lemaire, J., *Predicting polymer durability.* Chemitech, 1996(October).

24. Quaschning, V., *The sun as an energy resource.* Renewable Energy World, 2003(September-October).
25. Kinmonth, R.A.J., Norton, J.E., *Effect on Spectral Energy Distribution on Degradation of Organic Coatings.* Journal of Coatings Technology, 1977. **49**(633).
26. Hirt, R.C., Searle, N. Z. *Energy characteristics of outdoor and indoor exposure sources and their relation to the weatherability of plastics.* in *Applied Polymer Symposium No 4 Interscience.* 1967.
27. Mascia, L., *The role of additives in plastics.* 1974, Edward Arnold Ltd.: London.
28. Yassin, A.A., Sabaa, M.W., J. Pol. Sci. Polym. Chem. Ed., 1980. **18**: p. 2513-21 and 2523-33.
29. Braun, D., *Degradation and stabilisation of polymers*, ed. G. Geuskens. 1975, London: Applied Science Publishers.
30. Nass, L.I., *Encyclopedia of PVC*, ed. L.I. Nass. 1976, New York: Dekker, M.
31. Grossman, D.M., *Correlation questions and answers*, Q-Panel Lab Products: Cleveland.
32. Grossman, D.M., *The weather and how to reproduce it in the laboratory*, Q-Panel Lab Products: Cleveland.
33. DeCoste, J.B., Wallder, V.T., *Weathering of Polyvinyl Chloride.* Ind. Eng. Chem., 1955. **47**: p. 314-22.
34. DeCoste, J.B., Wallder, V.T., Howard, J.B., *Weathering of Polyvinyl Chloride: The effect of composition.* Chem. Eng. Data Ser., 1958. **3**(1): p. 131-140.
35. DeCoste, H., R.H., *Coloured Polyvinyl chloride plastics for outdoor applications.* SPE J., 1962. **18**: p. 431-439.
36. Allen, N.S., *Action of light on dyed and pigmented polymers.*, in *Polymers in Conservation.* 1992, Royal Society of Chemistry:London.
37. Evans, M., *To weather or not to weather.* Surface world, 1999(June).
38. Ellinger, M.L., *Correlation of weathering results.* Journal of coatings technology, 1977. **49**(627).
39. Garner, B.L., Papillo, P. J., *Accelerated outdoor exposure testing in evaluation of ultraviolet light stabilisers for plastics.* I&EC Product Research and Development, 1962. **1**(4).
40. *A choice of lamps for the QUV.* 1994, Q-Panel Lab Products: Cleveland.
41. Skerry, B.S., Alvi, A., Lindren, K. I., *Environmental and electrochemical tests methods for the evaluation of protective organic coatings.* Journal of coatings technology, 1988. **60**(765).
42. Torikai, A., Hasegawa, H., *Accelerated photodegradation of poly(vinyl chloride).* Polymer Degradation and Stability, 1999(63): p. 441-445.
43. Timmins, F.D., *Avoiding paint failures by prohesion.* Oil and Colour Chemists Assoc., 1979. **62**(4).
44. Brennan, P.J., Grossman, S. J. *Combined corrosion/weathering exposures: a status report.* in *16th Annual Symposium of the South African Division of the Oil and Colour Chemists Association.* 1996. Cape Town, South Africa.
45. Meekin, G.E., Hill, H.E., *Applied techniques in statistics for selected industries; coatings, paints and pigments.* 1984: John Wiley & Sons.
46. Nelson, W., *Applied life data analysis.* 1982, New York: John Wiley & Sons.

47. Guseva, O., Brunner, S., Richner, P., *Service life prediction for aircraft coatings.* Polymer Degradation and Stability, 2003(82): p. 1–13.
48. Cunningham, G.P., Hansen, C. M. *Examination of weathered coatings by photoelectron spectroscopy and Fourier transform infrared spectroscopy.* in *59th Annual Meeting of the Federation of Societies for Coatings Technology.* 1981. Detroit.
49. Cho, S., Choi, W., *Solid-phase photocatalytic degradation of PVC–TiO_2 polymer composites.* Journal of Photochemistry and Photobiology A, 2001(Chemistry 143): p. 221–228.
50. Birer, O., Suzera, S. , Sevil, U.A. , Guven, O., *UV–VIS, IR and XPS analysis of UV induced changes in PVC composites.* Journal of Molecular Structure, 1999(482–483): p. 515–518.
51. Beltran, M., Marcilla, A., *PVC Plastisols decomposition by FT-IR spectroscopy.* Eur. Polym. J. Vol., 1997. **33**(8): p. 1271-1280.
52. Gesenhues, U., *Influence of titanium dioxide pigments on the photodegradation of poly(vinyl chloride).* Polymer Degradation and Stability, 2000(68): p. 185-196.
53. Bierwagen, G.P., Tallman, D.E., *Choice and measurement of crucial aircraft coatings system properties.* Progress in Organic Coatings, 2001(41): p. 201–216.
54. Bierwagen, G.P., *Increased durability of aircraft coatings by the use of pigmented polymer beads.* J. Coat. Technol., 1982. **54**(695): p. 19–24.
55. Hunt, R.W.G., *Measuring Colour.* 1984: Ellis Horwood.
56. Hughes, W. *Photodegradation of paint films containing Titanium Dioxde Pigments.* in *10th FATIPEC Congress.* 1970: Verlag Chemie GmbH.
57. Martin, J.W., Saunders, S.C., Floyd, F.L., Wineburg, J.P., *Methodologies for predicting the service lifetimes of coating systems*, D. Brezinsky, Miranda, T.J., Editor. 1996, Federation of Societies for Coatings Technology.
58. Ashton, H.E., *Evaluating the performance of organic coatings and building materials in ASTM*, in *Permanence of Organic Coatings, STP 781.* 1982, American Society for Testing and Materials.: Philadelphia. p. 67–85.
59. Brand, B.G., Nowacki, L.J, Mirick, W., Mueller, E.R., *Predicting service life of organic coatings. A state of the art review.* Journal Paint Technology, 1968. **62**: p. 37–42.
60. Berg, C.J., Jarosz, |W.R., Salanthe, G.F., *Performance of polymers in pigmented systems.* Journal Paint Technology, 1967. **39**: p. 436–53.
61. Clark, F.G., *Accelerated and outdoor weathering of colored vinyl films.* Industrial Engineering Chemistry, 1952. **44**: p. 2697–709.
62. White, J.R., Turnbull, A., *Weathering of polymers: mechanisms of degradation and stabilization, testing strategies and modelling.* Journal of Materials Science, 1994. **29**: p. 584-613.
63. Allen, N.S., *A study of the light absorption properties of polymer films using UV-visible derivative spectroscopy.* Polymer Photochemistry 1, 1981: p. 43–55.
64. Andrady, A.L., Torikai, A., Fueki, K., *Photodegradation of rigid PVC formulations Part I. Wavelength sensitivity to lightinduced yellowing by monochromatic light.* Journal Applied Polymer Science, 1989. **37**: p. 935–46.

65. Andrady, A.L., Searle, N.Z., *Photodegradation of rigid PVC formulations. Part II. Spectral sensitivity of light-induced yellowing by polychromatic light.* Polymer Degradation and Stability, 1989. **37**: p. 2789–2802.
66. Arney, J.S., Jacobs, A.J., *Accelerated aging of paper—the relative importance of atmospheric oxidation.* Tappi, 1979. **62**: p. 89–91.
67. Feller, R.L., Lee, S.B, Bogaard, J., *The darkening and bleaching of paper by various wavelengths in the visible and ultraviolet.*, B.a.P.G. Postprints, Editor. 1982, American Institute for Conservation of Historic and Artistic Works: Milwaukee.
68. Feller, R.L., *Accelerated Aging, Photochemical and Thermal Aspects.* 1994: The J. Paul Getty Trust.
69. Feller, R.L., *The deteriorating effect of light on museum objects: Principles of photochemistry, the effect on varnishes and paint vehicles and on paper.* Museum News, Technical Supplement, 1964. **3**(June).
70. Arney, J.S., A. Jacobs, A.J., Newman, R. and :. *The influence of oxygen on the fading of organic colorants.* Journal American Institute for Conservation, 1979. **18**: p. 108–17.
71. Down, J.L., *The yellowing of epoxy resin adhesives: Report on natural dark aging.* Studies in Conservation, 1984. **29**: p. 63–76.
72. Down, J.L., *The yellowing of epoxy resin adhesives: Report on high-intensity light aging.* Studies in Conservation, 1986. **31**: p. 159–70.
73. Allen, N.S., *Factors influencing the photostability of reactive dyes in polymers.* Polymer Photochemistry, 1981. **1**: p. 275–83.
74. Allen, N.S., *Photofading mechanisms of dyes in solution and polymer media.* Review Progress in Coloration, 1987. **17**: p. 61–71.
75. Kubelka, P., Munk, F., *Ein Beitrag zur Optik der Farbenstriche.* Z. Tech. Phys., 1931. **12**: p. 593.
76. Schuster, A., *Radiation through a foggy atmosphere.* Astrophys, J., 1905. **21**(1).
77. Walowitt, E., McCarthy, C.J., Berns, R.S., *An algorithm for the optimisation of Kubelka-Munk absorption ans scattering coeficients.* Color Res. and Appl., 1987. **12**: p. 340.
78. Nobbs, J.H., *Kubelka-Munk theory and the prediction of reflactance.* Rev. Prog. Coloration, 1985. **15**: p. 66.
79. Williams, D.H., Fleming, I., *Spectroscopic methods in organic chemistry.* 5 ed. 1995, England: McGraw-Hill.
80. Matauna, L.M., Kamdem, D.P., Zhang, J., *Photoaging and Stabilization of Rigid PVC/Wood-Fiber Composites.* Journal of Applied Polymer Science, 2001. **80**: p. 1943–1950.
81. Pouchert, C.J., ed. *The Aldrich Library of FTIR Spectra.*
82. *QUV Accelerated Weathering Tester with Solar Irradiance Control,operating manual.* 1992, Q-Panel Company: Bolton, England.
83. *http://www.metoffice.com/climate/uk/averages/19712000/index.html.* Met Office.
84. Rozenberg, G.V., *Twilight: A Study in Atmospheric Optics.* 1966, New York: Plenum Press.
85. Dam, O.v., *http://www.geo.vu.nl/~damo/potrad/potrad_calcul.htm.* 2002.

86. Gueymard, C., *Parameterized transmittance model for direct beam and circumsolar spectral irradiance.* Solar Energy, 2001. **71**(5): p. 325-346.
87. Gueymard, C., Myers, D.,Emery, K., *Proposed reference irradiance spectra for solar energy systems testing.* Solar Energy, 2002. **73**(6): p. 443-467.
88. Emery, K., Myers, D., *http://rredc.nrel.gov/solar/spectra/am1.5/.* 2004.
89. Gueymard, C., *The sun's total and spectral irradiance for solar energy applications and solar radiation models.* Solar Energy, 2004. **76**(4): p. 423-453.
90. Rosendahl, F. in *XIII FATIPEC Congress*. 1976. Juan les Pins.
91. Bourroughs, W.J., *Weather cycles: Real or Imaginary*. 1992, New York: Cambridge University Press.
92. Masters, L.W., Brandt, E., *Prediction of service life of building materials and components.* Materials and Structures, 1987. **20**: p. 55.
93. Wicks, Z.W., *Research challenges in coating science.* Proc. ACS Division of Polymeric Materials: Science and Engineering, 1988. **59**: p. 269.
94. Martin, J.W., McKnight, M.E.,, *Prediction of the service life coatings on steel part II: Quantitative prediction of the service life of a coating system.* Journal of Coatings Technology, 1985. **62**(724): p. 39.
95. O'Regan, B., Grätzel, M., Nature, 1991. **353**: p. 737-739.
96. Smestad, G.P., Grätzel, M., *J. Chem. Educ.* 1998. **75**: p. 752.
97. Kay, A., Grätzel,M., J. Phys. Chem., 1993. **97**: p. 6272.
98. *www.mansolar.nl.*

Appendix I

Appendix I

MAD and error tables

Shade	pigmentation	QUV	Rye	2000 NonC		2000 Cond		2000 C hor		22 months Rye	
		MAD	MAD	max diff	ratio	max diff	ratio	max diff	ratio	max diff	ratio
R1	0.1 red 0 TiO2	0.046	0.055	**0.027**	0.577	0.002	0.047	**0.071**	**1.532**	0.017	0.311
R2	0.1 red 1 TiO2	0.046	0.038	0.007	0.161	0.005	0.120	0.002	0.054	0.015	0.401
R3	0.1 red 5 TiO2	0.044	0.068	0.013	0.289	0.006	0.131	0.004	0.102	0.006	0.086
R4	0.25 red 0 TiO2	0.048	0.018	0.003	0.064	0.004	0.093	**0.089**	**1.836**	0.018	0.978
R5	0.25 red 1 TiO2	0.032	0.051	0.014	0.438	0.010	0.301	0.014	0.435	0.008	0.157
R6	0.25 red 5 TiO2	0.047	0.014	0.006	0.135	0.007	0.156	0.018	0.388	0.013	0.937
R7	0.5 red 0 TiO2	0.031	0.013	0.006	0.192	0.012	0.394	0.019	0.632	0.010	0.766
R8	0.5 red 1 TiO2	0.042	0.029	0.006	0.147	0.006	0.137	0.012	0.281	**0.031**	1.041
R9	0.5 red 5 TiO2	0.031	0.013	0.004	0.127	**0.031**	**1.002**	0.016	0.507	0.014	1.084
R10	0.5 red 10 TiO2	0.043	0.011	0.006	0.144	0.018	0.414	0.005	0.123	0.008	0.732
R11	0.5 red 15 TiO2	0.025	0.032	0.005	0.211	0.007	0.299	**0.022**	0.894	0.017	0.528
R12	1.5 red 0 TiO2	0.031	0.027	0.005	0.168	0.011	0.366	0.017	0.557	0.011	0.421
R13	1.5 red 1 TiO2	0.023	0.010	0.005	0.220	0.002	0.078	**0.023**	0.995	0.006	0.624
R14	1.5 red 5 TiO2	0.037	0.036	0.004	0.110	0.009	0.248	0.015	0.412	0.007	0.199
R15	1.5 red 10 TiO2	0.495	0.039	0.017	0.034	**0.029**	0.059	0.013	0.027	0.027	0.680
R16	1.5 red 15 TiO2	0.026	0.027	0.002	0.070	0.012	0.462	0.014	0.540	0.013	0.462
R17	2.5 red 0 TiO2	0.064	0.021	0.006	0.095	0.007	0.114	0.015	0.227	0.010	0.467
R18	2.5 red 1 TiO2	0.043	0.018	0.016	0.367	0.018	0.425	0.008	0.181	0.010	0.545
R19	2.5 red 5 TiO2	0.041	0.050	0.005	0.134	0.009	0.215	0.009	0.210	0.025	0.491
R20	2.5 red 10 TiO2	0.058	0.052	0.004	0.063	0.006	0.097	0.010	0.172	0.014	0.271
R21	2.5 red 15 TiO2	0.057	0.021	0.004	0.066	0.007	0.114	**0.032**	0.558	0.016	0.746
B1	0.05 blue 0 TiO2	0.031	0.025	0.013	0.428	0.008	0.251	0.004	0.132	0.019	0.760
B2	0.05 blue 1 TiO2	0.113	0.055	0.005	0.046	0.007	0.058	0.003	0.030	0.007	0.131
B3	0.05 blue 5 TiO2	0.109	0.054	0.013	0.119	**0.020**	0.185	0.012	0.107	0.008	0.152
B4	0.1 blue 0 TiO2	0.042	0.034	0.004	0.105	0.004	0.097	0.010	0.231	0.009	0.253
B5	0.1 blue 1 TiO2	0.101	0.026	0.006	0.064	0.012	0.118	0.005	0.044	0.014	0.513
B6	0.1 blue 5 TiO2	0.038	0.018	0.005	0.139	0.004	0.118	**0.037**	0.966	0.004	0.205
B7	0.2 blue 0 TiO2	0.120	0.034	0.015	0.128	0.008	0.063	0.004	0.032	0.005	0.139
B8	0.2 blue 1 TiO2	0.063	0.017	0.007	0.118	**0.020**	0.322	0.011	0.175	0.013	0.806
B9	0.2 blue 5 TiO2	0.079	0.042	0.003	0.032	0.012	0.154	0.005	0.067	0.003	0.061
B10	0.2 blue 10 TiO2	0.060	0.047	0.018	0.303	0.005	0.080	**0.020**	0.334	0.007	0.149
B11	0.2 blue 15 TiO2	0.091	0.073	0.008	0.090	0.003	0.036	0.011	0.122	0.008	0.107
B12	0.6 blue 0 TiO2	0.050	0.020	0.002	0.042	0.002	0.036	0.004	0.078	0.006	0.299
B13	0.6 blue 1 TiO2	0.061	0.021	0.002	0.036	0.005	0.077	**0.031**	0.513	**0.034**	**1.638**
B14	0.6 blue 5 TiO2	0.071	0.044	0.002	0.027	0.008	0.115	**0.048**	0.683	0.020	0.447
B15	0.6 blue 10 TiO2	0.035	0.057	0.002	0.045	0.003	0.096	0.003	0.099	0.007	0.120
B16	0.6 blue 15 TiO2	0.064	0.055	0.004	0.064	0.012	0.180	0.007	0.113	0.006	0.113
B17	1 blue 0 TiO2	0.044	0.010	0.001	0.023	0.001	0.030	0.002	0.043	0.009	0.893
B18	1 blue 1 TiO2	0.055	0.011	0.001	0.018	0.002	0.034	0.003	0.047	0.004	0.378
B19	1 blue 5 TiO2	0.030	0.028	0.001	0.033	0.004	0.147	0.003	0.093	0.003	0.112
B20	1 blue 10 TiO2	0.032	0.015	0.006	0.170	0.005	0.148	0.006	0.173	0.014	0.972
B21	1 blue 15 TiO2	0.026	0.019	0.004	0.161	0.012	0.463	0.006	0.245	0.008	0.412

Shade	pigmentation	QUV	Rye	2000 NonC		2000 Cond		2000 C hor		22 months Rye	
		MAD	MAD	max diff	ratio	max diff	ratio	max diff	ratio	max diff	ratio
G1	0.05 green 0 TiO2	0.163	0.067	0.009	0.056	0.010	0.060	**0.020**	0.123	0.026	0.394
G2	0.05 green 1 TiO2	0.105	0.043	0.002	0.017	0.008	0.081	0.006	0.053	0.005	0.110
G3	0.05 green 5 TiO2	0.209	0.105	0.012	0.055	0.008	0.037	0.008	0.038	0.005	0.049
G4	0.1 green 0 TiO2	0.099	0.022	0.010	0.101	0.003	0.027	0.007	0.074	0.006	0.287
G5	0.1 green 1 TiO2	0.136	0.014	0.006	0.044	0.005	0.034	0.006	0.046	0.005	0.393
G6	0.1 green 5 TiO2	0.036	0.010	0.019	0.520	0.004	0.101	0.003	0.076	0.017	**1.760**
G7	0.2 green 0 TiO2	0.148	0.023	0.007	0.046	0.002	0.010	0.003	0.019	0.008	0.326
G8	0.2 green 1 TiO2	0.039	0.023	0.001	0.018	0.005	0.116	0.014	0.348	0.014	0.607
G9	0.2 green 5 TiO2	0.056	0.025	0.003	0.045	0.003	0.050	0.012	0.206	0.016	0.631
G10	0.2 green 10 TiO2	0.059	0.036	0.002	0.039	0.007	0.116	0.006	0.110	0.007	0.197
G11	0.2 green 15 TiO2	0.154	0.053	0.006	0.036	0.009	0.056	0.009	0.060	0.019	0.366
G12	0.6 green 0 TiO2	0.054	0.042	0.001	0.013	0.003	0.048	0.018	0.334	0.007	0.159
G13	0.6 green 1 TiO2	0.034	0.018	0.004	0.107	0.003	0.101	0.007	0.202	0.009	0.508
G14	0.6 green 5 TiO2	0.295	0.020	0.019	0.066	0.012	0.039	0.015	0.050	**0.062**	**3.064**
G15	0.6 green 10 TiO2	0.073	0.029	0.002	0.029	0.002	0.020	**0.043**	0.584	0.005	0.160
G16	0.6 green 15 TiO2	0.133	0.093	0.002	0.014	0.001	0.009	0.013	0.100	0.007	0.076
G17	1 green 0 TiO2	0.061	0.028	0.003	0.049	0.002	0.034	0.002	0.026	0.013	0.457
G18	1 green 1 TiO2	0.022	0.021	0.002	0.105	0.004	0.160	0.003	0.133	0.006	0.270
G19	1 green 5 TiO2	0.021	0.010	0.001	0.058	0.005	0.244	0.014	0.697	0.008	0.800
G20	1 green 10 TiO2	0.153	0.021	0.002	0.012	0.002	0.010	0.015	0.095	0.008	0.388
G21	1 green 15 TiO2	0.028	0.026	0.010	0.334	0.005	0.186	0.012	0.408	**0.032**	1.213
P1	0.25 1-yellow 0 TiO2	0.067	0.110	0.013	0.187	**0.021**	0.310	0.013	0.193	0.028	0.253
P2	0.25 1-yellow 1 TiO2	0.083	0.075	0.006	0.075	**0.036**	0.436	0.010	0.116	0.015	0.195
P3	0.25 1-yellow 5 TiO2	0.177	0.054	0.012	0.068	0.009	0.050	0.016	0.088	**0.055**	1.024
P4	1 1-yellow 0 TiO2	0.063	0.054	0.006	0.096	0.002	0.030	0.012	0.192	0.012	0.219
P5	1 1-yellow 1 TiO2	0.063	0.053	0.014	0.216	**0.026**	0.413	0.015	0.235	0.023	0.423
P6	1 1-yellow 5 TiO2	0.035	0.059	0.005	0.149	0.009	0.264	0.005	0.132	0.008	0.135
P7	2 1-yellow 0 TiO2	0.069	0.039	0.003	0.042	0.006	0.079	**0.031**	0.450	0.009	0.236
P8	2 1-yellow 1 TiO2	0.038	0.043	0.002	0.042	**0.029**	0.755	0.007	0.169	0.004	0.102
P9	2 1-yellow 5 TiO2	0.057	0.047	0.003	0.060	0.014	0.245	0.017	0.307	0.011	0.242
P10	2 1-yellow 10 TiO2	0.053	0.068	0.004	0.076	0.006	0.106	0.010	0.187	0.011	0.161
P11	2 1-yellow 15 TiO2	0.131	0.033	0.016	0.120	0.014	0.104	0.007	0.051	**0.041**	1.239
P12	6 1-yellow 0 TiO2	0.060	0.047	0.012	0.207	0.005	0.078	0.003	0.058	**0.035**	0.749
P13	6 1-yellow 1 TiO2	0.076	0.045	0.004	0.056	0.010	0.128	**0.025**	0.328	0.017	0.378
P14	6 1-yellow 5 TiO2	0.043	0.048	0.015	0.337	0.010	0.226	0.006	0.127	0.008	0.177
P15	6 1-yellow 10 TiO2	0.049	0.038	0.009	0.181	0.007	0.151	0.012	0.236	0.012	0.317
P16	6 1-yellow 15 TiO2	0.046	0.041	0.010	0.219	0.013	0.285	**0.077**	**1.678**	**0.037**	0.889
P17	10 1-yellow 0 TiO2	0.096	0.056	0.019	0.193	0.018	0.191	0.006	0.064	**0.048**	0.856
P18	10 1-yellow 1 TiO2	0.059	0.051	0.012	0.201	**0.020**	0.345	0.012	0.205	0.015	0.303
P19	10 1-yellow 5 TiO2	0.034	0.076	0.020	0.579	0.011	0.323	0.006	0.166	0.023	0.307
P20	10 1-yellow 10 TiO2	0.084	0.031	0.010	0.123	0.012	0.140	0.011	0.125	0.011	0.360
P21	10 1-yellow 15 TiO2	0.072	0.037	0.013	0.181	0.005	0.071	**0.021**	0.289	**0.035**	0.943

Shade	pigmentation	QUV	Rye	2000 NonC		2000 Cond		2000 C hor		22 months Rye	
		MAD	MAD	max diff	ratio	max diff	ratio	max diff	ratio	max diff	ratio
S1	0.25 2-yellow 0 TiO2	0.070	0.056	0.006	0.084	0.013	0.189	0.006	0.092	0.025	0.452
S2	0.25 2-yellow 1 TiO2	0.104	0.043	0.007	0.065	0.012	0.114	0.018	0.173	0.011	0.244
S3	0.25 2-yellow 5 TiO2	0.062	0.044	0.017	0.279	0.010	0.168	0.008	0.133	0.013	0.295
S4	1 2-yellow 0 TiO2	0.090	0.077	**0.043**	0.476	0.013	0.143	**0.027**	0.298	0.026	0.338
S5	1 2-yellow 1 TiO2	0.051	0.026	0.013	0.252	**0.028**	0.552	0.010	0.201	0.008	0.286
S6	1 2-yellow 5 TiO2	0.041	0.017	0.016	0.379	**0.026**	0.627	0.015	0.350	0.006	0.365
S7	2.5 2-yellow 0 TiO2	0.109	0.122	**0.114**	**1.040**	**0.056**	0.513	**0.045**	0.412	**0.076**	0.626
S8	2.5 2-yellow 1 TiO2	0.050	0.024	**0.034**	0.683	0.013	0.270	0.006	0.111	0.017	0.693
S9	2.5 2-yellow 5 TiO2	0.036	0.028	0.004	0.118	0.007	0.195	0.002	0.047	0.027	0.957
S10	2.5 2-yellow 10 TiO2	0.045	0.037	0.005	0.102	0.002	0.044	0.006	0.136	0.022	0.583
S11	2.5 2-yellow 15 TiO2	0.061	0.040	0.017	0.278	0.009	0.144	0.018	0.292	0.030	0.739
S12	5 2-yellow 0 TiO2	0.033	0.029	0.014	0.438	0.007	0.217	0.007	0.227	0.013	0.457
S13	5 2-yellow 1 TiO2	0.041	0.013	0.010	0.232	0.008	0.191	0.005	0.121	0.011	0.850
S14	5 2-yellow 5 TiO2	0.038	0.029	0.007	0.187	0.008	0.221	**0.031**	0.824	0.005	0.158
S15	5 2-yellow 10 TiO2	0.036	0.034	0.009	0.258	0.003	0.087	0.008	0.222	0.005	0.149
S16	5 2-yellow 15 TiO2	0.029	0.028	0.006	0.216	0.007	0.237	0.004	0.144	0.007	0.267
S17	10 2-yellow 0 TiO2	0.016	0.020	0.005	0.321	0.005	0.334	0.005	0.327	0.012	0.618
S18	10 2-yellow 1 TiO2	0.022	0.009	0.004	0.185	0.004	0.180	0.006	0.262	0.005	0.511
S19	10 2-yellow 5 TiO2	0.011	0.014	0.007	0.611	0.003	0.275	0.008	0.709	0.004	0.286
S20	10 2-yellow 10 TiO2	0.029	0.013	0.003	0.119	0.010	0.351	0.019	0.630	0.009	0.721
S21	10 2-yellow 15 TiO2	0.037	0.012	0.005	0.144	0.010	0.273	0.006	0.155	0.008	0.712
N1	base PVC 0 TiO2	0.338	0.350	**0.066**	0.194	**0.026**	0.077	0.016	0.048	**0.105**	0.299
N2	base PVC 1 TiO2	0.422	0.175	0.005	0.012	0.009	0.021	0.008	0.019	0.023	0.131
N3	base PVC 5 TiO2	0.191	0.126	**0.023**	0.119	0.006	0.031	0.015	0.077	**0.143**	1.135
N4	base PVC 10 TiO2	0.281	0.082	**0.145**	0.516	0.004	0.016	0.014	0.050	0.008	0.101
N5	base PVC 15 TiO2	0.082	0.086	0.015	0.184	0.008	0.093	0.017	0.204	**0.157**	**1.821**
Y1	0.5 2-yellow 0.05 green	0.019	0.022	0.009	0.486	0.003	0.164	**0.023**	**1.194**	0.018	0.801
Y2	2 2-yellow 0.2 green	0.010	0.009	0.002	0.175	0.002	0.214	0.005	0.487	0.003	0.304
Y3	5 2-yellow 0.5 green	0.009	0.004	0.003	0.340	0.001	0.148	0.006	0.681	0.001	0.318
Y4	10 2-yellow 1 green	0.011	0.003	0.001	0.044	0.001	0.122	0.003	0.227	0.003	0.871
Y5	0.5 2-yellow 0.02 green	0.055	0.038	0.013	0.227	0.003	0.054	**0.020**	0.366	0.015	0.387
Y6	2 2-yellow 0.08 green	0.022	0.007	0.003	0.130	0.002	0.080	0.005	0.237	0.015	**2.097**
Y7	5 2-yellow 0.2 green	0.011	0.004	0.002	0.188	0.002	0.198	0.009	0.885	0.005	1.209
Y8	10 2-yellow 0.4 green	0.010	0.003	0.002	0.228	0.001	0.139	0.001	0.119	0.002	0.821
Y9	0.25 2-yellow 0.05 green	0.091	0.060	**0.026**	0.285	0.004	0.046	0.007	0.074	0.019	0.309
Y10	0.5 2-yellow 0.1 green	0.063	0.026	0.002	0.024	0.004	0.055	0.009	0.147	0.013	0.504
Y11	2.5 2-yellow 0.5 green	0.009	0.006	0.002	0.266	0.001	0.116	0.001	0.116	0.001	0.196
Y12	5 2-yellow 1 green	0.006	0.004	0.004	0.569	0.002	0.237	0.001	0.174	0.001	0.324

Shade	pigmentation	QUV	Rye	2000 NonC		2000 Cond		2000 C hor		22 months Rye	
		MAD	MAD	max diff	ratio	max diff	ratio	max diff	ratio	max diff	ratio
M1	0.05 blue 0.25 red	0.024	0.009	0.001	0.025	0.003	0.132	0.003	0.124	0.006	0.724
M2	0.1 blue 0.5 red	0.010	0.003	0.001	0.084	0.000	0.032	0.002	0.179	0.002	0.815
M3	0.5 blue 2.5 red	0.002	0.001	0.000	0.192	0.001	0.288	0.004	**1.726**	0.001	1.200
M4	1 blue 5 red	0.003	0.001	0.001	0.190	0.000	0.114	0.001	0.190	0.002	1.250
M5	0.05 blue 0.1 red	0.017	0.006	0.005	0.284	0.001	0.046	0.003	0.145	0.003	0.531
M6	0.1 blue 0.2 red	0.009	0.005	0.001	0.086	0.004	0.460	0.002	0.193	0.001	0.196
M7	0.5 blue 1 red	0.001	0.002	0.001	0.401	0.001	0.882	0.002	**1.364**	0.001	0.765
M8	1 blue 2 red	0.003	0.001	0.001	0.228	0.001	0.419	0.001	0.342	0.001	1.125
M9	0.01 blue 0.25 red	0.068	0.018	0.003	0.040	0.004	0.064	0.005	0.073	0.006	0.342
M10	0.04 blue 1 red	0.042	0.013	0.001	0.029	0.001	0.012	0.004	0.100	0.003	0.225
M11	0.08 blue 2 red	0.018	0.009	0.000	0.022	0.001	0.071	0.002	0.104	0.001	0.128
M12	0.2 blue 5 red	0.016	0.006	0.004	0.233	0.000	0.018	0.001	0.061	0.003	0.429
C1	0.05 green 0.05 blue	0.156	0.050	0.005	0.033	0.019	0.121	0.010	0.062	**0.033**	0.660
C2	0.1 green 0.1 blue	0.153	0.013	0.019	0.123	0.010	0.063	0.011	0.074	0.011	0.888
C3	0.5 green 0.5 blue	0.085	0.007	0.010	0.122	0.008	0.098	0.002	0.019	0.004	0.507
C4	1 green 1 blue	0.040	0.011	0.011	0.271	0.004	0.088	0.012	0.298	0.004	0.366
C5	0.05 green 0.02 blue	0.114	0.048	0.009	0.079	0.002	0.017	**0.032**	0.282	**0.045**	0.944
C6	0.1 green 0.04 blue	0.047	0.021	0.005	0.095	0.006	0.116	0.006	0.133	0.008	0.392
C7	0.5 green 0.2 blue	0.072	0.023	0.009	0.119	0.004	0.053	0.006	0.086	0.008	0.321
C8	1 green 0.4 blue	0.279	0.007							0.004	0.547
C9	0.02 green 0.05 blue	0.064	0.009	0.012	0.187	0.013	0.205	**0.025**	0.385	0.017	**1.977**
C10	0.04 green 0.1 blue	0.090	0.006	0.017	0.193	0.006	0.067	0.012	0.131	**0.034**	**5.895**
C11	0.2 green 0.5 blue	0.052	0.020	0.002	0.039	0.014	0.264	0.002	0.033	0.011	0.569
C12	0.4 green 1 blue	0.031	0.013	0.001	0.029	0.001	0.038	0.005	0.169	0.017	1.313
O1	1 red 0.1 1-yellow	0.085	0.013	0.008	0.095	0.006	0.073	0.009	0.102	**0.071**	**5.508**
O2	2 red 0.2 1-yellow	0.497	0.069	0.008	0.016	0.015	0.030	0.015	0.029	0.018	0.265
O3	3 red 0.3 1-yellow	0.190	0.036	**0.026**	0.135	0.012	0.063	**0.043**	0.224	**0.064**	**1.801**
O4	5 red 0.5 1-yellow	0.057	0.059	**0.031**	0.547	0.013	0.228	**0.044**	0.766	0.025	0.420
O5	0.25 red 0.1 1-yellow	0.061	0.077	0.011	0.175	0.008	0.130	0.014	0.228	**0.046**	0.594
O6	0.5 red 0.2 1-yellow	0.060	0.030	0.005	0.075	0.018	0.295	0.015	0.245	**0.031**	1.017
O7	0.75 red 0.3 1-yellow	0.068	0.062	0.010	0.141	0.007	0.106	0.005	0.069	0.013	0.210
O8	1.25 red 0.5 1-yellow	0.064	0.033	0.005	0.087	**0.022**	0.351	0.007	0.115	0.018	0.548
O9	0.05 red 0.1 1-yellow	0.046	0.056	0.017	0.356	0.008	0.164	**0.072**	**1.563**	0.027	0.480
O10	0.1 red 0.2 1-yellow	0.047	0.108	0.007	0.152	0.009	0.186	**0.023**	0.477	0.011	0.104
O11	0.15 red 0.3 1-yellow	0.047	0.031	0.011	0.225	0.013	0.280	0.016	0.336	0.028	0.928
O12	0.25 red 0.5 1-yellow	0.047	0.084	0.014	0.297	**0.024**	0.521	0.006	0.135	0.028	0.331

Appendix I

Red

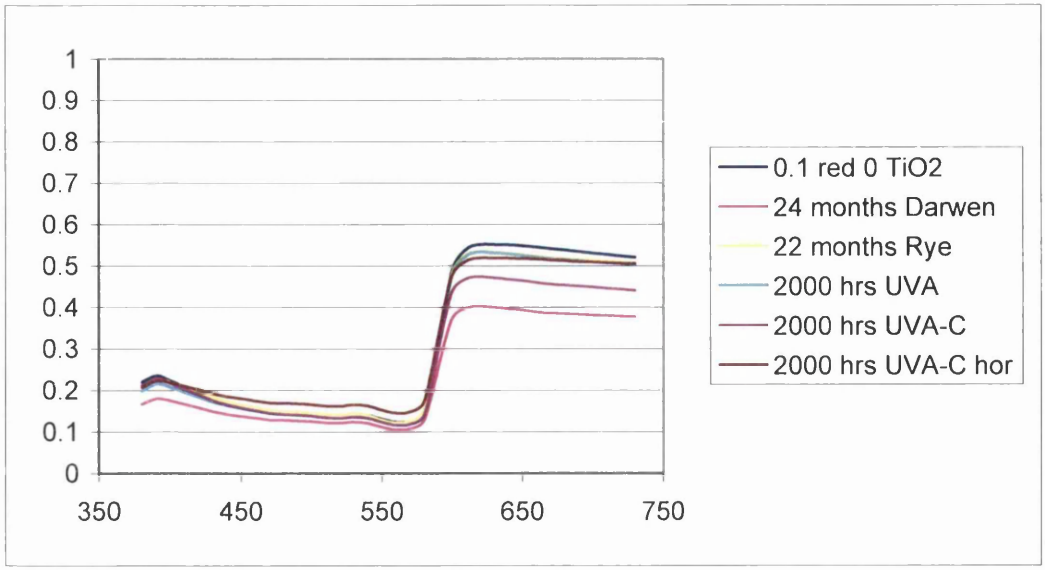
1
0.9
0.8
0.7
0.6
0.5
0.4
0.3
0.2
0.1
0
350
450
550
650
750
0.1 red 0 TiO2
24 months Darwen
22 months Rye
2000 hrs UVA
2000 hrs UVA-C
2000 hrs UVA-C hor

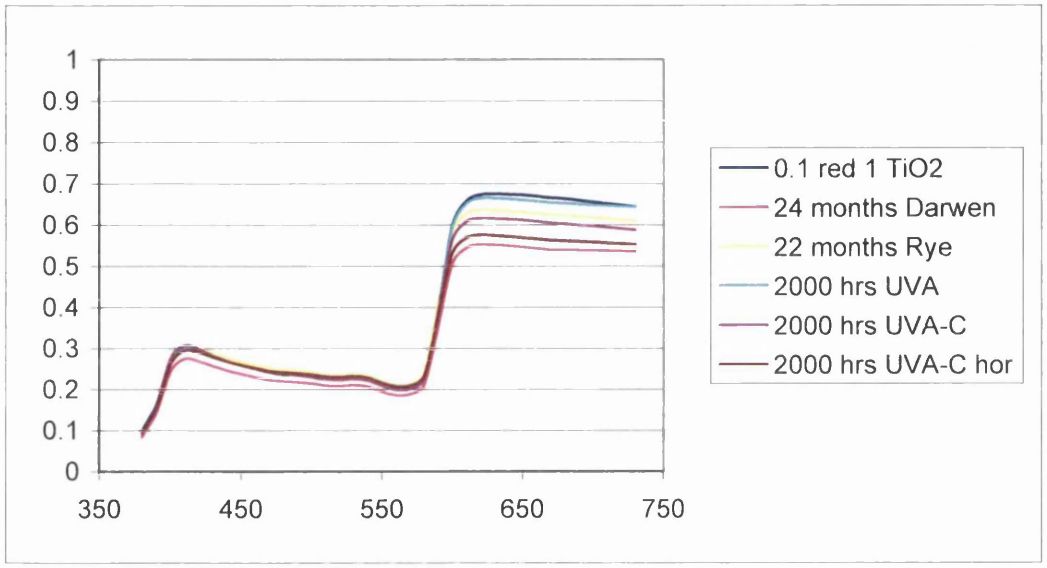
1
0.9
0.8
0.7
0.6
0.5
0.4
0.3
0.2
0.1
0
350
450
550
650
750
0.1 red 1 TiO2
24 months Darwen
22 months Rye
2000 hrs UVA
2000 hrs UVA-C
2000 hrs UVA-C hor

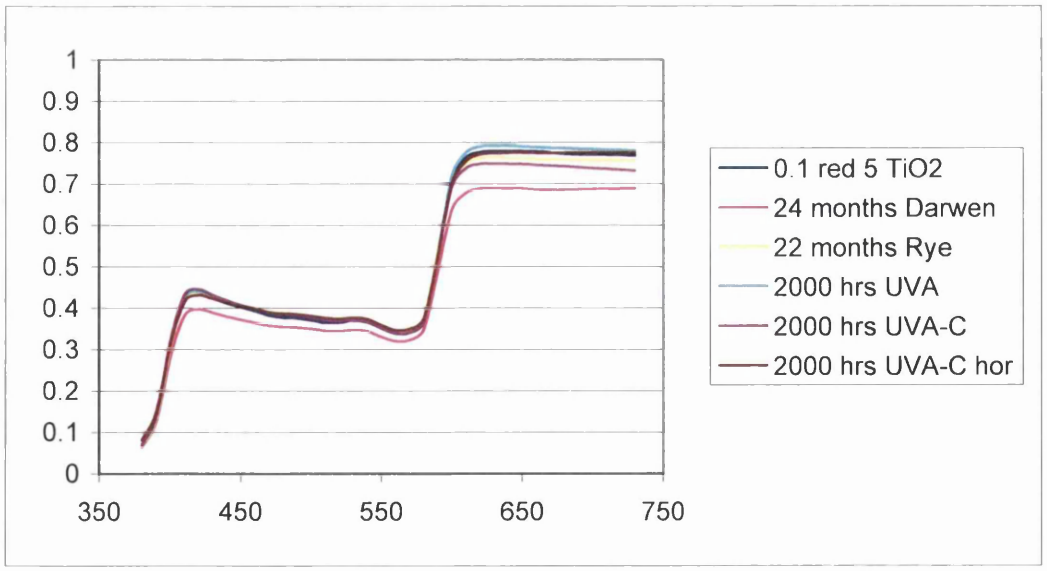
1
0.9
0.8
0.7
0.6
0.5
0.4
0.3
0.2
0.1
0
350
450
550
650
750
0.1 red 5 TiO2
24 months Darwen
22 months Rye
2000 hrs UVA
2000 hrs UVA-C
2000 hrs UVA-C hor

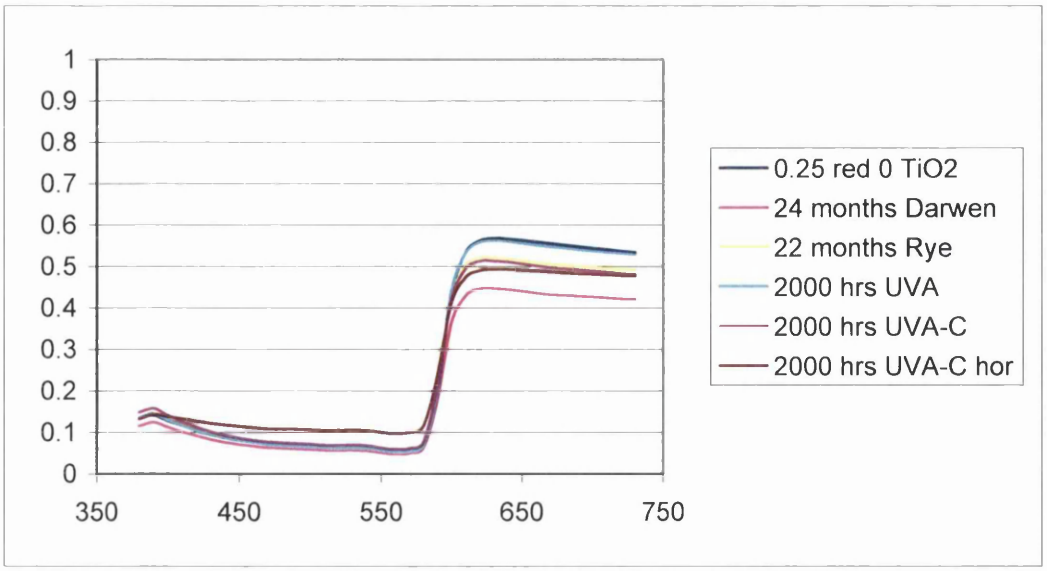
1
0.9
0.8
0.7
0.6
0.5
0.4
0.3
0.2
0.1
0
350
450
550
650
750
0.25 red 0 TiO2
24 months Darwen
22 months Rye
2000 hrs UVA
2000 hrs UVA-C
2000 hrs UVA-C hor

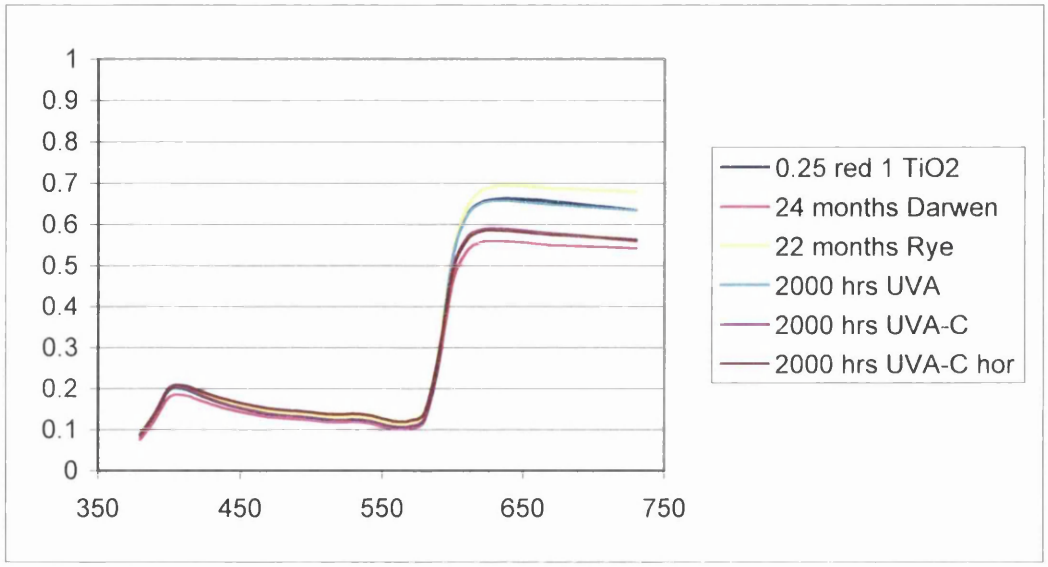
1
0.9
0.8
0.7
0.6
0.5
0.4
0.3
0.2
0.1
0
350
450
550
650
750
0.25 red 1 TiO2
24 months Darwen
22 months Rye
2000 hrs UVA
2000 hrs UVA-C
2000 hrs UVA-C hor

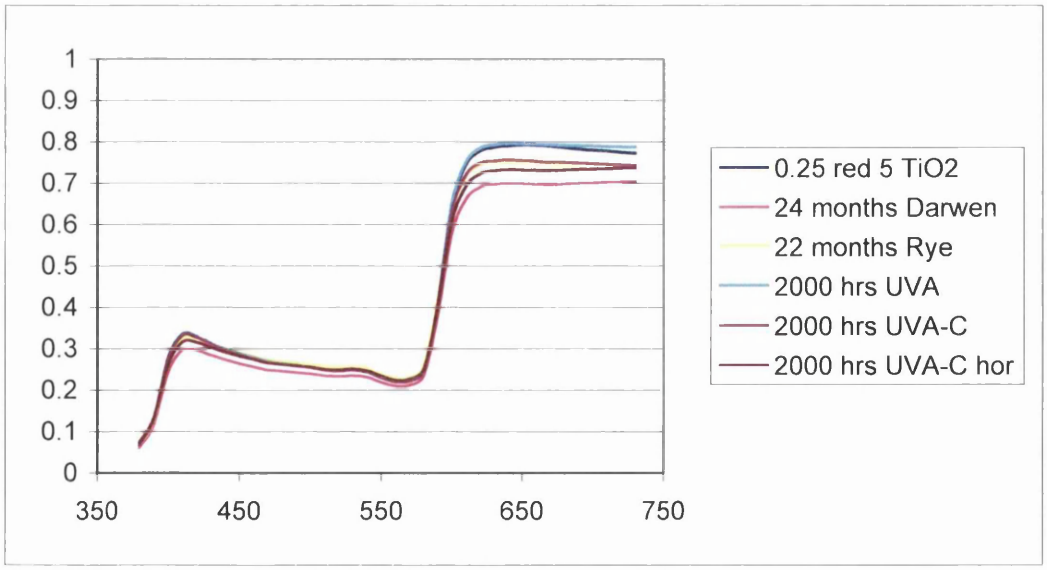
1
0.9
0.8
0.7
0.6
0.5
0.4
0.3
0.2
0.1
0
350
450
550
650
750
0.25 red 5 TiO2
24 months Darwen
22 months Rye
2000 hrs UVA
2000 hrs UVA-C
2000 hrs UVA-C hor

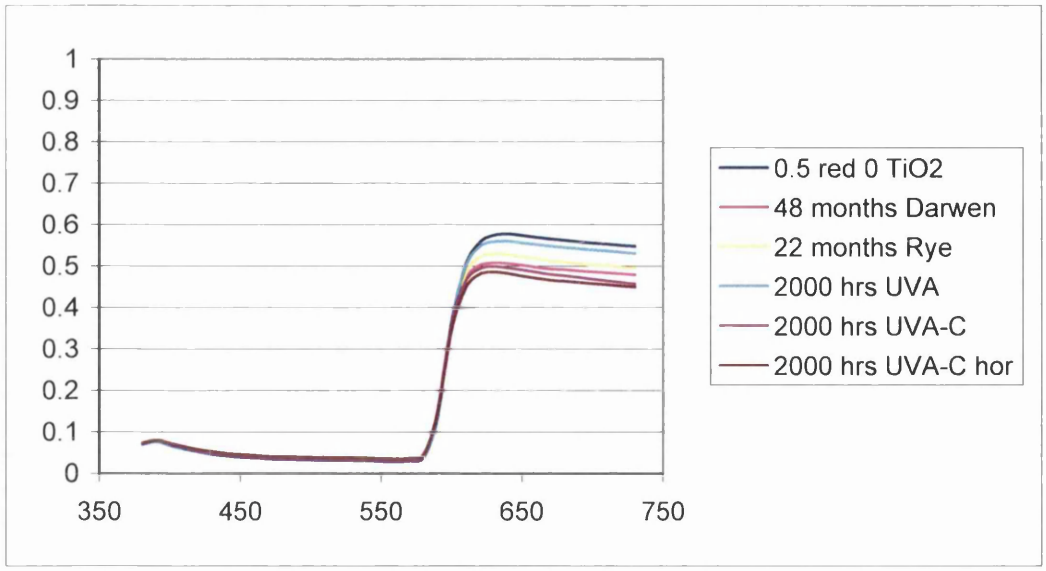
1
0.9
0.8
0.7
0.6
0.5
0.4
0.3
0.2
0.1
0
350
450
550
650
750
0.5 red 0 TiO2
48 months Darwen
22 months Rye
2000 hrs UVA
2000 hrs UVA-C
2000 hrs UVA-C hor

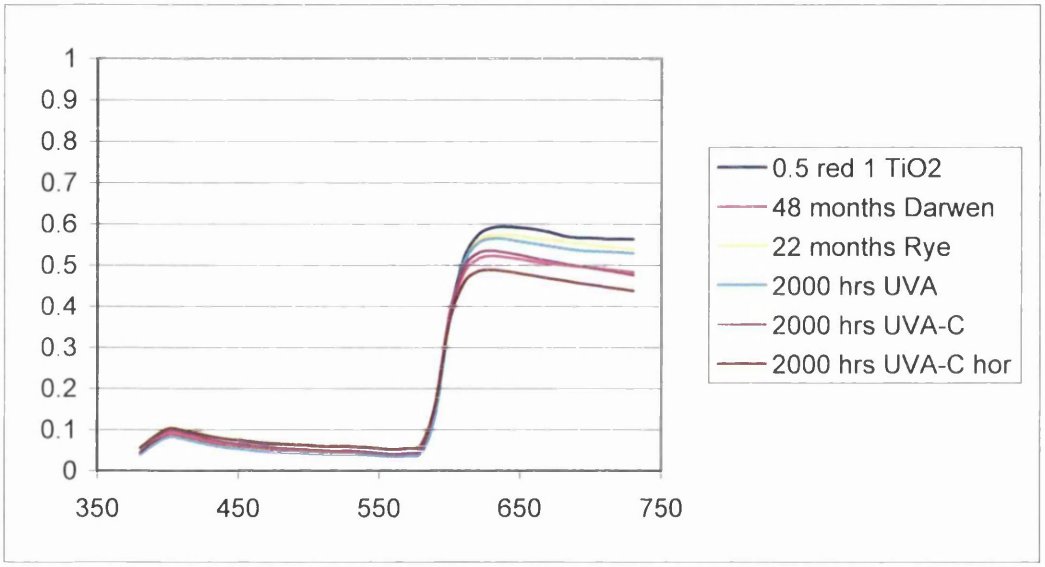
1
0.9
0.8
0.7
0.6
0.5
0.4
0.3
0.2
0.1
0
350
450
550
650
750
0.5 red 1 TiO2
48 months Darwen
22 months Rye
2000 hrs UVA
2000 hrs UVA-C
2000 hrs UVA-C hor

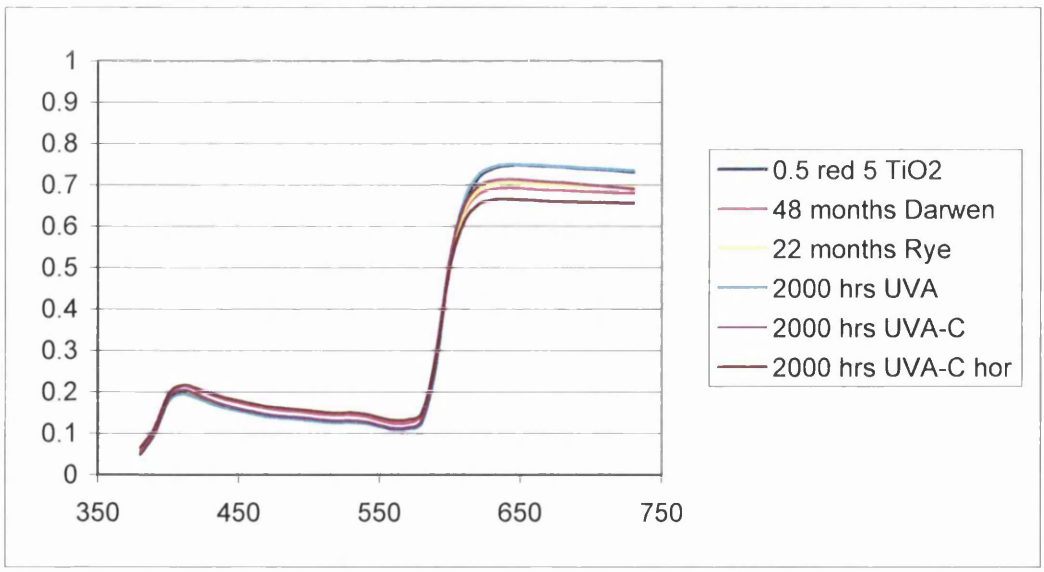
1
0.9
0.8
0.7
0.6
0.5
0.4
0.3
0.2
0.1
0
350
450
550
650
750
0.5 red 5 TiO2
48 months Darwen
22 months Rye
2000 hrs UVA
2000 hrs UVA-C
2000 hrs UVA-C hor

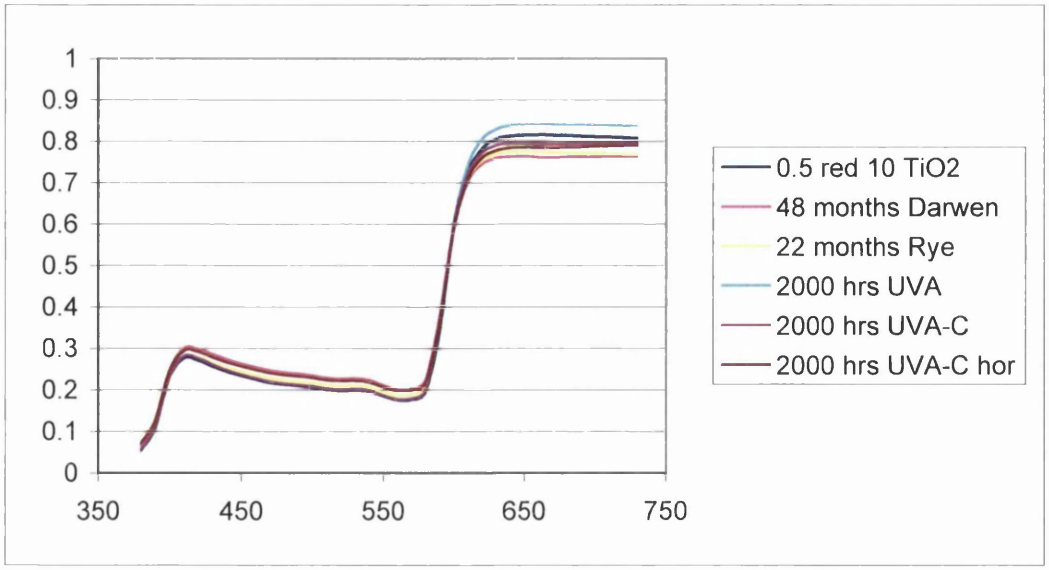
1
0.9
0.8
0.7
0.6
0.5
0.4
0.3
0.2
0.1
0
350
450
550
650
750
0.5 red 10 TiO2
48 months Darwen
22 months Rye
2000 hrs UVA
2000 hrs UVA-C
2000 hrs UVA-C hor

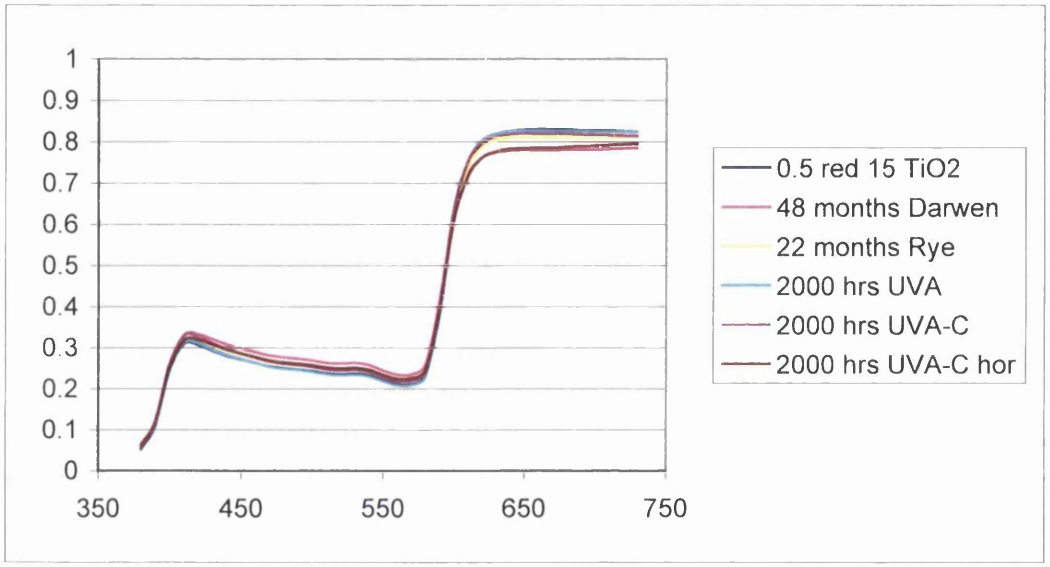
1
0.9
0.8
0.7
0.6
0.5
0.4
0.3
0.2
0.1
0
350
450
550
650
750
0.5 red 15 TiO2
48 months Darwen
22 months Rye
2000 hrs UVA
2000 hrs UVA-C
2000 hrs UVA-C hor

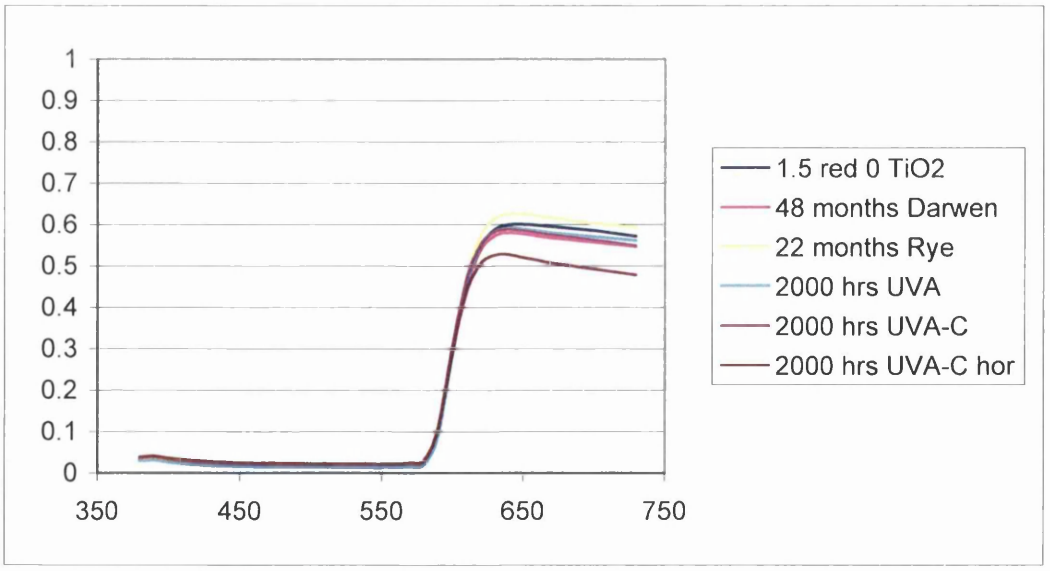
1
0.9
0.8
0.7
0.6
0.5
0.4
0.3
0.2
0.1
0
350
450
550
650
750
1.5 red 0 TiO2
48 months Darwen
22 months Rye
2000 hrs UVA
2000 hrs UVA-C
2000 hrs UVA-C hor

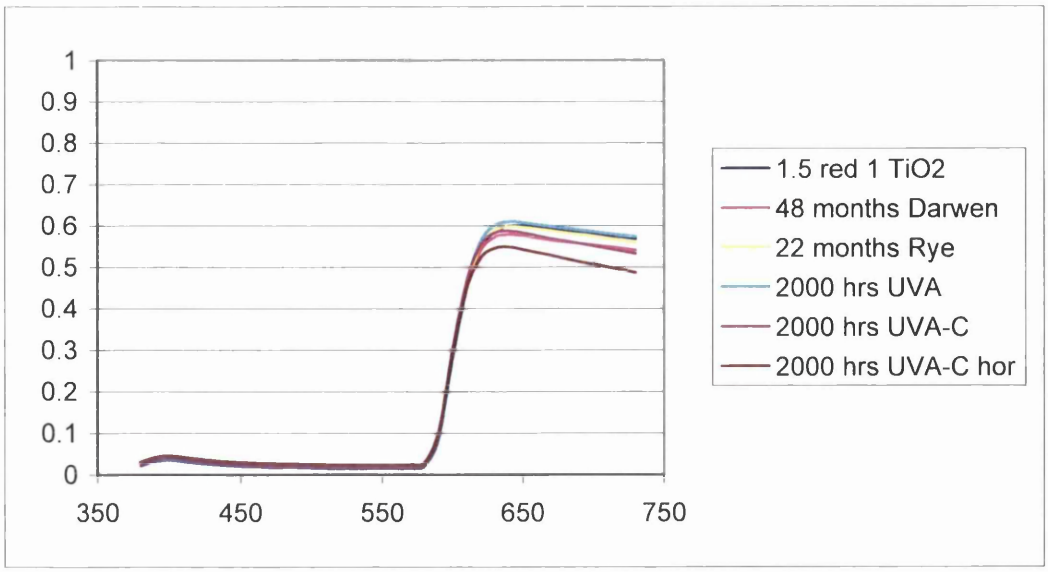
1
0.9
0.8
0.7
0.6
0.5
0.4
0.3
0.2
0.1
0
350
450
550
650
750
1.5 red 1 TiO2
48 months Darwen
22 months Rye
2000 hrs UVA
2000 hrs UVA-C
2000 hrs UVA-C hor

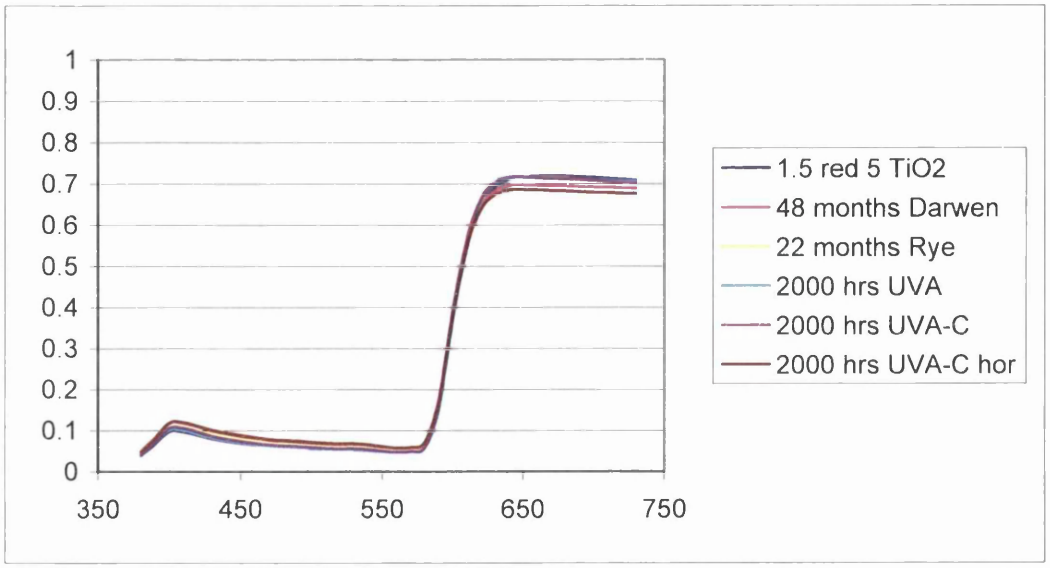
1
0.9
0.8
0.7
0.6
0.5
0.4
0.3
0.2
0.1
0
350
450
550
650
750
1.5 red 5 TiO2
48 months Darwen
22 months Rye
2000 hrs UVA
2000 hrs UVA-C
2000 hrs UVA-C hor

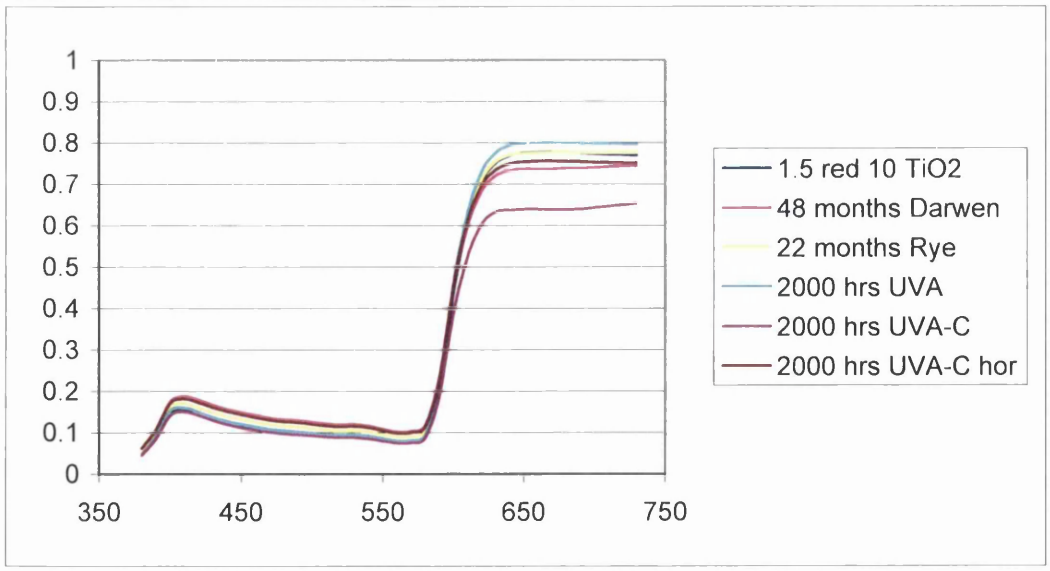
1
0.9
0.8
0.7
0.6
0.5
0.4
0.3
0.2
0.1
0
350
450
550
650
750
1.5 red 10 TiO2
48 months Darwen
22 months Rye
2000 hrs UVA
2000 hrs UVA-C
2000 hrs UVA-C hor

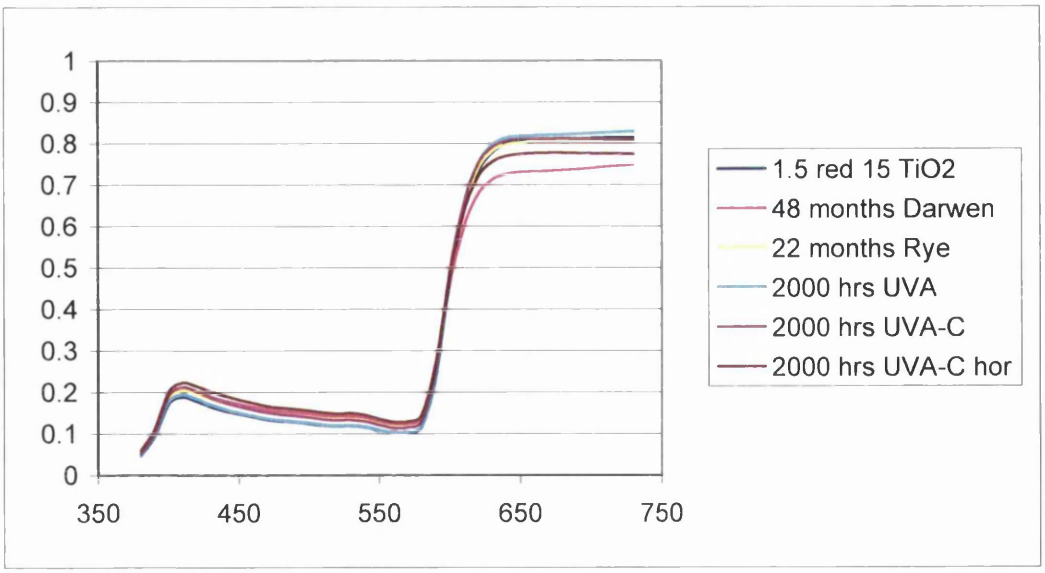
1
0.9
0.8
0.7
0.6
0.5
0.4
0.3
0.2
0.1
0
350
450
550
650
750
1.5 red 15 TiO2
48 months Darwen
22 months Rye
2000 hrs UVA
2000 hrs UVA-C
2000 hrs UVA-C hor

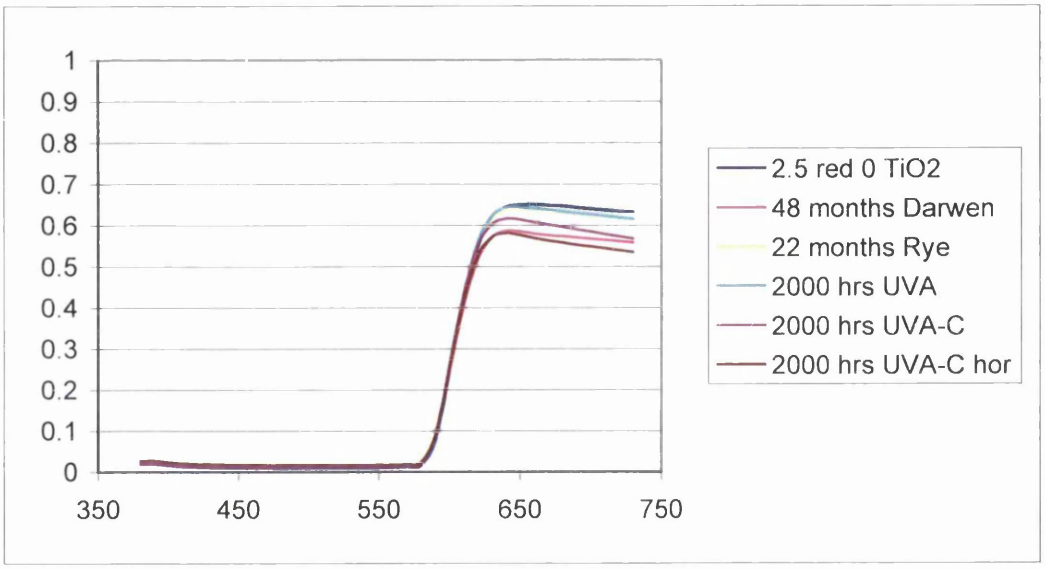
1
0.9
0.8
0.7
0.6
0.5
0.4
0.3
0.2
0.1
0
350
450
550
650
750
2.5 red 0 TiO2
48 months Darwen
22 months Rye
2000 hrs UVA
2000 hrs UVA-C
2000 hrs UVA-C hor

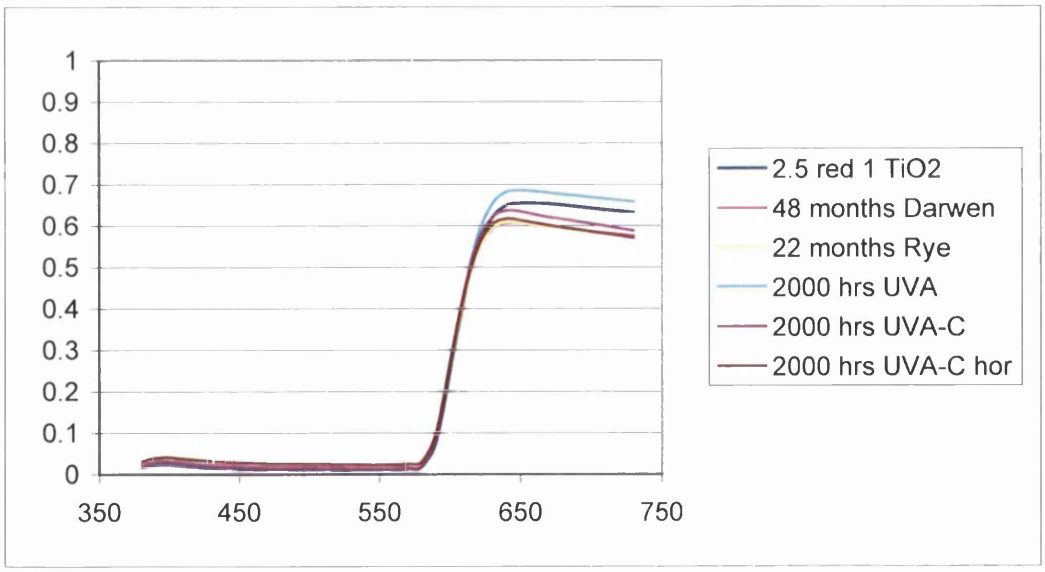
1
0.9
0.8
0.7
0.6
0.5
0.4
0.3
0.2
0.1
0
350
450
550
650
750
2.5 red 1 TiO2
48 months Darwen
22 months Rye
2000 hrs UVA
2000 hrs UVA-C
2000 hrs UVA-C hor

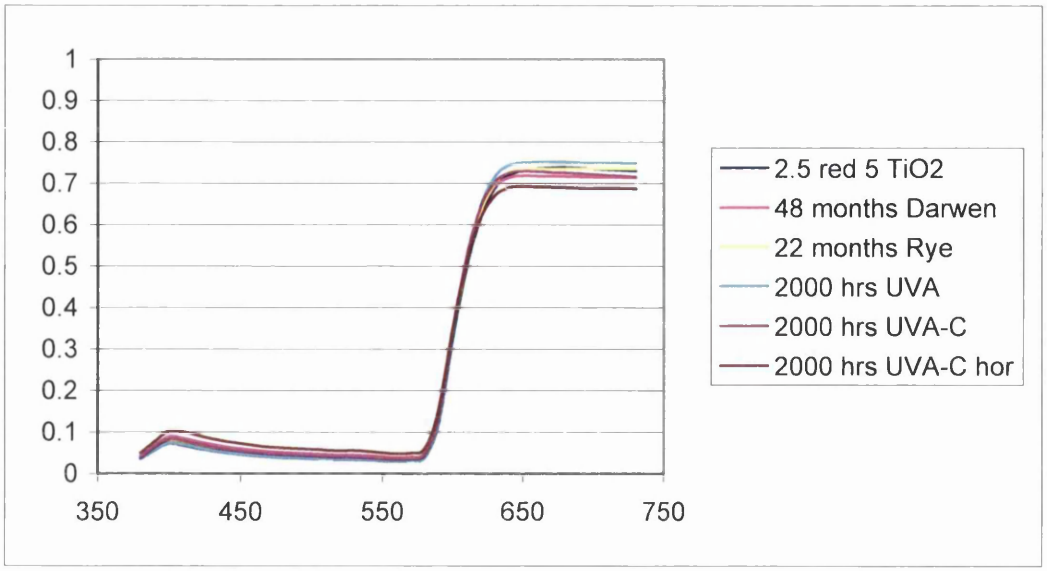
1
0.9
0.8
0.7
0.6
0.5
0.4
0.3
0.2
0.1
0
350
450
550
650
750
2.5 red 5 TiO2
48 months Darwen
22 months Rye
2000 hrs UVA
2000 hrs UVA-C
2000 hrs UVA-C hor

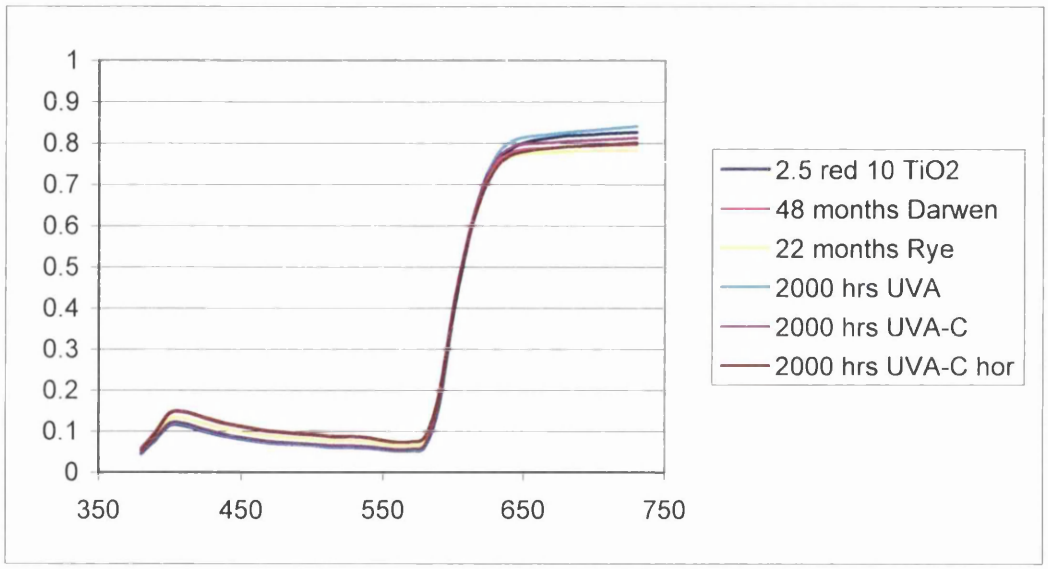
1
0.9
0.8
0.7
0.6
0.5
0.4
0.3
0.2
0.1
0
350
450
550
650
750
2.5 red 10 TiO2
48 months Darwen
22 months Rye
2000 hrs UVA
2000 hrs UVA-C
2000 hrs UVA-C hor

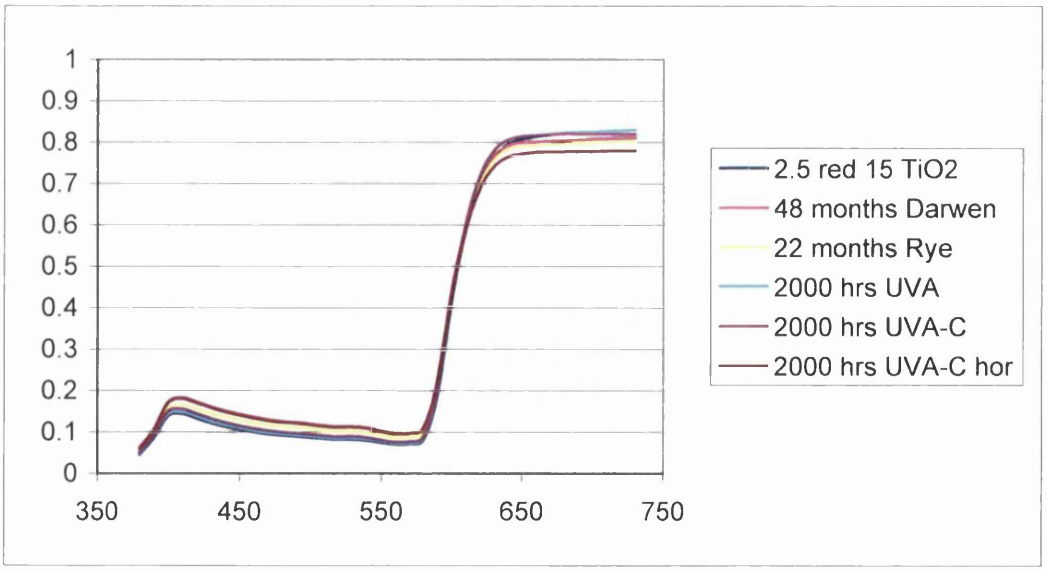
1
0.9
0.8
0.7
0.6
0.5
0.4
0.3
0.2
0.1
0
350
450
550
650
750
2.5 red 15 TiO2
48 months Darwen
22 months Rye
2000 hrs UVA
2000 hrs UVA-C
2000 hrs UVA-C hor

Appendix I

Blue

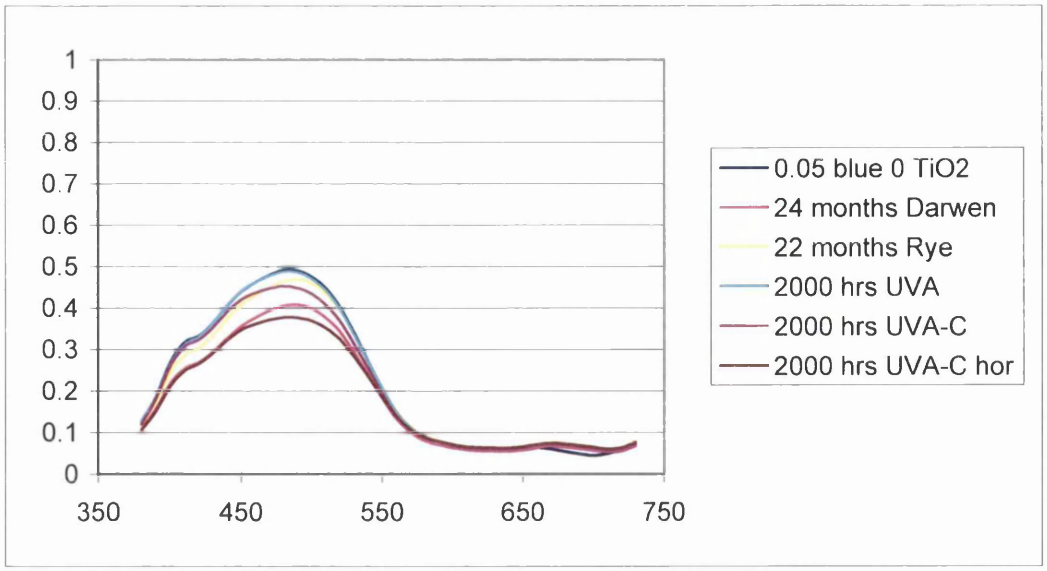
1
0.9
0.8
0.7
0.6
0.5
0.4
0.3
0.2
0.1
0
350
450
550
650
750
0.05 blue 0 TiO2
24 months Darwen
22 months Rye
2000 hrs UVA
2000 hrs UVA-C
2000 hrs UVA-C hor

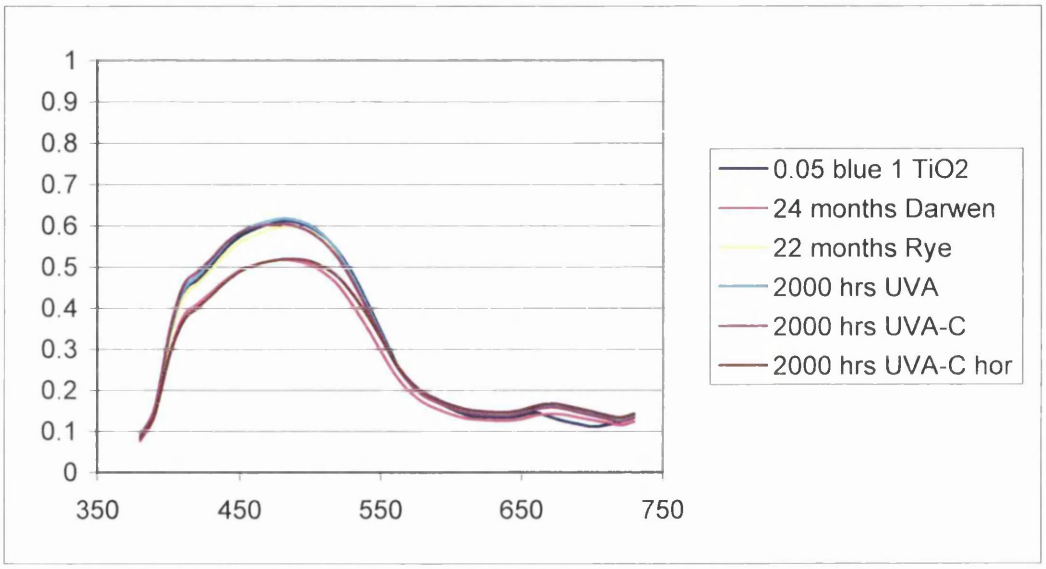
1
0.9
0.8
0.7
0.6
0.5
0.4
0.3
0.2
0.1
0
350
450
550
650
750
0.05 blue 1 TiO2
24 months Darwen
22 months Rye
2000 hrs UVA
2000 hrs UVA-C
2000 hrs UVA-C hor

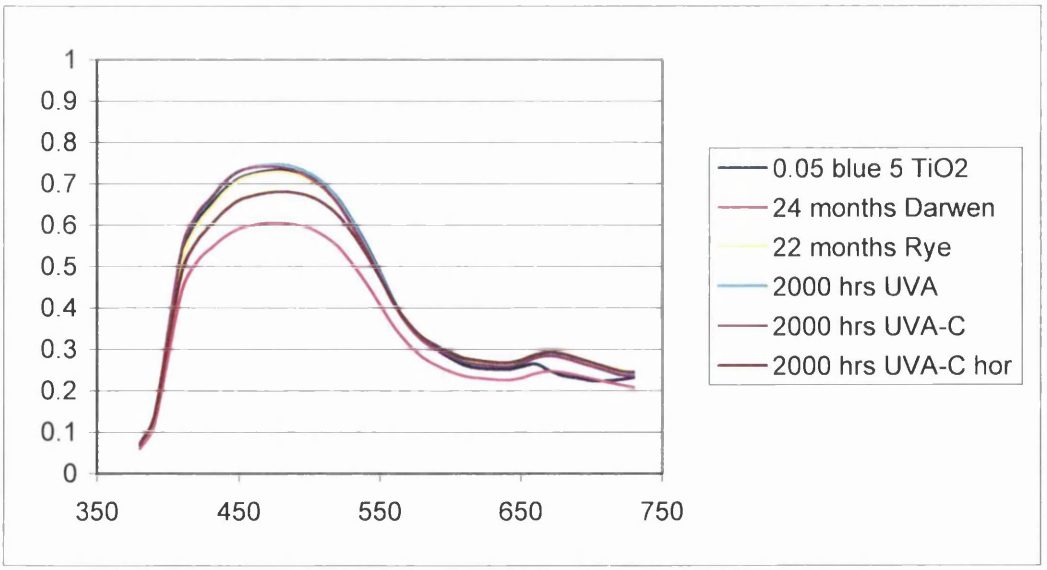
1
0.9
0.8
0.7
0.6
0.5
0.4
0.3
0.2
0.1
0
350
450
550
650
750
0.05 blue 5 TiO2
24 months Darwen
22 months Rye
2000 hrs UVA
2000 hrs UVA-C
2000 hrs UVA-C hor

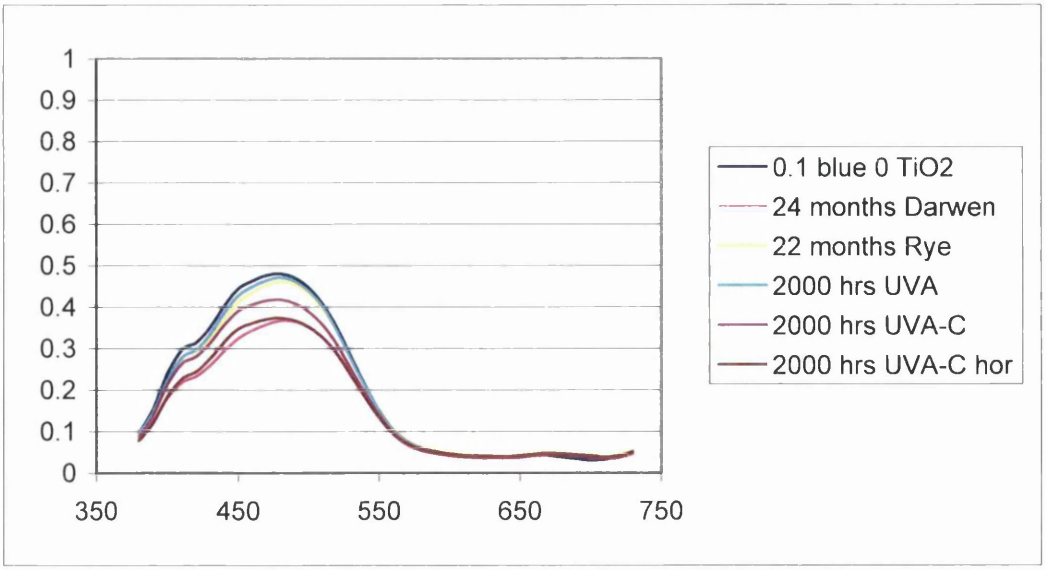
1
0.9
0.8
0.7
0.6
0.5
0.4
0.3
0.2
0.1
0
350
450
550
650
750
0.1 blue 0 TiO2
24 months Darwen
22 months Rye
2000 hrs UVA
2000 hrs UVA-C
2000 hrs UVA-C hor

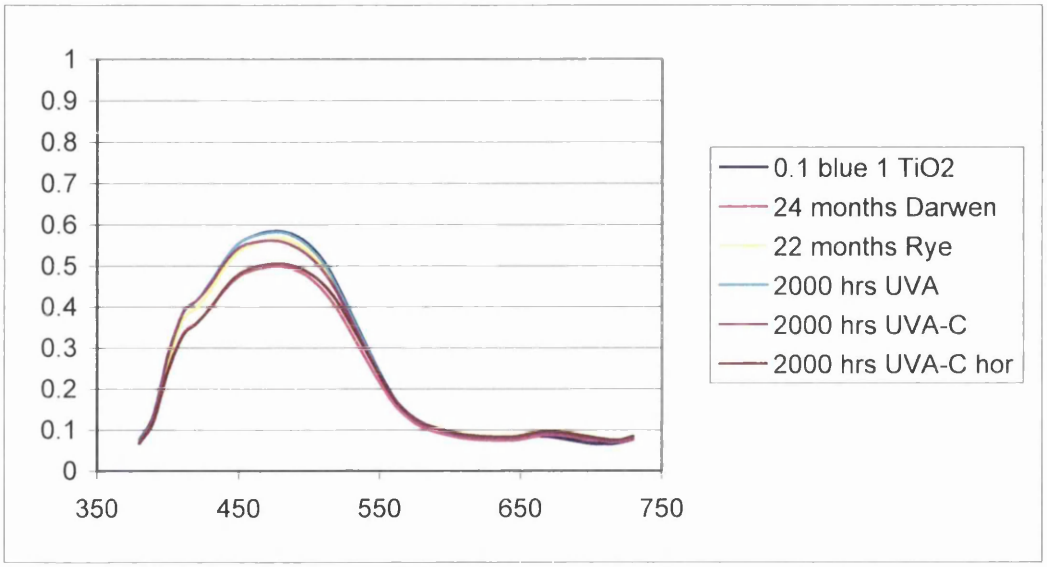
1
0.9
0.8
0.7
0.6
0.5
0.4
0.3
0.2
0.1
0
350
450
550
650
750
0.1 blue 1 TiO2
24 months Darwen
22 months Rye
2000 hrs UVA
2000 hrs UVA-C
2000 hrs UVA-C hor

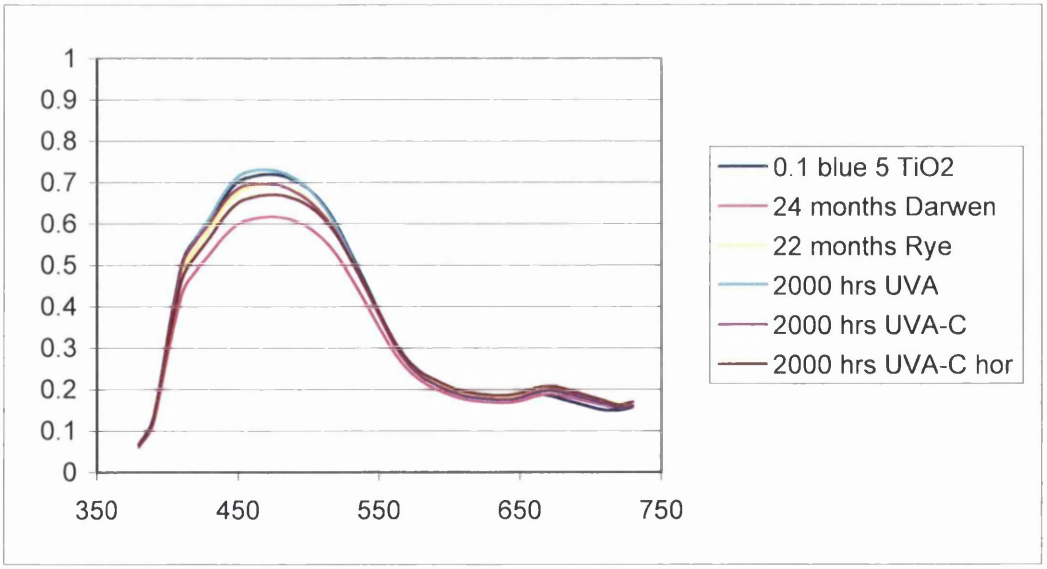
1
0.9
0.8
0.7
0.6
0.5
0.4
0.3
0.2
0.1
0
350
450
550
650
750
0.1 blue 5 TiO2
24 months Darwen
22 months Rye
2000 hrs UVA
2000 hrs UVA-C
2000 hrs UVA-C hor

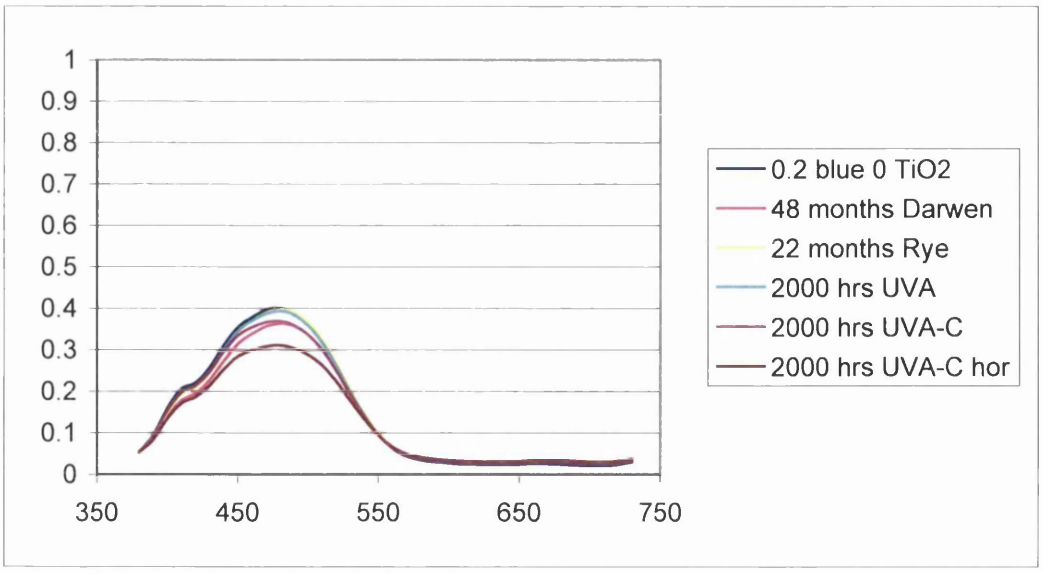
1
0.9
0.8
0.7
0.6
0.5
0.4
0.3
0.2
0.1
0
350
450
550
650
750
0.2 blue 0 TiO2
48 months Darwen
22 months Rye
2000 hrs UVA
2000 hrs UVA-C
2000 hrs UVA-C hor

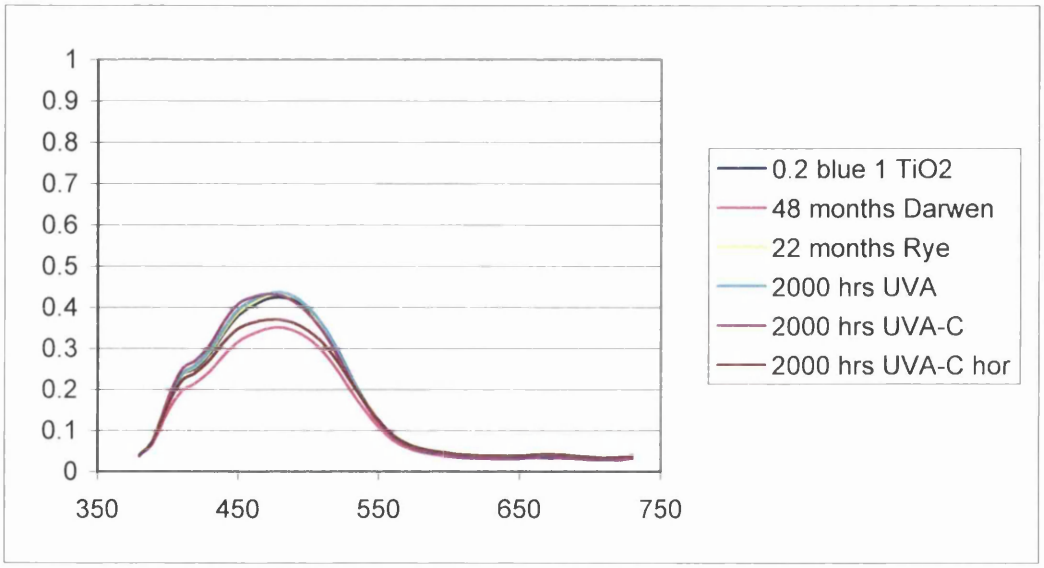
1
0.9
0.8
0.7
0.6
0.5
0.4
0.3
0.2
0.1
0
350
450
550
650
750
0.2 blue 1 TiO2
48 months Darwen
22 months Rye
2000 hrs UVA
2000 hrs UVA-C
2000 hrs UVA-C hor

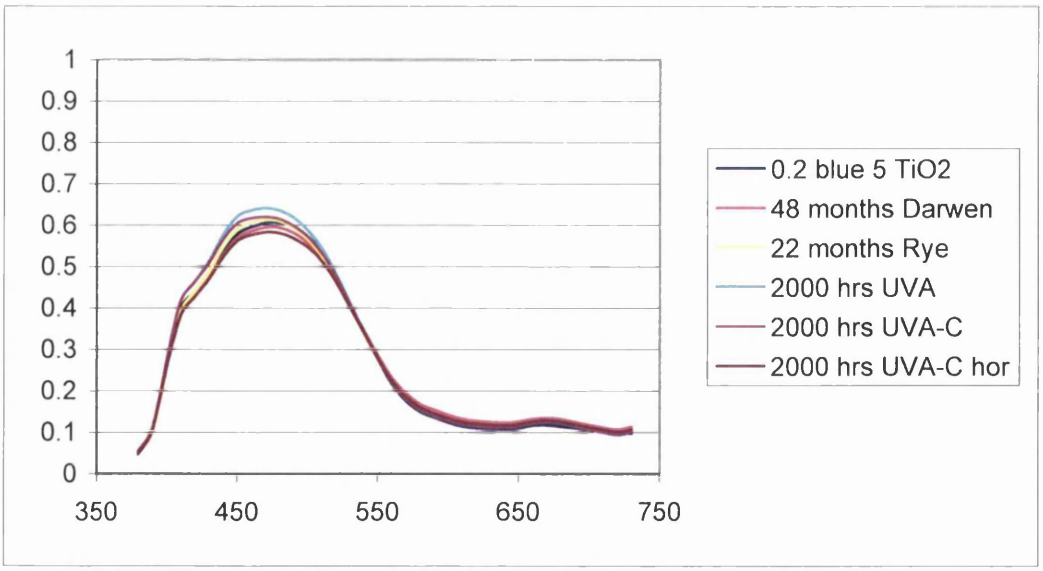
1
0.9
0.8
0.7
0.6
0.5
0.4
0.3
0.2
0.1
0
350
450
550
650
750
0.2 blue 5 TiO2
48 months Darwen
22 months Rye
2000 hrs UVA
2000 hrs UVA-C
2000 hrs UVA-C hor

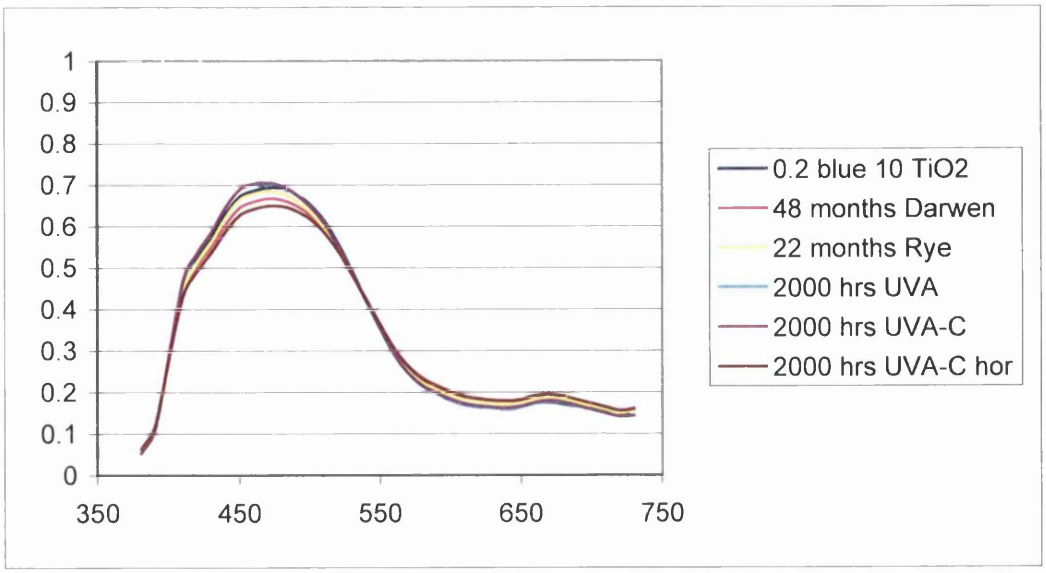
1
0.9
0.8
0.7
0.6
0.5
0.4
0.3
0.2
0.1
0
350
450
550
650
750
0.2 blue 10 TiO2
48 months Darwen
22 months Rye
2000 hrs UVA
2000 hrs UVA-C
2000 hrs UVA-C hor

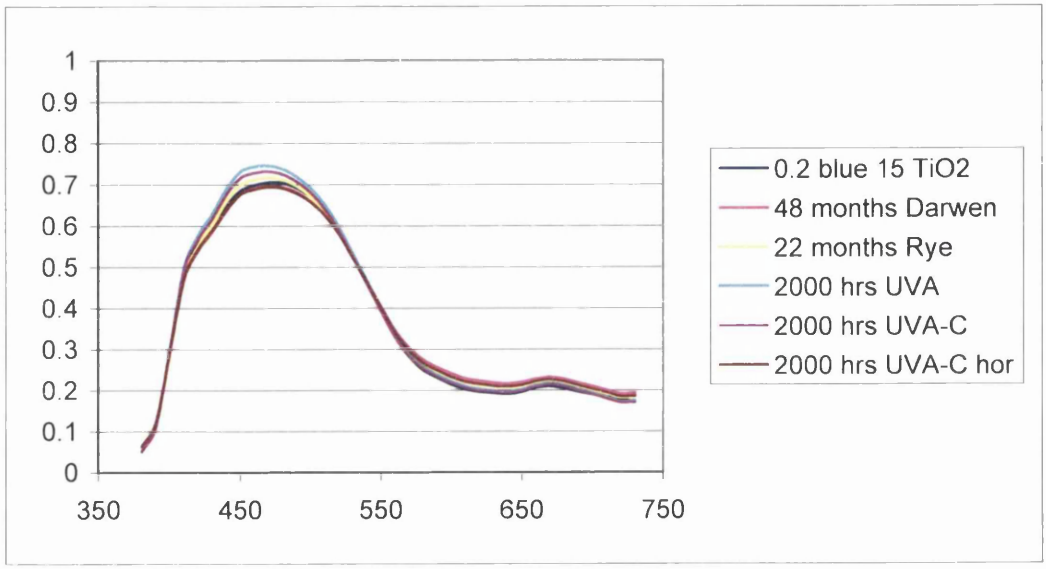
1
0.9
0.8
0.7
0.6
0.5
0.4
0.3
0.2
0.1
0
350
450
550
650
750
0.2 blue 15 TiO2
48 months Darwen
22 months Rye
2000 hrs UVA
2000 hrs UVA-C
2000 hrs UVA-C hor

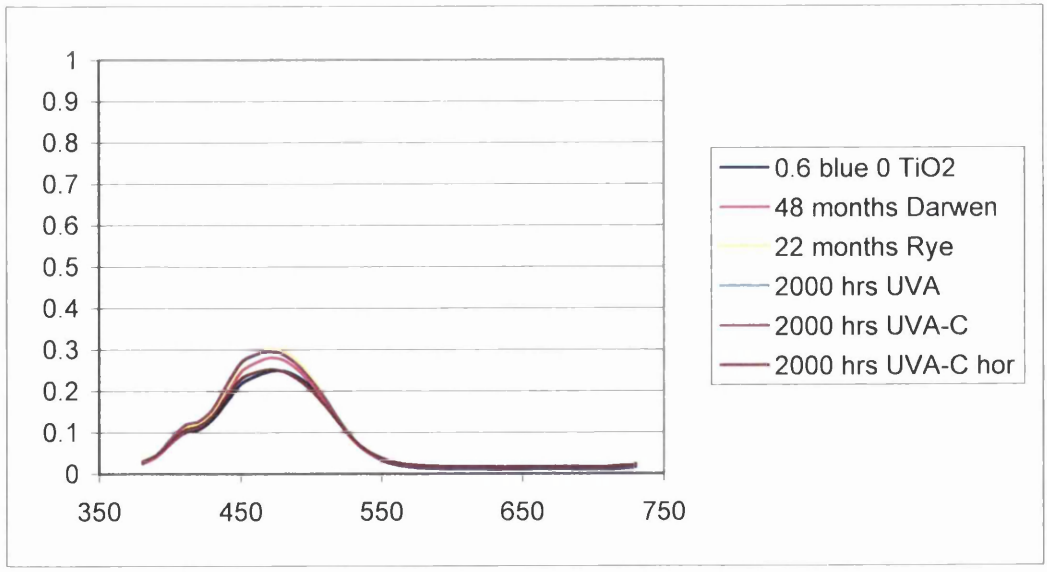
1
0.9
0.8
0.7
0.6
0.5
0.4
0.3
0.2
0.1
0
350
450
550
650
750
0.6 blue 0 TiO2
48 months Darwen
22 months Rye
2000 hrs UVA
2000 hrs UVA-C
2000 hrs UVA-C hor

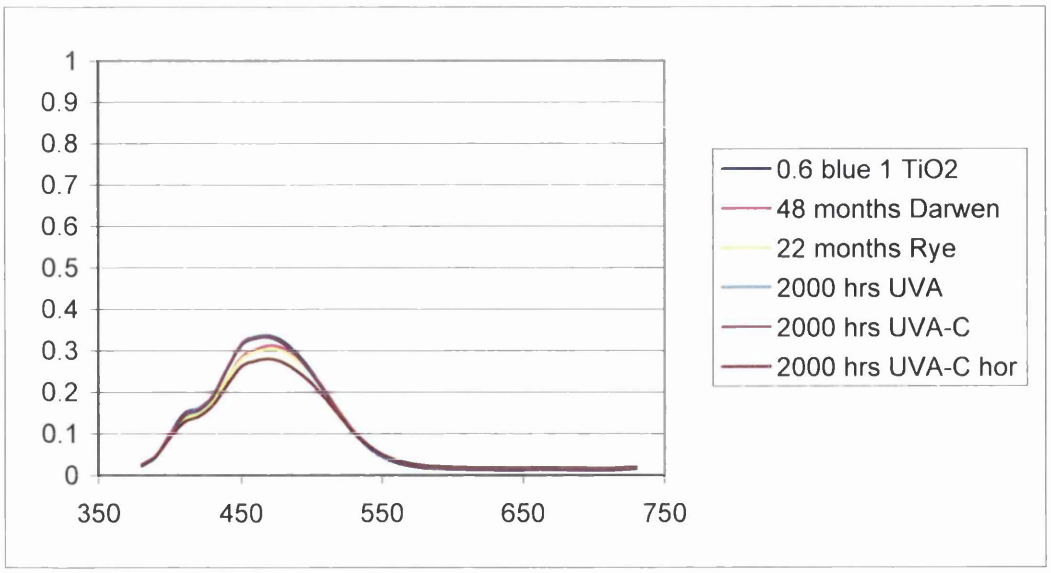
1
0.9
0.8
0.7
0.6
0.5
0.4
0.3
0.2
0.1
0
350
450
550
650
750
0.6 blue 1 TiO2
48 months Darwen
22 months Rye
2000 hrs UVA
2000 hrs UVA-C
2000 hrs UVA-C hor

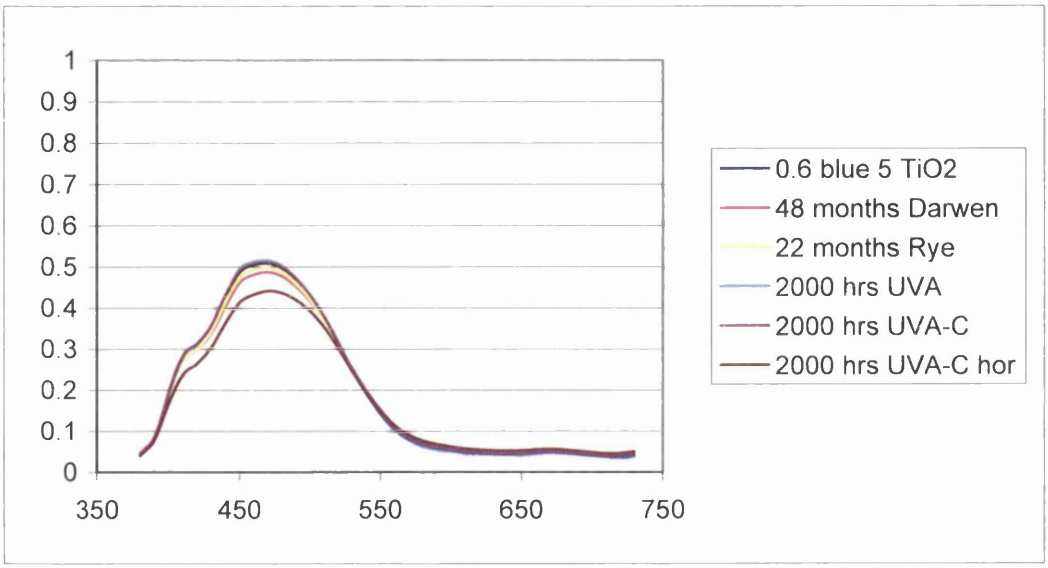
1
0.9
0.8
0.7
0.6
0.5
0.4
0.3
0.2
0.1
0
350
450
550
650
750
0.6 blue 5 TiO2
48 months Darwen
22 months Rye
2000 hrs UVA
2000 hrs UVA-C
2000 hrs UVA-C hor

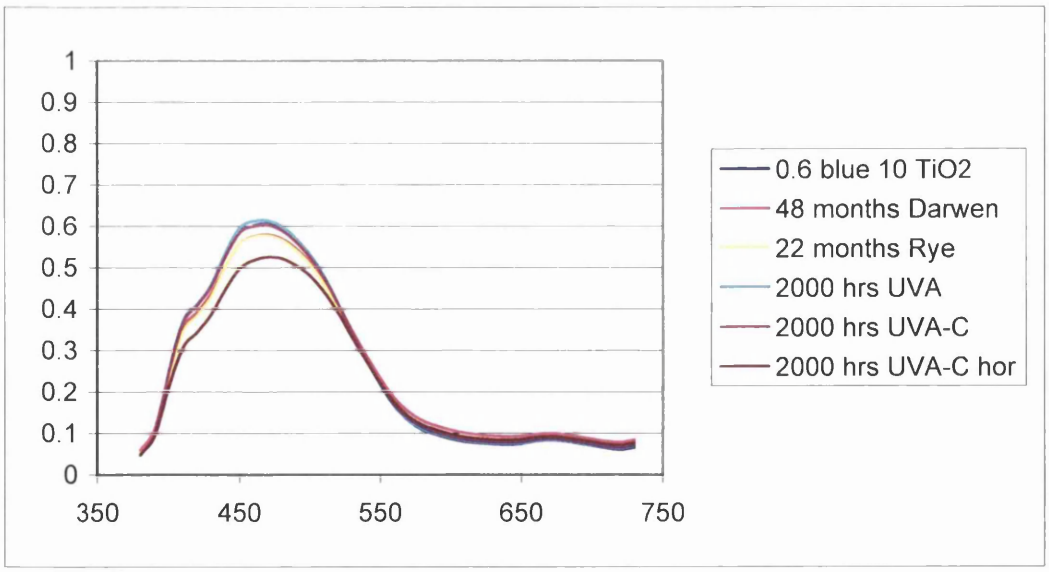
1
0.9
0.8
0.7
0.6
0.5
0.4
0.3
0.2
0.1
0
350
450
550
650
750
0.6 blue 10 TiO2
48 months Darwen
22 months Rye
2000 hrs UVA
2000 hrs UVA-C
2000 hrs UVA-C hor

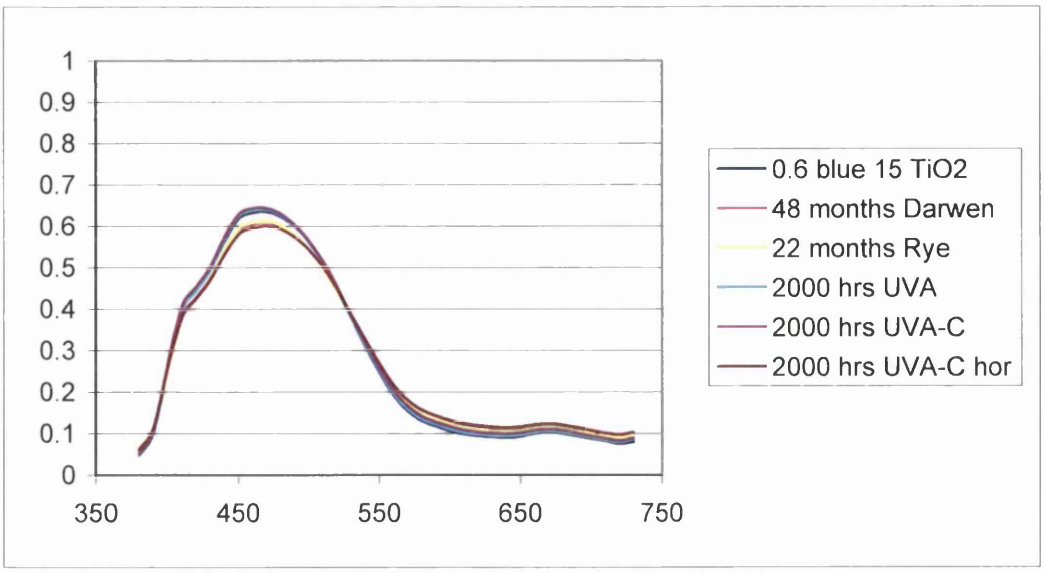
1
0.9
0.8
0.7
0.6
0.5
0.4
0.3
0.2
0.1
0
350
450
550
650
750
0.6 blue 15 TiO2
48 months Darwen
22 months Rye
2000 hrs UVA
2000 hrs UVA-C
2000 hrs UVA-C hor

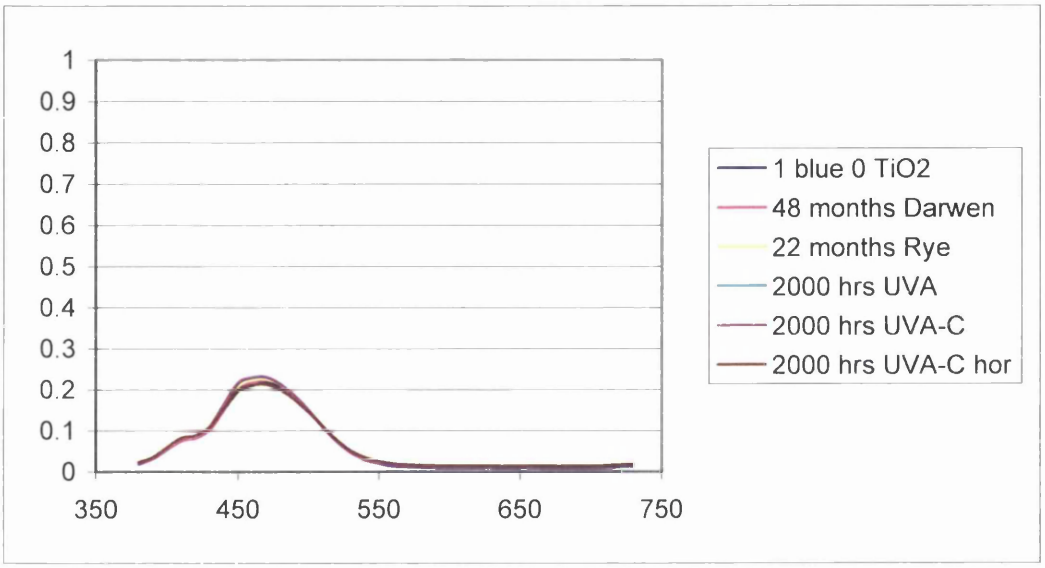
1
0.9
0.8
0.7
0.6
0.5
0.4
0.3
0.2
0.1
0
350
450
550
650
750
1 blue 0 TiO2
48 months Darwen
22 months Rye
2000 hrs UVA
2000 hrs UVA-C
2000 hrs UVA-C hor

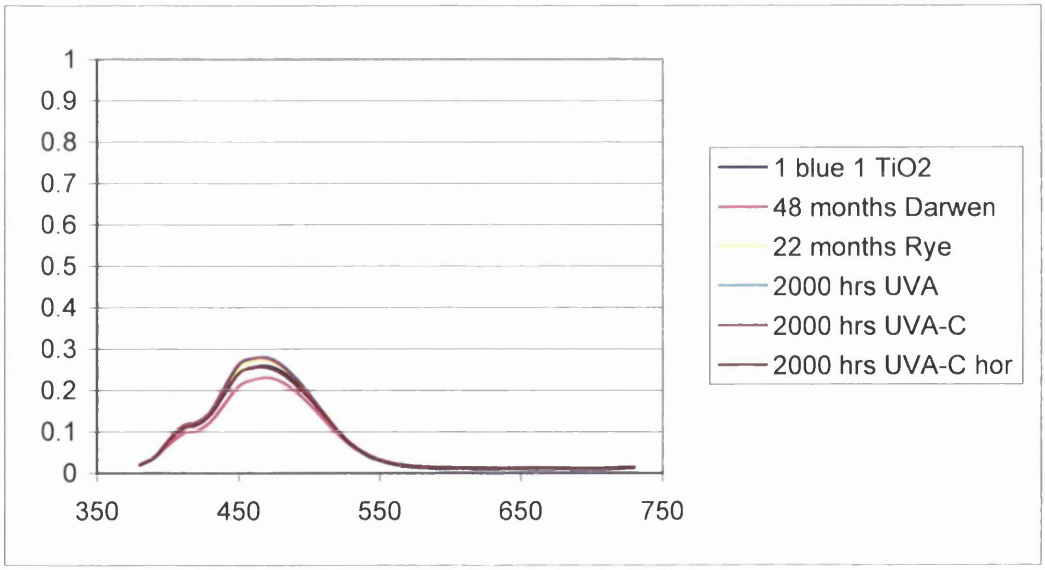
1
0.9
0.8
0.7
0.6
0.5
0.4
0.3
0.2
0.1
0
350
450
550
650
750
1 blue 1 TiO2
48 months Darwen
22 months Rye
2000 hrs UVA
2000 hrs UVA-C
2000 hrs UVA-C hor

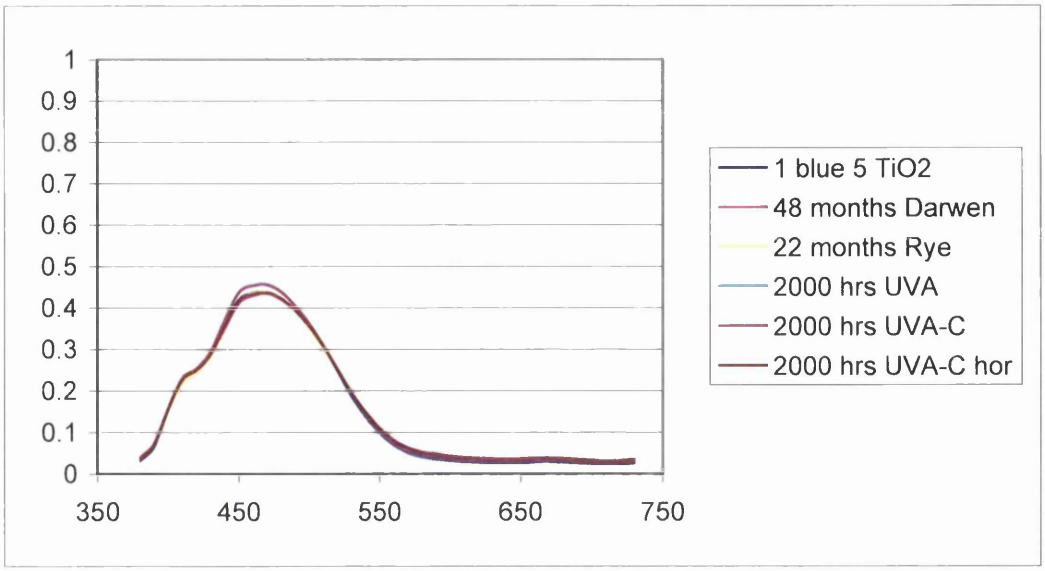
1
0.9
0.8
0.7
0.6
0.5
0.4
0.3
0.2
0.1
0
350
450
550
650
750
1 blue 5 TiO2
48 months Darwen
22 months Rye
2000 hrs UVA
2000 hrs UVA-C
2000 hrs UVA-C hor

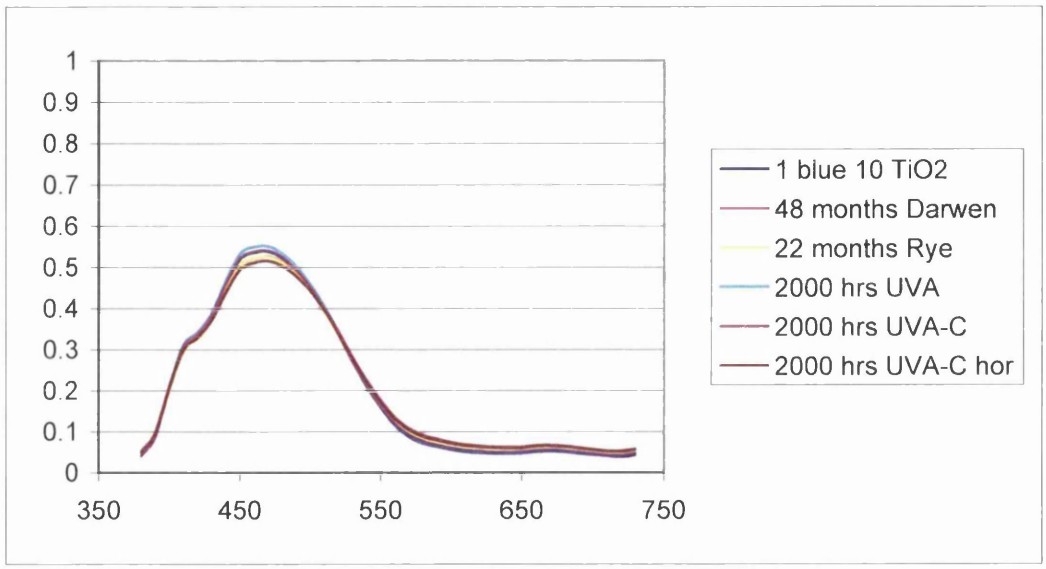
1
0.9
0.8
0.7
0.6
0.5
0.4
0.3
0.2
0.1
0
350
450
550
650
750
1 blue 10 TiO2
48 months Darwen
22 months Rye
2000 hrs UVA
2000 hrs UVA-C
2000 hrs UVA-C hor

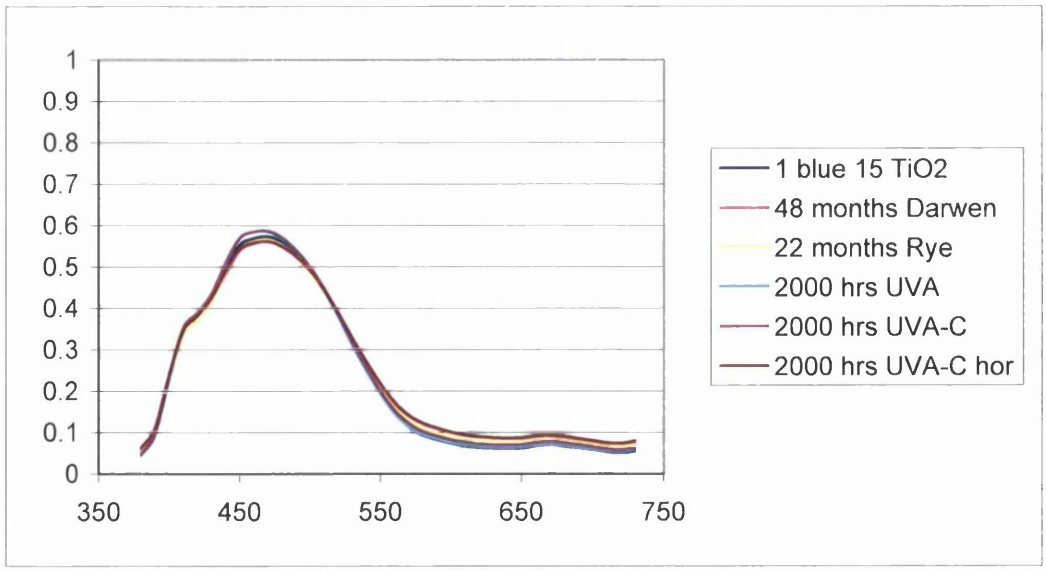
1
0.9
0.8
0.7
0.6
0.5
0.4
0.3
0.2
0.1
0
350
450
550
650
750
1 blue 15 TiO2
48 months Darwen
22 months Rye
2000 hrs UVA
2000 hrs UVA-C
2000 hrs UVA-C hor

Appendix I

Green

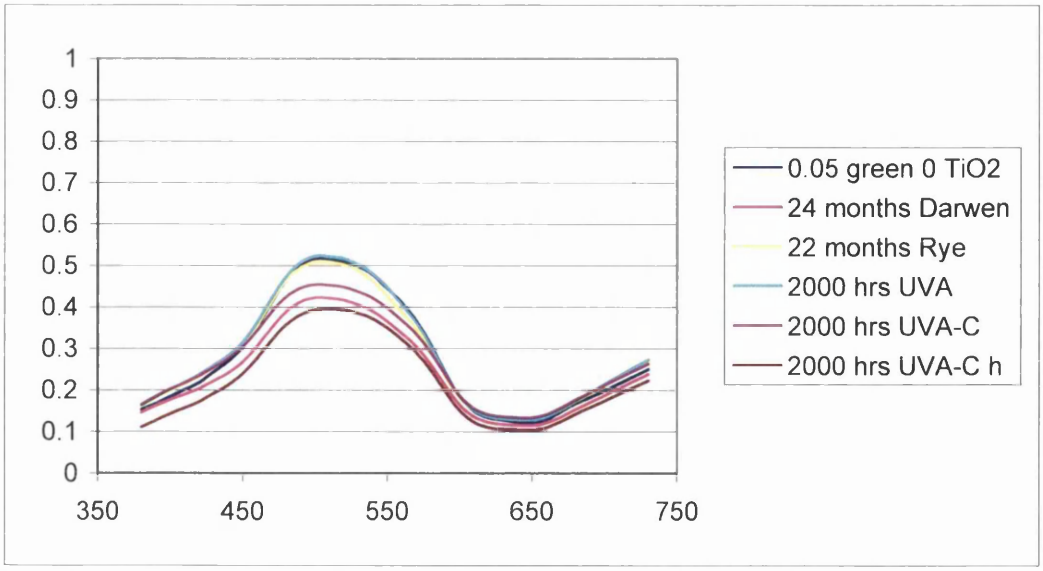
1
0.9
0.8
0.7
0.6
0.5
0.4
0.3
0.2
0.1
0
350
450
550
650
750
0.05 green 0 TiO2
24 months Darwen
22 months Rye
2000 hrs UVA
2000 hrs UVA-C
2000 hrs UVA-C h

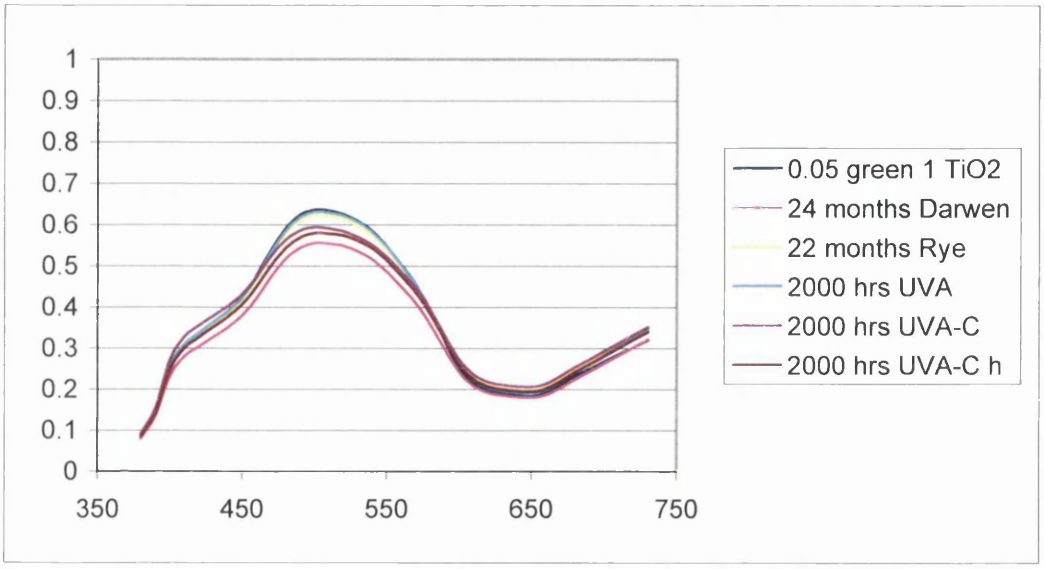
1
0.9
0.8
0.7
0.6
0.5
0.4
0.3
0.2
0.1
0
350
450
550
650
750
0.05 green 1 TiO2
24 months Darwen
22 months Rye
2000 hrs UVA
2000 hrs UVA-C
2000 hrs UVA-C h

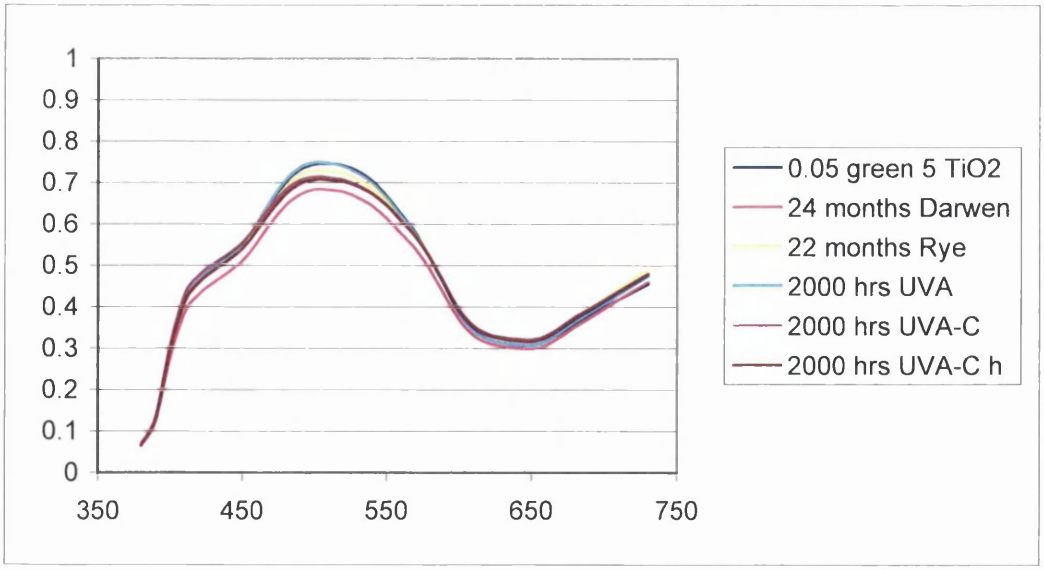
1
0.9
0.8
0.7
0.6
0.5
0.4
0.3
0.2
0.1
0
350
450
550
650
750
0.05 green 5 TiO2
24 months Darwen
22 months Rye
2000 hrs UVA
2000 hrs UVA-C
2000 hrs UVA-C h

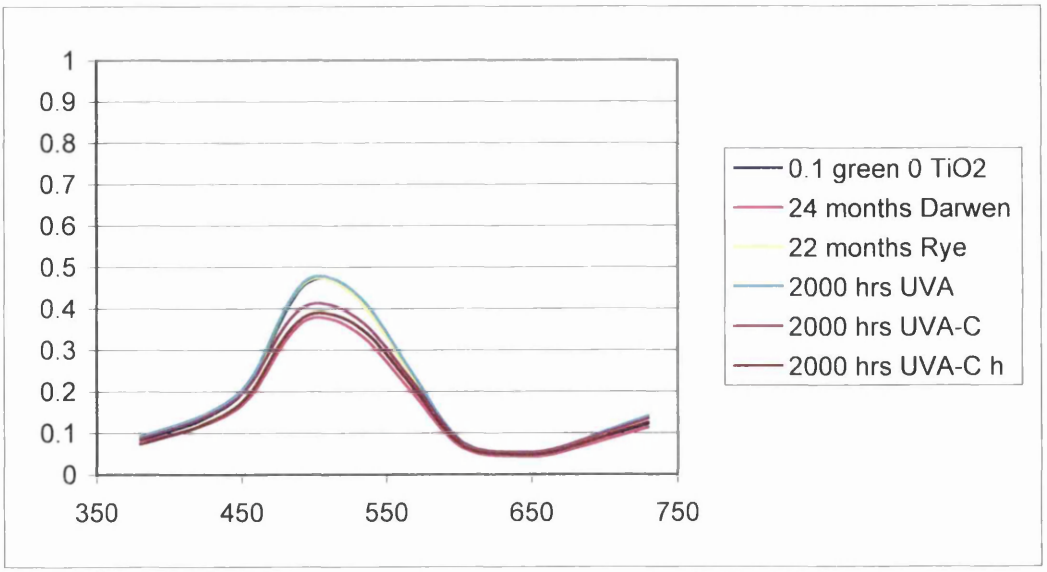
1
0.9
0.8
0.7
0.6
0.5
0.4
0.3
0.2
0.1
0
350
450
550
650
750
0.1 green 0 TiO2
24 months Darwen
22 months Rye
2000 hrs UVA
2000 hrs UVA-C
2000 hrs UVA-C h

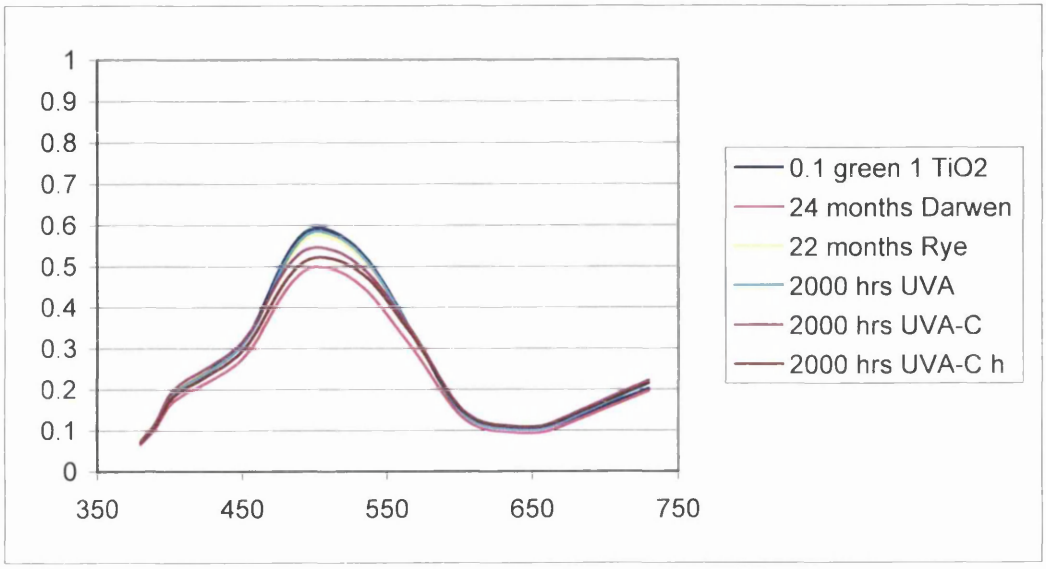
1
0.9
0.8
0.7
0.6
0.5
0.4
0.3
0.2
0.1
0
350
450
550
650
750
0.1 green 1 TiO2
24 months Darwen
22 months Rye
2000 hrs UVA
2000 hrs UVA-C
2000 hrs UVA-C h

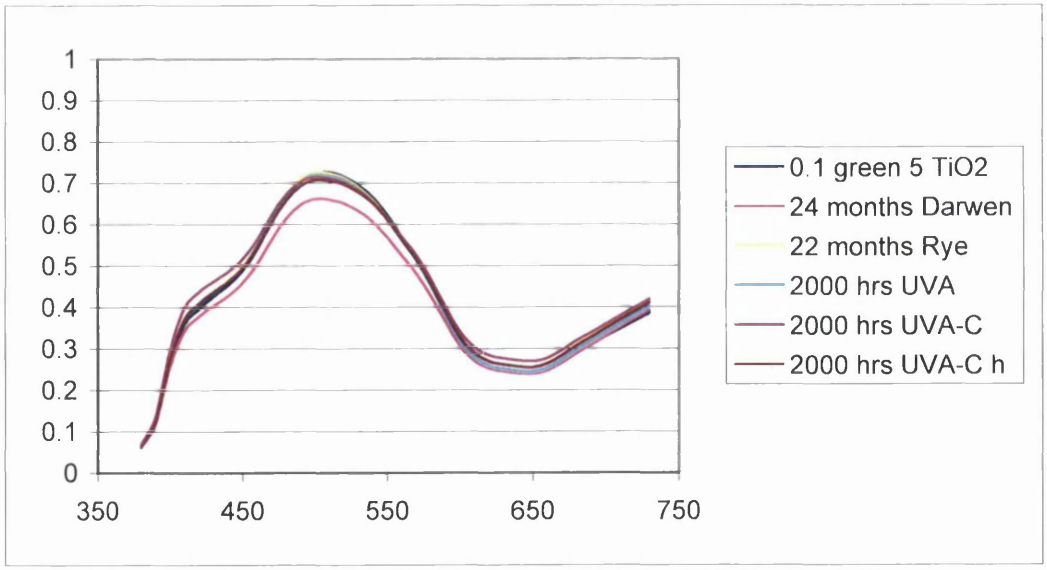
1
0.9
0.8
0.7
0.6
0.5
0.4
0.3
0.2
0.1
0
350
450
550
650
750
0.1 green 5 TiO2
24 months Darwen
22 months Rye
2000 hrs UVA
2000 hrs UVA-C
2000 hrs UVA-C h

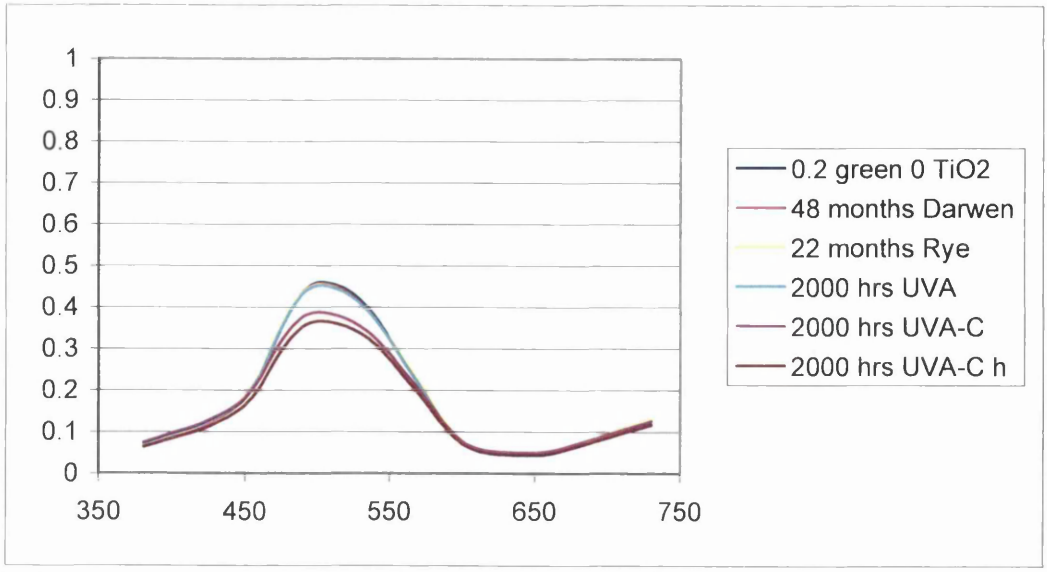
1
0.9
0.8
0.7
0.6
0.5
0.4
0.3
0.2
0.1
0
350
450
550
650
750
0.2 green 0 TiO2
48 months Darwen
22 months Rye
2000 hrs UVA
2000 hrs UVA-C
2000 hrs UVA-C h

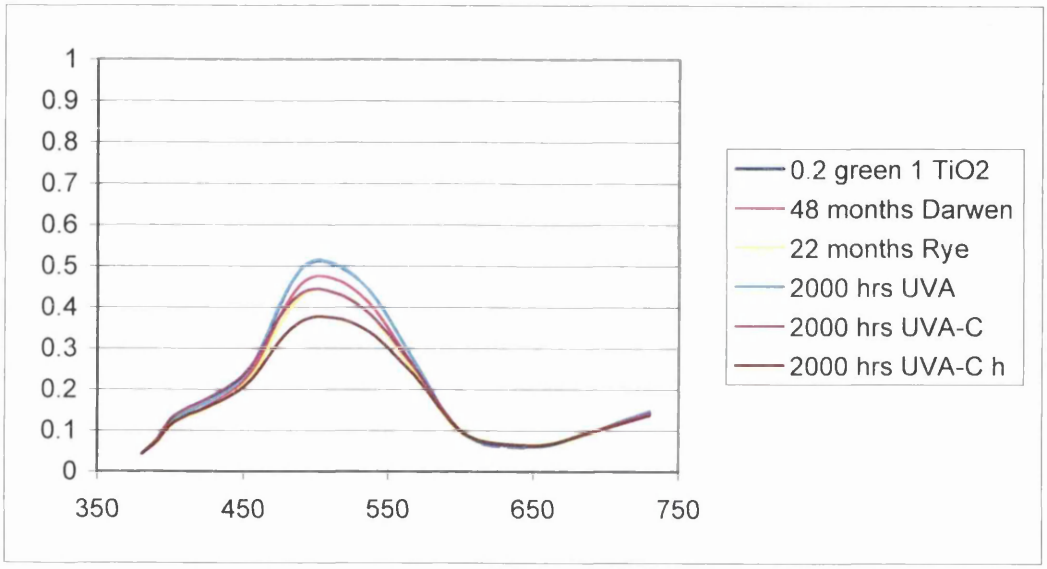
1
0.9
0.8
0.7
0.6
0.5
0.4
0.3
0.2
0.1
0
350
450
550
650
750
0.2 green 1 TiO2
48 months Darwen
22 months Rye
2000 hrs UVA
2000 hrs UVA-C
2000 hrs UVA-C h

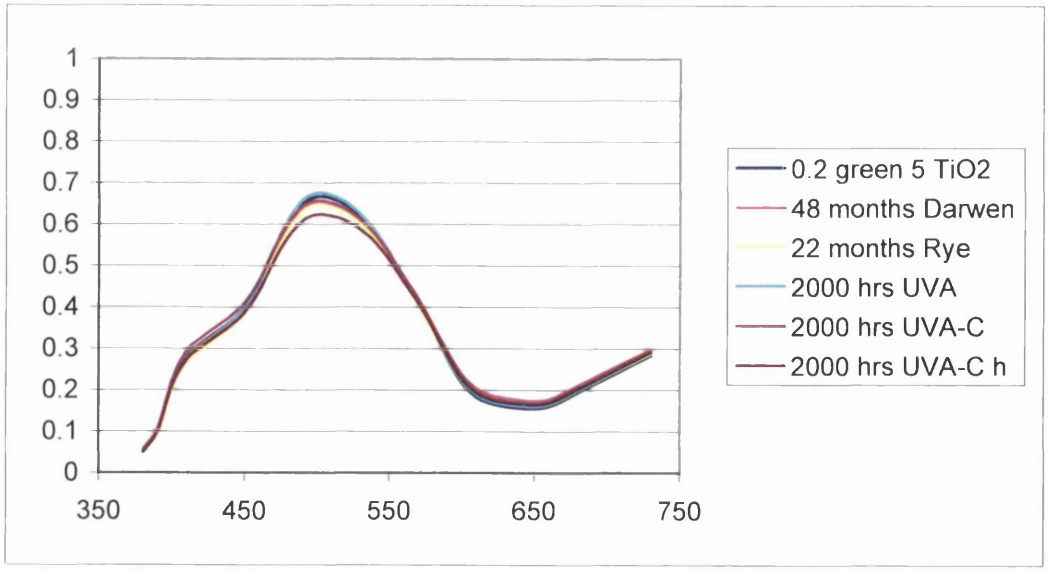
1
0.9
0.8
0.7
0.6
0.5
0.4
0.3
0.2
0.1
0
350
450
550
650
750
0.2 green 5 TiO2
48 months Darwen
22 months Rye
2000 hrs UVA
2000 hrs UVA-C
2000 hrs UVA-C h

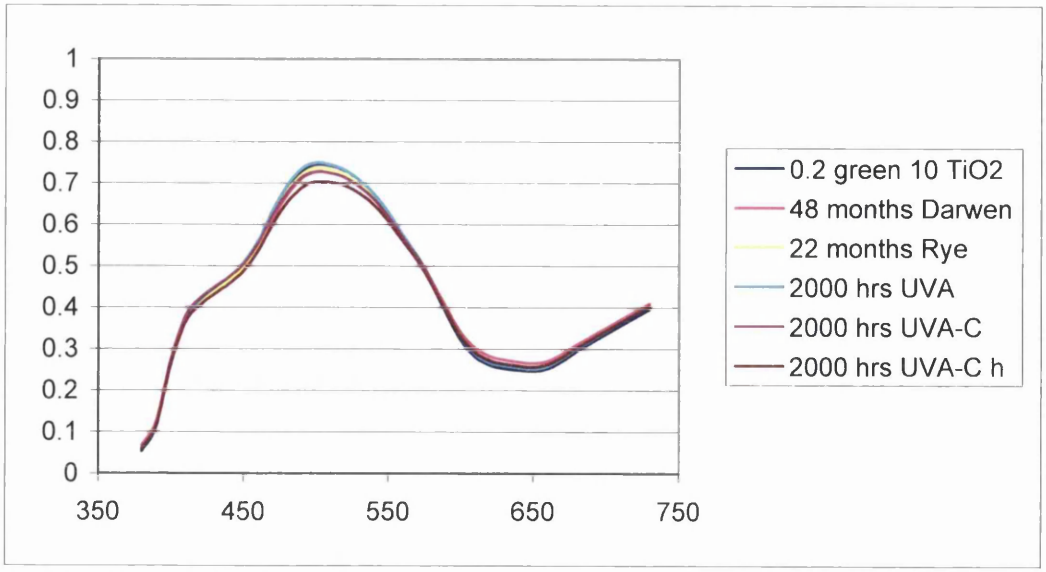
1
0.9
0.8
0.7
0.6
0.5
0.4
0.3
0.2
0.1
0
350
450
550
650
750
0.2 green 10 TiO2
48 months Darwen
22 months Rye
2000 hrs UVA
2000 hrs UVA-C
2000 hrs UVA-C h

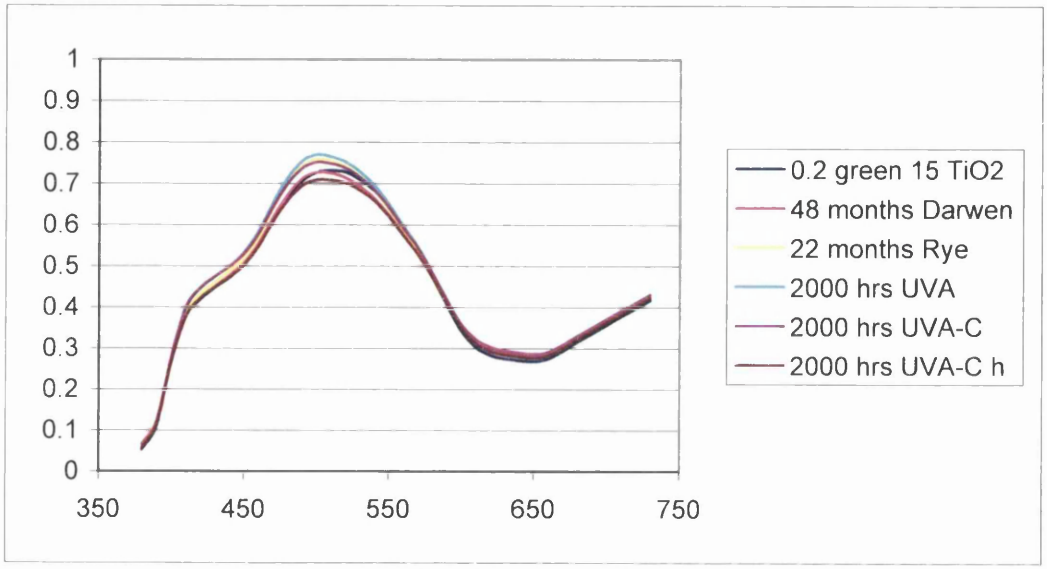
1
0.9
0.8
0.7
0.6
0.5
0.4
0.3
0.2
0.1
0
350
450
550
650
750
0.2 green 15 TiO2
48 months Darwen
22 months Rye
2000 hrs UVA
2000 hrs UVA-C
2000 hrs UVA-C h

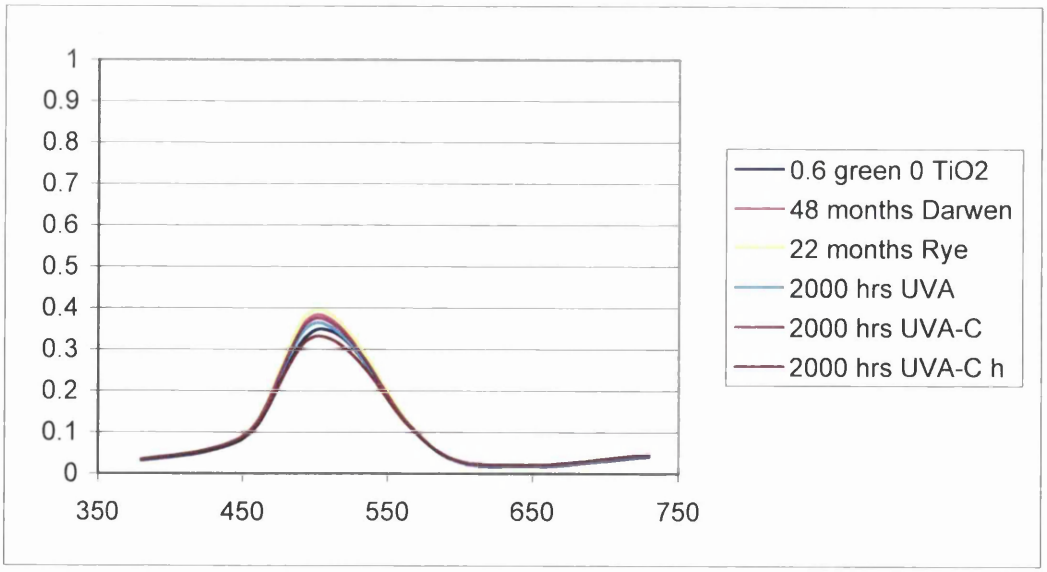
1
0.9
0.8
0.7
0.6
0.5
0.4
0.3
0.2
0.1
0
350
450
550
650
750
0.6 green 0 TiO2
48 months Darwen
22 months Rye
2000 hrs UVA
2000 hrs UVA-C
2000 hrs UVA-C h

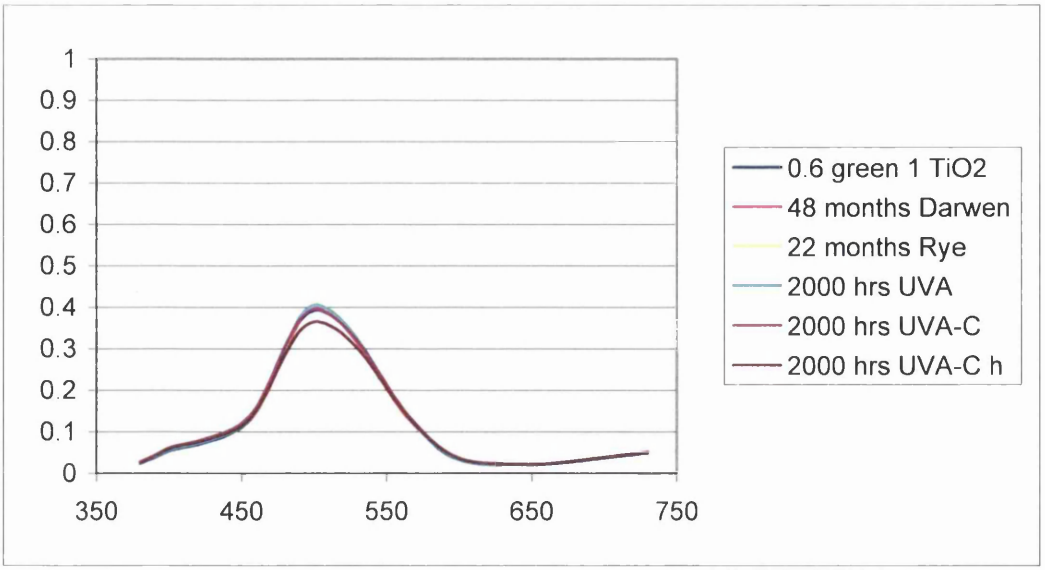
1
0.9
0.8
0.7
0.6
0.5
0.4
0.3
0.2
0.1
0
350
450
550
650
750
0.6 green 1 TiO2
48 months Darwen
22 months Rye
2000 hrs UVA
2000 hrs UVA-C
2000 hrs UVA-C h

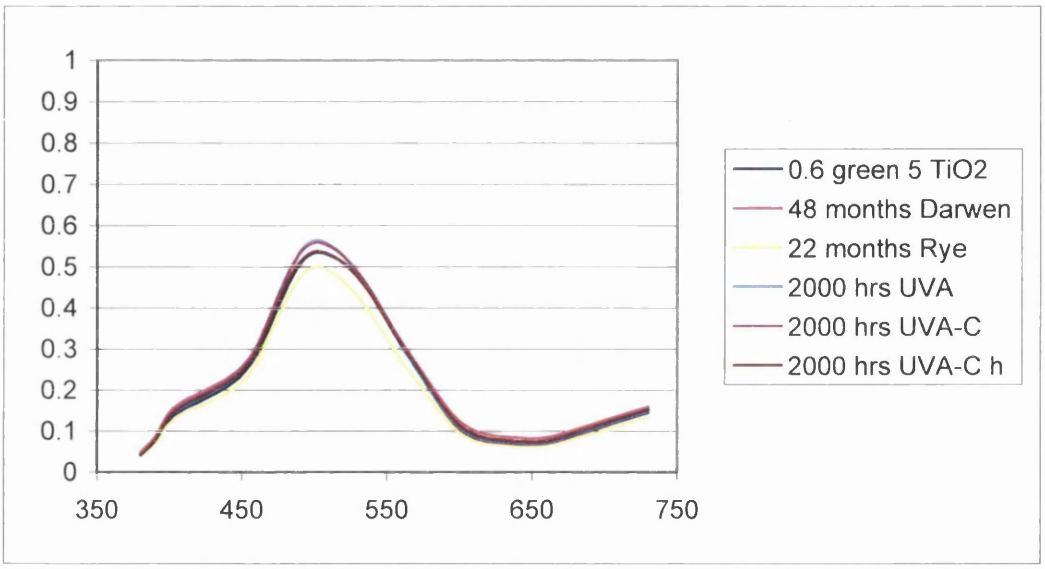
1
0.9
0.8
0.7
0.6
0.5
0.4
0.3
0.2
0.1
0
350
450
550
650
750
0.6 green 5 TiO2
48 months Darwen
22 months Rye
2000 hrs UVA
2000 hrs UVA-C
2000 hrs UVA-C h

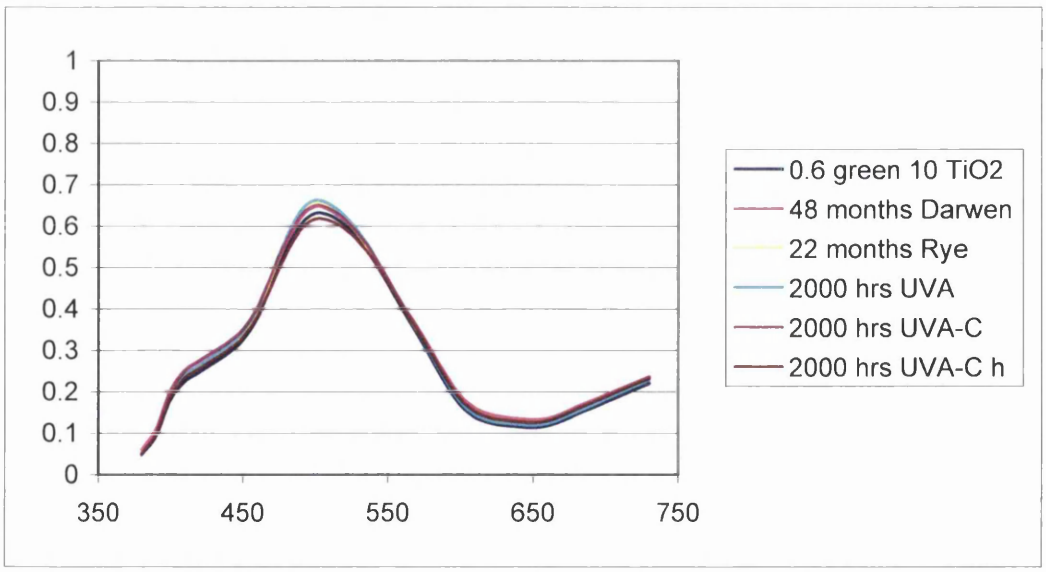
1
0.9
0.8
0.7
0.6
0.5
0.4
0.3
0.2
0.1
0
350
450
550
650
750
0.6 green 10 TiO2
48 months Darwen
22 months Rye
2000 hrs UVA
2000 hrs UVA-C
2000 hrs UVA-C h

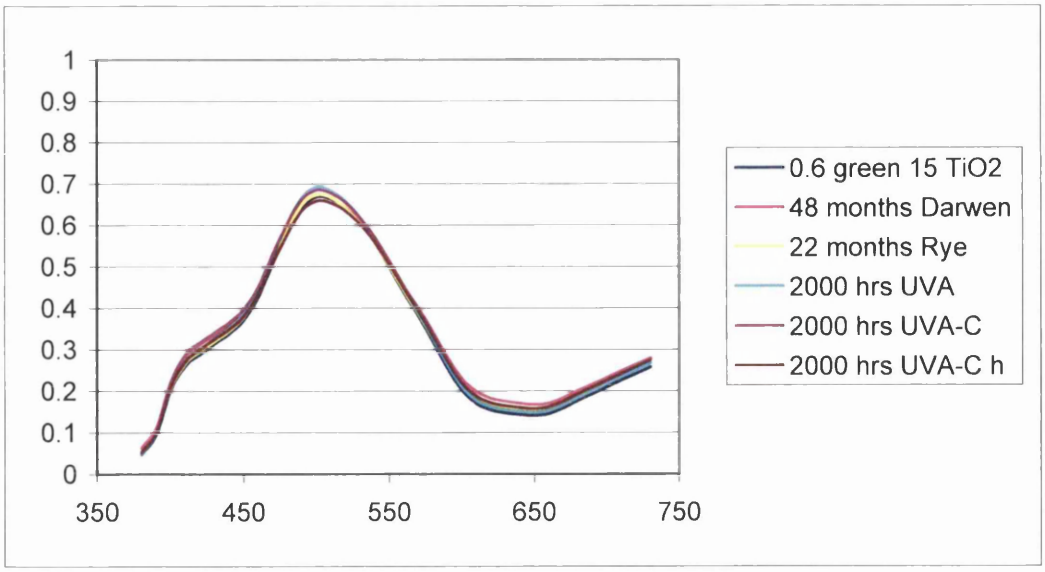
1
0.9
0.8
0.7
0.6
0.5
0.4
0.3
0.2
0.1
0
350
450
550
650
750
0.6 green 15 TiO2
48 months Darwen
22 months Rye
2000 hrs UVA
2000 hrs UVA-C
2000 hrs UVA-C h

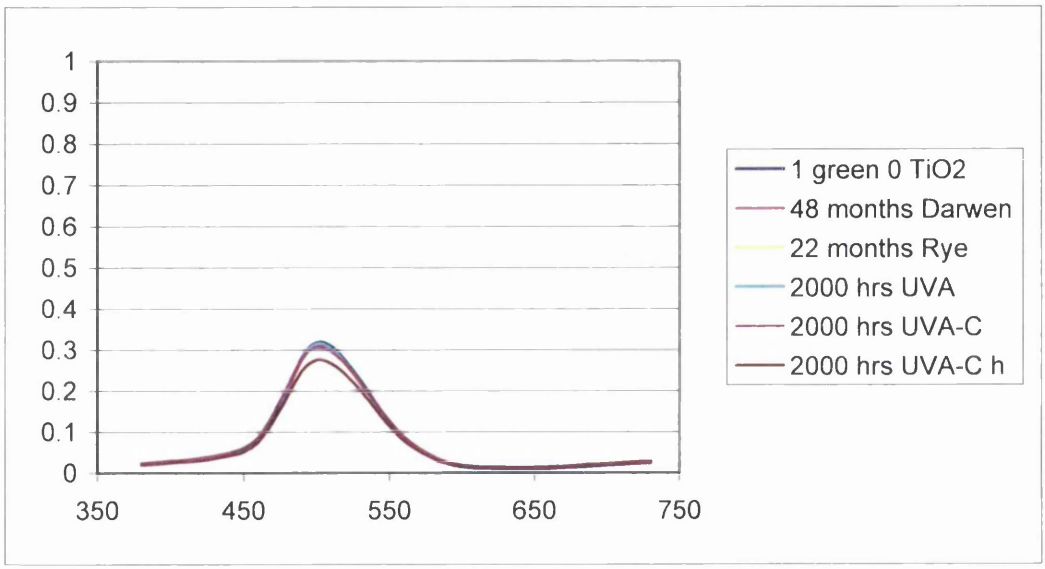
1
0.9
0.8
0.7
0.6
0.5
0.4
0.3
0.2
0.1
0
350
450
550
650
750
1 green 0 TiO2
48 months Darwen
22 months Rye
2000 hrs UVA
2000 hrs UVA-C
2000 hrs UVA-C h

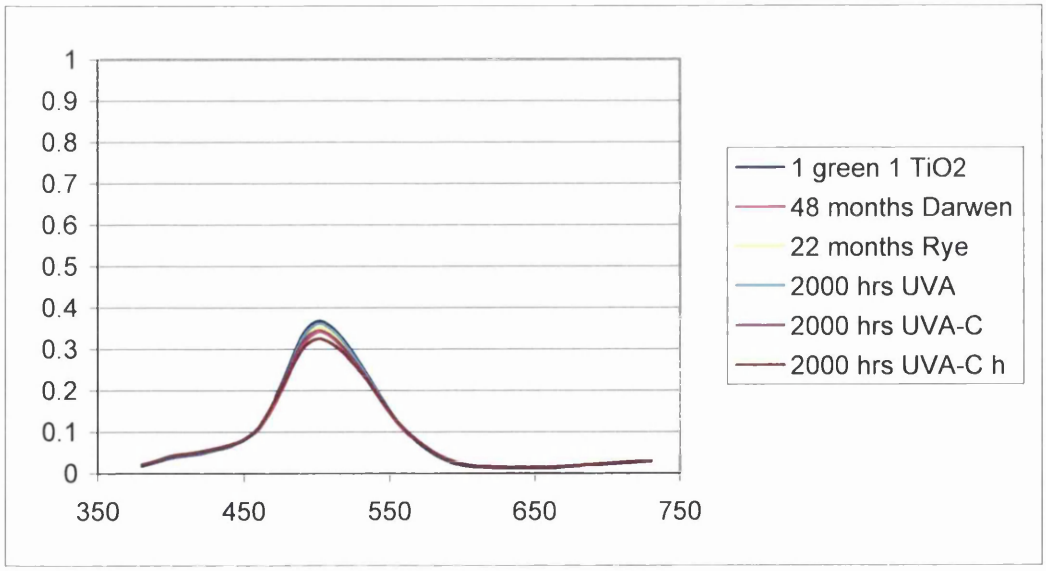
1
0.9
0.8
0.7
0.6
0.5
0.4
0.3
0.2
0.1
0
350
450
550
650
750
1 green 1 TiO2
48 months Darwen
22 months Rye
2000 hrs UVA
2000 hrs UVA-C
2000 hrs UVA-C h

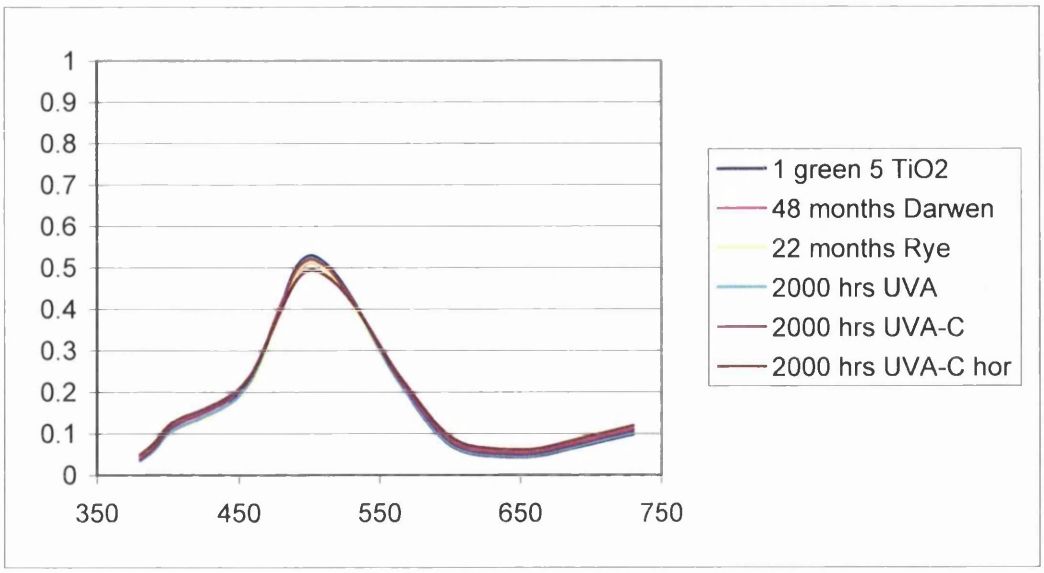
1
0.9
0.8
0.7
0.6
0.5
0.4
0.3
0.2
0.1
0
350
450
550
650
750
1 green 5 TiO2
48 months Darwen
22 months Rye
2000 hrs UVA
2000 hrs UVA-C
2000 hrs UVA-C hor

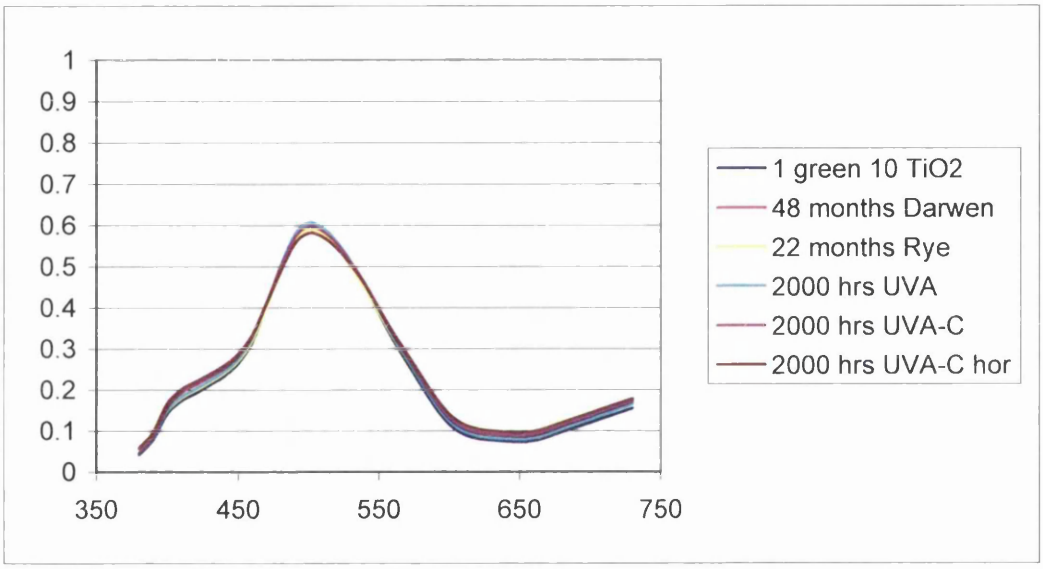
1
0.9
0.8
0.7
0.6
0.5
0.4
0.3
0.2
0.1
0
350
450
550
650
750
1 green 10 TiO2
48 months Darwen
22 months Rye
2000 hrs UVA
2000 hrs UVA-C
2000 hrs UVA-C hor

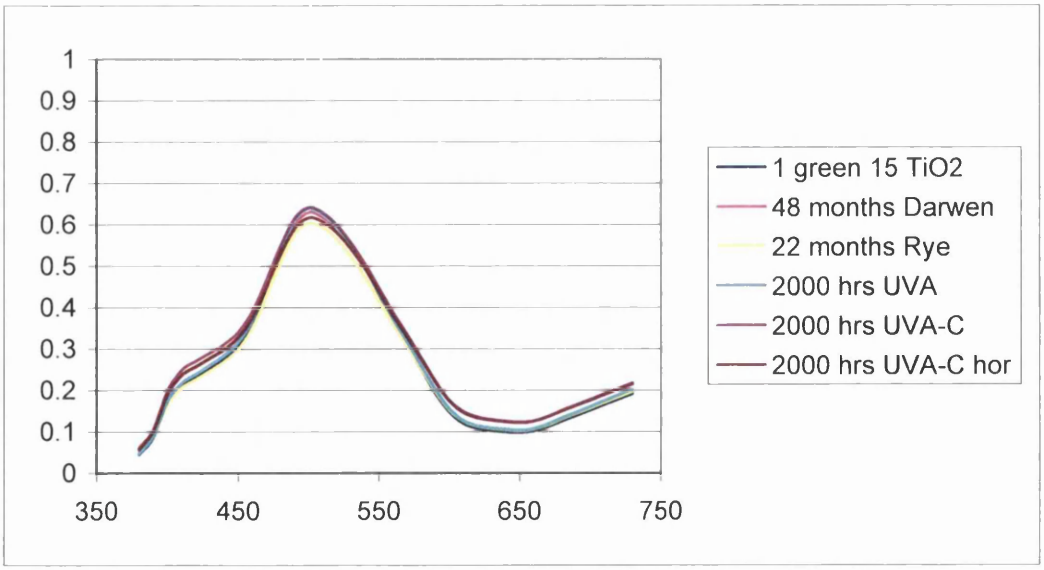
1
0.9
0.8
0.7
0.6
0.5
0.4
0.3
0.2
0.1
0
350
450
550
650
750
1 green 15 TiO2
48 months Darwen
22 months Rye
2000 hrs UVA
2000 hrs UVA-C
2000 hrs UVA-C hor

Appendix I

1-Yellow

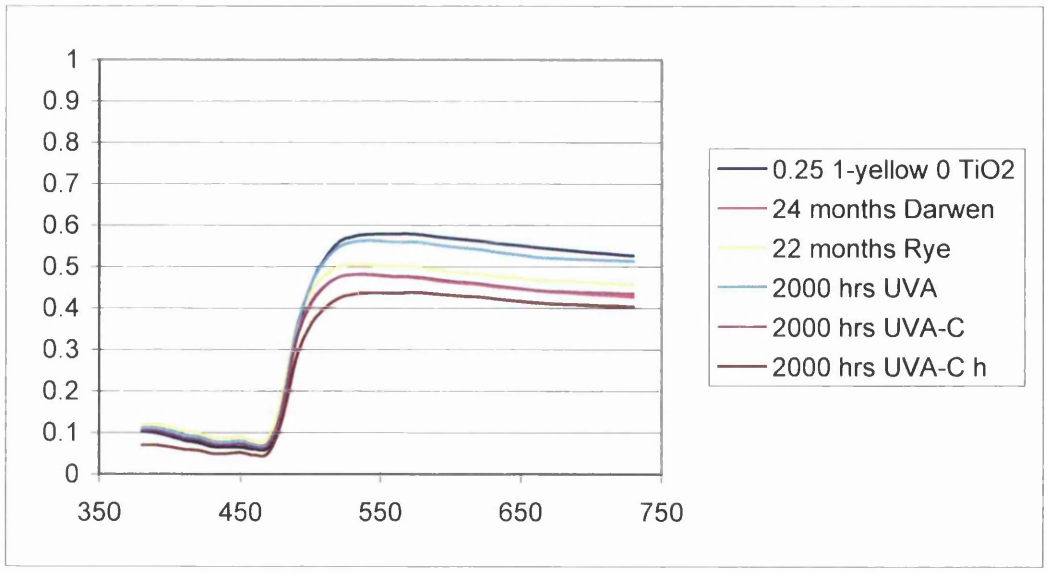
1
0.9
0.8
0.7
0.6
0.5
0.4
0.3
0.2
0.1
0
350
450
550
650
750
0.25 1-yellow 0 TiO2
24 months Darwen
22 months Rye
2000 hrs UVA
2000 hrs UVA-C
2000 hrs UVA-C h

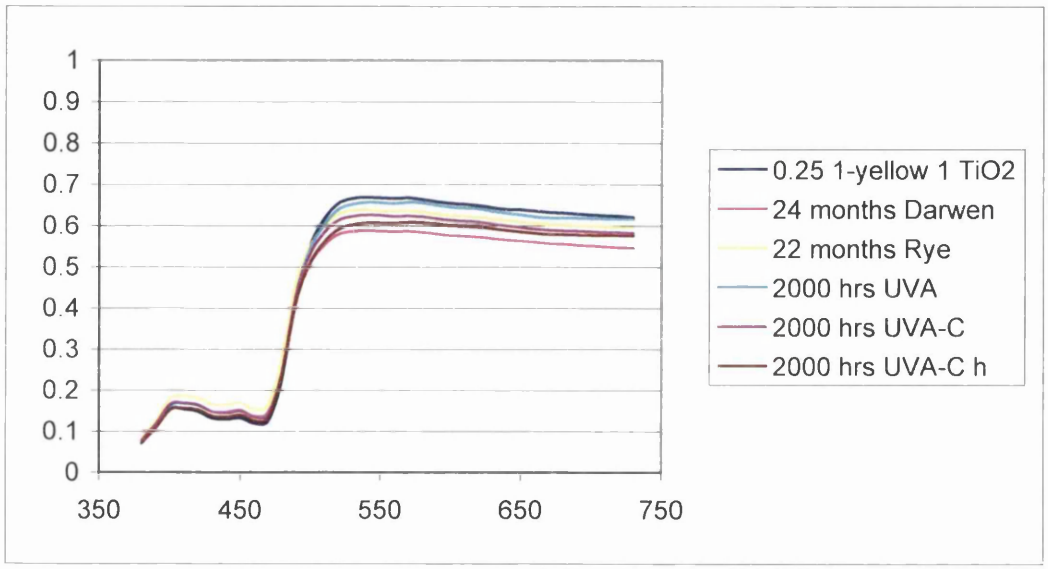
1
0.9
0.8
0.7
0.6
0.5
0.4
0.3
0.2
0.1
0
350
450
550
650
750
0.25 1-yellow 1 TiO2
24 months Darwen
22 months Rye
2000 hrs UVA
2000 hrs UVA-C
2000 hrs UVA-C h

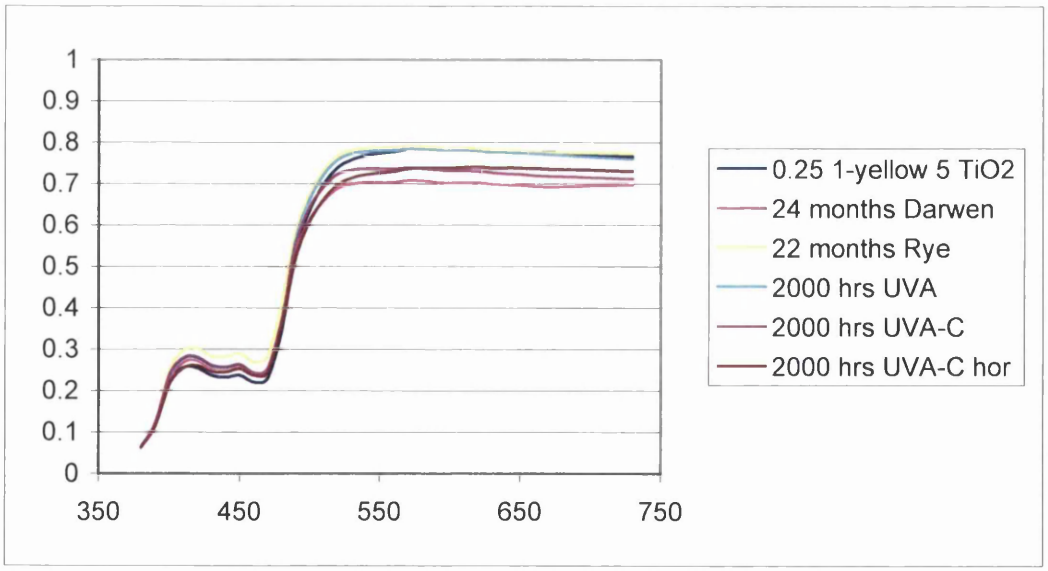
1
0.9
0.8
0.7
0.6
0.5
0.4
0.3
0.2
0.1
0
350
450
550
650
750
0.25 1-yellow 5 TiO2
24 months Darwen
22 months Rye
2000 hrs UVA
2000 hrs UVA-C
2000 hrs UVA-C hor

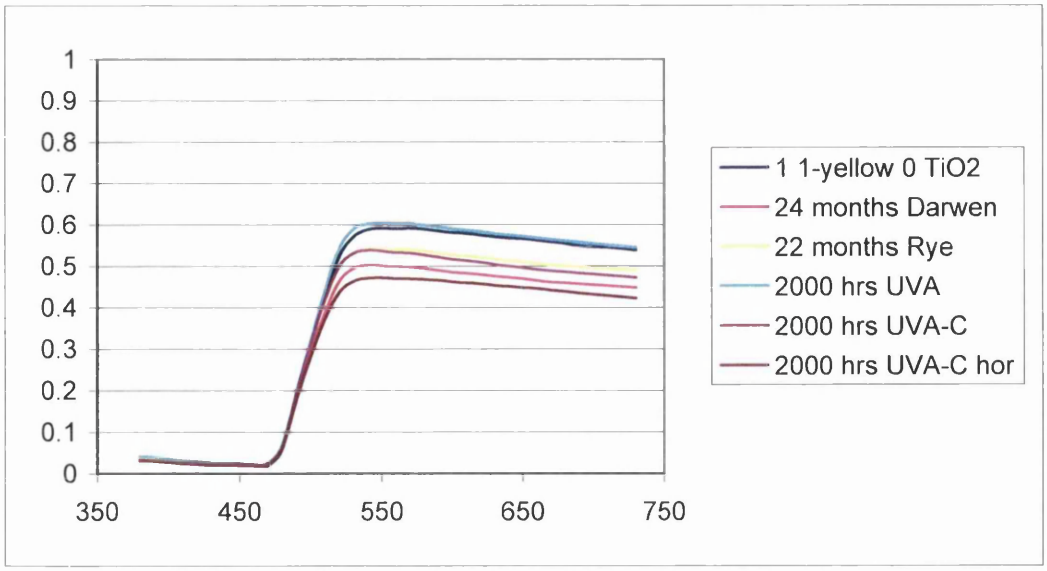
1
0.9
0.8
0.7
0.6
0.5
0.4
0.3
0.2
0.1
0
350
450
550
650
750
1 1-yellow 0 TiO2
24 months Darwen
22 months Rye
2000 hrs UVA
2000 hrs UVA-C
2000 hrs UVA-C hor

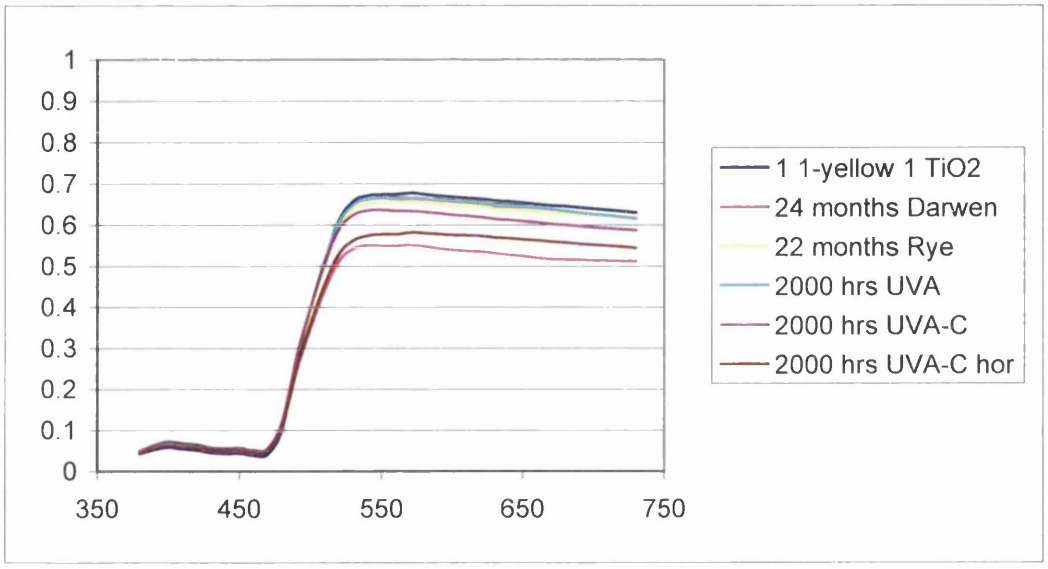
1
0.9
0.8
0.7
0.6
0.5
0.4
0.3
0.2
0.1
0
350
450
550
650
750
1 1-yellow 1 TiO2
24 months Darwen
22 months Rye
2000 hrs UVA
2000 hrs UVA-C
2000 hrs UVA-C hor

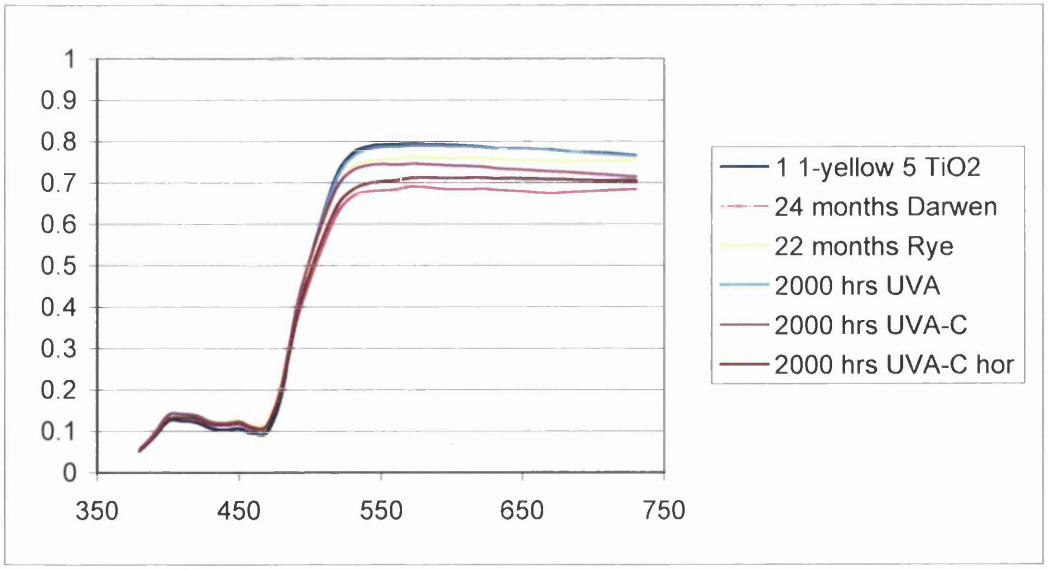
1
0.9
0.8
0.7
0.6
0.5
0.4
0.3
0.2
0.1
0
350
450
550
650
750
1 1-yellow 5 TiO2
24 months Darwen
22 months Rye
2000 hrs UVA
2000 hrs UVA-C
2000 hrs UVA-C hor

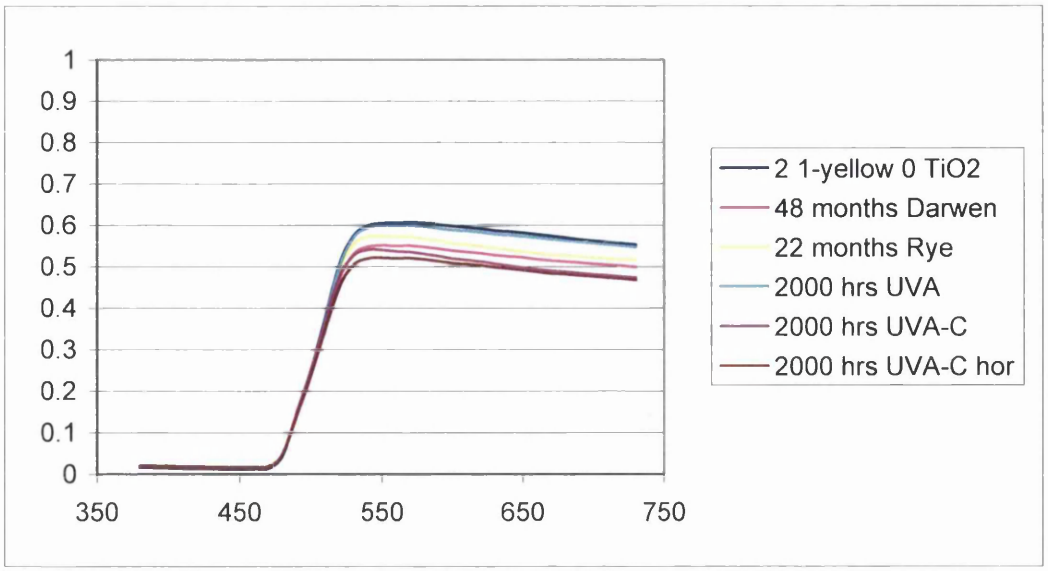
1
0.9
0.8
0.7
0.6
0.5
0.4
0.3
0.2
0.1
0
350
450
550
650
750
2 1-yellow 0 TiO2
48 months Darwen
22 months Rye
2000 hrs UVA
2000 hrs UVA-C
2000 hrs UVA-C hor

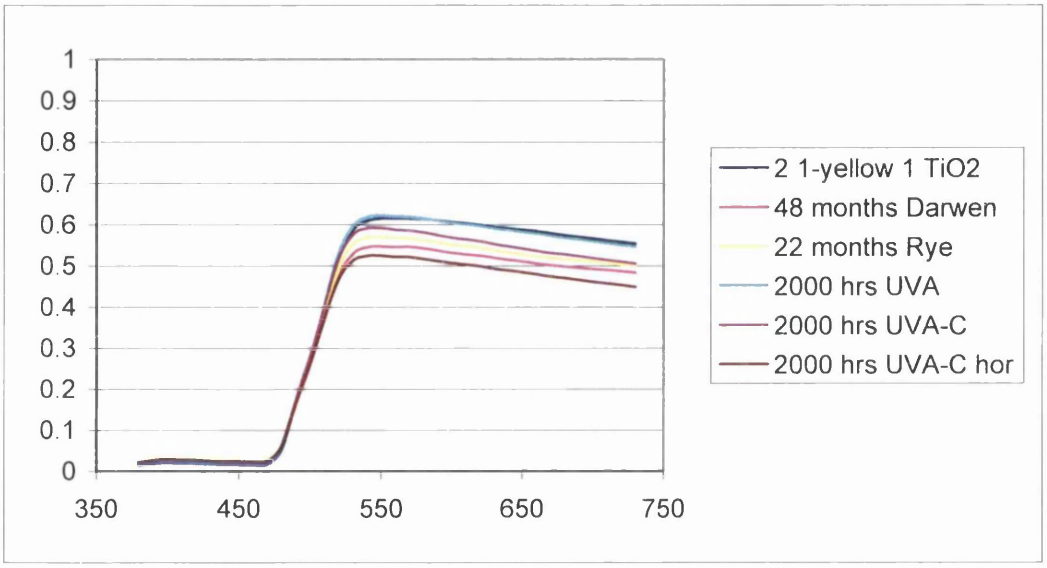
1
0.9
0.8
0.7
0.6
0.5
0.4
0.3
0.2
0.1
0
350
450
550
650
750
2 1-yellow 1 TiO2
48 months Darwen
22 months Rye
2000 hrs UVA
2000 hrs UVA-C
2000 hrs UVA-C hor

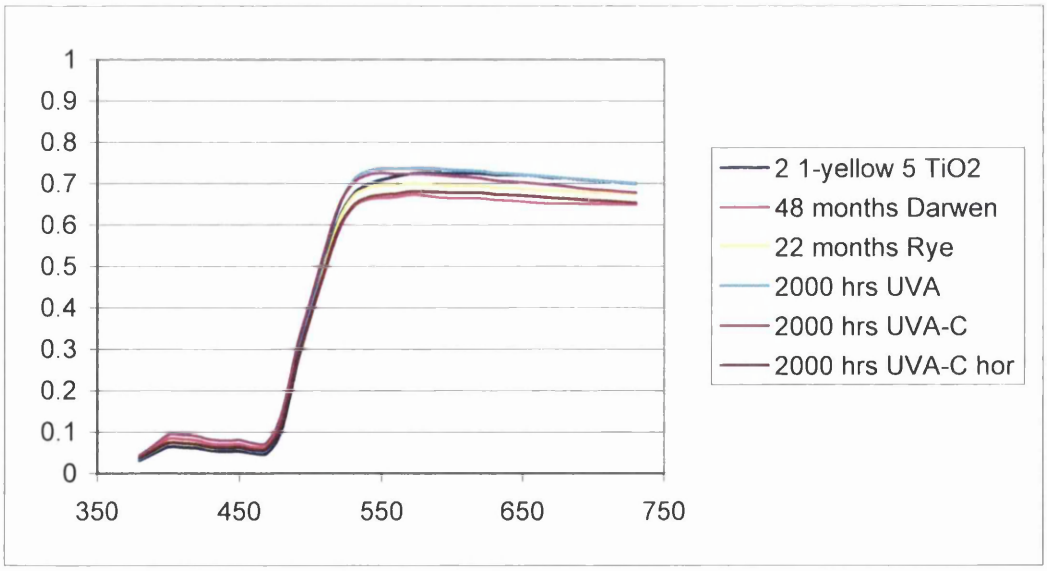
1
0.9
0.8
0.7
0.6
0.5
0.4
0.3
0.2
0.1
0
350
450
550
650
750
2 1-yellow 5 TiO2
48 months Darwen
22 months Rye
2000 hrs UVA
2000 hrs UVA-C
2000 hrs UVA-C hor

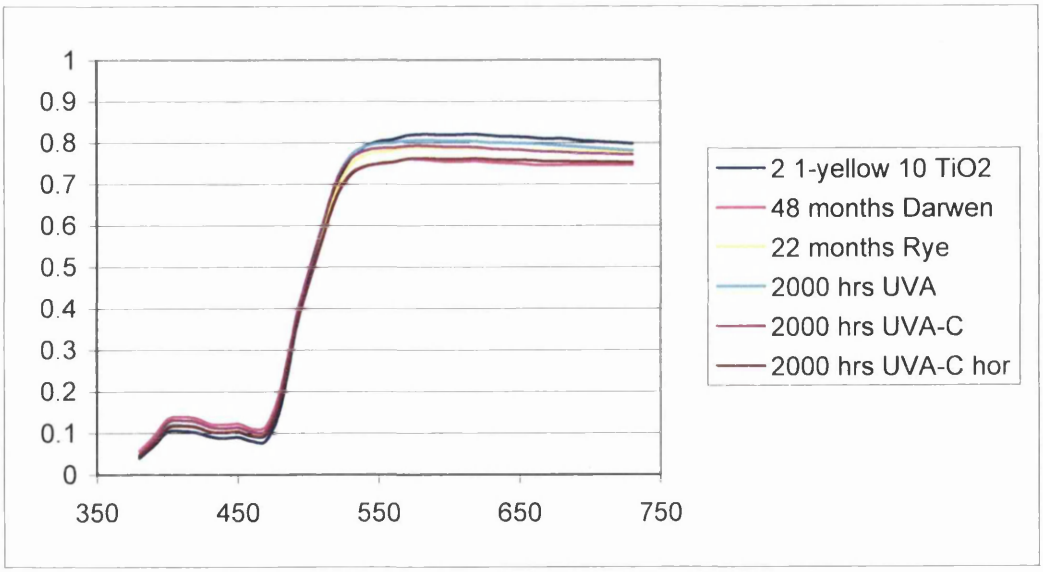
1
0.9
0.8
0.7
0.6
0.5
0.4
0.3
0.2
0.1
0
350
450
550
650
750
2 1-yellow 10 TiO2
48 months Darwen
22 months Rye
2000 hrs UVA
2000 hrs UVA-C
2000 hrs UVA-C hor

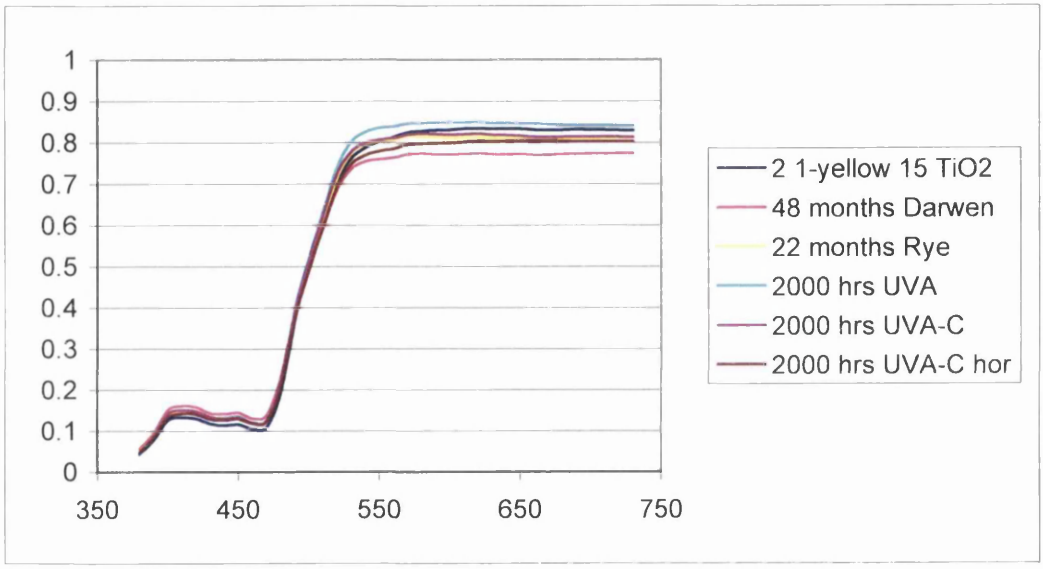
1
0.9
0.8
0.7
0.6
0.5
0.4
0.3
0.2
0.1
0
350
450
550
650
750
2 1-yellow 15 TiO2
48 months Darwen
22 months Rye
2000 hrs UVA
2000 hrs UVA-C
2000 hrs UVA-C hor

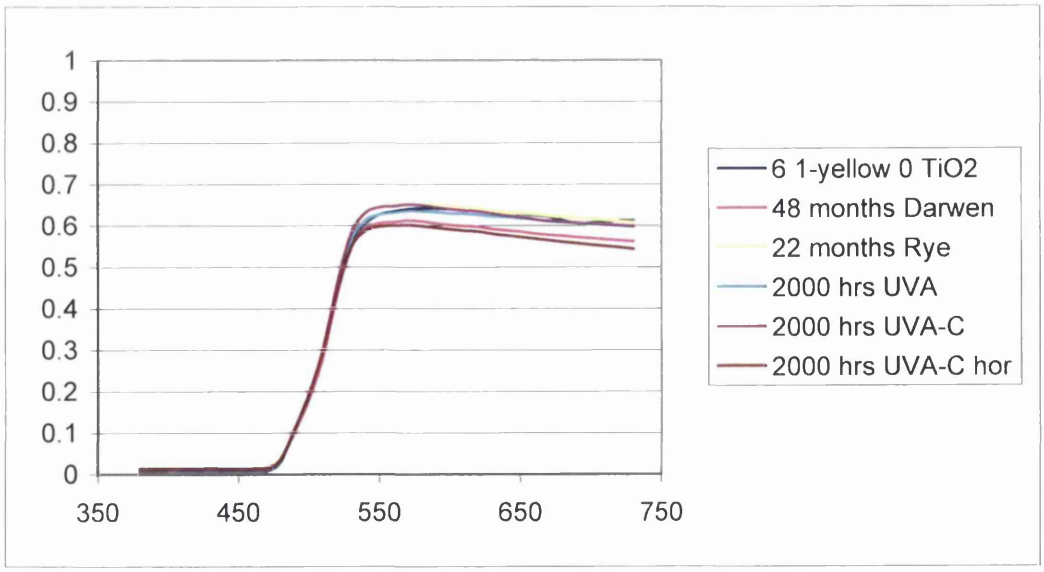
1
0.9
0.8
0.7
0.6
0.5
0.4
0.3
0.2
0.1
0
350
450
550
650
750
6 1-yellow 0 TiO2
48 months Darwen
22 months Rye
2000 hrs UVA
2000 hrs UVA-C
2000 hrs UVA-C hor

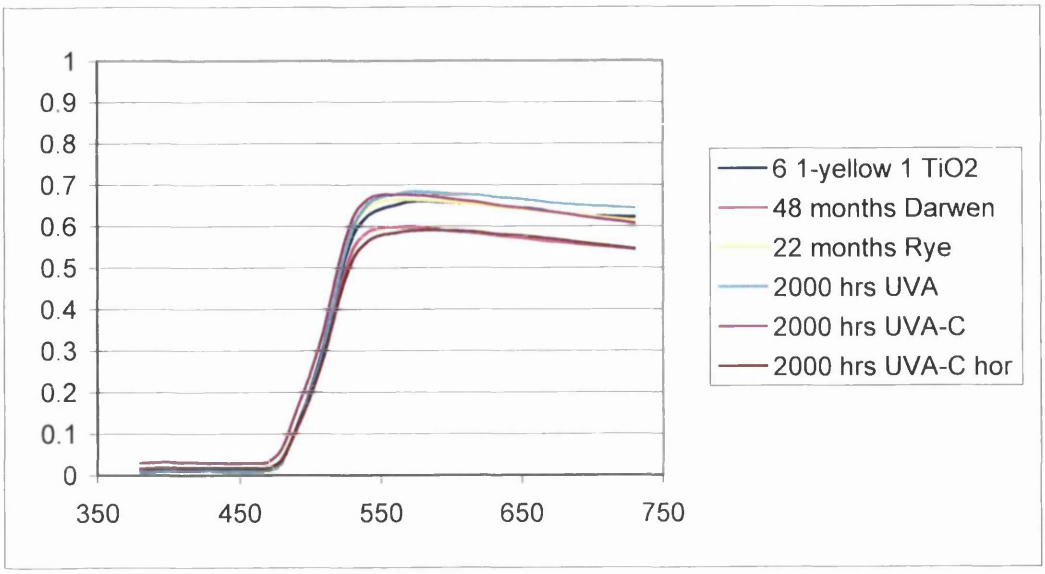
1
0.9
0.8
0.7
0.6
0.5
0.4
0.3
0.2
0.1
0
350
450
550
650
750
6 1-yellow 1 TiO2
48 months Darwen
22 months Rye
2000 hrs UVA
2000 hrs UVA-C
2000 hrs UVA-C hor

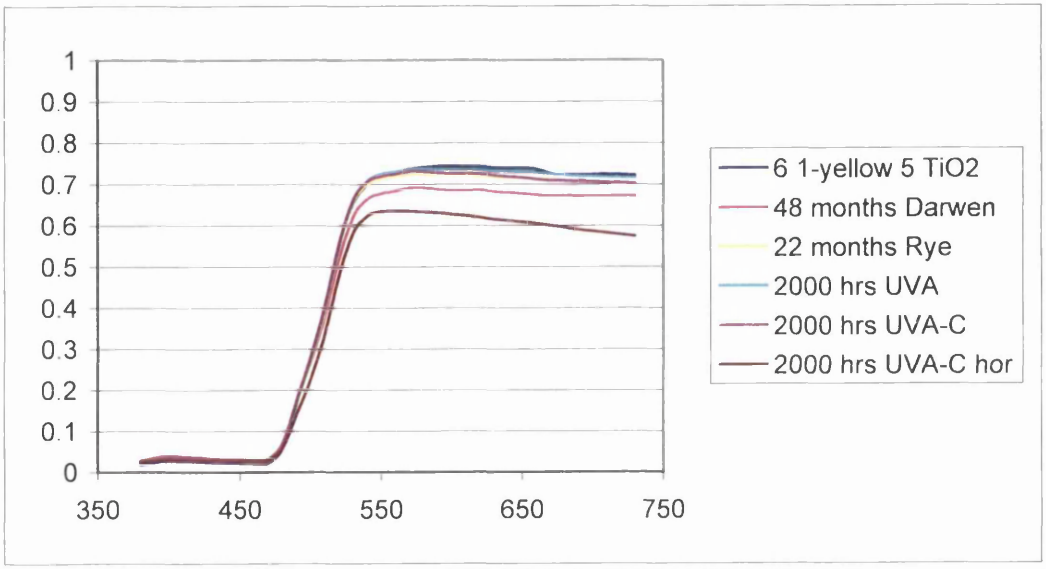
1
0.9
0.8
0.7
0.6
0.5
0.4
0.3
0.2
0.1
0
350
450
550
650
750
6 1-yellow 5 TiO2
48 months Darwen
22 months Rye
2000 hrs UVA
2000 hrs UVA-C
2000 hrs UVA-C hor

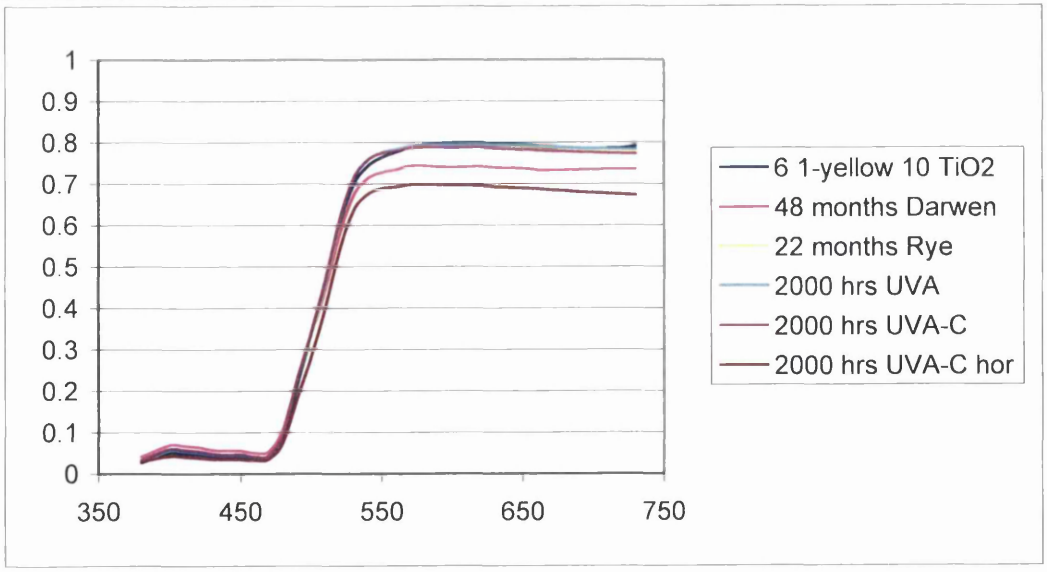
1
0.9
0.8
0.7
0.6
0.5
0.4
0.3
0.2
0.1
0
350
450
550
650
750
6 1-yellow 10 TiO2
48 months Darwen
22 months Rye
2000 hrs UVA
2000 hrs UVA-C
2000 hrs UVA-C hor

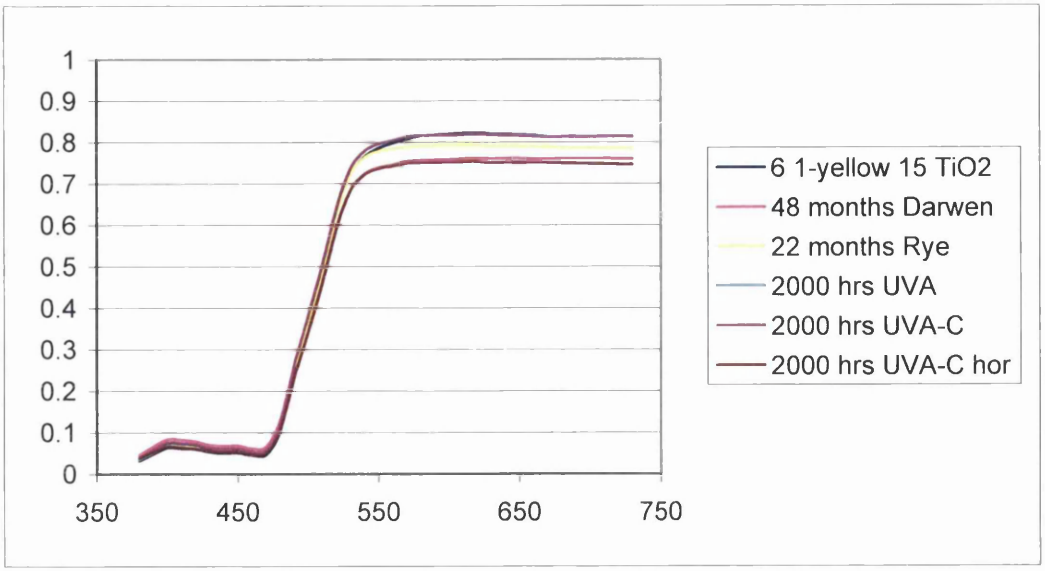
1
0.9
0.8
0.7
0.6
0.5
0.4
0.3
0.2
0.1
0
350
450
550
650
750
6 1-yellow 15 TiO2
48 months Darwen
22 months Rye
2000 hrs UVA
2000 hrs UVA-C
2000 hrs UVA-C hor

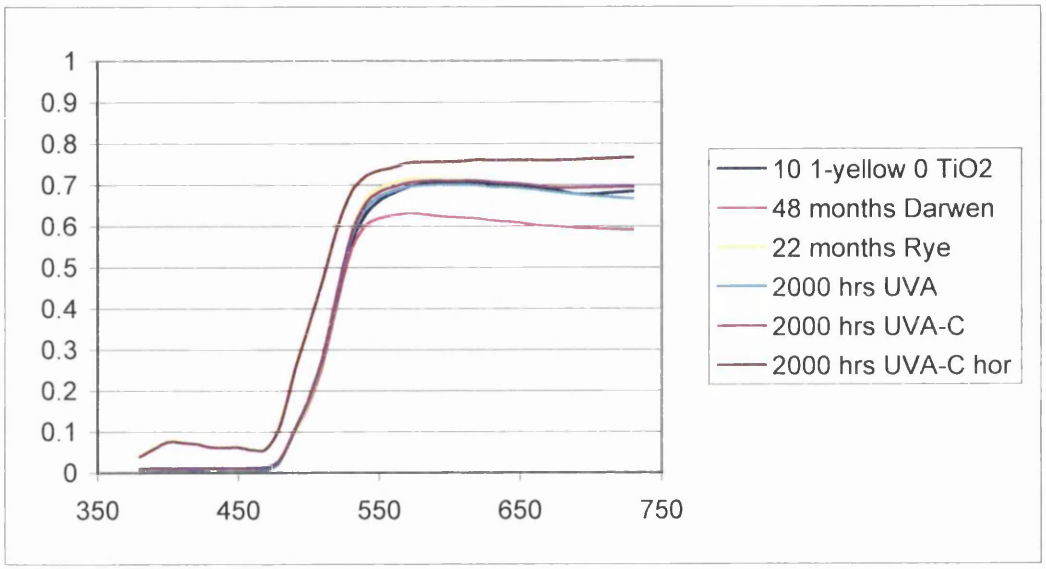
1
0.9
0.8
0.7
0.6
0.5
0.4
0.3
0.2
0.1
0
350
450
550
650
750
10 1-yellow 0 TiO2
48 months Darwen
22 months Rye
2000 hrs UVA
2000 hrs UVA-C
2000 hrs UVA-C hor

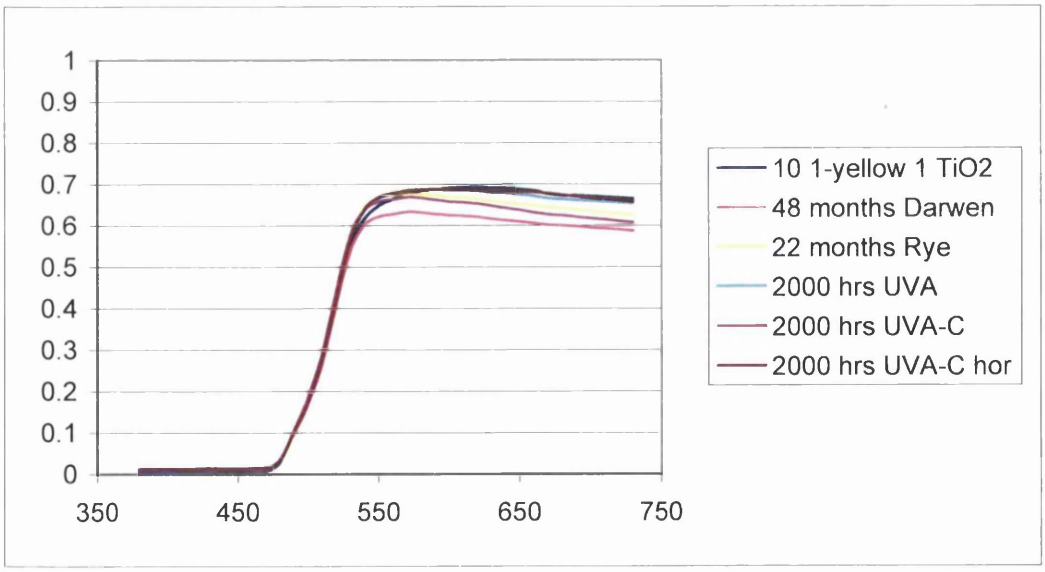
1
0.9
0.8
0.7
0.6
0.5
0.4
0.3
0.2
0.1
0
350
450
550
650
750
10 1-yellow 1 TiO2
48 months Darwen
22 months Rye
2000 hrs UVA
2000 hrs UVA-C
2000 hrs UVA-C hor

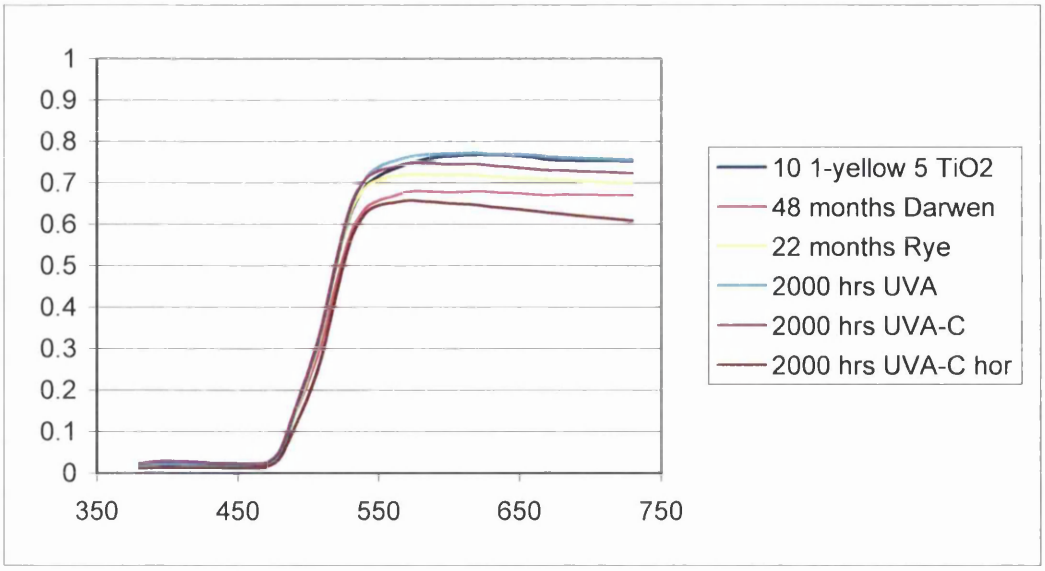
1
0.9
0.8
0.7
0.6
0.5
0.4
0.3
0.2
0.1
0
350
450
550
650
750
10 1-yellow 5 TiO2
48 months Darwen
22 months Rye
2000 hrs UVA
2000 hrs UVA-C
2000 hrs UVA-C hor

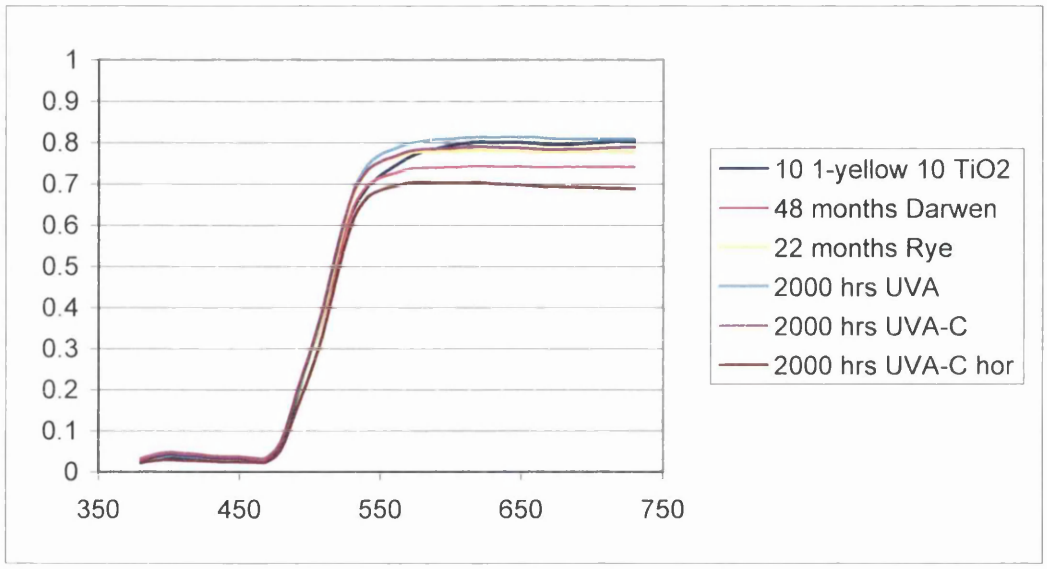
1
0.9
0.8
0.7
0.6
0.5
0.4
0.3
0.2
0.1
0
350
450
550
650
750
10 1-yellow 10 TiO2
48 months Darwen
22 months Rye
2000 hrs UVA
2000 hrs UVA-C
2000 hrs UVA-C hor

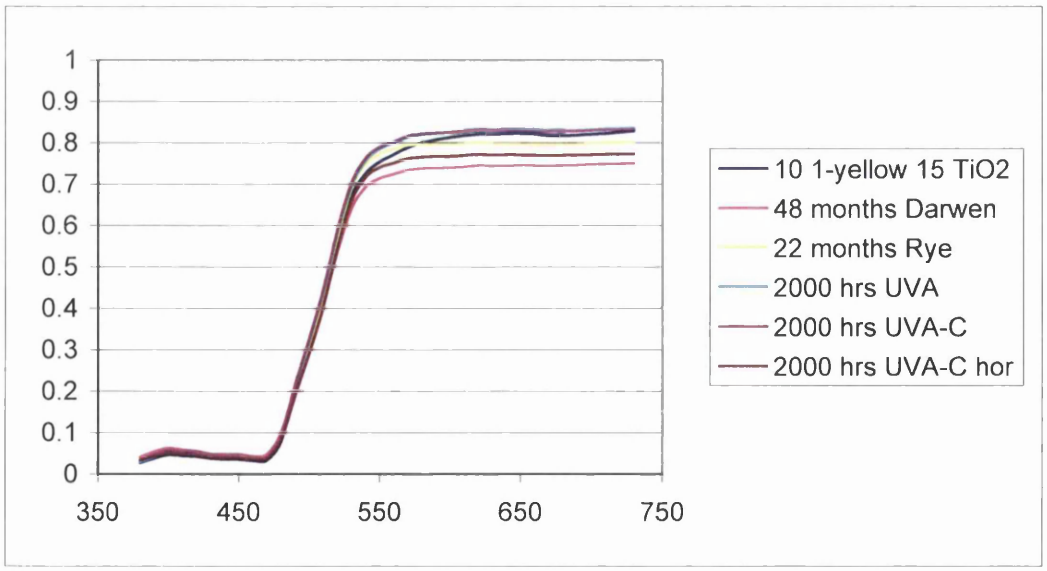
1
0.9
0.8
0.7
0.6
0.5
0.4
0.3
0.2
0.1
0
350
450
550
650
750
10 1-yellow 15 TiO2
48 months Darwen
22 months Rye
2000 hrs UVA
2000 hrs UVA-C
2000 hrs UVA-C hor

Appendix I

2-Yellow

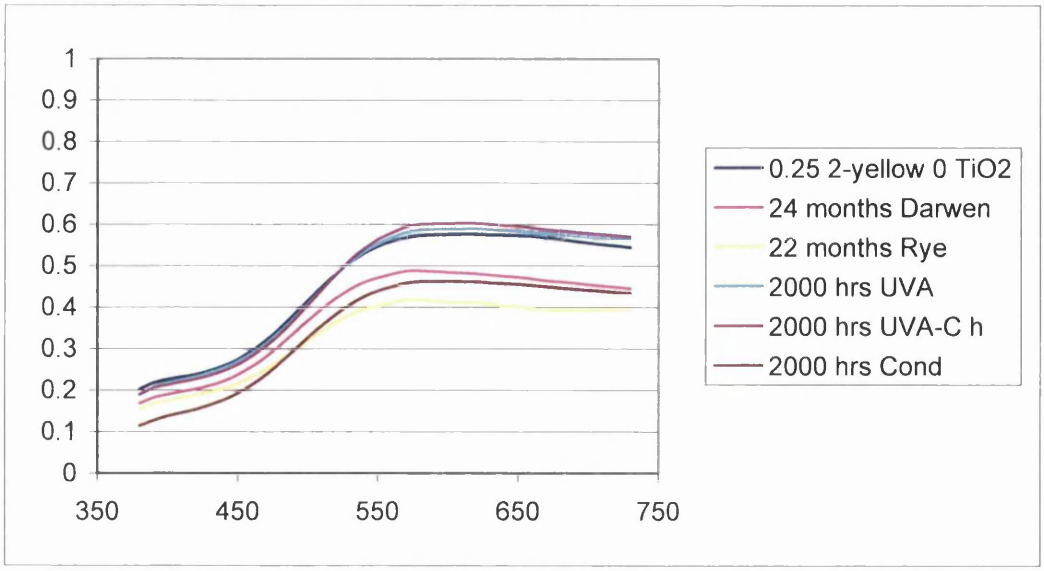
1
0.9
0.8
0.7
0.6
0.5
0.4
0.3
0.2
0.1
0
350
450
550
650
750
0.25 2-yellow 0 TiO2
24 months Darwen
22 months Rye
2000 hrs UVA
2000 hrs UVA-C h
2000 hrs Cond

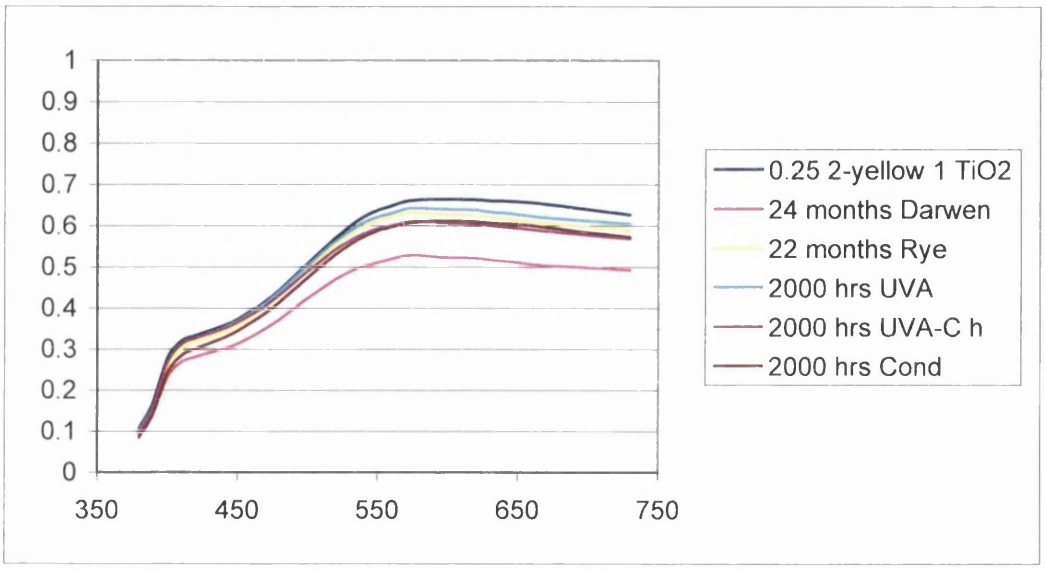
1
0.9
0.8
0.7
0.6
0.5
0.4
0.3
0.2
0.1
0
350
450
550
650
750
0.25 2-yellow 1 TiO2
24 months Darwen
22 months Rye
2000 hrs UVA
2000 hrs UVA-C h
2000 hrs Cond

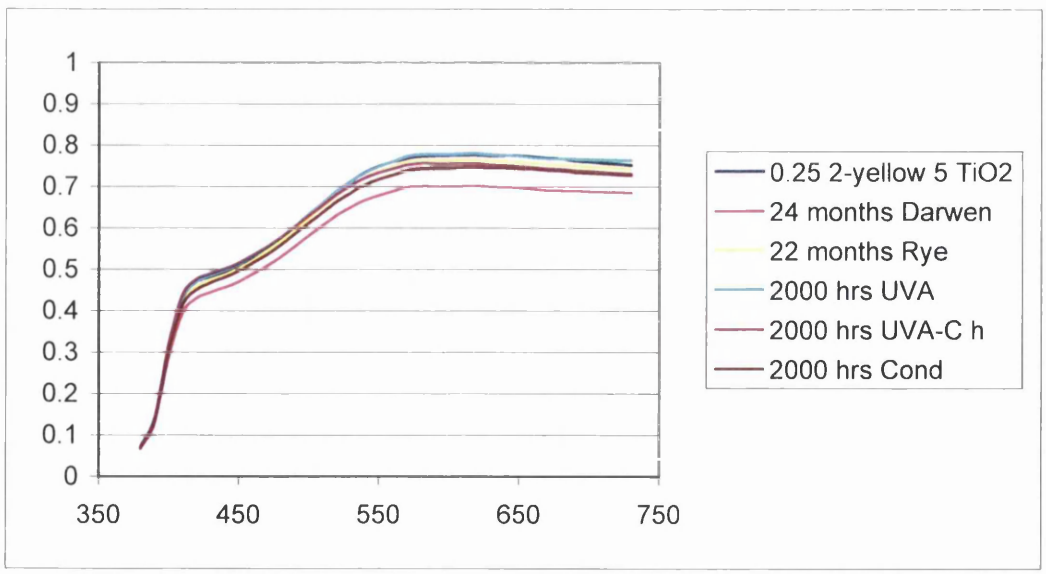
1
0.9
0.8
0.7
0.6
0.5
0.4
0.3
0.2
0.1
0
350
450
550
650
750
0.25 2-yellow 5 TiO2
24 months Darwen
22 months Rye
2000 hrs UVA
2000 hrs UVA-C h
2000 hrs Cond

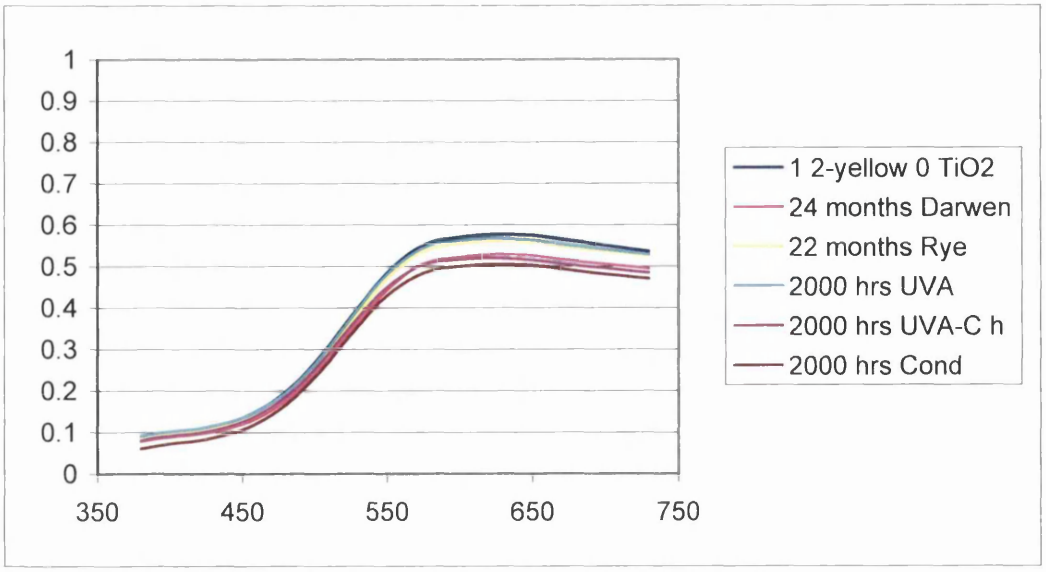
1
0.9
0.8
0.7
0.6
0.5
0.4
0.3
0.2
0.1
0
350
450
550
650
750
1 2-yellow 0 TiO2
24 months Darwen
22 months Rye
2000 hrs UVA
2000 hrs UVA-C h
2000 hrs Cond

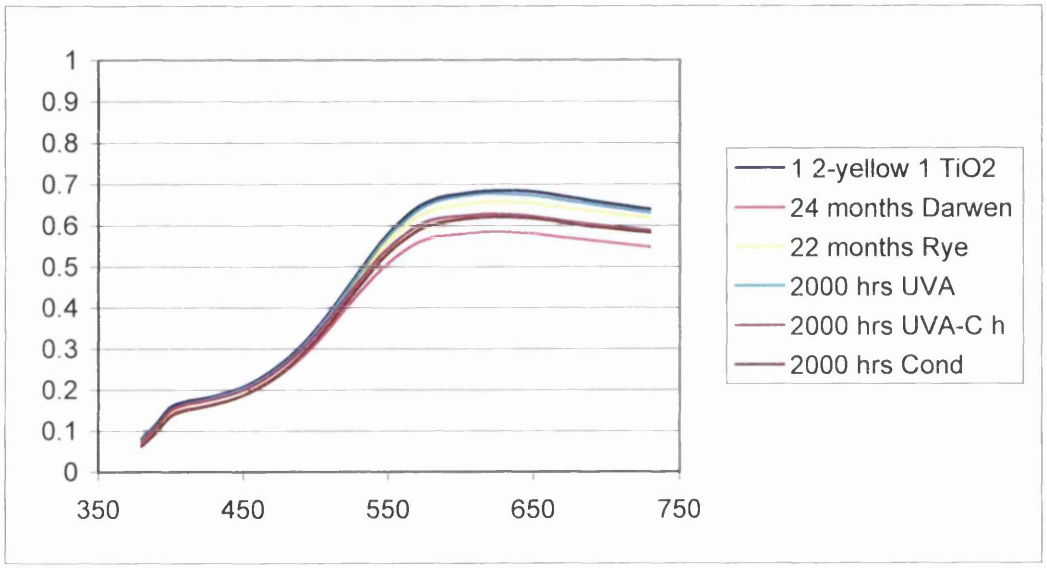
1
0.9
0.8
0.7
0.6
0.5
0.4
0.3
0.2
0.1
0
350
450
550
650
750
1 2-yellow 1 TiO2
24 months Darwen
22 months Rye
2000 hrs UVA
2000 hrs UVA-C h
2000 hrs Cond

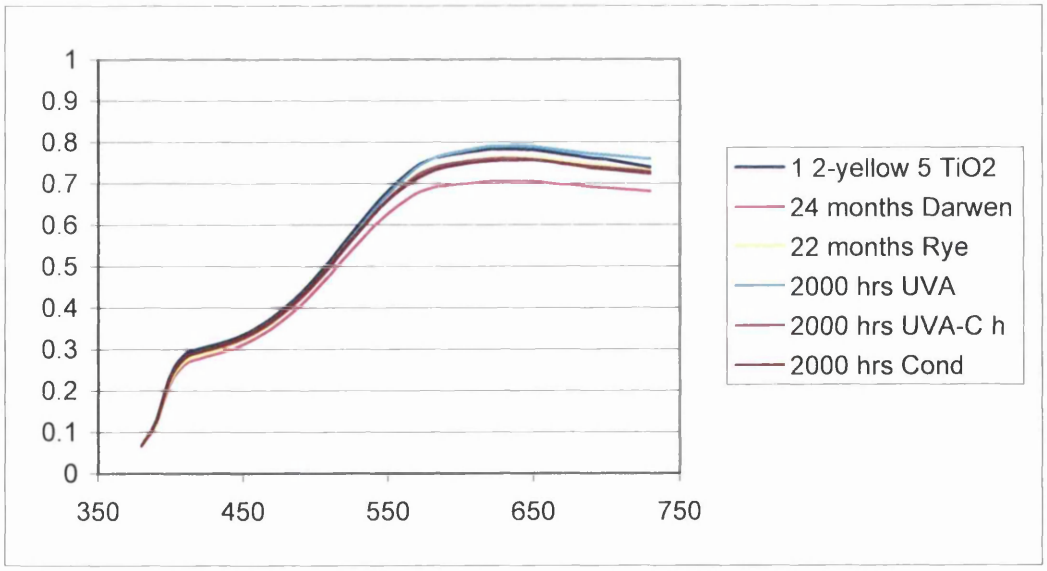
1
0.9
0.8
0.7
0.6
0.5
0.4
0.3
0.2
0.1
0
350
450
550
650
750
1 2-yellow 5 TiO2
24 months Darwen
22 months Rye
2000 hrs UVA
2000 hrs UVA-C h
2000 hrs Cond

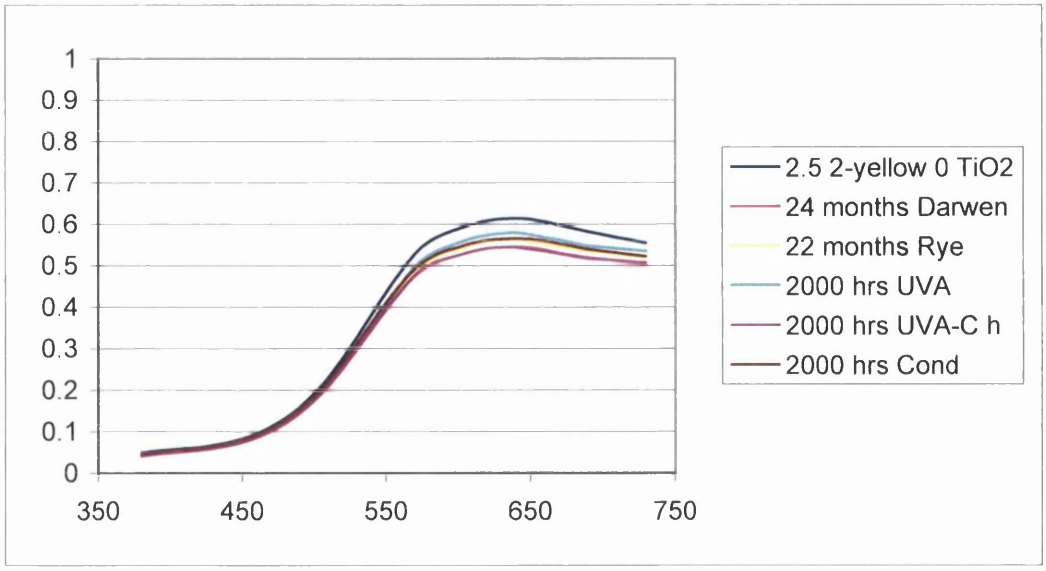
1
0.9
0.8
0.7
0.6
0.5
0.4
0.3
0.2
0.1
0
350
450
550
650
750
2.5 2-yellow 0 TiO2
24 months Darwen
22 months Rye
2000 hrs UVA
2000 hrs UVA-C h
2000 hrs Cond

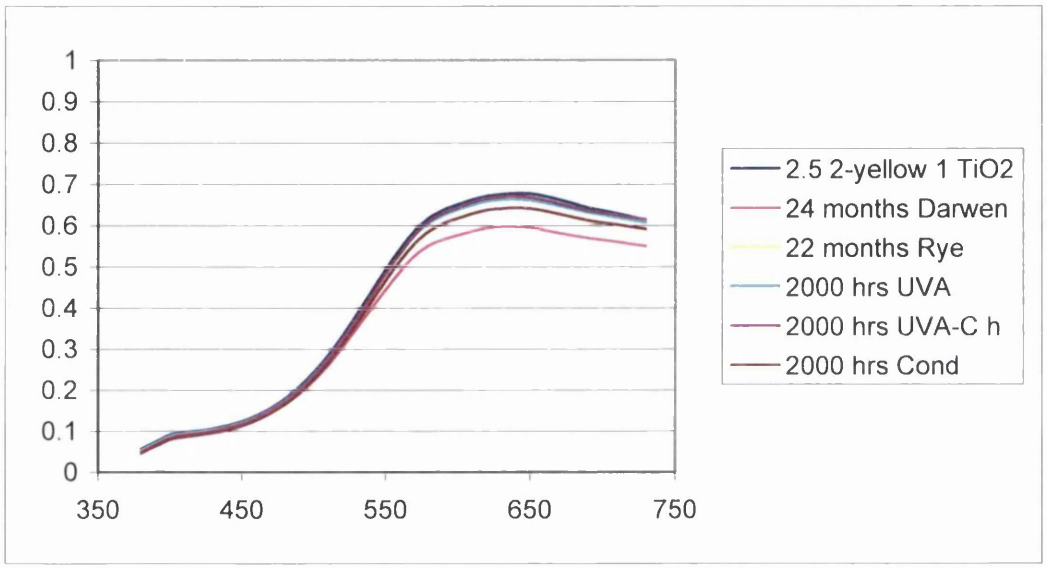
1
0.9
0.8
0.7
0.6
0.5
0.4
0.3
0.2
0.1
0
350
450
550
650
750
2.5 2-yellow 1 TiO2
24 months Darwen
22 months Rye
2000 hrs UVA
2000 hrs UVA-C h
2000 hrs Cond

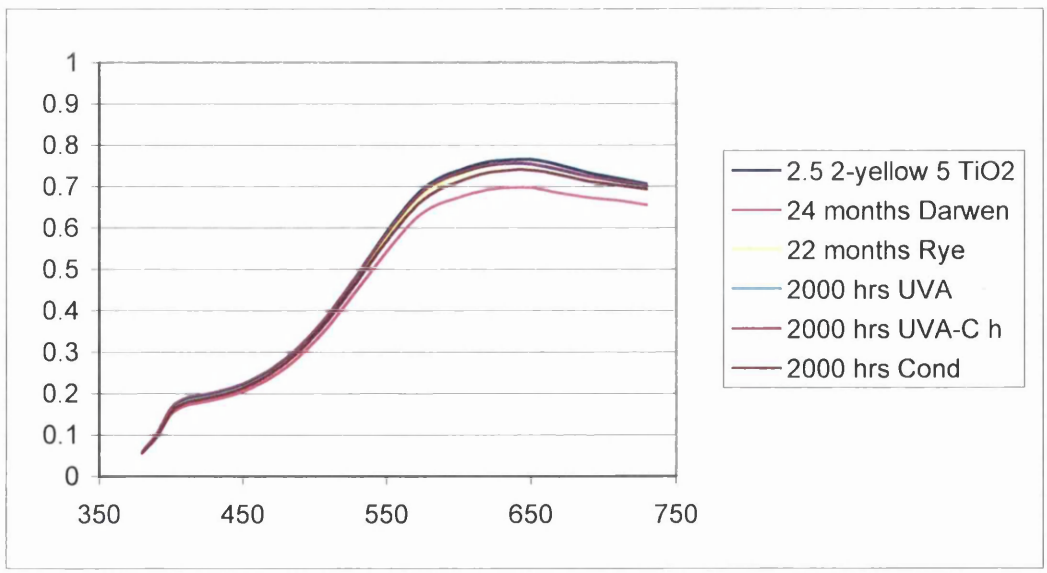
1
0.9
0.8
0.7
0.6
0.5
0.4
0.3
0.2
0.1
0
350
450
550
650
750
2.5 2-yellow 5 TiO2
24 months Darwen
22 months Rye
2000 hrs UVA
2000 hrs UVA-C h
2000 hrs Cond

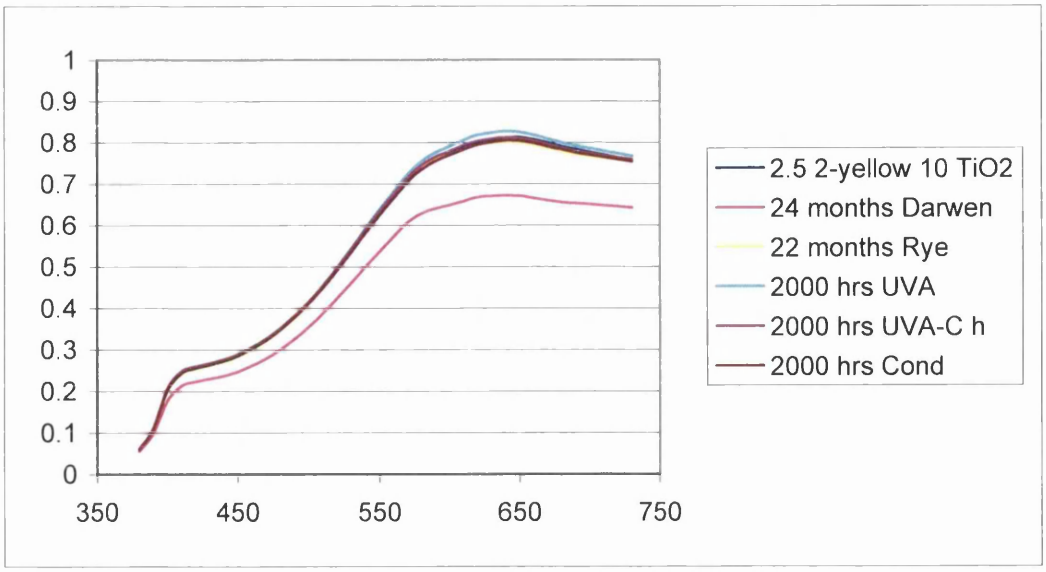
1
0.9
0.8
0.7
0.6
0.5
0.4
0.3
0.2
0.1
0
350
450
550
650
750
2.5 2-yellow 10 TiO2
24 months Darwen
22 months Rye
2000 hrs UVA
2000 hrs UVA-C h
2000 hrs Cond

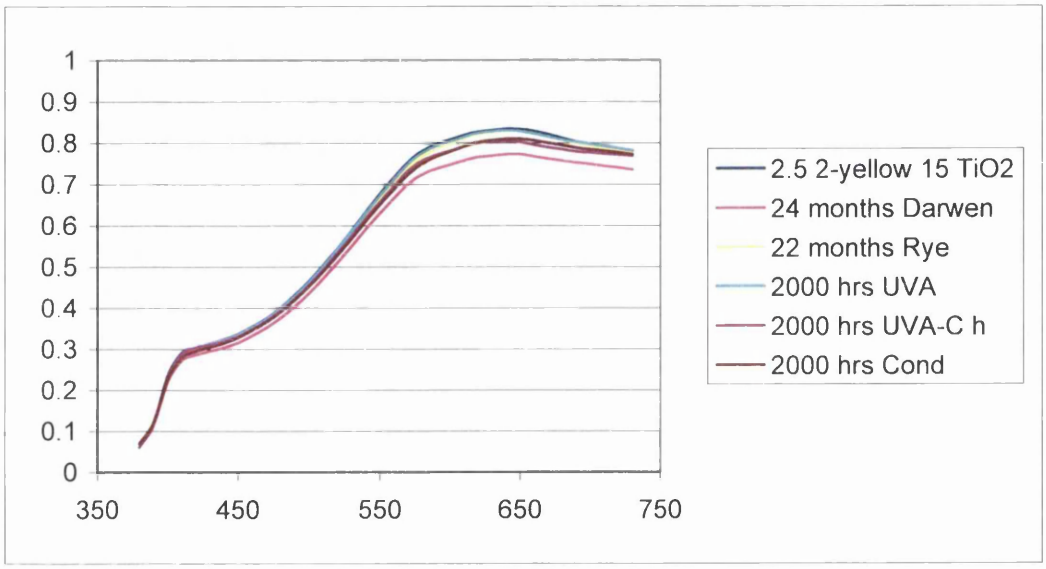
1
0.9
0.8
0.7
0.6
0.5
0.4
0.3
0.2
0.1
0
350
450
550
650
750
2.5 2-yellow 15 TiO2
24 months Darwen
22 months Rye
2000 hrs UVA
2000 hrs UVA-C h
2000 hrs Cond

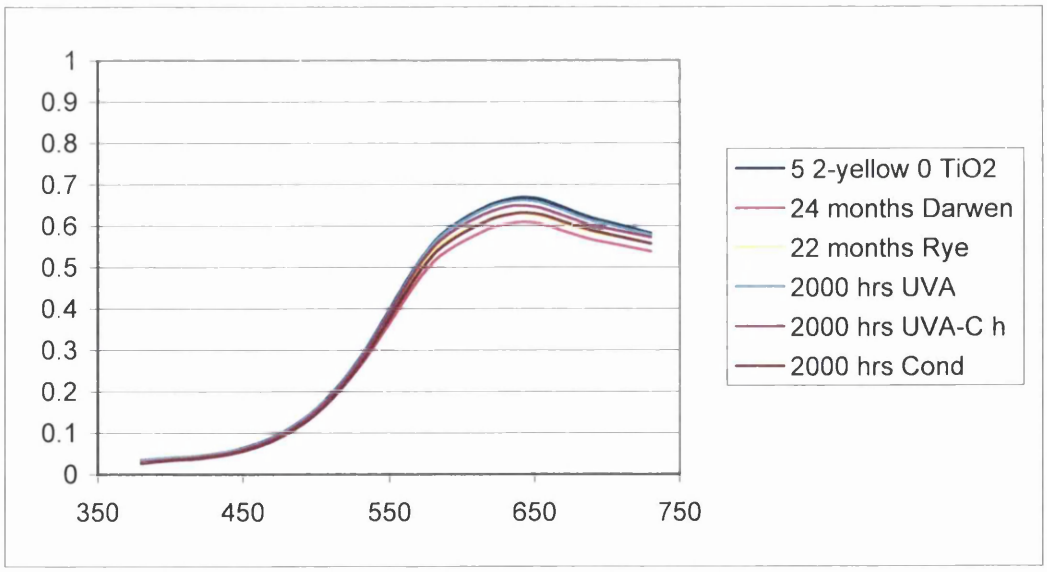
1
0.9
0.8
0.7
0.6
0.5
0.4
0.3
0.2
0.1
0
350
450
550
650
750
5 2-yellow 0 TiO2
24 months Darwen
22 months Rye
2000 hrs UVA
2000 hrs UVA-C h
2000 hrs Cond

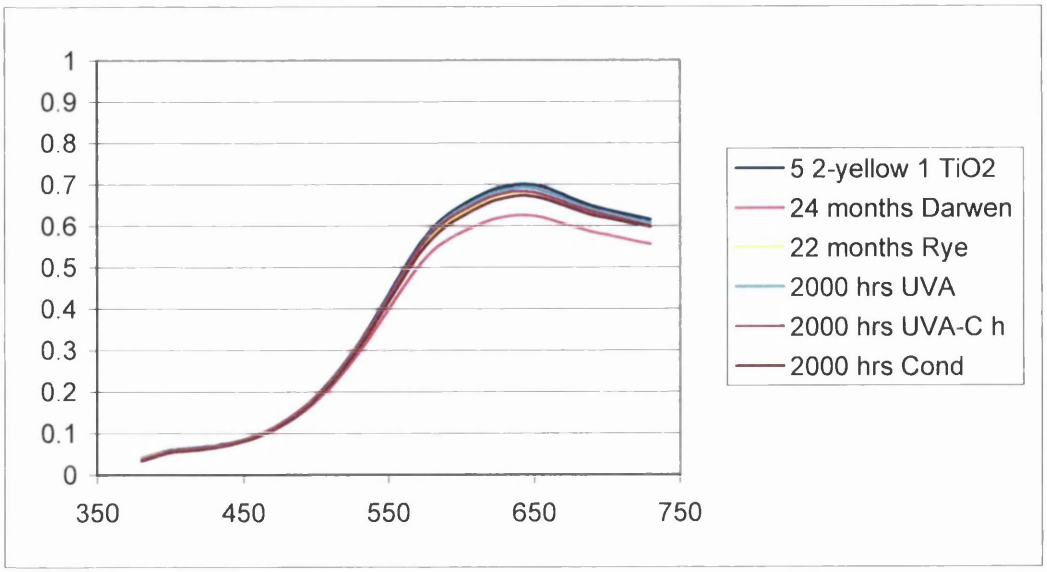
1
0.9
0.8
0.7
0.6
0.5
0.4
0.3
0.2
0.1
0
350
450
550
650
750
5 2-yellow 1 TiO2
24 months Darwen
22 months Rye
2000 hrs UVA
2000 hrs UVA-C h
2000 hrs Cond

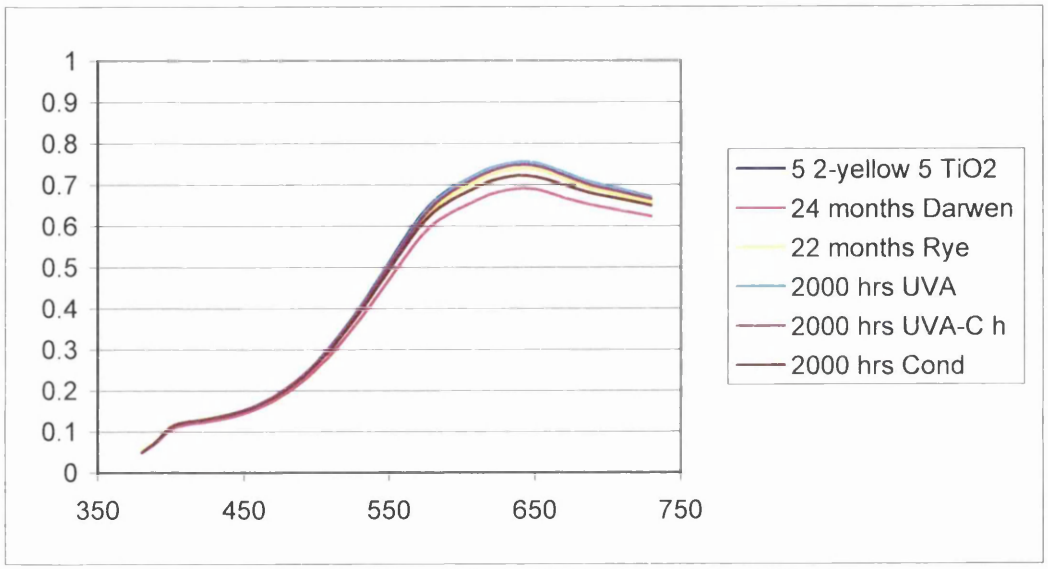
1
0.9
0.8
0.7
0.6
0.5
0.4
0.3
0.2
0.1
0
350
450
550
650
750
5 2-yellow 5 TiO2
24 months Darwen
22 months Rye
2000 hrs UVA
2000 hrs UVA-C h
2000 hrs Cond

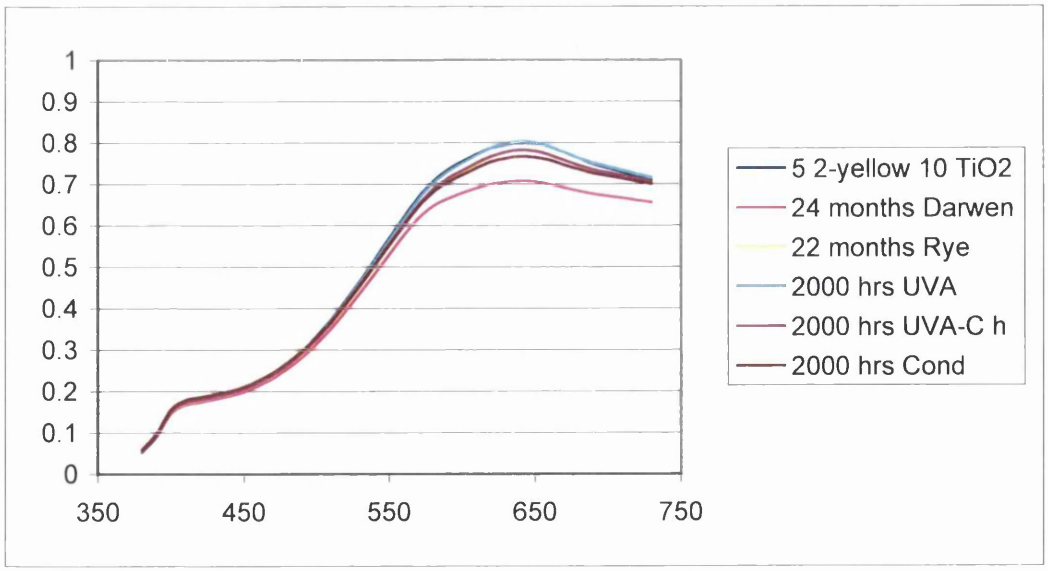
1
0.9
0.8
0.7
0.6
0.5
0.4
0.3
0.2
0.1
0
350
450
550
650
750
5 2-yellow 10 TiO2
24 months Darwen
22 months Rye
2000 hrs UVA
2000 hrs UVA-C h
2000 hrs Cond

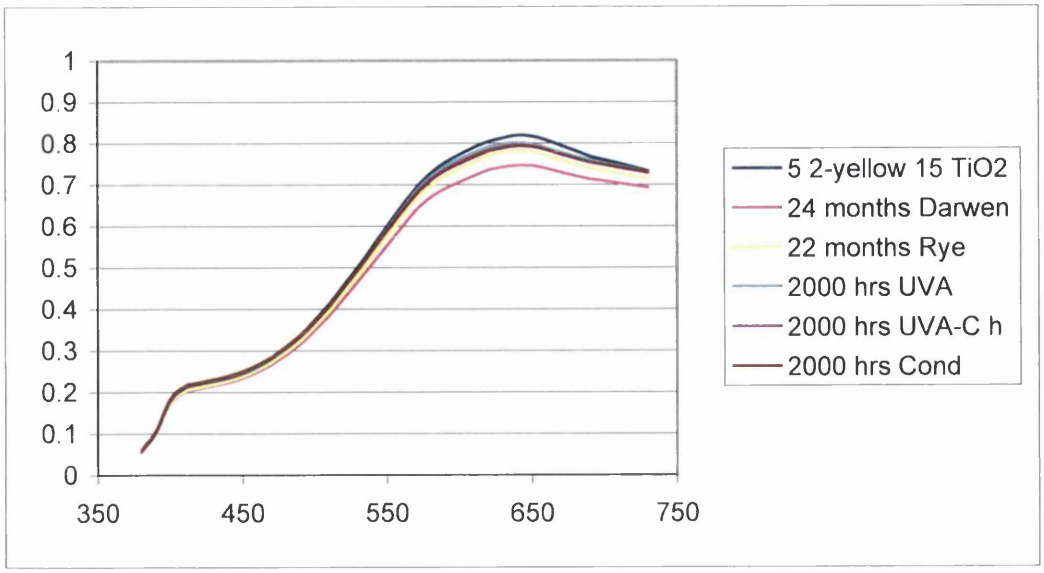
1
0.9
0.8
0.7
0.6
0.5
0.4
0.3
0.2
0.1
0
350
450
550
650
750
5 2-yellow 15 TiO2
24 months Darwen
22 months Rye
2000 hrs UVA
2000 hrs UVA-C h
2000 hrs Cond

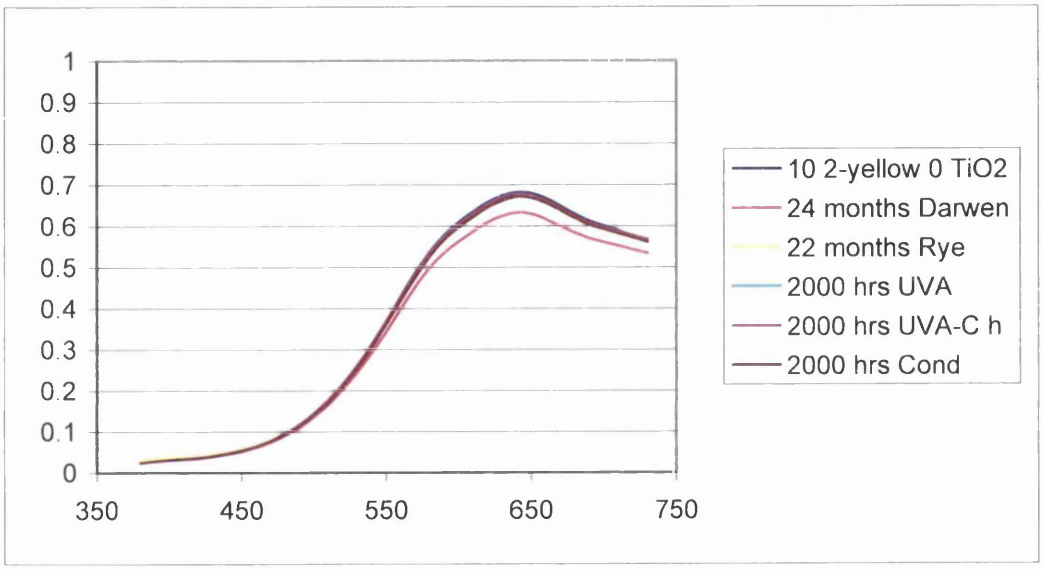
1
0.9
0.8
0.7
0.6
0.5
0.4
0.3
0.2
0.1
0
350
450
550
650
750
10 2-yellow 0 TiO2
24 months Darwen
22 months Rye
2000 hrs UVA
2000 hrs UVA-C h
2000 hrs Cond

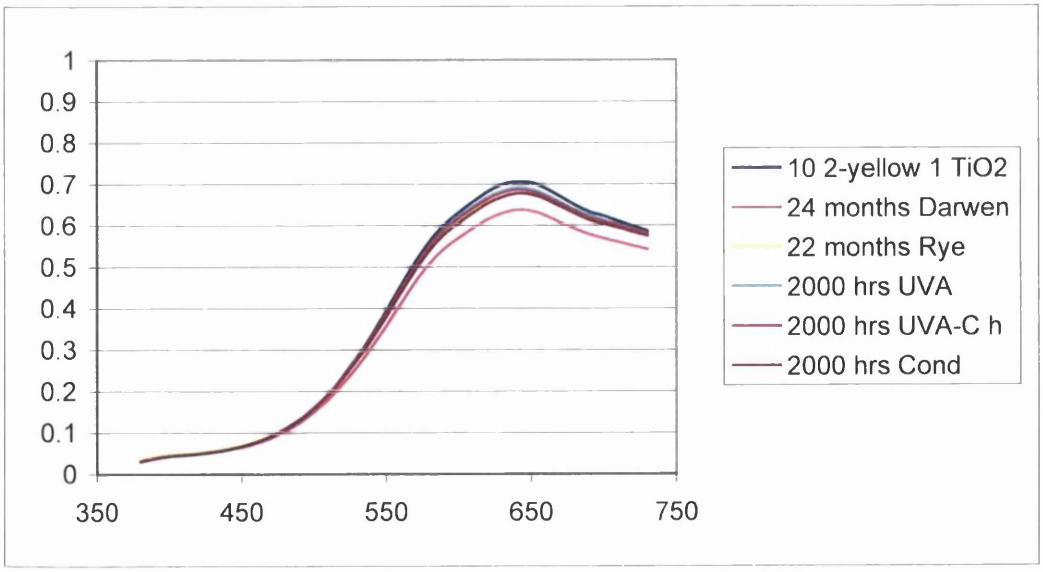
1
0.9
0.8
0.7
0.6
0.5
0.4
0.3
0.2
0.1
0
350
450
550
650
750
10 2-yellow 1 TiO2
24 months Darwen
22 months Rye
2000 hrs UVA
2000 hrs UVA-C h
2000 hrs Cond

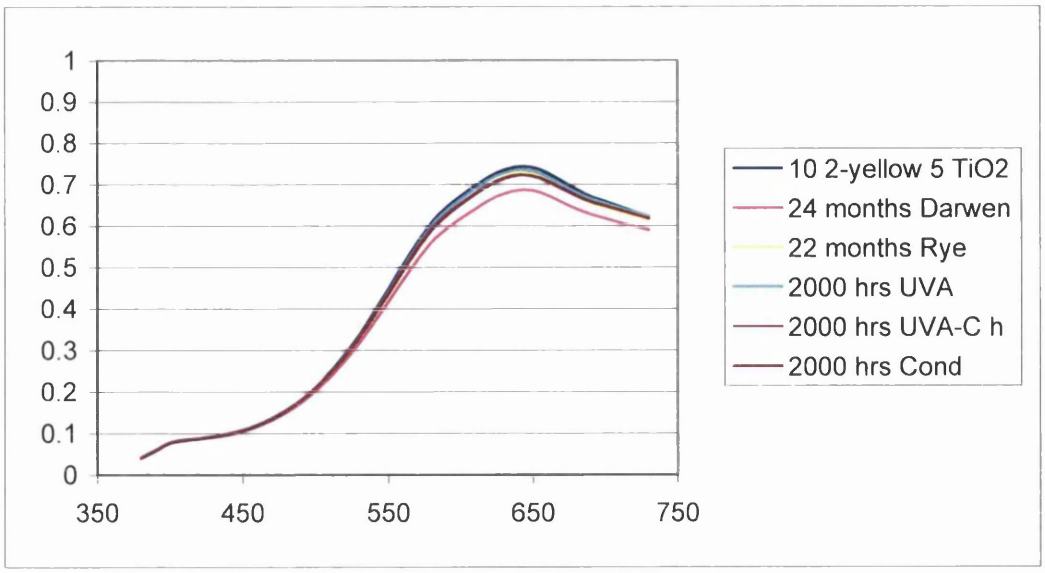
1
0.9
0.8
0.7
0.6
0.5
0.4
0.3
0.2
0.1
0
350
450
550
650
750
10 2-yellow 5 TiO2
24 months Darwen
22 months Rye
2000 hrs UVA
2000 hrs UVA-C h
2000 hrs Cond

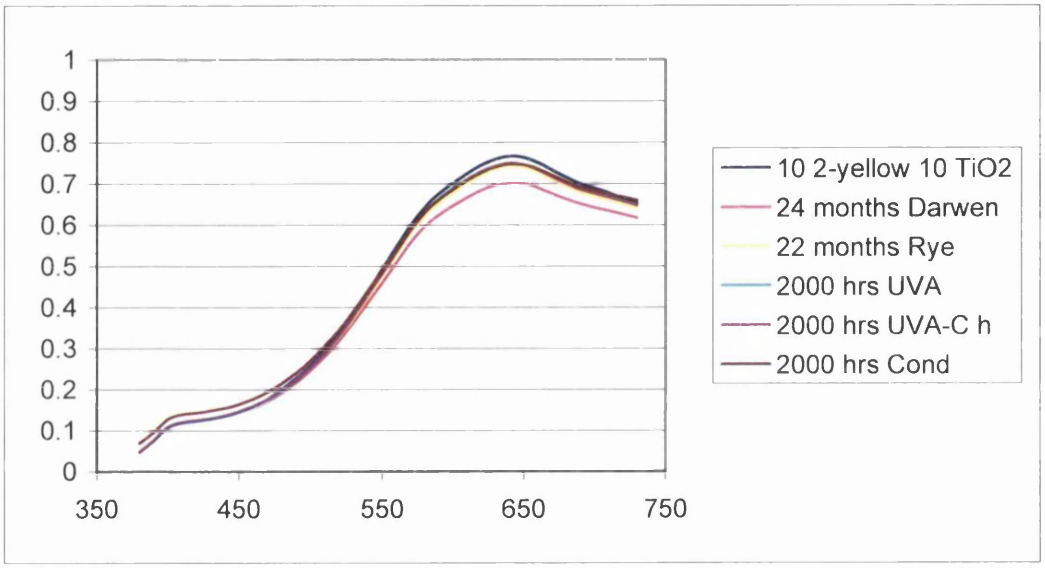
1
0.9
0.8
0.7
0.6
0.5
0.4
0.3
0.2
0.1
0
350
450
550
650
750
10 2-yellow 10 TiO2
24 months Darwen
22 months Rye
2000 hrs UVA
2000 hrs UVA-C h
2000 hrs Cond

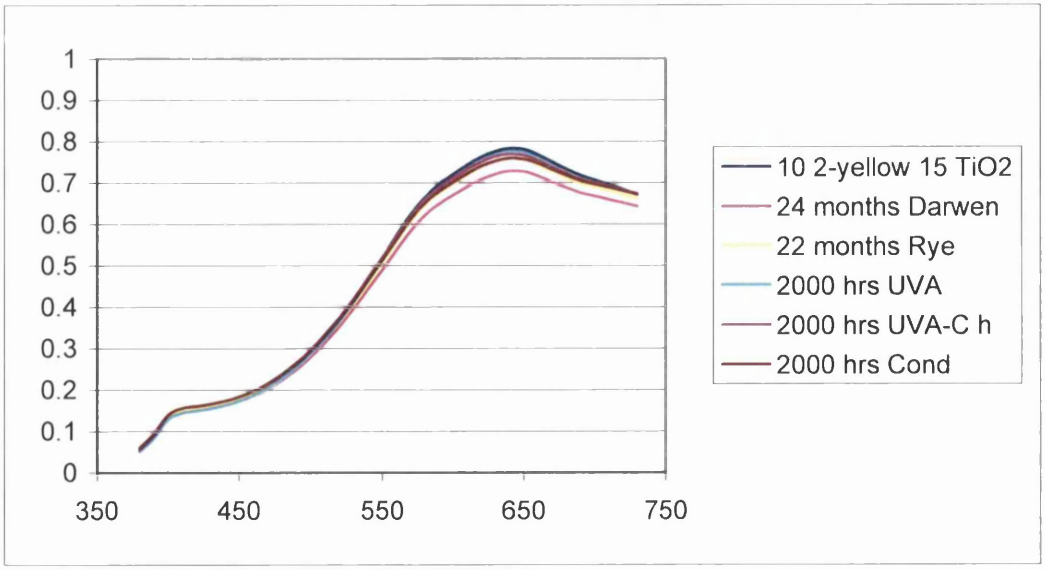
1
0.9
0.8
0.7
0.6
0.5
0.4
0.3
0.2
0.1
0
350
450
550
650
750
10 2-yellow 15 TiO2
24 months Darwen
22 months Rye
2000 hrs UVA
2000 hrs UVA-C h
2000 hrs Cond

Appendix I

Base + TiO2

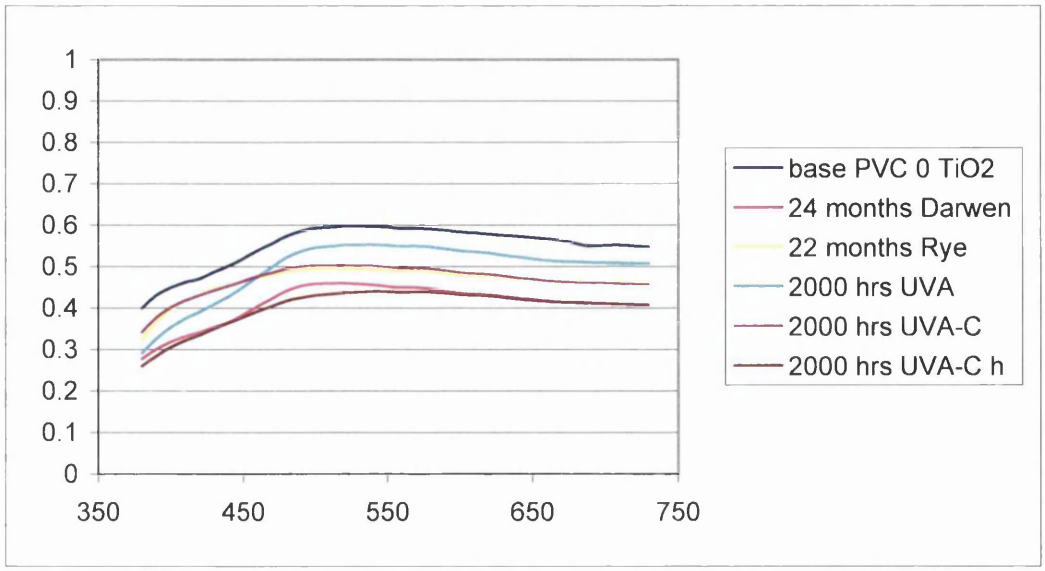
1
0.9
0.8
0.7
0.6
0.5
0.4
0.3
0.2
0.1
0
350
450
550
650
750
base PVC 0 TiO2
24 months Darwen
22 months Rye
2000 hrs UVA
2000 hrs UVA-C
2000 hrs UVA-C h

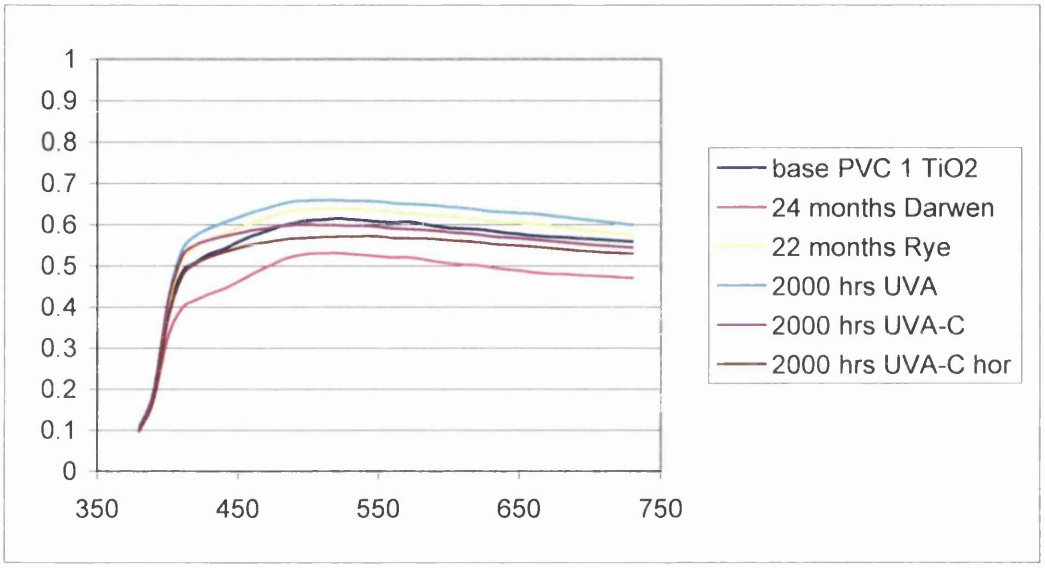
1
0.9
0.8
0.7
0.6
0.5
0.4
0.3
0.2
0.1
0
350
450
550
650
750
base PVC 1 TiO2
24 months Darwen
22 months Rye
2000 hrs UVA
2000 hrs UVA-C
2000 hrs UVA-C hor

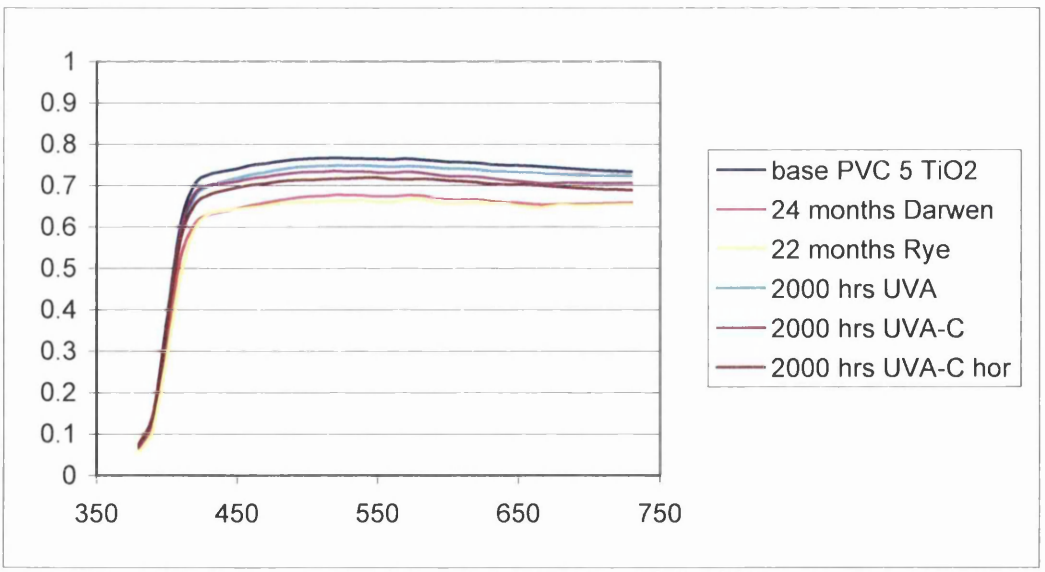
1
0.9
0.8
0.7
0.6
0.5
0.4
0.3
0.2
0.1
0
350
450
550
650
750
base PVC 5 TiO2
24 months Darwen
22 months Rye
2000 hrs UVA
2000 hrs UVA-C
2000 hrs UVA-C hor

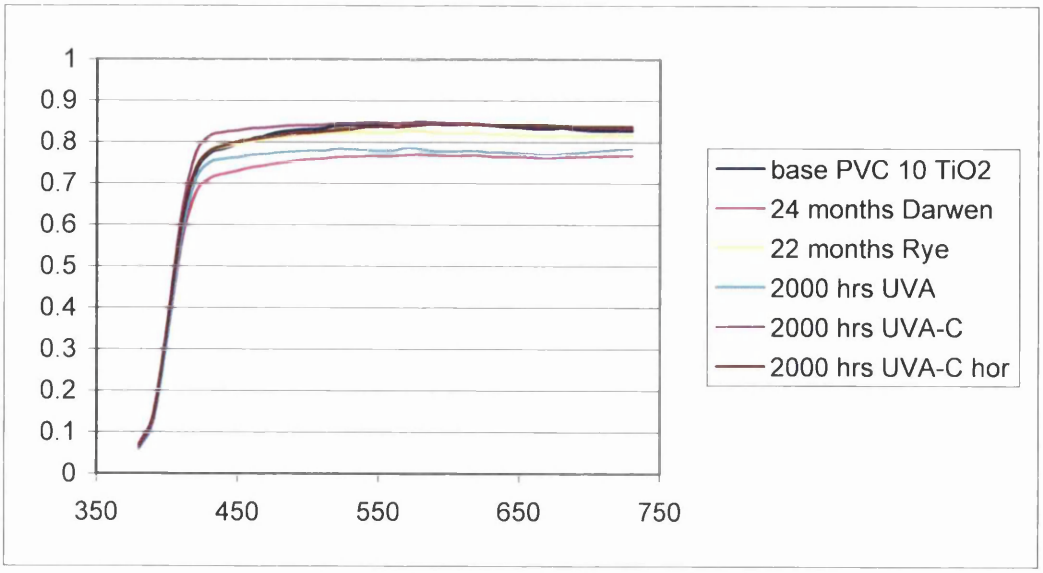
1
0.9
0.8
0.7
0.6
0.5
0.4
0.3
0.2
0.1
0
350
450
550
650
750
base PVC 10 TiO2
24 months Darwen
22 months Rye
2000 hrs UVA
2000 hrs UVA-C
2000 hrs UVA-C hor

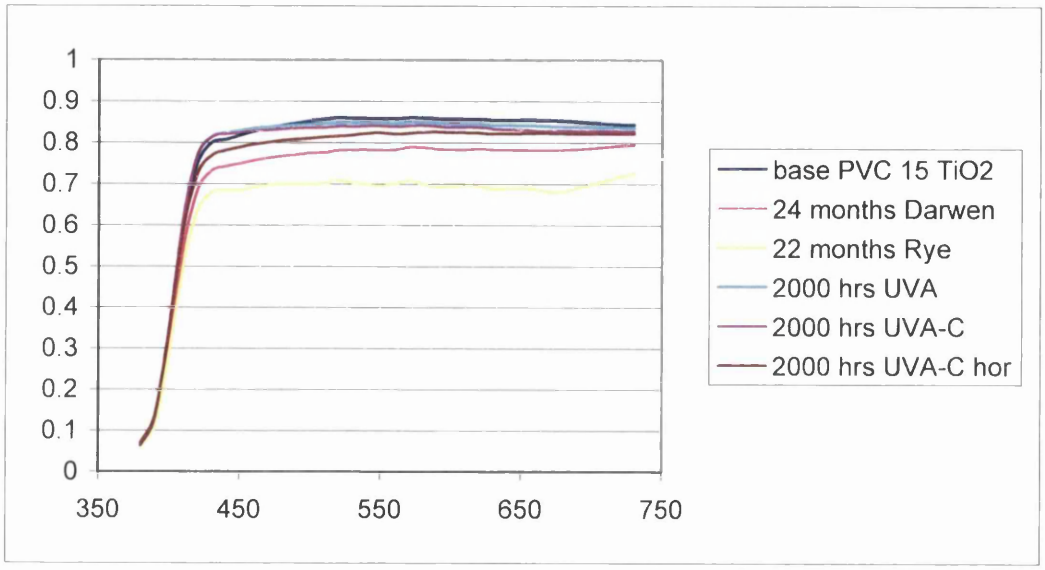
1
0.9
0.8
0.7
0.6
0.5
0.4
0.3
0.2
0.1
0
350
450
550
650
750
base PVC 15 TiO2
24 months Darwen
22 months Rye
2000 hrs UVA
2000 hrs UVA-C
2000 hrs UVA-C hor

Appendix I

Yellow-Green

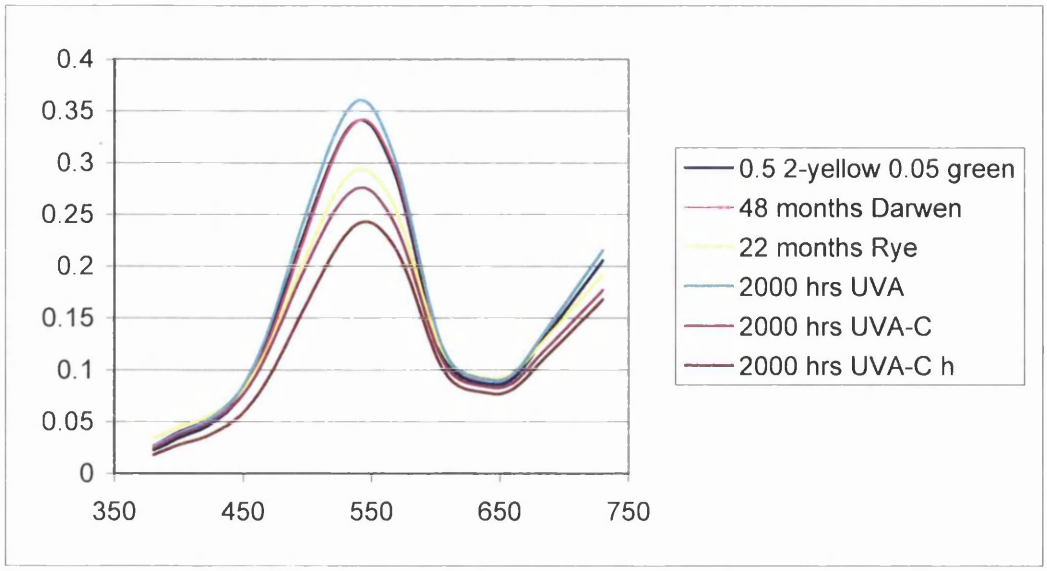
0.4
0.35
0.3
0.25
0.2
0.15
0.1
0.05
0
350
450
550
650
750
0.5 2-yellow 0.05 green
48 months Darwen
22 months Rye
2000 hrs UVA
2000 hrs UVA-C
2000 hrs UVA-C h

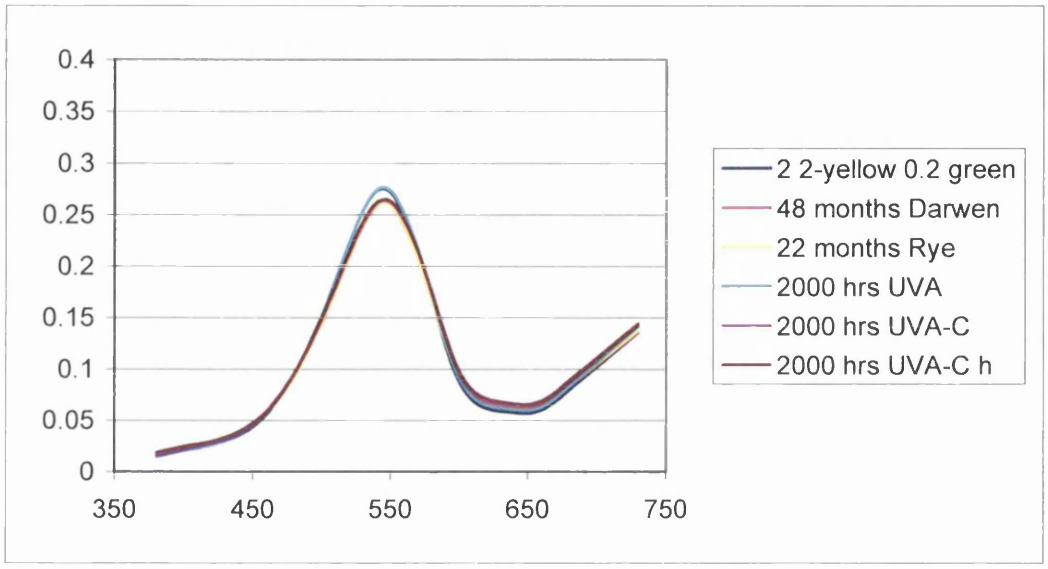
0.4
0.35
0.3
0.25
0.2
0.15
0.1
0.05
0
350
450
550
650
750
2 2-yellow 0.2 green
48 months Darwen
22 months Rye
2000 hrs UVA
2000 hrs UVA-C
2000 hrs UVA-C h

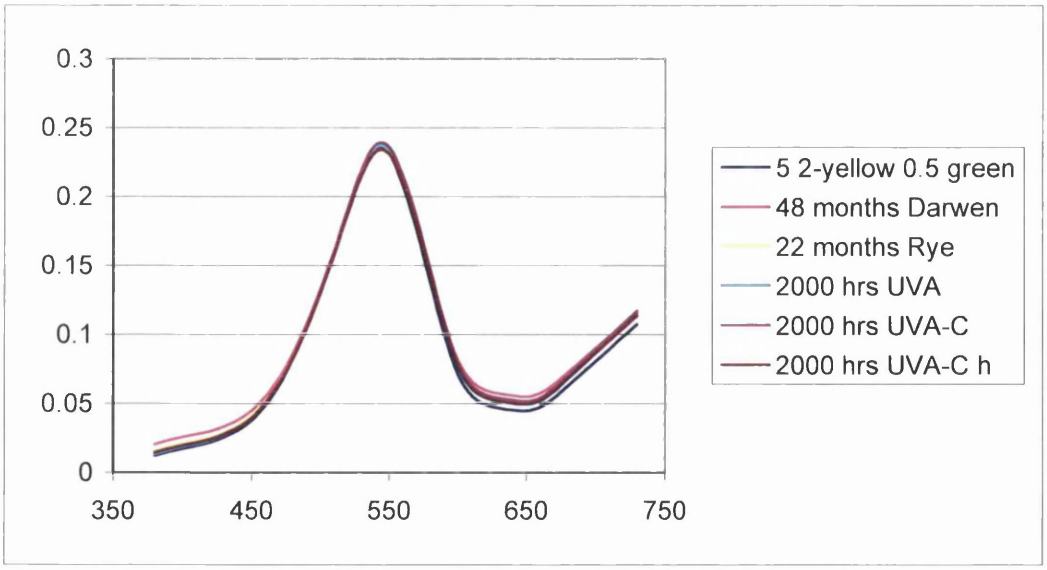
0.3
0.25
0.2
0.15
0.1
0.05
0
350
450
550
650
750
5 2-yellow 0.5 green
48 months Darwen
22 months Rye
2000 hrs UVA
2000 hrs UVA-C
2000 hrs UVA-C h

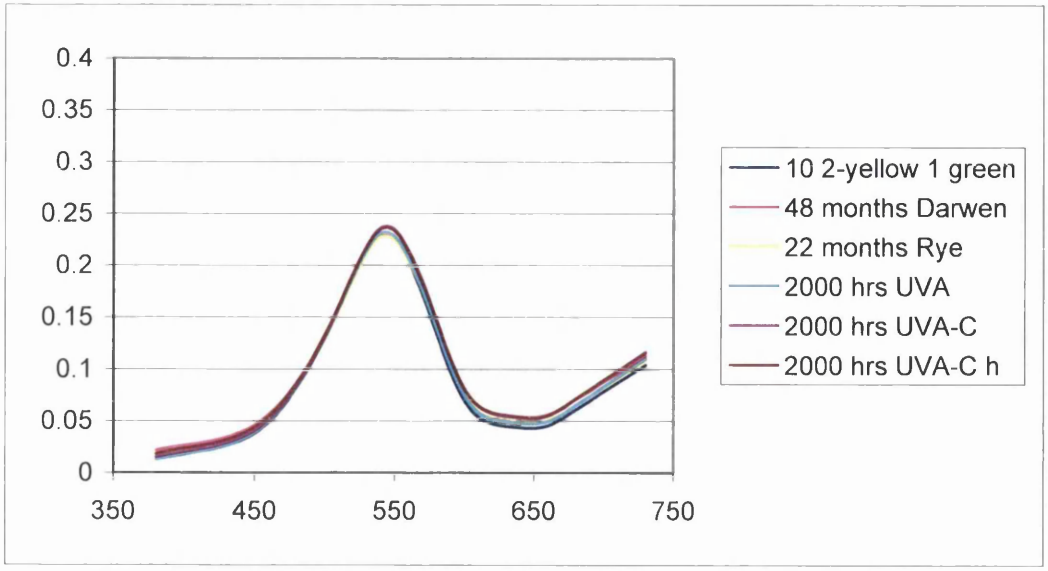
0.4
0.35
0.3
0.25
0.2
0.15
0.1
0.05
0
350
450
550
650
750
10 2-yellow 1 green
48 months Darwen
22 months Rye
2000 hrs UVA
2000 hrs UVA-C
2000 hrs UVA-C h

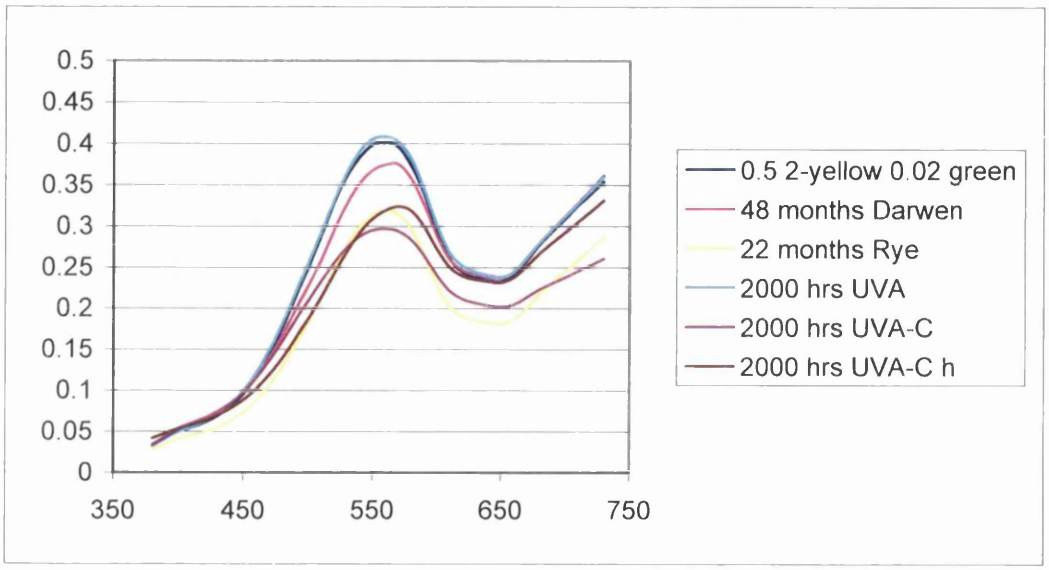
0.5
0.45
0.4
0.35
0.3
0.25
0.2
0.15
0.1
0.05
0
350
450
550
650
750
0.5 2-yellow 0.02 green
48 months Darwen
22 months Rye
2000 hrs UVA
2000 hrs UVA-C
2000 hrs UVA-C h

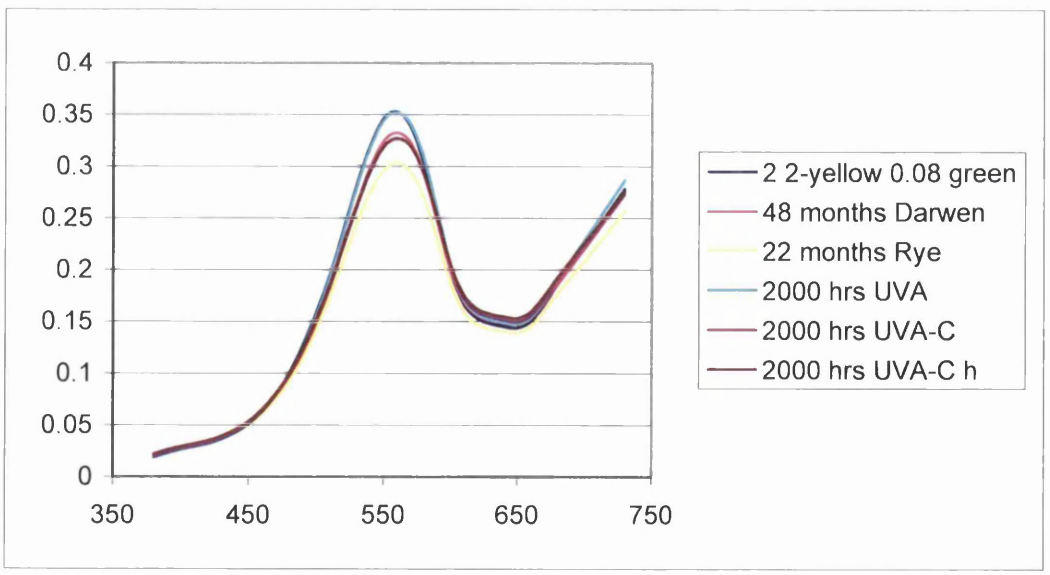
0.4
0.35
0.3
0.25
0.2
0.15
0.1
0.05
0
350
450
550
650
750
2 2-yellow 0.08 green
48 months Darwen
22 months Rye
2000 hrs UVA
2000 hrs UVA-C
2000 hrs UVA-C h

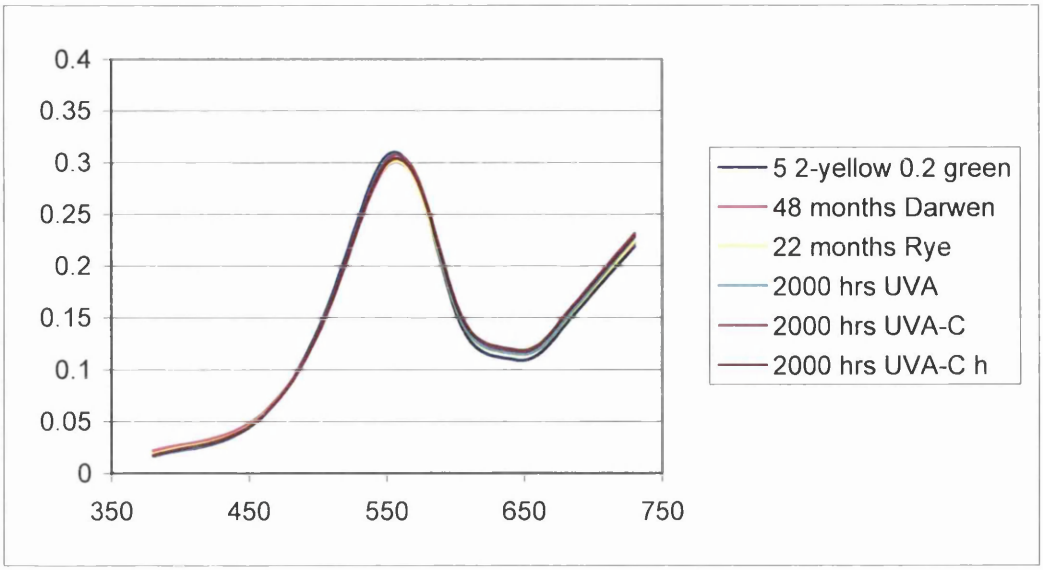
0.4
0.35
0.3
0.25
0.2
0.15
0.1
0.05
0
350
450
550
650
750
5 2-yellow 0.2 green
48 months Darwen
22 months Rye
2000 hrs UVA
2000 hrs UVA-C
2000 hrs UVA-C h

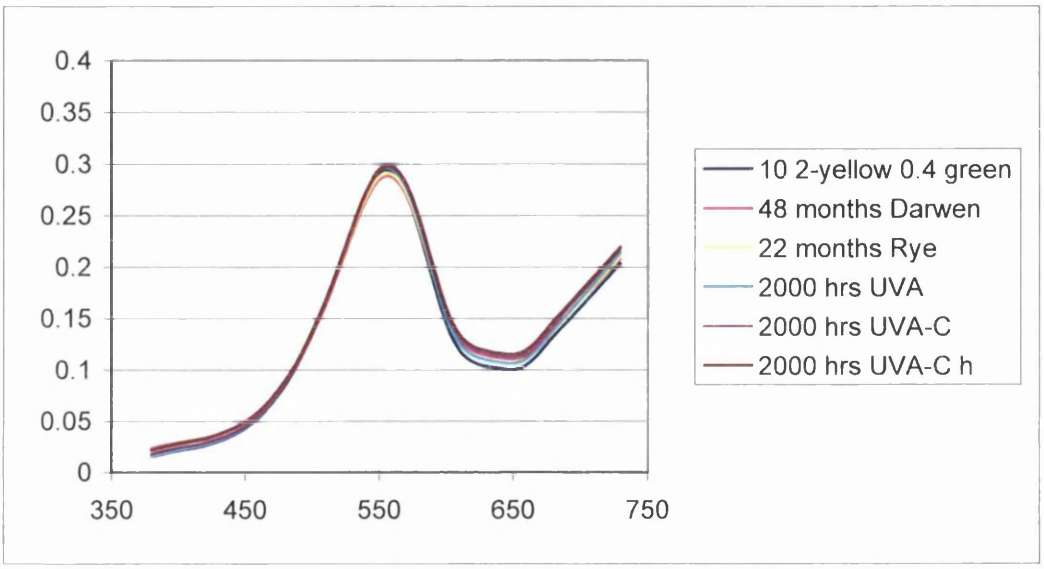
0.4
0.35
0.3
0.25
0.2
0.15
0.1
0.05
0
350
450
550
650
750
10 2-yellow 0.4 green
48 months Darwen
22 months Rye
2000 hrs UVA
2000 hrs UVA-C
2000 hrs UVA-C h

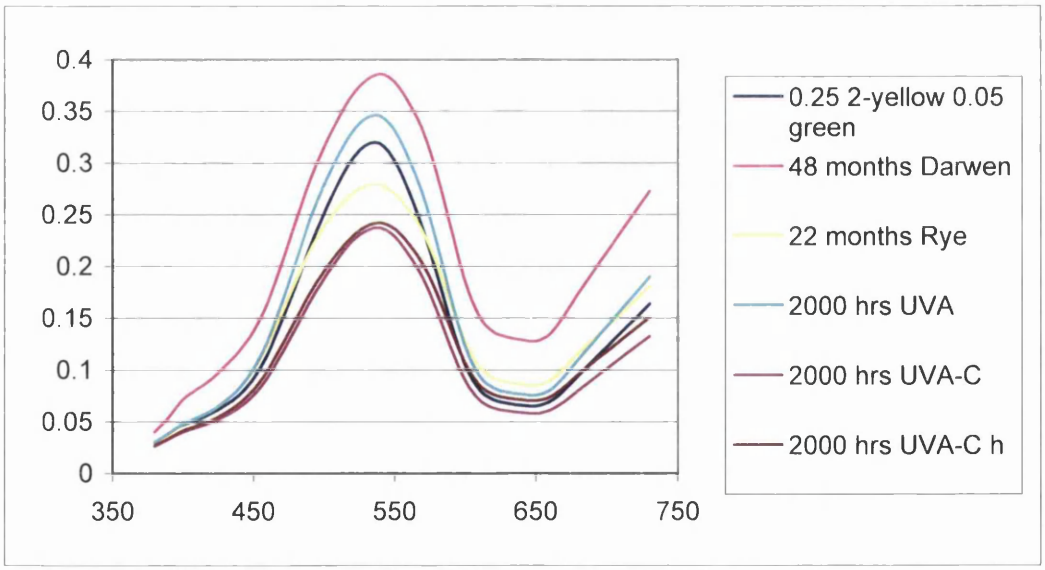
0.4
0.35
0.3
0.25
0.2
0.15
0.1
0.05
0
350
450
550
650
750
0.25 2-yellow 0.05 green
48 months Darwen
22 months Rye
2000 hrs UVA
2000 hrs UVA-C
2000 hrs UVA-C h

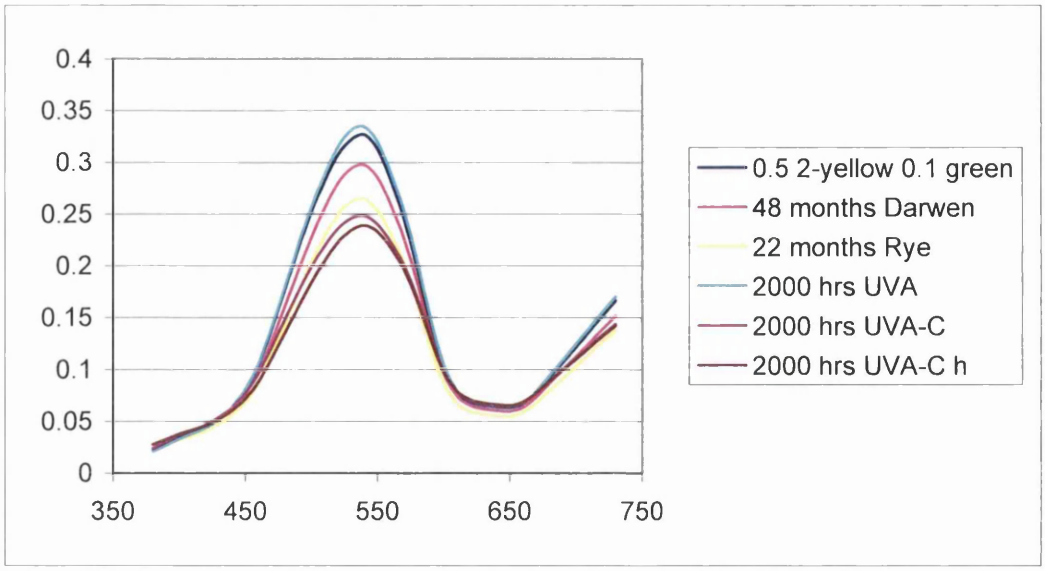
0.4
0.35
0.3
0.25
0.2
0.15
0.1
0.05
0
350
450
550
650
750
0.5 2-yellow 0.1 green
48 months Darwen
22 months Rye
2000 hrs UVA
2000 hrs UVA-C
2000 hrs UVA-C h

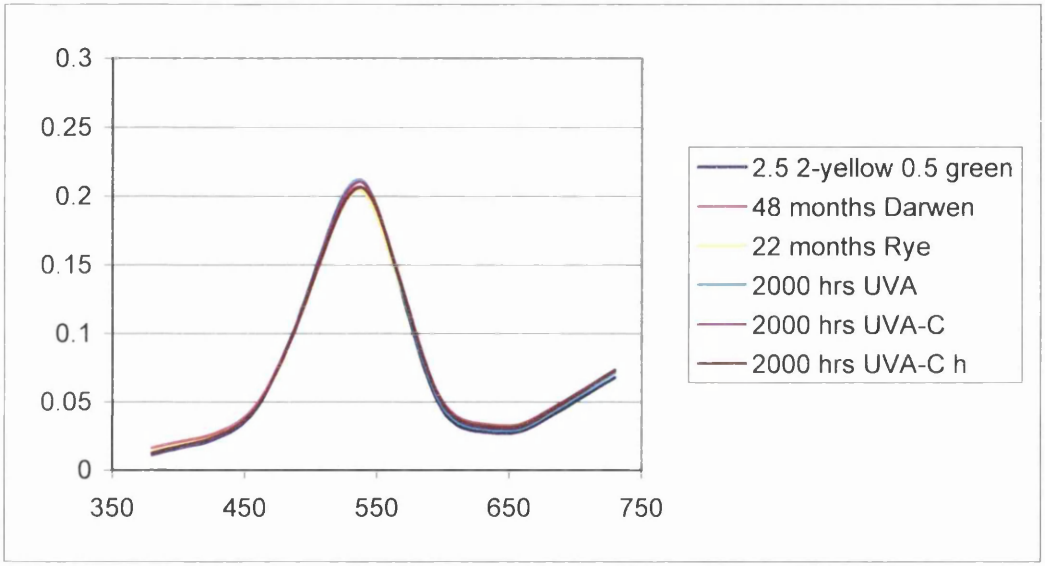
0.3
0.25
0.2
0.15
0.1
0.05
0
350
450
550
650
750
2.5 2-yellow 0.5 green
48 months Darwen
22 months Rye
2000 hrs UVA
2000 hrs UVA-C
2000 hrs UVA-C h

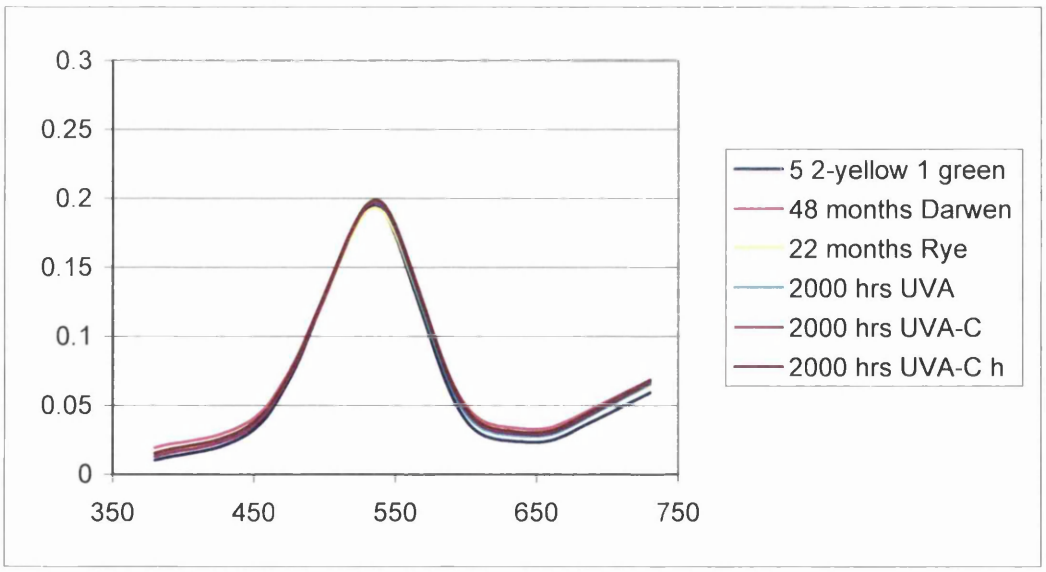
0.3
0.25
0.2
0.15
0.1
0.05
0
350
450
550
650
750
5 2-yellow 1 green
48 months Darwen
22 months Rye
2000 hrs UVA
2000 hrs UVA-C
2000 hrs UVA-C h

Appendix I

Magenta

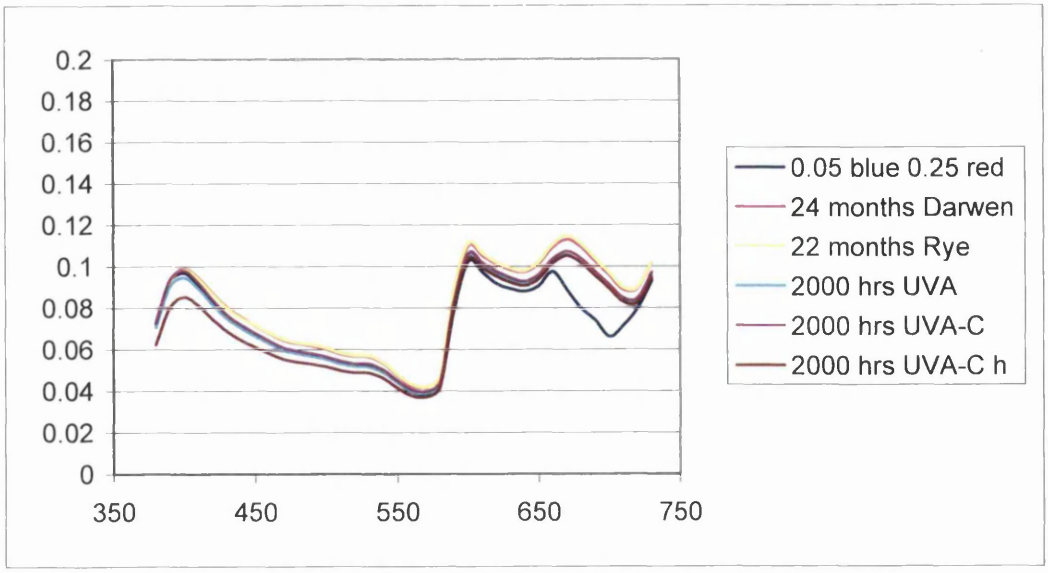
0.2
0.18
0.16
0.14
0.12
0.1
0.08
0.06
0.04
0.02
0
350
450
550
650
750
0.05 blue 0.25 red
24 months Darwen
22 months Rye
2000 hrs UVA
2000 hrs UVA-C
2000 hrs UVA-C h

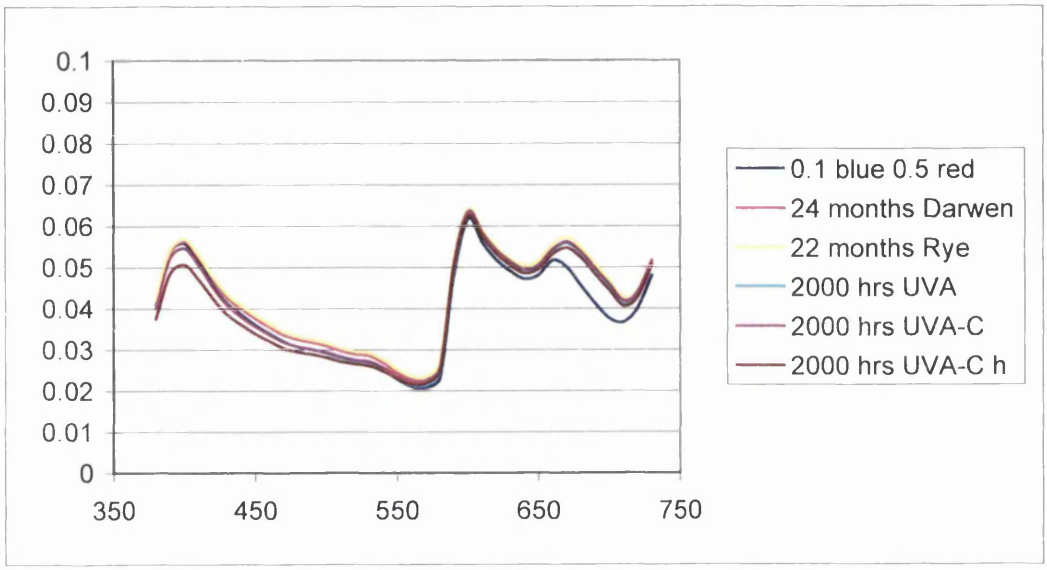
0.1
0.09
0.08
0.07
0.06
0.05
0.04
0.03
0.02
0.01
0
350
450
550
650
750
0.1 blue 0.5 red
24 months Darwen
22 months Rye
2000 hrs UVA
2000 hrs UVA-C
2000 hrs UVA-C h

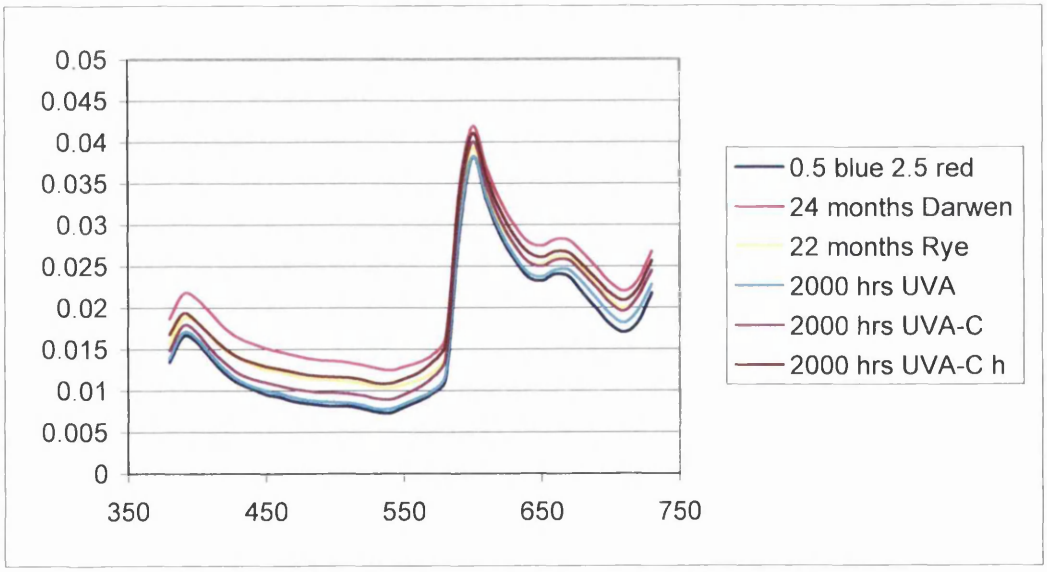
0.05
0.045
0.04
0.035
0.03
0.025
0.02
0.015
0.01
0.005
0
350
450
550
650
750
0.5 blue 2.5 red
24 months Darwen
22 months Rye
2000 hrs UVA
2000 hrs UVA-C
2000 hrs UVA-C h

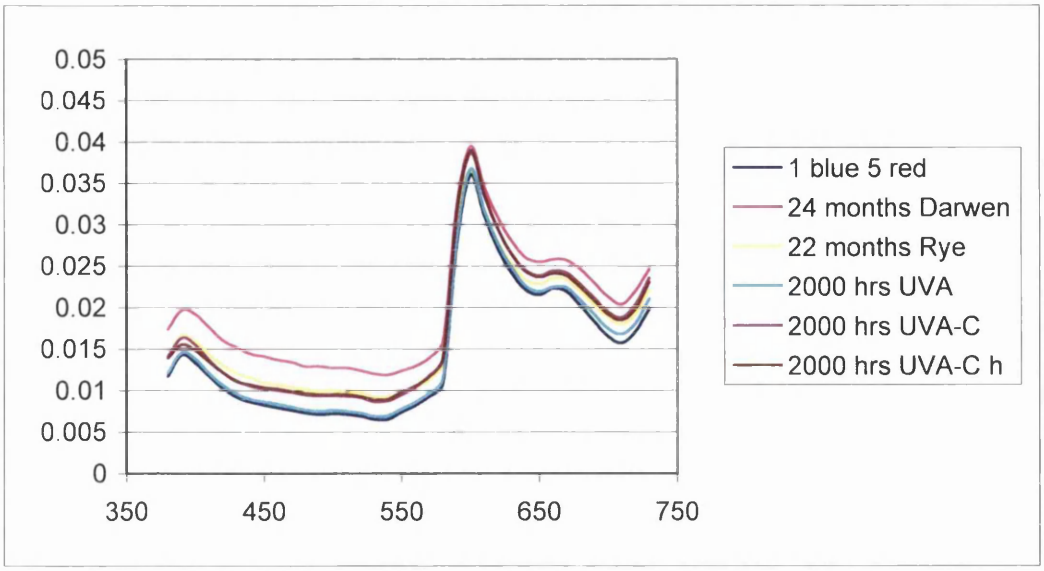
0.05
0.045
0.04
0.035
0.03
0.025
0.02
0.015
0.01
0.005
0
350
450
550
650
750
1 blue 5 red
24 months Darwen
22 months Rye
2000 hrs UVA
2000 hrs UVA-C
2000 hrs UVA-C h

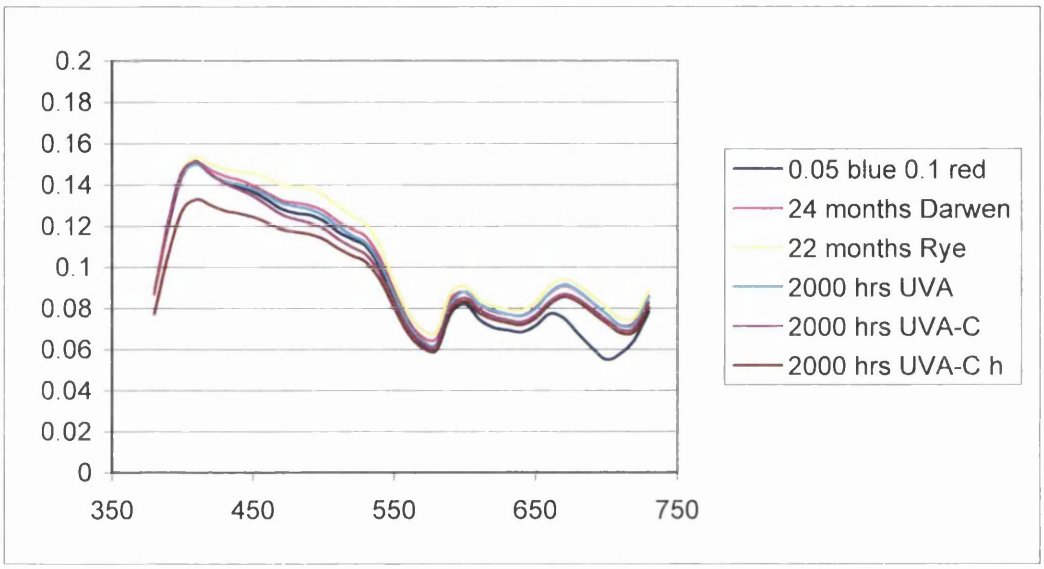
0.2
0.18
0.16
0.14
0.12
0.1
0.08
0.06
0.04
0.02
0
350
450
550
650
750
0.05 blue 0.1 red
24 months Darwen
22 months Rye
2000 hrs UVA
2000 hrs UVA-C
2000 hrs UVA-C h

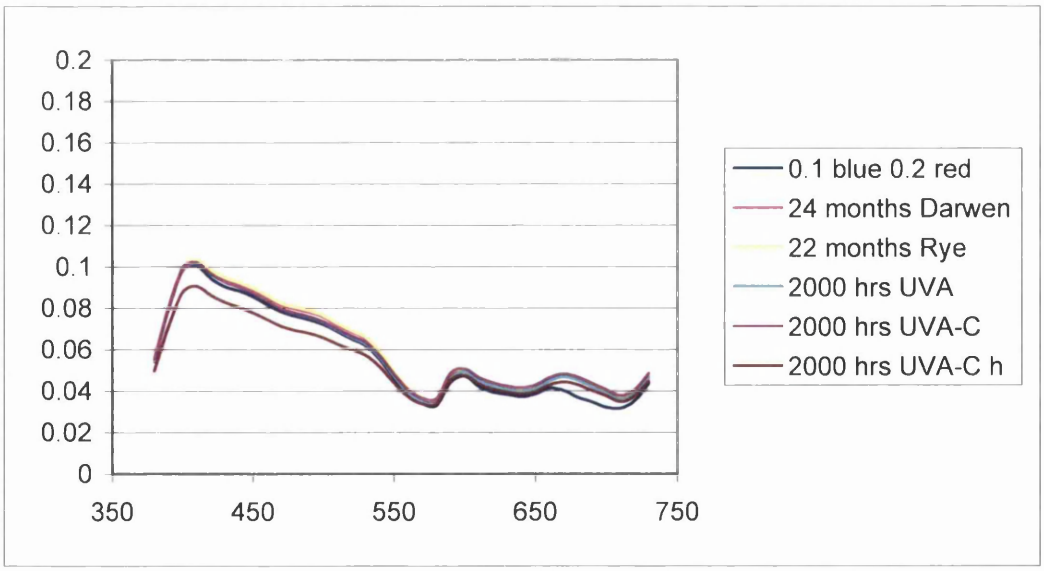
0.2
0.18
0.16
0.14
0.12
0.1
0.08
0.06
0.04
0.02
0
350
450
550
650
750
0.1 blue 0.2 red
24 months Darwen
22 months Rye
2000 hrs UVA
2000 hrs UVA-C
2000 hrs UVA-C h

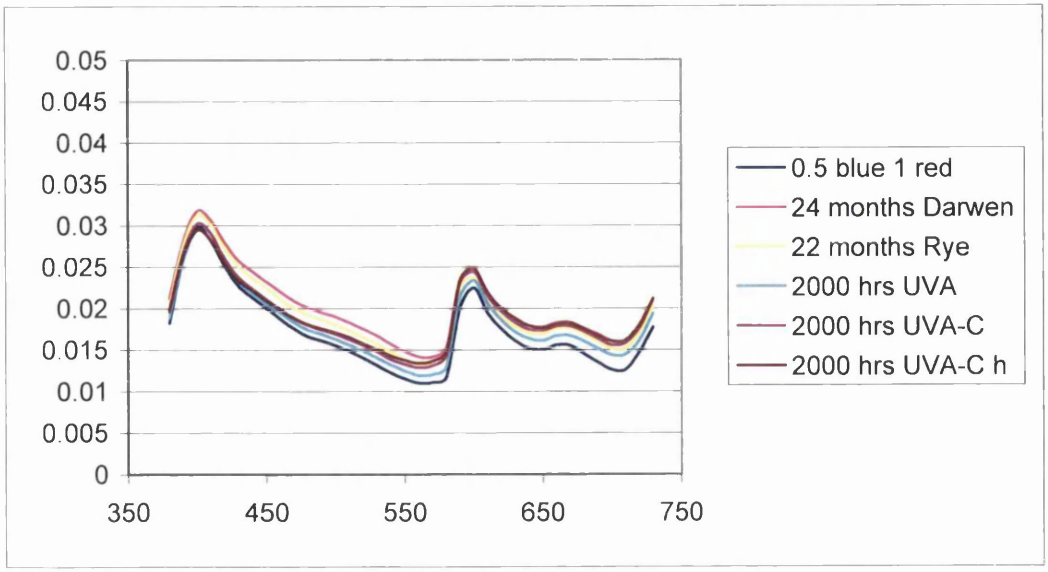
0.05
0.045
0.04
0.035
0.03
0.025
0.02
0.015
0.01
0.005
0
350
450
550
650
750
0.5 blue 1 red
24 months Darwen
22 months Rye
2000 hrs UVA
2000 hrs UVA-C
2000 hrs UVA-C h

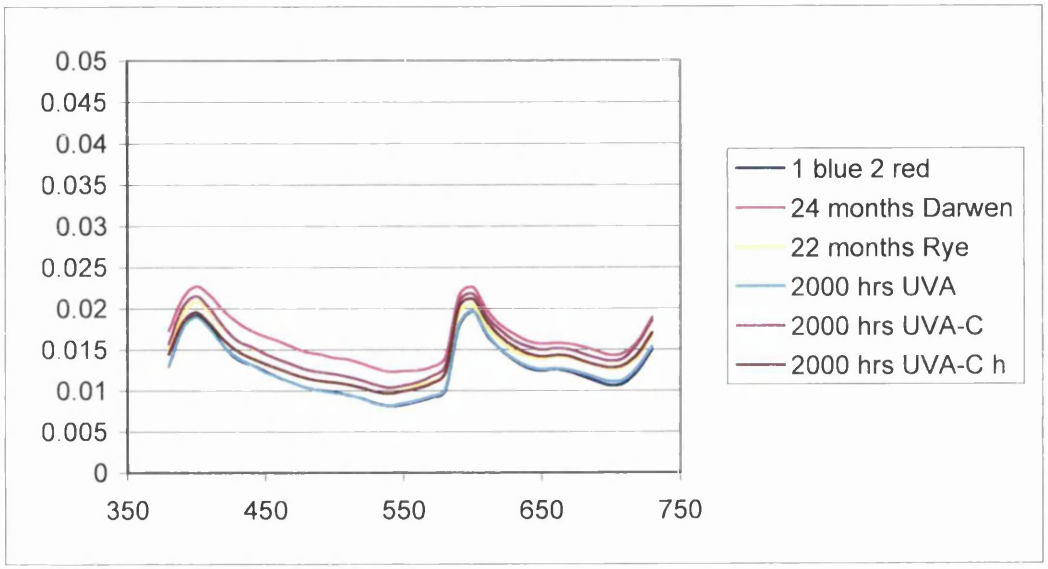
0.05
0.045
0.04
0.035
0.03
0.025
0.02
0.015
0.01
0.005
0
350
450
550
650
750
1 blue 2 red
24 months Darwen
22 months Rye
2000 hrs UVA
2000 hrs UVA-C
2000 hrs UVA-C h

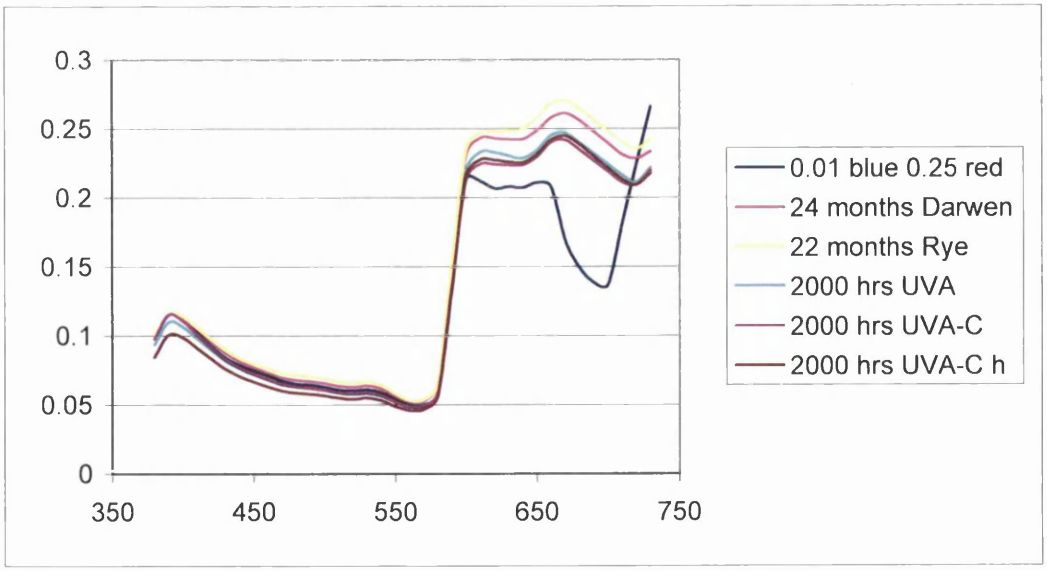
0.3
0.25
0.2
0.15
0.1
0.05
0
350
450
550
650
750
0.01 blue 0.25 red
24 months Darwen
22 months Rye
2000 hrs UVA
2000 hrs UVA-C
2000 hrs UVA-C h

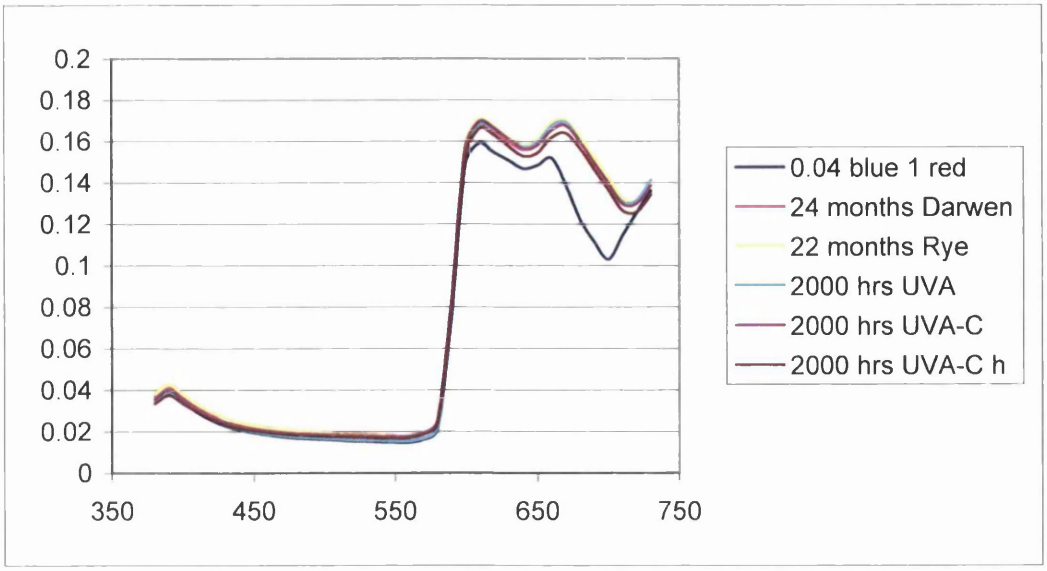
0.2
0.18
0.16
0.14
0.12
0.1
0.08
0.06
0.04
0.02
0
350
450
550
650
750
0.04 blue 1 red
24 months Darwen
22 months Rye
2000 hrs UVA
2000 hrs UVA-C
2000 hrs UVA-C h

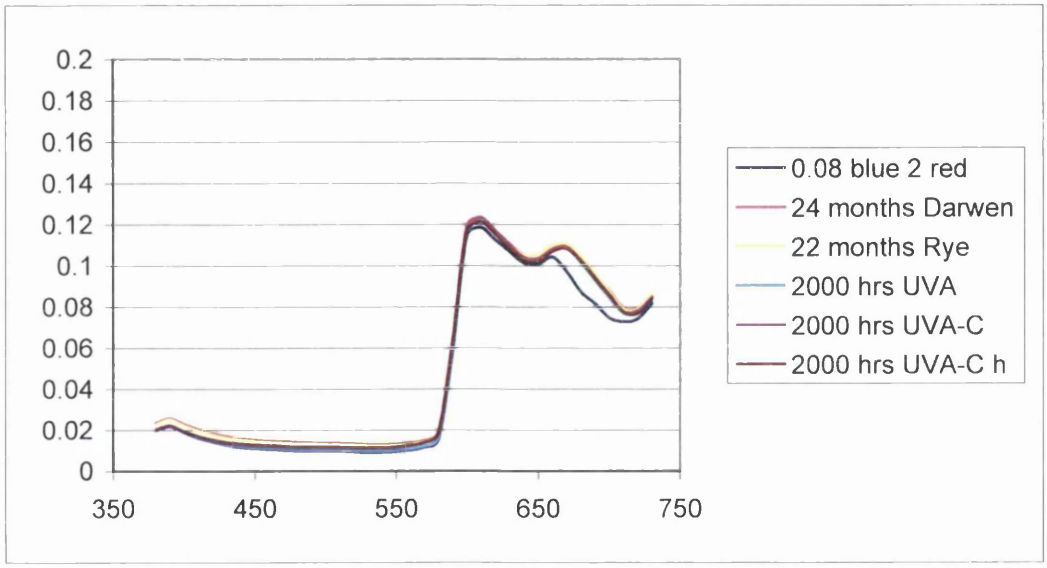
0.2
0.18
0.16
0.14
0.12
0.1
0.08
0.06
0.04
0.02
0
350
450
550
650
750
0.08 blue 2 red
24 months Darwen
22 months Rye
2000 hrs UVA
2000 hrs UVA-C
2000 hrs UVA-C h

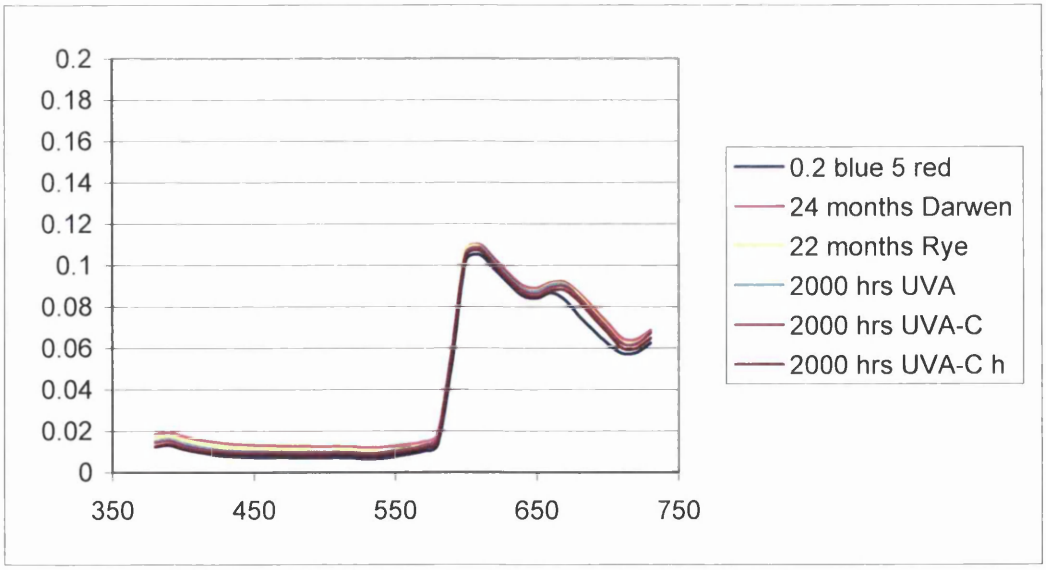
0.2
0.18
0.16
0.14
0.12
0.1
0.08
0.06
0.04
0.02
0
350
450
550
650
750
0.2 blue 5 red
24 months Darwen
22 months Rye
2000 hrs UVA
2000 hrs UVA-C
2000 hrs UVA-C h

Appendix I

Cyan

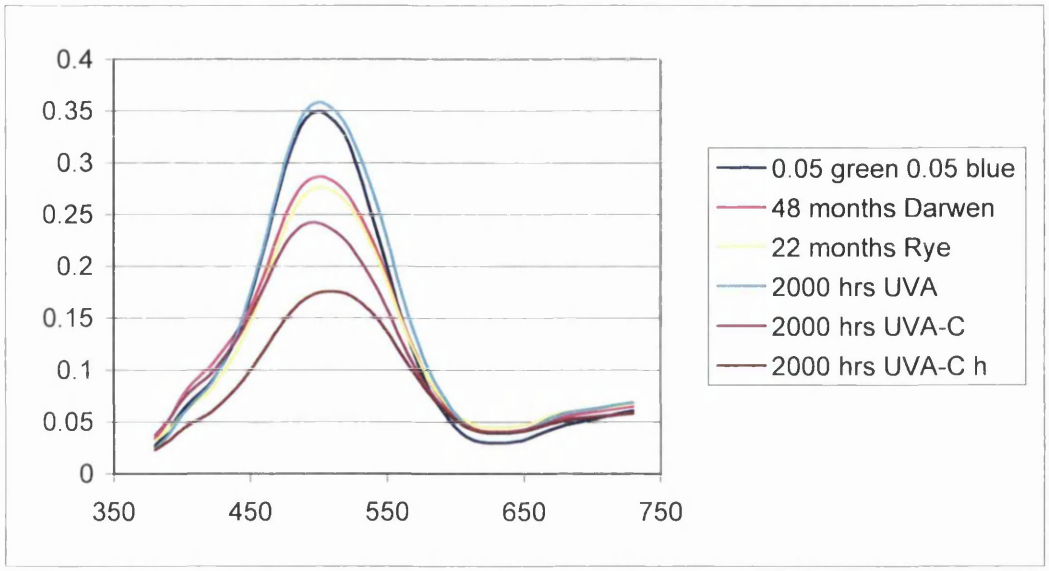
0.4
0.35
0.3
0.25
0.2
0.15
0.1
0.05
0
350
450
550
650
750
0.05 green 0.05 blue
48 months Darwen
22 months Rye
2000 hrs UVA
2000 hrs UVA-C
2000 hrs UVA-C h

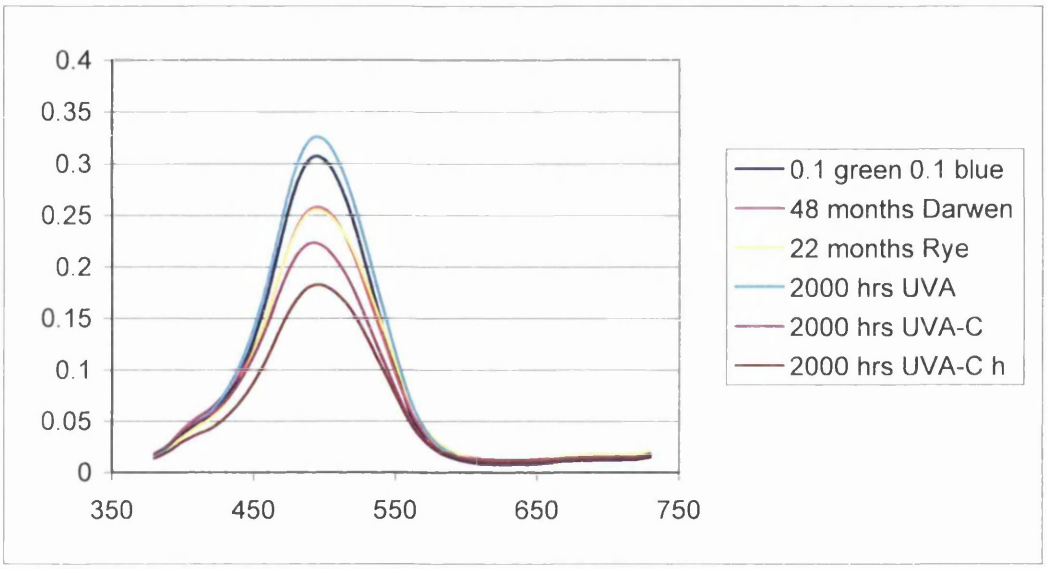
0.4
0.35
0.3
0.25
0.2
0.15
0.1
0.05
0
350
450
550
650
750
0.1 green 0.1 blue
48 months Darwen
22 months Rye
2000 hrs UVA
2000 hrs UVA-C
2000 hrs UVA-C h

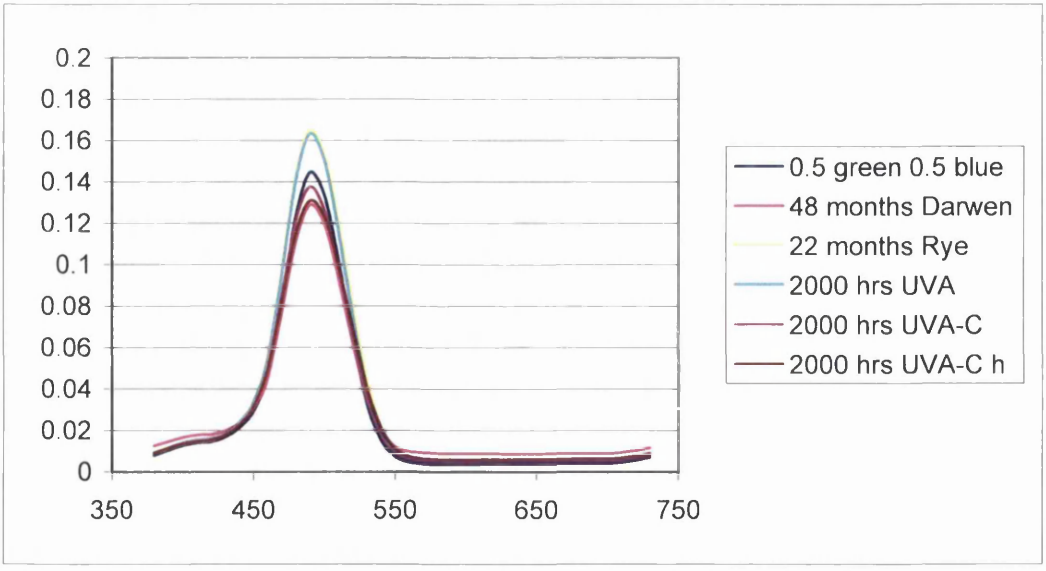
0.2
0.18
0.16
0.14
0.12
0.1
0.08
0.06
0.04
0.02
0
350
450
550
650
750
0.5 green 0.5 blue
48 months Darwen
22 months Rye
2000 hrs UVA
2000 hrs UVA-C
2000 hrs UVA-C h

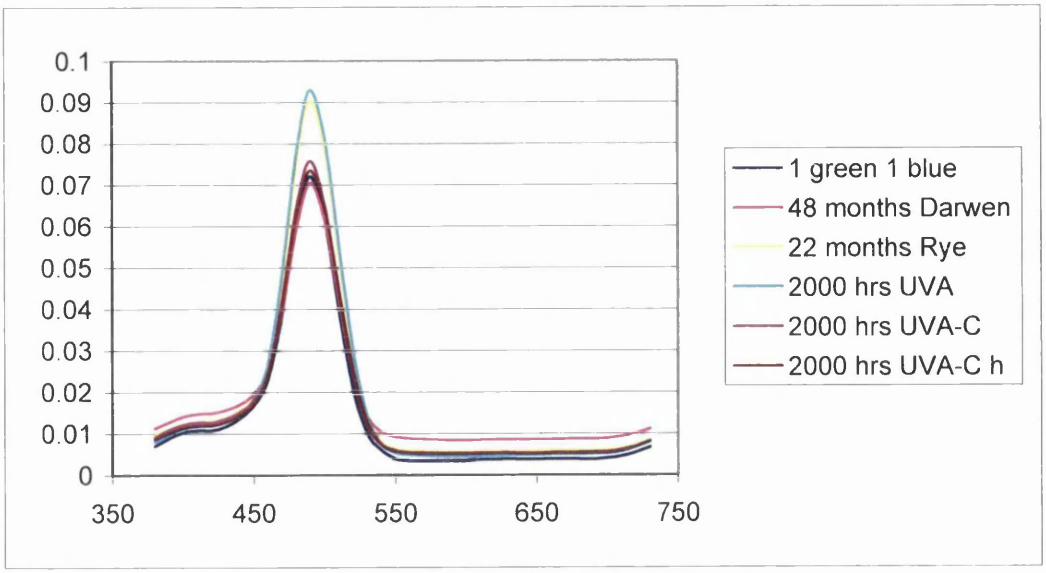
0.1
0.09
0.08
0.07
0.06
0.05
0.04
0.03
0.02
0.01
0
350
450
550
650
750
1 green 1 blue
48 months Darwen
22 months Rye
2000 hrs UVA
2000 hrs UVA-C
2000 hrs UVA-C h

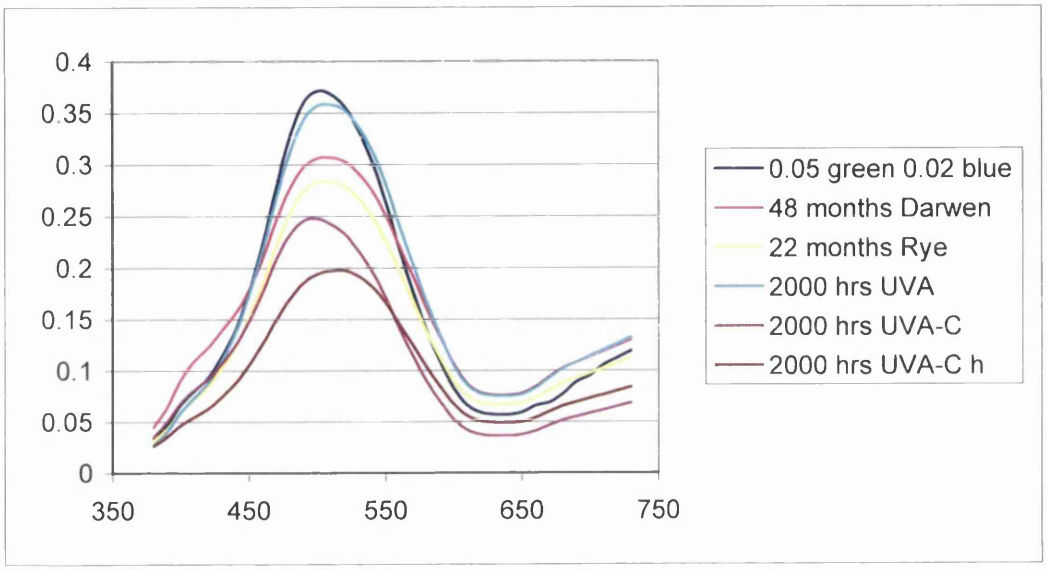
0.4
0.35
0.3
0.25
0.2
0.15
0.1
0.05
0
350
450
550
650
750
0.05 green 0.02 blue
48 months Darwen
22 months Rye
2000 hrs UVA
2000 hrs UVA-C
2000 hrs UVA-C h

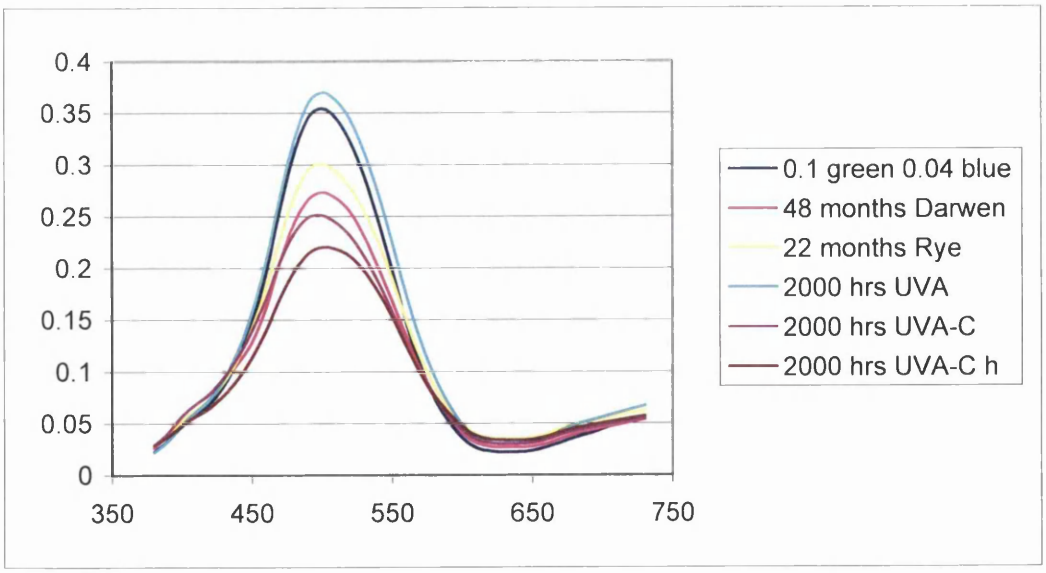
0.4
0.35
0.3
0.25
0.2
0.15
0.1
0.05
0
350
450
550
650
750
0.1 green 0.04 blue
48 months Darwen
22 months Rye
2000 hrs UVA
2000 hrs UVA-C
2000 hrs UVA-C h

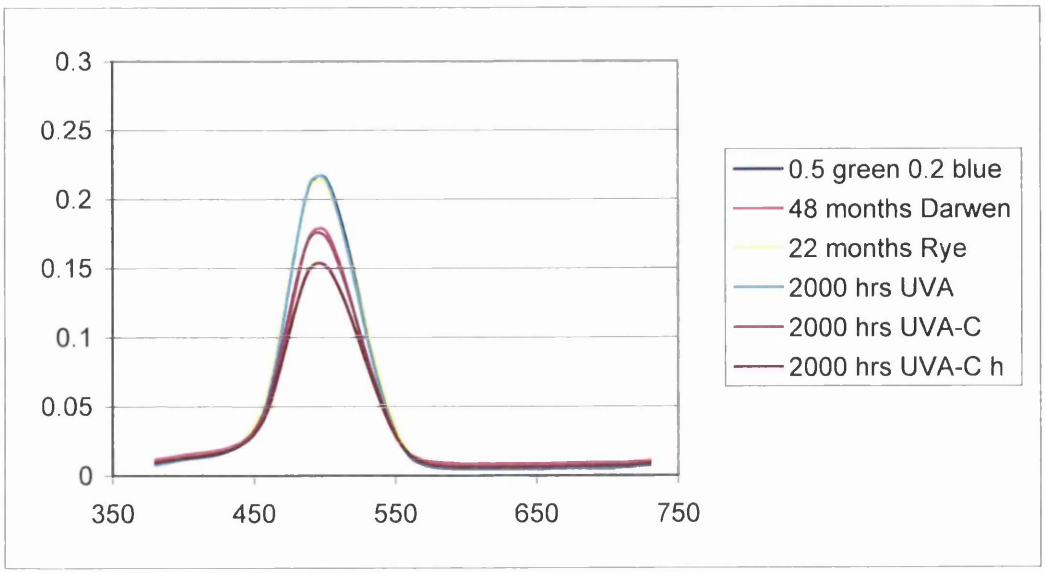
0.3
0.25
0.2
0.15
0.1
0.05
0
350
450
550
650
750
0.5 green 0.2 blue
48 months Darwen
22 months Rye
2000 hrs UVA
2000 hrs UVA-C
2000 hrs UVA-C h

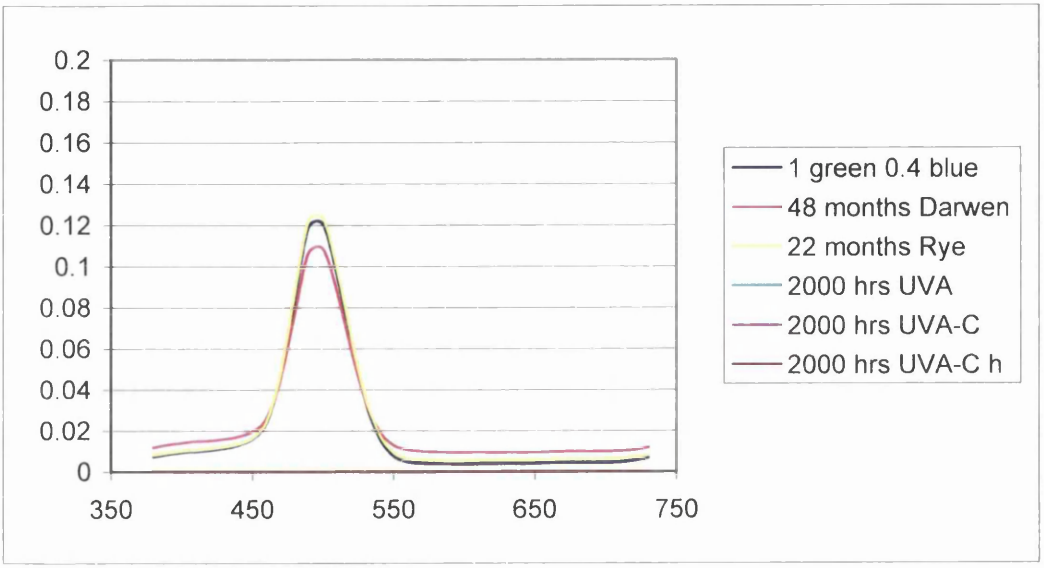
0.2
0.18
0.16
0.14
0.12
0.1
0.08
0.06
0.04
0.02
0
350
450
550
650
750
1 green 0.4 blue
48 months Darwen
22 months Rye
2000 hrs UVA
2000 hrs UVA-C
2000 hrs UVA-C h

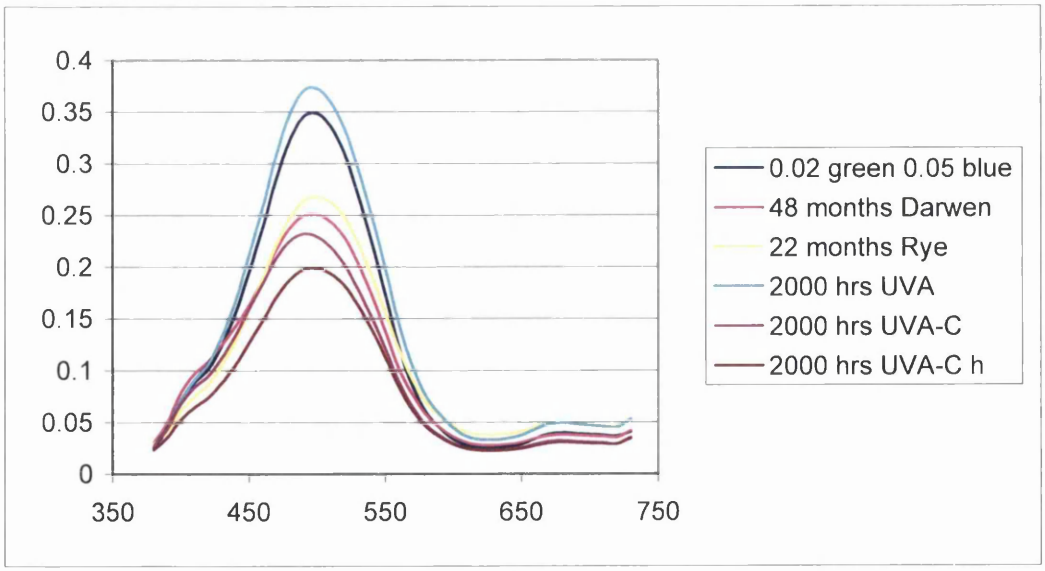
0.4
0.35
0.3
0.25
0.2
0.15
0.1
0.05
0
350
450
550
650
750
0.02 green 0.05 blue
48 months Darwen
22 months Rye
2000 hrs UVA
2000 hrs UVA-C
2000 hrs UVA-C h

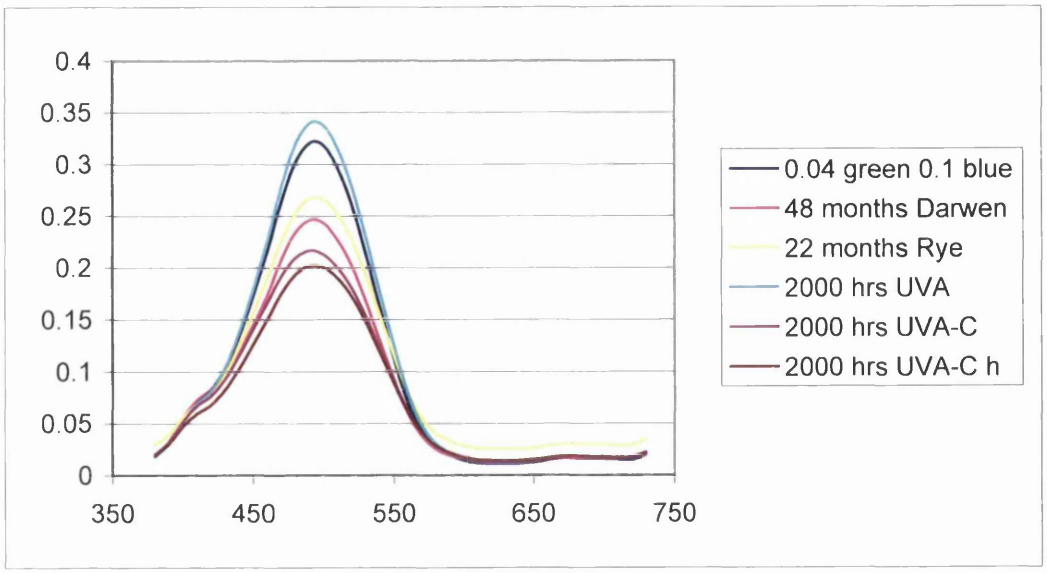
0.4
0.35
0.3
0.25
0.2
0.15
0.1
0.05
0
350
450
550
650
750
0.04 green 0.1 blue
48 months Darwen
22 months Rye
2000 hrs UVA
2000 hrs UVA-C
2000 hrs UVA-C h

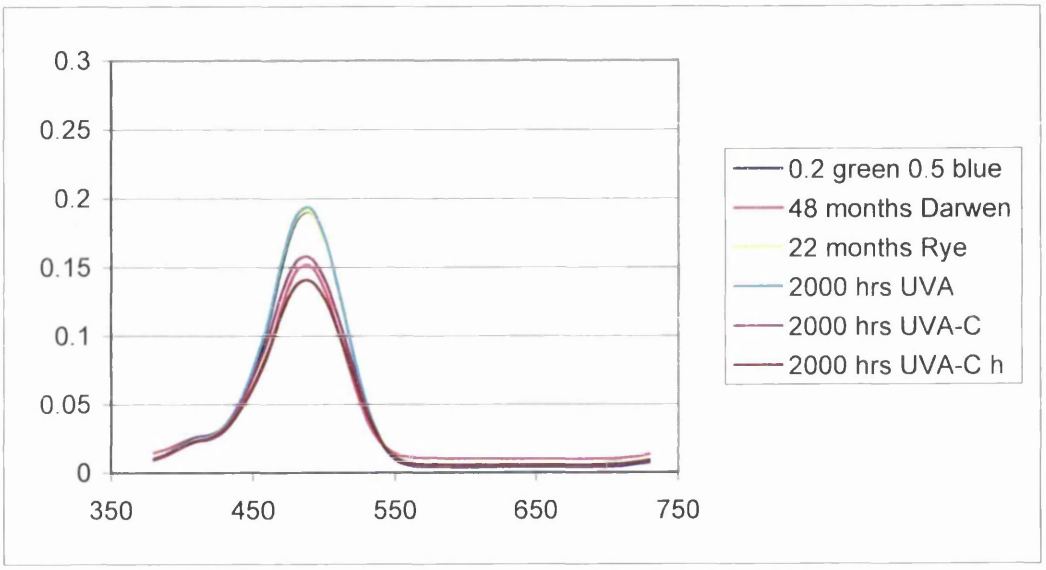
0.3
0.25
0.2
0.15
0.1
0.05
0
350
450
550
650
750
0.2 green 0.5 blue
48 months Darwen
22 months Rye
2000 hrs UVA
2000 hrs UVA-C
2000 hrs UVA-C h

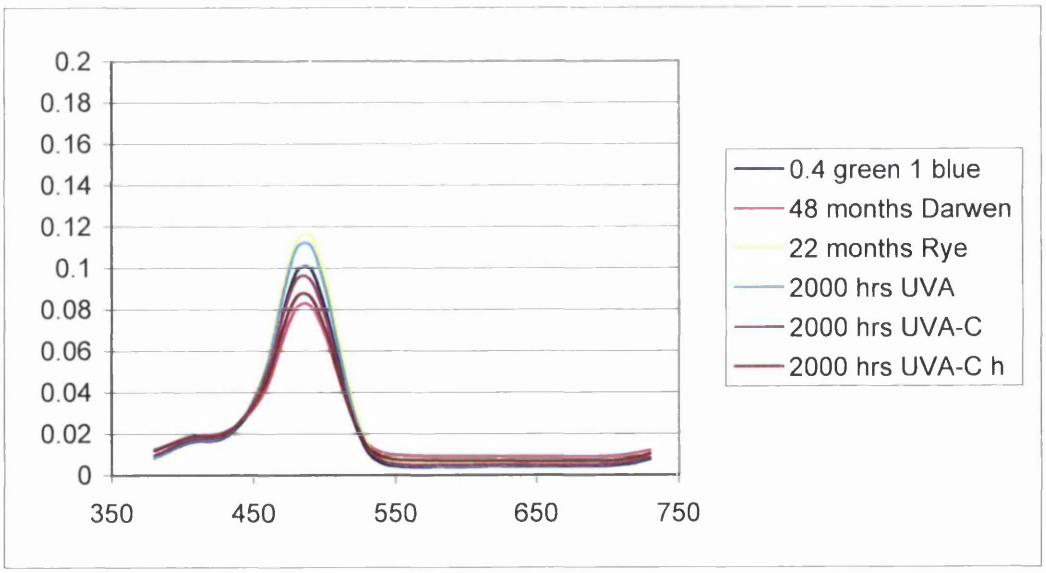
0.2
0.18
0.16
0.14
0.12
0.1
0.08
0.06
0.04
0.02
0
350
450
550
650
750
0.4 green 1 blue
48 months Darwen
22 months Rye
2000 hrs UVA
2000 hrs UVA-C
2000 hrs UVA-C h

Appendix I

Orange

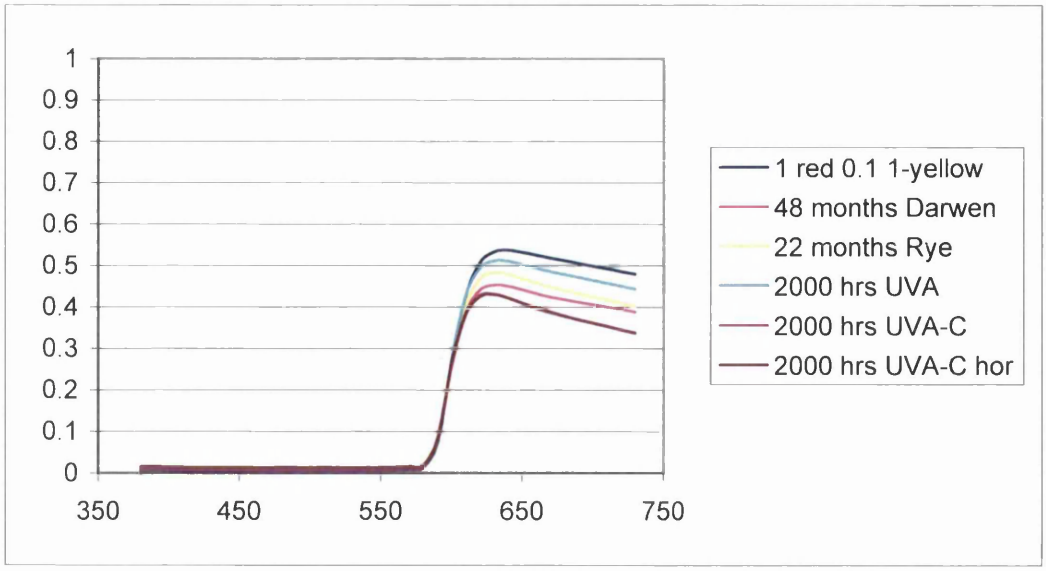
1
0.9
0.8
0.7
0.6
0.5
0.4
0.3
0.2
0.1
0
350
450
550
650
750
1 red 0.1 1-yellow
48 months Darwen
22 months Rye
2000 hrs UVA
2000 hrs UVA-C
2000 hrs UVA-C hor

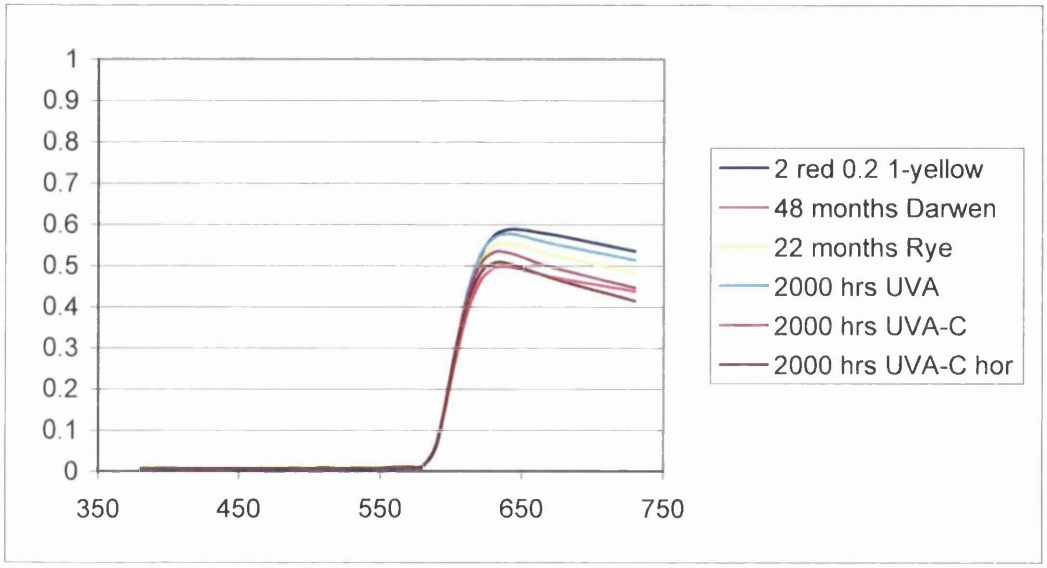
1
0.9
0.8
0.7
0.6
0.5
0.4
0.3
0.2
0.1
0
350
450
550
650
750
2 red 0.2 1-yellow
48 months Darwen
22 months Rye
2000 hrs UVA
2000 hrs UVA-C
2000 hrs UVA-C hor

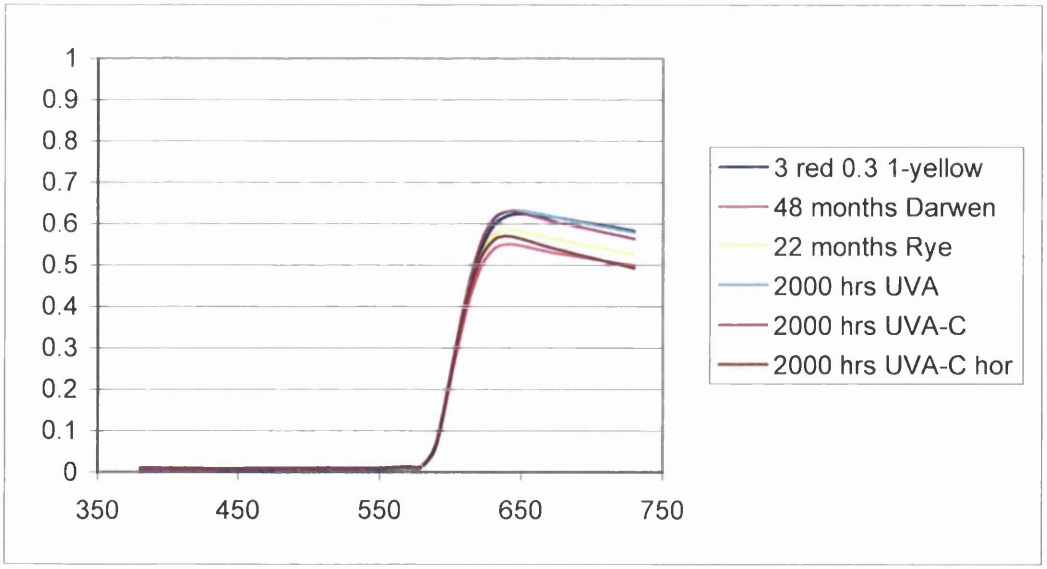
1
0.9
0.8
0.7
0.6
0.5
0.4
0.3
0.2
0.1
0
350
450
550
650
750
3 red 0.3 1-yellow
48 months Darwen
22 months Rye
2000 hrs UVA
2000 hrs UVA-C
2000 hrs UVA-C hor

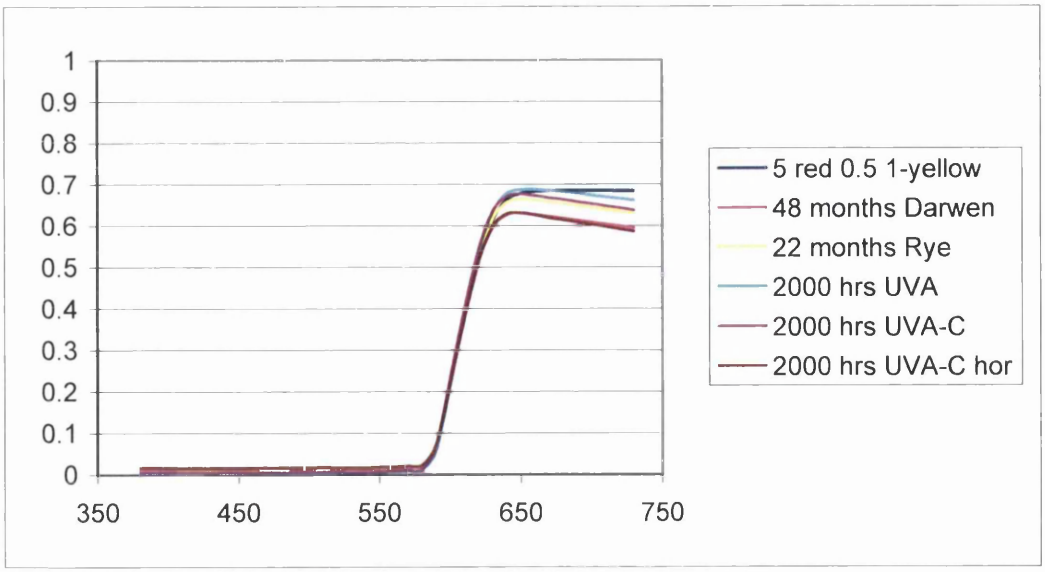
1
0.9
0.8
0.7
0.6
0.5
0.4
0.3
0.2
0.1
0
350
450
550
650
750
5 red 0.5 1-yellow
48 months Darwen
22 months Rye
2000 hrs UVA
2000 hrs UVA-C
2000 hrs UVA-C hor

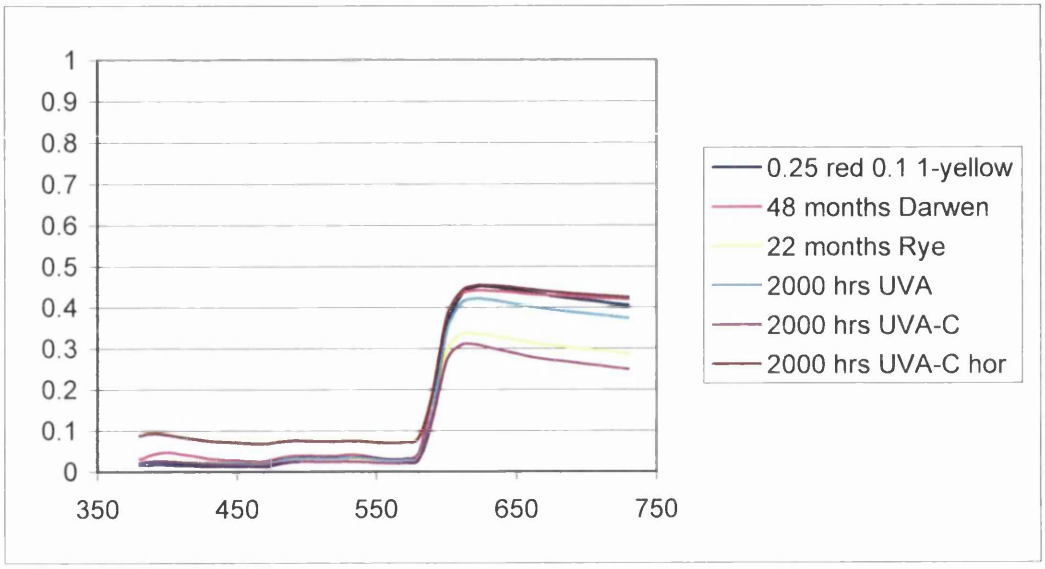
1
0.9
0.8
0.7
0.6
0.5
0.4
0.3
0.2
0.1
0
350
450
550
650
750
0.25 red 0.1 1-yellow
48 months Darwen
22 months Rye
2000 hrs UVA
2000 hrs UVA-C
2000 hrs UVA-C hor

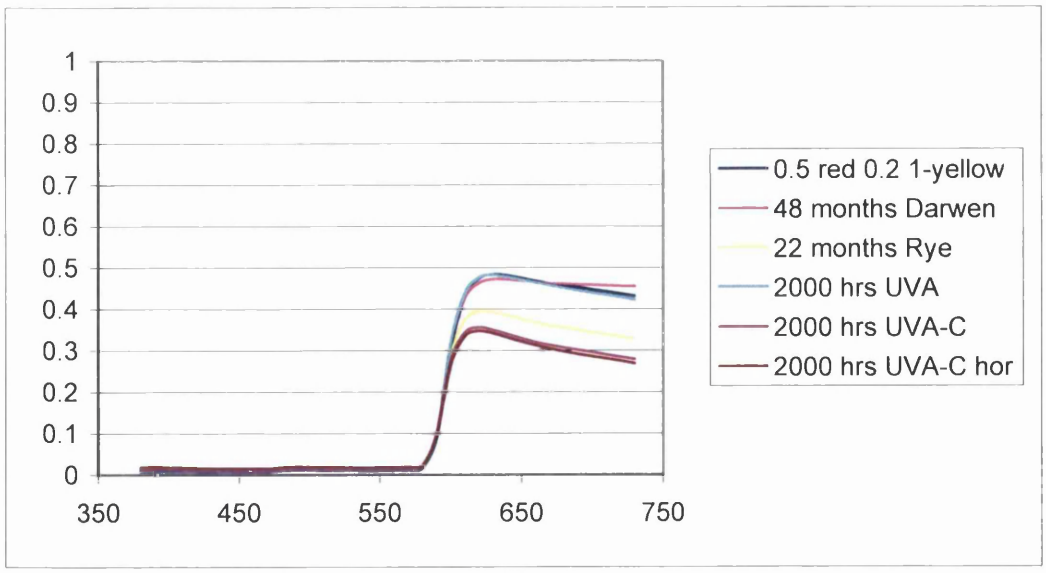
1
0.9
0.8
0.7
0.6
0.5
0.4
0.3
0.2
0.1
0
350
450
550
650
750
0.5 red 0.2 1-yellow
48 months Darwen
22 months Rye
2000 hrs UVA
2000 hrs UVA-C
2000 hrs UVA-C hor

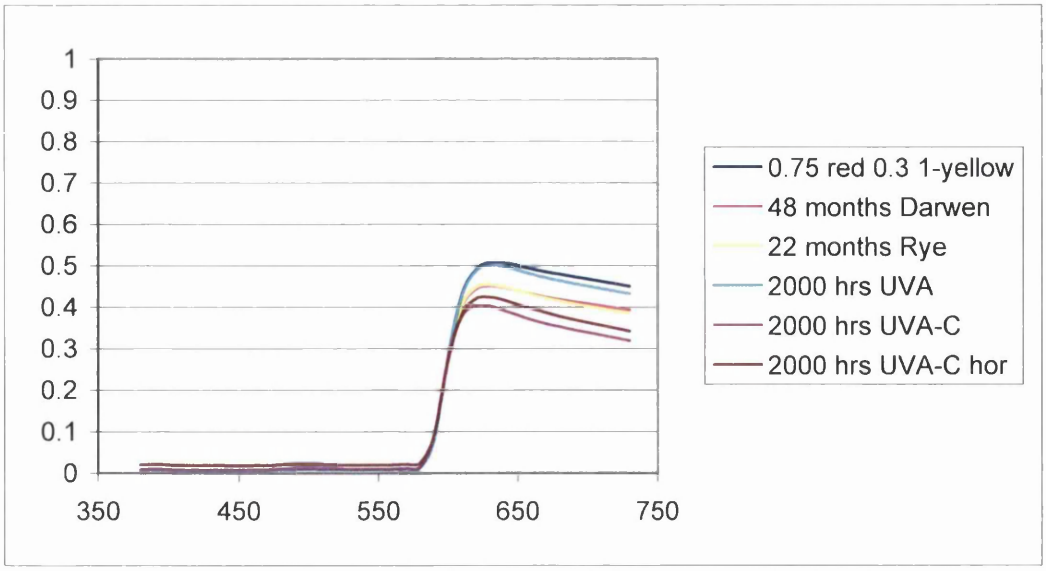
1
0.9
0.8
0.7
0.6
0.5
0.4
0.3
0.2
0.1
0
350
450
550
650
750
0.75 red 0.3 1-yellow
48 months Darwen
22 months Rye
2000 hrs UVA
2000 hrs UVA-C
2000 hrs UVA-C hor

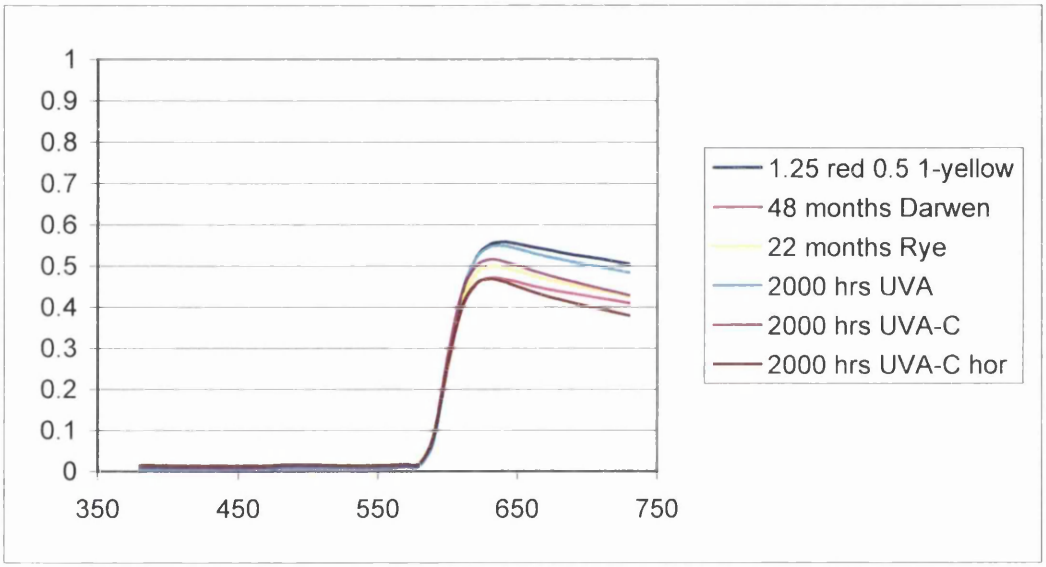
1
0.9
0.8
0.7
0.6
0.5
0.4
0.3
0.2
0.1
0
350
450
550
650
750
1.25 red 0.5 1-yellow
48 months Darwen
22 months Rye
2000 hrs UVA
2000 hrs UVA-C
2000 hrs UVA-C hor

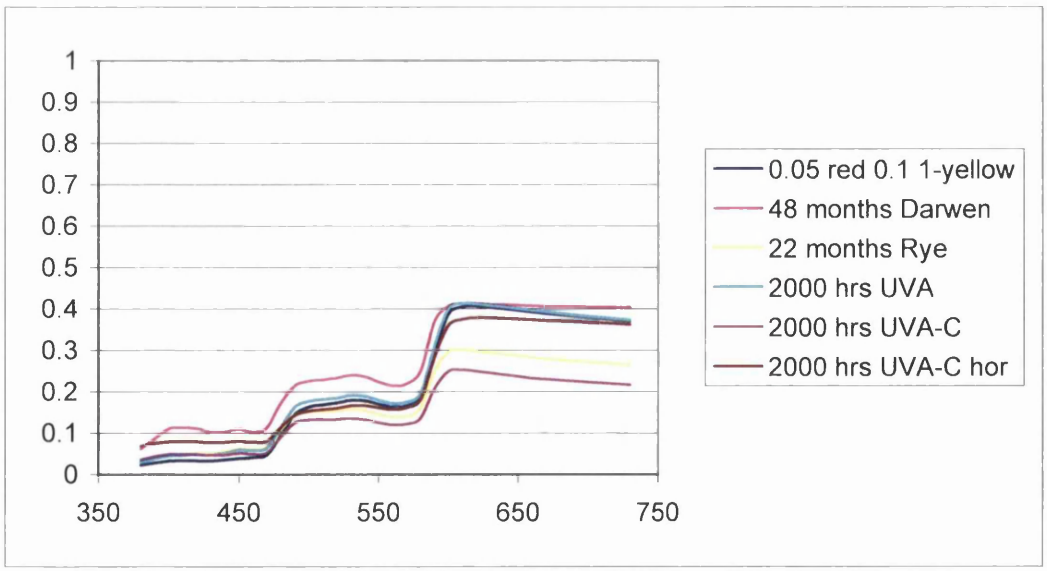
1
0.9
0.8
0.7
0.6
0.5
0.4
0.3
0.2
0.1
0
350
450
550
650
750
0.05 red 0.1 1-yellow
48 months Darwen
22 months Rye
2000 hrs UVA
2000 hrs UVA-C
2000 hrs UVA-C hor

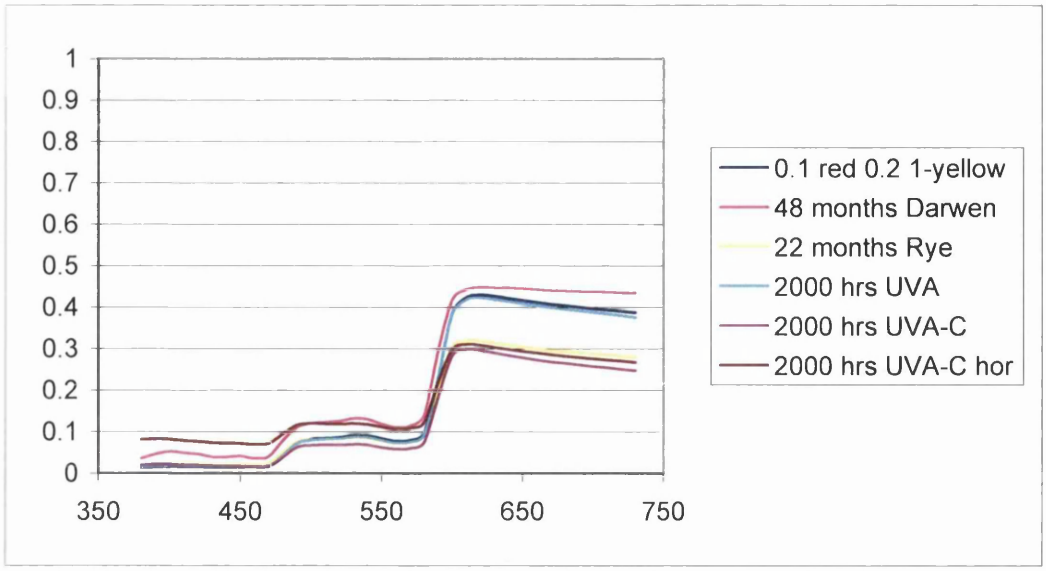
1
0.9
0.8
0.7
0.6
0.5
0.4
0.3
0.2
0.1
0
350
450
550
650
750
0.1 red 0.2 1-yellow
48 months Darwen
22 months Rye
2000 hrs UVA
2000 hrs UVA-C
2000 hrs UVA-C hor

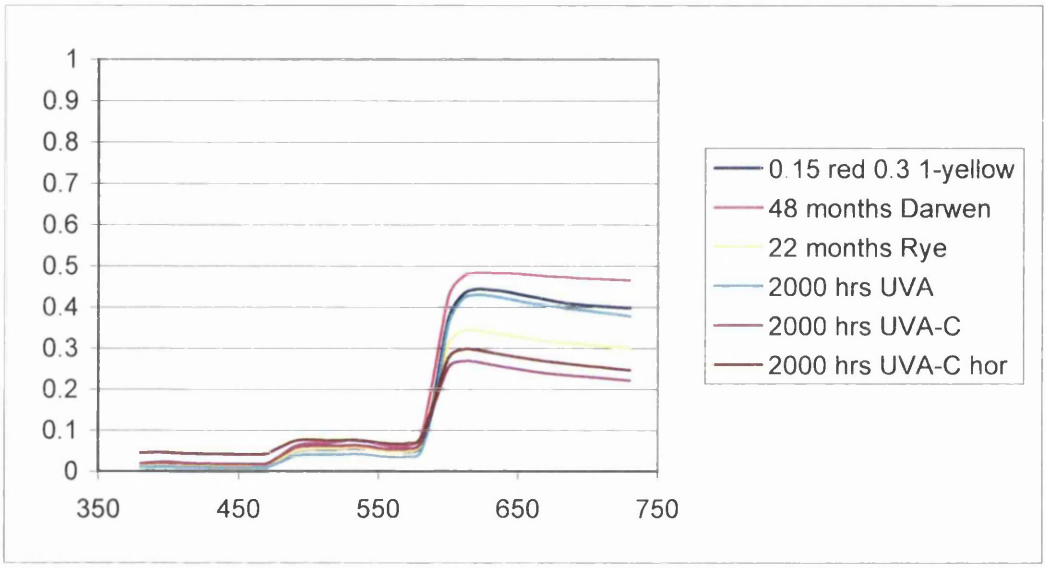
1
0.9
0.8
0.7
0.6
0.5
0.4
0.3
0.2
0.1
0
350
450
550
650
750
0.15 red 0.3 1-yellow
48 months Darwen
22 months Rye
2000 hrs UVA
2000 hrs UVA-C
2000 hrs UVA-C hor

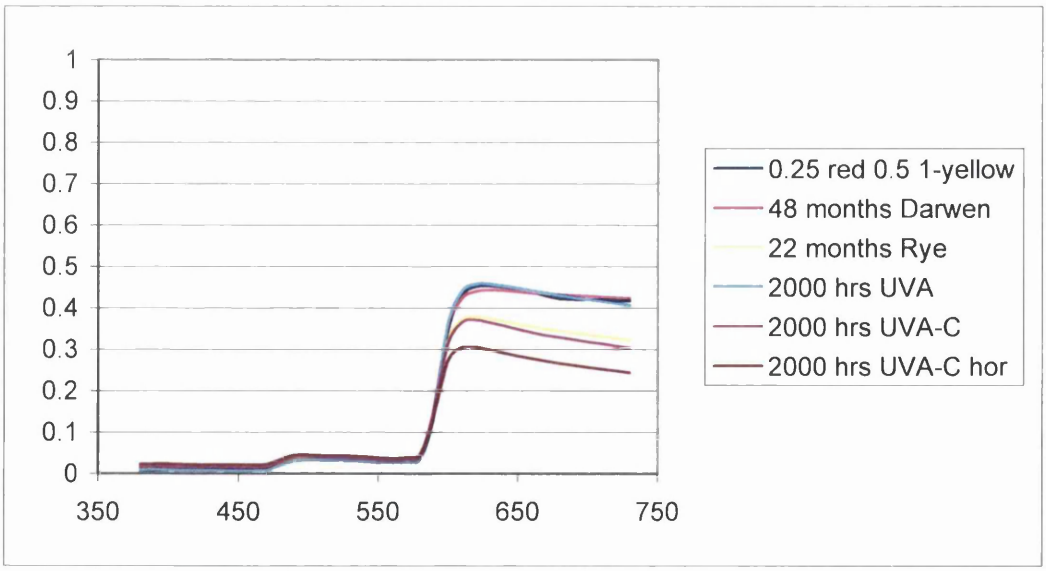
1
0.9
0.8
0.7
0.6
0.5
0.4
0.3
0.2
0.1
0
350
450
550
650
750
0.25 red 0.5 1-yellow
48 months Darwen
22 months Rye
2000 hrs UVA
2000 hrs UVA-C
2000 hrs UVA-C hor

Appendix II

	Rye				Darwen		
Shade	no weathering	11 months	22 months		no weathering	12 months	24 months
	Gloss 60	Gloss ret.	Gloss ret.		Gloss 60	Gloss ret.	Gloss ret.
R1	71.8	86.2	69.1		52.0		77.9
R2	68.2	104.4	75.2		50.6		87.4
R3	65.4	109.8	93.3		41.5		84.3
R4	64.2	85.4	89.4		53.3		79.5
R5	65.8	98.3	86.3		74.2		64.8
R6	65.2	109.0	89.9		80.7		74.2
R7	69.1	91.0	88.1		81.8	92.9	86.7
R8	88.6	101.0	89.6		86.1	95.5	93.0
R9	82.3	106.8	87.7		86.6	96.0	92.3
R10	81.6	103.3	96.8		89.2	95.1	93.9
R11	61.1	140.3	125.0		87.6	93.8	94.2
R12	77.4	101.9	90.7		80.3	89.7	84.6
R13	90.6	98.2	85.8		83.7	98.7	94.7
R14	89.6	98.2	92.5		89.4	95.7	94.0
R15	86.8	100.5	99.5		87.1	94.9	95.5
R16	67.3	126.0	82.3		87.8	95.4	94.2
R17	68.0	109.9	88.2		81.5	90.9	84.7
R18	79.3	100.1	88.4		87.8	94.0	92.3
R19	80.6	99.6	92.3		88.4	94.2	92.8
R20	67.8	112.2	105.0		88.5	97.2	91.4
R21	41.0	193.4	143.2		89.0	94.6	92.4
B1	71.8	98.9	77.6		64.3		75.6
B2	50.6	135.6	100.6		65.3		70.6
B3	65.3	102.3	98.3		42.7		85.5
B4	74.4	100.5	70.6		66.9		74.0
B5	47.9	145.7	82.9		56.2		79.2
B6	63.4	108.4	86.4		58.7		86.0
B7	73.6	96.9	86.0		76.2	76.2	87.8
B8	77.8	101.0	95.5		84.3	84.3	91.7
B9	78.0	106.0	102.1		80.4	80.4	96.6
B10	82.4	93.4	100.2		89.0	89.0	96.0
B11	67.4	123.6	113.9		84.4	84.4	95.1
B12	63.7	102.2	93.9		71.8	71.8	90.0
B13	73.4	109.8	109.4		81.0	81.0	91.9
B14	73.5	110.9	108.8		82.6	82.6	92.9
B15	59.8	137.5	134.1		88.2	88.2	95.0
B16	37.3	219.3	208.0		88.2	88.2	94.0
B17	69.0	102.9	92.8		74.1	74.1	88.8
B18	84.6	100.6	96.1		83.8	83.8	91.2
B19	84.8	99.8	95.6		84.5	84.5	93.3
B20	77.8	108.6	109.8		84.4	84.4	97.6
B21	71.8	107.1	105.0		82.5	82.5	94.4

	Rye				Darwen		
Shade	no weathering	11 months	22 months		no weathering	12 months	24 months
	Gloss 60	Gloss ret.	Gloss ret.		Gloss 60	Gloss ret.	Gloss ret.
G1	67.5	104.4	70.5		71.5		76.9
G2	71.0	100.7	85.2		47.6		89.7
G3	61.6	123.9	95.8		59.0		79.7
G4	69.3	93.8	76.5		68.5		81.8
G5	49.0	68.8	91.4		52.5		77.1
G6	59.6	104.2	97.1		59.1		93.4
G7	56.1	90.0	111.2		80.6	92.4	87.8
G8	77.0	99.5	96.8		87.3	95.8	93.4
G9	73.4	93.9	108.2		83.2	93.9	95.7
G10	69.9	124.6	108.4		91.1	95.2	94.5
G11	65.9	126.3	110.5		84.9	97.2	92.9
G12	69.1	97.5	84.8		80.0	91.5	89.0
G13	83.8	99.6	91.6		86.0	95.7	91.0
G14	86.3	103.7	97.7		84.7	96.3	94.8
G15	84.8	103.5	89.6		87.5	94.9	93.3
G16	77.9	96.1	95.1		84.3	95.5	95.1
G17	61.4	99.5	110.6		79.7	93.9	87.1
G18	86.3	106.0	94.1		86.6	96.3	92.4
G19	68.4	71.8	105.8		85.3	96.5	93.1
G20	73.1	114.2	101.0		89.1	95.5	92.9
G21	74.6	107.8	102.3		85.8	95.8	95.8
P1	72.0	108.8	66.8		64.7		72.0
P2	66.1	110.1	82.8		61.0		77.5
P3	52.0	133.1	112.9		74.4		75.4
P4	58.5	121.0	84.3		60.8		74.7
P5	70.2	107.4	78.1		43.1		89.8
P6	61.3	120.1	95.1		59.4		70.7
P7	62.8	115.4	82.5		84.1	86.6	83.8
P8	84.3	102.1	89.2		90.8	93.5	91.4
P9	76.9	104.0	102.9		92.6	90.0	90.3
P10	78.3	104.5	100.3		92.0	91.5	92.5
P11	53.9	157.9	152.3		91.7	91.9	90.3
P12	55.6	121.9	114.2		82.5	87.3	84.1
P13	80.5	101.7	103.2		90.1	89.9	90.6
P14	48.4	173.6	160.1		89.6	90.7	89.7
P15	33.7	230.3	210.1		87.7	89.9	90.6
P16	16.2	480.9	431.5		87.3	90.6	89.9
P17	25.1	253.0	241.4		72.1	92.2	87.2
P18	23.3	349.8	315.9		87.0	90.9	88.6
P19	16.8	461.9	419.0		85.5	91.1	84.9
P20	15.8	488.0	400.0		84.3	93.5	88.7
P21	9.8	617.3	458.2		79.5	89.6	88.8

	Rye				Darwen		
Shade	no weathering	11 months	22 months		no weathering	12 months	24 months
	Gloss 60	Gloss ret.	Gloss ret.		Gloss 60	Gloss ret.	Gloss ret.
S1	65.0	96.8	76.2		76.8		79.2
S2	50.4	148.0	106.5		72.1		75.3
S3	39.3	161.8	125.2		83.2		116.5
S4	54.7	128.5	96.2		61.1		74.1
S5	63.9	88.6	85.6		75.1		75.9
S6	52.1	121.9	110.0		67.0		74.6
S7	55.0	116.5	105.1		66.4		83.7
S8	59.1	123.5	109.3		77.2		85.4
S9	34.4	201.5	193.6		83.1		84.8
S10	28.9	253.6	256.7		56.6		109.7
S11	17.9	371.5	341.9		46.5		69.7
S12	51.2	130.3	115.4		62.2		78.5
S13	37.7	177.2	154.4		76.5		83.5
S14	24.3	270.8	226.3		61.3		82.9
S15	34.0	186.2	176.8		67.2		78.0
S16	11.8	398.3	504.2		53.8		93.9
S17	48.2	143.2	102.1		52.2		83.7
S18	33.3	201.8	169.1		78.8		84.0
S19	37.3	186.9	157.9		82.3		80.1
S20	17.5	393.1	341.1		66.7		84.7
S21	10.0	595.0	348.0		55.3		74.7
N1	75.1	94.3	77.5		80.1		78.5
N2	77.9	94.2	39.8		57.3		82.2
N3	75.8	104.6	88.4		75.4		76.4
N4	71.0	105.6	103.9		57.6		90.3
N5	34.0	186.8	129.7		57.7		79.0
Y1	74.4	103.2	53.0		78.0	90.8	94.1
Y2	73.3	102.2	102.6		67.3	101.3	101.5
Y3	73.7	107.5	100.9		66.9	101.5	97.6
Y4	74.6	107.5	105.9		58.1	111.2	106.2
Y5	81.7	102.3	54.1		75.1	95.3	94.7
Y6	82.4	101.3	82.6		78.7	93.9	94.8
Y7	79.6	103.6	97.6		78.1	94.4	93.0
Y8	74.5	105.0	93.0		80.9	91.0	90.2
Y9	77.0	106.0	36.6		82.6	90.6	88.7
Y10	78.5	105.6	78.2		81.4	88.6	88.7
Y11	74.1	104.0	102.4		79.6	88.8	89.3
Y12	72.2	114.8	102.4		69.1	100.3	96.7

	Rye				Darwen		
Shade	no weathering	11 months	22 months		no weathering	12 months	24 months
	Gloss 60	Gloss ret.	Gloss ret.		Gloss 60	Gloss ret.	Gloss ret.
M1	81.2	101.1	70.6		74.3	83.8	80.5
M2	75.5	84.8	77.7		79.0	83.5	76.6
M3	53.4	134.3	121.9		77.8	83.3	77.2
M4	42.7	155.5	142.4		78.2	75.4	73.5
M5	71.2	42.3	75.7		72.4	84.4	83.4
M6	75.3	95.1	73.8		77.9	81.3	79.8
M7	68.1	106.6	95.7		77.7	80.8	76.8
M8	50.2	149.8	131.5		77.5	78.1	74.6
M9	78.1	86.4	87.7		80.5	81.0	78.8
M10	81.4	97.7	75.4		77.8	79.7	77.2
M11	65.3	112.3	84.8		70.9	80.8	80.1
M12	63.3	105.1	83.7		70.8	83.8	82.6
C1	82.8	91.3	14.4		73.2	97.8	94.8
C2	80.0	108.4	63.0		72.7	98.4	97.7
C3	82.7	101.8	99.3		71.6	97.6	97.4
C4	54.7	143.7	145.9		68.6	101.8	98.7
C5	79.8	95.0	14.4		75.0	102.3	96.3
C6	83.1	100.6	40.2		71.3	104.2	102.7
C7	81.8	105.5	99.3		78.6	98.7	99.2
C8	70.7	110.9	102.8		81.6	95.0	96.7
C9	83.6	102.9	13.9		80.3	92.2	91.9
C10	83.8	101.4	13.7		81.9	87.1	88.4
C11	69.8	114.9	116.3		80.0	88.6	92.9
C12	72.4	107.7	109.9		74.7	96.3	96.5
O1	61.1	127.8	103.3		68.9	85.1	82.9
O2	68.1	113.5	102.2		65.1	85.3	85.1
O3	50.4	126.0	137.7		82.2	85.5	86.9
O4	48.3	149.9	131.3		64.1	84.6	85.3
O5	68.3	106.3	107.3		73.6	83.2	84.6
O6	62.8	107.5	100.3		65.8	81.6	87.4
O7	72.7	109.4	99.4		72.4	79.4	83.3
O8	45.3	165.3	155.0		71.7	80.3	82.1
O9	71.7	104.6	92.6		64.6	85.1	85.4
O10	72.7	101.5	87.9		71.0	81.0	80.4
O11	70.0	110.6	98.4		69.3	77.3	75.3
O12	62.8	116.2	104.3		73.5	78.5	76.7

QUV			No Condensation			
Shade	no weathering		500 (UV-A hrs)	1000 (UV-A hrs)	1500 (UV-A hrs)	2000 (UV-A hrs)
	Gloss 60		Gloss ret.	Gloss ret.	Gloss ret.	Gloss ret.
R1	67.3		83.5		86.6	80.7
R2	69.9		115.7		104.1	96.4
R3	67		96.1		95.2	85.1
R4	63.9		100.2		100.0	89.0
R5	73.8		105.6		98.4	90.7
R6	55.4		111.2		106.7	105.2
R7	78.1		107.6		100.9	97.4
R8	78.1		115.0		114.5	107.4
R9	79.5		104.3		98.7	92.6
R10	79		103.3		100.8	90.1
R11	74.8		116.6		110.7	103.9
R12	77.1		102.3		97.3	90.7
R13	87.1		104.1		99.0	93.7
R14	90.7		94.5		90.8	81.4
R15	84.1		98.3		88.5	80.6
R16	61.2		144.9		138.9	129.4
R17	69.5		95.3		90.2	86.0
R18	83.5		103.6		95.1	87.8
R19	82.5		112.1		110.2	105.0
R20	81		101.7		100.6	95.4
R21	55.9		144.2		132.7	119.5
B1	72.2		105.3		98.8	96.1
B2	67.4		113.8		107.1	99.3
B3	67.8		89.5		84.7	83.8
B4	64.6		97.4		88.7	89.3
B5	68.3		98.5		87.8	84.0
B6	69.1		105.2		98.0	95.7
B7	75.5		108.3		95.1	94.6
B8	86.9		105.6		94.0	93.9
B9	83.1		106.3		96.8	94.1
B10	86.5		100.2		92.0	91.2
B11	78.8		110.2		98.5	95.6
B12	68.4		106.1		97.5	97.5
B13	80		109.1		101.1	100.6
B14	81.2		112.2		96.9	93.2
B15	73.8		114.9		100.9	98.2
B16	55.2		156.2		139.7	137.9
B17	66.8		117.1		109.4	109.3
B18	86.9		100.6		87.2	92.5
B19	79.3		94.8		71.1	76.4
B20	72.4		114.6		109.3	105.4
B21	55.3		117.4		103.1	96.0

QUV			No Condensation			
Shade	no weathering		500 (UV-A hrs)	1000 (UV-A hrs)	1500 (UV-A hrs)	2000 (UV-A hrs)
	Gloss 60		Gloss ret.	Gloss ret.	Gloss ret.	Gloss ret.
G1	66.8		94.3	98.8	90.9	84.9
G2	78.1		98.5	101.2	95.5	94.6
G3	69.1		87.8	88.9	80.9	80.2
G4	67.8		97.5	98.1	91.4	78.5
G5	65.9		93.2	95.6	88.8	90.1
G6	68.4		109.1	112.6	103.4	103.4
G7	63.2		127.5	131.3	125.3	124.8
G8	65.7		104.1	132.0	99.1	99.7
G9	81		103.3	105.7	99.0	95.8
G10	82.7		78.0	79.8	66.4	71.8
G11	74.7		99.7	105.6	97.7	92.1
G12	73.3		103.1	107.4	96.6	95.2
G13	82.3		106.6	109.5	102.6	99.0
G14	85.9		92.7	93.7	87.8	80.9
G15	83.5		98.0	100.5	91.4	86.8
G16	73.4		107.5	110.8	101.0	96.0
G17	74		96.8	97.3	93.6	91.2
G18	69.8		120.3	120.9	112.2	109.5
G19	74.7		104.3	103.6	90.6	83.0
G20	80.5		75.0	77.4	68.0	65.7
G21	56		132.0	137.1	126.1	118.8
P1	69.3		101.4	97.5	101.2	93.7
P2	73.7		89.0	85.5	77.3	78.3
P3	69.7		119.2		109.0	103.0
P4	72.9		120.3		106.3	106.6
P5	70.1		109.6		98.4	97.1
P6	63.7		112.1		100.2	91.5
P7	66.6		120.0		114.3	108.6
P8	81.1		110.4		97.2	97.3
P9	87.3		101.1		78.6	89.7
P10	73.4		85.0		104.6	96.5
P11	74.9		116.8		101.1	96.7
P12	76.7		107.0		96.9	95.2
P13	86.2		105.8		72.3	95.7
P14	50.3		137.6		118.5	110.7
P15	25.1		310.0		274.1	275.7
P16	15.3		479.1		433.3	434.0
P17	17.9		359.8		292.7	314.0
P18	38.7		226.9		171.8	157.6
P19	17.3		487.9		374.0	357.8
P20	15.3		483.7		394.1	372.5
P21	12.3		517.9		489.4	494.3

	QUV		No Condensation			
Shade	no weathering		500 (UV-A hrs)	1000 (UV-A hrs)	1500 (UV-A hrs)	2000 (UV-A hrs)
	Gloss 60		Gloss ret.	Gloss ret.	Gloss ret.	Gloss ret.
S1	69.4		105.8	108.1	100.0	103.7
S2	67.1		114.2	108.8	102.1	90.6
S3	52.5		143.0	142.1	128.8	123.8
S4	55.6		130.0	133.1	121.2	117.8
S5	64		114.8	120.2	111.4	113.8
S6	47.8		143.5	144.1	131.8	123.2
S7	52.8		126.7	133.1	118.8	116.1
S8	53.9		147.1	151.2	138.6	134.9
S9	32.3		200.6	201.2	183.6	184.2
S10	51.6		140.3	138.8	139.5	136.4
S11	17.8		362.9	363.5	351.1	311.8
S12	42.2		163.3	177.5	161.6	152.4
S13	50.1		140.7	145.1	134.7	127.7
S14	37.2		183.1	185.2	171.0	168.3
S15	17.6		386.4	415.3	382.4	355.7
S16	11.8		389.0	350.0	355.1	333.9
S17	42.3		167.4	186.5	175.2	172.6
S18	18		342.2	342.2	332.8	335.6
S19	23.4		300.0	309.4	287.6	267.1
S20	14.7		320.4	300.0	304.8	313.6
S21	9.5		575.8	588.4	547.4	546.3
N1	68.8		90.4	92.2	82.6	86.5
N2	78.7		111.4		91.9	96.8
N3	78		108.2		80.5	83.5
N4	68.8		107.6		99.3	99.0
N5	37.1		171.7		167.7	159.0
Y1	82.1		100.1	105.0	91.8	67.6
Y2	84.9		97.6	99.6	93.8	90.8
Y3	82.2		75.9	75.1	67.0	64.0
Y4	81		100.7	105.7	99.0	96.9
Y5	79.6		101.1	104.1	94.3	95.4
Y6	75.3		102.8	104.5	98.7	95.0
Y7	73.7		58.5	61.2	50.7	50.9
Y8	80.8		93.2	96.4	89.0	86.4
Y9	81.2		76.8	91.9	84.7	68.0
Y10	77.5		99.0	102.1	92.0	94.1
Y11	82.1		99.6	99.5	96.2	92.9
Y12	77.2		82.1	89.4	80.3	72.3

	QUV		No Condensation			
Shade	no weathering		500 (UV-A hrs)	1000 (UV-A hrs)	1500 (UV-A hrs)	2000 (UV-A hrs)
	Gloss 60		Gloss ret.	Gloss ret.	Gloss ret.	Gloss ret.
M1	76.3		101.6	105.5	100.0	101.4
M2	73.7		94.0	95.8	90.8	92.7
M3	67.4		112.2	115.4	110.4	105.8
M4	60.9		123.2	128.1	120.9	119.0
M5	76.1		91.7	94.0	90.4	90.5
M6	77.2		98.6	99.6	93.3	90.5
M7	76.7		68.8	68.6	68.8	67.3
M8	59.1		132.7	140.3	123.9	126.7
M9	81.8		57.1	53.9	49.1	50.4
M10	72.4		103.0	105.7	99.3	96.8
M11	73.2		107.9	110.2	99.3	97.0
M12	61.8		104.4	110.5	103.7	101.3
C1	80.4		103.4	105.7	95.5	105.3
C2	81.8		107.1	110.4	104.3	92.1
C3	76.3		107.7	114.0	104.1	102.2
C4	61.1		130.9	136.3	127.5	113.7
C5	81.7		102.2	102.4	98.4	104.3
C6	76		102.2	107.0	96.7	101.7
C7	80.2		105.4	109.7	103.1	102.0
C8	76					
C9	85.8		99.7	105.2	98.5	96.6
C10	82.7		104.0	108.5	90.8	85.7
C11	84.7		98.6	100.6	93.5	91.3
C12	65		121.5	123.8	100.5	93.8
O1	62.8		118.5		99.0	101.6
O2	63.3		120.5		98.9	95.4
O3	49		150.2		120.4	118.6
O4	55.2		154.2		125.2	122.1
O5	65.4		119.7		110.4	106.0
O6	74.4		100.8		87.8	87.1
O7	60.7		130.1		106.8	105.3
O8	68.6		125.9		108.2	103.5
O9	63.9		112.2		103.4	102.5
O10	73.5		119.7		107.9	100.0
O11	20.7		119.3		101.4	101.4
O12	69.1		115.5		109.0	110.4

	QUV		8 hrs UV-A / 4 hrs condensation			
Shade	no weathering		500 (UV-A hrs)	1000 (UV-A hrs)	1500 (UV-A hrs)	2000 (UV-A hrs)
	Gloss 60		Gloss ret.	Gloss ret.	Gloss ret.	Gloss ret.
R1	67.3		77.1	84.0	76.4	73.0
R2	69.9		79.0	80.5	79.1	73.1
R3	67		86.1	94.2	88.5	79.4
R4	63.9		87.9	91.1	85.9	75.3
R5	73.8		76.7	83.3	76.3	72.9
R6	55.4		93.7	100.0	93.9	92.8
R7	78.1		71.7	75.0	74.0	72.5
R8	78.1		102.4	109.3	106.0	103.7
R9	79.5		103.3	110.9	107.9	109.4
R10	79		97.3	111.8	103.8	95.6
R11	74.8		109.0	115.2	116.2	114.6
R12	77.1		65.6	70.7	66.5	57.2
R13	87.1		90.1	97.0	93.7	91.7
R14	90.7		88.1	93.2	92.1	90.4
R15	84.1		84.2	92.0	89.1	87.2
R16	61.2		121.7	130.7	127.8	126.1
R17	69.5		75.1	75.3	75.3	71.9
R18	83.5		90.8	98.9	95.6	95.3
R19	82.5		89.8	97.1	92.6	94.2
R20	81		89.5	97.5	99.8	90.1
R21	55.9		125.9	134.7	136.9	124.9
B1	72.2		66.5	62.3	64.5	62.7
B2	67.4		82.9	81.8	75.5	72.6
B3	67.8		85.7	85.5	86.1	79.6
B4	64.6		70.9	66.3	69.2	67.2
B5	68.3		84.5	80.7	78.0	73.9
B6	69.1		78.0	80.6	77.7	72.5
B7	75.5		77.5	73.6	72.7	69.7
B8	86.9		84.0	92.1	92.1	91.8
B9	83.1		96.8	103.2	102.4	97.4
B10	86.5		97.0	101.3	105.1	104.7
B11	78.8		99.7	107.9	109.4	109.3
B12	68.4		81.4	75.1	76.0	73.1
B13	80		97.8	100.8	102.3	102.5
B14	81.2		100.2	99.1	102.8	104.8
B15	73.8		107.7	115.6	119.0	117.1
B16	55.2		138.0	150.0	150.2	156.2
B17	66.8		86.4	88.0	82.2	78.3
B18	86.9		78.4	82.5	75.7	78.7
B19	79.3		87.0	90.2	90.0	91.0
B20	72.4		112.8	120.6	116.7	118.8
B21	55.3		129.8	140.5	140.9	138.5

QUV			8 hrs UV-A / 4 hrs condensation			
Shade	no weathering		500 (UV-A hrs)	1000 (UV-A hrs)	1500 (UV-A hrs)	2000 (UV-A hrs)
	Gloss 60		Gloss ret.	Gloss ret.	Gloss ret.	Gloss ret.
G1	66.8			71.9	64.2	34.4
G2	78.1			62.2	60.9	47.5
G3	69.1			82.3	75.1	72.9
G4	67.8			73.5	64.2	37.0
G5	65.9			95.4	88.5	63.9
G6	68.4			85.7	79.1	75.3
G7	63.2			88.4	78.2	57.9
G8	65.7			117.8	106.4	95.4
G9	81			107.4	104.4	100.6
G10	82.7			109.9	112.0	111.1
G11	74.7			110.4	108.8	105.2
G12	73.3			74.6	70.1	56.3
G13	82.3			77.8	98.4	90.2
G14	85.9			104.7	103.5	100.6
G15	83.5			101.8	100.1	94.4
G16	73.4			109.0	107.8	108.2
G17	74			70.8	68.2	55.9
G18	69.8			124.6	122.3	116.8
G19	74.7			80.2	75.9	70.7
G20	80.5			101.7	103.0	102.7
G21	56			120.0	130.4	112.9
P1	69.3			88.9	67.7	42.6
P2	73.7			68.2	72.9	52.8
P3	69.7		83.4	85.9	82.1	77.0
P4	72.9		77.8	82.9	83.4	79.7
P5	70.1		66.2	75.9	64.5	59.6
P6	63.7		70.8	89.6	94.8	95.3
P7	66.6		78.4	84.2	79.4	75.2
P8	81.1		95.7	106.5	103.2	99.9
P9	87.3		88.7	91.4	92.2	82.8
P10	73.4		95.1	104.1	106.0	108.2
P11	74.9		104.8	114.0	114.3	112.3
P12	76.7		77.4	85.9	82.8	77.8
P13	86.2		88.3	98.4	90.5	62.3
P14	50.3		142.9	152.3	148.3	144.5
P15	25.1		299.6	314.3	297.6	286.5
P16	15.3		449.0	480.4	480.4	498.0
P17	17.9		298.9	304.5	286.6	308.4
P18	38.7		201.6	212.9	203.1	205.4
P19	17.3		411.0	434.1	436.4	408.1
P20	15.3		434.6	469.9	430.1	426.1
P21	12.3		446.3	478.0	540.7	495.1

	QUV		8 hrs UV-A / 4 hrs condensation			
Shade	no weathering		500 (UV-A hrs)	1000 (UV-A hrs)	1500 (UV-A hrs)	2000 (UV-A hrs)
	Gloss 60		Gloss ret.	Gloss ret.	Gloss ret.	Gloss ret.
S1	69.4			72.3	74.9	64.7
S2	67.1			67.7	67.8	55.0
S3	52.5			109.9	100.2	96.0
S4	55.6			93.5	98.4	66.5
S5	64			87.3	83.1	77.2
S6	47.8			135.4	120.5	122.0
S7	52.8			99.4	85.4	74.6
S8	53.9			113.2	104.6	98.3
S9	32.3			186.1	167.5	158.5
S10	51.6			138.4	131.8	124.0
S11	17.8			346.6	330.3	318.0
S12	42.2			135.3	128.7	114.0
S13	50.1			114.8	109.4	96.2
S14	37.2			167.5	153.2	146.2
S15	17.6			367.6	343.2	320.5
S16	11.8			400.0	433.9	427.1
S17	42.3			141.6	133.8	129.1
S18	18			332.8	302.2	301.1
S19	23.4			262.0	271.8	254.7
S20	14.7			359.2	380.3	362.6
S21	9.5			421.1	393.7	418.9
N1	68.8		0.0	74.0	66.7	44.5
N2	78.7		63.7	83.2	72.8	61.6
N3	78		89.5	93.8	88.3	86.8
N4	68.8		99.7	105.1	102.8	102.3
N5	37.1		166.8	174.9	167.4	170.1
Y1	82.1			106.7	93.5	73.0
Y2	84.9			106.7	103.1	90.7
Y3	82.2			110.0	108.4	97.3
Y4	81			94.2	99.4	82.7
Y5	79.6			91.0	77.0	50.0
Y6	75.3			113.4	106.5	84.5
Y7	73.7			113.4	103.7	90.8
Y8	80.8			110.1	104.7	96.3
Y9	81.2			55.5	60.0	52.6
Y10	77.5			101.7	89.0	61.2
Y11	82.1			104.5	102.3	92.9
Y12	77.2			107.6	101.7	89.6

	QUV		8 hrs UV-A / 4 hrs condensation			
Shade	no weathering		500 (UV-A hrs)	1000 (UV-A hrs)	1500 (UV-A hrs)	2000 (UV-A hrs)
	Gloss 60		Gloss ret.	Gloss ret.	Gloss ret.	Gloss ret.
M1	76.3			76.4	72.9	59.0
M2	73.7			79.0	71.4	56.9
M3	67.4			85.6	82.5	74.8
M4	60.9			90.6	86.4	84.2
M5	76.1			75.3	67.8	53.5
M6	77.2			74.9	65.4	48.4
M7	76.7			86.0	69.8	64.9
M8	59.1			96.1	100.5	86.8
M9	81.8			80.0	70.7	59.2
M10	72.4			82.7	72.8	55.9
M11	73.2			82.2	74.7	63.5
M12	61.8			79.8	80.7	71.5
C1	80.4			96.6	79.2	61.9
C2	81.8			105.4	99.4	83.3
C3	76.3			110.2	109.8	98.4
C4	61.1			137.6	135.2	121.3
C5	81.7			106.4	72.9	62.5
C6	76			95.5	81.8	51.8
C7	80.2			102.5	99.0	81.9
C8	76					
C9	85.8			99.3	88.1	52.2
C10	82.7			102.2	94.1	71.5
C11	84.7			101.5	101.9	92.8
C12	65			121.2	118.3	109.4
O1	62.8		116.1	119.1	116.1	119.1
O2	63.3		89.4	99.1	97.9	100.9
O3	49		106.3	106.3	119.0	135.1
O4	55.2		132.6	136.1	126.8	127.9
O5	65.4		109.3	110.1	99.7	90.7
O6	74.4		93.4	94.9	89.4	85.8
O7	60.7		104.8	114.3	107.4	100.0
O8	68.6		99.4	107.0	102.8	95.3
O9	63.9		98.4	94.4	81.1	76.2
O10	73.5		98.2	103.0	94.0	81.5
O11	20.7		99.0	101.4	96.6	91.3
O12	69.1		93.8	102.6	95.2	89.1

horizontal QUV			8 hrs UV-A / 4 hrs condensation			
Shade	no weathering		500 (UV-A hrs)	1000 (UV-A hrs)	1500 (UV-A hrs)	2000 (UV-A hrs)
	Gloss 60		Gloss ret.	Gloss ret.	Gloss ret.	Gloss ret.
R1	67.3		70.9	59.4	37.1	18.0
R2	69.9		76.4	68.4	52.4	39.2
R3	67		86.9	85.7	75.8	45.8
R4	63.9		77.8	65.6	38.3	16.1
R5	73.8		74.9	66.3	56.1	45.5
R6	55.4		101.1	101.4	90.8	78.9
R7	78.1		71.7	64.0	51.1	45.1
R8	78.1		101.0	89.4	56.2	40.8
R9	79.5		102.8	100.1	83.4	77.1
R10	79		92.3	94.9	89.1	69.4
R11	74.8		95.5	105.3	96.3	99.2
R12	77.1		57.3	66.4	59.5	52.5
R13	87.1		87.1	87.1	77.2	73.6
R14	90.7		55.9	89.1	85.3	78.5
R15	84.1		75.7	68.0	65.4	55.3
R16	61.2		87.3	119.3	103.4	105.4
R17	69.5		62.0	68.6	66.3	62.4
R18	83.5		73.4	83.2	68.7	46.6
R19	82.5		78.9	90.4	83.8	47.3
R20	81		66.7	92.0	95.1	78.1
R21	55.9		108.2	112.2	111.6	97.0
B1	72.2		66.2	55.1	53.7	30.3
B2	67.4		84.6	70.3	58.9	40.4
B3	67.8		92.8	90.7	87.2	78.0
B4	64.6		77.9	64.9	59.0	46.0
B5	68.3		68.4	57.4	56.4	53.9
B6	69.1		59.5	62.7	67.6	57.7
B7	75.5		76.4	64.9	57.5	55.2
B8	86.9		87.8	87.6	82.5	75.4
B9	83.1		104.7	96.8	83.9	90.3
B10	86.5		96.5	97.8	95.1	81.3
B11	78.8		92.8	88.6	79.4	67.0
B12	68.4		76.9	70.0	65.5	63.9
B13	80		107.0	94.4	100.6	99.9
B14	81.2		102.3	98.3	99.5	94.7
B15	73.8		96.9	97.0	106.0	102.0
B16	55.2		148.6	144.4	141.8	134.1
B17	66.8		75.0	68.4	69.9	62.4
B18	86.9		50.2	38.9	50.6	54.2
B19	79.3		104.0	100.4	101.9	98.7
B20	72.4		115.9	95.3	116.2	112.4
B21	55.3		133.8	109.4	123.5	112.3

horizontal QUV			8 hrs UV-A / 4 hrs condensation			
Shade	no weathering		500 (UV-A hrs)	1000 (UV-A hrs)	1500 (UV-A hrs)	2000 (UV-A hrs)
	Gloss 60		Gloss ret.	Gloss ret.	Gloss ret.	Gloss ret.
G1	66.8		77.8	78.7	68.3	50.1
G2	78.1		79.6	75.8	72.3	60.7
G3	69.1		83.4	86.8	83.6	78.3
G4	67.8		86.1	86.9	74.9	54.6
G5	65.9		82.9	72.5	74.8	60.7
G6	68.4		80.1	90.8	86.3	101.8
G7	63.2		90.0	92.2	80.7	52.5
G8	65.7		45.4	42.6	30.9	47.0
G9	81		108.0	113.6	105.6	98.3
G10	82.7		91.8	102.4	102.3	87.8
G11	74.7		75.5	74.8	75.5	73.5
G12	73.3		65.1	73.9	64.1	58.1
G13	82.3		102.6	105.6	96.1	90.8
G14	85.9		97.6	97.6	93.8	87.2
G15	83.5		95.7	101.2	92.7	74.1
G16	73.4		97.3	101.9	86.9	91.4
G17	74		91.6	88.9	76.4	74.7
G18	69.8		113.9	112.6	108.5	102.7
G19	74.7		102.4	95.9	88.6	60.1
G20	80.5		96.6	97.5	87.2	78.9
G21	56		134.6	143.4	120.9	119.5
P1	69.3		85.6	81.1	70.4	51.7
P2	73.7		67.6	75.0	71.5	65.1
P3	69.7		78.6	66.6	60.5	69.7
P4	72.9		85.3	53.9	64.1	59.5
P5	70.1		72.2	55.8	67.0	64.8
P6	63.7		87.1	52.9	77.4	79.9
P7	66.6		74.8	47.0	73.7	71.3
P8	81.1		95.4	76.2	93.7	80.9
P9	87.3		76.4	44.4	77.8	78.5
P10	73.4		78.5	43.6	95.1	89.8
P11	74.9		69.3	59.7	104.8	107.9
P12	76.7		66.8	48.0	65.8	63.5
P13	86.2		98.4	93.0	89.9	82.4
P14	50.3		121.5	114.5	109.7	79.9
P15	25.1		219.9	184.1	214.3	180.1
P16	15.3		320.3	289.5	341.2	315.0
P17	17.9		251.4	280.4	258.7	250.8
P18	38.7		164.1	146.3	162.0	122.5
P19	17.3		282.1	285.5	312.1	275.7
P20	15.3		334.6	330.1	366.7	310.5
P21	12.3		414.6	462.6	419.5	322.0

horizontal QUV			8 hrs UV-A / 4 hrs condensation			
Shade	no weathering		500 (UV-A hrs)	1000 (UV-A hrs)	1500 (UV-A hrs)	2000 (UV-A hrs)
	Gloss 60		Gloss ret.	Gloss ret.	Gloss ret.	Gloss ret.
S1	69.4		90.5	96.1	54.8	37.0
S2	67.1		91.4	85.7	85.4	76.2
S3	52.5		97.3	98.5	102.1	91.2
S4	55.6		125.4	127.7	79.0	83.1
S5	64		89.2	89.4	85.9	76.1
S6	47.8		120.1	129.3	125.1	121.3
S7	52.8		103.4	105.3	93.9	44.5
S8	53.9		121.3	122.1	108.2	94.1
S9	32.3		139.3	152.3	125.1	133.4
S10	51.6		142.1	131.4	105.2	116.1
S11	17.8		386.5	384.8	287.6	284.3
S12	42.2		66.4	126.5	107.1	117.1
S13	50.1		118.4	112.0	87.6	108.8
S14	37.2		163.2	163.2	135.2	119.4
S15	17.6		236.4	264.2	255.7	206.8
S16	11.8		332.2	313.6	305.9	360.2
S17	42.3		138.1	142.1	129.6	83.5
S18	18		209.4	239.4	227.2	264.4
S19	23.4		250.9	193.2	225.2	120.1
S20	14.7		304.1	333.3	318.4	234.0
S21	9.5		238.9	328.4	338.9	320.0
N1	68.8		74.0	82.3	49.7	25.1
N2	78.7		78.1	60.1	44.5	49.6
N3	78		57.8	56.9	46.8	39.9
N4	68.8		107.8	104.4	87.4	84.0
N5	37.1		139.1	131.0	128.0	123.2
Y1	82.1		100.5	71.4	68.9	77.6
Y2	84.9		98.5	100.5	93.2	28.7
Y3	82.2		88.2	103.9	97.6	94.4
Y4	81		93.7	103.0	90.1	74.8
Y5	79.6		96.2	66.6	50.9	38.7
Y6	75.3		87.5	103.9	90.0	52.1
Y7	73.7		100.5	109.5	101.4	74.6
Y8	80.8		91.7	102.0	94.4	71.3
Y9	81.2		84.6	96.6	44.2	53.1
Y10	77.5		92.0	69.8	51.9	49.4
Y11	82.1		83.1	101.2	82.0	87.2
Y12	77.2		87.7	94.4	97.2	96.1

horizontal QUV			8 hrs UV-A / 4 hrs condensation			
Shade	no weathering		500 (UV-A hrs)	1000 (UV-A hrs)	1500 (UV-A hrs)	2000 (UV-A hrs)
	Gloss 60		Gloss ret.	Gloss ret.	Gloss ret.	Gloss ret.
M1	76.3		66.3	87.7	74.7	65.8
M2	73.7		90.5	85.9	70.7	70.8
M3	67.4		86.5	75.8	68.0	74.2
M4	60.9		97.0	101.6	93.8	99.3
M5	76.1		77.4	72.4	62.2	61.0
M6	77.2		76.7	35.1	47.2	62.6
M7	76.7		88.8	82.3	66.4	66.6
M8	59.1		99.8	92.9	85.1	83.9
M9	81.8		81.3	81.7	66.4	68.2
M10	72.4		86.3	83.7	60.1	66.4
M11	73.2		82.7	77.7	68.3	72.3
M12	61.8		94.5	92.2	90.5	85.1
C1	80.4		99.4	81.5	47.8	43.8
C2	81.8		99.4	84.1	79.2	44.6
C3	76.3		108.0	110.1	103.9	99.6
C4	61.1		129.1	136.8	123.1	120.1
C5	81.7		96.9	73.6	63.6	66.8
C6	76		99.1	69.6	59.7	50.8
C7	80.2		98.6	103.4	95.0	84.3
C8	76					
C9	85.8		95.0	85.8	69.8	44.8
C10	82.7		103.1	90.9	70.7	17.0
C11	84.7		99.5	103.3	97.0	91.0
C12	65		114.0	113.5	100.9	96.6
O1	62.8		128.3	117.4	95.4	72.1
O2	63.3		131.8	116.9	114.4	107.9
O3	49		160.2	141.2	127.6	128.6
O4	55.2		146.0	142.2	134.1	119.0
O5	65.4		108.4	79.1	60.9	26.8
O6	74.4		98.5	86.2	69.8	29.3
O7	60.7		117.1	118.9	102.5	32.3
O8	68.6		100.6	90.8	82.4	62.7
O9	63.9		115.8	85.9	63.1	22.5
O10	73.5		106.4	97.1	52.4	22.6
O11	20.7		83.1	81.6	81.6	49.8
O12	69.1		98.0	80.0	60.2	44.1

Appendix III

		DIDP concentrations (weight %)					
		horizontal QUV				normal QUV	
						cond.	no cond.
pigmentation		500 (UV-A hrs)	1000 (UV-A hrs)	1500 (UV-A hrs)	2000 (UV-A hrs)	2000 (UV-A hrs)	2000 (UV-A hrs)
N1	base PVC 0 TiO2	11	7.8	7.8	8.7	7.6	13.4
N2	base PVC 1 TiO2	9.8	9.9	8.2	7.7	25.2	9.9
N3	base PVC 5 TiO2	11.4	9.3	7.8	10.1	11.6	
N3b	base PVC 5 TiO2					12.3	
N4	base PVC 10 TiO2	12.7	11.5	10.6	9.6	11.2	
N5	base PVC 15 TiO2	11.5	9.4	7.6	7.3	8.8	
S1	0.25 2-yellow 0 TiO2	12.4	8.2	7.5	18.5	12.9	13.4
S2	0.25 2-yellow 1 TiO2			16.8	16.3	12.4	12.2
S3	0.25 2-yellow 5 TiO2			16.8	4.7	15.1	21.3
S4	1 2-yellow 0 TiO2	7.5	8.6	12.9	3	13.6	12.3
S5	1 2-yellow 1 TiO2			10.9	12.9	12.7	14.5
S6	1 2-yellow 5 TiO2			17.7	12.8	14	15.5
S7	2.5 2-yellow 0 TiO2			15.4	12.9	12	10.2
R1	0.1 red 0 TiO2			4.1	3.3		
R4	0.25 red 0 TiO2			4.9	5.9		
R13a	1.5 red 1 TiO2				7.7		
R13b	1.5 red 1 TiO2				7		
B8a	0.2 blue 1 TiO2				8.7		
B8b	0.2 blue 1 TiO2				8.6		
P1	0.25 1-yellow 0 TiO2				7.2		
P2	0.25 1-yellow 1 TiO2				11.6		
P4	1 1-yellow 0 TiO2			6.2	6.3		
P13a	6 1-yellow 1 TiO2				7.8		
P13b	6 1-yellow 1 TiO2				11.4		
G1	0.05 green 0 TiO2			14.9	7.4		
G2	0.05 green 1 TiO2			14.2	11.1		
G3	0.05 green 5 TiO2			11.9	6.7		
G4	0.1 green 0 TiO2			10.9	8.3		
G5	0.1 green 1 TiO2			14.2	10.2		
G6	0.1 green 5 TiO2			8.3	10.9		
O1	1 red 0.1 1-yellow			7.2	5.2		
O2	2 red 0.2 1-yellow			7.7	3.1		
O5	0.25 red 0.1 1-yellow			4.2	3.9		
O6	0.5 red 0.2 1-yellow			5.9	3.1		
O7a	0.75 red 0.3 1-yellow				5.1		
O7b	0.75 red 0.3 1-yellow				5.4		
O9	0.05 red 0.1 1-yellow			3.3	2.3		
O10	0.1 red 0.2 1-yellow			4.3	3.8		
C1	0.05 green 0.05 blue				4.4		
C2	0.1 green 0.1 blue				6.6		
C3	0.5 green 0.5 blue				15.7		
C4	1 green 1 blue				18.3		
C5	0.05 green 0.02 blue				5.3		
C6	0.1 green 0.04 blue				5.4		
C7	0.5 green 0.2 blue				15.4		
C9	0.02 green 0.05 blue				7		
C10	0.04 green 0.1 blue				7.7		
C11	0.2 green 0.5 blue				17.3		
C12	0.4 green 1 blue				18.6		
Y1	0.5 2-yellow 0.05 green			7.2	2		
Y2	2 2-yellow 0.2 green			11.6	9.1		
Y3	5 2-yellow 0.5 green			17.7	17.1		
Y4	10 2-yellow 1 green			18.4	13		
Y5	0.5 2-yellow 0.02 green			2.1	1.2		
Y6	2 2-yellow 0.08 green			14.4	2.9		
Y7	5 2-yellow 0.2 green			18.5	13.3		
Y8	10 2-yellow 0.4 green			21.5	10.4		
Y9	0.25 2-yellow 0.05 green			16.1	1.8		
Y10	0.5 2-yellow 0.1 green			8.6	3.5		
Y11	2.5 2-yellow 0.5 green			18.3	1.3		
Y12	5 2-yellow 1 green			19.3	11.2		

Appendix IV

Vibration Wavenumber (cm-1)		O-H **3400**	C-H **2900**	C=O **1730**	HC=H2 **1600**
0.05 green		19	80	98	13
11 months Rye		26	67	81	11
22 months Rye		15	64	87	14
24 months Darwen		9	75	100	17
2000 hrs UVA		28	61	75	12
2000 hrs UVA hor cond		20	53	71	15
2500 hrs UVA cond,		18	55	75	12
0.1 green		16	80	103	12
11 months Rye		25	68	90	13
22 months Rye		16	64	83	12
24 months Darwen		8	82	91	12
2000 hrs UVA		28	61	71	13
2000 hrs UVA hor cond		40	51	53	27
2500 hrs UVA cond,		16	60	77	15
0.25 2-yel 0.05 green		17	85	100	12
11 months Rye		25	74	94	16
22 months Rye		28	59	79	15
2000 hrs UVA		61	44	57	29
2000 hrs UVA hor cond		22	45	69	18
2500 hrs UVA cond,		17	70	85	20
0.5 2-yellow 0.02 green		15	80	101	14
11 months Rye		26	75	94	17
22 months Rye		29	54	79	15
2000 hrs UVA		25	53	72	12
2000 hrs UVA hor cond		25	23	40	9
2500 hrs UVA cond,		17	35	64	16
0.25 2-yellow		15	76	98	10
11 months Rye		25	73	94	14
22 months Rye		18	65	84	13
24 months Darwen		10	67	95	12
2000 hrs UVA		28	70	73	14
2000 hrs UVA hor cond		20	35	62	19
2500 hrs UVA cond,		20	70	85	18

Vibration Wavenumber (cm-1)		O-H **3400**	C-H **2900**	C=O **1730**	HC=H2 **1600**
0 TiO2		20	80	98	21
11 months Rye		30	72	87	15
22 months Rye		20	67	87	11
24 months Darwen		8	72	98	11
2000 hrs UVA		29	66	69	11
2000 hrs UVA hor cond		34	44	50	28
2500 hrs UVA cond,		18	65	80	11
1 TiO2		18	69	90	21
11 months Rye		21	61	87	15
22 months Rye		17	62	84	11
24 months Darwen		7	66	91	10
2000 hrs UVA		27	64	75	18
2000 hrs UVA hor cond		22	61	71	16
2500 hrs UVA cond,		15	67	84	15
5 TiO2		17	65	87	19
11 months Rye		22	57	83	12
22 months Rye		12	55	82	12
24 months Darwen		6	59	88	9
2000 hrs UVA		29	59	76	11
2000 hrs UVA hor cond		15	58	75	16
2500 hrs UVA cond,		13	55	78	13
10 TiO2		12	54	78	16
11 months Rye		29	48	70	15
22 months Rye		10	50	74	8
24 months Darwen		6	53	84	8
2000 hrs UVA		27	50	69	10
2000 hrs UVA hor cond		17	52	73	13
2500 hrs UVA cond,		12	48	72	10
15 TiO2		16	54	66	25
11 months Rye		17	45	70	10
22 months Rye		10	46	73	9
24 months Darwen		7	47	80	7
2000 hrs UVA		25	47	70	9
2000 hrs UVA hor cond		24	47	68	15
2500 hrs UVA cond,		17	49	66	18

Vibration Wavenumber (cm-1)		O-H **3400**	C-H **2900**	C=O **1730**	HC=H2 **1600**
1 2-yellow		16	79	100	15
11 months Rye		22	67	90	13
22 months Rye		18	67	90	13
24 months Darwen		9	74	99	13
2000 hrs UVA		27	65	73	11
2000 hrs UVA hor cond		22	48	78	20
2500 hrs UVA cond,		20	65	84	21
2.5 2-yellow		13	67	93	12
11 months Rye		21	65	92	10
22 months Rye		19	66	86	15
24 months Darwen		7	71	99	11
2000 hrs UVA		30	64	76	13
2000 hrs UVA hor cond		62	42	42	70
2500 hrs UVA cond,		18	61	82	22
0.25 2-yellow 1 TiO2		15	72	96	11
11 months Rye		23	71	94	11
22 months Rye		16	65	97	7
24 months Darwen		7	66	92	10
2000 hrs UVA		26	67	78	15
2000 hrs UVA hor cond		30	59	76	30
2500 hrs UVA cond,		13	65	88	15
1 2-yellow 1 TiO2		13	74	101	11
11 months Rye		20	63	87	10
22 months Rye		15	65	87	10
24 months Darwen		8	71	86	11
2000 hrs UVA		38	68	89	13
2000 hrs UVA hor cond		20	65	83	21
2500 hrs UVA cond,		20	62	85	20
0.25 2-yellow 5 TiO2		14	61	89	10
11 months Rye		16	61	88	12
22 months Rye		18	54	78	12
24 months Darwen		7	60	90	10
2000 hrs UVA		27	54	81	13
2000 hrs UVA hor cond		17	56	78	17
2500 hrs UVA cond,		15	54	77	17

Vibration Wavenumber (cm-1)		O-H **3400**	C-H **2900**	C=O **1730**	HC=H2 **1600**
1 2-yellow 5 TiO2		12	65	92	9
11 months Rye		17	57	84	9
22 months Rye		14	61	80	10
24 months Darwen		8	61	88	11
2000 hrs UVA		40	58	86	8
2000 hrs UVA hor cond		17	54	75	16
2500 hrs UVA cond,		17	51	75	8

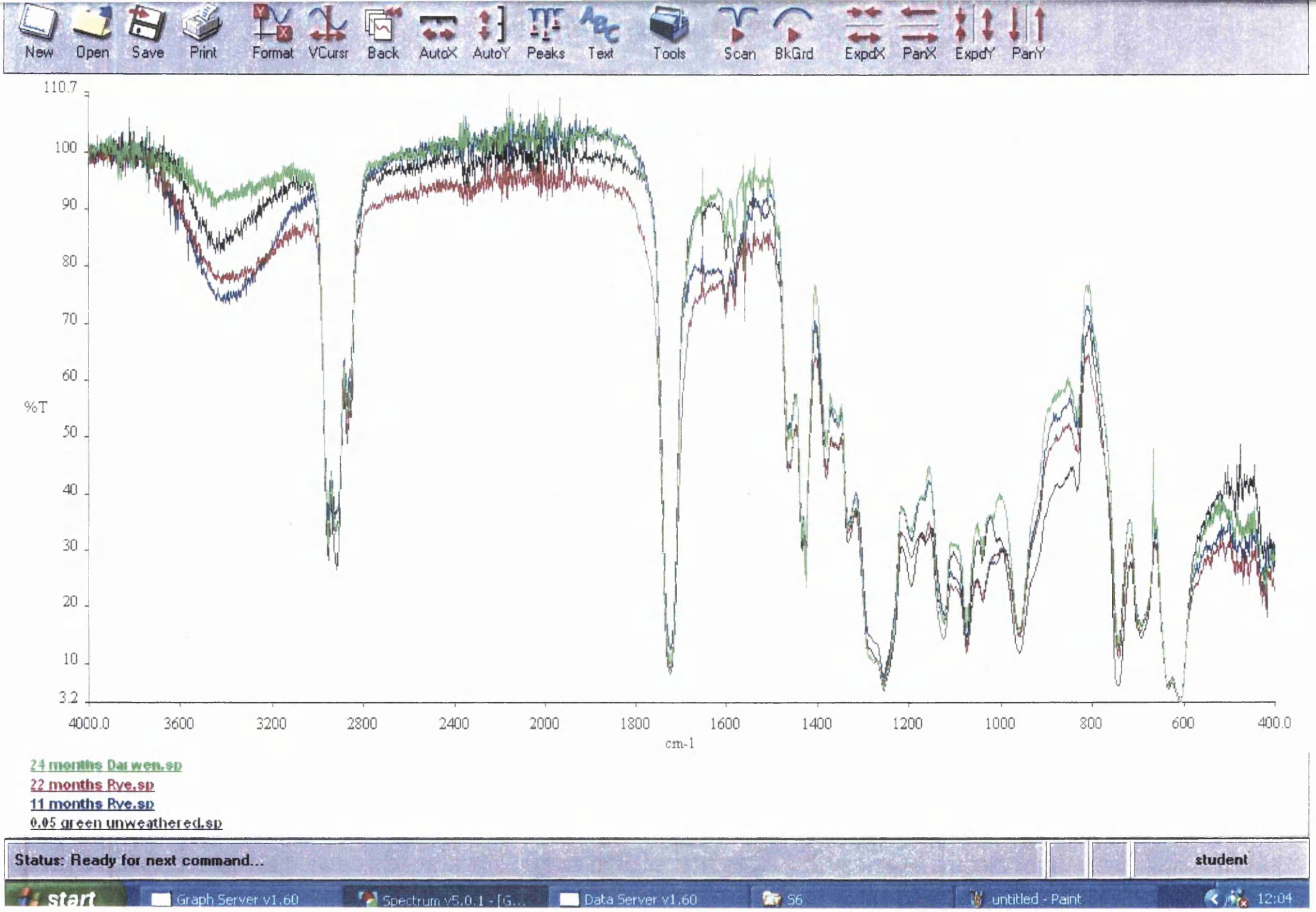
New
Open
Save
Print
Format
VCursr
Back
AutoX
AutoY
Peaks
Text
Tools
Scan
BkGrd
ExpdX
PanX
ExpdY
PanY
110.7
100
90
80
70
60
%T
50
40
30
20
10
3.2
4000.0
3600
3200
2800
2400
2000
1800
1600
1400
1200
1000
800
600
400.0
cm-1
24 months Dai wen.sp
22 months Rye.sp
11 months Rye.sp
0.05 green unweathered.sp
Status: Ready for next command...
student
start
Graph Server v1.60
Spectrum v5.0.1 - [G...
Data Server v1.60
S6
untitled - Paint
12:04

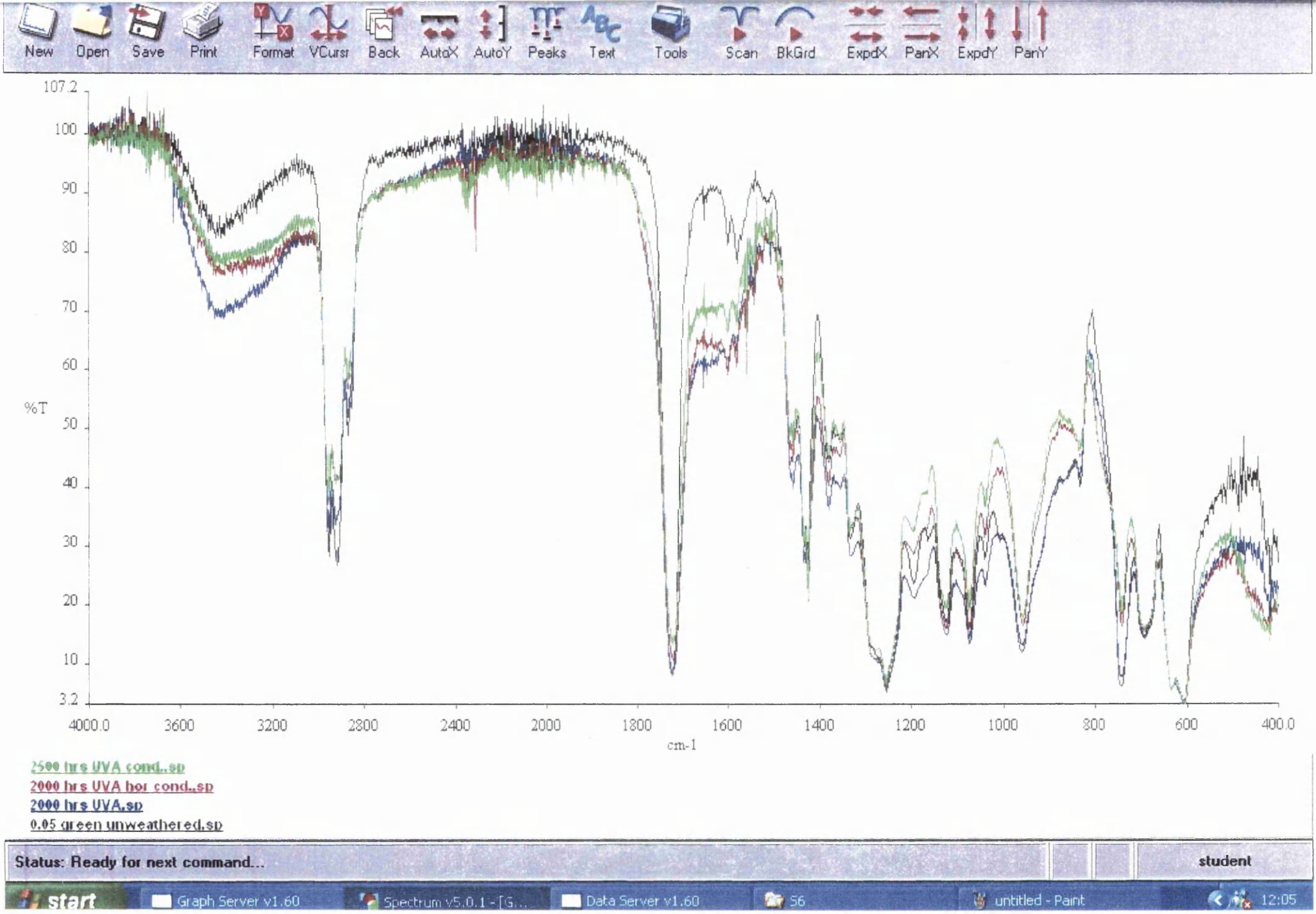
New
Open
Save
Print
Format
VCursr
Back
AutoX
AutoY
Peaks
Text
Tools
Scan
BkGrd
ExpdX
PanX
ExpdY
PanY
107.2
100
90
80
70
60
%T
50
40
30
20
10
3.2
4000.0
3600
3200
2800
2400
2000
1800
1600
1400
1200
1000
800
600
400.0
cm-1
2500 hrs UVA cond..sp
2000 hrs UVA hor cond..sp
2000 hrs UVA.sp
0.05 green unweathered.sp
Status: Ready for next command...
student
start
Graph Server v1.60
Spectrum v5.0.1 - [G...
Data Server v1.60
S6
untitled - Paint
12:05

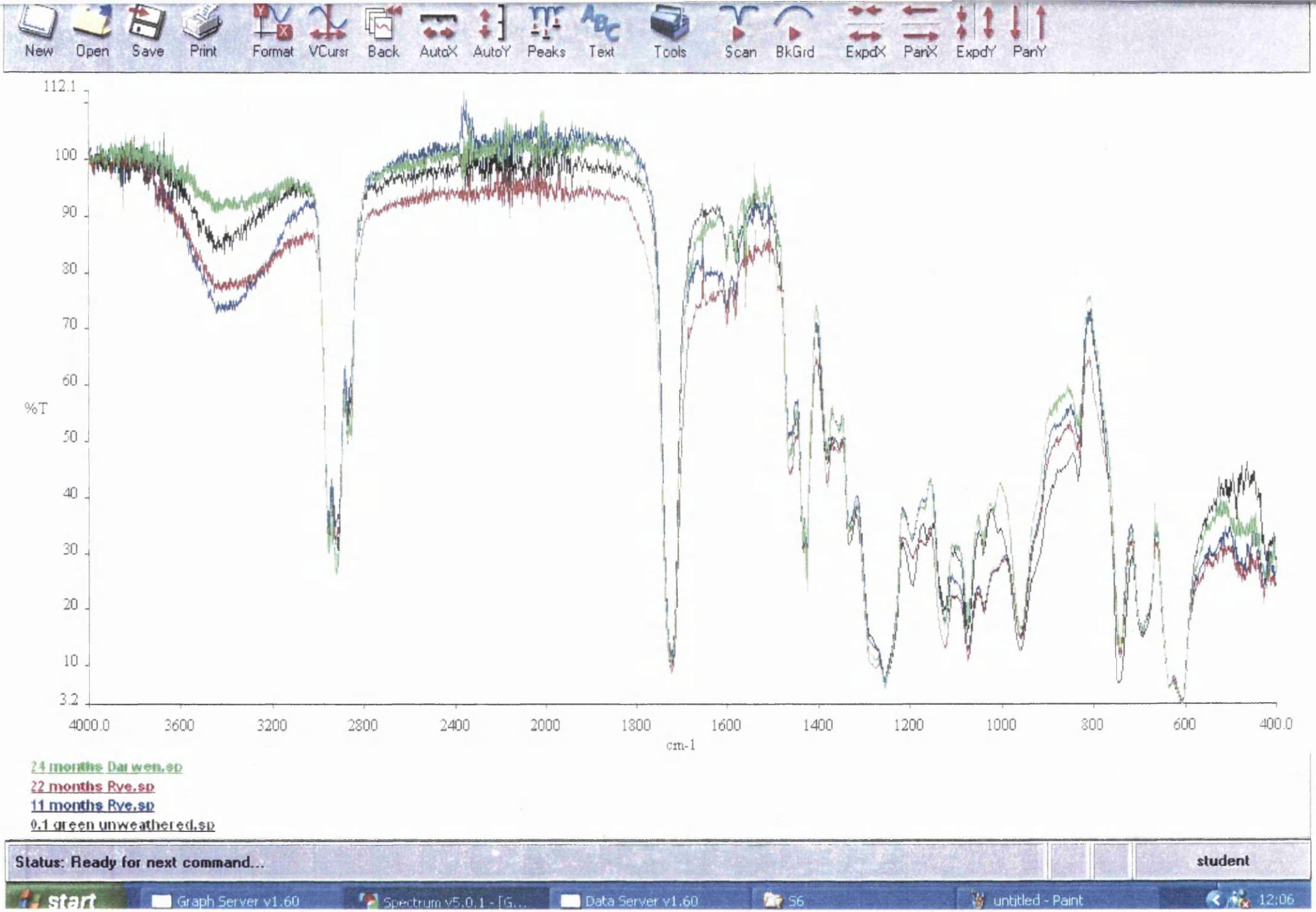
New
Open
Save
Print
Format
VCursr
Back
AutoX
AutoY
Peaks
Text
Tools
Scan
BkGrd
ExpdX
PanX
ExpdY
PanY
112.1
100
90
80
70
60
%T
50
40
30
20
10
3.2
4000.0
3600
3200
2800
2400
2000
1800
1600
1400
1200
1000
800
600
400.0
cm-1
24 months Darwen.sp
22 months Rye.sp
11 months Rye.sp
0.1 green unweathered.sp
Status: Ready for next command...
student
start
Graph Server v1.60
Spectrum v5.0.1 - [G...
Data Server v1.60
S6
untitled - Paint
12:06


New
Open
Save
Print
Format
VCursr
Back
AutoX
AutoY
Peaks
Text
Tools
Scan
BkGrd
ExpdX
PanX
ExpdY
PanY
105.6
100
90
80
70
60
%T
50
40
30
20
10
3.2
4000.0
3600
3200
2800
2400
2000
1800
1600
1400
1200
1000
800
600
400.0
cm-1
2500 hrs UVA cond..sp
2000 hrs UVA hor cond..sp
2000 hrs UVA.sp
0.1 green unweathered.sp
Status: Ready for next command...
student
start
Graph Server v1.60
Spectrum v5.0.1 - [G...
Data Server v1.60
S6
untitled - Paint
12:07

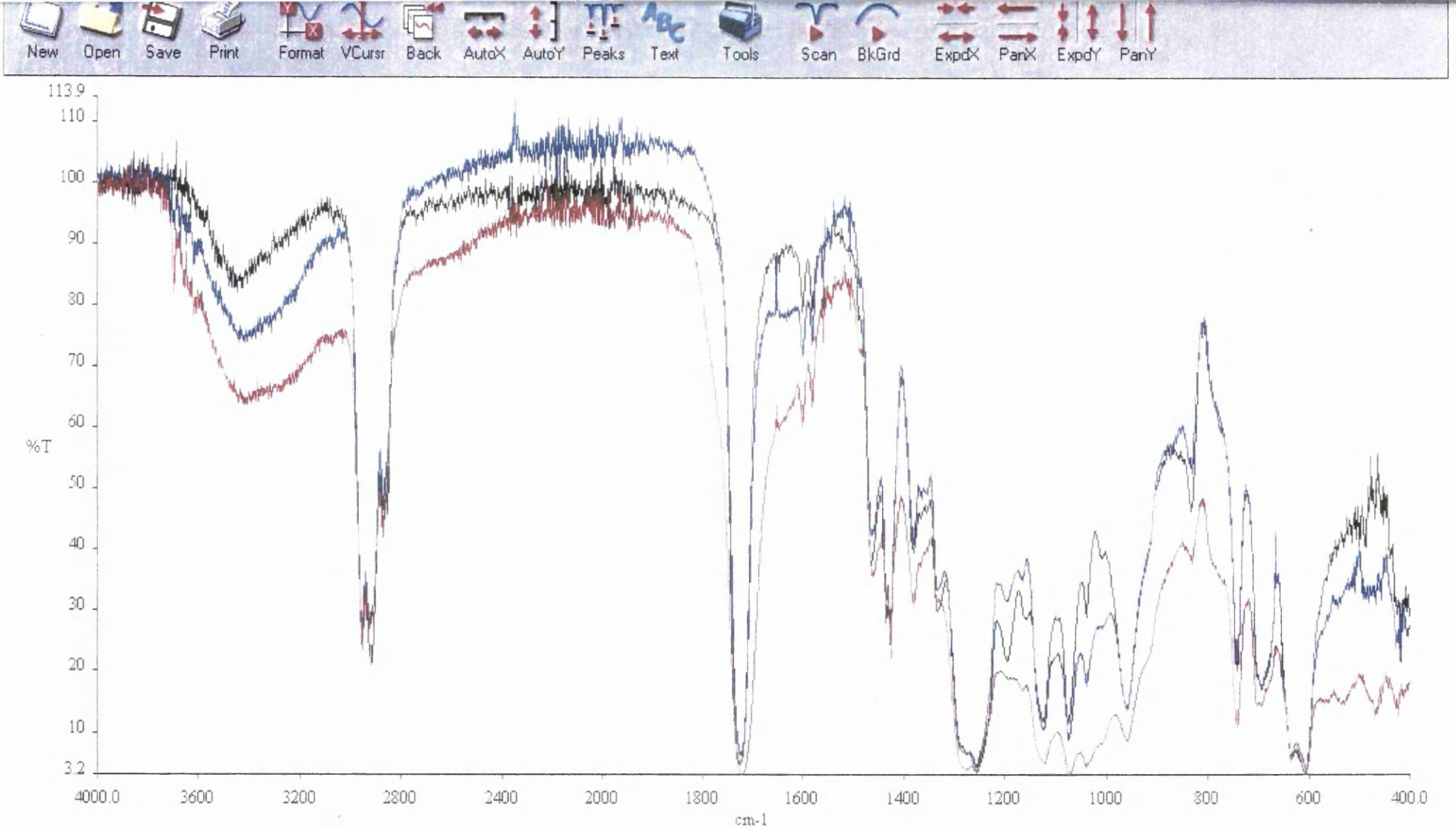
New
Open
Save
Print
Format
VCursr
Back
AutoX
AutoY
Peaks
Text
Tools
Scan
BkGrd
ExpdX
PanX
ExpdY
PanY
113.9
110
100
90
80
70
60
%T
50
40
30
20
10
3.2
4000.0
3600
3200
2800
2400
2000
1800
1600
1400
1200
1000
800
600
400.0
cm-1
22 months Rye.sp
11 months Rye.sp
0.25 svellow 0.05 green unweather...
Status: Ready for next command...
student
start
Graph Server v1.60
Spectrum v5.0.1 - [G...
Data Server v1.60
Y5
untitled - Paint
10:57

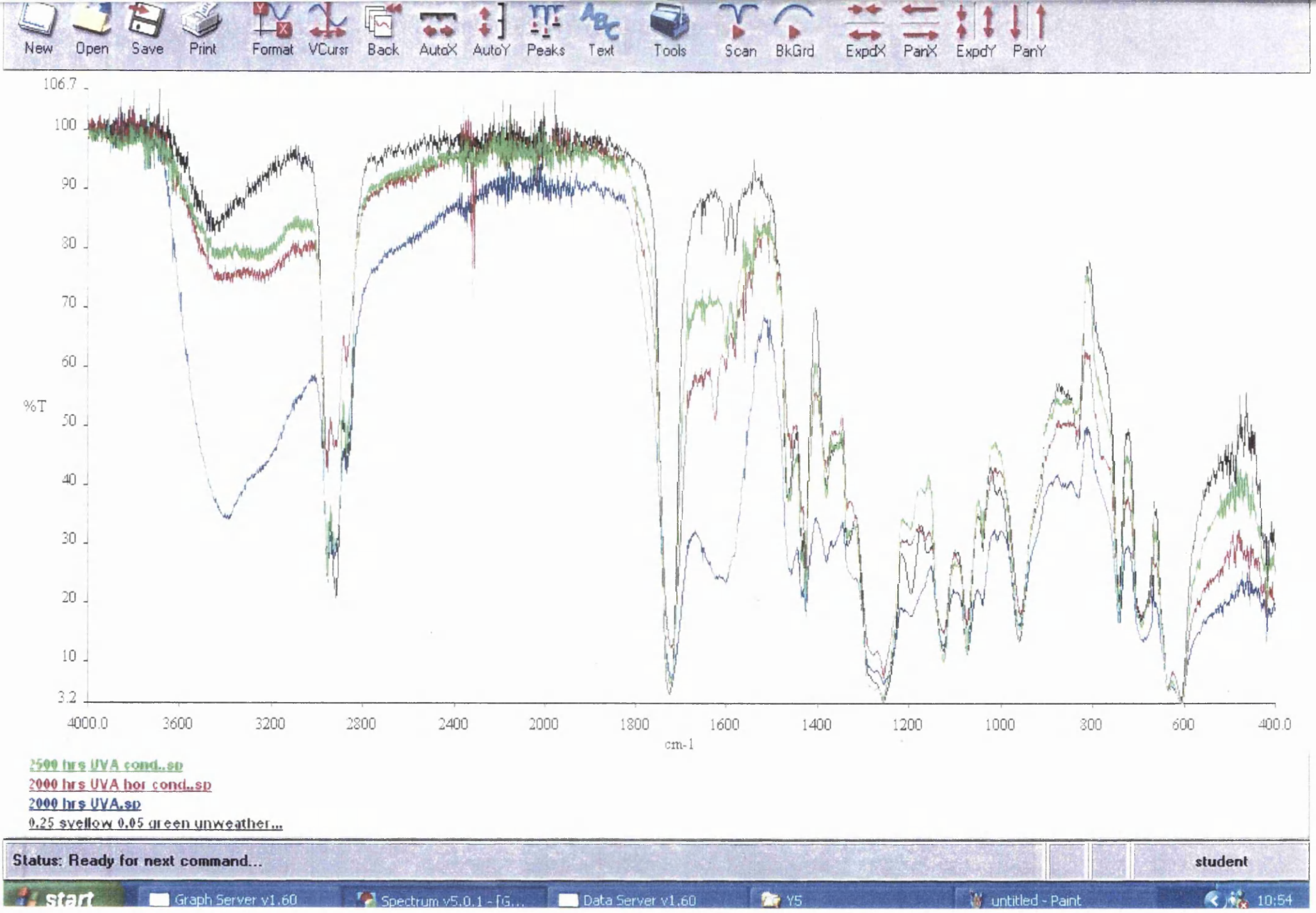
New
Open
Save
Print
Format
VCursr
Back
AutoX
AutoY
Peaks
Text
Tools
Scan
BkGrd
ExpdX
PanX
ExpdY
PanY
106.7
100
90
80
70
60
%T
50
40
30
20
10
3.2
4000.0
3600
3200
2800
2400
2000
1800
1600
1400
1200
1000
800
600
400.0
cm-1
2500 hrs UVA cond..sp
2000 hrs UVA hor cond..sp
2000 hrs UVA.sp
0.25 svellow 0.05 green unweather...
Status: Ready for next command...
student
start
Graph Server v1.60
Spectrum v5.0.1 - [G...
Data Server v1.60
Y5
untitled - Paint
10:54

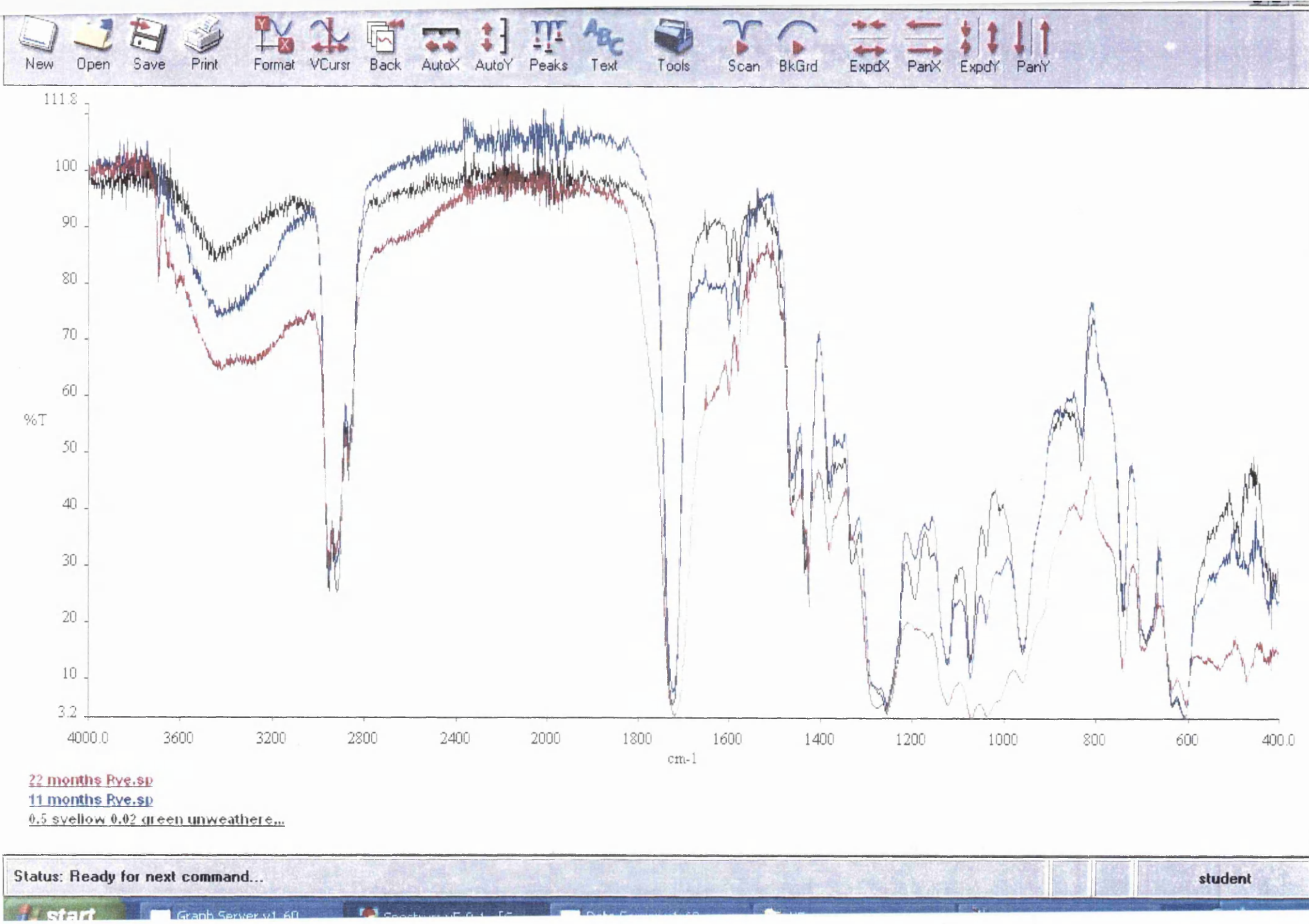
New
Open
Save
Print
Format
VCursr
Back
AutoX
AutoY
Peaks
Text
Tools
Scan
BkGrd
ExpdX
PanX
ExpdY
PanY
111.8
100
90
80
70
60
%T
50
40
30
20
10
3.2
4000.0
3600
3200
2800
2400
2000
1800
1600
1400
1200
1000
800
600
400.0
cm-1
22 months Rye.sp
11 months Rye.sp
0.5 syellow 0.02 green unweathere...
Status: Ready for next command...
student

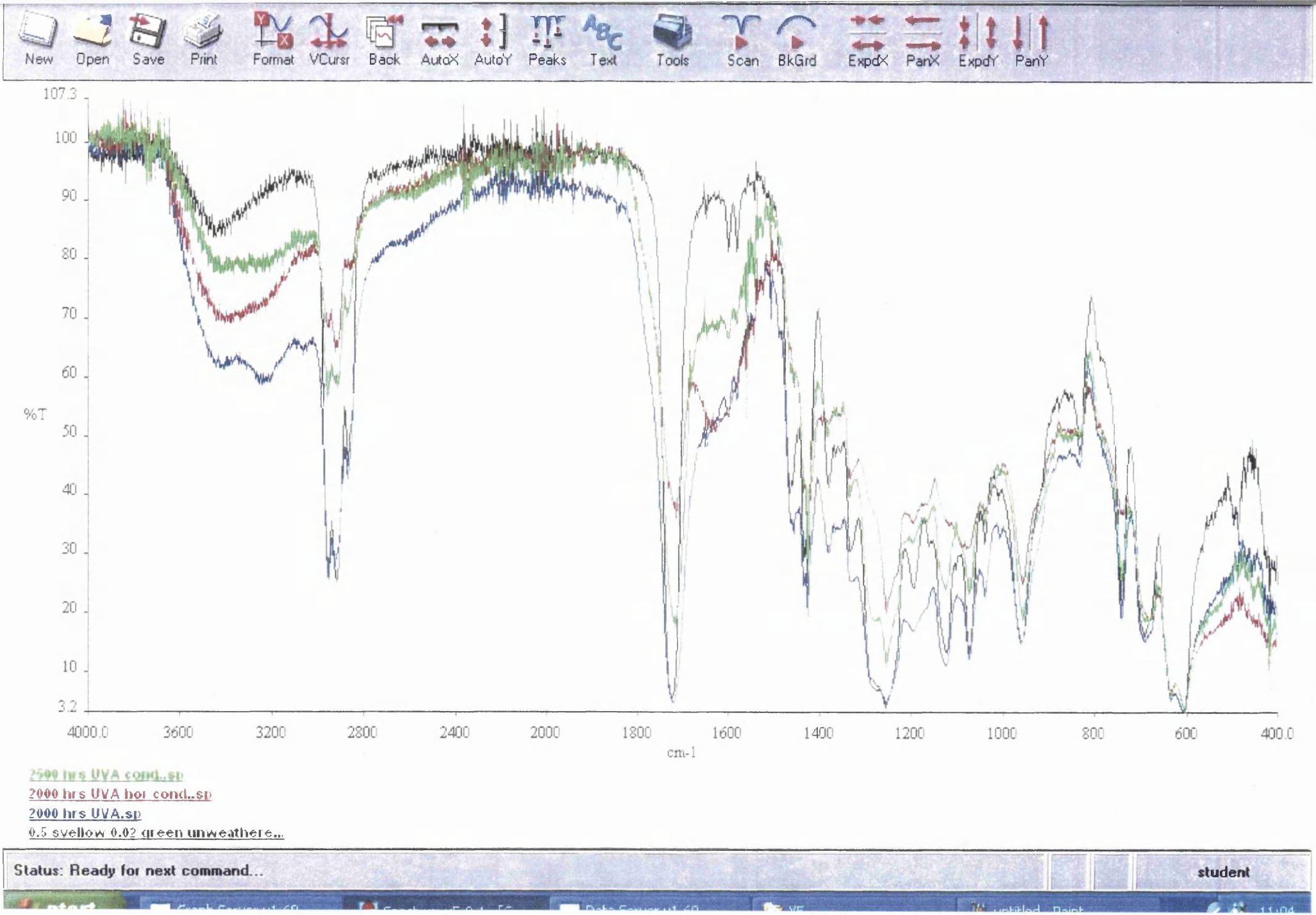
New
Open
Save
Print
Format
VCursr
Back
AutoX
AutoY
Peaks
Text
Tools
Scan
BkGrd
ExpdX
PanX
ExpdY
PanY
107.3
100
90
80
70
60
%T
50
40
30
20
10
3.2
4000.0
3600
3200
2800
2400
2000
1800
1600
1400
1200
1000
800
600
400.0
cm-1
2500 hrs UVA cond..sp
2000 hrs UVA hor cond..sp
2000 hrs UVA.sp
0.5 svellow 0.02 green unweathere...
Status: Ready for next command...
student

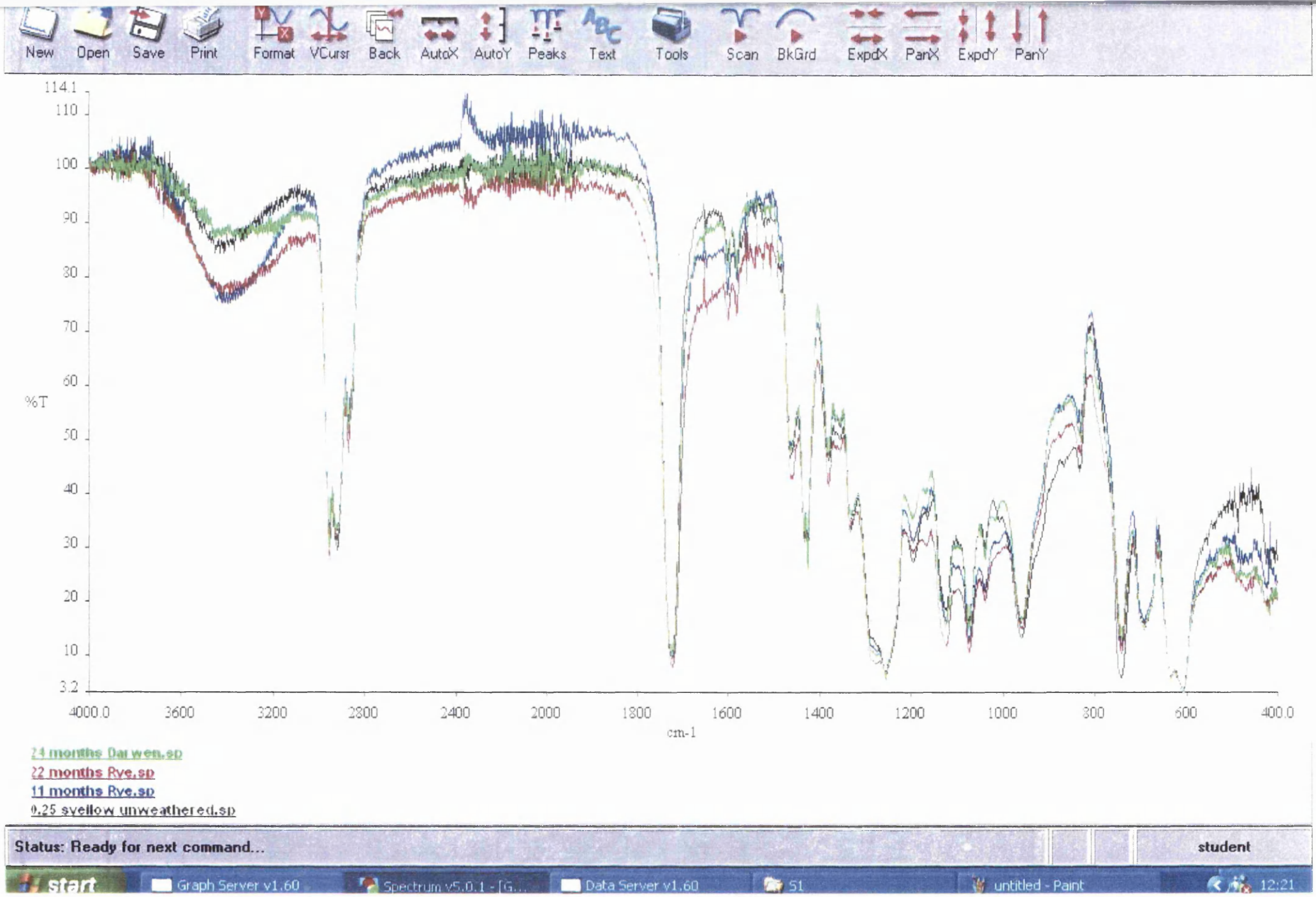
New
Open
Save
Print
Format
VCursr
Back
AutoX
AutoY
Peaks
Text
Tools
Scan
BkGrd
ExpdX
PanX
ExpdY
PanY
114.1
110
100
90
80
70
60
%T
50
40
30
20
10
3.2
4000.0
3600
3200
2800
2400
2000
1800
1600
1400
1200
1000
800
600
400.0
cm-1
24 months Darwen.sp
22 months Rye.sp
11 months Rye.sp
0.25 svellow unweathered.sp
Status: Ready for next command...
student
start
Graph Server v1.60
Spectrum v5.0.1 - [G...
Data Server v1.60
51
untitled - Paint
12:21

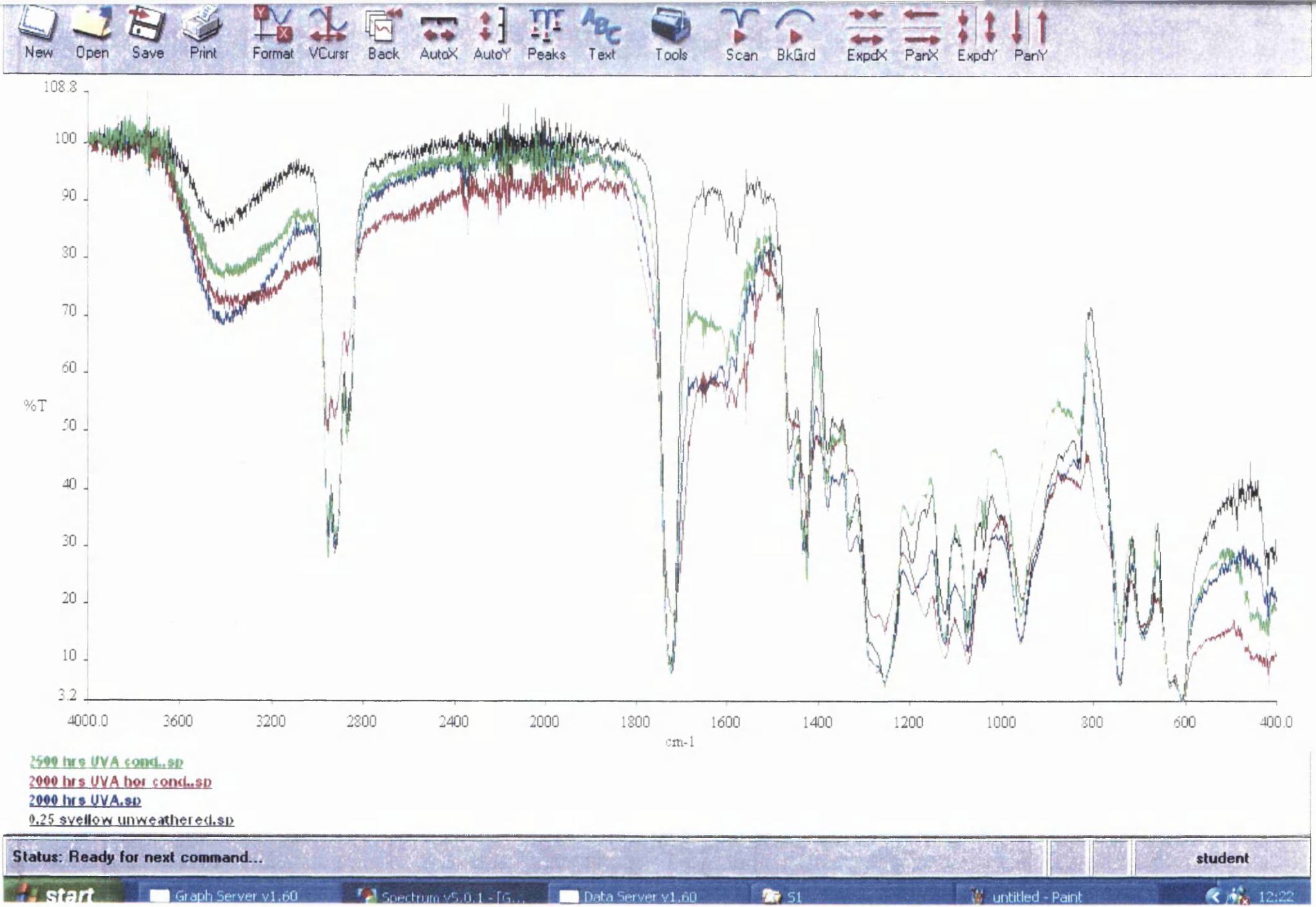
New
Open
Save
Print
Format
VCursr
Back
AutoX
AutoY
Peaks
Text
Tools
Scan
BkGrd
ExpdX
PanX
ExpdY
PanY
108.8
100
90
80
70
60
%T
50
40
30
20
10
3.2
4000.0
3600
3200
2800
2400
2000
1800
1600
1400
1200
1000
800
600
400.0
cm-1
2500 hrs UVA cond..sp
2000 hrs UVA hor cond..sp
2000 hrs UVA.sp
0.25 svellow unweathered.sp
Status: Ready for next command...
student
start
Graph Server v1.60
Spectrum v5.0.1 - [G...
Data Server v1.60
S1
untitled - Paint
12:22

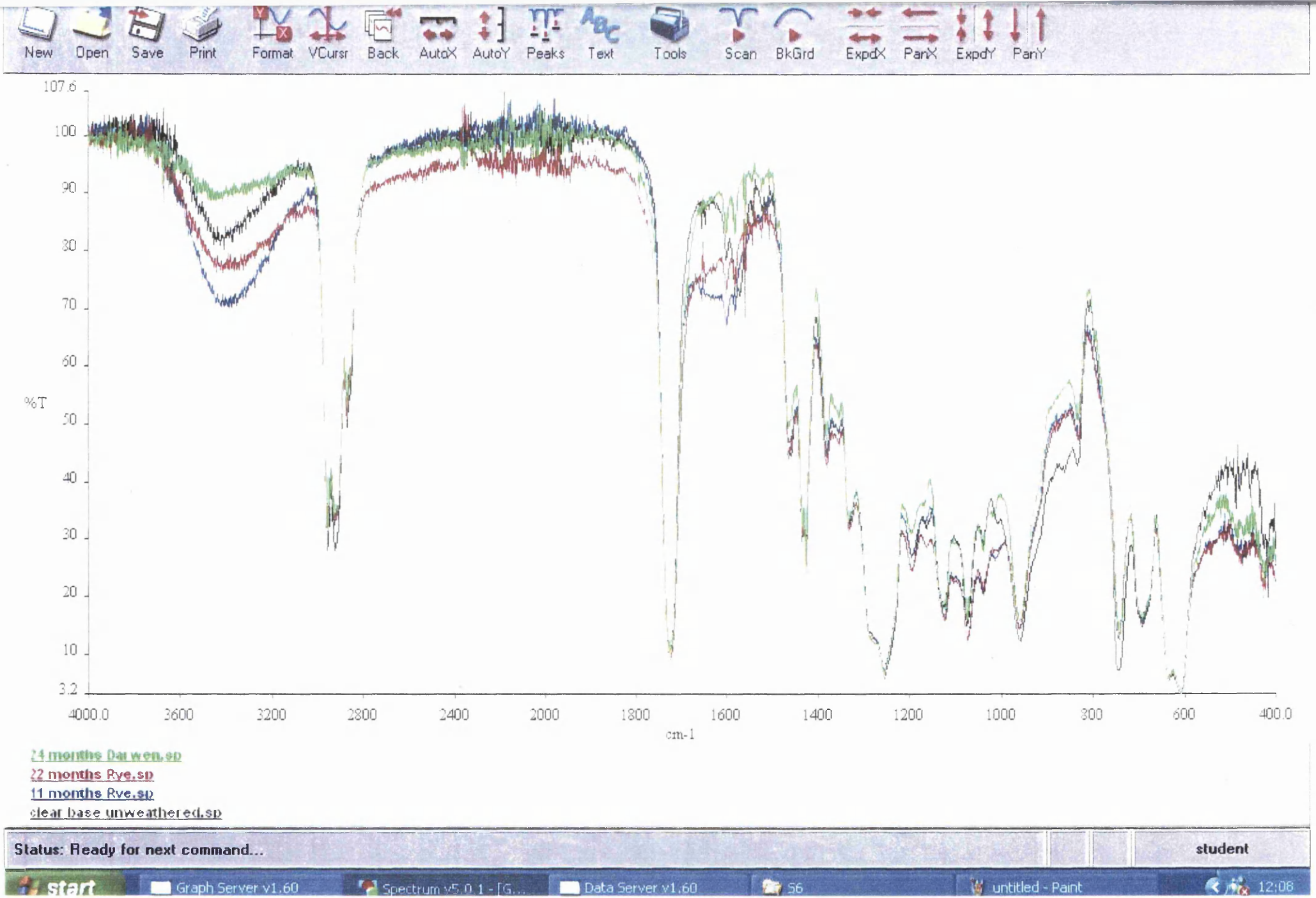
New
Open
Save
Print
Format
VCursr
Back
AutoX
AutoY
Peaks
Text
Tools
Scan
BkGrd
ExpdX
PanX
ExpdY
PanY
107.6
100
90
80
70
60
%T
50
40
30
20
10
3.2
4000.0
3600
3200
2800
2400
2000
1800
1600
1400
1200
1000
800
600
400.0
cm-1
24 months Darwen.sp
22 months Rye.sp
11 months Rye.sp
clear base unweathered.sp
Status: Ready for next command...
student
start
Graph Server v1.60
Spectrum v5.0.1 - [G...
Data Server v1.60
S6
untitled - Paint
12:06

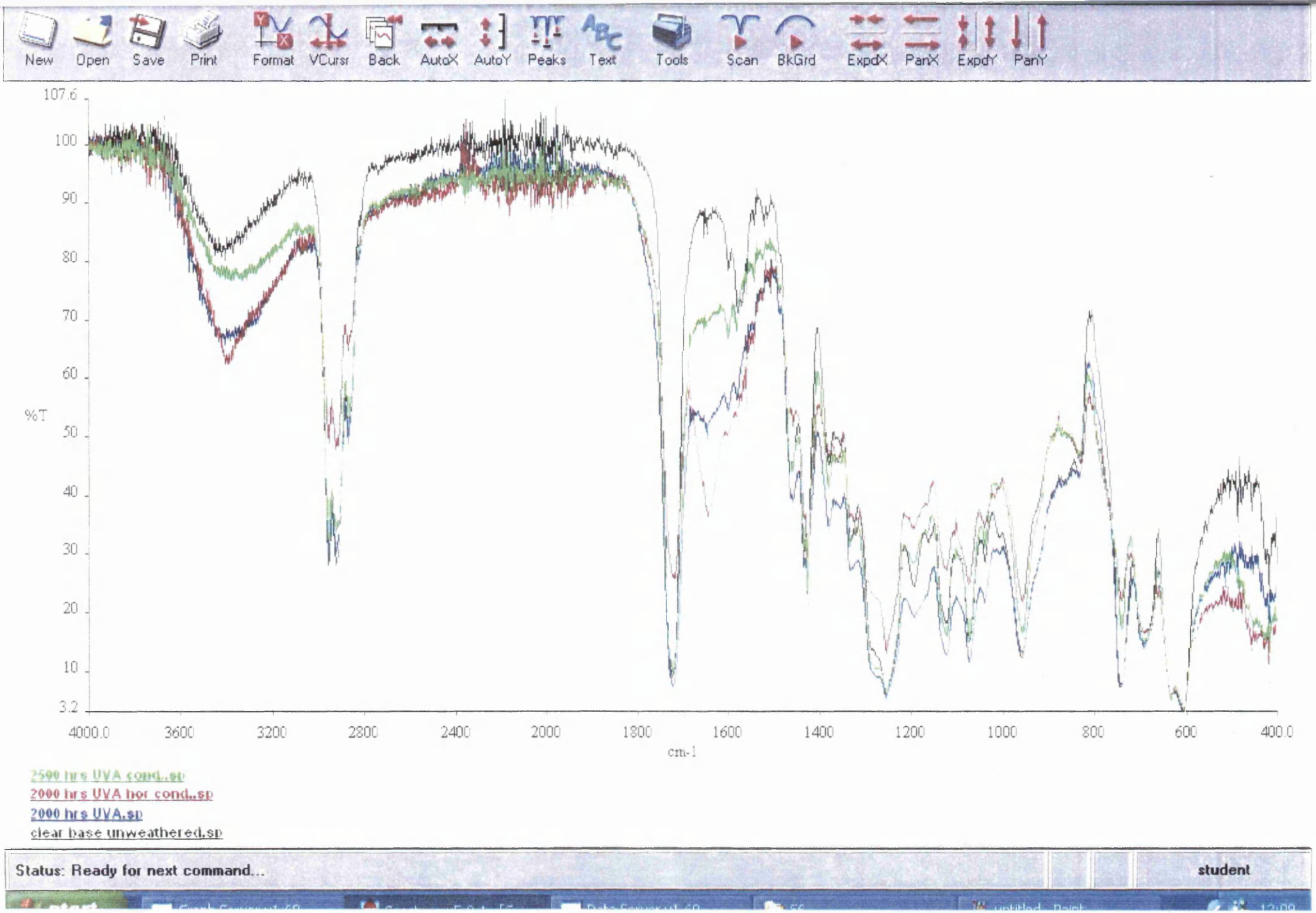
New
Open
Save
Print
Format
VCursr
Back
AutoX
AutoY
Peaks
Text
Tools
Scan
BkGrd
ExpdX
PanX
ExpdY
PanY
107.6
100
90
80
70
60
%T
50
40
30
20
10
3.2
4000.0
3600
3200
2800
2400
2000
1800
1600
1400
1200
1000
800
600
400.0
cm-1
2500 hrs UVA cond..sp
2000 hrs UVA hor cond..sp
2000 hrs UVA.sp
clear base unweathered.sp
Status: Ready for next command...
student

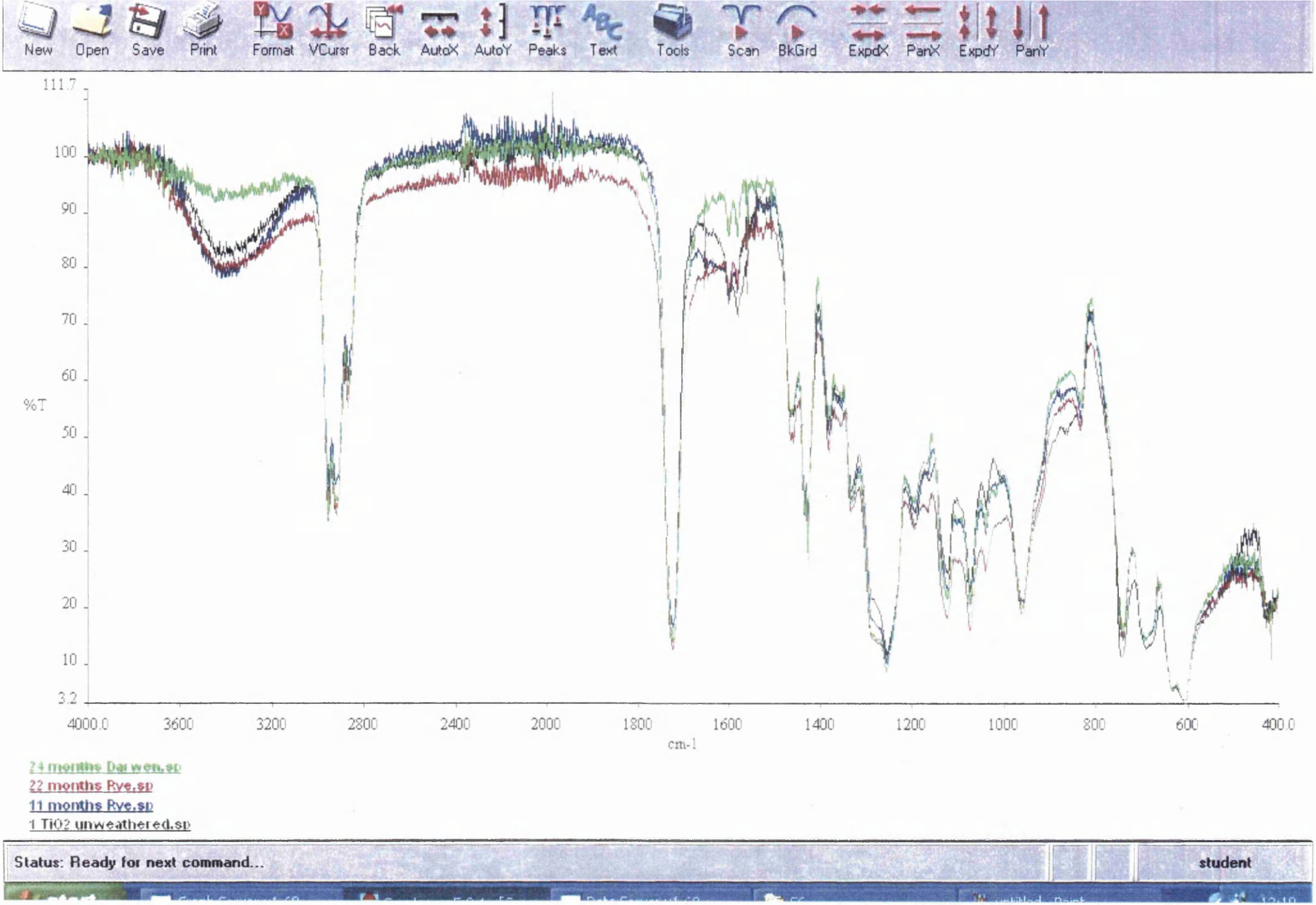
New
Open
Save
Print
Format
VCursr
Back
AutoX
AutoY
Peaks
Text
Tools
Scan
BkGrd
ExpdX
PanX
ExpdY
PanY
111.7
100
90
80
70
60
%T
50
40
30
20
10
3.2
4000.0
3600
3200
2800
2400
2000
1800
1600
1400
1200
1000
800
600
400.0
cm-1
24 months Darwen.sp
22 months Rye.sp
11 months Rye.sp
1 TiO2 unweathered.sp
Status: Ready for next command...
student

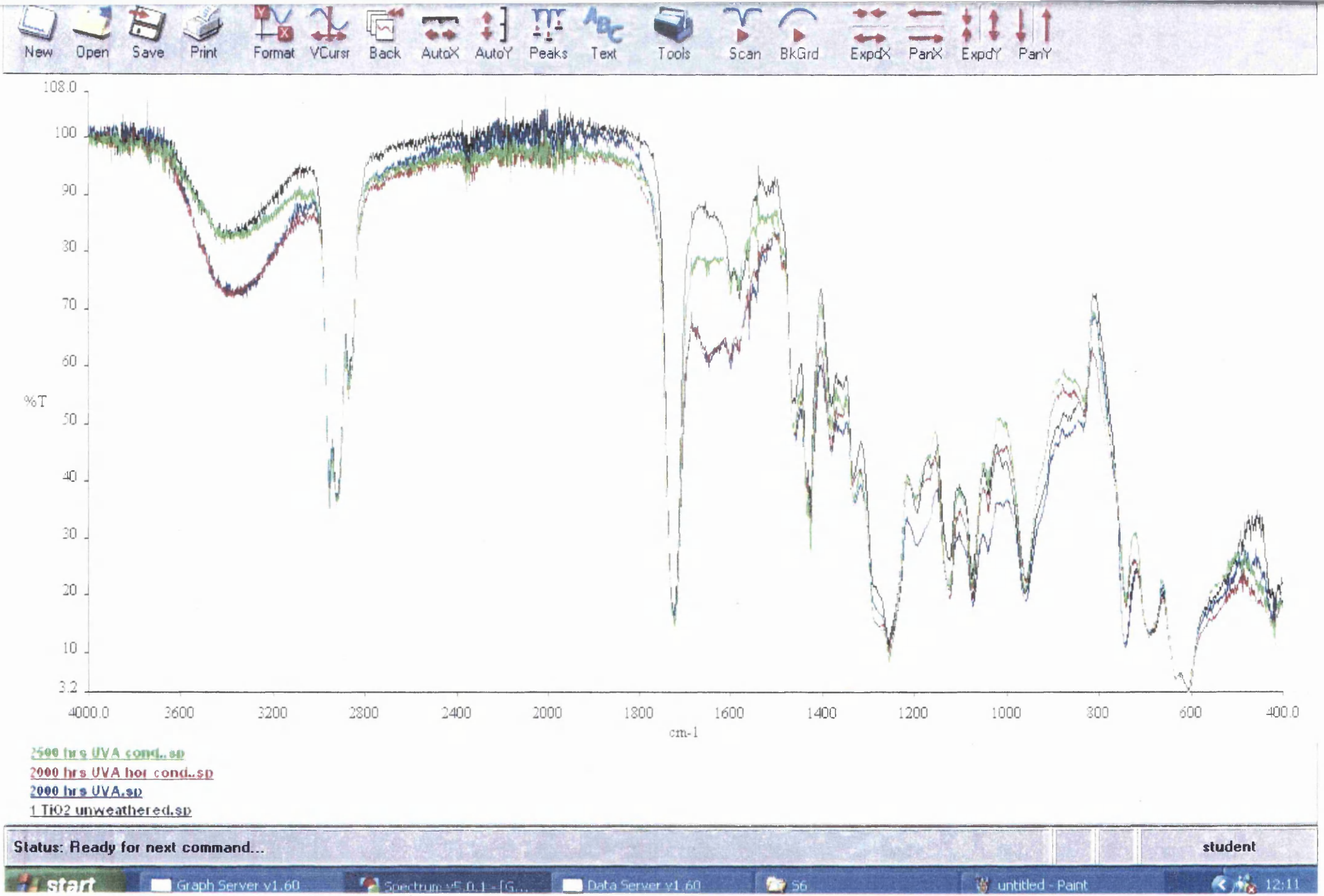
New
Open
Save
Print
Format
VCursr
Back
AutoX
AutoY
Peaks
Text
Tools
Scan
BkGrd
ExpdX
PanX
ExpdY
PanY
108.0
100
90
30
70
60
%T
50
40
30
20
10
3.2
4000.0
3600
3200
2800
2400
2000
1800
1600
1400
1200
1000
800
600
400.0
cm-1
2500 hrs UVA cond..sp
2000 hrs UVA hot cond..sp
2000 hrs UVA.sp
1 TiO2 unweathered.sp
Status: Ready for next command...
student
start
Graph Server v1.60
Spectrum-v5.0.1-[G...
Data Server v1.60
S6
untitled - Paint
12:11

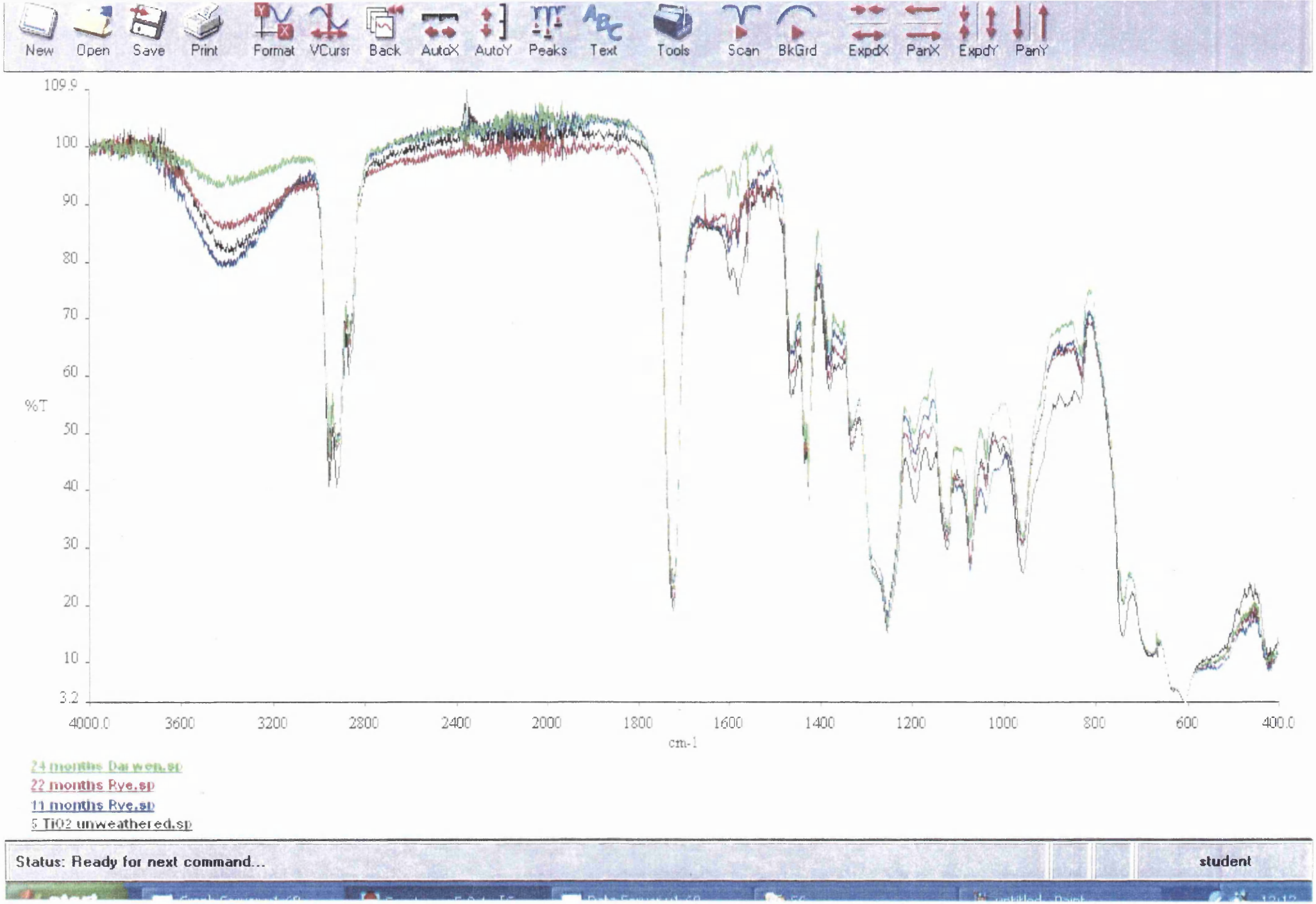
New
Open
Save
Print
Format
VCursr
Back
AutoX
AutoY
Peaks
Text
Tools
Scan
BkGrd
ExpdX
PanX
ExpdY
PanY
109.9
100
90
80
70
60
%T
50
40
30
20
10
3.2
4000.0
3600
3200
2800
2400
2000
1800
1600
1400
1200
1000
800
600
400.0
cm-1
24 months Darwen.sp
22 months Rye.sp
11 months Rye.sp
5 TiO2 unweathered.sp
Status: Ready for next command...
student

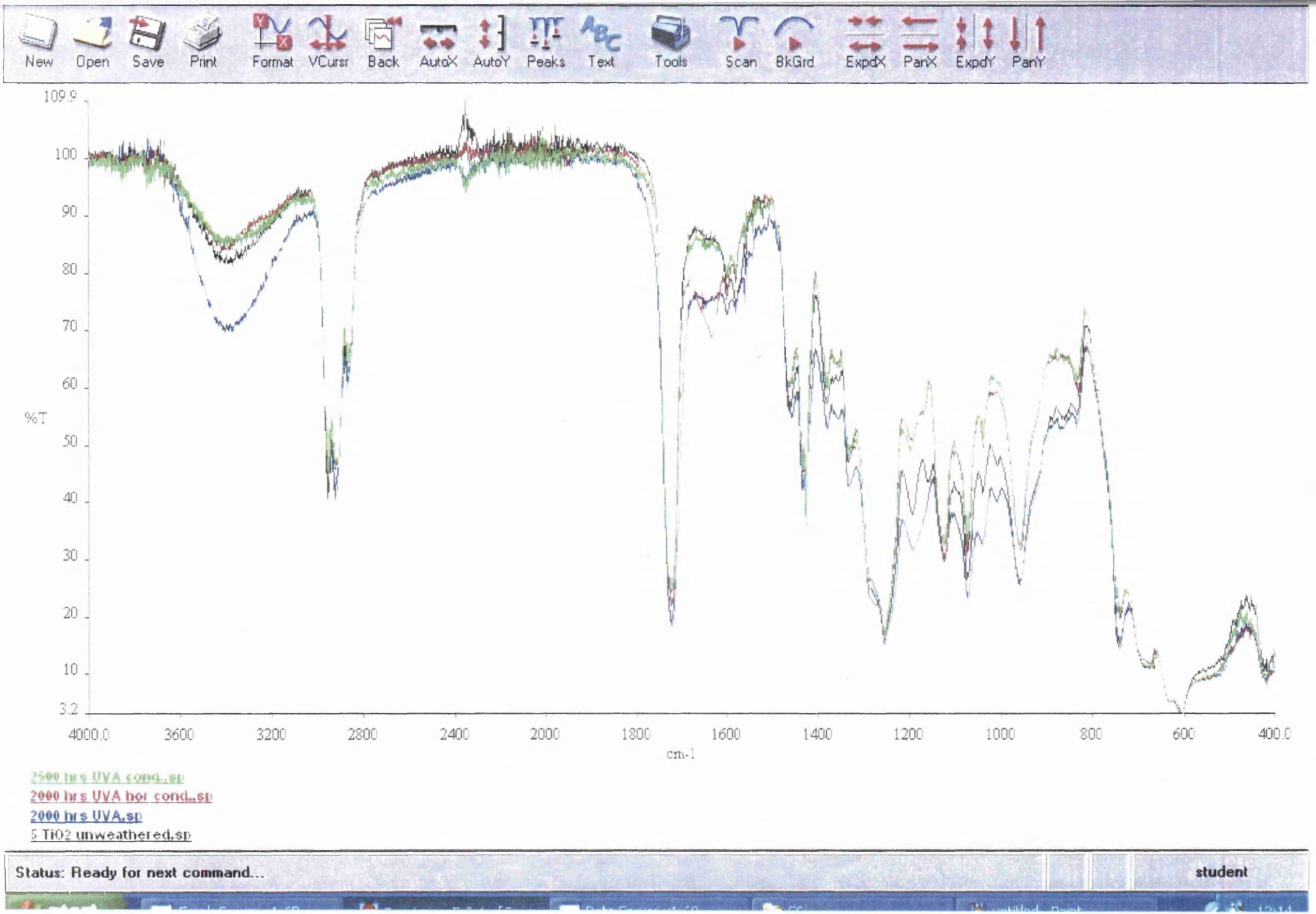
New
Open
Save
Print
Format
VCursr
Back
AutoX
AutoY
Peaks
Text
Tools
Scan
BkGrd
ExpdX
PanX
ExpdY
PanY
109.9
100
90
80
70
60
%T
50
40
30
20
10
3.2
4000.0
3600
3200
2800
2400
2000
1800
1600
1400
1200
1000
800
600
400.0
cm-1
2500 hrs UVA cond..sp
2000 hrs UVA hor cond..sp
2000 hrs UVA.sp
5 TiO2 unweathered.sp
Status: Ready for next command...
student

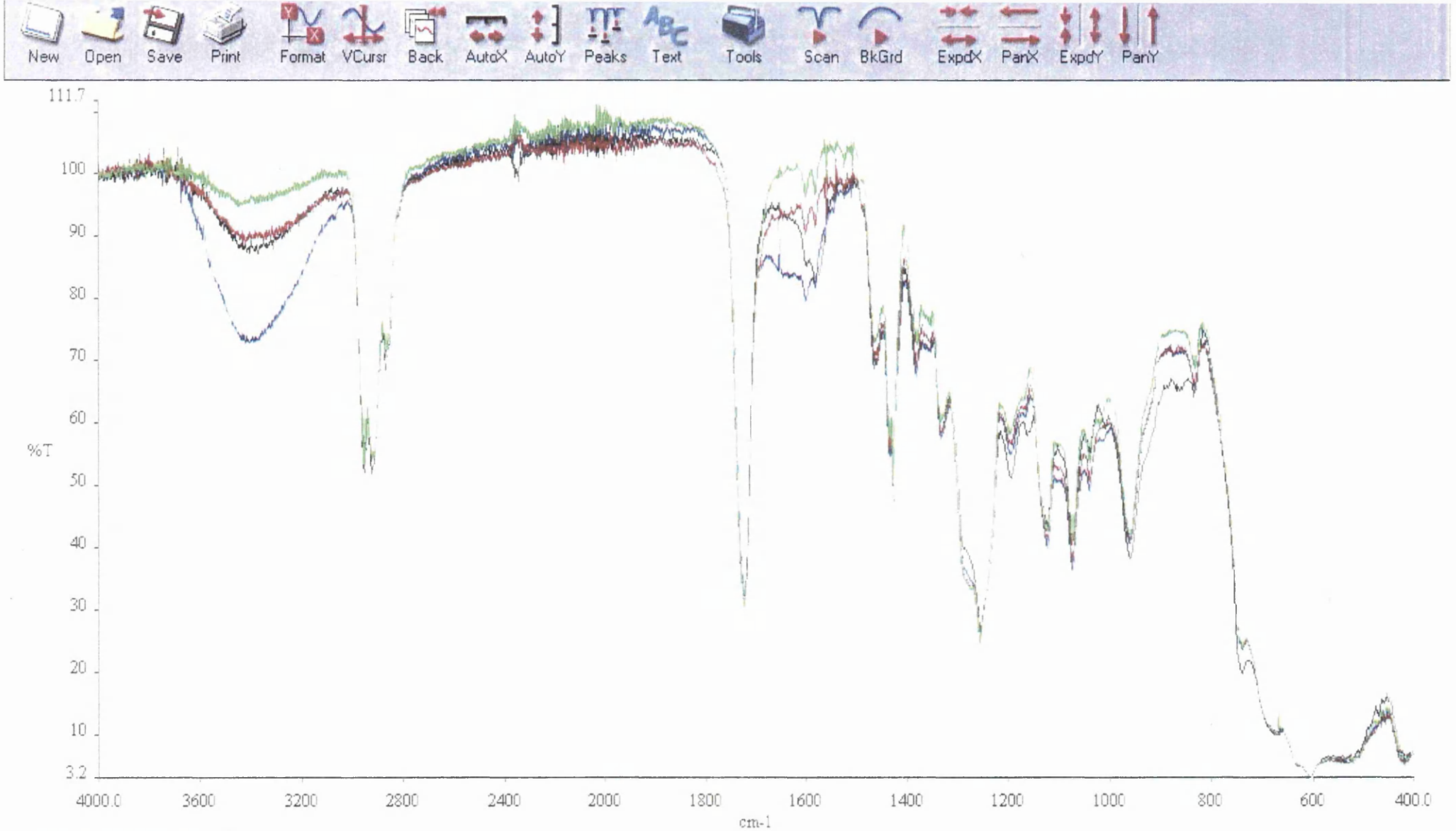

Status: Ready for next command...

student

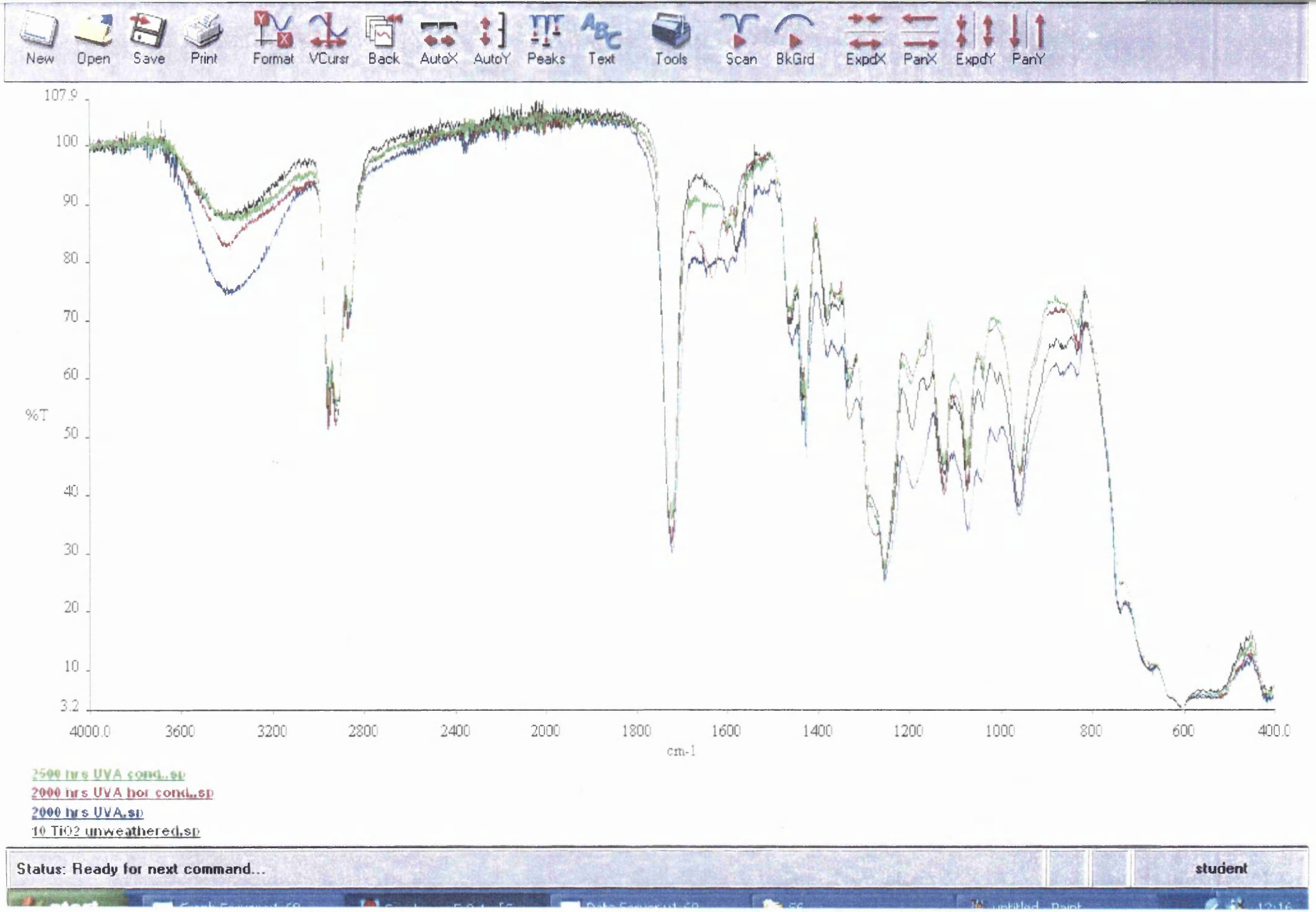
New
Open
Save
Print
Format
VCursr
Back
AutoX
AutoY
Peaks
Text
Tools
Scan
BkGrd
ExpdX
PanX
ExpdY
PanY
107.9
100
90
80
70
60
%T
50
40
30
20
10
3.2
4000.0
3600
3200
2800
2400
2000
1800
1600
1400
1200
1000
800
600
400.0
cm-1
2500 hrs UVA cond..sp
2000 hrs UVA hor cond..sp
2000 hrs UVA.sp
10 TiO2 unweathered.sp
Status: Ready for next command...
student

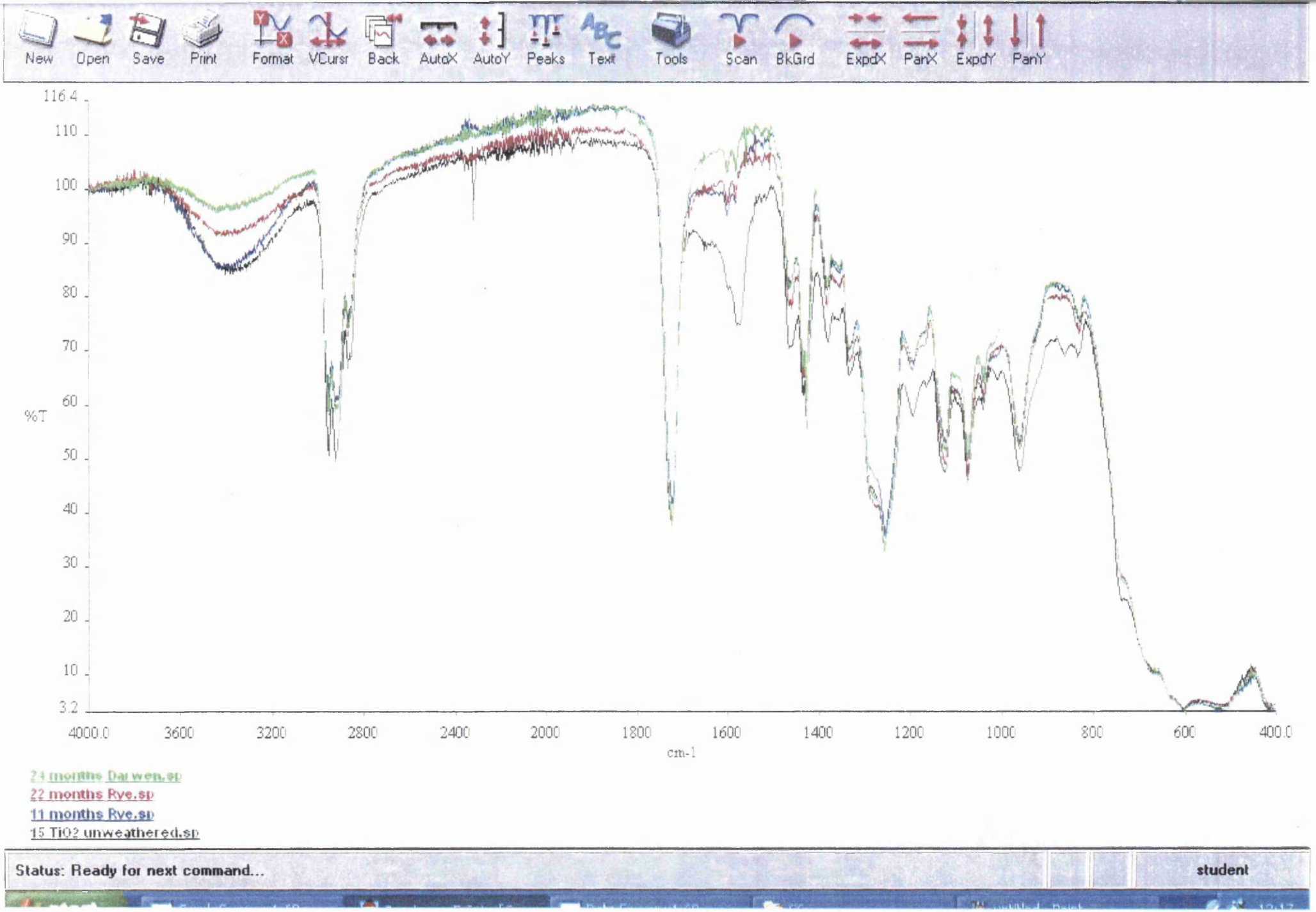
New
Open
Save
Print
Format
VCursr
Back
AutoX
AutoY
Peaks
Text
Tools
Scan
BkGrd
ExpdX
PanX
ExpdY
PanY
116.4
110
100
90
80
70
60
50
40
30
20
10
3.2
%T
4000.0
3600
3200
2800
2400
2000
1800
1600
1400
1200
1000
800
600
400.0
cm-1
24 months Darwen.sp
22 months Rye.sp
11 months Rye.sp
15 TiO2 unweathered.sp
Status: Ready for next command...
student


New
Open
Save
Print
Format
VCursr
Back
AutoX
AutoY
Peaks
Text
Tools
Scan
BkGrd
ExpdX
PanX
ExpdY
PanY
111.7
100
90
80
70
60
%T
50
40
30
20
10
3.2
4000.0
3600
3200
2800
2400
2000
1800
1600
1400
1200
1000
800
600
400.0
cm-1
2500 hrs UVA cond..sp
2000 hrs UVA hor cond..sp
2000 hrs UVA.sp
15 TiO2 unweathered.sp
Status: Ready for next command...
student

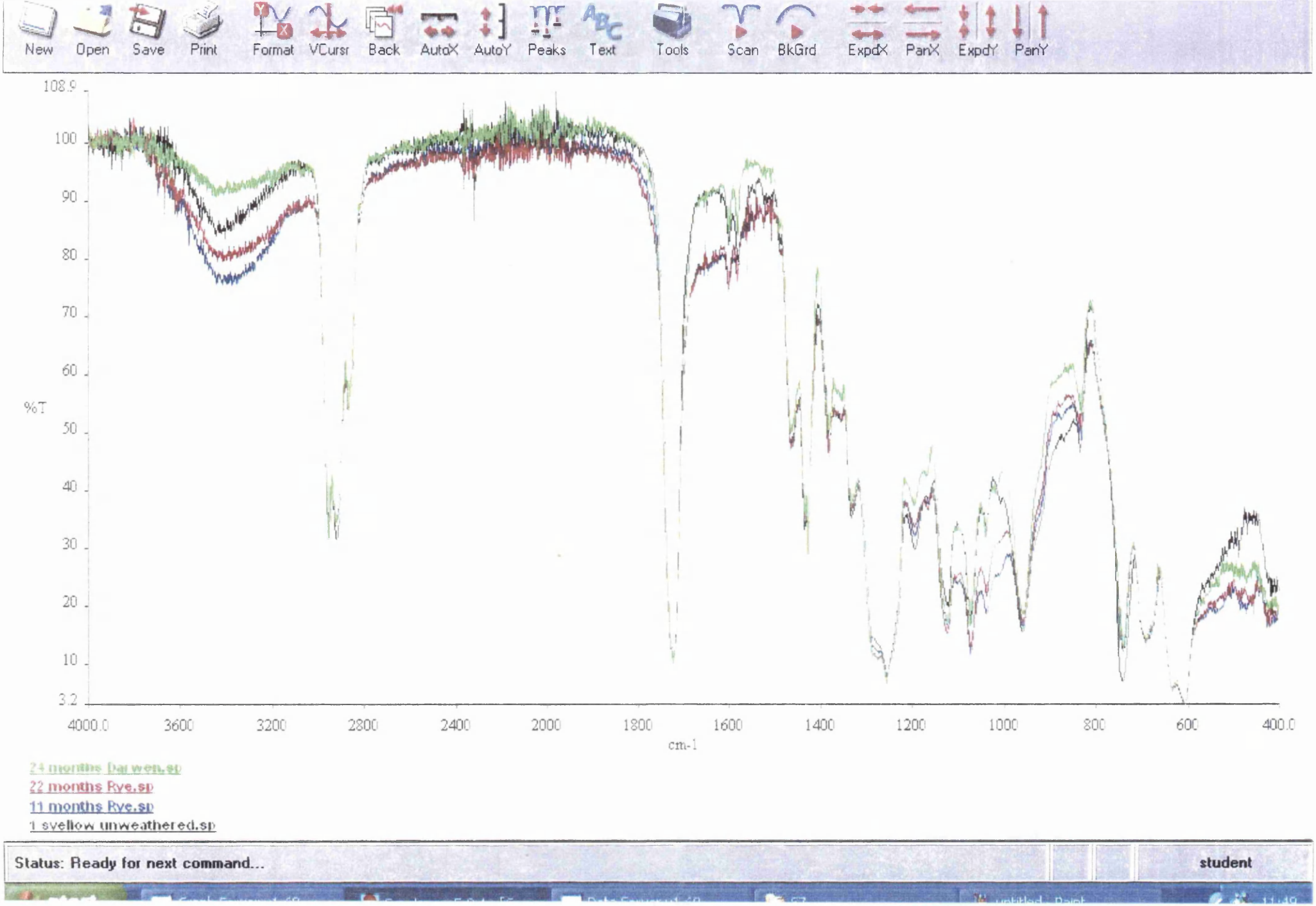
New
Open
Save
Print
Format
VCursr
Back
AutoX
AutoY
Peaks
Text
Tools
Scan
BkGrd
ExpdX
PanX
ExpdY
PanY
108.9
100
90
80
70
60
%T
50
40
30
20
10
3.2
4000.0
3600
3200
2800
2400
2000
1800
1600
1400
1200
1000
800
600
400.0
cm-1
24 months Darwen.sp
22 months Rye.sp
11 months Rye.sp
1 svellow unweathered.sp
Status: Ready for next command...
student

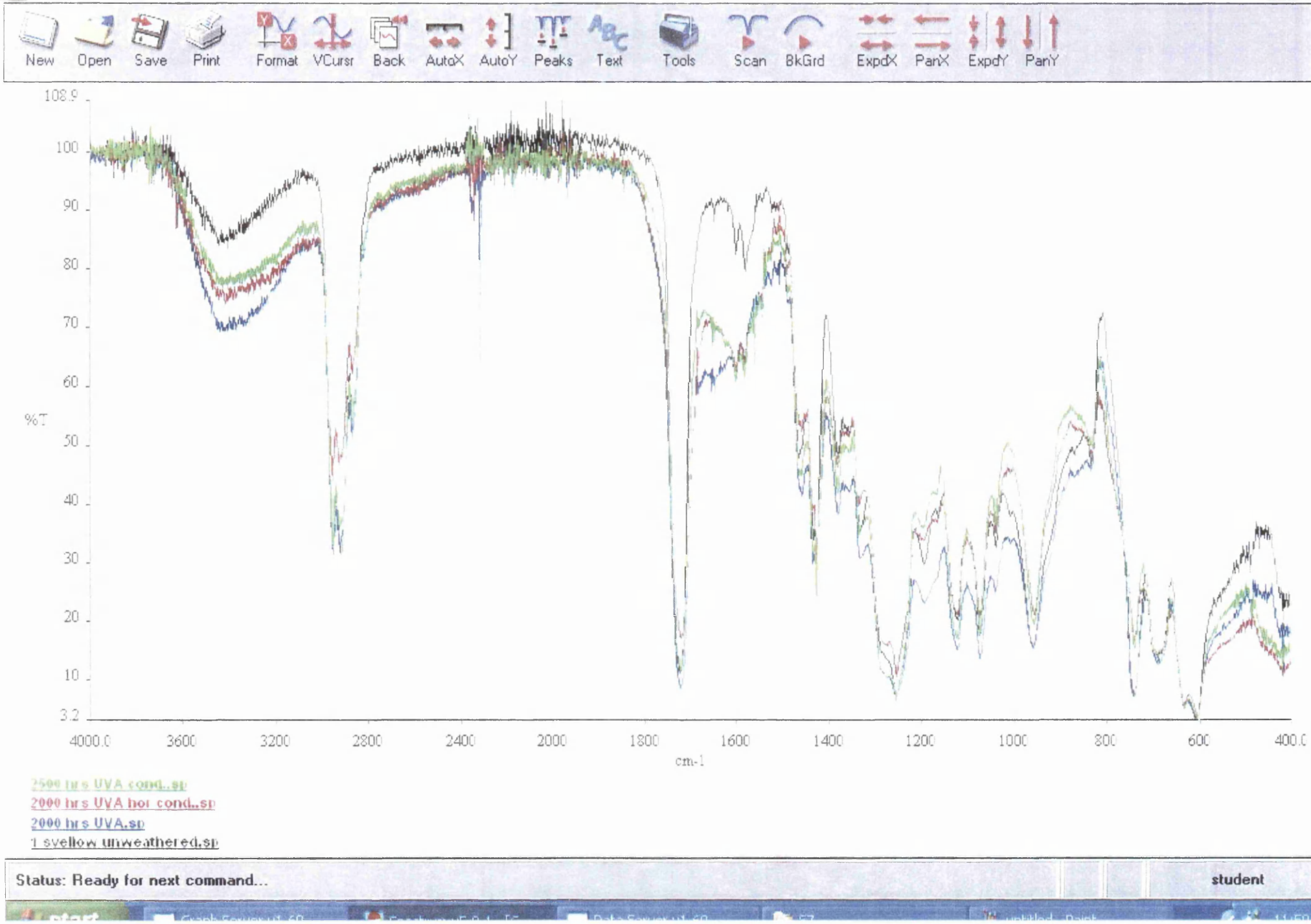
New
Open
Save
Print
Format
VCursr
Back
AutoX
AutoY
Peaks
Text
Tools
Scan
BkGrd
ExpdX
PanX
ExpdY
PanY
108.9
100
90
80
70
60
%T
50
40
30
20
10
3.2
4000.0
3600
3200
2800
2400
2000
1800
1600
1400
1200
1000
800
600
400.0
cm-1
2500 hrs UVA cond..sp
2000 hrs UVA hot cond..sp
2000 hrs UVA.sp
1 svellow unweathered.sp
Status: Ready for next command...
student

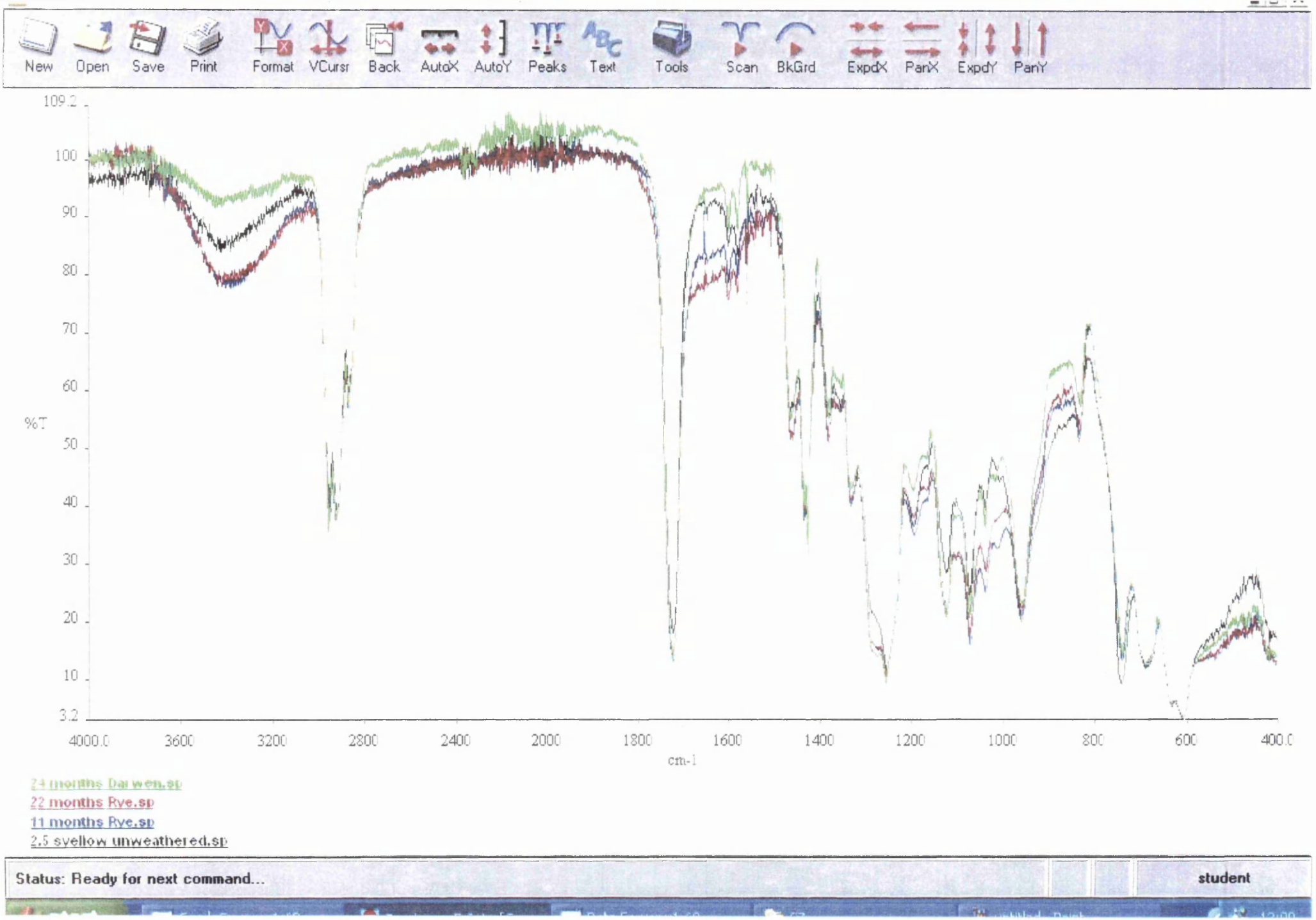
New
Open
Save
Print
Format
VCursr
Back
AutoX
AutoY
Peaks
Text
Tools
Scan
BkGrd
ExpdX
PanX
ExpdY
PanY
109.2
100
90
80
70
60
%T
50
40
30
20
10
3.2
4000.0
3600
3200
2800
2400
2000
1800
1600
1400
1200
1000
800
600
400.0
cm-1
24 months Darwen.sp
22 months Rye.sp
11 months Rye.sp
2.5 syellow unweathered.sp
Status: Ready for next command...
student

File Edit View Process Instrument Setup Procedures Window Help

New Open Save Print Format VCursr Back AutoX AutoY Peaks Text Tools Scan BkGrd ExpdX ParX ExpdY ParY

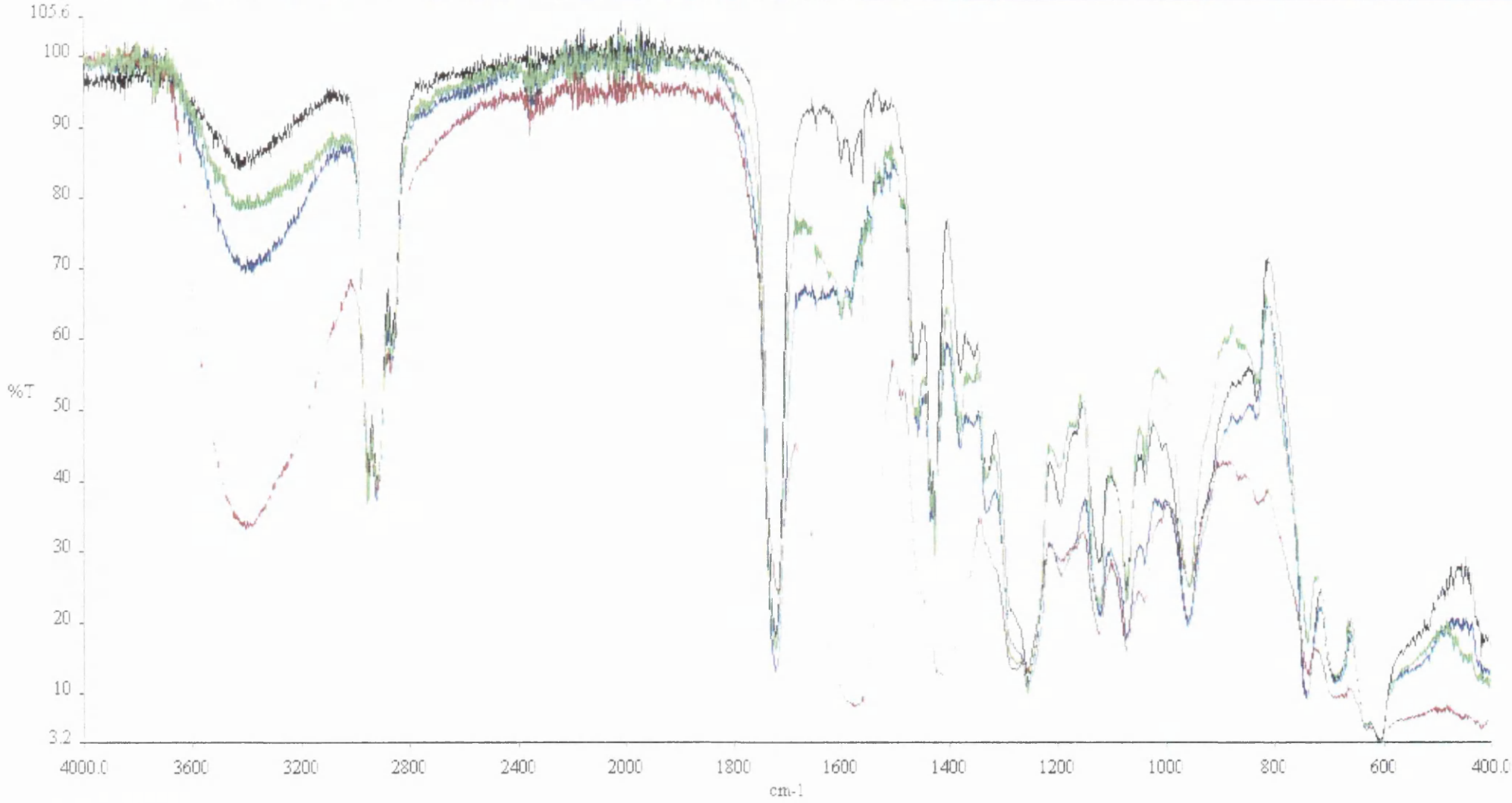

2500 hrs UVA cond..sp
2000 hrs UVA hor cond..sp
2000 hrs UVA.sp
2.5 svellow unweathered.sp

Status: Ready for next command...

student

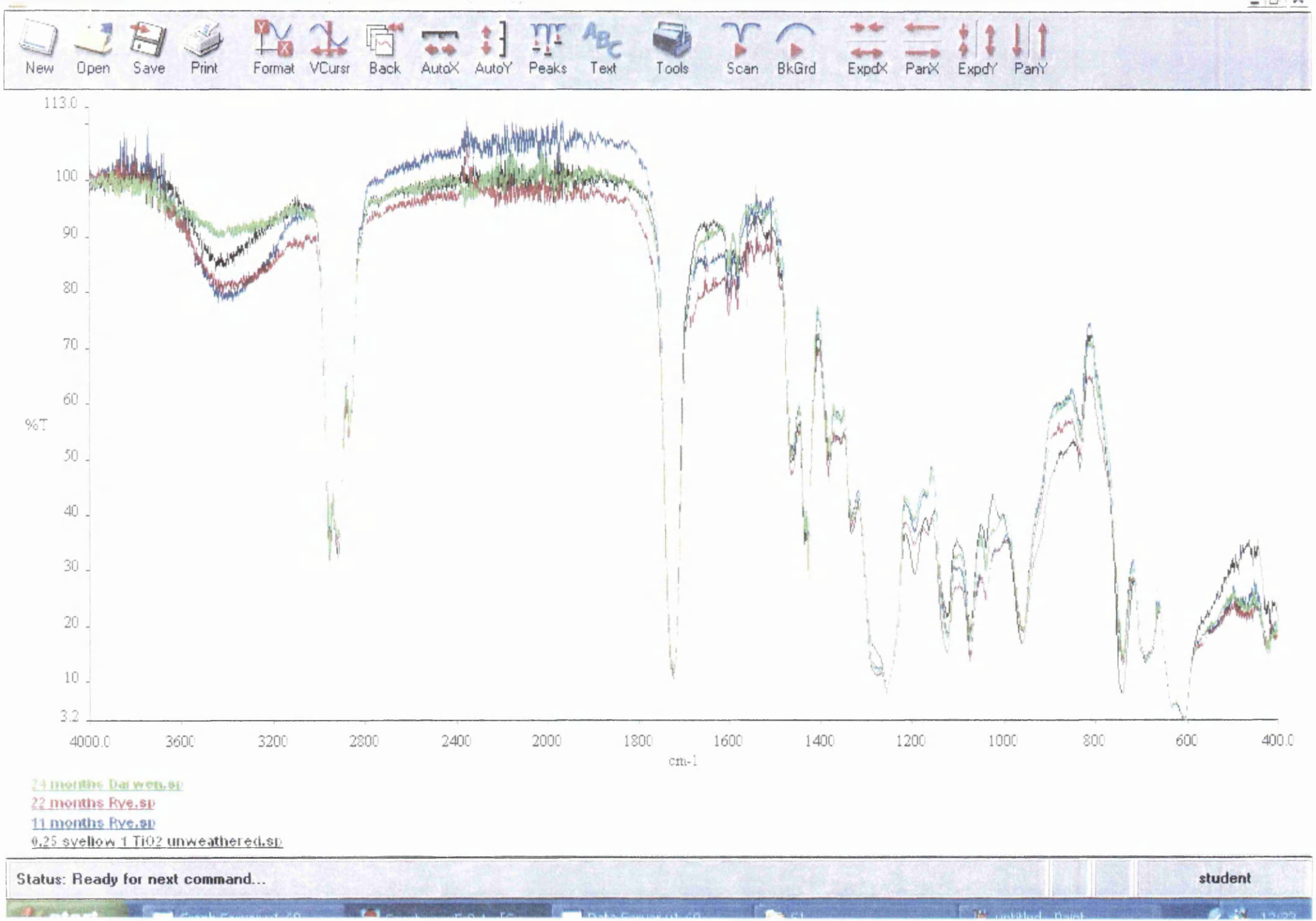
New
Open
Save
Print
Format
VCursr
Back
AutoX
AutoY
Peaks
Text
Tools
Scan
BkGrd
ExpdX
PanX
ExpdY
PanY
113.0
100
90
80
70
60
%T
50
40
30
20
10
3.2
4000.0
3600
3200
2800
2400
2000
1800
1600
1400
1200
1000
800
600
400.0
cm-1
24 months Darwen.sp
22 months Rye.sp
11 months Rye.sp
0.25 syellow 1 TiO2 unweathered.sp
Status: Ready for next command...
student

File Edit View Process Instrument Setup Procedures Window Help

New Open Save Print Format VCursr Back AutoX AutoY Peaks Text Tools Scan BkGrd ExpdX PanX ExpdY PanY

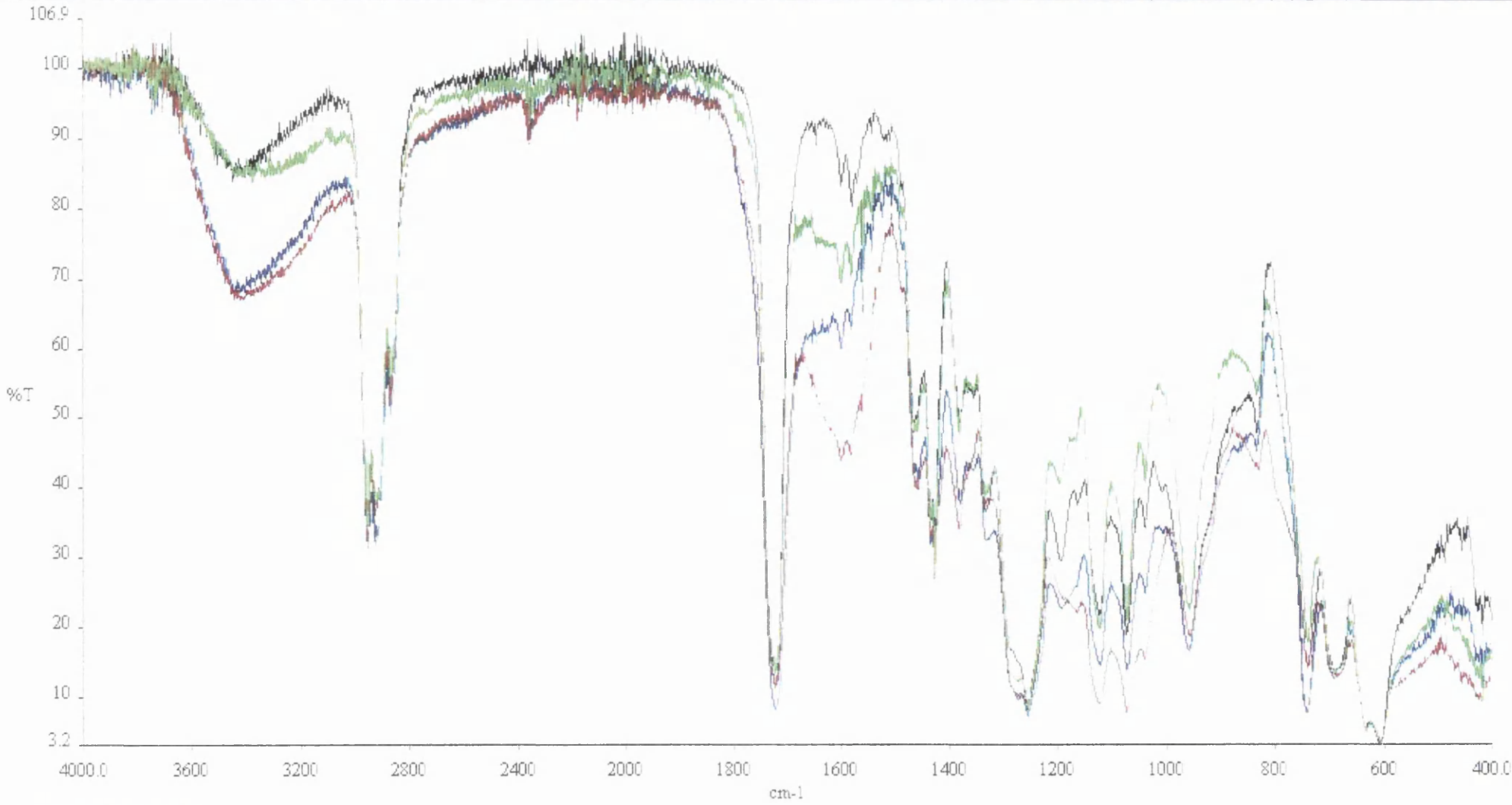

2500 hrs UVA cond..sp
2000 hrs UVA hor cond..sp
2000 hrs UVA.sp
0.25 svellow 1 TiO2 unweathered.sp

Status: Ready for next command...

student

File Edit View Process Instrument Setup Procedures Window Help

New Open Save Print Format VCursr Back AutoX AutoY Peaks Text Tools Scan BkGrd ExpdX PanX ExpdY PanY

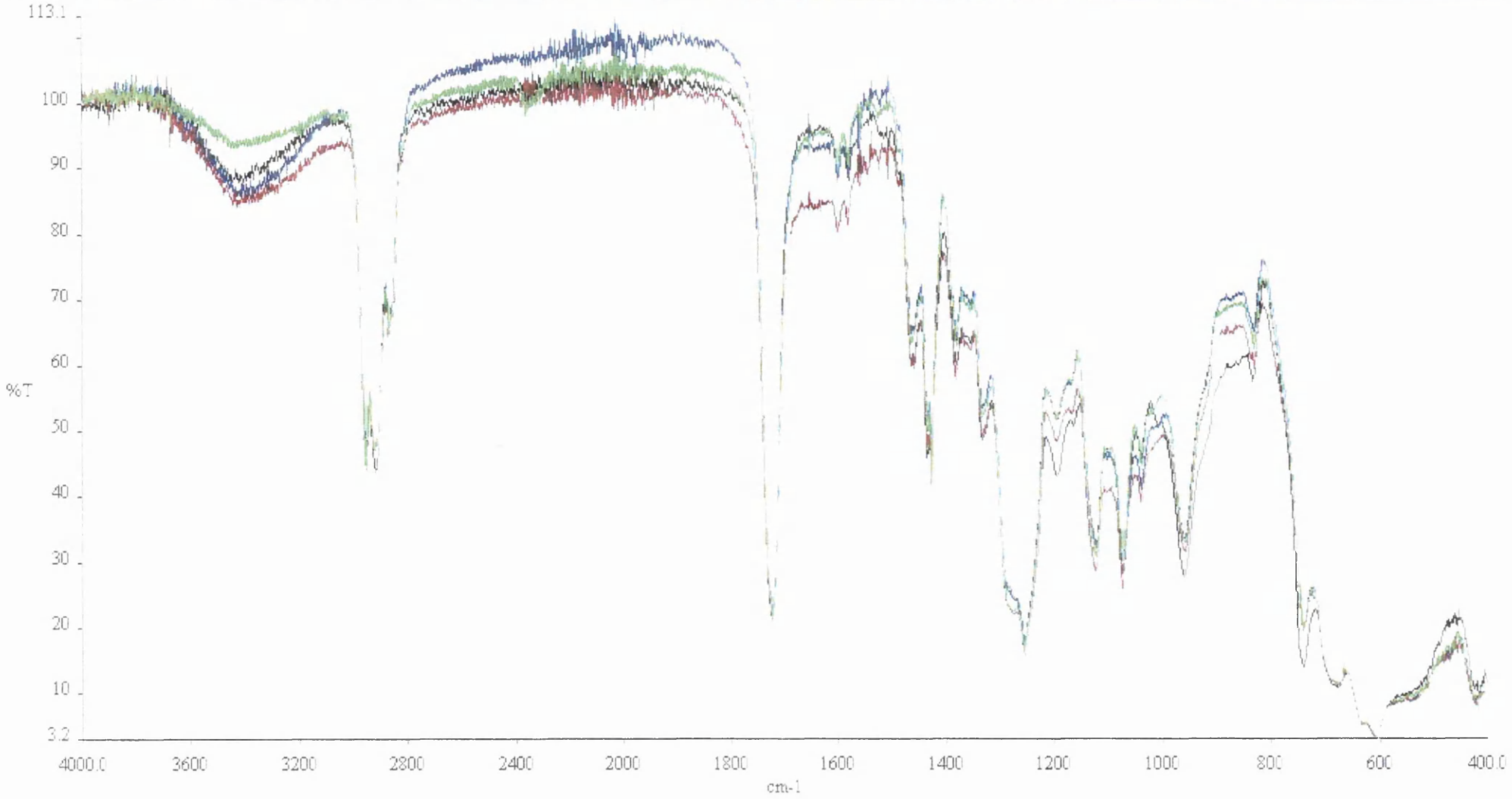

24 months Darwen.sp
22 months Rye.sp
11 months Rye.sp
0.25 svellow 5 TiO2 unweathered.sp

Status: Ready for next command...

student

File Edit View Process Instrument Setup Procedures Window Help

New Open Save Print Format VCursr Back AutoX AutoY Peaks Text Tools Scan BkGrd ExpdX PanX ExpdY PanY

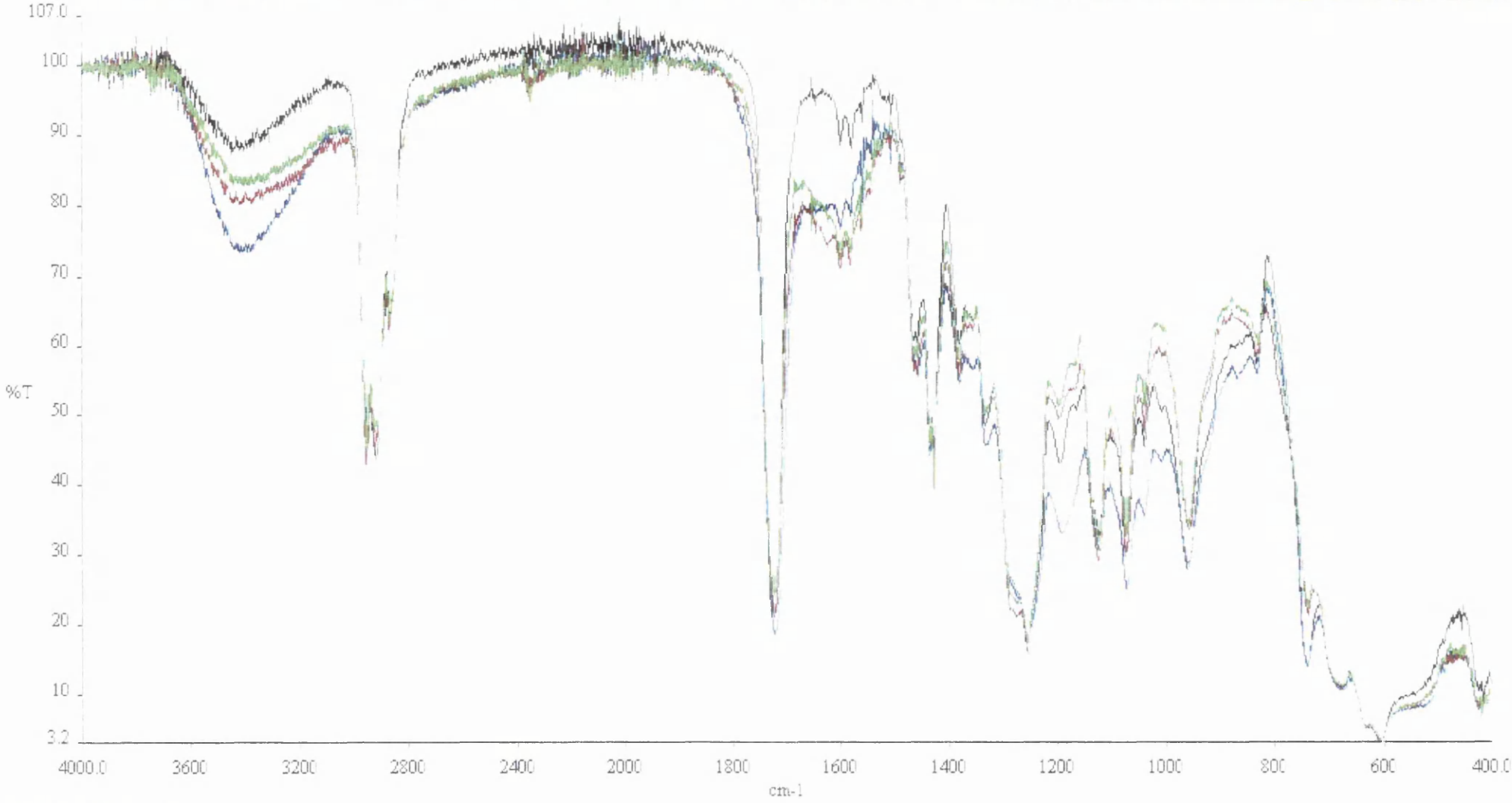

2500 hrs UVA cond..sp
2000 hrs UVA hor cond..sp
2000 hrs UVA.sp
0.25 svellow 5 TiO2 unweathered.sp

Status: Ready for next command...

student

File Edit View Process Instrument Setup Procedures Window Help

New Open Save Print Format VCursr Back AutoX AutoY Peaks Text Tools Scan BkGrd ExpdX PanX ExpdY PanY

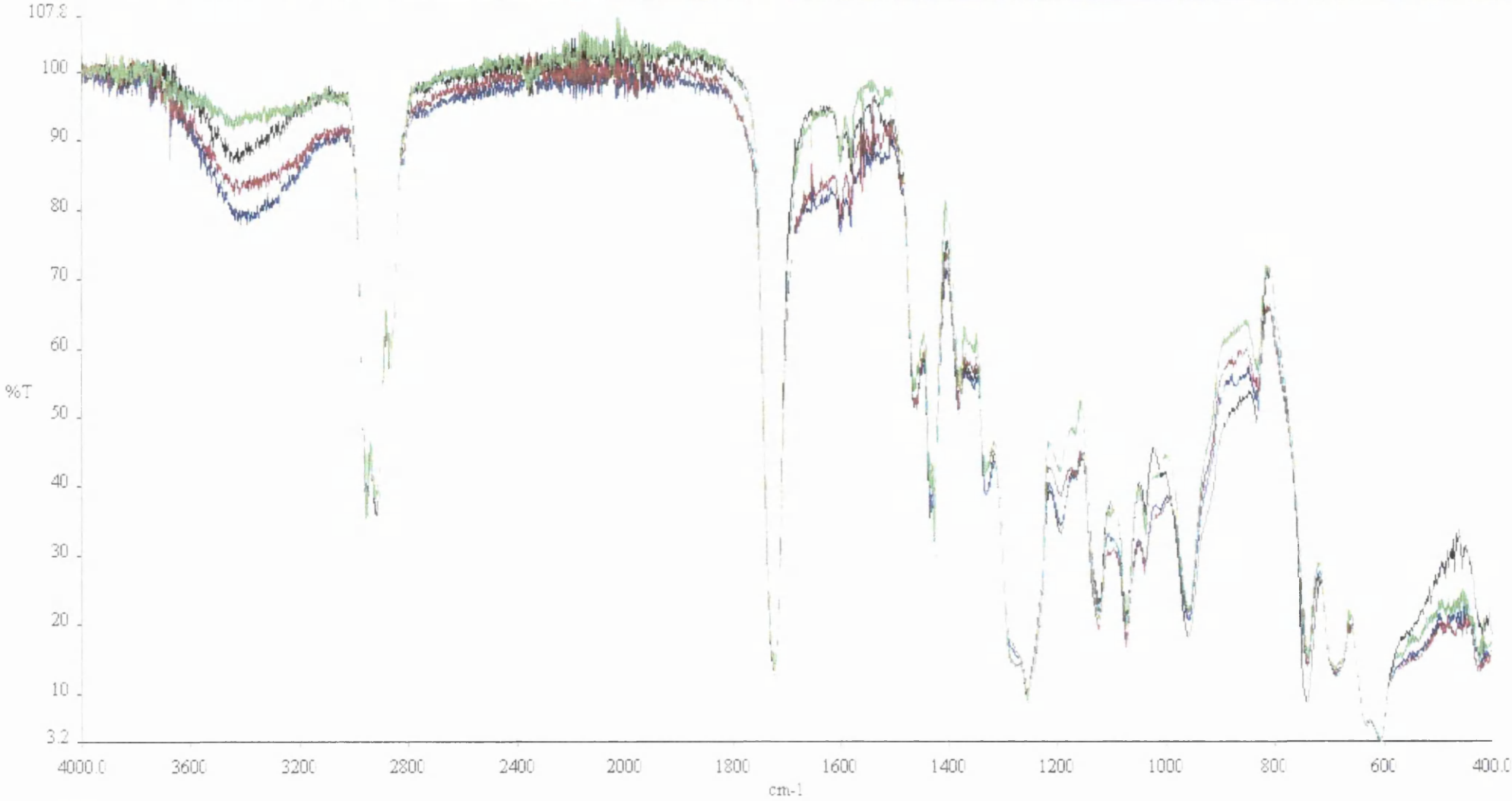

24 months Darwen.sp
22 months Rye.sp
11 months Rye.sp
1 svellow 1 TiO2 unweathered.sp

Status: Ready for next command...

student

File Edit View Process Instrument Setup Procedures Window Help

New Open Save Print Format VCursr Back AutoX AutoY Peaks Text Tools Scan BkGrd ExpdX PanX ExpdY PanY

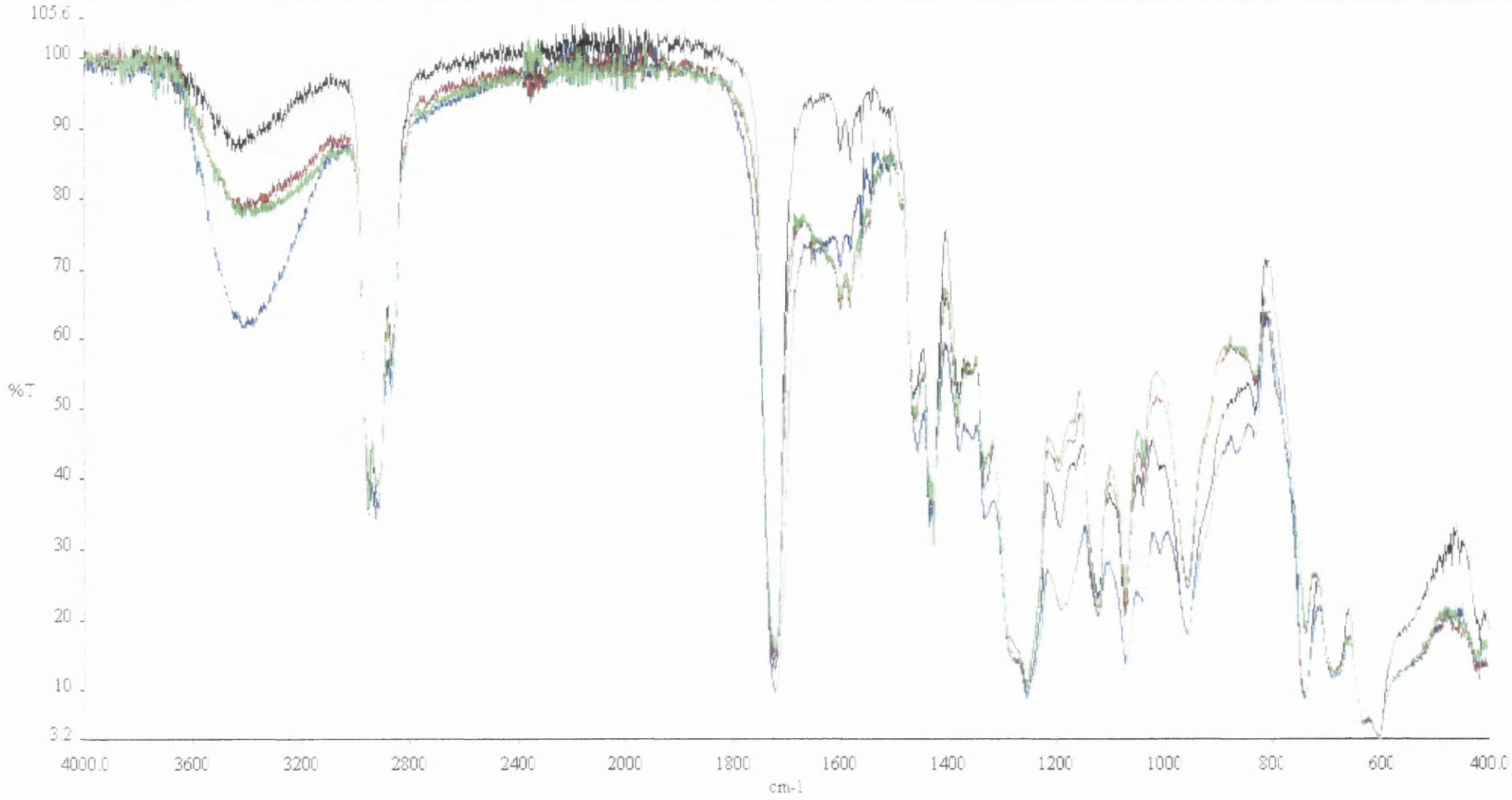

2500 hrs UVA cond..sp
2000 hrs UVA hor cond..sp
2000 hrs UVA.sp
1 svellow 1 TiO2 unweathered.sp

Status: Ready for next command...

student

File Edit View Process Instrument Setup Procedures Window Help

New Open Save Print Format VCursr Back AutoX AutoY Peaks Text Tools Scan BkGrd ExpdX PanX ExpdY PanY

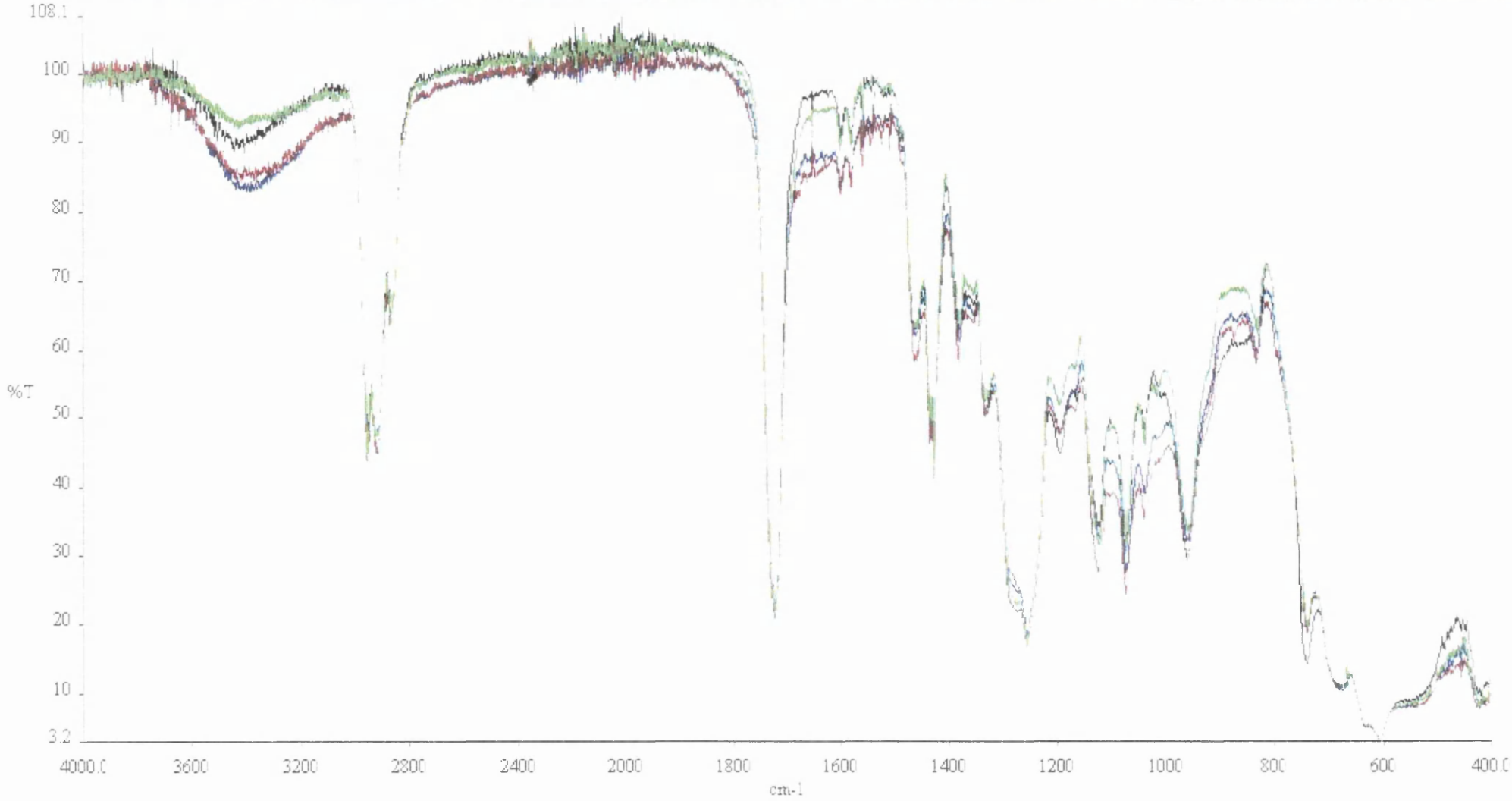

24 months Darwen.sp
22 months Rye.sp
11 months Rye.sp
1 svellow 5 TiO2 unweathered.sp

Status: Ready for next command...

student

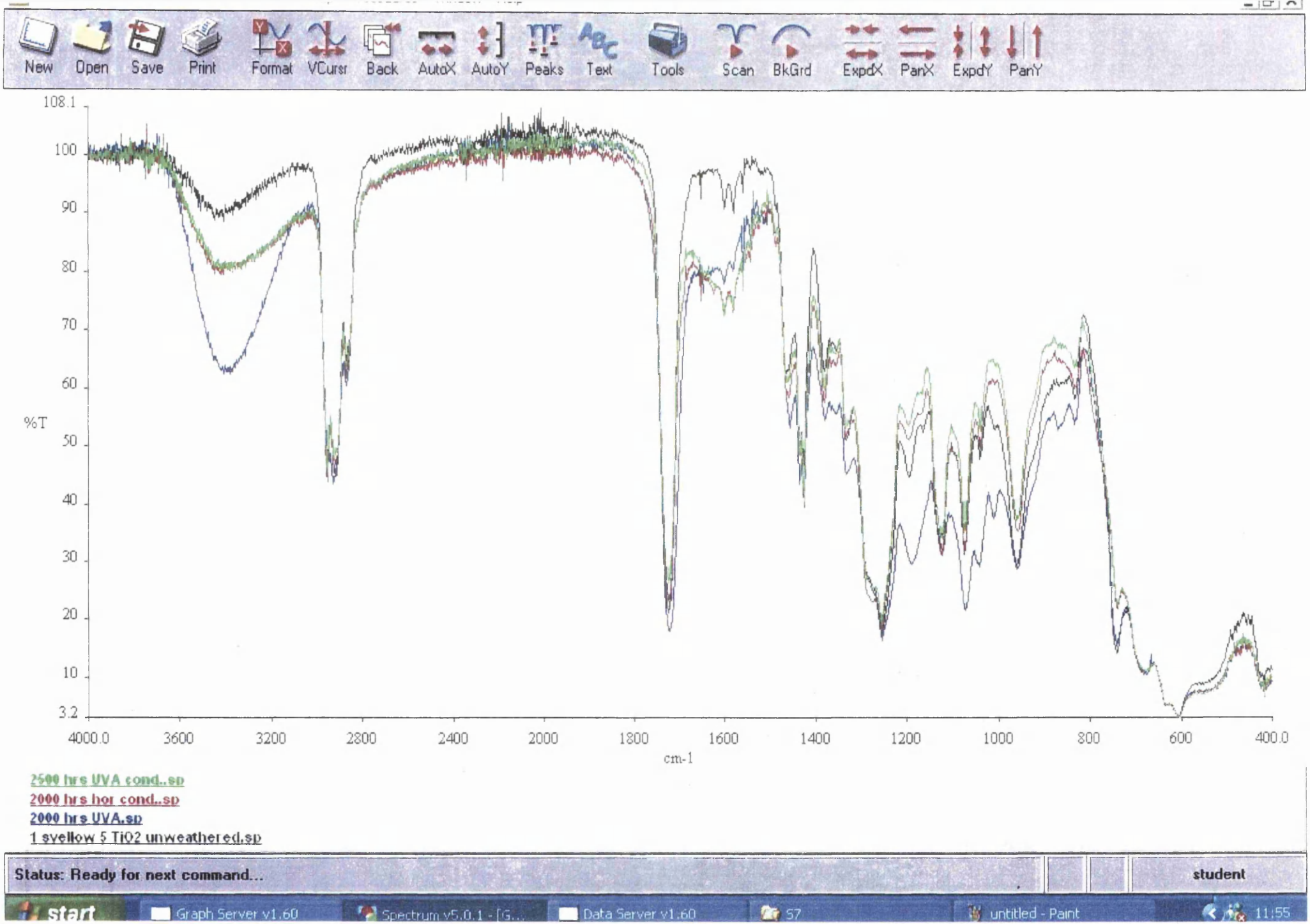
New
Open
Save
Print
Format
VCursr
Back
AutoX
AutoY
Peaks
Text
Tools
Scan
BkGrd
ExpdX
PanX
ExpdY
PanY
108.1
100
90
80
70
60
%T
50
40
30
20
10
3.2
4000.0
3600
3200
2800
2400
2000
1800
1600
1400
1200
1000
800
600
400.0
cm-1
2500 hrs UVA cond..sp
2000 hrs hor cond..sp
2000 hrs UVA.sp
1 syellow 5 TiO2 unweathered.sp
Status: Ready for next command...
student
start
Graph Server v1.60
Spectrum v5.0.1 - [G...
Data Server v1.60
S7
untitled - Paint
11:55